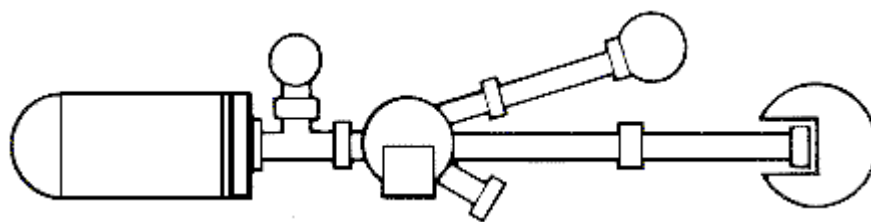


Welcome!
to the

**22nd International Conference
on the Application of Accelerators
in Research and Industry
(CAARI 2012)**



August 5 – 10, 2012

Renaissance Worthington Hotel

Fort Worth, Texas USA

Contact Details

Holly Decker
Conference Secretary
University of North Texas
1155 Union Circle, # 311427
Denton, Texas 76203-5017 USA

Phone: +1-940-565-3256
Fax: +1-940-565-2227
E-mail: holly.decker@unt.edu
Web: www.caari.com

Using this Abstract Book

Please, use the “find” field at the top of the pdf document to search for a single abstract or all the abstracts in a particular session. You can also search this entire document for words in the abstracts that relate to your areas of interest.

This listing contains information about each presentation including all of the authors and their affiliations. If one wants to find out when Barney Doyle’s talk is to be given, just look up his name in the index at the end of this book:

Doyle, Barney L. MON-AT03-1

Then go to the “PRESENTATIONS” listing to find

MON (i.e. the Monday presentations)

AT03 (the session codes are listed alphabetical, in this case AT is Accelerator Technology)

1 (the first talk of this session)

The details in this PRESENTATION listing includes the Presentation Number: #82

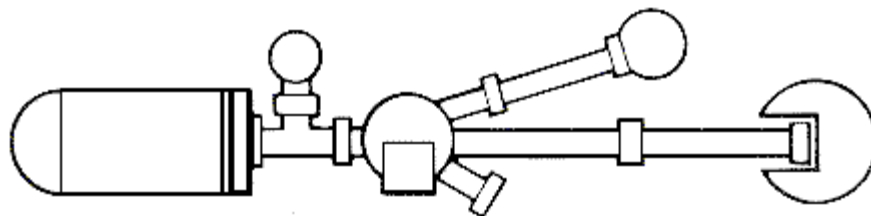
The type of presentation: Invited Talk

The day and time Session AT01 starts: Monday 1:00 PM

The location: The Bur Oak room

TABLE OF CONTENTS

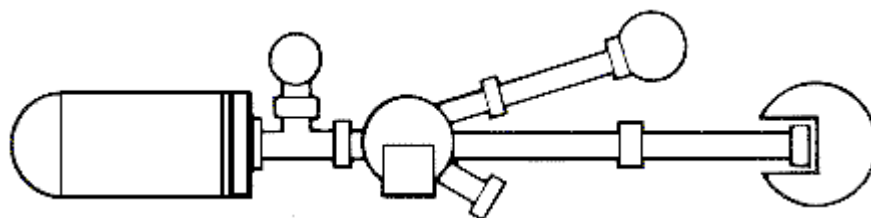
	<u>Page No.</u>
Monday Abstracts	5
Tuesday Abstracts	55
Wednesday Abstracts	125
Thursday Abstracts	188
Friday Abstracts	221
Author Index	223



ABSTRACTS

PLENARY, INVITED, CONTRIBUTED TALKS AND POSTERS

In Order by Day of the Week



MONDAY

Modeling X-ray Emission due to Charge Exchange

Phillip C. Stancil

Department of Physics and Astronomy, University of Georgia, Athens GA 30602, United States

Since the advent of Cravens' [1] proposal that the observed X-ray emission from comet Hyakutake was due to charge exchange (CX) of highly-charged solar wind ions with cometary neutrals, the CX mechanism has been identified as a possible dominant contributor to the X-ray emission observed in the heliosphere, planetary exospheres, the geocorona, supernova remnants, starburst galaxies, and molecular cooling flows in galaxy clusters. To provide reliable CX-induced X-ray spectra models to simulate these and other astrophysical environments, we have undertaken a project to compute quantum-state-resolved CX cross sections of highly-charged ions colliding with H and He. Here we summarize current results for $C^{(5-6)+}$, N^{6+} , and $O^{(6-8)+}$ obtained with the molecular-orbital close coupling (CC), atomic-orbital CC, and classical trajectory Monte Carlo methods. Utilizing the theoretical CX cross sections, cascade models are computed to generate X-ray spectra and compared to available measurements and observations. Comparison is also made to models assuming excitation by thermal electrons to identify diagnostics to distinguish CX-induced and electron-impact-induced X-ray emission. [1] T. E. Cravens, *Geophys. Res. Lett.* 25, 105 (1997).

This work was partially supported by NASA grant NNX09AV46G. Work performed in collaboration with Y. Wu, J. L. Nolte, D. R. Schultz, Y. Hui, M. Rakovic, H. P. Liebermann, and R. J. Buenker.

Fragmentation dynamics of complex molecules and their clusters

Patrick Rousseau¹, Sylvain Maclot¹, Michael Capron¹, Rémi Maisonnay¹, Elie Lattouf¹, Alicja Domaracka², Alain Méry¹, Jean-Christophe Pouilly¹, Jimmy Rangama², Jean-Yves Chesnel¹, Ann IS Holm³, Henning Zettergren³, Henrik AB Johansson³, Fabien Seitz³, Stefan Rosen³, Henning Schmidt³, Henrik Cederquist³, Bernd A Huber⁴,
Lamri Adoui¹

⁽¹⁾*Université de Caen Basse-Normandie, CIMAP, Bd Henri Becquerel, Caen F-14070, France*

⁽²⁾*CNRS, CIMAP, Bd Henri Becquerel, Caen F-14070, France*

⁽³⁾*Dpt of Physics, Atomic Physics, Stockholm University, Alba Nova University Ctr, Stockholm S-10691, Sweden*

⁽⁴⁾*CEA, CIMAP, Bd Henri Becquerel, Caen F-14070, France*

Complex molecular systems such as large molecules, clusters or nano-particles, consist of many atoms and are characterised by a large number of degrees of freedom. Energies well in excess of individual thresholds for fragmentation can be stored for long times and metastable excited states become important. We will concentrate in this talk on the study of the response of such nanoscale systems, **i.e.** we will study excitation and fragmentation mechanisms induced by highly charged ion (HCI) radiation, reflecting dynamic energy and charge flow processes. We will illustrate these relaxation processes for different molecular systems from Polycyclic Aromatic Hydrocarbons, water or biomolecule targets and their clusters in collision with HCI. We will emphasize that slow HCI provide an efficient way to study the stability of complex systems. Indeed, such ions are known to remove electrons at large impact parameters resulting in a fast and gentle ionisation. Moreover, in a less conventional way, HCI can also be used as a tool to form new bonds and induce the formation of even more complex molecules.

Classical treatment of ionization and electron capture in water by ion impact

Clara Illescas

Departamento de Química, Universidad Autonoma de Madrid, Cantoblanco Universidad, Madrid 28049, Spain

Ion-beam cancer therapy is a valuable alternative to conventional photon radiotherapy. In this field, collisions of water molecules by energetic ions play a very important role to the contribution of the stopping power of ions in biological tissues [1]. Moreover, ionization processes from multielectron and multicenter targets are also relevant in a broad range of disciplines such as fusion research and astrophysics.

In this work, we calculate electron production and electron capture total cross sections for H^+ , He^{2+} and C^{6+} + H_2O collisions in the impact energy range of $10 \text{ keV/amu} < E < 10 \text{ MeV/amu}$. The basic assumptions of our ion-molecule CTMC (Classical Trajectory Monte-Carlo) treatment [2] are: (i) the electrons are independent, so each electron is moving in an effective field created by the nuclei and the remaining electrons; (ii) the interaction of the active electron with the H_2O^+ core is described by a three-center model potential, so we explicitly consider the anisotropy of the molecular target; (iii) we apply the IEVM (Independent Event Model) for evaluating the inelastic multielectron probabilities from the mono-electronic ones.

In this talk, I will summarize this approach, emphasizing the description of the initial electron densities associated with the molecular orbitals of the H_2O molecule and, discuss our results for ionization and electron capture. I will also illustrate the validity of the postcollisional fragmentation mechanism by comparing calculated fragmentation yields with the available measurements for $H^+ + H_2O$ collisions. A stringent test of our CTMC method is provided by the good agreement of the calculated emitted electron spectra with the experimental data that will be shown at the Conference.

[1] D. Schardt et al., Rev. Mod. Phys. 82, 383 (2010)

[2] Clara Illescas et al., Phys. Rev. A 83, 52704 (2011)

ION IMPACT INDUCED IONIZATION/FRAGMENTATION DYNAMICS OF RARE GAS DIMERS

Markus S. Schoeffler¹, H.K. Kim¹, J. Titzel¹, F. Trinter¹, M. Waitz¹, J. Voigtsberger¹, H. Sann¹, M. Meckel¹, C. Stuck¹, U. Lenz¹, D. Metz¹, A. Jung¹, M. Odenweller¹, N. Neumann¹, B. Ulrich¹, R. Costa-Fraga¹, N. Petridis¹, S. Schoessler¹, K. Ullmann-Pfleger¹, R. Grisenti¹, A. Czasch¹, O. Jagutzki¹, L. Schmidt¹, T. Jahnke¹, H. Schmidt-Boecking¹, J. Bech¹, H. Gassert¹, H. Merabet², J. Rangama³, C. L. Zhou³, A. Cassimi³, R. Doerner¹

⁽¹⁾Institut fuer Kernphysik, J. W. Goethe Universitaet Frankfurt, Max-von-Laue-Str. 1, Frankfurt 60438, Germany

⁽²⁾Department of Mathematics, Statistics and Physics, College of Arts and Sciences, P.O. Box: 2713, Doha, Qatar

⁽³⁾CIMAP Caen, GANIL, Bd Henri Becquerel, BP 55027, Caen 14076, France

Rare gas atoms can form weakly bound molecules, held together by the van-der-Vaals-force. We investigated the ionization/fragmentation-dynamics of He_2 and Ne_2 caused by ion impact with a COLTRIMS reaction microscope. Dependent on how electrons are removed from the dimer's atomic sites different decay pathways are open. We focus on the following two:

1.) The direct mechanism, where the projectile ionizes both atoms via 2 separate projectile-atom interactions. The dimer's constituents have ionization properties similar to those of a single atom. Up to now, large impact parameters b , which dominate ionization are believed not to be an observable that can be measured. For large impact parameters Rutherford scattering leads to momentum transfers, that are smaller than the momenta transferred by the ejected electrons. This makes the impact parameter inaccessible through any momentum transfer measurement between the nuclei. The large internuclear distance of the dimer open a new way to access the impact parameter. The impact parameter dependent ionization probability $P(b)$ will lead to a maximum tilt angle of the molecular axis to the ion beam up to which both atoms can be ionized. Measuring this molecular orientation allows to test the predictions of impact parameter dependence of ionization [1].

2.) In addition to the direct ionization mechanism, where the dimer's atoms are subsequently ionized there is also a second mechanism, which is called the Interatomic Coulombic Decay (ICD). Predicted in 1997 [2] and in photoionization experimentally shown in 2004 [3], ICD probably plays a significant role for radiation damage in living tissue and for ion radiation therapy [4,5].

- [1] Titze et al., PRL, 106, 033201, (2011)
- [2] Cederbaum et al., PRL, 79, 4778, (1997)
- [3] Jahnke et al., PRL, 93, 163401-1, (2004)
- [4] Boudaïffa, et al., Science 287, 1658, (2000)
- [5] H.-K. Kim et al., PNAS, 108, 29, (2011)

MON-AP01-5

#384 - Invited Talk - Monday 1:00 PM - Elm Fork

Supercritical Dirac Resonances in Heavy-Ion Systems

Alain Marsman, Marko Horbatsch

Physics and Astronomy, York University, 4700 Keele St., Toronto Ontario M3J 1P3, Canada

The intense fields that develop during collisions of highly-charged heavy ions give rise to a range of electrodynamic phenomena, including ionization and electron-positron creation, due to the time-varying nuclear potentials. If the nuclear separation is sufficiently close, the combined electrostatic field can even become **supercritical**, strong enough to destabilize the vacuum and cause it to spontaneously decay by pair creation to a charged state.

This process can be understood in terms of supercritical Dirac resonances, whereby an initially vacant $1S\sigma$ bound-state becomes embedded in the negative-energy continuum, forming a resonance which gradually decays to a bound-electron/free-positron pair. These resonance states are characterized by their mean energy position E_{res} , and width Γ . The position determines the kinetic energy of the emitted positron, while the width is related to the lifetime of the state by the uncertainty principle. An accurate determination of these parameters is therefore of interest in order to model the supercritical component of the positron spectrum. The current work is based on numerically solving the Dirac equation to high precision, combined with analytic continuation of the Hamiltonian, giving the position and width of the resonance in terms of a complex eigenenergy. The equations, which contain the multipole decomposition of the two-center potential, are augmented by a complex absorbing potential and truncated at various orders in the partial wave expansion to demonstrate convergence of the resonance parameters in the limit of vanishing absorber. The convergence of the partial-wave spinor and of the multipole potential expansions is demonstrated in the supercritical regime.

MON-AP01-P1

#45 - Poster - Monday 5:30 PM - Rio Grande

Single electron capture in K^+ - H_2 reaction

FB Alarcon¹, FB Yousif², H Martinez¹, BE Fuentes³

⁽¹⁾*Instituto de Ciencias Fisicas, Universidad Nacional Autonoma de Mexico, Apdo. Postal 48-3, Cuernavaca Morelos 62210, Mexico*

⁽²⁾*Facultad de Ciencias, Universidad Autonoma del Estado de Morelos, Av. Universidad 1001, Cuernavaca Morelos 62210, Mexico*

⁽³⁾*Facultad de Ciencias, Universidad Nacional Autonoma de Mexico, Circuito Exterior, Ciudad Universitaria, Mexico Distrito Federal 04510, Mexico*

In collisions of alkali metal ions with rare gas atoms at energies ranging from a hundred to a thousand electron volts, various inelastic processes are involved effectively. However, obtaining reliable data about the cross-sections of these processes is still difficult. This is mainly due to the characteristics of the colliding particles having closed electron shells, and leading to the formation of energetic secondary particles. To reveal the mechanism of the inelastic processes, it is necessary to determine the contribution of the separate inelastic channels for the investigated processes. For example in capture processes, the contribution of capture at different states, involving either the target or the projectile electrons, plays a significant role, so that the dominant process is not always the direct electron capture to the ground state.

In this work a beam of K^+ -ions from a surface-ionization source was accelerated, focused and then passed through the collision chamber filled with the target gas (H_2), to measure the absolute total cross sections for the production K^0 in collisions of K^+ ions with H_2 molecules. We present measurements of absolute cross section of single electron capture for the $K^+ - H_2$ reaction in the energy range of 0.5 to 4 keV. Capture cross section increased with an increase in energy. Present results overlap with previously measured data of other investigators [1, 2] and extend down in energy.

This research was partially sponsored by DGAPA IN-109511, CONACyT 128714.

[1] Ignacio Alvarez, Carmen Cisneros, C.F. Barnett and J.A. Ray, Phys. Rev. A13 (1976) 1728.

[2] M. Gochitashvili, B.Kikiani and R. Lomsadze, Hyperfine Interactions 132 (2001) 517.

MON-AP01-P2

#247 - Poster - Monday 5:30 PM - Rio Grande

Calculations for electron removal and fragmentation in proton-water-molecule collisions

Mitsuko Murakami¹, Tom Kirchner¹, Marko Horbatsch¹, Hans Juergen Luedde²

⁽¹⁾Department of Physics and Astronomy, York University, 4700 Keele Street, Toronto Ontario M3J1P3, Canada

⁽²⁾Institut fuer Theoretische Physik, Goethe-Universitaet, Max-von-Laue Str. 1, Frankfurt 60438, Germany

Charge-state correlated cross sections for single- and multiple-electron removal processes due to capture and ionization in proton-water-molecule collisions are calculated by using the non-perturbative basis generator method adapted for ion-molecule collisions [1,2]. Orbital-specific cross sections for vacancy production are evaluated using this method to predict the yields of charged fragments according to branching ratios known to be valid at high impact energies. At intermediate and low energies, we obtain fragmentation results on the basis of predicted multi-electron removal cross sections, and explain most of the available experimental data. The cross sections for charge transfer and for ionization are also compared with recent multi-center classical-trajectory Monte Carlo calculations for impact energies from 20 keV to several MeV.

[1] H.J. Luedde et al, Phys. Rev. A 80, 060702(R) (2009)

[2] M. Murakami et al, Phys. Rev. A 85, 052704 (2012)

MON-AP01-P3

#258 - Poster - Monday 5:30 PM - Rio Grande

Classical treatment of ionization and capture in ion- H_2O collisions at intermediate energies

Clara Illescas¹, L. F. Errea¹, L. Méndez¹, B. Pons², I. Rabadán¹

⁽¹⁾Departamento de Química, Universidad Autónoma de Madrid, Cantoblanco Universidad, Madrid 28049, Spain

⁽²⁾CELIA, Université de Bordeaux I-CNRS-CEA, Cours de la Libération, Talence, Bordeaux 33405, France

Ionization of water molecules by energetic ions are relevant processes in hadron therapy, which is a valuable alternative to conventional photon therapy. They are also benchmark systems for ionization of other multielectron and multicenter targets, needed to understand biological damage of ionizing radiations.

Several experiments have provided detailed information on ionizing proton-water collisions, but data are scarce for multicharged ion impact. Therefore, we have performed calculations for H^+ , He^{2+} and $C^{6+} + H_2O$ collisions in the energy range of $15 \text{ keV/amu} < E < 10 \text{ MeV/amu}$ employing our ion-molecule CTMC (Classical Trajectory Monte-Carlo) treatment described in [1]. We have calculated total cross sections for single and double inelastic processes as well as single (SDCS) and double (DDCS) differential cross sections of electron emission in the ionization of H_2O bombarded by stripped projectiles. The energy and angular distributions of the electron have been calculated at collision energies of the experiments. Preliminary results for proton- H_2O collisions show a good agreement of the classical SDCS and DDCS with the experimental data [2,3] and other theoretical results obtained in the frame of the first Born approximation [4].

[1] C. Illescas et al., Phys. Rev. A 83, 52704 (2011)

[2] M. A. Bolorizadeh and M. E. Rudd, Phys. Rev. A 33, 888 (1986)

[3] L. H. Toburen and W. E. Wilson, J. Chem. Phys. 66, 5202 (1977)

[4] O. Boudrioua et al., Phys. Rev. A 75, 22720 (2007)

Oscillatory patterns in angular differential ion-atom charge exchange cross sections: the role of electron saddle swaps

Sebastian Otranto¹, Ina Blank², Ronald E Olson³, Ronnie Hoekstra²

⁽¹⁾*IFISUR and Departamento de Física, Universidad Nacional del Sur, Av. Alem 1253, Bahía Blanca Buenos Aires 8000, Argentina*

⁽²⁾*KVI Atomic Physics, Zernikelaan 25, NL-9747 AA, Groningen, Netherlands*

⁽³⁾*Physics Department, Missouri University of Science and Technology, Rolla MO 65409, United States*

We present a theoretical and experimental study of state selective and angular differential cross sections of single electron transfer in collisions of Ne^{8+} with ground state $\text{Na}(3s)$ in the collision energy range 1-10 keV/amu. The experiments were performed by means of the MOTRIMS technique which provides high resolution data for the Na^+ recoil momentum spectrum. The theoretical description is based on the 3-body classical trajectory Monte Carlo (CTMC) method with a Garvey model central potential for the electron- Na^+ ion interaction. We find the total cross section of charge exchange to be a smooth function of the impact energy but oscillatory patterns emerge as we investigate further the angular differential cross sections. In particular, for electron capture to n-levels > 10 the transverse momentum distributions exhibit an oscillatory structure which is very sensitive on the impact energy. Our theoretical analysis suggests that this feature is a direct consequence of the number of swaps the electron undergoes across the potential energy saddle during the charge exchange process. Although different numbers of swaps also contribute to $n < 9$, their contributions overlap in such a way that no oscillatory pattern can be identified. A closer theoretical inspection of the collision dynamics for electron capture to n-levels > 10 suggests that the last saddle crossing for the 1 (3)-swap mechanism takes place in the outgoing (incoming) path of the projectile. We argue that this effect is a general feature of low-energy collisions of highly charged ions with atoms.

Alternative Approaches for Achieving Antihydrogen Recombination

Carlos A. Ordonez

Department of Physics, University of North Texas, 1155 Union Circle #311427, Denton Texas 76203-5017, United States

Research by a number of collaborations at the CERN Antiproton Decelerator facility is aimed at testing fundamental symmetries between the properties of hydrogen and antihydrogen. Antihydrogen is currently produced by using nested Penning traps to confine antihydrogen plasma, within which three-body recombination occurs. Matter-antimatter symmetry studies with antihydrogen requires the production of antihydrogen atoms with sufficiently low kinetic energy. However, plasma drifts within nested Penning traps represent a formidable problem. An antihydrogen atom is born with the kinetic energy of its antiproton, and plasma drifts can increase the kinetic energy of antiprotons. An ideal plasma confinement approach for antihydrogen studies would avoid plasma drifts and be capable of providing long confinement times for a cold, dense non-drifting (e.g., non-rotating) plasma of any desired size. We are studying alternatives that may ultimately provide such confinement. For many of the configurations, a minimum-B magnetic field could be produced that could serve for trapping antihydrogen atoms. However, configurations that do not produce a minimum-B magnetic field are also being studied, because it is not necessary to trap antihydrogen for conducting gravity symmetry studies. Alternatives being studied include configurations that employ an artificially structured boundary, dual levitated coils, or two pairs of parallel wires that are crossed. The possibility of using the configurations for other applications, such as for confining fusion plasmas, is discussed.

Kohn Variational Calculations of Positronium-Hydrogen Scattering

Denton Woods¹, S. J. Ward¹, P. Van Reeth²

⁽¹⁾*Physics Department, University of North Texas, 1155 Union Circle, #311427, Denton TX 76203-1427, United States*

⁽²⁾*Department of Physics and Astronomy, University College London, Gower Street, London WC1E 6BT, United Kingdom*

We are investigating positronium-hydrogen (Ps-H) scattering, which is a fundamental four-body Coulomb process. Using the Kohn, inverse Kohn, generalized Kohn and complex Kohn variational methods, we computed preliminary $^{1,3}\text{S}$ and $^{1,3}\text{P}$ -wave phase shifts for Ps-H scattering. We implemented different numerical techniques to reduce linear dependence, and we have been able to use larger basis sets than used in the previous Kohn and inverse Kohn variational calculations [1,2]. For the $^{1,3}\text{P}$ -wave trial functions, as in the previous variational calculations, we considered Hylleraas-type short-range terms in which the angular momentum is on both the positron and on the electron of the Ps atom. We have also considered using Hylleraas-type terms in which the angular momentum is on the Ps atom and on the electron of the H atom. Using a quantum defect theory for the van der Waals interaction [3], we determined the $^{1,3}\text{S}$ scattering lengths and effective ranges. **D**-wave calculations of Ps-H scattering are underway.

S.J.W. acknowledges support from NSF under grant no. PHYS-968638.

[1.] P. Van Reeth and J. W. Humberston, J. Phys. B **36**, 1923 (2003).

[2.] P. Van Reeth and J. W. Humberston, Nucl. Instr. and Methods Phys. Res. B **221**, 140 (2004).

[3.] Bo Gao, Phys. Rev. A **58**, 4222 (1998).

Time-Dependent Close-Coupling Study of Antiproton-Impact Ionization of Atoms and Molecules

Teck Ghee Lee¹, M S Pindzola¹, J Colgan²

⁽¹⁾*Physics, Auburn University, Auburn AL 36949, United States*

⁽²⁾*Theoretical, Los Alamos National Laboratory, Los Alamos NM, United States*

Over the years significant effort has been made in order to better understand the interactions between antiproton and atoms or molecules. One reason being such fundamental knowledge may serve as a key to the formation and production of antihydrogen at CERN for testing CPT invariance and disclosing the nature of gravity. Another being low-energy antiproton beam has been suggested as a possible radiation therapy for cancer treatment. More precisely, atomic and molecular ionization processes due to antiprotons may help to better understand the radiation damage of biological cells. With the construction of the Facility for Low-Energy Antiproton and Ion Research at GSI, new experiments will be performed for antiproton collisions with various atoms and molecules. In this talk I shall present a time-dependent close-coupling (TDCC) method that was used to study the atomic and molecular ionization due to antiproton-impact. Samples of TDCC calculated energy-dependent ionization cross sections for H, He, Li, H₂⁺ and H₂ will be shown and compared with the available theories and experiments.

This work is supported by Department of Energy and National Science Foundation. The computational work was carried out under a DOE ERCAP award at the National Energy Research Scientific Computing Center in Oakland, California, USA, and under a NSF Tera-grid award at the National Institute for Computational Science (NICS) in Knoxville, Tennessee, USA.

Antiproton, proton and electron impact multiple ionization of rare gases

Claudia C Montanari, Jorge E Miraglia

Institute of Astronomy and Space Physics, CONICET and University of Buenos Aires, Pabellon IAFE, Ciudad Universitaria, Buenos Aires, Argentina

Multiple-ionization is one of the most challenging subjects within the field of the atomic collisions. Experimental measurements require highly advanced techniques to get absolute values of all possible channels and final states. For positive ions, they must separate pure ionization from capture channels, which enhance the data in the intermediate energy region [1]. The case of antiproton impact is quite different. Despite the experimental difficulty to achieve a low energy antiproton-beam, it is the simplest ionization dynamic to describe [2]: no possible capture channel or electron exchanges to consider. On the other hand, the study of antiproton impact ionization has the additional interest of being projectiles produced in high-energy physics sources.

We present a theoretical study on multiple-ionization [3], which involves four different aspects:

i) the theoretical calculations of single to sextuple ionization cross sections, using the CDW-EIS and the first Born approximation in an extended energy region (50 keV-15 MeV).

ii) the inclusion of Auger-type post-collisional contributions through experimental photoionization data.

iii) the comparison with the available experimental data on multiple-ionization by protons and antiprotons, but also by electron impact at high velocities. In this energy region the post-collisional ionization is the main contribution to multiple-ionization.

iv) the review of the total ionization cross sections, gross and count, showing that Auger-type contributions should be included in total-ionization cross sections too. Our results demonstrate that this contribution is very small for Ne or Ar but increases with the target atomic number, being 30 % for total-ionization of Xe at high energies [3].

[1] DuBois R D, **Phys. Rev. Lett.** **52**, 2348-2351 (1984).

[2] Kirchner T and Knudsen H, **J. Phys. B: At. Mol. Opt. Phys.** **44**, 122001 (2011).

[3] Montanari C C and Miraglia J E **J. Phys. B: At. Mol. Opt. Phys.** **45**, in press (2012).

An Overview of the Activities and Developments at the Surrey Ion Beam Centre

R. P. Webb, B. N. Jones, V. V. Palitsin, G. W. Grime, J. L. Colaux, M. J. Bailey, C. Jeynes, K. C. Heasman, N. Peng, R. M. Gwilliam, M. Merchant, J. C. Jeynes, K. J. Kirkby
Surrey Ion Beam Centre, University of Surrey, Guildford Surrey, United Kingdom

The Surrey Ion Beam Centre (IBC) is the National Centre for ion beam applications in the UK. It provides facilities for ion implantation and analysis to more than 100 companies and academic departments around the world. The IBC houses three accelerators, used for ion beam modification of materials and one used for ion beam analysis and radiation biology. A brief description of the interactions with industry and academia will be given, with some case histories.

The unique combination of facilities housed at the IBC are described, including: the implantation facilities (from 2 keV to 4 MeV); IBA beamlines for channelling microbeam and in air measurement; the vertical nanobeam used for radiation biology experiments; and the horizontal nanobeam line under development for proton beam lithography. Examples of the developments and use of these lines will be given.

A new beam line for MeV-SIMS (Secondary Ion Mass Spectrometry), which is expected to be fully operational by the end of this year, will be described. The expectations and development of this new MeV-SIMS beam line, which will provide molecular concentration mapping at ambient pressure, will be given.

The Ion Implantation Laboratory at IF-UFRGS

P. L. Grande, J. F. Dias, P. F. Fichtner, C. Radkte, F. C. Stedile, C. Krug, G. V. Soares, L. Amaral, G. M. de Azevedo, R. Papaleo

Institute of Physics, Federal University of Rio Grande do Sul, Porto Alegre RS, Brazil

The Ion Implantation Laboratory is an ion beam center belonging to the Institute of Physics (IF) at the Federal University of Rio Grande do Sul (UFRGS). This facility is fully dedicated to research in materials research, fundamental and applied physics. The activities with ion beams started in 1981 with the acquisition of a 400 kV particle accelerator, which was upgraded to 500 kV in 1996. In 1997, a 3 MV TANDEM accelerator from High Voltage Engineering Europa B.V (HVEE) became operational at this facility. Both machines provide a wide variety of positive ions covering a broad energy range. Several beam lines with different analytical techniques (PIXE, RBS, NRA and ERDA) are available to scientists from different fields. In the past ten years, two other beam lines were installed at this facility: MEIS (Medium Energy Ion Scattering) and ion microprobe. MEIS is a high-resolution ($DE/E \sim 3E-3$) backscattering technique, which allows to characterize nanostructures like nanoparticles, nanoislands and quantum-dots located either on the surface of at buried interfaces. The ion microprobe system consists of an Oxford triplet lenses coupled to a scanner, allowing the measurement of different materials at micrometer scale. Microprobe techniques like STIM (on- and off-axis), micro-RBS and micro-PIXE are fully operational at this beam line.

In this talk, a brief review of leading research pursued at the Ion Implantation Laboratory will be presented. The capabilities of the MEIS technique with some recent results will be discussed as well.

Upgrade to the East Carolina University Accelerator Laboratory

Jefferson L. Shinpaugh, James M Joyce, Chris A Bonnerup, Larry H Toburen
Department of Physics, East Carolina University, Greenville NC 27858, United States

The ECU Accelerator Laboratory has recently undergone major upgrades to the ion beam system and extensive renovations to the facility infrastructure. This has included the addition of a new National Electrostatics Corporation 2-MV Pelletron accelerator to replace the 1970s-vintage High Voltage Engineering tandem accelerator. The new accelerator and high-energy beam transport system will allow us to expand our current studies of fundamental processes in ion-atom and ion-molecule collisions, atomic interactions in solids, and radiation effects in biological systems. In addition, our multidisciplinary research using ion beam analysis techniques should benefit significantly from the laboratory upgrades. The new ion beam system will be described along with the current research supported in the laboratory.

This work is supported in part by the National Science Foundation and the National Institutes of Health, National Cancer Institute.

Upgrade of the Ion Beam Modification and Analysis Laboratory at the University of North Texas

Gary A. Glass, Floyd D. McDaniel, Bibhudutta Rout, Duncan L. Weathers, Tilo Reinert, Jerome L. Duggan, Naresh T. Deoli, Mangal Dhoubhadel, Venkata C. Kummari, Jack E. Manuel, Jose L. Pacheco, Stephen J. Mulware, W. J. Lakshantha, Nafiseh Aflakian
Ion Beam Modification and Analysis Laboratory, Physics Department, University of North Texas, Denton TX 76203, United States

The Ion Beam Modification and Analysis Laboratory (IBMAL) of the University of North Texas utilizes four electrostatic accelerators for work in ion beam modification and analysis and ion beam systems development. A National Electrostatics Corporation (NEC) 9SDH-2 3.0 MV tandem Pelletron with SNICS and RF ion sources has several dedicated beamlines for low and high energy ion implantation, ion analysis and ion microscopy.

An NEC 9SH 3.0 MV single-ended Pelletron was recently installed and will have beamlines for ion microscopy/microlithography and high resolution ion beam analysis including channeling. Additionally, a Texas Nuclear 200 kV Cockcroft-Walton accelerator and a HVEC 2.5 MV Van de Graaff accelerator are available for ion beam analysis and surface studies. This report will outline the ongoing work at IBMAL, upgrades to accelerator systems and future plans.

MON-IBA01-1

#428 - Invited Talk - Monday 1:00 PM - Brazos I

Ion Beam Analysis of Highly Mismatched Alloy Films

Rachel S. Goldman

Materials Science and Engineering, University of Michigan, 2300 Hayward Street, Ann Arbor MI 48109, United States

Highly mismatched alloys (HMAs) consist of highly immiscible solute atoms in a solvent. Due to the resonant interactions between the conduction and/or valence band of the solvent and energy levels of the solute, HMAs provide an "intermediate band" for solar cells based upon multi-photon excitation. The effective bandgap narrowing is also useful for ultra-high efficiency tandem solar cells. In addition, the resonant levels in HMAs have been proposed as potential candidates for high efficiency thermoelectrics based upon tuning of the electron density of states. The properties of HMAs are often described with a model focusing on the influence of individual solute atoms, assuming that all solute atoms "see" the same atomic environment. In the case of GaAsN alloys, single local environment models predict a N composition-dependent energy band gap which agrees **qualitatively** with experiment. However, such models do not **quantitatively** explain non-monotonic composition-dependent effective masses [1] and persistent photoconductivity [2].

Using Rutherford Backscattering Spectrometry and Nuclear Reaction Analysis, we recently revealed significant composition-dependent incorporation of N into non-substitutional sites, as either (N-N)_{As} or (N-As)_{As} interstitials [3]. In addition, the fraction of substitutional N was highest (lowest) for growth at the lowest (highest) temperatures, presumably due to the high areal density of Group V sites available for N-As exchange on the (2x1) reconstructed GaAs (001) surface. To date, we have identified a N interstitial related deep electronic level and confirmed its Raman signature [4]. We will discuss these results and progress towards distinguishing (N-N)_{As} and (N-As)_{As} split interstitials using [001] and [111] channeling measurements.

[1] T. Dannecker, et al, **Phys. Rev. B** 82, 125203 (2010).

[2] R.L. Field, III, et al., submitted (2012).

[3] M. Reason, et al., **Appl. Phys. Lett.** 85, 1692 (2004).

[4] Y. Jin, et al. **Appl. Phys. Lett.** 95, 062109 (2009).

MON-IBA01-2

#206 - Invited Talk - Monday 1:00 PM - Brazos I

Ion implantation in ZnO crystals: defect interactions and impurity diffusion

Faisal Yaqoob¹, Mengbing Huang²

⁽¹⁾*Department of Physics, State University of NY-University at Albany, 1400 Washington Ave, Albany NY 12222, United States*

⁽²⁾*College of Nanoscale Science and Engineering, State University of NY-University at Albany, 1400 Washington Ave, Albany NY 12222, United States*

ZnO is a wide band gap semiconductor material with many potential applications such as blue and UV light emitters, transparent thin film transistors, high temperature and high power devices and sensors. Controllable doping of both p- and n-type impurities in ZnO is crucial to many of its applications. Ion implantation is well established method for impurity doping and defect engineering in silicon microelectronics, but its application in the case of ZnO has not been fully explored. In this work, we study the effects of ion implantation of indium (n-type) and silver (p-type) in ZnO crystals. The crystal quality as well as the distribution and occupation of dopant atoms in ZnO lattice are characterized with Rutherford backscattering spectrometry combined with ion channeling, for various post-implantation annealing conditions. It is observed that during ion implantation most of the impurity dopants are placed at interstitial positions. The fraction of substitutional impurity atoms increases with thermal annealing temperatures.

The thermal process also causes diffusion of the substitutional and interstitial impurity atoms. Through modeling of RBS/ion channeling data, the effective activation energies for interstitial and substitutional dopant atoms are determined. To evaluate the concept of defect engineering in ZnO, we also study silver doping in hydrogen implanted ZnO crystals. It is found that the damage created to the crystal lattice by the Ag implant is smaller in the samples with a prior H implant than the samples without H. As the samples are annealed at high temperatures, a larger fraction of Ag atoms is found to be on zinc substitutional sites in samples with H than in the samples without H. These experimental results may offer a pathway to understand atomic mechanisms for interactions between dopants and defects in ion implanted ZnO crystals.

MON-IBA01-3

#103 - Invited Talk - Monday 1:00 PM - Brazos I

RBS-channeling in characterizing H-platelet and "dynamic annealing" effect in H-implanted Si

Zengfeng Di¹, Miao Zhang¹, Xi Wang¹, Yongqiang Wang², Michael Nastasi²

⁽¹⁾*State Key Laboratory of Functional Materials for Informatics, Shanghai Institute of Microsystem and Information Technology, No. 865 Changning Road, Shanghai 200050, China*

⁽²⁾*Los Alamos National Laboratory, Bikini Atoll Road, SM 30, Los Alamos New Mexico 87545, United States*

With annealing treatment, hydrogen incorporated into Si by implantation is known to precipitate in extended planar defects in the form of platelets named "H-platelets". Understanding how H-platelets nucleate and grow in H implanted Si is important since they play key role in ion cutting and layer transfer. The evolution of H-platelets under conventional thermal annealing has been studied intensively, it is found that in (100) H-platelets are mostly formed on the (001) plane parallel to the surface in H-implanted (100) Si. However, the effect of annealing other than thermal annealing has not been investigated. In this study, we compare dynamic annealing and thermal annealing effects on the nucleation and growth of H-platelets and find that dynamic annealing promotes the formation of HIPs even more efficiently than thermal annealing. Furthermore, in addition to the (001) platelets normally formed in H-implanted (100) Si, massive nucleation on {111} crystallographic planes is observed in the presence of dynamic annealing. RBS-channeling performed along different crystallographic directions is capable of distinguishing H-platelet defects with different orientation from conventional vacancy-interstitial (V-H) defects, which may be introduced by He or Si implantation. From the unique atomistic nature of hydrogen platelet, which has a shift in the registry of off-normal lattice planes on either side, a model is proposed to interpret the mechanism of this technique. The different observations of defective region formation after either thermal annealing or dynamic annealing in H-implanted (001) Si, along different axial directions, are predicted by the model and re-verify the model proposed.

MON-IBA01-4

#314 - Invited Talk - Monday 1:00 PM - Brazos I

Irradiation induced changes in small angle grain boundaries in mosaic Cu thin films

E.G. Fu¹, Y.Q. Wang¹, M. Nastasi²

⁽¹⁾*Materials Science and Technology, Los Alamos National Laboratory, Los Alamos NM 87544, United States*

⁽²⁾*Mechanical & Materials Engineering, University of Nebraska-Lincoln, Lincoln NE 68588, United States*

We have studied the effect of ion irradiation on small angle grain boundaries in mosaic structured Cu thin films. The Cu films were deposited on Si (110) substrates by magnetron sputtering at room temperature. X-ray diffraction (XRD) and Rutherford backscattering spectroscopy (RBS) were used to characterize the crystalline structure of the films before and after ion irradiation. After 200 keV helium ion irradiations to a fluence of 5×10^{17} ions/cm², the films showed a decrease in mosaic spread via a narrowing of the Full Width at Half Maximum (FWHM) in rocking curves of XRD and a smaller minimum yield of RBS channeling. These data indicate that the ion irradiation decreased the mis-orientation angles between mosaic crystal separated by small angle grain boundaries in these films. Possible mechanisms involving interactions between grain boundary dislocations and ion irradiation induced point defects are discussed.

The role of flux super-focusing in the origin of shoulders in channeling angular scans and possible applications in ion beam analysis

Dharshana Nayanajith Wijesundera¹, Ki Ma¹, Xuemei Wang¹, Buddhi P Tilakaratne¹, Lin Shao², Wei-Kan Chu¹

⁽¹⁾Physics and Texas Center for Superconductivity, University of Houston, 4800 Calhoun Rd, Houston TX 77004, United States

⁽²⁾Department of Nuclear Engineering, Texas A&M University, College Station TX 77843, United States

We have studied the effect of ion channeling flux super-focusing in originating near-surface shoulders in channeling angular scans observed in ion beam analysis of crystalline materials. By simulation, we observe that at the angle of incidence corresponding to the channeling shoulder, the primary channeling super-focus overlaps with lattice atoms, dramatically enhancing the ion flux density at atomic sites, thereby increasing the ion-atom close encounter probability. We show that the so increased close encounter probability originates high near-surface shoulders in channeling.

Our explanation of the origin of the channeling shoulders opens the possibility of utilizing the same as a tool in ion beam analysis. We demonstrate such an application in determining the atomic planar stacking sequence and thereby the direction of crystallographic polarity of wurtzite structured ZnO.

Determination of ordering effect in InGaP by Rutherford Backscattering Spectroscopy/Channeling

Lin Li^a, Huiping Pan^a, Fengfeng Cheng^a, Shude Yao^{a*}, Hao-Hsiung Lin^b, Yu-Chung Chin^b, Chijing Hong Liao^b

^a.State Key Laboratory of Nuclear Physics and Technology, Peking University, Beijing 100871, PR China

^b.Graduate Institute of Photonics and Optoelectronics and Department of Electrical Engineering, National Taiwan University, Taipei 106-17, Taiwan

Spontaneous long-range CuPt ordering in InGaP has been well studied. The ordering affects the electronic properties of the alloy and makes InGaP a most suitable emitter material for HBTs used in mobile phones and tablets. In this contribution, a new method has been developed by Rutherford Backscattering Spectroscopy/Channeling (RBS/C) to analyze the ordering effect in InGaP. The principle is as follows. It is well known that bonds in an alloy ensemble their lengths in binaries and thus suffer from bending and stretching. If the alloy is disordering, the distortion is randomly distributed. However, in InGaP with CuPt ordering, according to super cell calculation using valence force field model, the distortion will accommodate to the ordering direction. As a result, the randomization is reduced and increase in channel yield is expected. The order parameter η of GaInP₂ is defined by the composition of the alternating Ga- and In-rich monolayers: Ordered material consists of a sequence of layers (Ga_{1+ η} In_{1- η} P₂) and (Ga_{1- η} In_{1+ η} P₂) oriented perpendicularly to a <111> direction [1]. Channeling effect and angular RBS/C scans have been carried out to test the ordering effect along four <111> direction. From RBS/C measurement, different channeling yield and angular RBS/C scan spectra have been observed along four different directions, which indicates that the four <111> directions present different ordering effects. Such conclusion is further supported by TED and SR-XRD results.

[1] P. Ernst, C. Geng, F. Scholz, H. Schweizer, Y. Zhang, and A. Mascarenhas, Appl. Phys. Lett. 67, 2347 (1995)

Elemental detection limits for heavy-ion ERDA using TOF-E telescope

Timo Sajavaara, Mikko Laitinen, Jaakko Julin

Department of Physics, University of Jyväskylä, P.O.Box 35, Jyväskylä 40014, Finland

The elemental detection and quantification limits in ion beam analysis can in a coarse classification be depended on incident ion fluence, scattering or X-ray emission cross-section, elemental losses, and spectrum background. Although these all are to some degree depended on each other, optimized measurement parameters can in most cases be selected if the aim is to get either as high depth resolution, high depth of range, or as low quantification limit as possible. A vehicle for this case study is a TOF-ERDA setup installed to a 1.7 MV Pelletron accelerator in Jyväskylä, Finland. With TOF-ERDA all the sample elements can in principle be quantified in one measurement as different detected particles are separated by means of their different masses. The easily changeable measurement parameters are incident ion selection, incident energy, sample tilt angle, beam spot size, and also to some degree incident ion current. Normally the detector telescope is fixed to an angle between 35 and 45 degrees with respect to the incoming beam.

In this paper we discuss the different factors governing the elemental detection limits for light and heavy elements in different matrices based on experimental results and Monte Carlo simulations. A special attention is given to show the importance of good time and energy resolution of detectors, and high performance data acquisition system.

MON-IBA01-P1

#5 - Poster - Monday 5:30 PM - Rio Grande

Production of SiO_n^- and $(\text{SiO}_2)_n^-$, $n=2, 3, 4$ molecular and cluster anion beams from a cesium-sputter-type negative ion source

V. T. Davis¹, D. D. Davis², K. Chartkunchand¹, J. S. Thompson¹, A. C. Covington¹

⁽¹⁾*University of Nevada, Reno, MS 0220, Reno NV 89557-0220, United States*

⁽²⁾*ATK Launch Systems Group, Magna UT 84044, United States*

Theoretical models have been developed for many decades to describe the sputtering process. These models have used various explanations to account for the mechanisms that lead to secondary ion beam production via sputtering from solid surfaces. Experimental studies of negative ion beam production, although dependent on source design and geometry, reveal trends which can, in turn, assist theorists in identifying the important microscopic events involved in sputtering. The study described in this report characterizes the yields of SiO_n^- and $(\text{SiO}_2)_n^-$, $n=2, 3, 4$ molecules and clusters from a cylindrical-geometry, cesium-sputter-type negative ion source. Mass- and charged-analyzed beam currents ranging from several picoamperes to several nanoamperes were observed.

MON-IBA01-P2

#59 - Poster - Monday 5:30 PM - Rio Grande

Energy distribution of sputtered atoms and ions from energetic ion bombardment of GaAs

Angelin Ebanazar John, Rainer Hippler

Institute of Physics, University of Greifswald, Felix-Hausdorff-Str. 6, Greifswald, Germany

The energy distributions of secondary neutral Ga and As atoms and positively and negatively charged ions sputtered from a GaAs(100) surface after energetic Ar^+ ion bombardment are reported. The incident ion energy was 150keV. A charge analysis shows that Ga species are preferentially sputtered as neutral Ga atoms or as positively charged Ga^+ ions. By contrast, As is preferentially sputtered as negatively charged As^- ions. The energy distribution of sputtered Ga and As monomers is close to an E^{-3} dependence. In general, the energy distribution of sputtered Ga_n and As_n clusters is significantly steeper than compared to the monomers. Results will be presented at the Conference.

Measurements of $^4\text{He}+^{14}\text{N}$ elastic scattering cross sections for TOF-ERDA using He beam

Keisuke Yasuda¹, Hidetsugu Tsuchida², Takuya Majima²

⁽¹⁾*The Wakasa Wan Energy Research Center, 64-52-1 Nagatani, Tsuruga Fukui 914-0192, Japan*

⁽²⁾*Quantum Science and Engineering Center, Kyoto University, Gokasho, Uji Kyoto 611-0011, Japan*

A Time-of-flight Elastic Recoil Detection Analysis (TOF-ERDA) is one of the promising methods for the simultaneous measurements of multi light elements with good depth resolution. We are developing a TOF-ERDA measurement system using He beams. For quantitative measurements of elemental concentrations by the TOF-ERDA, reliable data of recoil cross sections are needed. For the TOF-ERDA using He beams of above about 2 MeV, the recoil cross sections are known to be non-Rutherford. In such case, experimental data for the recoil cross sections are necessary. Therefore, we plan to measure recoil cross sections for light elements such as Li, B, C, N, O bombarded by ^4He ions. This paper presents measurements of cross sections for $^4\text{He}+^{14}\text{N}$ elastic scattering.

The experiments were performed using the 2MV tandem Pelletron accelerator at the Quantum Science and Engineering Center, Kyoto University. An energy range of ^4He ions was between 4.3 MeV and 5.5 MeV. A silicon-nitride membrane of 50 nm thickness with a coated thin Au layer was used as a target. The ^4He ion beams bombarded the target and scattered ions were detected with silicon detectors at scattering angles of 83.6° and 165° . The scattering angle of 83.6° corresponds to the recoil angle of 40° , and recoil cross sections at 40° were evaluated from scattering cross sections at 83.6° using the kinematical calculation. We measured the scattering cross sections at 165° for the backscattering experiments of nitrogen. This paper will present results of cross section measurements as well as details of the experimental setup. Comparison between the present data and calculations will also be indicated.

Design and performance of the HVE electrostatic nuclear microprobe

Nicolae C. Podaru, F.L. van de Hoef, A. Gottdang, D.J.W. Mous

High Voltage Engineering B.V., P.O. Box 99, Amersfoort, Netherlands

Nuclear microprobes with spatial resolution in the micrometer range are commonly used in research fields such as medicine, biology, environmental sciences, archeology, to name a few. For example, micro-PIXE is used to determine elemental distributions and concentrations in biological samples, providing insight into tissue morphology, drug penetration in tissue or biochemical changes caused by diseases. Typically, the required spatial resolution of the nuclear microprobes used for these applications is 1-10 μm . To serve these applications High Voltage Engineering has developed, built and tested a nuclear microprobe based on the Russian quadruplet concept, with a spatial resolution of $<10 \mu\text{m}$. The microprobe is constructed in a single compact assembly, 350 mm long. Its nominal focal distance is 325 mm, its demagnification factor 16.2 and it supports beam energy to charge ratio of up to 4 MV. Three dimensional finite element methods coupled with raytracing capabilities were used to quantify parasitic aberrations introduced by e.g. electrode imperfections or misalignments. This was used to determine the best geometric design and the level of tolerance required, in order to avoid complex alignment and tuning procedures. As a consequence, focus and astigmatism are the only parameters that require adjustment, a substantial advantage for its use. The microprobe was connected to a 3 MV TandetronTM and its performance has been measured by high resolution knife edge scans. With an object size of $100 (\pm 2) \mu\text{m} \times 100 (\pm 2) \mu\text{m}$, and a 0.23 mrad half-angle divergence, the beam size at the focal plane was $6.8 (\pm 0.2) \mu\text{m} \times 6.1 (\pm 0.2) \mu\text{m}$ (FWHM). Based on these results, it is anticipated that a beam size of $\sim 2 \mu\text{m}$ (FWHM) can be achieved. A core brightness of $2 \text{ A m}^{-2} \text{ rad}^{-2} \text{ eV}^{-1}$ for 3 MeV H^+ ions, and $0.8 \text{ A m}^{-2} \text{ rad}^{-2} \text{ eV}^{-1}$ for 3 MeV He^{2+} ions is measured.

Digital Electronics for a ToF-ERD telescope

Jaakko Julin, Mikko Laitinen, Timo Sajavaara

Department of Physics, University of Jyväskylä, POB 35, University of Jyväskylä FI-40014, Finland

Digital electronics for pulse processing in nuclear and particle physics experiments is well established. In IBA traditional analogue electronics chain for example with CFDs, spectroscopy amplifiers and MCAs is commonly used. Recently the cost of digitizers with sampling rate near and above 1 GS/s has become low enough for digital electronics to be cost effective. Additionally pulse processing of several measurement channels is possible in real time with regular modern PCs. The major advantage of digital electronics is the ability to store the original waveform of the acquired signal. This is a powerful tool in the development of instrumentation and evaluation of data. The time-of-flight ERDA telescope of the Accelerator Laboratory of the Department of Physics, University of Jyväskylä (JYFL) has been installed to the Pelletron accelerator in 2009 with a data acquisition system based on an FPGA, which reads out conventional ADCs. An entirely new electronics system based on CAEN digitizers is currently being tested and will replace the existing system in late 2012. The setup consists of two digitizer modules, a CAEN N6751 is used in two channel 2 GS/s mode to read the signals from two electrostatic MCP timing detectors. A timing resolution of 170 ps, which is similar to the resolution achieved with analogue electronics, has been demonstrated. The advantage over analogue CFD+TAC setup is advanced rejection of multiple hits in timing window. A four channel CAEN N6724 digitizer is used to read out the preamplified signals of the energy detector, which can be either a Si detector or a gas ionization chamber. The software signal processing makes it possible to extract rise-time and timing information in addition to pulse-height information for example from cathode and anode signals of a gas ionization chamber.

Design of a time-of-flight telescope for ion beam analysis

Mikko Laitinen, Jaakko Julin, Timo Sajavaara

Department of Physics, University of Jyväskylä, P.O.Box 35, Jyväskylä 40014, Finland

Time-of-flight (TOF) telescope, comprising of two time pick-up detectors based on a detection of secondary electrons created by ion passing a thin carbon foil, is one of the most versatile and useful detectors in the field of ion beam analysis. It can be used for all ions and energies down to few tens of keVs. The well-known limitations of TOF-detectors are detection efficiency for hydrogen and scattering in the first carbon foil. Also so called tandem effect - the acceleration or deceleration due to the change in ion charge state while passing through the first carbon foil in high potential - causes extra energy spread which is most visible for low energy ions. To totally avoid tandem effect, grounded carbon foils in both time pick-up detectors should face each other.

We have made both experiments and simulations to study the magnitude of the tandem effect and to what degree it affects the actual measurement results. The timing resolution of our TOF detector has been measured to be as good as 155 ps for scattered 4.8 MeV He beam, and this yields to an energy resolution better than 0.4 % for particle energies higher than one MeV. For H and He ions our resolution is measured to be 2-3 keV for the particle energy range of 200-500 keV, where tandem effect is often claimed to be clearly visible. Significant energy resolution worsening due to the tandem effect could not be reproduced for heavier low energy ions either, which promotes the use of TOF detectors in the high resolution work as an option for charge state sensitive magnetic spectrometers. The SIMION simulations also showed that the bending of low energy light ions in the electric fields of the first time pick-up detector needs to be taken seriously in the detector design.

Efficiency Calibration of a HPGe X-ray Detector for Quantitative PIXE Analysis

Stephen J Mulware, Wickramaarachchige Lakshantha, Bibhudutta Rout, Tilo Reinert

Ion Beam Modification and Analysis Laboratory, Physics Department, University of North Texas, 1155 Union Circle #311427, Denton TX 76203, United States

Particle Induced X-ray Emission (PIXE) is an analytical technique, which provides reliably and accurately quantitative results without the need of standards when the efficiency of the X-ray detection system is calibrated. The ion beam microprobe of the Ion Beam Modification and Analysis Laboratory at the University of North Texas has recently purchased a 100 mm² high purity germanium X-ray detector (Canberra GUL0110 Ultra-LEGe). In order to calibrate the efficiency of the detector for standardless PIXE analysis we have measured the X-ray yield of a set of commercially available X-ray fluorescence standards. The set contained elements from low atomic number $Z=11$ (sodium) to higher atomic numbers to cover the X-ray energy region from 1 keV to about 20 keV where the detector is most efficient. The charge measurement was done by collected charge integration as well as from the proton backscattering yield of a calibrated particle detector. The calibration is tested on reference samples.

Geochemistry and Health Burden of Radionuclides and Trace Metals in Shale Samples from North-Western Niger Delta: A PIXE Approach

Felix S. Olise¹, Adaeze C. Onumojor¹, Akinsehinwa Akinlua², Oyediran K. Owoade¹, Hezekiah B. Olaniyi¹

⁽¹⁾*Department of Physics, Obafemi Awolowo University, Ede Road, Ile-Ife Osun 220005, Nigeria*

⁽²⁾*Department of Chemistry, Obafemi Awolowo University, Ede Road, Ile-Ife Osun 220005, Nigeria*

Organic sedimentary rock samples were collected from three Oil wells in the North-Western Niger Delta, Nigeria in order to determine their natural radioactivity concentration and elemental geochemistry, with the aim of determining the major radionuclides and their radiological and environmental health implication. Despite the well-established capability of gamma spectrometry in determining the radionuclides, the PIXE method of IBA technique and an accurately calibrated Si(Li) detector system has been successfully used to determine the radionuclides. This has been attested to by the high level of agreement between measured and certified values for the CRM IAEA-SL-3 and IAEA -405 standard reference materials used to verify the experimental procedures. The radionuclides identified belong to the decay series of naturally occurring radionuclides headed by ²³⁸U and ²³²Th along with the non-decay series radionuclide, ⁴⁰K. The radionuclides' activity concentrations and their derived dose were then calculated. ⁴⁰K average activity concentrations were 250 Bq/kg for Well A, 260 Bq/kg for Well B and 270 Bq/kg for Well C. For ²³²Th, the activity concentrations were 1045 Bq/kg for Well A, 1400 Bq/kg for Well B, 1430 Bq/kg for Well C. ²³⁸U activity concentrations were 2210 Bq/kg, 3510 Bq/kg and 250 Bq/kg for the Oil Wells A, B and C respectively. The detected trace metals were majorly V, Ni, Pb, Fe, Cr, Cu, Zn, Co and their concentrations together with those of the radionuclides are compared with the relevant world standard limits. The results obtained were high, and hence, the radioactivity level and trace element content of the sediment samples could constitute health hazard to occupationally exposed workers and the public if not properly disposed. However, despite the careful disposal practice claims by the oil industries and given the high concentrations, the sediments could still pose an intrinsic health hazard considering their cumulative effects in the environment.

Measuring parameters of dynamic annealing in ion-irradiated solids

M. T. Myers^{1,2}, S. Charnvanichborikarn¹, L. Shao², S. O. Kucheyev¹
⁽¹⁾*Lawrence Livermore National Laboratory, Livermore CA 94550, United States*
⁽²⁾*Texas A&M University, College Station TX 77843, United States*

Under ion irradiation, all crystalline materials display some degree of dynamic annealing when defects experience evolution after the thermalization of collision cascades. The exact time and length scales of such defect relaxation processes are, however, unknown even for Si at room temperature. Here, we propose a method to measure effective diffusion lengths and relaxation times of mobile defects that dominate the formation of stable post-irradiation disorder. A defect lifetime of about 10 ms is measured for Si at room temperature, essentially independent of the average density of ballistic collision cascades. Defect relaxation appears to be dominated by a second order kinetic process. We discuss implications of these findings for the development of predictive models of radiation damage buildup in solids.

This work was performed under the auspices of the U.S. DOE by LLNL under Contract DE-AC52-07NA27344.

Plasma-Surface Interactions in Hollow Cathodes

James Polk¹, Angela Capece², Ioannis Mikellides¹
⁽¹⁾*Propulsion and Materials Engineering, Jet Propulsion Laboratory, MS 125-109, 4800 Oak Grove Dr., Pasadena CA 91109, U.S.*
⁽²⁾*Materials Characterization Laboratory, Princeton Plasma Physics Laboratory, 100 Stellarator Road, Princeton NJ 08540, U.S.*

Electric thrusters using xenon gas discharges for space propulsion employ hollow cathodes with porous tungsten emitters impregnated with barium-containing compounds. In a number of long duration tests of hollow cathodes significant changes in the interior surface morphology have occurred. Deposition of tungsten crystals at the downstream end of the emitter is typically observed after long periods of operation. These deposits appear to form a dense tungsten layer on the surface in the emitting zone which inhibits barium transport from the interior. Despite the restricted flow of barium from the interior directly under the emission zone, the cathodes appear to function normally. This suggests that the barium on oxygen surface complex that reduces the work function in the emission zone is maintained by barium from the gas phase. This barium must be supplied by flow from the porous tungsten substrate upstream of the region where the dense tungsten surface deposits form. A model of barium gas phase diffusion has been developed to better understand the transport in the internal hollow cathode plasma. A 2D axisymmetric model of the hollow cathode interior plasma has been developed. Neutral and ionized barium and barium oxide are considered minor species that do not significantly perturb the plasma density or temperature calculated in the xenon plasma model. Diffusion equations for these minor species including ionization source/sink terms are solved in the interior domain. Models of barium flow from the emitter interior and adsorption/desorption kinetics of barium on tungsten provide boundary conditions. This model has been extended recently to include gas phase reactions and transport of oxygen, which may appear as an impurity in the xenon propellant and can poison the emitter when adsorbed on the surface. The transport of these species and the interactions with the electron emitter surface will be discussed in this presentation.

Channeling of Low Energy Ions on Hydrogen-Covered Surfaces: Modeling and Experiments

Robert D Kolasinski, Josh A Whaley

Hydrogen and Metallurgy Science Department, Sandia National Laboratories, P.O. Box 969, MS 9161, Livermore CA 94551, United States

Detecting adsorbed hydrogen presents numerous experimental challenges, especially because it is invisible to most surface analysis techniques. Low energy ion scattering (LEIS) and direct recoil spectroscopy (DRS) are among the only tools capable of directly detecting hydrogen on surfaces and characterizing its behavior at an atomic scale. However, surface scattering is complex and difficult to model accurately, particularly at grazing angles of incidence where adsorbates are most readily observed. To address these limitations, we have applied modeling and experimental approaches that expand the range of conditions over which LEIS and DRS may be applied. Rigorous modeling of scattering at grazing incidence requires the use of molecular dynamics to account for how ions are gently steered along open surface channels. By incorporating improved scattering potentials and an accurate thermal vibrational model into our simulations, we are able to reproduce recoiled hydrogen signals for both heavy substrates (e.g. W(001)+H) as well as lighter systems (Be(0001)+H and Al(001)+H.) To further improve the fidelity of such measurements, we have recently implemented a time of flight spectroscopy system. Using a technique that detects and differentiates between both charged and neutral particles eliminates the need to account for neutralization in our models. This makes the prospect of applying sophisticated computational techniques to simulate scattering experiments particularly promising.

Sandia National Laboratories is a multi-program laboratory managed and operated by Sandia Corporation, a wholly owned subsidiary of Lockheed Martin Corporation, for the U.S. Department of Energy's National Nuclear Security Administration under contract DE-AC04-94AL85000.

Forward Elastic Scattering of 13 MeV ${}^6\text{Li}^{3+}$ by ${}^1\text{H}$, ${}^7\text{Li}$, ${}^{12}\text{C}$, ${}^{16}\text{O}$, ${}^{19}\text{F}$, ${}^{28}\text{Si}$ and ${}^{197}\text{Au}$

Federico E Portillo¹, Jacinto A Liendo¹, Aleida C Gonzalez², Dave D Caussyn³, Neil R Fletcher³, O. A. Momotyuk³, Brian T Roeder³, Ingo Wiedenhoever³, Kirby W Kemper³, Powell Barber³, Laszlo Sajo-Bohus¹

⁽¹⁾*Physics Department, Simon Bolivar University, Caracas, Venezuela*

⁽²⁾*Centro de Fisica, Instituto Venezolano de Investigaciones Cientificas, Caracas, Venezuela*

⁽³⁾*Physics Department, Florida State University, Tallahassee Florida, United States*

Targets containing ${}^1\text{H}$, ${}^7\text{Li}$, ${}^{12}\text{C}$, ${}^{16}\text{O}$, ${}^{19}\text{F}$, ${}^{28}\text{Si}$ and ${}^{197}\text{Au}$ have been bombarded with 13 MeV ${}^6\text{Li}^{3+}$ and 20 MeV ${}^{16}\text{O}^{5+}$ beams. The ${}^{16}\text{O} + {}^1\text{H}$, ${}^{16}\text{O} + {}^{12}\text{C}$, ${}^{16}\text{O} + {}^{16}\text{O}$, ${}^{16}\text{O} + {}^{19}\text{F}$, ${}^{16}\text{O} + {}^{28}\text{Si}$ and ${}^{16}\text{O} + {}^{197}\text{Au}$ cross sections, shown to be consistent with the Rutherford formula predictions at 15° and 20° , have been used to determine cross sections for the ${}^6\text{Li} + {}^1\text{H}$, ${}^6\text{Li} + {}^{12}\text{C}$, ${}^6\text{Li} + {}^{16}\text{O}$, ${}^6\text{Li} + {}^{19}\text{F}$, ${}^6\text{Li} + {}^{28}\text{Si}$ and ${}^6\text{Li} + {}^{197}\text{Au}$ reactions respectively at 24° , 26° , 28° and 30° . Although ${}^6\text{Li} + {}^7\text{Li}$ cross sections have not been obtained from ${}^{16}\text{O} + {}^7\text{Li}$ cross sections, they have been determined from measured ${}^6\text{Li} + {}^{19}\text{F}$ cross sections and, in addition, used to obtain ${}^{16}\text{O} + {}^7\text{Li}$ cross sections at 15° and 20° . All the cross sections determined in this work are relevant for applied and basic physics.

Recent applications of low energy ion implantation in nanoscience and novel devices

John Vedomuthu Kennedy^{1,2}

⁽¹⁾National Isotope Centre, GNS Science, 30 Gracefield Road, PO Box 31312,, Lower Hutt, Wellington 5010, New Zealand

⁽²⁾The MacDiarmid Institute for Advanced Materials and Nanotechnology, Victoria University of Wellington, PO Box 600, , Wellington, New Zealand

Surface nanostructuring with ion implantation has led to the development of materials with unique properties which have opened the door to novel applications. Recently we have established a dual low-energy ion implantation facility based on Penning ion sources. In my talk, I will highlight the use and advantages of low energy ion implantations for modern applications.

(a). Nanoparticles synthesis for magnetic sensors: Shallow low-fluence Fe implantation along with electron beam annealing induced the formation of Fe nanoparticles on a SiO₂ surface[1]. This materials exhibit large room temperature magnetoresistance [2] and have potential for "on-chip" applications.

(b). Metallic ion doping in polymer surfaces: In an effort to develop hybrid organic inorganic tungstates as novel functional electronic materials, single crystals and films of WO₃-polymer have been doped with Na, Ca, and K ions by ion implantation [3]. The properties of DNA sensors from polypyrrole films were also improved through Pt implantation. The resulting Pt nanoparticles were shown to serve as anchoring points for DNA attachment as well as enhancing the film's conductivity [4].

(c). Surface superconductivity: Controlling the superconductive behaviour of material can be achieved through low-energy implantation. K and Ca implanted SrFe₂As₂ show a superconducting transition below 25K in magnetisation and resistivity measurements with implantation above a threshold of 2 at.%. Results suggest that the observed superconductivity is principally confined to the surface or sub-surface level and is induced by surface or sub-surface crystallographic strain resulting from the adaptation of foreign atoms into the lattice from shallow implantation [5].

[1] J. Kennedy, et.al **Nanotechnology**, 22 (2011) 115602.

[2] J. Leveneur, et.al **Appl. Phys. Lett.** 98 (2011) 053111.

[3] Islah-u-din, et.al, **J. Phys. Chem. C**, 116 (2012) 3787.

[4] M.A. Booth, et.al **J. Phys. Chem. C**, 116 (2012) 8236.

[5] S.V. Chong, et.al, **Euro. Phys. Lett** 94 (2011) 37009.

SUBSURFACE SYNTHESIS AND CHARECTERIZATION OF Ag EMBEDDED MgO METALLODIELECTRIC COMPOSITE

Subramanian Vilayurganapathy, Arun Devaraj², Robert Colby², Archana Pandey², Shutthanandan Vaithiyalingam², Sandeep Manandhar², Suntharampillai Thevuthasan², Asghar Kayani¹

⁽¹⁾Physics Department, Western Michigan University, 1903 West Michigan Ave., Kalamazoo MI 49008, United States

⁽²⁾Environmental and Molecular Sciences Laboratory,, Pacific Northwest National Laboratory,, 902 Battelle Boulevard P. O. Box 999, MSIN K8-93, Richland WA 99354, United States

Metal nanostructures embedded in dielectric media exhibit interesting linear and non-linear optical properties finding applications in the field of optoelectronics. The optical properties of these composites is dominated by localized surface Plasmon resonance and this resonant frequency depends strongly on size, shape, distribution and the surrounding dielectric medium. By controlling the physical and chemical properties of the embedded nanostructures the electronic and optical properties of the material can be tuned for appropriate applications. The method of ion implantation with subsequent annealing is a good candidate for developing embedded nanoclusters because it provides a certain degree of control over the above mentioned parameters in addition to providing high metal filling factor beyond the solubility limit of host matrix.

We employed a two-step process to synthesize Ag nanoclusters in MgO matrix. In the first step 200 KeV Ag ions were ion implanted in MgO (100) substrate with fluence 1×10^{17} ions/cm² at 650°C. The implanted samples were subsequently annealed at a temperature of 1000°C for 10, 20, 30 hours to facilitate the growth of Ag nanoclusters. Rutherford Backscattering Spectrometry (RBS) along the channeling and random geometries was carried out to investigate the crystalline quality of the clusters and Ag concentration profile in MgO. The Ag Plasmon resonance peak red-shifted and became narrower with increasing annealing times indicating the Ag nanocluster size is increasing. This is corroborated with Transmission Electron Microscopy which shows the clear size evolution of the Ag nanoclusters with increasing annealing time. Finally Atom probe Tomography studies were performed to obtain a 3D map of the Ag nanoclusters in the MgO oxide matrix and this technique is employed to confirm that Ag exists in the form of a pure metal inside the nanocluster.

MON-IBM01-3

#210 - Contributed Talk - Monday 3:30 PM - Pecos II

Effects of low-energy electron irradiation on the formation of color centers in nitrogen implanted diamond

Julian Schwartz, Shaul Aloni, Frank Ogletree, Thomas Schenkel

Lawrence Berkeley National Laboratory, 1 Cyclotron Road, 5-121, Berkeley CA 94720, United States

Color centers in diamond, e. g. the nitrogen-vacancy center (NV-) are promising quantum bit candidates and they enable advanced magnetometry schemes. The reliable formation of NV-centers with high spatial resolution is challenging. Implantation of nitrogen ions into single crystal diamonds followed by thermal annealing is an established approach that leads to the formation of some NV-centers. We report an unexpected effect of exposure to low energy electrons on the formation of NV-centers in nitrogen implanted single crystal diamonds. Exposure to beams of low-energy electrons (2-30 keV) in a scanning electron microscope locally induces formation of NV-centers without any thermal annealing. We find that non-thermal, electron-beam-induced NV-formation is about four times less efficient than thermal annealing. But NV-center formation in a consecutive thermal annealing step (800 C) following exposure to low-energy electrons increases by a factor of up to 1.8 compared to thermal annealing alone. These observations point to reconstruction of nitrogen-vacancy complexes induced by electronic excitations from low-energy electrons as an NV-center formation mechanism and identify local electronic excitations as a means for spatially controlled room-temperature NV-center formation [1].

[1] J. Schwartz, S. Aloni, D. F. Ogletree and T. Schenkel, New Journal of Physics 14 (2012) 043024.

This work was supported by the Office of Science of the US Department of Energy under contract no. DE-AC02-05CH11231 and by Darpa.

MON-IBM01-4

#191 - Contributed Talk - Monday 3:30 PM - Pecos II

Observation of paramagnetic Fe in Mn/Fe implanted metal oxides

Krish Bharuth-Ram¹, Haraldur Palle Gunnlaugsson², Torben Esman Molholt³, Deena Naidoo⁴, Hilary Masenda⁴, Roberto Mantovan⁵, Haflidi Gislason³, Guido Langouche⁶, Karl Johnston⁷, Svein Olafsson³, Morten Bo Madsen⁸, Rainer Sielemann⁹, Gerd Weyer²

⁽¹⁾*School of Physics, University of KwaZulu-Natal, Durban 4000, South Africa*

⁽²⁾*Department of Physics and Astronomy, Aarhus University, Aarhus, Denmark*

⁽³⁾*Science Institute, University of Iceland, Reykjavik, Iceland*

⁽⁴⁾*School of Physics, University of Witwatersrand, Johannesburg, South Africa*

⁽⁵⁾*Laboratorio MDM, IMM-CNR, Agrate Brianza (MB), Italy*

⁽⁶⁾*Department of Physics, Katholieke Universiteit- Leuven, Leuven, Belgium*

⁽⁷⁾*PH Department, ISOLDE/CERN, Geneva, Switzerland*

⁽⁸⁾*Niels Bohr Institute, University of Copenhagen, Copenhagen, Denmark*

⁽⁹⁾*Helmholtz Zentrum-Berlin, Berlin, Germany*

Theoretical prediction of room temperature ferromagnetism in ZnO (and GaN) implanted with low concentrations of transition metal (TM) ions has excited considerable experimental activity in the search for dilute magnetic semiconducting (DMS) behaviour in conventional semiconductors with the cations partially replaced with TM ions. Such DMSs have potential applications in spintronic devices. While several authors have reported observation of magnetic complexes in TM implanted substrates, no clarity exists on the origin of the observed magnetism, which has been attributed to dopant-defect complexes, unintentional precipitation, or formation of secondary phases.

We have investigated the state of Fe in ZnO and other metal oxides implanted with extremely low concentrations of ^{57}Mn , employing ^{57}Fe Moessbauer spectroscopy following the implantation of radioactive ^{57}Mn ($T_{1/2} = 1.5$ min). $^{57}\text{Mn}^{+12}$ ions, produced at the online RIB facility ISOLDE at CERN, were accelerated to 60 keV and implanted to fluences up to 10^{12} ions/cm² into commercially available single crystals substrates, held at temperatures between 100-700 K in an implantation chamber. ^{57}Fe Moessbauer measurements, following the ^{57}Mn to ^{57}Fe β -decay, were made with a parallel plate avalanche counter mounted on a conventional drive outside the implantation chamber. Spectra obtained after implantation into ZnO show, in addition to spectral components due to Fe^{2+} at Zn lattice sites, sextets originating from iron in the ferric (Fe^{3+}) state. Angle dependent measurements in an external magnetic field confirm that the Fe^{3+} are paramagnetic in nature. Similar results were found in MgO and $\alpha\text{-Al}_2\text{O}_3$. The spin-lattice relaxation of Fe^{3+} is found to be unexpectedly long (> 20 ns), and follows a T^9 temperature dependence in ZnO, in contrast to the T^2 dependence expected for a two-phonon Raman process as observed in both MgO and $\alpha\text{-Al}_2\text{O}_3$. Results will be presented and discussed.

MON-IBM01-5

#358 - Contributed Talk - Monday 3:30 PM - Pecos II

Damage studies in 4H-SiC after Si and C low energy implantation

Venkata C. Kummari, Mangal S. Dhoubhadel, Bibhudutta Rout, Tilo Reinert, Floyd D. McDaniel, Weilin Jiang

⁽¹⁾Department of Physics, University of North Texas, 1155 Union Circle #311427, Denton Texas 76203, United States

⁽²⁾Pacific Northwest National Laboratory, Richland Washington 99352, United States

Single crystals of 4H-SiC were implanted with 60 keV carbon or silicon ions separately at four different fluences: for carbon implantation from 1.85×10^{14} cm⁻² to 1×10^{15} cm⁻² (0.05 dpa to 0.28 dpa at the damage peak) and for silicon implantation from 5.5×10^{13} cm⁻² to 3.2×10^{14} cm⁻² (0.05 dpa to 0.30 dpa at the damage peak). All implantations were done at room temperature. Before implantation the depth distribution of primary displacements and implanted ions were calculated using SRIM/TRIM-2011. The displacement energies for simulations were taken as 20 eV and 35 eV for C and Si respectively. Damage accumulation after implantation was studied using two complementary techniques, Rutherford Backscattering Spectroscopy in channeling mode (RBS-C) and Raman spectroscopy.

RBS-C was done using 2 MeV He^+ beam along (0001) crystallographic axis in SiC. The damage accumulation was studied only in Si sub-lattice region. The measured depth profiles for Si sublattice damage determined from RBS-C are compared with TRIM simulations for both C and Si implantation. Raman measurements were performed with 532 nm Ar-ion laser. The decrease of the Raman signal intensity, measured at the transverse and longitudinal optical peaks in Si-C vibrational range, with increasing ion fluence shows the influence of implantation-induced damage.

Complete amorphization has not been achieved for the maximum fluence implanted for both C and Si ion implantation. The amount of damage after implantation, determined by both the techniques, is in good agreement with each other. In this paper we report the theoretical simulations from TRIM-2011 and experimental results obtained from both the techniques in Si and C implanted 4H-SiC.

Acknowledgements: Authors would like to thank the CART facility at UNT for Raman spectroscopy measurements. RBS-C experiment was performed at EMSL, a national scientific user facility sponsored by the DOE's OBER located at PNNL. Jiang was supported by DOE BES.

MON-IBM01-6

#65 - Contributed Talk - Monday 3:30 PM - Pecos II

Swift heavy ions for synthesis of the light-emitting Si nanostructures in Si/SiO₂ multilayers

G. A. Kachurin¹, S. G. Cherkova^{1,2}, V. A. Skuratov³, D. V. Marin^{1,2}, V. A. Volodin^{1,2}, A. G. Cherkov^{1,2}, G. N. Kamaev^{1,2}, A. H. Antonenko^{1,2}

⁽¹⁾SO RAN, Institute of Semiconductor Physics, Pr. Lavrentjeva 13, Novosibirsk 630090, Russia

⁽²⁾Novosibirsk State University, Pirogova 2, Novosibirsk 630090, Russia

⁽³⁾Joint Institute for Nuclear Research, Joliot-Curie, 6, Dubna 141980, Russia

The ability of quantum-size Si nanocrystals (Si-ncs) to emit light opens the door to the Si-based optoelectronics. Usually Si-ncs are prepared by furnace annealing of the Si-rich SiO₂ layers, however that results in their relatively broad size distribution, and their size and density cannot be controlled independently. We attempted to use swift heavy ions for the highly local formation of Si-ncs. The stopping of swift heavy ions in the near-surface layers occurs predominantly by the ionization losses. That leads to formation of the tracks, where the carrier concentrations may reach 10^{22} cm⁻³ and the temperature may exceed 5000 K for 10^{-13} - 10^{-11} s. Thus, the structural transformations in the target may be stimulated either by heat or by ionization. Several pairs of the alternating ~4-8 nm-thick amorphous Si and ~10 nm-thick SiO₂ layers on the

Si substrates were irradiated with 167 MeV Xe ions to the doses of 10^{12} - 10^{14} cm⁻². The ionization and nuclear losses of the ions were ~14.5 keV/nm and ~0.3 displacements/nm, respectively. It was supposed that thickness of Si layers and diameters of the tracks will define the sizes of Si-ncs. After irradiation the electron microscopy revealed an appearance of numerous 3-5 nm size dark spots. The layers gave yellow-orange photoluminescence (PL), which intensity grew with the ion dose. It is traditionally considered as of the different non-crystalline Si nanoinclusions in SiO₂. After annealing the PL strongly increased with a shift of maximum intensity to ~800nm, typical of the Si-ncs emission. The highest intensity was observed after 1100°C anneal, still remaining proportional to the ion dose. Also the Raman spectroscopy evidenced the disappearance of the amorphous Si phase in compliance with the ion doses. It is concluded, that irradiation stimulates synthesis of the light-emitting Si-ncs in SiO₂ during the subsequent annealing. The mechanism of the stimulation is discussed.

MON-IBM01-P1

#213 - Poster - Monday 5:30 PM - Rio Grande

Correlation between microstructural and magnetic properties of Tb implanted ZnO

P P Murmu^{1,2}, J Kennedy^{1,2}, B J Ruck², G.V.M Williams², A Markwitz^{1,2}, S Rubanov³, A A Suvorova⁴

⁽¹⁾National Isotope Centre, GNS Science, 30 Gracefield Road, PO Box 31312, Lower Hutt, Wellington 5010, New Zealand

⁽²⁾The MacDiarmid Institute for Advanced Materials and Nanotechnology, Victoria University of Wellington, PO Box 600, Wellington 5010, New Zealand

⁽³⁾Inst Bio21, University of Melbourne, Vic, Melbourne 3010, Australia

⁽⁴⁾Centre for Microscopy, The University of Western Australia, Crawley, Perth Western Australia 6009, Australia

Rare-earth (RE) elements doped semiconductors are potential dilute magnetic semiconductors (DMSs) for spintronic applications, which are reported to exhibit large magnetic moment [1]. Zinc oxide (ZnO) is predicted to be a promising host material for DMS systems [2], however, research has mainly been focussed into transition metals doped ZnO [3]. Reports of magnetic properties of RE doped ZnO are scarce and lack consistency. Moreover, magnetic properties are very sensitive to microstructures of the film, and require a careful correlation between microstructural and magnetic properties.

We report microstructural and magnetic properties of Tb implanted ZnO single crystals. Tb ions were implanted at 40 keV at RT with fluences ranging from 6.7×10^{14} to 3.0×10^{16} cm⁻², resulting around 0.7 to 12% Tb atoms at an average depth of ~12 nm with a maximum depth of 25 nm. RBS and channeling for 6.7×10^{14} cm⁻² implanted ZnO revealed that around 85% Tb atoms occupied at Zn substitutional lattice sites, unlike Gd implanted ZnO with similar fluence, where almost all the Gd atoms resided at substitutional lattice sites [4]. Energy-filtered TEM micrographs revealed Tb atoms were primarily located at an average depth of ~10 nm and suggested to form Tb-related nanoclusters. Raman spectroscopy results indicated that annealing assisted implantation induced disorder recovery in ZnO lattice by driving Tb atoms out of the substitutional sites. Room temperature ferromagnetic ordering was observed in ZnO:Tb samples annealed at 650 oC. Temperature dependent magnetization results suggested contributions from ferromagnetic and paramagnetic phases, a trend also observed in ZnO:Gd [5].

[1] S. Dhar et.al, Phys. Rev. Lett. 94 (2005) 037205.

[2] T. Dietl et.al, Science, 287 (2000) 1019.

[3] S. J. Pearton et.al, J. Elec. Mater. 36 (2007) 462.

[4] P. P. Murmu et.al, J. Appl. Phys. 110 (2011) 033534.

[5] P. P. Murmu et.al, J. Mater. Sci. 47 (2012) 1119.

Formation and structure of Zn and ZnO nanoparticles in Si by ion implantation and thermal annealing

Bimal Pandey, Prakash R Poudel, Duncan L Weathers

Ion Beam Modification and Analysis Laboratory, Department of Physics, University of North Texas, 1115 Union Circle # 311427, Denton TX 76203, United States

Zinc Oxide (ZnO) nanostructures were synthesized by the implantation of ZnO molecular ions into Si followed by high temperature thermal annealing. ZnO ions at a fluence of 1×10^{17} atoms/cm² and energy of 35 keV were implanted into Si at room temperature. The implanted sample was annealed for 1 hour in a mixture of argon (96%) and hydrogen (4%) gases environment at 700 °C to allow the growth of ZnO precipitates. In the as-implanted sample, Zn nanoparticles ~ 4 nm in diameter were observed. The highest concentration of Zn during the implantation was at a depth of 26 nm in the Si. During annealing, Zn diffused in both directions, and after annealing the maximum concentration of Zn was at 38 nm from the surface. After annealing, Zn and ZnO nanostructure formation was confirmed, with diameters up to 17 nm and 13 nm, respectively. High resolution transmission electron microscope (HRTEM), energy dispersive x-ray spectroscopy (EDS), x-ray diffraction spectroscopy (XRD) and x-ray photoelectron spectroscopy (XPS) were used to characterize the sample.

Antibacterial and Surface Characterizations of Hybrid Ion Implanted ePTFE Samples for Vascular Graft Applications

Senem Ongel¹, Ahmet Oztarhan^{2,3}, Emel Sokullu Urkac⁴

⁽¹⁾*Biotechnology, Ege University, Izmir, Turkey*

⁽²⁾*Ege University, Surface Modification Laboratory, Izmir, Turkey*

⁽³⁾*Bioengineering, Ege University, Izmir, Turkey*

⁽⁴⁾*Ege University, Surface Modification Laboratory, Izmir, Turkey*

In this work antibacterial and surface characterizations of hybrid ion implanted ePTFE samples for vascular graft applications were investigated and the results were presented. Expanded Polytetrafluoroethylene (ePTFE) is widely used as vascular grafts, due to its mechanical strength, chemical inertness, non-adhesiveness and infection resistant properties.

In this work the samples were implanted with both Ag and Zn+O ions (with $1 \times 10^{13-14}$ ion/cm² fluences, 20 kV extraction voltage) by using MEVVA ion implantation system. The antibacterial activities of ion implanted samples were examined against both S.aureus and E.coli according to AATCC Test Method 100-1999. The S. aureus bacteria reduction of Ag ion implanted samples (for vascular graft applications) were found 100% , and 97% for Zn+O. But E.coli bacteria reduction of Ag and Zn+O hybrid ion implanted samples were found 70%. Contact angle measurements were done by using goniometer and found that sample surfaces became hydrophobe after Ag implantation and Zn+O hybrid ion implantation . Surface morphology of ion implanted samples were investigated by SEM analysis. The results suggests new approach to functional ePTFE surfaces for biomedical applications.

Molecular Dynamics Modelling of Swift Heavy Ion Tracks in MeV SIMS of Organics and Semiconductors

Roger P Webb

Surrey Ion Beam Centre, University of Surrey, Guildford Surrey GU12 5LY, United Kingdom

Recently there has been an increasing interest in the use of MeV heavy ions for ion beam analysis purposes. Previously the majority of ion beam analysis work has been performed using either protons or helium ions except for ERD (Elastic Recoil Detection) analysis. PDMS (Plasma Desorption Mass Spectrometry) in the 1970s demonstrated that MeV Heavy ions are very efficient at sputtering insulating and organic samples and the resulting secondary ion mass spectra can be used for identification purposes. Recently it has been shown that this technique can be used in conjunction with a focussed beam to produce Molecular concentration maps on surfaces with high spatial resolution (now termed MeV-SIMS) with the potential to move into analysis at ambient pressure conditions. We use Molecular Dynamics simulations to show how the energy deposited from an MeV heavy ion in organic and semiconducting materials can result in substantial sputtering. The effect of changes in energy deposition density are investigated and the results of the MD simulations are parameterised to use in a simple Monte Carlo model for sputter erosion of insulating and semiconducting surfaces.

Swift heavy ion induced nano-dimensional phase separation in liquid immiscible metal binaries

Sanjeev Kumar Srivastava¹, Saif Ahmad Khan², Sudhherbabu Pavuluri¹, Devesh Kumar Avasthi²

⁽¹⁾*Department of Physics and Meteorology, Indian Institute of Technology Kharagpur, Kharagpur West Bengal 721302, India*

⁽²⁾*Inter University Accelerator Centre, Aruna Asaf Ali Marg, P.O. Box 10502, New Delhi Delhi 110067, India*

Materials composed of dispersed nanoparticles of metals in the matrix of another metal have potential applications as solid lubricants in advanced bearing systems [1]. Attempts are made to synthesize such structures by rapid thermal annealing, at earth and in space, of liquid immiscible binaries, but the density difference and Marangoni motion led to stratification and coarse phase separation. Another way is to utilize the capability of swift heavy ions that they produce transient molten nanocylindrical zones in matter and cool it at a rate of nearly 10^{14} K/s to elevate a mixture of liquid immiscible binary to liquid state and then get the rapid cooling [2]. We irradiated pulsed laser deposited homogeneous thin films of **MnBi**, **BiFe** and **BiCr** binaries, where elements in bold are impurities of about 5 percent, by 100 MeV Au ions. FESEM images reveal that the irradiation leads to formation of roughly 20 nm nanoparticles up to a fluence of 5×10^{13} ions/cm² in all samples. Coalesced nanoparticles are observed at higher fluences. Enhancement of impurity XRD peaks after irradiation is suggestive of phase separation of minority element. A reduction in the remanence and saturation magnetization of **MnBi** samples on irradiation, an evidence of Mn nanostructures formation, reveals the phase separation of Mn as well. A further XPS investigation on the **MnBi** samples shows nearly 1.5 eV binding energy shift in Mn peaks, indicative of isolation of Mn in nanodimensional form and/or some bonding with Bi, which, in turn, has been observed as a reduction in the intensities of Bi peaks. Ab-initio density functional theory calculations very well supplement the above observations.

[1] B. Predel **et al.** in **Decomposition of Alloys: The Early Stages**, ed. H.U. Walter and M.F. Ashby (Berlin: Springer, 1987) p. 517.

[2] S.K. Srivastava **et al.**, Phys. Rev. B 71 (2005) 193405.

Swift heavy ion induced material modifications in ferroelectrics: understanding molecular reorientation and strain development through temperature dependent Raman spectroscopy

Parmendra Kumar Bajpai

Advanced Material laboratory, Department of Pure & Applied Physics, Guru Ghasidas Vishwavidyalaya, Guru Ghasidas Vishwavidyalaya campus, Koni, Bilaspur Chattisgarh 495009, India

Energetic ion beams are widely used in material's modification. The ion beam effects on materials depend upon the type of materials, ion energy, fluence and ion species used. Heavy ions with energies so high that the electronic energy loss process dominates are known as swift heavy ions (SHI). SHI beams are used to study the novel effects in different materials such as metals, semiconductors, superconductors, organic crystals, polymers, etc. Ferroelectric crystals are basic materials used in pyroelectric, piezoelectric and optical devices for technological applications. Molecular orientation plays a critical role in many of the ferroelectrics, especially, in ferroelectric crystals having polyatomic units in the unit cell. Switching is significantly affected by the orientational change in molecular units. The Raman spectroscopy is one of the molecular level probes that are inherently orientation sensitive.

In the present talk, we review the material modifications using SHI irradiation in ferroelectrics and present the recent results of temperature dependent Raman spectral analysis on the Tri-glycine sulphate (TGS) single crystals and $\text{Ba}_x\text{Sr}_{1-x}\text{TiO}_3$ ceramics. Temperature dependent changes in line width, peak intensity and integrated intensities of Raman modes revealed molecular orientational change in glycine ions and oxygen octahedral tilting, lowering of cubic to tetragonal phase transition temperature in BST after irradiation. The results are analyzed in terms of change in dipolar long range order and are used to explain the dopant induced polarization switching inhibition and reduction in strain. It demonstrates the application of heavy ion beams as a tool to control polar ordering.

Porosity and plastic flow in swift heavy ion irradiated GaSb

Patrick Kluth¹, Leandro Araujo², Raquel Giulian², Boshra Afra¹, Matias Rodriguez¹, Thomas Bierschenk¹, James Sullivan¹, Aidan Byrne¹, Mark Ridgway¹

⁽¹⁾*Research School of Physics and Engineering, The Australian National University, Canberra ACT 0200, Australia*

⁽²⁾*Universidade Federal do Rio Grande do Sul, Porto Alegre, Brazil*

While it has previously been reported, that ion irradiation with dominant nuclear energy loss leads to amorphisation and the formation of a porous network in crystalline GaSb, little is known about the effect of swift heavy ion (SHI) irradiation on this material, i.e. where the energy transfer is virtually entirely due to electronic interactions. For this study we have irradiated 2 μm thin crystalline GaSb layers, grown on InP by metal organic chemical vapor deposition, with 185 MeV Au ions. We have investigated the resulting structure and morphology of the material using synchrotron x-ray absorption spectroscopy (XAS), scanning electron microscopy (SEM), surface profilometry and positron annihilation lifetime spectroscopy (PALS) as a function of the irradiation parameters. The irradiation renders the GaSb porous and induces structural disorder. Initially, vacancy clusters form, which evolve into large spherical voids that elongate along the ion beam direction. Continuing irradiation leads to the formation of irregularly shaped hollow pockets with thin sidewalls. This structure is significantly different from that observed previously for irradiation in the nuclear energy loss regime. When irradiation is performed under an angle of 45° with respect to the surface normal, plastic flow of the material is observed in the direction of the projection of the ion beam. The latter has previously only been observed for amorphous materials, however, XAS measurements reveal residual crystallinity after irradiation albeit with enhanced local disorder. The porous layer thickness and the related porous micro-structure is critically dependent on the angle of irradiation. We will present a systematical investigation of the morphology and local atomic structure of GaSb as a function of irradiation fluence and angle and discuss the possible underlying mechanisms for the transformation.

Structural and optical properties of Ge nanocrystals embedded in SiO₂ prepared by 1 MeV Ge implantation

Saikiran V¹, Srinivasa Rao N¹, Devaraju G¹, Sundaravel B², K G M Nair², Anand P Pathak¹

⁽¹⁾*School Of Physics, University Of Hyderabad, P.O. Central University, Gachibowli, Hyderabad, Andhra Pradesh, 500046, India*

⁽²⁾*Materials Science Division, Indira Gandhi Centre for Atomic Research, Kalpakkam, Tamilnadu, 603102, India*

Semiconductor nanocrystals (NCs) embedded in a dielectric matrix have attracted increasing attention due to their potential applications in optoelectronic devices. Researchers are looking for various synthesis methods in order to optimize structural and optical properties of embedded NCs for diverse applications. Among those, ion beam synthesis has received considerable interest due to its ease and simplicity in varying the ion beam parameters. One of the most versatile techniques for nanocrystal synthesis involves high-dose ion implantation followed by high temperature annealing, because the size and structure of NCs can be controlled by changing the ion dose, the energy of ion and the annealing temperatures. In this work, the structural and optical properties of Ge NCs embedded in SiO₂ prepared by 1 MeV Ge implantation and followed by rapid thermal annealing (RTA) at various temperatures will be discussed. The Ge implantation was done at various fluences ranging from 3×10^{16} to 1.5×10^{17} ions/cm² into SiO₂. The structural and optical properties of the as implanted and annealed samples have been investigated by using X-ray diffraction (XRD), Transmission Electron Microscopy (TEM), Raman spectroscopy and Photoluminescence (PL). The effects of annealing temperature on the structural and optical properties of Ge NCs obtained by Ge implantation at various fluences will be discussed in detail.

Effects of Ion irradiation on GeO₂ nanocrystals fluence dependence study

Saikiran V, Srinivasa Rao N, Devaraju G, Anand P Pathak

School Of Physics, University Of Hyderabad, Gachibowli, Hyderabad, Andhra Pradesh, 500046, India

Semiconductor nanocrystals (NCs) exhibit interesting electronic and optical properties which make them potential candidates for important applications. In addition to elemental semiconductor NCs, Germanium dioxide (GeO₂) also attracts immense attention due to its wide range applications such as optical waveguides, nano-connections in optoelectronic communication and vacuum technology. The properties of NCs are not only determined by their size but also by their shape, composition and structure. The modification of these materials plays a vital role in tuning their properties for various applications. In particular ion irradiation is established to be one of the versatile techniques for the modification of materials at nano-scale. Here we present the effects of 80 MeV Ni ions irradiation with different fluences on GeO₂ NCs. The GeO₂ NCs films were prepared by RF magnetron sputtering with Ge as sputtering target in argon and oxygen partial pressures. The samples have been characterized by X-ray Diffraction (XRD), Raman Spectroscopy, Field emission scanning electron Microscopy (FESEM) and Atomic Force Microscopy (AFM) before and after irradiation. The modifications due to ion irradiation observed from these results based on ion solid interaction will be discussed in detail.

Structural and Optical properties of Porous Silicon prepared by anodic etching of Irradiated Silicon

V S Vendamani¹, S V S Nageswara Rao², N Manikantha Babu², Saikiran V², Srinivasa Rao N², Devaraju G²,
Anand P Pathak²

⁽¹⁾*Department of Physics, Pondicherry University, Pondicherry, Pondicherry, Puducherry, 605014, India*

⁽²⁾*School of Physics, University of Hyderabad, Gachibowli, Hyderabad, Andhra Pradesh, 500046, India*

Porous silicon is considered to be a potential material in the field of electronics and optoelectronics because of its strong luminescence in visible region. Ion beam irradiation shows versatile effects on physical and optical properties of porous silicon. However there are only few reports on the structural and optical properties of porous silicon prepared from irradiated silicon. Here we present a study on the influence of swift heavy ion irradiation on the surface roughness of silicon and consequent effects on the formation of porous silicon. The p-type (100) Si was irradiated with 80 MeV Ni ions at various fluences ranging from 1×10^{11} to 5×10^{13} ions/cm². The irradiated samples were anodically etched to get porous Si. These ion induced effects are being investigated by Photoluminescence (PL), Raman Spectroscopy, Fourier Transform Infrared Spectroscopy (FTIR), AFM and FESEM and will be discussed in detail during the conference.

MON-MA01-1

#475 - Contributed Talk - Monday 1:00 PM - Pecos I

Important Considerations in the Use of Charged particles for Radiotherapy

Amato J. Giaccia

Department of Radiation Oncology, Stanford University School of Medicine, Stanford CA 94305, United States

In 1946, Wilson and colleagues from Berkley the use of protons to treat tumors after analyzing their depth dose profile. Treatment of patients with protons, and then other charged particles soon followed. The advantage of increased energy deposition with penetration depth was perceived as a distinct advantage of protons. and some charged particles such as carbon ions. In addition, charged ions such as carbon ions also possess increased ionization energy density that results in clustered DNA damage that is more difficult to repair. The ever-increasing numbers of Proton facilities and to a lesser extent Hadron facilities that are going on line represents an opportune time to investigate the radiobiology of these particles in more depth. The talks in this session will cover the basic biophysical and radiobiologic properties of charged particles. We will cover how tissues respond to charged particles, and how the cellular response to charged particles differs from conventional low LET irradiation such as X-rays. In particular, DNA damage and repair, the effects of tumor hypoxia, cell-cycle effects, stem cells and normal tissues effects will be discussed. There are still many questions about the use of charged particles in clinical radiotherapy that need to be addressed to better utilize them for the treatment of cancer.

MON-MA01-2

#474 - Invited Talk - Monday 1:00 PM - Pecos I

DNA damage responses induced by HZE particles in human cells

Aroumougame Asaithamby, David J. Chen

Department of Radiation Oncology, The University of Texas Southwestern Medical Center at Dallas, Dallas TX 75390, United States

The most important effect of radiation is damage to DNA, mainly DNA double-strand breaks (DSBs). Unrepaired or misrepaired DSBs will result in cytotoxic, mutagenic and carcinogenic effects of radiation. Substantial evidence indicates that high-LET radiation induces complex DNA damage or clustered DNA lesions in cells. Evidence indicates that complex lesions are difficult to repair than isolated lesions and therefore, associated with increased relative biological effectiveness (RBE) for cell killing, chromosomal aberrations, mutagenesis, and carcinogenesis. Using a novel live cell imaging combined with immunofluorescent approach, we have monitored the repair kinetics of DNA DSBs induced by HZE particles in human cells. We found that the induction of unrepaired DSBs is dependent on the physical quality of the HZE particles. Further more, we showed that the kinetics of loss of clustered DNA lesions was substantially compromised in human cells. The unique spatial distribution of different types of DNA lesions within the clustered damages, but not the physical location of these damages within the sub-nuclear domains, determined the cellular ability to repair these damages. Importantly, examination of metaphase cells derived from HZE particles irradiated cells revealed that the extent of chromosome aberrations directly correlated with the levels of unrepaired clustered DNA lesions.

In addition, we used a novel organotypic human lung three-dimensional (3D) model to investigate the biological consequences of unrepaired DNA lesions in differentiated lung epithelial cells. We found that, unlike simple DSBs, complex DNA lesions induced by iron particles were irreparable in organotypic 3D culture. As the organotypic 3D model mimics human lung, it opens up new experimental approaches to explore the effect of radiation **in vivo** and will have important implications for evaluating radiation risk on human lung carcinogenesis and cancer therapy.

MON-MA01-3

#469 - Invited Talk - Monday 1:00 PM - Pecos I

Long-term cellular response predicted by microdosimetry and DNA repair centers

Sylvain Costes, Ph.D.

Life Sciences Division, Lawrence Berkeley National Laboratory, 1 Cyclotron Road, MS 977, Berkeley CA 94720, United States

Our lab recently showed that DNA double strand breaks (DSB) induced by ionizing radiations could cluster into common regions of the nucleus to be repaired. We hypothesized that such a phenotype is probably genetically variable among the human population, and that people with strong “repair center” phenotypes would be at higher risk from the effects of ionizing radiation. Our rationale was that when two or more DSB moved into one common repair center, this would increase the probability of DNA misrejoining, leading to chromosomal rearrangements and potentially cell death. If we assumed the following: 1. a nucleus is an hemisphere; 2. DNA damage are randomly generated in the DNA; 3. DNA damage migrate to the closest repair center for repair, then we also concluded that DSB clustering would be non linear with dose, with much more clustering at higher doses. We recently developed a simple Monte Carlo model to simulate the movement of DSB into common repair centers in hypothetical nuclear hemispheres for various doses. In this model, the average distance between nearest repair centers was determined experimentally for X-ray, and was estimated to be $\sim 1.2 \mu\text{m}$ in human breast cells. Using such parameters, we then determined cell survival curves after exposure to X-rays to estimate the lethal impact of DSB clustering using simple target theory. When the geometrical property of “repair centers” were combined with the microdosimetric description of high-LET tracks, we could then predict cell death and chromosomal rearrangements after exposure to high-LET ions. Our prediction matched very accurately experimental data for high-LET radiation. Therefore, such approach is very promising to refine clinical treatment planning at the individual level.

Supported by the U.S. Department of Energy under Contract No. DE-AC02-05CH11231 and the DoE Low Dose Research Program

Impact of HEZ Particle Irradiation on Adult Neural Stem Cells and Neurogenesis In Vivo

Benjamin Chen

Radiation Oncology, University of Texas, Southwestern Medical Center, 2201 Inwood Road, Dallas TX 75390, United States

The high-LET HZE particles from galactic cosmic radiation pose tremendous health risks to astronauts, including risks to the central nervous system (CNS) and potential cognitive impairment. One CNS cell population that warrants close analysis for their response to radiation is adult neural stem cells in subgranular zone (SGZ) of hippocampal dentate gyrus (DG) since adult hippocampal neurogenesis has been linked to learning and spatial memory and is critical for cognitive recovery after brain injury. To examine the response and potential recovery of adult neural stem cells after low- and high-LET irradiation, we utilize two transgenic mouse models based on Nestin promote as Nestin-expressing stem cells are thought to be the source of a continuous supply of neural progenitor cells, which eventually mature into neurons. Nestin-GFP mouse could label neural stem cells based on expression of green fluorescent protein and morphology and Nestin-CreERT2/R26R-YFP (KxY) mouse allows permanent YFP-labeling of adult neural stem cells and their progeny. In this study, we analyze cell proliferation and adult neural stem cells survival at SGZ after ⁵⁶Fe particle irradiation. Nestin-GFP and Nestin-CreERT2/R26R-YFP mice were subjected to whole body irradiation with ⁵⁶Fe particles. Our analyses reveal that ⁵⁶Fe particle exposure transiently decreases DG proliferation and induces long-term changes in overall neurogenesis. We also observe the persistence of DNA damage (53BP1 foci, suggesting long-term genomic instability) and an inverse correlation with the number of immature DCX+ neurons. However, the number of Type-1 neural stem cells remains constant, suggesting that the slow-proliferating Type-1 cells are more resilient than the fast-proliferating progenitor cells. These results highlight that, despite the persistence of putative neural stem cells, ⁵⁶Fe particle exposure could deliver a long-term impairment in adult hippocampal neurogenesis not by influencing the number of neural stem cells but their ability in proliferation and/or differentiation.

Development of an External Beam Setup for the Ion-Beam-Microprobe at the University of North Texas

Jacob D Baxley, Tilo Reinert

Ion Beam Modification and Analysis Laboratory, Physics Department, University of North Texas, 1155 Union Circle #311427, Denton TX 76203, United States

The University of North Texas (UNT) has an ion beam microprobe beam line at the 9SDH-2 3.0 MV Tandem Pelletron® accelerator capable of focusing also heavy ions. The variety of ion species at MeV energies represents a source of ionizing radiation of a broad range of linear energy transfer. The microprobe at UNT is therefore well suited to study the effects of localized low dose ionizing radiation in biological systems.

Since radiobiological research requires living model systems we are developing an external beam set up based on a beam exit nozzle, which will be installed in the existing microprobe analysis chamber. The intended biological model system is the egg of **drosophila melanogaster**. Our goal is to use the Bragg-peak of maximum ionization density for particle radiation to induce a localized hot spot of ionizing radiation inside the egg. The hot spot shall deliver an energy dose above the level for triggering radiation response, especially the activation of the tumor suppressor protein p53, whereby p53 remain silent along the radiation entrance path.

We will present the design of the external beam setup and simulations of the energy dose distribution.

Predicting the enhanced effect of ions compared to X-rays: The local effect model and its application

Thomas Friedrich¹, Uwe Scholz¹, Rebecca Grün¹, Olaf Steinsträter¹, Marco Durante^{1,2}, Michael Scholz¹

⁽¹⁾Department of Biophysics, GSI Helmholtz Centre for Heavy Ion Research GmbH, Planckstrasse 1, Darmstadt 64291, Germany

⁽²⁾Institute of solid state physics, Darmstadt University of Technology, Hochschulstrasse 6-8, Darmstadt 64289, Germany

Compared to gamma- or X-rays ions show an increased effectiveness when irradiated to biologic targets such as cultured cells or tissues. This enhancement is one of the rationales for ion cancer therapy and is quantified as the relative biological effectiveness (RBE). The RBE has been investigated in radiobiology since decades, and a manifold dependence on radiation quality (i.e. energy and ion species), dose, depth in tissue, and on the biologic response of cells or tissues under investigation has been found. For therapeutic purposes with ion beams mixed radiation fields have to be considered and a sufficiently accurate set of RBE values for each specific tissue type and radiation quality is needed. The Local Effect Model (LEM) is one of the few models capable to predict the RBE and hence allowing biologically oriented treatment planning. It is successfully applied in carbon ion therapy and also used for designing and understanding radiobiological experiments with different endpoints.

In the talk the conceptual basis of the LEM is discussed. The response of cells after photon irradiation is used to calculate its response to ion beams. For that purpose a mechanistic modeling of the induction and the spatial distribution of double strand breaks is performed. For photons the distribution is based on Poissonian statistics and for ions an amorphous track structure model is applied. This allows predicting RBE values for all ion species relevant for ion therapy with one comprehensive set of input parameters. We show several examples of how the LEM is used to model in-vitro and in-vivo results of radiobiological experiments, and how the model was validated. The interpretation of the LEM in treatment planning is described, and the consistency of model predictions with clinical outcomes is demonstrated. Finally a short qualitative comparison of the LEM with other RBE models is given.

RBE enhancement by sub micrometer focusing of low LET protons

Christoph Greubel¹, Thomas E Schmid², Stefanie Girst¹, Volker Hable¹, Dörte Michalski², Michael Molls², Gabriele Multhoff², Ernst Schmid³, Judith Seel¹, Christian Siebenwirth¹, Olga Zlobinskaya², Günther Dollinger¹

⁽¹⁾Institut für Angewandte Physik und Messtechnik, Universität der Bundeswehr München, Neubiberg, Germany

⁽²⁾Department of Radiation Oncology, Technische Universität München, München, Germany

⁽³⁾Institute for Cell Biology, Ludwig-Maximilians Universität München, München, Germany

High LET radiation like heavy ions is well known to induce a higher RBE than low LET radiation for almost all endpoints. However, in order to obtain more insight into heavy ion tumor therapy some major features of the biological effectiveness of high energy and high LET ions are essential to analyze in more detail.

High LET radiation deposits doses in the order of few gray into a cell nucleus by only few hits, whereas for low LET particle several hundred hits are necessary. As a result the spatial dose distribution of low LET protons is nearly homogenous with dose enhancements up to 10^2 Gy around the proton tracks. In contrast, for carbon ions the dose is concentrated around the few ion tracks exceeding the maximum dose of protons by two orders of magnitudes.

To study the influence of spatial dose distribution on RBE we use the ion microprobe SNAKE to concentrate the deposited dose in cells by focusing a certain number of low LET protons to a sub micrometer spot which approximate a high LET dose distribution. In detail, human hamster hybrid (AL) cells have been exposed to an average dose of 1.7 Gy using randomly distributed 20 MeV protons, single 55 MeV carbon ions in a $5.4 \times 5.4 \mu\text{m}^2$ matrix and 20 MeV protons in the same matrix with 117 protons per matrix point. The RBE values for induction of micronuclei ($\text{RBE}_{\text{Mn}} = 1.48 \pm 0.07$) and dicentric chromosome ($\text{RBE}_{\text{Dc}} = 1.92 \pm 0.15$) are significantly higher in focused proton mode than for randomly distributed protons ($\text{RBE}_{\text{Mn}} = 1.28 \pm 0.07$; $\text{RBE}_{\text{Dc}} = 1.41 \pm 0.14$). The RBE enhancement toward the value of high LET 55 MeV carbon ions ($\text{RBE}_{\text{Mn}} = 2.20 \pm 0.09$ and $\text{RBE}_{\text{Dc}} = 3.21 \pm 0.27$) is attributed to the modified dose distribution.

Estimate of the clinical impact of the RBE variations in proton and carbon ion treatments: a radiobiological modeling approach

Andrea Attili¹, Germano Russo¹, Felix Ms Milian¹, Flavio Marchetto¹, Laura Iannotti¹, Damien Bertrand², Yves Jongen²

⁽¹⁾Experimental Physics, Istituto Nazionale di Fisica Nucleare, Via Giuria 1, Turin 10125, Italy

⁽²⁾Ion Beam Applications (IBA), Chemin du Cyclotron, 3, Louvain-la-Neuve 1348, Belgium

Purpose: An important aspect in the field of advanced radiotherapy with ion beams is the implementation of a Treatment Planning System (TPS) which includes the evaluation of the biological effects. In this work we present an analysis of the clinical impact of the biological effects in Charged Particle therapy with protons and Carbon ion beams. The analysis was performed using a TPS prototype for hadrontherapy that is currently being developed at INFN in partnership with Ion Beam Applications (IBA).

Methods: The TPS prototype dose and RBE distributions are computed by the superposition of kernel look-up tables generated using MC simulations. These were performed using the Fluka toolkit plus an implementation of the Local Effect Model (developed by the GSI Biophysics group [1]), and an original improved version of the Microdosimetric Kinetic Model (MKM) [2]. A set of treatment plans of clinical cases are analyzed using the RBE weighted dose volume histograms (DVHs), the tumour control probability (TCP) and the normal tissue complication probability (NTCP) values.

Result: The RBE weighted DVH for organs at risk is significantly increased due to the RBE variation, even in the case of irradiation with protons which clinically are assumed to have a constant RBE = 1.1. As a consequence lower NTCP values for the non-target normal tissue were obtained when applying the computed RBE.

Conclusion: In the case of protons, we observed a difference when the RBE is modeled with respect to applying a generic RBE of 1.1. This observation suggests that in some clinical cases it is worth considering such a variability in clinical proton therapy planning, especially when risk organs are located immediately behind the target volume.

[1] T.Elsasser, M.Kramer, M.Scholz, Int. J. Radiation Oncology Biol. Phys, 71 no.3 (2008) 866-872;

[2] Y.Kase et al., Phys. Med. Biol. 53 (2008) 37-59.

Revision of the status of proton relative biological effectiveness and its uncertainties

Alejandro Carabe

Department of Radiation Oncology, Hospital of the University of Pennsylvania, 3400 Civic Center Blvd, Philadelphia Pennsylvania 19104, United States

The improvement of the delivery techniques in proton radiotherapy to increase conformality and accuracy of the delivered dose should always be accompanied by a detailed knowledge of the radiobiological principles guiding the design of the treatment. Without a full description of the radiobiological properties of protons when used in different treatment sites and with different doses, it is not possible to think of tailor made, personalized, proton radiotherapy treatment. The current radiobiological data supporting the universally accepted 10% difference in biological effectiveness (measured in terms of the relative biological effectiveness, RBE) between protons and x-rays will be discussed, with particular emphasis on the variability of this biological effectiveness with standard radiotherapy quantities such as dose/fraction, Linear Energy Transfer and α/β ratios. On the basis of this discussion, the justification of the use of a constant RBE for doses/fraction of any size, or for tissues with very different radiosensitivities or at every depth along the proton depth-dose profile will be assessed. The potential advantages of the use of a 'variable' RBE in proton radiotherapy compared to a 'constant' RBE will be shown in prostate and brain cases. The uncertainties associated to the RBE weighted dose distributions will be then discussed on the bases of the current biological uncertainties, as well as how these uncertainties affect the proton physical range uncertainty.

Overview on Photon Activation Analysis and Recent Results on Particulate Matter from the Idaho Accelerator Center

Philip Lawrence Cole^{1,2}, Christian Segebade¹, Mayir Mamtimin²

⁽¹⁾*Idaho Accelerator Center, Idaho State University, 1500 Alvin Ricken Drive, Pocatello Idaho 83201, United States*

⁽²⁾*Dept of Physics, Idaho State University, Pocatello Idaho 83209, United States*

Instrumental analytical methods are preferable in studying the expected sub-milligram quantities of airborne particulates collected in dust filters. The multi-step analytical procedure used in treating samples chemically is complicated. Moreover, due to the expected small masses of the "dust particles" (10 to 100 ugram) collected on filters, such a chemical treatment can easily lead to significant contamination levels. Radio-analytical techniques, and in particular, activation analysis methods offer a far cleaner alternative. Activation methods require minimal sample preparation and provide sufficient sensitivity for detecting the vast majority of the elements throughout the periodic table.

In this talk, we will give a general overview of the technique of photon activation analysis (PAA). We will show that by activating dust particles with 10- to 30-MeV bremsstrahlung photons, we can ascertain their elemental composition. The samples are embedded in dust-collection filters and are irradiated "as is" by these photons. The radioactivity of the photonuclear reaction products is measured with appropriate spectrometers and the respective analytes are quantified using multi-component calibration materials. We will give specific examples of identifying the elemental components of airborne dust particles, volcanic ash, and lunar dust simulants by making use of bremsstrahlung photons from the electron linear accelerator at the Idaho Accelerator Center.

Trace Element Analysis of Airborne Particulates, Volcanic Ash and Moon Dust Simulants by Photon Activation

Mayir Mamtimin¹, Philip Cole¹, Christian Segebade²

⁽¹⁾*Department of Physics, Idaho State University, 921 S 8th Ave, Pocatello IDAHO 83209, United States*

⁽²⁾*Idaho Accelerator Center, Idaho State University, 921 S 8th Ave, Pocatello IDAHO 83209, United States*

The quality of the air suffers from contaminants: the industrial world releases tremendous amounts of pollution into the atmosphere around the world, volcanic eruption and volcanic ash often cause sudden environmental change, and the events like the Fukushima nuclear power plant incident releases radioactive particles into the air which could eventually spread around the globe. Studies of these environmental facts not only tell us what we are inhaling everyday, but are also strong telltale signs of environmental change, industrial impact, and global warming. As a feasibility study, we investigate the technique of Photon Activation Analysis (PAA) on airborne particulates, volcanic ash, and Moon dust simulant samples. PAA is multi-element activation analysis method which is based on photonuclear interaction. Using the facilities at the Idaho Accelerator Center, it is possible to determine the elemental composition of the various samples. These results can assist us in better understanding the change in environment, the impact of industrialization, and the contribution of natural events like volcanos. At the same time, we are applying the technique of Photon Activation Analysis on a more fundamental topic as determining the elemental composition of various materials. It is our aim to demonstrate that PAA is a successful alternative method. At the end, we compare our preliminary results to that of some other analytical methods.

Optimization of Commercial Scale Photonuclear Production of Radioisotopes

Bindu KC, Frank Harmon, Valeriia N. Starovoitova, Jon Stoner, Douglas P. Wells
Idaho Accelerator Center, Idaho State University, 1500 Alvin Ricken Drive, Pocatello ID 83201, United States

Photonuclear production of radioisotopes driven by bremsstrahlung photons using a linear electron accelerator in the suitable energy range is a promising method for manufacturing radioisotopes. The photonuclear production method is capable of making radioisotopes more conveniently, cheaply and with much less radioactive waste compared to existing methods. Historically, photo-nuclear reactions have not been exploited for isotope production because of the low specific activity that is generally associated with this production process, although the technique is well-known to be capable of producing large quantities of certain radio-isotopes. We describe an optimization technique for a set of parameters to maximize specific activity of the final product. This set includes the electron beam energy and current, the end station design (an integrated converter and target as well as cooling system), the purity of materials used, and the activation time. These parameters are mutually dependent and thus their optimization is not trivial. ^{67}Cu photonuclear production via $^{68}\text{Zn}(\gamma, p)^{67}\text{Cu}$ reaction was used as an example of such and optimization process.

Thin Layer Activation (TLA) analysis of different materials for wear, corrosion and erosion measurement

Ferenc Ditrői, Sándor Takács, Ferenc Tárkányi
Cyclotron Application, Institute of Nuclear Research, Bem ter 18-c, Debrecen H-4026, Hungary

In the modern industrial research sophisticated tools are required in order to elaborate, test and check a new development (new material, surface treatment, design, lubricant, etc.) and introduce it into the routine production. One of these tools is the radioisotope tracing by Thin Layer Activation (TLA). Charged Particle Activation Analysis is routinely used in several accelerator laboratories producing radioisotopes with medium (from hours to days) half-lives. From this method has the TLA developed. The basic material to be investigated is mainly metal (being the most frequent construction materials in industry) and the most convenient way of TLA if one or more of the alloy components can be activated directly, producing longer-lived radioisotopes having strong enough gamma-radiation for wear measurements. If none of the components can be activated in such a way, the more sophisticated secondary implantation or radioactive beams can be used. The secondary implantation can be performed in any accelerator laboratory (producing much lower activity than in the direct activation case), but for radioactive beams a dedicated accelerator/laboratory is required. We demonstrate in the present study through some real cases the applicability of the method and discuss the problem of "radioactive isotopes" introduced in industrial sites, providing solution by introducing the activities under the "free handling limit" (FHL).

Testing the Quasi-absolute Method in Photon Activation Analysis

Z. J. Sun^{1,2}, D. Wells^{1,2}, V. Starovoitova^{1,2}, C. Segebade²

⁽¹⁾Department of Physics, Idaho State University, 921 S. 8th Ave., Pocatello ID 83209, United States

⁽²⁾Idaho Accelerator Center, 1500 Alvin Ricken Drive, Pocatello ID 83201, United States

In photon activation analysis (PAA), relative methods are widely used because of their accuracy and precision. Absolute methods, which are conducted without any assistance from calibration materials, are seldom applied for the difficulty in obtaining photon flux in measurements. This research is an attempt to perform a new absolute approach in PAA - quasi-absolute method - by retrieving photon flux in the sample through Monte Carlo simulation. With simulated photon flux and database of experimental cross sections, it is possible to calculate the concentration of target elements in the sample directly. The QA/QC procedures to solidify the research are discussed in detail. Our results show that the accuracy of the method for certain elements is close to a useful level in practice. Furthermore, the future results from the quasi-absolute method can also serve as a validation technique for experimental data on cross sections. The quasi-absolute method looks promising.

Edward's Sword? - A non-destructive study of a medieval king's swordChristian Segebade*Idaho Accelerator Centre, Idaho State University, Pocatello ID 83201, United States*

Non-destructive methods including photon activation analysis were applied in an examination of an ancient sword. It was tried to find indication of forgery or, if authentic, any later processing and alteration. Metal components of the hilt and the blade were analysed by instrumental and non-destructive photon activation, respectively. Metallurgical studies (hardness measurements, microscopic microstructure analysis) are described, too. The results of these investigations did not yield indication of non-authenticity. This stood in agreement with the results of stylistic and scientific studies by weapon experts.

Applications of the associated-particle neutron-time-of-flight interrogation technique - From Sheep to Unexploded OrdnanceSudeep Mitra*Environmental Sciences Department, Brookhaven National Laboratory, Upton NY 11973, United States*

The associated-particle technique (APT) will be presented for some diverse applications that include on the one hand, analyzing the body composition of live sheep and on the other, identifying the fillers of unexploded ordnance (UXO). What began with proof-of-concept studies using a large laboratory based 14 MeV neutron generator of the "associated-particle" type, soon became possible for the first time to measure total body protein, fat and water simultaneously in live sheep using a compact field deployable associated-particle sealed-tube neutron generator (APSTNG). This non-invasive technique offered the animal physiologist a tool to monitor the growth of an animal in response to new genetic, nutritional and pharmacologic methods for livestock improvement. While measurement of carbon (C), nitrogen (N) and oxygen (O) determined protein, fat and water because of the fixed stoichiometric proportions of these elements in these body components, the unique C/N and C/O ratios of high explosives revealed their identity in UXO. The algorithm that was developed and implemented to extract C, N and O counts from an APT generated gamma-ray spectrum will be presented together with the UXO investigations that involved preliminary proof-of-concept studies and modeling with Monte Carlo produced synthetic spectra of 57-155 mm projectiles.

An integrated mobile system for non-destructive analysis with tagged neutronsD. Cester¹, G. Nebbia², L. Stevanato¹, G. Viesti¹, F. Neri³, S. Petrucci³, S. Selmi³, C. Tintori³⁽¹⁾*Dipartimento di Fisica ed Astronomia, Università di Padova, Via Marzolo 8, padova 35131, Italy*⁽²⁾*Sezione di Padova, INFN, Via Marzolo 8, padova 35131, Italy*⁽³⁾*CAEN S.p.A., Via Vetràia 11, Viareggio (LU) 55049, Italy*

The SMANDRA inspection system has been recently developed within an Italian national program. It is conceived as a multi-task tool for non-destructive analysis, to search and identify sources of ionizing radiation or identify dangerous and/or illegal materials inside volumes tagged as "suspect" by conventional surveys. The system is made of two pieces: 1) a passive unit including two gamma-ray detectors (5"x5" NaI(Tl) and 2"x2" LaBr) and two neutron counters (liquid scintillator and ³He proportional counter for fast/slow neutrons). The unit hosts batteries, power supplies, front-end electronics and CPU; 2) an active unit including a portable sealed neutron generator based on the Associated Particle Imaging (API) technique (EADS SODERN TPA17). The first unit can be used in standalone mode to search and identify radioactive material as well as Special Nuclear Material (SNM). It can be used as well as detector package connected to the second unit for active interrogation of voxels.

SMANDRA is designed to be transported by a light vehicle, easily operated by non-specialized personnel. The front end electronics consist of a single VME card hosting FADC units (CAEN-V1720) used to perform digital pulse processing by FPGA. The passive unit passed laboratory tests aimed at verifying the compliance with IEC standards. Moreover the detection of SNM has been the subject of a specific experimental study [1]. Possible applications of the present system will be discussed.

[1] D. Cester et al., NIM A663 (2012) 55

MON-NBAE02-3

#111 - Invited Talk - Monday 3:30 PM - Brazos II

Application of the Associated Particle Imaging Technique for Induced Fission Imaging

Seth McConchie, Paul Hausladen, Matthew Blackston, James Mullens, John Mihalcz
Oak Ridge National Laboratory, 1 Bethel Valley Rd, Oak Ridge TN 37831, United States

The associated particle imaging (API) technique is well suited for performing fast neutron transmission imaging to determine the configuration of materials within an object. By detection of the alpha particle from the deuterium-tritium reaction, the time and direction tagging of individual 14 MeV neutrons can be sufficiently precise to enable of order millimeter spatial resolution when using an appropriately sized fast neutron detector. Determination of an object's material configuration is accomplished by measuring the attenuation along many paths through the portion of the object in view of tagged neutron cone. Rotating the object enables the use of tomographic image reconstruction methods for three-dimensional image analysis. However, those instances where the 14 MeV neutrons interact in the object somewhere along their individual trajectories can also yield interesting information. For those neutrons that induce fission, one or more neutrons will be emitted isotropically that are correlated in time with each other and with the original alpha event that normally would have been used to reconstruct the neutron transmission data. If the fissioning material has multiplication, then all of the fission chain neutrons will be correlated with the alpha event. These neutrons typically have energies on the order of 2 MeV, so that time-of-flight can be used to distinguish between transmitted 14 MeV neutrons and the late-arriving fission chain neutrons. Such a measurement would be useful for imaging the location of fissioning material within a configuration and distinguishing highly enriched uranium from depleted uranium, especially when high Z shielding is present. A methodology for reconstructing the induced fission locations and measurements of various configurations of uranium are presented.

MON-NBAE02-4

#339 - Contributed Talk - Monday 3:30 PM - Brazos II

Associated Particle Neutron Imaging for Elemental Analysis in Medical Diagnostics

David Koltick¹, Huiling Nie²

⁽¹⁾*Physics Department, Purdue University, 525 Northwestern Avenue, West Lafayette Indiana 47907, United States*

⁽²⁾*School of Health Sciences, Purdue University, 550 Stadium Mall Drive, West Lafayette Indiana 47907, United States*

Associated particle neutron elemental imaging (API) for in vivo and invitro diagnostic analysis is a candidate to measure elemental disease signatures. Results suggest API can produce elemental images with spatial resolution as small as 1-mm even when limiting patient radiation exposure to 5-rem. While API technology has been developed and used in detecting explosive materials and mining resources for over three decades, its development for medical imaging has been minimal.

While the human body is composed of complex mechanical, chemical and organizational interactions involving molecules with up to 100s of billions of atoms, it is surprising localized elemental content presents diagnostic information on disease presence. Anomalous elemental concentrations have been observed to depend on cancer location for breast, liver, colon, kidney, lung and prostate. In vivo observation of these elemental anomalies would provide a diagnostic tool for disease presence. In vitro observation may provide rapid margin analysis during surgery to reduce the need for surgical reintervention. Investigation into the pathways underlying these anomalous elemental concentrations may provide new and possible novel therapeutic targets. Measured elemental disease signatures range from 1-ppm to over 1000-ppm.

The paucity of API development for medical diagnoses is due to the limited obtainable spatial resolution by (1) the timing of the associated particle used to form the image. However, we have developed a working API neutron generator with measured timing resolution of less than 500-picosecond based on an in place ZnO-Fluor. (2) Initial commercial API generator developments required beam diameters ~ 1-cm in order to provide good neutron flux at low power target-densities for extended generator lifetime. We present data using a focusing beam with diameter to less than 2-mm. These features will allow spatial elemental details, on order of 1-mm for projective imaging and less than 1-cm depth resolution for 3-dimensional images.

Prompt Gamma Analysis of Blended Cement Concrete Samples utilizing a Portable Neutron Generator

Akhtar A. Naqvi¹, Faris A. Al-Matouq¹, Zameer Kalakada², M. Maslehuddin³, Omar O. S. Al-Amoudi²

⁽¹⁾Physics, King Fahd University of Petroleum and Minerals, Dhahran, Dhahran Eastern Province 31261, Saudi Arabia

⁽²⁾Civil Engineering, King Fahd University of Petroleum and Minerals, Dhahran, Dhahran Eastern Province 31261, Saudi Arabia

⁽³⁾Center for Engineering Research, King Fahd University of Petroleum and Minerals, Dhahran, Dhahran Eastern Province 31261, Saudi Arabia

A prompt gamma-ray neutron activation (PGNAA) setup has been developed utilizing a D(d,n) reaction based portable neutron generator model MP320 (Thermo Fisher Company, USA) to determine the concentration of elements in blended cement concretes. The main feature of the developed PGNAA setup is its source - detector geometry that allows one to detect prompt gamma-rays emitted from bulk specimens at a backward angle. In spite of low yield of gamma-rays at a backward angle, this type of PGNAA setup geometry is highly desirable for developing a portable PGNAA-based chlorine detector. The setup has been tested by detecting chlorine concentration in chloride-contaminated blast furnace slag (BFS), fly ash (FA) and superpozz (SPZ) cement concrete specimens. In spite of strong interference between the chlorine prompt gamma-rays and those from other constituents in concrete, the chlorine concentration was successfully determined utilizing 6116 and 3935 keV chlorine prompt-gamma rays. A linear correlation ($R^2 > 0.94$) between the gamma-ray experimental yield and chloride concentration in the BFS, FA and SPZ cement concrete specimens was obtained. The results of this study will be discussed in detail the full length paper.

Water Salinity Analysis using a Portable Neutron Generator Based PGNAA Setup

Akhtar A. Naqvi¹, Faris A. Al-Matouq¹, M. A. Gondal¹, A. A. Issab²

⁽¹⁾Physics, King Fahd University of Petroleum and Minerals, Dhahran, Dhahran Eastern Province 31261, Saudi Arabia

⁽²⁾Chemistry, King Fahd University of Petroleum and Minerals, Dhahran, Dhahran Eastern Province 31261, Saudi Arabia

Performance of a portable neutron generator based PGNAA setup has been evaluated for prompt gamma analysis of water salinity using a large cylindrical 125 mm x 125 mm (diameter x height) BGO detector. The yield of 3.06, 5.57, 6.11 and 6.67 MeV chlorine prompt gamma rays was measured from water samples contaminated with 1.0 to 4.0 wt. % chlorine to determine the samples water salinity. The excellent agreement between the measured and calculated yield of chlorine gamma-rays from water samples as a function of chlorine concentration in water indicates satisfactory performance of the MP320 portable neutron generator in PGNAA studies.

Quantitative comparison between PGNAA measurements and MCNP calculations in view of the characterization of radioactive wastes in Germany and France

Eric Mauerhofer¹, Andreas Havenith¹, Cedric Carasco², Emmanuel Payan², John Kettler¹, Thomas Kring¹, Jean-Luc Ma², Bertrand Perot²

⁽¹⁾Institut für Energie- und Klimaforschung Nukleare Entsorgung und Reaktorsicherheit, Forschungszentrum Jülich, Wilhelm-Johnen-Straße, Jülich 52428, Germany

⁽²⁾DEN, Nuclear Measurement Laboratory, CEA, Cadarache, Saint Paul Lez Durance 13108, France

The Forschungszentrum Jülich (FZJ, Germany) and the Commissariat à l'Energie Atomique et aux Energies Alternatives (CEA Cadarache, France) are involved in a cooperation aiming at characterizing toxic and reactive elements in radioactive waste packages by means of Prompt Gamma Neutron Activation Analysis (PGNAA) [1]. The French and German waste management agencies have indeed defined acceptability limits concerning these elements in view of their respective geological repositories. A first measurement campaign was performed in the new MEDINA PGNAA graphite cell, at FZJ, to assess the capture gamma-ray signatures of some elements of interest.

The paper will present MCNP calculations of the MEDINA system and quantitative comparison between measurement and simulation. Passive gamma-ray spectra performed with the high purity germanium detector and calibration sources are used to qualify its detailed numerical model. Experimental PGNA spectra taken in MEDINA with a chlorine sample will then allow qualifying the global numerical model of the measurement cell. Chlorine indeed constitutes a usual reference due to its reliable capture gamma-ray production data. The goal is to qualify the whole simulation protocol (geometrical model, nuclear data, and post-processing tools) in view to design, optimize and predict the performances of future measurement cells.

[1] J.-L. Ma, C. Carasco, B. Perot, E. Mauerhofer, J. Kettler, A. Havenith, Prompt Gamma Neutron Activation Analysis of toxic elements in radioactive waste packages, IRRMA-8, 8th Topical Meeting on Industrial Radiation and Radioisotopes Measurement Applications, Kansas City, USA, June 26 - July 1, 2011, doi:10.1016/j.apradiso.2012.02.011, to be published in Applied Radiation and Isotopes.

MON-NBAE02-P3

#120 - Poster - Monday 5:30 PM - Rio Grande

Faster Identification of Explosives Using a Lanthanum Bromide Gamma-Ray Detector & D-D Neutron Generator

C Jayson Wharton, Edward H Seabury, Augustine J Caffrey
Idaho National Laboratory, 1765 N. Yellowstone Hwy, Idaho Falls ID 83415, United States

Gamma ray detection instruments are a critical component in the identification of explosives, special nuclear material, chemical weapons and other materials of interest in the non-proliferation arena. A new type of detector, LaBr₃(Ce), has been developed that has a 38.4% higher density and 65.8% higher light yield than the accepted standard scintillation material for routine gamma-ray spectroscopy, NaI(Tl). This is particularly valuable in PGNA explosives measurements where detection relies on the identification of a 10.8 MeV gamma ray from thermal neutron capture on nitrogen. If LaBr₃(Ce) detectors are to be considered a viable option in an explosive detection application, their response to the high-energy nitrogen gamma rays must be determined.

Idaho National Laboratory conducted a set of experiments to determine whether identification times for explosives can be significantly reduced by the use of a LaBr₃(Ce) detector. PGNA spectra were taken on different explosive simulants using different neutron sources, ²⁵²Cf and a Thermo-Electron P385 deuterium-deuterium neutron generator, and three different detector types, LaBr₃(Ce), NaI(Tl), and HPGe to determine how identification times varied for each experimental setup.

Results will be presented comparing the explosives minimum detection times required for all three detector types.

MON-NP01-1

#463 - Invited Talk - Monday 1:00 PM - Trinity Central

Recent activities of RIKEN RIBF (RI Beam Factory)

Hideyuki Sakai
RIKEN Nishina Center, RIKEN, 2-1, Hirosawa, Wako Saitama 351-0198, Japan

The RIKEN RIBF (RI Beam Factory) is an accelerator complex providing a wide range of light- to heavy-ion beams with several tens to 350 MeV/u in energy. It is equipped with the projectile-fragment separator BigRIPS, zero degree spectrometer(ZD) for analysis of reaction products, high-resolution spectrometer SHARAQ, and large solid angle superconducting spectrometer SAMURAI. Those instruments are used to study various properties of nuclei far from the stability.

To realize electron scattering off short-lived unstable nuclei, the SCRIT (Self Confining RI Target) facility is constructed and being commissioned. It is installed at an electron storage ring for Synchrotron radiation coupled with a recetrack microtron accelerator (150MeV) and ISOL in RIBF.

In this talk, I will present some highlights of recent results and introduce new instruments, SAMURAI, SCRIT etc.

High Current H_2^+ Cyclotrons for Neutrino Physics: the IsoDAR and DAE δ ALUS Projects

Jose R Alonso, for the DAE δ ALUS Collaboration

Physics Department, Massachusetts Institute of Technology, 77 Massachusetts Avenue, 26-537, Cambridge MA 02139, United States

A new concept for compact neutrino sources is being developed with INFN-LNS Catania (Calabretta), using high-current cyclotrons accelerating H_2^+ ions to 800 MeV/amu. Designs provide currents a factor of 5 to 10 higher than existing cyclotrons: H_2^+ offers space-charge advantages over protons (and provides two protons for every charge), and stripping provides efficient extraction without need for clean turn separation.

800 MeV protons with peak power of 6 MW produce pions in a low-Z target; π^- are captured in high-Z blankets while π^+ undergo neutrino-producing decays. The resulting neutrino spectrum has negligible intrinsic electron antineutrinos. The DAE δ ALUS experiment complements planned Long Baseline experiments that use large (100 kiloton-scale) detectors with high hydrogen content (water Cherenkov or liquid scintillator) by detecting, via inverse beta decay, the appearance of electron antineutrinos oscillating from muon antineutrinos emerging from the target. While each experiment provides a good measurement of CP violation, running both experiments in the same detector (cancelling systematic errors) provides a great increase in measurement sensitivity as the strengths of each technique complement the weaknesses of the other.

The main cyclotron, a superconducting ring cyclotron similar in size to the SRC at RIKEN, is injected by a 60 MeV/amu cyclotron. This injector can be used in stand-alone mode for producing large fluxes of electron antineutrinos from ^8Li decay produced from $p+^9\text{Be}$ reactions, enhanced by surrounding the beryllium target with a lithium-7 blanket to use the copious neutrons produced in the primary reaction. IsoDAR (Isotope Decay at Rest) will use this configuration, with the target placed a few meters from a kiloton-scale detector for a high-sensitivity sterile-neutrino search.

This staged approach, with compelling physics programs for both energy ranges, allows for progressive development of the new cyclotron technology in a phased manner with realistic goals at each step.

An Update on Notre Dame's New Accelerator Facility

Edward Stech, Manoel Couder, Joachim Goerres, Daniel Robertson, Michael Wiescher

Department of Physics, University of Notre Dame, 225 Nieuwland Science Hall, Notre Dame Indiana 46556, United States

During early 2012, a new 5MV single ended pelletron was installed in the newly expanded Nuclear Science Laboratory at the University of Notre Dame. With its ECR source, this machine provides the beams to the St. George recoil mass separator which was installed in early 2011. The vertical accelerator replaced the aging KN accelerator and required the construction of a new tower within the existing laboratory. Together, this system is perfectly suited for the measurements of alpha radiative capture reactions in inverse kinematics. In addition, the 5U can also deliver proton and alpha beams to other beamlines. A summary of the design goals and objectives as well as the latest results will be presented.

TRIUMF Rare Isotope Beam Program: Developments and the ARIEL Project

Yuri Bylinski

Accelerator Division, TRIUMF, 4004 Wesbrook Mall, Vancouver British Columbia B6T2A3, Canada

TRIUMF is Canada's national laboratory for Nuclear and Particle Physics. In this talk I will review recent highlights and near-term developments of ISAC, TRIUMF's Rare Isotope Beam (RIB) facility. TRIUMF has recently embarked on the construction of ARIEL, the Advanced Rare Isotope Laboratory, with the goal to ultimately triple the current RIB capability. I will present an overview of the ARIEL project and status of design and construction activities.

Establishment of an Accelerator Based Research, Education and Services Facility at the Fayetteville State University

Daryush ILA, Robert Lee Zimmerman

Department of Chemistry and Physics, Fayetteville State University, 1200 Murchison Rd, Fayetteville NC 28301-4297, United States

Fayetteville State University (FSU) a constituent of University of North Carolina (UNC) have initiated the establishment of a Research and Development Center of Excellence (RDCE), centered around a 3MV tandem accelerator, Ion Beam Assisted Deposition, a large number of other major instrumentation, in addition to sensors and thermoelectric device prototyping capabilities while building relationship with local government and industries for joint research and tech-transfer. This research and development center of excellence is being established to function as one of the unique materials and devices prototyping capabilities in the region with ability to financially self sustain. The first three beam-lines of the accelerator facility will be dedicated to Rutherford Backscattering Spectrometry (RBS), Ion-Implantation and NRA, while the plans are underway to secure high precision hydrogen profiling beam-line, as well as a beam writing capabilities. The dedicated building for RDCE is designed to host a 100 attendee in an amphitheater structure and four small parallel session meeting rooms, a Board room, and a dozen offices and a large number of interconnect labs. Presently the initial joint efforts with local government and industries includes: Thermoelectric Device and Sensor Prototyping, materials for extreme environment prototyping, as well as capabilities complementing the Forensic, Micro-Probe, and Electron Microscopic capabilities of the FSU.

Irradiation studies of ferrofluidic feedthroughs for FRIB under fast neutrons, gamma and protons

Sandrina Fernandes¹, Nickolas Simos², Wolfgang Mittig^{1,3}, Frederique Pellemoine¹, Mikhail Avilov¹,
Leonard Mausner², Joseph O'Connor², Reg Ronningen¹, Mike Schein¹

⁽¹⁾*Facility for Rare Isotope Beams FRIB, Michigan State University, 1 Cyclotron, East Lansing MI 48824-1321, United States*

⁽²⁾*Brookhaven National Laboratory, Upton NY 11973, United States*

⁽³⁾*National Superconducting Cyclotron Laboratory NSCL, Michigan State University, 1 Cyclotron, East Lansing MI 48824-1321, United States*

Ferrofluid sealed rotary feedthroughs have been chosen for Facility for Rare Isotope Beams (FRIB) production target and beam dump systems. To study the limits of using these ferrofluid feedthroughs in the high radiation environment of FRIB, three units were irradiated at Brookhaven Linac Isotope Producer (BLIP). The test beam consisted primarily of mixed fast neutrons, protons, gamma rays and electrons with an average absorbed dose of 0.2, 2 and 20 MGy. These radiation types, intensity and energy are close to the ones expected under FRIB conditions in the target and beam dump systems area. Most of the irradiation studies found in the literature for typical ferrofluid feedthrough materials components are for one or two types of radiation and limited to thermal neutrons. During the post-irradiation analysis, we measured the seal vacuum tightness and friction torque under static and dynamic rotational conditions. It was found that the seal vacuum tightness was kept for all doses and that the friction torque of the ferrofluid feedthroughs irradiated with a radiation dose of 0.2 MGy and 2 MGy increases slightly in comparison to a non-irradiated ferrofluid feedthrough of the same model for FRIB typical operation rotational speed of 3000-5000 RPM. However both ferrofluid feedthroughs remained in the operational domain, whereas the one irradiated with 20 MGy was irreparably damaged. The seal vacuum tightness was kept for all doses. These results will be used in the design of the FRIB production target and the primary beam dump to determine the radiation shielding requirements.

Nuclear structure near the N=50 shell closure

Meredith Howard¹, J. Cizewski¹, B. Manning¹, E. Merino¹, P. D. O'Malley¹, D. Bazin², Z. Chajecki², D. Coupland^{2,3}, T. K. Ghosh⁴, R. Hodges^{2,3}, J. Lee^{2,3}, W. Lynch^{2,3}, A. Sanetullaev^{2,3}, M. B. Tsang², J. Winkelbauer^{2,3}, M. Youngs^{2,3}, R. R.C. Clement⁵, D. W. Bardayan^{6,7}, K. Y. Chae⁶, D. Shapira⁶, S. H. Ahn⁷, K. Schmitt⁷, M. A. Famiano⁸

⁽¹⁾Department of Physics and Astronomy, Rutgers University, Piscataway NJ 08854, United States

⁽²⁾National Superconducting Cyclotron Laboratory, Michigan State University, East Lansing MI 48824, United States

⁽³⁾Department of Physics and Astronomy, Michigan State University, East Lansing MI 48824, United States

⁽⁴⁾Variable Energy Cyclotron Centre, 1/AF, Bidhannagar Kolkata 700064, India

⁽⁵⁾Los Alamos National Laboratory, Los Alamos NM 87545, United States

⁽⁶⁾Physics Department, Oak Ridge National Laboratory, Oak Ridge TN 37831, United States

⁽⁷⁾Department of Physics and Astronomy, University of Tennessee, Knoxville TN 37831, United States

⁽⁸⁾Department of Physics, Western Michigan University, Kalamazoo MI, United States

While nuclear astrophysicists eagerly await availability of new beams of increased neutron richness, nuclear structure data in hand near the N=50 shell closure closer to the valley of stability offer immediate tests of the nuclear theory used as input to r-process models. Nuclear experiments will never be able to measure all of the thousands of quantities astrophysics need. As the majority of nuclear quantities fed to astrophysics models come from theory rather than measurement, the immediate goal is to both constrain and verify theoretical calculations. The $^{84}\text{Se}(p,d)^{83}\text{Se}$ and $^{86}\text{Kr}(p,d)^{85}\text{Kr}$ reactions at 45 MeV/u in inverse kinematics were measured at the National Superconducting Cyclotron Laboratory, using the charged particle detector HiRA and the S800 spectrometer.

This experiment is the first to use the full complement of 20 HiRA telescopes. The primary goal is to extract angular momentum quantum numbers and neutron spectroscopic factors for the ground and first excited states of ^{83}Se . Details of the experiment and preliminary analysis results will be discussed. (This work is supported in part by the U.S. National Science Foundation and Department of Energy.)

Probing Neutron Capture Off Stability

Aaron Couture², Matthew Devlin², Toshihiko Kawano¹, Hye Young Lee², John M. O'Donnell², Patrick Talou¹

⁽¹⁾T-2, Los Alamos National Laboratory, PO Box 1663, Los Alamos NM 87545, United States

⁽²⁾LANSCE-NS, Los Alamos National Laboratory, PO Box 1663, Los Alamos NM 87545, United States

For over fifty years, we have known that the heavy elements were created through neutron induced reactions in stellar environments. Abundances of the elements indicated that there were at least two classes of environments. The first environment takes place on or near the valley of stability. Because of the long time scales for the nucleosynthesis, it is referred to as the "slow" neutron capture process, or s-process. In contrast, the second process needs to take place on very neutron-rich, unstable nuclei in order to explain the observed abundances. This process on nuclei far from stability is referred to as the "rapid" neutron capture process, or r-process, as it is predicted to take place very quickly.

At present, our understanding of the heavy elements is dominated by what we understand of the s-process. For the r-process, almost all of the isotopes of interest are unstable. Our experimental knowledge of the nuclear physics is typically limited to nuclear masses on a subset of the isotopes of interest. Several thousand nuclei are expected to participate in the nucleosynthesis, making for vast reaction networks. The reaction rates are almost entirely determined from nuclear theory, **but we have not yet been able to test the accuracy of the underlying nuclear theory on nuclei so far from stability.**

The ATLAS facility at Argonne has just installed the CARIBU ion source to produce high intensity beams of select unstable isotopes---we can start to make indirect measurements today on some unstable isotopes. I will discuss a new LANL LDRD-led effort to couple a gamma detection array Apollo to the Helical Orbit Spectrometer (HELIOS) in order to extract information about the gamma-cascades following neutron transfer with radioactive ion beams. These measurements will provide constraints on the underlying nuclear theory used to predict neutron capture rates for the r-process.

Coupling Gammasphere and ORRUBA

A. Ratkiewicz¹, S. D. Pain², J. A. Cizewski¹, D. W. Bardayan², J. C. Blackmon³, K. A. Chipps⁴, S. Hardy^{1,5},
M. E. Howard¹, K. L. Jones⁶, R. L. Kozub⁷, C. J. Lister⁸, B. Manning¹, M. Matos³, W. A. Peters⁹, D. Seweryniak⁸,
C. Shand^{1,5}

⁽¹⁾*Department of Physics and Astronomy, Rutgers University, New Brunswick NJ 08903, United States*

⁽²⁾*Physics Division, Oak Ridge National Laboratory, Oak Ridge TN 37831, United States*

⁽³⁾*Department of Physics and Astronomy, Louisiana State University, Baton Rouge LA 70803, United States*

⁽⁴⁾*Department of Physics, Colorado School of Mines, Golden CO 80401, United States*

⁽⁵⁾*Department of Physics, University of Surrey, Guildford Surrey GU2 7XH, United Kingdom*

⁽⁶⁾*Department of Physics and Astronomy, University of Tennessee, Knoxville TN 37996, United States*

⁽⁷⁾*Physics Department, Tennessee Technological University, Cookeville TN 38505, United States*

⁽⁸⁾*Physics Division, Argonne National Laboratory, Argonne IL 60439, United States*

⁽⁹⁾*Oak Ridge Associated Universities, Oak Ridge TN 37830, United States*

The coincident detection of gamma rays and particles facilitates high-resolution studies of single-particle states in exotic nuclei. While the energy resolution obtainable from measuring charged particles alone is strongly constrained by target thickness effects, the energy resolution of gamma rays emitted in-flight is relatively unaffected by typical target thicknesses, allowing thicker targets to be employed with relatively weak beam intensities. Additionally, the de-excitation gamma rays emitted from excited states populated by a nuclear reaction carry important structure information, information which is lost in a particle-only measurement.

The ideal detector system for such studies combines a high-efficiency, high-resolution gamma-ray detector and a particle detector with good angular resolution, high energy resolution, and covering a large solid angle. Such a detector system can be used to study many interesting physics cases, e.g. (via neutron transfer reactions) the fragmentation of single-particle strength and the onset of deformation away from shell closures, and the determination of excited state energies with smaller systematic uncertainties than is possible in a particle-only measurement. Applications of this detector system include the study of surrogate reactions for neutron capture, collective excitations via inelastic scattering, of pickup reactions (e.g. (d,t)), and stripping reactions, such as (d,p).

The high gamma-ray detection efficiency and high energy resolution of Gammasphere make it an excellent gamma-ray detector, while its large internal geometry allows it to be coupled to the Oak Ridge Rutgers Barrel Array (ORRUBA) particle detector without compromising the large solid angle coverage and high angular resolution of this device. We report on the progress of a project to couple these two arrays in order to make measurements with beams from CARIBU at ATLAS.

This work is supported in part by the US Department of Energy Office of Nuclear Physics, the National Science Foundation, and the National Nuclear Security Administration.

Nuclear reaction rates for the study of X-ray bursts

Wanpeng Tan, Sergio Almaraz-Calderon, Ani Aprahamian, Michael Wiescher

Department of Physics, University of Notre Dame, 225 Nieuwland Science Hall, Notre Dame IN 46556, United States

Neutron stars in close binary star systems often accrete matter from their companion star. Thermonuclear ignition of the accreted material on the surface of the neutron star leads to a thermonuclear explosion which is observed as an X-ray burst occurring periodically. In this talk, I will discuss recent experimental progress on the underlying nuclear reactions that power the X-ray bursts, in particular, the efforts at Notre Dame. Recent measurements on alpha-induced nuclear reactions in the hot CNO cycles and on the waiting points of the rp-process will be presented. Experimental results and their astrophysical implications will be discussed.

Recent results on intermediate-energy nucleon knockout reactionsKathrin Wimmer*NSCL, Michigan State University, 640 S. Shaw Lane, East Lansing MI 48824, United States*

The explanation of the magic numbers for nuclei in the valley of stability was one of the milestones in the understanding of nuclear structure. However, in recent years, several theoretical and experimental investigations found evidence that these magic numbers change when going away from stability towards more exotic nuclei. Nucleon knockout reactions using fast rare isotope beams are a well suited tool to study single-particle properties of exotic nuclei and the evolution of nuclear shell structure towards the drip-lines. Recently, a series of experiments has been performed at the National Superconducting Cyclotron Laboratory at Michigan State University in order to study reaction mechanism in nucleon knockout reactions. Such experiments are key for validation of the theoretical description of the reaction mechanism and use for quantitative spectroscopy of very exotic nuclei. In this talk I will present recent results from experiments at the interplay of nuclear structure and reactions performed at the NSCL.

ION BEAM-INDUCED BIOFUNCTIONAL SURFACESGiovanni Marletta¹, Gabriela Ciapetti²⁽¹⁾*Laboratory for Molecular Surfaces and Nanotechnology (LAMSUN) - Dept. of Chemical Sciences, University of Catania and CSGL, Viale A.Doria 6, Catania I-95125, Italy*⁽²⁾*Laboratory of Orthopedic Physiopathology and Regenerative Medicine, Istituto Ortopedico Rizzoli, Via di Barbiano 1/10, Bologna 50001, Italy*

Surface modifications by ion beams have been shown to be an election tool to increase the biocompatibility of many materials, enhancing cell adhesion, proliferation and differentiation, but also inducing peculiar aggregation modes of biomolecules relevant to the structuring of biological tissues. This lecture is aimed to discuss the basic factors driving the cell response to ion irradiated surfaces. Relevant case studies will be discussed in details, focusing the role of the modification of the chemical structure, nano-morphology, surface free energy, density of spins, etc., in view of the changes observed in the behavior of cells seeded onto ion beam modified polymeric surfaces.

A particular attention will be devoted to the discussion and analysis of the processes of irradiated surfaces in modifying the protein and gene expression of interacting cells. Thus, for instance, the behavior of mesenchimal cells (MSC) obtained from patients undergoing routine hip replacement surgery, will be discussed in view of their response to seeding onto untreated PCL and low-energy He⁺-irradiated polymer films, showing that irradiation-induced modification enhances the adhesion and differentiation. Also, the enhancement of osteoblast activity onto ion irradiated surfaces will be discussed in view of the modification of integrin expression. Finally, the relative weight of chemical structure and electric domains at the irradiated surfaces will be discussed in view of the behavior of pericellular matrix on irradiated surfaces. The possible transduction mechanisms relaying the modified physico-chemical features of surfaces and the cell behavior will be discussed.

Ion Implanted, Radical-rich Surfaces for the Rapid Covalent Immobilization of Active Biomolecules

Stacey L. Hirsh¹, Marcela MM Bilek¹, Daniel V Bax², Alexey Kondyurin¹, Elena Kosobrodova¹, Kostadin Tsoutas¹, Clara TH Tran¹, Anna Waterhouse², Youngbai Yin¹, Neil J Nosworthy¹, David R McKenzie¹, Christobal G dos Remedios⁴, Martin KC Ng³, Anthony S Weiss²

⁽¹⁾*Applied and Plasma Physics, University of Sydney, Rm 227, School of Physics A28, Sydney NSW 2006, Australia*

⁽²⁾*School of Molecular Biosciences, University of Sydney, G08, Sydney NSW 2006, Australia*

⁽³⁾*School of Medical Sciences, University of Sydney, F13, Sydney NSW 2006, Australia*

⁽⁴⁾*Heart Research Institute, Sydney NSW 2042, Australia*

Recent work has revealed that radicals embedded in carbon rich organic surface layers by energetic ion bombardment can covalently immobilize bioactive proteins*. The ability to strongly attach proteins to surfaces whilst retaining their biological activity underpins a host of biotechnologies, such as biosensors for medical and environmental applications and protein or antibody diagnostic arrays for early disease detection. This new approach delivers the strength and stability of covalent coupling without the need for time-consuming, wet chemical processes. The immobilization occurs in a single step directly from solution and the hydrophilic nature of the surface ensures that the bioactive 3D shapes of the protein molecules are not disturbed.

This presentation will describe how energetic ion treatments conferring protein immobilization capability can be applied to any underlying material, which also makes it possible to achieve covalent protein immobilization whilst maintaining the physical properties (including mechanical and electrical) of an underlying material. A kinetic theory model is presented and compared to experimental results to describe the covalent protein immobilization process **via** the mobility of free-radicals in a reservoir generated by the ion implantation process. We show that covalent protein immobilization using this method obtains high covalent coverage within 1 minute of incubation. This rapid covalent attachment process, which is non-specific with respect to amino acid side-chains, can also be used to control the composition of the adsorbed protein layer from a mixture. Preliminary applications of this technology to direct cell growth, to create biosensors and protein microarrays, and to engineer the surfaces of implantable biodevices will be reviewed.

* **Proc. Nat. Acad. Sci** **108**(35) pp.14405-14410 (2011)

Plasma Treatment on 3D Cell Culture Environment

Emel Sokullu Urkac, Umut Atakan Gurkan, Utkan Demirci

Health Science & Technology HST, Harvard Medical School - M.I.T., 65 Landsdowne St. Cambridge, Boston MA 02139, United States

One of the major challenges of tissue engineering is to design a matrix that is capable of mimicking the natural properties of extracellular environment while providing a temporary scaffold for tissue regeneration. The current focus in tissue engineering has intended towards the design of deliberately 'bioactive' materials that integrate with biological molecules or cells and regenerate tissues in 3D environment. Literature reports support the fact that changes in scaffold surface chemistry and topography alter cellular activity.

Surface modification of biomaterials with Plasma Treatment is highly popular technique in literature. By plasma treatment we can introduce different chemical groups to the polymer surfaces and thus make surfaces either hydrophilic or hydrophobic; we can also change surface crystallinity, surface energy, roughness and morphology. All these factors thus even play important or synergistic role in surface interactions. However in literature plasma treatment effects on 3D surfaces is still not evaluated although it is very important in order to mimicking extracellular environment especially tissue regeneration studies involving co-culture experiments.

Here in this work we evaluated plasma treatment effects on 3D Methacrylated hydrogels (GELMA) which are encapsulating 3T3 and HUVEC cells. Resulting materials are promoting cell attachments in 3D applications and also providing appropriate environments for co-culture studies.

Precise mold fabrication using proton beam writing for Cell and DNA manipulation

Jeroen Anton van Kan

Physics, CIBA, 2 Science Dr 3, Singapore 117542, Singapore

Proton beam writing (PBW) is a new direct write 3D nano lithographic technique which has been developed at the Centre for Ion Beam CIBA, in the Physics Department of the National University of Singapore. PBW employs a focused MeV proton beam which is scanned in a predetermined pattern over a resist, which is subsequently chemically developed. PBW exhibits low proximity effects coupled with the straight trajectory and high penetration of the proton beam enables the production of high aspect ratio, high density 3D micro and nano structures, allowing surface structuring down to the sub 100 nm level. In this review we present the versatility of the proton beam fabricated master molds for applications in tissue engineering and nanofluidics study of single DNA molecules.

In tissue engineering cells are grown on PMMA substrates that have been produced via PBW. Aligned and elongated cells are observed on well defined ridges and grooves. The underlying mechanism responsible of this cellular behaviour is assumed to be induced by the mechanical restrictions imposed by the topographic features on cellular migration, cell adhesion and concomitant changes in the cytoskeleton. The use of topographical stimuli to regulate cell function is an area of high potential in tissue engineering.

Master molds obtained via PBW are used to produce PDMS nanofluidic lab-on-chip devices through nano imprint lithography. The master molds can be used many times to replicate nanofluidic devices capable of detecting single DNA molecules. This method reduces fabrication and packaging complexity, allowing end users to fabricate lab on a chip devices through simple PDMS casting. The extensions of YOYO-1 stained T4 bacteriophage and lambda-phage DNA inside these PDMS nano-channels have been experimentally investigated using fluorescence microscopy.

The authors acknowledge the support from A-Star (R-144-000-261-305), MOE Singapore (R-144-000-265-112) and the US Air Force.

Ion Implantation on Electrospun Fabricated Poly (L-lactide/Caprolactone) (PLC) Nanofibers for Cell Proliferation in Tissue Scaffolds

Secil Kurtalan¹, Mustafa Ahmet Oztarhan², Emel Sokullu Urkac³, Taner Dagci⁴

⁽¹⁾Biotechnology, Ege University, Surface Modification Laboratory, Ege University Campus, Bornova, Izmir 35100, Turkey

⁽²⁾Bioengineering, Ege University, Bioengineering Department, Ege University Campus, Bornova, Izmir 35100, Turkey

⁽³⁾Bioengineering, Ege University, Surface Modification Laboratory, Ege University Campus, Bornova, Izmir 35100, Turkey

⁽⁴⁾Medical Faculty, Ege University, Medical Faculty, Ege University Campus, Bornova, Izmir 35100, Turkey

The use of polymeric materials produced by the electrospinning technique has gained considerable interest for tissue engineering applications. It was found by many researchers that the interaction of cells and material's surface is the most important factor affecting cell adhesion and proliferation. Ion beam modification of material's surfaces is an alternative technique for improving the surface properties of polymeric materials for tissue engineering applications.

In an attempt for enhancing cell adhesion and proliferation, Poly (L-lactide/Caprolactone) 70/30 (PLC) nanofibrous scaffolds were fabricated by an electrospinning process and implanted by Au and Au+O ions. In the first part of this work, biodegradable PLC polymer was used for the fabrication of nanofibers. PLC polymer was dissolved in chloroform and 8%, 10% and 12% (w/v, g/mL) PLC-Chloroform solutions were prepared. Nanofibers were produced by electrospinning with a voltage of 20kV and flow rate of 1.5 mL/h, and deposited on a drum which was rotating with 1500 rpm and at a distance 12 cm from the spinneret tip for aligned nanofiber production. In the second part of this work, PLC nanofibers were implanted with Au and Au+O ions with fluencies of 1×10^{14} , 1×10^{15} , 1×10^{16} ion/cm² and extraction voltages of 20kV, 30kV.

Finally, cell culture tests were performed on Au and Au+O implanted PLC electrospun samples and the results compared with unimplanted ones. Samples were incubated with neuroblastoma cells for 1, 4 and 7 days in a culture medium at 37 °C, and viewed with Scanning Electron Microscope (SEM) micrographs. Also, for identifying the elemental composition, unimplanted and implanted surfaces were analyzed with Energy Dispersive X-ray (EDX). The wettability of implanted and unimplanted surfaces were evaluated by contact angle tests. Surface compositions of PLC nanofibrous, Au and Au+O implanted and unimplanted samples were analyzed by X-ray photoelectron spectroscopy (XPS) for surface chemical characterisation.

Cell Attachment Study of Zr+O Hybrid Ion Implanted Dental Implants by MEVVA Ion Implantation

Ali Erdem Turanli¹, Mustafa Ahmet Oztarhan², Emel Sokullu Urkac¹, Taner Dagci³, Orhan Öztürk⁴

⁽¹⁾Bioengineering, Ege University, Surface Modification Laboratory, Ege University Campus, Bornova, Izmir 35100, Turkey

⁽²⁾Bioengineering, Ege University, Bioengineering Department, Ege University Campus, Bornova, Izmir 35100, Turkey

⁽³⁾Medical Faculty, Ege University, Medical Faculty, Ege University Campus, Bornova, Izmir 35100, Turkey

⁽⁴⁾Physics, Izmir Institute of Technology, Izmir Institute of Technology, Urla, Izmir 35430, Turkey

Titanium and Titanium alloys have been used extensively as implant material because of their remarkable mechanical and chemical properties such as high strength-to-weight ratio and high corrosion resistance and biocompatibility. The biocompatibility of a biomaterial is highly related to the behavior of the cells in contact and in particular the cell adhesion to its surface. The surface characteristics of a material, including its topography and physical and chemical properties at a micro and nano-scale, play an important role in osteoblast cell adhesion on biomaterials. Ion implantation technique was identified as a good candidate for improving the osseointegration properties of the implants in patient's bone.

In this work, the effects of Zr+O hybrid ion implanted cp Ti (grade 4) dental implant samples on cell attachment and cell growth were studied. It was aimed to gain bioactive and biocompatible surfaces to contribute to duration of treatment of patients who have low quantity and low quality alveolar bone or are osteoporosis. CpTi (grade-4) dental implants samples with 6 mm diameter and 3 mm thick were implanted by Zr + O ions simultaneously with the extraction voltage of 50kV and fluency of 1×10^{17} ions/cm² to see cell viability. Ti samples were implanted in home built MEVVA Ion Implantation System. Unimplanted and implanted surfaces were analyzed with Energy Dispersive X-ray (EDX) to identify the elemental composition. Surface topography of the samples was studied by AFM and also the wettability of implanted and unimplanted surfaces were evaluated by contact angle measurements. Cell culture tests were performed on Zr+O implanted and unimplanted samples. Samples are incubated with osteoblast cells (SAOS-2) for 12 and 24 hours in culture medium at 37 °C and visualized with Scanning Electron Microscope (SEM) and the results are presented.

Nanofabrication with the helium ion microscope

Bipin Singh

Carl Zeiss NTS, One Corporation Way, Peabody MA 01960, United States

Invented for high resolution imaging, the helium ion microscope has emerged as a class leading FIB tool that is capable of making structures that are not possible to make using traditional gallium FIB. While making sub-10 nanometer structures is challenging for other technologies, this is the core strength of the helium ion microscope. Characteristics and features that make the helium ion microscope such a powerful nanofabrication tool will be discussed. Examples from research groups that have used the helium ion microscope for nanofabrication will be presented.

Can one make devices with a helium ion microscope?

Paul F.A. Alkemade

Kavli Institute of Nanoscience, Delft University of Technology, Lorentzweg 1, Delft 2628 CJ, Netherlands

The recent invention of the helium ion microscope stimulated several research groups to use the microscope's subnanometer beam probe for high-resolution nanofabrication. Four routes for have been explored so far: helium ion beam milling, beam-induced chemical processing, lithography, and materials modification. First results were promising, e.g. in lithography studies simple patterns were made in resist material and -as compared to electron beam lithography- higher sensitivity, similar resolution, and much lower proximity effects were obtained. However, coupling to other components and integration in actual devices are not trivial and require careful design, optimization and testing.

This presentation will summarize the recent progress of device fabrication with a focused helium ion beam. Examples of all four explored routes will be given. Emphasis is on those studies in which physical phenomena have been observed under unique conditions.

Bit-Patterned Magnetic Arrays for Data Storage Applications

Dmitri Litvinov¹, Long Chang¹, Paul Ruchhoeft¹, Sakhrat Khizroev²

⁽¹⁾*Electrical & Computer Engineering, University of Houston, N308 Engineering Building 1, Houston TX 77204, United States*

⁽²⁾*Electrical & Computer Engineering, Florida International University, 10555 W. Flagler Street, Miami FL 33174, United States*

Conventional magnetic recording systems based on longitudinal magnetic recording are rapidly approaching their superparamagnetic limit. A shift to perpendicular recording is taking place due to its superiority with respect to data thermal stability. Yet, perpendicular recording will face its own superparamagnetic limit, which calls for further innovation. Magnetic recording based on patterned media, as compared to continuous media used in today's hard drives, allows to further extend areal bit densities due to a significant increase of the thermal activation volume.

In this work, we present recording physics, design considerations, and fabrication of bit-patterned magnetic medium for next generation data storage systems. (Co/Pd)_N magnetic multilayers are evaluated as candidates for bit-patterned medium recording layer materials for their high and easily tunable magnetic anisotropy. Optimized patterned multilayers used in this study had coercivities in excess of 12-14kOe. Bit patterning was accomplished using ion-beam proximity printing, a high-throughput direct write lithography where a large array of ion beamlets shaped by a stencil mask is used to write an arbitrary device pattern. It is found that the nature of magnetization reversal strongly depends on bit edge imperfections and is likely to contribute to switching field distribution.

This presentation will detail the finding on the design considerations, fabrication, recording physics, and characterization of bit-patterned media prototypes fabricated using ion-beam proximity lithography. Optimized patterned multilayers used in this study had coercivities in excess of 12-14kOe, suitable to for recording densities far in excess of 1Tbit/in². It is found that the nature of magnetization reversal strongly depends on bit edge imperfections and the texturing of the underlying multilayers and is likely to contribute to switching field distribution.

IRRADIATED SURFACES AS PLATFORMS FOR SMART DEVICES

Giovanni Marletta

Laboratory for Molecular Surfaces and Nanotechnology (LAMSun) - Dept. of Chemical Sciences, University of CATANIA, Viale A.Doria 6, Catania 95129, Italy

Particle beam treatments have been shown having a huge impact in prompting innovative device technologies in a variety of fields, due to the possibility of inducing controlled properties modification of materials. This includes both the properties depending on the local chemical structure, as well as those depending on the structure and morphology. Thus, in a somewhat traditional way, particle beam treatments have been widely employed as one of the election tools to tailoring the induction/change of optical, magnetic and electrical properties, adhesion and wearing behavior, chemical reactivity, biocompatibility, molecular stitching at surfaces, etc. All these treatments were essentially aimed to produce the active or passive part of functional devices. In recent years, the research effort has been progressively shifted towards the integration of different functions in a single micrometric platform. Particle beams have an intrinsic, tremendous potentiality in this context, due to the inherently nanometric scale of the primary particle-materials events. In fact, tool based on highly focused beam, as FIB apparatus and He(+)-microscope, have been developed and integrated in frontier technological processes to produce highly integrated devices.

The present Lecture wish to address the opportunities provided by particle beams in building highly integrated devices. Examples spanning from the simple integration of different inorganic material domains to the integration of organic-inorganic and biological functions will be discussed, in view of the parameters relevant to enable effective integration.

MON-PS01-1

#460 - Plenary Talk - Monday 8:30 AM - Pecos I & II

Current Status of Inertial Confinement Fusion Research

Jeffrey P Quintenz, on behalf of The National Inertial Confinement Fusion Team
National Nuclear Security Administration, Washington DC, United States

The Inertial Confinement Fusion (ICF) program has made significant progress toward creating the extreme conditions necessary to produce fusion ignition at the National Ignition Facility (NIF). In addition, the ICF program has developed other unique High Energy Density (HED) facilities to explore alternate paths to ignition. Facilities such as the NIF at Lawrence Livermore National Laboratory, the Omega laser at the Laboratory for Laser Energetics, and the Z machine at Sandia National Laboratories are capable of producing environments that, in addition to laboratory fusion, are of relevance to a wide range of topics in fundamental science. This presentation will discuss recent progress made in ICF and the challenges remaining and will describe some other applications of these powerful and energetic HED facilities.

MON-PS02-1

#79 - Plenary Talk - Monday 9:15 AM - Pecos I & II

PIXE and XRF analysis on the Mars Science Laboratory mission

John L Campbell
Physics, University of Guelph, 50 Stone Road East, Guelph Ontario N1G 2W1, Canada

MSL's primary goal is to explore and quantitatively assess Mount Sharp in the Gale Crater on Mars as a potential habitat for life, past or present. Among its many instruments, the Curiosity rover has a chemistry lab to study organic detritus and a neutron spectrometer to look for hydrogen-bearing materials in the ground. The Canadian alpha-particle X-ray spectrometer is mounted on an arm, and performs in-situ elemental analysis via PIXE and XRF, effectively combining a positive ion accelerator and a synchrotron in a soup-can sized device.

This talk will detail the calibration of APXS and the resultant understanding of the dependence of the elemental analysis results on the mineral make-up of the sample. APXS will work closely with several other MSL instruments responsible for visual imaging, X-ray diffraction and laser-induced breakdown analysis, in order to seek elemental and mineralogical evidence for past aqueous processes that would indicate a habitable phase in the Martian history.

MaRIE, an experimental facility concept for revolutionizing materials in extreme environmentsJohn L Sarrao*LANL, MS A121, Los Alamos NM 87545, United States*

MaRIE, for Matter-Radiation Interactions in Extremes, is Los Alamos National Laboratory's facility concept for addressing decadal challenges in materials, especially in extreme environments, through a focus on predicting and controlling materials microstructure. MaRIE will be an international user facility and will enable unprecedented in-situ, transient measurements of "real" mesoscale materials in relevant extremes, especially dynamic loading and irradiation extremes. Concurrent advances in multi-scale modeling and computational resources hold great promise for rapid progress toward these goals. To achieve this vision, MaRIE will construct a high-energy, low-average-intensity source of x-ray photons (pre-conceptually, a 50 keV XFEL) and couple it to an existing high intensity proton linear accelerator (800 MeV at 1 MW) through three measurement halls: the Multi-Probe Diagnostic Hall (MPDH), the Fission-Fusion Materials Facility (F³), and the Making, Measuring and Modeling Materials Facility (M4). In this presentation we will discuss both the science questions that motivate such a facility and our vision for realizing it, including the essential role of advanced accelerators.

Deuterium retention at displacement damage in tungstenWilliam R Wampler*Radiation-Solid Interactions, Sandia National Laboratories, MS 1056, Albuquerque NM 87185, United States*

Displacement damage from fusion neutrons in plasma-facing materials may increase tritium inventory in tritium-fueled fusion devices such as ITER. Experiments were conducted to quantify this effect in tungsten, in which damage was produced by irradiation with 12 MeV silicon ions. Damaged samples were exposed to high flux deuterium (D) plasma in the PISCES linear plasma device at UCSD. Depth profiles of retained D were measured by ³He nuclear reaction analysis. The effect of damage on D retention was determined by comparing D profiles in adjacent damaged and undamaged regions. D retention is expected to strongly depend on temperature, so experiments were done with the tungsten at various temperatures during exposure to the plasma. The D retention at damage decreased with increasing temperature, notably by nearly two orders of magnitude between 300°C and 400°C. This is the temperature range where vacancies in tungsten become mobile. To determine whether this reduction in D retention was due to defect annealing, a sample was annealed at 500°C after irradiation but prior to D plasma exposure at 220°C. This anneal produced only a modest decrease in D retention. This shows that damage-associated traps are still present after annealing at 500°C, which indicates that factors other than defect annealing influence the temperature dependence of D retention. Here we discuss the influences of precipitation and the binding energy of D to the traps on D retention. Results from experiments and modeling indicate that D retention may be maximum near 300-400°C where binding is still strong and permeation is fast enough for D retention to reach significant depths.

Sandia National Laboratories is a multi-program laboratory managed and operated by Sandia Corporation, a wholly owned subsidiary of Lockheed Martin Corporation, for the U.S. Department of Energy's National Nuclear Security Administration under contract DE-AC04-94AL85000.

Overview of the US-Japan collaborative investigation on tritium behavior in radiation damaged fusion reactor materials

Masashi Shimada¹, Yuji Hatano², Yasuhisa Oya³, Masanori Hara², Guoping Cao⁴, Makoto Kobayashi³, Mihail Sokolov⁵

⁽¹⁾*Fusion Safety Program, Idaho National Laboratory, 2525 N. Fremont Ave., Idaho Falls ID 83415-7113, United States*

⁽²⁾*Hydrogen Isotope Research Center, University of Toyama, Toyama, Japan*

⁽³⁾*Radioscience Research Laboratory, Shizuoka University, Shizuoka, Japan*

⁽⁴⁾*Department of Engineering Physics, University of Wisconsin-Madison, Madison WI, United States*

⁽⁵⁾*Oak Ridge National Laboratory, Oak Ridge TN, United States*

Tritium behavior in fusion reactor materials plays a major role in the material choice for future fusion reactors, because tritium retention and permeation determines in-vessel inventory levels and ex-vessel releases in reactor safety assessments. D-T fusion reactions produce 14.1 MeV neutrons that activate plasma facing components (PFCs) and cause defects in the structural materials of these components. To date, the effect of radiation damage has been mainly simulated using high-energy ion bombardment, which offers the advantage of simulating high damage (>10 dpa) levels in a few days that usually take several years to achieve in a fission reactor without activating materials significantly, allowing us to handle the specimens much more easily than with neutron-irradiation. It, however, does not encompass the full range of effects that must be considered in a practical fusion environment due to short penetration depth, damage gradient, high damage rate, and high PKA energy spectrum of the ion bombardment. In addition, neutrons change the elemental composition via transmutations, and create a high radiation environment inside PFCs, which influence the behavior of hydrogen isotopes in PFCs.

Under the framework of the US-Japan TITAN program, tungsten specimens (99.99 at. % purity from A.L.M.T. Co.) were irradiated by neutron in the High Flux Isotope Reactor (HFIR), ORNL, at 50 and 300°C to 0.025, 0.3, and 1.2 dpa, and the investigation of hydrogen isotope retention in neutron-irradiated tungsten was performed in the INL Tritium Plasma Experiment (TPE), the unique high-flux linear plasma facility that can handle tritium, beryllium and activated materials. This paper will give an overview of this collaborative investigation on tritium behavior in neutron-irradiated tungsten, and discuss the similarities and differences among ion-damaged tungsten and neutron-irradiated tungsten along with the INL Tritium Migration Analysis Program (TMAP) modeling.

Nanoporous Materials Response to Radiation Damage

Engang Fu², Magdalena Caro², Yongqiang Wang², Mike Nastasi¹, Alfredo Caro²

⁽¹⁾*Nebraska Center for Energy Sciences Research, University of Nebraska - Lincoln, 230 Whittier Research Center, 2200 Vine Street, Lincoln NE 68583, United States*

⁽²⁾*Materials Science in Radiation and Dynamics Extremes, Los Alamos National Laboratory (LANL), 38 Bikini Atoll Road, Los Alamos NM 87545, United States*

In a recent paper we showed using computer simulations that length and time scales determine the overall behavior of nanoporous materials under irradiation [1]. These scale lengths are the size of the ligament in the foam compared to the collision cascade size and the characteristic time scale for defect annihilation relative to dose rate. The model defines a window of radiation endurance and predicts conditions for Au nanofoams to be radiation resistance.

Support to the model was provided by 45 keV Ne⁺ ion irradiation of nanoporous gold (np-Au) at room temperature (RT) and 77 K up to a dose of 1.5 dpa at a dose-rate of 0.033 dpa/s. To help further the understanding of defect evolution during irradiation of nanoporous materials, ion beam irradiations of nanoporous Au has been undertaken at the Ion Beam Materials Laboratory (IBML) in Los Alamos National Laboratory (LANL). In this work, we explore the behavior of np-Au under 400 keV Ne⁺ ions at a dose-rate of 0.0052 dpa/s for a total of 1.5 dpa. We discuss the mechanisms that could explain the behavior change under irradiation at two different temperatures; i.e. room temperature (RT) and 77 K. These observations agree with the model predictions and provide further insight on the existence of a window for radiation tolerance.

Work supported by the Laboratory Directed Research and Development Program at Los Alamos National Laboratory.

[1] E. M. Bringa, J. D. Monk, A. Caro, A. Misra, L. Zepeda-Ruiz, M. Duchaineau, F. Abraham, M. Nastasi, S. T. Picraux, Y. Q. Wang, and D. Farkas, "Are Nanoporous Materials Radiation Resistant?", to appear in Nano Letters July (2012). dx.doi.org/10.1021/nl201383u

MON-REP01-4

#250 - Invited Talk - Monday 1:00 PM - West Fork

Isotope exchange experiments in tungsten after ion induced damage

Joseph Barton¹, Yongqiang Wang², Matthew Baldwin¹, Russell Doerner¹, George Tynan¹

⁽¹⁾Center for Energy Research, University of California, San Diego, 9500 Gilman Drive #0417, La Jolla CA 92093, United States

⁽²⁾Ion Beam Materials Laboratory, Los Alamos National Laboratory, P.O. Box 1663, Los Alamos NM 87545, United States

Hydrogen isotope exchange experiments in tungsten samples were conducted in the PISCES linear plasma device to study tritium migration in plasma facing components (PFCs). Tungsten samples were first exposed to deuterium plasma in typical magnetic fusion experiment divertor conditions to a fluence of 10^{26} ions/m² while maintaining a sample temperature below 373 K and subsequently exposed to hydrogen plasma at varying fluences (10^{23} to 10^{26} ions/m²). Bulk retention was measured by thermal desorption spectroscopy (TDS), and the D(³He,p)⁴He reaction was used to obtain concentration profiles of deuterium. The effects of neutron damage were simulated by ion irradiation. Ion induced damage increases deuterium inventory in the near surface region, decreasing diffusion into the bulk. Although displacement damage allows more deuterium to be retained near the surface where much of the isotope exchange takes place, the efficiency of isotope exchange in the bulk was reduced. Current work on modeling solute deuterium atom transport in tungsten using the simulation software TMAP will be discussed.

MON-REP01-5

#453 - Contributed Talk - Monday 1:00 PM - West Fork

Small scale mechanical testing and Microstructural investigation of triple beam irradiated ODS alloys for Inertial Fusion Energy Application

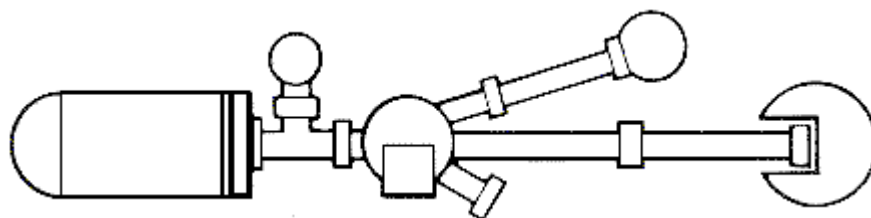
Peter Hosemann², Michael J. Fluss¹, Luke Hsiung¹, Jaime Marian¹, Scott Tumey¹, Bill Choi¹, Jeff Latkowski¹, Michael Dunne¹, S.A. Maloy³, Y. Wang³

⁽¹⁾Lawrence Livermore National Laboratory, Livermore CA, United States

⁽²⁾Department of Nuclear Engineering, University of California, Berkeley, Berkeley CA, United States

⁽³⁾Los Alamos National Laboratory, Los Alamos NM, United States

Inertial fusion energy application has similar issues in terms of materials selection as fission or magnetic fusion application. No large scale fusion neutron spectrum materials irradiation facility exists today to accurately test components and materials. For decades accelerator based ion irradiations have been conducted to study the effect of implantation and dose on candidate materials. However, usually the penetration depth is restricted due to the limited energy available, especially using heavy ions which can push to high dose but have very limited penetration depth. In this work materials considered for fusion application (ODS alloys) are irradiated with single, double and triple ion beams. While single and dual ion beam experiments have been conducted in the past, new results are shown here using the triple ion beam so as to evaluate the synergistic consequences of simultaneously implanted dpa dose, He and H. This approach thus emulates the damage that may develop in a fusion spectrum environment. However, due to the requirements of high dose heavy ions were used leading to shallow beam penetration. Microstructural information (TEM) is gained on FIB processed materials but also initial in-situ mechanical tests (in the SEM) are conducted. The multi beam irradiations pose novel challenges on the micromechanical testing methods due to the fact that position of the test needs to be selected very precise. The rather new micromechanical tests shows that no significant changes in yield strength are found in the irradiated region in the ODS alloys proving their superior radiation tolerance in this environment. Currently measurements on H and He implanted regions of the materials are ongoing which do show significant microstructural changes.



TUESDAY

Application of keV and MeV ion microbeams through tapered glass capillaries

Tokihiro Ikeda

Atomic Physics Laboratory, RIKEN, 2-1 Hirosawa, Wako Saitama 351-0198, Japan

We have developed a method to produce microbeams of keV energy highly charged ions (HCIs) and MeV energy protons/helium ions with tapered glass capillary optics for the applications of micro-/nano-meter sized surface modifications and a biological tool, respectively. Slow (keV energy) HCIs have high ability to modify surfaces and cause efficient sputtering without damaging the substrate very much. Once a microbeam is available, these functions specific to slow HCIs can be used to realize, e.g., micro-patterning of modifications and element-sensitive micro-imaging. However, microbeam of slow HCIs is not yet practically available because HCI beams are sometimes so weak for using a collimator or slit. In addition, when magnetic and/or electrostatic lenses are combined, good emittance is required. The tapered glass capillary is one of the feasible techniques to produce the microbeam because of the following advantages. (1) The taper can enhance the density of the output beam. (2) The size of the output beam is the same size of the outlet inner diameter. (3) Slow HCI can be reflected from the inner wall without a close collision due to a self-organized charge up on the wall, keeping its initial charge state and kinetic energy. The combination of MeV ion beams and the capillary with a thin end window at its outlet can realize three-dimensionally pinpoint energy deposition by observing the outlet through an optical microscope with a precision of a micron or better in an arbitrary position in a living cell or in any liquid object. In this talk, the mechanism of the beam transport through the capillary, the quality of the output microbeams, and some applications such as guiding of slow HCI's with bent Teflon tubes, irradiation of MeV ions to human cancer cells and Escherichia coli bacteria, and micro-patterned coating on polymer surfaces, will be presented.

TUE-AP03-3

#162 - Invited Talk - Tuesday 8:30 AM - Elm Fork

Dynamical evolution of 27 keV Ar⁹⁺ guiding through insulating glass capillaries: tapered and conical shape

ChunLin ZHOU¹, Amine CASSIMI¹, John A TANIS^{1,2}, Abdenacer BENYAGOUR¹, Clara GRYGIEL¹, Stéphane GUILLOUS¹, Henning LEBIUS¹, Daniel LELIEVRE¹, Toiamou MADI¹, Alain MERY¹, Isabelle MONNET¹, Jean-Marc RAMILLON¹, Frédéric ROPARS¹, Tokihiro IKEDA³, Yasunori YAMAZAKI^{3,4}, Hussein KHEMLICHE⁵, Philippe RONCIN⁵, Marius Johannes SIMON⁶, Arnold Milenko MÜLLER⁶, Max DOEBELI⁶

⁽¹⁾CIMAP CEA/CNRS/ENSICAEN, BP5133, Caen 14070, France

⁽²⁾Department of Physics, Western Michigan University, Kalamazoo Michigan 49008, United States

⁽³⁾Atomic Physics Laboratory, Riken, 2-1 Hirosawa, Wako, Saitama 351-0198, Japan

⁽⁴⁾University of Tokyo, Meguro, Tokyo 153-8902, Japan

⁽⁵⁾ISMO, CNRS/Universit Paris-Sud 11, Orsay 91405, France

⁽⁶⁾ETH Swiss Federal Institute of Technology, Rämistrasse 101, Zurich 8092, Switzerland

In the field of ion-surface interactions, slow highly charged ion (HCI) transmission through capillaries has attracted extensive attention for both fundamental and applied aspects in the last decade [1]. The accepted transmission scenario is ion 'guiding' by the charge up process of the capillary inner wall deduced from HCI transmission through nanocapillary foils [2] and tapered glass capillaries [3]. In applications, highly charged micro beams have been achieved with a tapered glass insulating capillary [4]. To study the dynamical features, an individual glass capillary avoids the collective effect and the inevitable divergence of the capillary foil. We have performed an experiment at the GANIL facility (Caen, France) with 27 keV Ar⁹⁺ ions transmitted through tapered and conical glass capillaries, respectively. There is no essential difference between the two types of capillary except for the taper angle. However, different behaviors were found for the transmission and blocking under the same beam conditions. A symmetric electrostatic potential barrier is proposed at the tapered part as responsible for the beam blocking. Furthermore, the evolution of the transmitted beam intensity and position for the conical capillary at a tilt angle of 1.1° was measured using a two-dimensional position sensitive detector. The most striking finding is the time evolution of a double peak structure due to charge patch guiding. A scenario involving three charge patches is proposed to interpret the charge up guiding behaviors. These findings lead to further understanding of the guiding effect and micro beam shaping.

This work has been supported by the European Community as an Integrating Activity' Support of Public and Industrial Research Using Ion Beam Technology (SPIRIT)' under EC contract no. 227012.

Dynamics of electron transmission through a micro-size tapered glass capillary

Samanthi Jayamini Wickramarachchi¹, Buddhika Senarath Dassanayake¹, Darshika Keerthisinghe¹, Tokihiro Ikeda², John Tanis¹

⁽¹⁾*Department of Physics, Western Michigan University, Kalamazoo MI 49008, United States*

⁽²⁾*Atomic physics Laboratory, RIKEN, 2-1 Hirosawa, Wako Saitama 351-0198, Japan*

The interaction and transmission of highly charged ions and electrons through insulating nano- and micro-sized capillaries has been studied experimentally and theoretically in the last few years. These capillaries have several promising applications in the areas of nano-fabrications and nano-structures, material modifications, tightly focused charge particle beams and medical applications¹. Using insulating capillaries to produce a particle beam of very small dimensions is simpler and less expensive than needing expensive and large electromagnetic devices to produce such small beams. Recently micro-sized tapered glass capillaries attracted the attention of the field because of their high focusing ability². In the present work we report the transmission of 500 and 1000 eV electrons through tapered Borosilicate glass capillaries with inlet/outlet diameters of 720 μm /22 μm and 800 μm /100 μm and a tapered length of 25 mm. Interestingly, almost no transmission was seen for the lowest energy (500 eV) for the capillary with the smaller outlet diameter (22 μm), while transmission was observed up to a 5.5° sample tilt angle with respect to the incident electron beam for the capillary with an outlet diameter of 100 μm . Additionally, the time dependence of the transmission has been examined for the energies at selected tilt angles, and evidence of charge accumulation and discharge were observed. Transmission never reached a stable equilibrium but sudden bursts of elastic transmission at the smallest tilt angles studied were seen for 1000 eV. The results reveal distinctive features of electron transmission through tapered glass capillaries compared to what has been observed for slow HCIs.

¹Y. Iwa et al., *App. Phys. Lett.* **92**, 023509 (2008)

²T. Nebiki et al., *J. Vac. Sci. Technol. A* **21**, 1671 (2003)

Transmission of fast electrons through PET nanocapillaries

D. Keerthisinghe¹, B S Dassanayake¹, S Wickramarachchi¹, A Ayyad¹, N Stolterfoht², J A Tanis¹

⁽¹⁾*Department of Physics, Western Michigan University, 1903, W. Michigan Ave, Kalamazoo MI 49008-5252, United States*

⁽²⁾*Materialien und Energie, Helmholtz-Zentrum Institute, D-14109, Berlin, Germany*

In 2002 the transmission and guiding of slow highly charged ions (HCIs) through insulating polyethylene terephthalate (PET) nanocapillaries was reported [1], while the first electron transmission through PET was published in 2007 [2]. Later the transmission of electrons through single glass microcapillaries was also studied [3]. The aim of the present work is directed towards the energy and time dependence of electron transmission through PET nanocapillaries. The PET foil used in this study had capillaries with diameters of 100 nm and an aspect ratio 120. Measurements were made for energies of 500 and 800 eV. Unlike the previous work [2], the present results show three electron transmission regions corresponding to the direct, indirect and direct-indirect transitions. For the direct region with sample tilt angles near zero degrees, the observation angle is constant for the two energies and equal to about zero. In the indirect region the observation angle equals the tilt angle, and in the direct-indirect region there are two observation angles showing characteristics of both. The characteristic guiding angle, i.e., the angle at which the transmission falls to 1/e of its initial value, is found to increase in the indirect region with increasing energy in contrast to the previous results [2]. Time dependence measurements were performed by blocking the beam for ~24 hours for a particular tilt angle and the corresponding spectrometer centroid angle. Results for both 500 and 800 eV, normalized to the current on the sample, clearly show that transmission of electrons through PET strongly depends on the time (charge) with the transmission eventually reaching equilibrium.

[1] N. Stolterfoht et al., *Phys. Rev. Lett.* **88** 133201 (2002).

[2] S. Das et al., *Phys. Rev. A* **76** 042716 (2007).

[3] B. S. Dassanayake et al., *Phys. Rev. A* **81** 020701 (R) (2010).

TIME EVOLUTION OF THE PROTON MICROBEAM TRANSMISSION THROUGH AN INSULATING MICROCAPILLARY

G.U. L. Nagy, I. Rajta, R. J. Bereczky, K. Tokesi

Institute of Nuclear Research of the Hungarian Academy of Sciences (Atomki), Debrecen H-4001, Hungary

Charged particles, keeping their initial charge states, can be transmitted through an insulating capillary even if the capillary axis is tilted with respect to the incident beam axis larger than the geometrical limit. This phenomenon is called charged particle guiding. In the past few years, since the discovery of the guiding effect, a number of experimental as well as theoretical works have been published on various insulating nanocapillaries of aspect ratios around 100 using slow highly charged ions.

In this work, as a unique feature, we used the combination of single charged projectiles and single capillaries. We investigated the time dependent behaviour of a 1 MeV proton microbeam passing through a polytetrafluoroethylene (Teflon) single microcapillary. A Faraday-cup placed behind the capillary exit has been used to measure the transmitted beam current as a function of time at different incident currents and tilt angles. We have found significant transmissions after the charge-up of the inner wall of the capillary. We have also analysed the energy distributions of the transmitted protons at different stages of the charge-up process. We identified three completely different regions in the transmission as a function of time. At first, at the beginning of the creation of the charge patch on the inner wall of the capillary, the energy spectra of the transmitted protons contained only inelastic contributions. This is due to Coulomb scattering on the inner wall atoms. Later the elastic peak also appears and becomes more and more significant. Finally, in the third region, after the amount of deposited charge on the wall reached a dynamical equilibrium, stable guided transmission was obtained. The dominant contribution in the energy distribution of the transmitted protons was the elastically scattered peak.

The work was supported in part by the Hungarian Scientific Research Fund OTKA No. NN 103279.

Multiple capture contributions in charge exchange induced X-ray spectra and their relevance to astrophysical applications

Sebastian Otranto¹, Ronald E Olson²

⁽¹⁾*IFISUR and Departamento de Física, Universidad Nacional del Sur, Av. Alem 1253, Bahía Blanca Buenos Aires 8000, Argentina*

⁽²⁾*Physics Department, Missouri University of Science and Technology, Rolla MO 65409, United States*

In recent years, there has been a renewed interest in the study of charge exchange processes within the atomic physics community prompted to a large extent by the demands and needs of the astrophysical community. The fortuitous discovery of the X-ray emission from comets in 1996 by Lisse et al., opened the door to the study of cometary and planetary X-ray emissions which were found to strongly rely upon charge exchange processes. Soon after this discovery, Earth-based laboratories started to study charge exchange processes for collision systems and impact energies of direct relevance to contrast the astrophysical observations. Ions of interest were those populating the solar wind ($C^{5+,6+}$, $O^{7+,8+}$, $N^{4+,5+}$ among others) and also highly charged ions of Ne, Ar and Fe. As the projectile charge increases, multiple capture events (MEC) increase in importance as well. The description of these multiple capture processes represents a challenging but unavoidable theoretical problem for a complete understanding of the underlying physics.

In this work, we present line emission cross sections for Ar^{18+} and Ne^{10+} ions colliding on Ar and Ne targets using a 5-body classical trajectory Monte Carlo (CTMC) code that utilizes three active electrons. These electrons are described from quantal momentum distributions with sequential binding energies. The range of impact energies considered is 5 eV/amu-10 keV/amu which covers typical EBIT-traps as well as Solar wind energies. The implemented scheme for the multiple capture analysis is the following: for double capture to levels (n_1, n_2) of the projectile with $n_1 - n_2 = \pm 1$, autoionizing double capture is assumed. Otherwise the event is recorded as double radiative decay. For three electron capture to states (n_1, n_2, n_3) of the projectile, autoionizing triple capture is assumed.

Our results are supported by recent extracted beam measurements made at Berlin and NIST, and by data from the Jet Propulsion Laboratory.

Charge Exchange X-ray Emission: Astrophysical Observations and Potential Diagnostics

Kelsey Morgan³, Ilija Draganic^{1,2}, Charles Havener¹, Mitchell Hokin³, Dan McCammon³, Patrick Sauter³

⁽¹⁾*Physics Division, Oak Ridge National Laboratory, Oak Ridge TN 37831, United States*

⁽²⁾*AOT-ABS, Los Alamos National Laboratory, Los Alamos NM 87545, United States*

⁽³⁾*Department of Physics, University of Wisconsin, 1150 University Ave, Madison WI 53706, United States*

Interest in astrophysical sources of charge exchange X-rays has been growing steadily since the discovery of X-ray emission from the comet Hyakutake with ROSAT in 1996. Since then, charge exchange has been observed between solar wind ions and neutrals in the Earth's geocorona and in the atmospheres of Mars and Jupiter. Charge exchange with interstellar neutrals within the heliosphere is now acknowledged as contributing a considerable (although currently unknown) fraction of the soft X-ray background. A brief survey of the heliospheric, Galactic, and extragalactic systems in which charge exchange has been observed or is predicted to take place will be presented. Experiments measuring velocity dependent cross-section and line ratios for Lyman-series lines and He-like triplets are needed to check current theoretical models of charge exchange emission and aid interpretation of observations. We point out a number of systems that are of particular astrophysical interest that could be the subject of future laboratory investigations.

Charge exchange experiments in electron beam ion traps

Joel Clementson, Peter Beiersdorfer, Gregory V. Brown

Physics Division, Lawrence Livermore National Laboratory, 7000 East Avenue, Livermore California 94550, United States

Charge exchange recombination, the transfer of one or more electrons from an atomic or molecular system to a positive ion, is believed to be an important line-formation mechanism in many astrophysical spectra [1]. The most important collision energy range for astrophysical charge exchange reactions reaches from single electron volts (eV) to maybe a few keV. While ion accelerators have problems to produce such low-energy ion beams, the situation is favorably reversed in electron beam ion traps (EBITs). Ions of a controllable charge state distribution can be produced and trapped with temperatures of a few hundreds of eV up to a few keV and can mingle with room temperature (meV) atoms or molecules in a very-low density environment. Thus measurements in an EBIT approximate well some astrophysical settings. Using solid-state detectors and x-ray calorimeter spectrometers developed at the NASA Goddard Space Flight Center [2], a number of such experiments involving highly charged ions and neutral gases have been performed at the Livermore EBIT facility and show drastic evidence of charge exchange in x-ray spectra [3-5].

Work performed under the auspices of the United States Department of Energy by Lawrence Livermore National Laboratory under contract No. DE-AC52-07NA-27344.

[1] A. Bhardwaj et al. Planet. Space Sci. 55(9), 1135 (2007)

[2] F. S. Porter et al. AIP Conf. Proc. 1185, 454 (2009)

[3] P. Beiersdorfer et al. Science 300(5625), 1558 (2003)

[4] M. Frankel et al. Astrophys. J. 702(1), 171 (2009)

[5] M. A. Leutenegger et al. Phys. Rev. Lett. 105(6), 063201 (2010)

Evidence for Radiative Double Electron Capture (RDEC) in F^{9+} on Carbon Collisions

T. Elkafrawy¹, A. Simon², A. Warczak³, J. A. Tanis¹

⁽¹⁾Physics Department, Western Michigan University, Kalamazoo MI 49008, United States

⁽²⁾NSCL, Michigan State University, East Lansing MI 48823, United States

⁽³⁾Institute of Physics, Jagiellonian University, Krakow, Poland

Projectile x-ray emission in the collision of fully-stripped ions with carbon foils provides insight into dynamical and structural problems. Radiative double electron capture (RDEC) is the time reversed process of double photoionization and can be measured when two target electrons are captured into a bound state of the projectile simultaneously with the emission of a single photon. For bare ions, this approach provides a proper way to explore electron-electron correlations in the absence of other electrons and also gives information to describe two-electron continuum wave functions. The first evidence for RDEC was found in 38 MeV $O^{8+} + C$ collisions [1] following other experimental [2,3] studies and theoretical calculations [4,5]. Recently, another theoretical work on RDEC was done [6]. The current work was conducted using the Van de Graaff accelerator at Western Michigan University. Radiative electron capture (REC) and RDEC were investigated in 42 MeV bare $F^{9+} + C$ collisions. Emitted x rays were measured at 90° to the beam line in coincidence with doubly (Q-2) and singly (Q-1) charge-changed projectile ions. Evidence of a small contribution from RDEC to the K-shell was observed. Moreover, the F K- α line was observed in the Q-1 time-gated x rays while no evidence for it was seen in case of the Q-2 time-gated x rays.

[1] A. Simon, A. Warczak, T. Elkafrawy, and J. A. Tanis, Phys. Rev. Lett. **104**, 123001 (2010).

[2] A. Warczak, et al., Nucl. Instr. Meth. Phys. Res. B **98**, 303 (1995).

[3] G. Bednarz et al., Nucl. Instr. Meth. Phys. Res. B **205**, 573 (2003).

[4] A. I. Mikhailov et al., Phys. Rev. A **69**, 032703 (2004).

[5] A. Nefiodov et al., Phys. Lett. A **346**, 158 (2005).

[6] E. A. Chernovskaya et al., Phys. Rev. A **84**, 062515 (2011).

High Resolution X-ray Emission Studies for C^{6+} on He, H₂ and Kr

V M Andrianarijaona¹, C I Guillen¹, S L Romano¹, A K Vasantachart¹, X Defay², K Morgan², D McCammon²,
M Fogle³, I N Draganic⁴, C C Havener⁴

⁽¹⁾Department of Physics, Pacific Union College, Angwin CA 94508, United States

⁽²⁾Department of Physics, University of Wisconsin, Madison WI 53706, United States

⁽³⁾Department of Physics, Auburn University, Auburn AL 36849, United States

⁽⁴⁾Physics Division, Oak Ridge National Laboratory, Oak Ridge TN 37831, United States

High-resolution X-ray emission studies are being performed at the Multicharged Ion Research Facility at Oak Ridge National Laboratory using the ion-atom beam line¹ and an X-ray calorimeter² from the University of Wisconsin. Fully stripped C^{6+} ions from an ECR ion source interact with a He, H₂ and Kr gas at collision energies corresponding to typical solar wind velocities (250 km/sec - 2500 km/sec). The recorded X-ray spectra with ~10 eV resolution clearly show a target and energy dependence for Lyman -alpha, -beta, and -gamma. The observed ratio of the different peaks depends on the initial population in n,l of the captured electron on C^{5+} and the subsequent cascading process. The theoretical n,l distribution of charge transfer is difficult to calculate³ at low energies with little total or state-selective cross section data for comparison.

1. C. C. Havener et al., NIMB 261 (2007) 129-132

2. D. McCammon et al., J Low Temp Phys, 151, 715 (2008)

3. Y. Wu et al., PRA 84, 022711 (2011)

Research supported by the NASA Solar & Heliospheric Physics Program NNN07ZDA001N, NASA Astrophysics NNX09AF09G, the U.S Department of Energy Office of Fusion Energy Sciences and the Office of Basic Energy Sciences under contract DE-AC05-00OR22725 with UT-Battelle, LLC. VA et al. is supported by the National Science Foundation through Grant No. PHY-106887.

Dielectronic recombination studies based on EBITs

Jun Xiao, Ke Yao, Wei Zhang, Roger Hutton, Yaming Zou
Modern Physics Institute, Fudan University, 220 Han Dan Road, Shanghai 200433, China

Dielectronic recombination (DR) process plays an important role in high temperature plasmas, where DR can affect charge balance and level populations significantly. At the same time DR of heavy elements can cause radiative energy loss in plasmas. On the other hand, DR satellite lines are used for plasma temperature and density diagnostic purpose, while un-resolvable satellite disturbs the determination of line shape, line intensity, and line position. Data of DR resonant strength is vital for accurate modeling of high temperature plasmas. DR Studies are also important for testing atomic structure and atomic collision theories, since it carries information on quantum electrodynamics, relativistic effects, electron correlations and so on. DR is a resonant process, in which a free electron is captured by an ion, at the same time a bound electron in the ion is promoted, forming a multiply excited intermediate state above auto-ionization threshold. Then the process is completed by stabilization through emitting one or more photons, so as to reducing the ion energy to below its auto-ionization limit.

In this talk, experimental studies based on EBIT will be presented.

Precision Mass Measurements with Radioactive Highly Charged Ions

Anna A. Kwiatkowski¹, C. Andreiou², T. Brunner³, A. Chaudhuri¹, U. Chowdhury^{1,4}, P. Delheij¹, S. Ettenauer^{1,5}, A. T. Gallant^{1,5}, A. Grossheim¹, G. Gwinner⁴, A. Lapierre⁶, A. Lennarz⁷, T. D. Macdonald^{1,5}, E. Mane¹, M. R. Pearson¹, R. Ringle⁶, B. E. Schultz¹, M. C. Simon¹, V. V. Simon^{1,8,9}, J. Dilling^{1,5}
⁽¹⁾TRIUMF, 4004 Wesbrook Mall, Vancouver BC V6T 2A3, Canada
⁽²⁾Dept. of Chemistry, Simon Fraser Univ., Burnaby BC V5A 1S6, Canada
⁽³⁾Dept. of Physics, Stanford Univ., Stanford CA 94305, United States
⁽⁴⁾Dept. of Physics and Astronomy, Univ. of Manitoba, Winnipeg MB R3T 2N2, Canada
⁽⁵⁾Dept. of Physics and Astronomy, Univ. of British Columbia, Vancouver BC V6T 1Z2, Canada
⁽⁶⁾National Superconducting Cyclotron Laboratory, Michigan State Univ., 1 Cyclotron, East Lansing MI 48824, United States
⁽⁷⁾Institut für Kernphysik, Westfälische-Wilhelms-Universität, Münster D-48149, Germany
⁽⁸⁾Max-Planck-Institut für Kernphysik, Saupfercheckweg 1, Heidelberg 69117, Germany
⁽⁹⁾Fakultät für Physik und Astronomie, Ruprecht-Karls-Universität, Heidelberg 69120, Germany

Measurements of the atomic mass further our understanding in many disciplines, from forensics to physics beyond the Standard Model. The reputation of Penning trap mass spectrometry for accuracy and precision was established with singly charged ions (SCI); nonetheless, the achievable precision and resolving power can be readily extended by using highly charged ions (HCI) as was demonstrated at SMILETRAP for stable ions. TRIUMF's Ion Trap for Atomic and Nuclear Science (TITAN) has recently demonstrated these enhancements are attainable for longer-lived ($T_{1/2} > 50$ ms) radioactive ions. Measurements include $^{71}\text{Ge}^{21+}$, $^{74}\text{Rb}^{8+}$, $^{78}\text{Rb}^{8+}$, and $^{98}\text{Rb}^{15+}$. The Q -value of ^{71}Ge enters into the neutrino cross section, and the use of HCI reduced the resolving power required to distinguish the isobars from 3×10^5 to 20. The precision achieved in the measurement of $^{74}\text{Rb}^{8+}$, a superallowed β -emitter and candidate to test the CVC hypothesis, rivaled earlier measurements with SCI in a fraction of the time. The 111.19(22) keV isomeric state in ^{78}Rb was resolved from the ground state. Mass measurements of neutron-rich Rb and Sr isotopes near $A = 100$ aid in determining the path of the r -process in the region. An overview of the technique and some resultant mass measurements will be presented.

Reference free, high-precision measurements of transition energies in few electron argon ions

Csilla I Szabo¹, Pedro Amaro², Mauro Guerra³, Sophie Schlessler⁴, Alex Gumberidze^{5,6}, Jose Paulo Santos³,
Paul Indelicato¹

⁽¹⁾Laboratoire Kastler Brossel, ENS, CNRS, UPMC, Université Pierre et Marie Curie, 4 Place Jussieu, Paris F-75005, France

⁽²⁾Physikalisches Institut, Heidelberg University, Heidelberg D-69120, Germany

⁽³⁾Centro de Física Atomica, CFA, Departamento de Física, Faculdade de Ciências e Tecnologia, FCT, Universidade Nova de Lisboa, Caparica 2829-516, Portugal

⁽⁴⁾KVI, Theory Group, University of Groningen, Groningen 9747 AA, Netherlands

⁽⁵⁾ExtreMe Matter Institute EMMI and Research Division, GSI Helmholtzzentrum für Schwerionenforschung, Darmstadt D-64291, Germany

⁽⁶⁾FIAS, Frankfurt Institute for Advanced Studies, Frankfurt am Main D-60438, Germany

The use of a vacuum double crystal spectrometer, coupled to an electron-cyclotron resonance ion source (ECRIS), allows to measure low-energy x-ray transitions energies in highly-charged ions with accuracies of the order of a few parts per million. This required an ab initio modeling of the instrument using a ray-tracing program that we developed. We have used this installation to measure $n=2$ to $n=1$ transitions energies in 2, 3 and 4-electron ions. In particular we have measured the $1s2p\ ^1P_1 - 1s^2\ ^1S_0$ diagram line and the $1s2s\ ^3S_1 - 1s^2\ ^1S_0$ forbidden M1 transition energies in heliumlike argon, the $1s2s2p\ ^2P_j - 1s^2\ 2s\ ^2S_{1/2}$ transitions in lithiumlike argon and the $1s2s^2p\ ^1P_1 - 1s^2\ 2s^2\ ^1S_0$ transition in berylliumlike argon. There transitions measurements have accuracies between 2 and 4 ppm depending on the line intensity. Thanks to the excellent agreement between the simulation and the measurements, we were also able to measure the transition width of all the allowed transitions. The results are compared to recent QED and relativistic many-body calculations

SPARC: The Stored Particle Atomic Research Collaboration at FAIR

Thomas Stoeckler^{1,3,7}, Heinrich Beyer¹, Angela Bräuning-Demian¹, Carsten Brandau², Alexandre Gumberidze², Robert Grisenti^{1,4}, Siegbert Hagmann, Frank Herfurth¹, Thomas Kühl¹, Yuri Litvinov¹, Renate Maertin^{3,7}, Wilfried Nörtershäuser¹, Oliver Kester¹, Nikos Petridis⁴, Wolfgang Quint¹, Ulrich Schramm⁵, Reinhold Schuch⁶, Uwe Spillmann^{1,3}, Serge Trotsenko, Günter Weber^{3,7}

⁽¹⁾Helmholtz-Zentrum für Schwerionenforschung, GSI, Planckstrasse 1, Darmstadt, Germany

⁽²⁾ExtreMe Matter Institute EMMI and Research Division, GSI, Planckstrasse 1, Darmstadt, Germany

⁽³⁾Helmholtz-Institut Jena, GSI, Planckstrasse 1, Darmstadt, Germany

⁽⁴⁾Frankfurt Institute for Advanced Studies FIAS, Johann Wolfgang Goethe Universität, Frankfurt, Germany

⁽⁵⁾HZDR Forschungszentrum, Dresden-Rossendorf, Dresden, Germany

⁽⁶⁾Department of Physics, Stockholm University, Stockholm University, Stockholm, Sweden

⁽⁷⁾Institut für Optik und Quantenelektronik, Friedrich-Schiller-Universität, Jena, Germany

An overview about the envisioned program of the research collaboration (Stored Particle Atomic Research Collaboration, at the future accelerator facility FAIR) will be given. This program exploits the key features of this future facility that offer a range of new and challenging opportunities for atomic physics and related fields. In SPARC we plan to perform experiments in two major research areas: collision dynamics in strong electromagnetic fields and fundamental interactions between electrons and heavy nuclei up to bare uranium. In the presentation special emphasis will be given to the newest developments where we focus on experiments at storage HESR where cooled heavy ions up to gamma factor of 5 are available for experiments.

Spectral Shape of Two-Photon Transitions in Heavy Highly Charged Ions

S. Trotsenko^{1,2}, A. Kumar³, D. Banas⁴, A. Volotka⁵, A. Gumberidze^{6,7}, C. Kozhuharov¹, H. F. Beyer¹, S. Fritzsche^{1,8}, S. Hagmann¹, S. Hess¹, P. Jagodzinski⁴, R. Reuschl^{1,6}, S. Salem¹, A. Simon⁹, U. Spillmann¹, M. Trassinelli¹¹, L. C. Tribedi¹⁰, G. Weber^{1,2}, D. Winters¹, Th. Stöhlker^{1,2,12}

⁽¹⁾Atomic Physics, GSI Helmholtzzentrum für Schwerionenforschung, Planckstr. 1, Darmstadt 64291, Germany

⁽²⁾Helmholtz-Institut Jena, Froebelstieg 3, Jena 07743, Germany

⁽³⁾Nuclear Physics Division, Bhabha Atomic Research Centre, Mumbai, India

⁽⁴⁾Institute of Physics, Jan Kochanowski University, Kielce, Poland

⁽⁵⁾Institut für Theoretische Physik, Technische Universität Dresden, Dresden, Germany

⁽⁶⁾ExtreMe Matter Institute EMMI, GSI, Planckstr. 1, Darmstadt 64291, Germany

⁽⁷⁾FIAS Frankfurt Institute for Advanced Studies, Frankfurt am Main, Germany

⁽⁸⁾Fysiikan Laitos, Oulun Yliopisto, Oulu, Finland

⁽⁹⁾Institute of Physics, Jagiellonian University, Krakow, Poland

⁽¹⁰⁾Tata Institute of Fundamental Research, Mumbai, India

⁽¹¹⁾Institute des Nanosciences de Paris, CNRS, Université Pierre et Marie Curie-Paris 6, Paris, France

⁽¹²⁾Physikalisches Institut, Ruprecht-Karls-Universität Heidelberg, Heidelberg, Germany

In the early days of quantum mechanics Maria Göppert-Mayer formulated a non-relativistic theory of two-photon process for hydrogen, which was later refined for the $1s2s\ ^1S_0 \rightarrow 1s^2\ ^1S_0$ two-photon decay in helium by Breit and Teller. Since then the study of this second order transition has been of particular interest for both theory and experiment. The study of two-photon transitions (2E1) in He-like heavy ions is of particular interest due to the sensitivity of its spectral shape to electron-electron correlation and relativistic effects. Numerous experimental and theoretical studies have attempted to explore this process, however due to a lack of experimental accuracy, sensitivity to relativistic effects on the two-photon spectral distribution has not yet been achieved.

We developed a novel experimental approach for studying such transitions in few-electron high-Z ions. In this approach, few-electron ions with a selectively produced hole in the K-shell are used for the investigation of the transition modes that follow the decay of the excited ions. It was found that K-shell ionization is a very selective process that leads to the production of only two excited states, namely the $1s2s\ 2^1S_0$ and $1s2s\ 2^3S_1$. This can be directly applied for studying accurately the two-photon decay in He-like ions. Up to now, the experimental method in conventional 2E1 experiments has been the photon-photon coincidence technique, which is required to separate the true 2E1 events from the x-ray background associated with single photon transitions.

In contrast, by exploiting the state selectivity of K-shell ionization, the spectral distribution of the two-photon decay could be obtained simply by a measurement of the photon emission, using only a single x-ray detector in coincidence with projectile ionization. The method allowed for a background-free measurement of the distribution of the two-photon decay ($2^1S_0 \rightarrow 1^1S_0$) in He-like tin.

A very low energy electron beam ion trap for spectroscopic research in Shanghai

Jun Xiao^{1,3}, Zejie Fei^{1,3}, Yang Yang^{1,3}, Xuelong Jin^{1,3}, Di Lu^{1,3}, Yang Shen^{1,3}, Leif Liljeby², Roger Hutton^{1,3}, Yaming Zou^{1,3}

⁽¹⁾Shanghai EBIT lab, Institute of Modern Physics, Fudan University, Shanghai 200433, China

⁽²⁾Manne Siegbahn Laboratory, Stockholm University, Stockholm 10691, Sweden

⁽³⁾The Key lab of Applied Ion Beam Physics, Ministry of Education, Shanghai 200433, China

We have developed a new compact low energy electron beam ion trap, SH-PermEBIT. This electron beam ion trap (EBIT) can operate in the electron energy range of 60-5000 eV, with a current density of up to 100 A/cm². The low energy limit of this machine sets the record among the reported works so far. The magnetic field in the central drift tube region of this EBIT is around 0.5 T, produced by permanent magnets and soft iron. In this work, transmission of the electron beam as well as the upper limit of the electron beam width under several conditions are measured. The performance of this EBIT has been investigated through x-ray spectroscopy, extreme ultra-violet (EUV) spectroscopy and visible spectroscopy of highly charged argon ions.

A new Electrostatic Storage Ring at KACST

Mohamed O. A. El Ghazaly¹, Suliman M. AlShammari¹, Carsten P. Welsch²

⁽¹⁾*National Center for Mathematics and Physics (NCMP) , King Abdulaziz City for Science and Technology (KACST), King Abdullah Road, P.O. Box 6086, Riyadh 11442, Saudi Arabia*

⁽²⁾*Cockcroft Institute, University of Liverpool, Warrington Cheshire WA4 4AD , United Kingdom*

Electrostatic Storage Rings (ESRs) are highly attractive tools for atomic and molecular physics, as well as in biophysics and biochemistry. The most interesting advantage of such storage devices is the no limitation to the mass of stored ions. A new ESR for beams at energies up to 30 keVq is currently under construction at the King Abdulaziz City for Science and Technology (KACST). The ring, of which the optical scheme follows the preceding electrostatic storage rings, is designed to be the core of a highly flexible experimental facility at KACST. This facility will combine many different, yet complementary beam techniques and experimental methods. The optical scheme of the ring thus had to accommodate the different experimental techniques that the ring will be equipped with, such as for example electron-ion, laser-ion, ion-ion or neutral- ion beams. Here, we present an overview of the layout of this new ESR.

Electronic Neutron Generator Technology and New Developments

David L. Chichester

Idaho National Laboratory, 2525 N. Fremont Avenue, Idaho Falls ID 83415, United States

Historically, basic compact ENG technology development has been driven by needs in the petroleum industry. However, over the last decade a distinct new set of instruments has been developed to meet needs for security screening and for industrial process control. Over the next decade instruments addressing these markets will continue to mature and specialize and, as a result of this specialization, commonality between sub-surface and above-surface ENGs will continue to decrease. Continued development and advancement of associated-particle ENGs is one example of this differentiation, another will be growing demand for turn-key instruments to serve as reliable neutron sources to replace radioisotope sources for education, training, and neutron-detector development. The development of practical, pulsed, high-yield ENG systems for commercial use remains a growth area that has not yet been adequately addressed by the commercial sector.

This paper will present a review of the development of commercial electronic neutron generator technology, an overview of current research and development in the field, and a discussion of technology pull from the user community that will shape future developments in ENG technology over the next five to ten years.

A neutron tube equipped with two alpha detectors for portable illicit material detection systems

Philippe Le Tourneur

Sodern, 20 avenue Descartes, LIMEIL BREVANES 94450, France

Sodern has developed a new compact sealed Associated Particle Imaging (API) neutron tube used in portable illicit material detection systems. The weight of the neutron tube is less than 900 grams and the entire neutron generator is less than 4kgs total. What makes this unique is having two alpha detectors. Alpha detection is needed inside the tube to detect alphas associated to neutrons after D + T reaction. One alpha detector is used for tagging the neutrons irradiating the object; the second alpha detector tags the neutron (unfortunately) irradiating the gamma detector, allowing for noise reduction by deleting fast neutron events in the gamma spectrum. This is useful for systems when the gamma detector must be near the neutron source. And when it is not possible to use heavy shielding to protect this detector. Typical specifications and results are given.

Applications and advantages of a high efficiency DD neutron generator platform

Matthew D. Coventry, Brian E. Jurczyk, Robert A. Stubbers, Kim L. Kloepper
Starfire Industries, 2109 S. Oak St., Ste 100, Champaign IL 61820, United States

DD neutron generators will find wider application with the realization of higher output levels and lifetimes. Key Starfire innovations in ion source and target technologies provide for higher neutron production efficiency with a longer life than existing DD technology. These factors enable DD neutron generators to be applied to situations where lower neutron energy and ease of licensing give them an advantage over DT units, but were not previously used due to output requirements. This talk will highlight the advantages of DD neutron generators over DT units and radionuclide-based sources and discuss the generators currently under development at Starfire Industries for oil/gas well evaluation, portable applications, and neutron radiography.

High Yield Neutron Generators using the DD reaction

Jaakko H Vainionpää¹, Jack L Harris¹, Melvin A Piestrup¹, Charles K Garry¹, David L Williams¹, Mac D Apodaca¹,
 Jay T Cremer¹, Qing Ji², Bernhard A Ludewigt², Glenn Jones³
⁽¹⁾*Adelphi Technology Inc., 2003 E Bayshore Rd, Redwood city California 94063, United States*
⁽²⁾*Lawrence Berkeley National Laboratory, 1 Cyclotron Rd, Berkeley California 94720, United States*
⁽³⁾*G&J Enterprise, 1258 Quarry Ln, Suite F, Pleasanton California 94566, United States*

A product line of high yield neutron generators has been developed that uses the D-D fusion reaction and operates with an ion beam supplied by a microwave plasma generator. Yields of up to 2×10^9 n/s have been achieved, which are comparable to those obtained using the more efficient D-T reaction. The microwave-driven plasma uses the electron cyclotron resonance effect to produce a high plasma density for high current and high Hydrogen atomic species. These generators have an actively pumped vacuum system that allows operation at reduced pressure at the target chamber, increasing the overall system reliability. Since no radioactive tritium is used the generators can be easily serviced, and components such as the target and plasma aperture, can be easily replaced to provide essentially an unlimited lifetime. Fast neutron source size can be adjusted by selecting the aperture and target geometries according to customer specifications. Pulsed and continuous operation has been demonstrated. Minimum pulse lengths of 50 μ s have been achieved. Since the generators are easily serviceable, they offer a long life-time neutron generator for laboratories and commercial systems requiring continuous operation.

Several of the generators have been enclosed in radiation shielding/moderator structures designed for customer specifications. In this mode of operation these generators have been proven to be useful for prompt gamma neutron activation analysis (PGNAA) and neutron activation analysis (NAA). Fast neutron radiography has also been demonstrated using a newly developed camera. Thus these moderated generators make excellent fast, epithermal and thermal neutron sources for laboratories and industrial applications that require neutrons with safe operation, small footprint, low cost and small regulatory burden.

Development of a compact, portable neutron generator for active interrogation applications

Amy Sy^{1,2}, Qing Ji¹, Arun Persaud¹, Bernhard Ludewigt¹, Thomas Schenkel¹

⁽¹⁾*Lawrence Berkeley National Laboratory, 1 Cyclotron Rd, Berkeley CA 94720, United States*

⁽²⁾*Department of Nuclear Engineering, University of California, Berkeley, Berkeley CA 94720, United States*

Compact, portable neutron generators have applications in radiological source replacement and field-portable interrogation systems. These generators benefit from efforts for increased power efficiency, atomic ion fraction, and neutron yield. Additional considerations are application-specific; for use with the associated particle imaging (API) method, narrow beam widths without the use of active focusing elements can improve the spatial resolution achievable in such systems. Penning ion sources have long been used for neutron generation through D-D and D-T fusion reactions due to their low power consumption, ease of operation, and compactness. Lawrence Berkeley National Laboratory is exploring methods for increased power efficiency and atomic ion fraction for improved neutron yields in a Penning source-based neutron generator. Efforts include optimization of size, power, and pressure, choice of plasma-facing materials, and improved plasma confinement using multi-cusp magnetic fields. Optimization efforts have resulted in an ion current density per unit power of 0.3 mA/cm²-W, with further optimization in progress. In an API system, a beam diameter of 1 mm at the neutron production target improves the system spatial resolution by a factor of four over commercially available systems. The use of passive focusing elements to reduce the ion beam diameter with minimal current loss is being explored. Initial results will be presented and discussed.

This work was performed under the auspices of the U. S. Department of Energy, NNSA Office of Nonproliferation and Verification Research & Development by Lawrence Berkeley National Laboratory under Contract No. DE-AC02-05CH11231.

A hydrocarbon fluid-based deuteron ion source for neutron generators

Paul R Schwoebel

Physical Sciences Division, SRI International, 333 Ravenswood Avenue, Menlo Park CA 94025, United States

A deuteron ion source based on a spark discharge between electrodes coated with a deuterated hydrocarbon fluid is investigated. In the prototypic example studied here ion currents extracted from the source were on the order of 0.5 A with a pulse duration of approximately 10 μ s. Operation in a laboratory neutron generator provided a neutron yield of $\sim 10^5$ neutrons/pulse with the deuterium-deuterium fusion reaction at a deuteron ion energy of 65 keV. This approach to ion sources for neutron generators has the potential to provide a compact, long-lived, high-output neutron generator for homeland security applications.

Neutron production using a pyroelectric driven target coupled with a gated field ionization source

Jennifer L Ellsworth¹, Vincent Tang¹, Steven Falabella¹, Brian Naranjo², Seth Putterman²

⁽¹⁾*Lawrence Livermore National Laboratory, 7000 East Ave., Livermore CA 94550, United States*

⁽²⁾*University of California Los Angeles, Los Angeles CA 90095, United States*

A palm sized, portable neutron source would be useful for widespread implementation of detection systems for shielded, special nuclear material. We report results from experiments using a decoupled pyroelectric, lithium tantalate crystal with a deuterated target clamped on top in a chamber filled with D₂. The target, 6 cm diameter crystal, and thermoelectric cooler are clamped together using a specially designed, electrically insulating tube which should prevent arcing across the crystal. Ion beam is produced through field ionization from single or multiple metal tips that are pointed towards the crystal. The effects of fill pressure, tip configuration and bias, crystal heating rates, and the distance between the tip and the crystal are considered.

This work was performed under the auspices of the U.S. Department of Energy by Lawrence Livermore National Laboratory under Contract DE-AC52-07NA27344 and supported by the U.S. Department of Energy NA-22 Office of Nonproliferation Research and Development under the Special Nuclear Materials Movement Detection portfolio.

TUE-AT03-P1

#195 - Poster - Tuesday 5:30 PM - Rio Grande

Pulsed D-D neutron source for compensated porosity well-logging

Allan Xi Chen, Arlyn J. Antolak, Ka-Ngo Leung

Sandia National Laboratories, 7011 East Ave., Livermore CA 94550, United States

Computational Monte Carlo analysis has shown that lower energy neutrons, such as from a ^{252}Cf source or a D-D neutron generator, provide the highest sensitivity to porosity in compensated well logging measurements. Neutrons from such sources do not penetrate the formation as deeply before becoming thermalized and, thus, are more easily detected. In addition, less shielding material is needed between the neutron source and detectors leading to a more compact logging tool. By operating the source in pulse mode, background noise is eliminated between pulses and the signal-to-noise ratio is improved in the detection system. This paper explores the operational functionality of a pulsed D-D neutron generator in terms of the required source intensity, optimized duty factor, and source-to-detector arrangements for compensated porosity well logging.

^aAllan Xi Chen is also affiliated with Department of Mechanical Engineering, University of California, Berkeley, CA 94720

²Ka-Ngo Leung is also affiliated with Department of Nuclear Engineering, University of California, Berkeley, CA 94720

Sandia National Laboratories is a multi-program laboratory managed and operated by Sandia Corporation, a wholly owned subsidiary of Lockheed Martin Corporation, for the U.S. Department of Energy's National Nuclear Security Administration under contract DE-AC04-94AL85000.

TUE-AT04-1

#329 - Invited Talk - Tuesday 1:00 PM - Bur Oak

Recent developments on ion beam diagnostics for research, healthcare and industry

Arnd Baurichter

Sales & Marketing, Danfysik A/S, Gregersensvej 8, Taastrup 2630, Denmark

Danfysik is dedicated to use its 50 years of experience in designing, manufacturing, installing, commissioning and testing of accelerator equipment to the benefit of its customers. We provide high-end components and turn-key systems for a large variety of ion and electron beam applications for research, healthcare and industry. As part of our product portfolio, we manufacture ion and electron beam diagnostics in the energy range from several KeV to a few GeV. Our diagnostics cover several ranges of beam power up to multiple KW.

The presentation will focus on recent developments on beam diagnostics for light ion beam applications like hadron cancer therapy. Our beam diagnostic program of current measurement devices, beam profile, position and beam loss monitors, as well as slits and beam blocking devices is mostly based on designs developed at GSI in Darmstadt.

Most recently, a doped scintillating optical fiber based beam profile monitor for light ion beams with intensities up to several 10^{10} p/s was developed in collaboration with Aarhus University and the Aarhus School of Engineering. The novel detector consists of horizontal and vertical grids of 0.2 mm diameter Yb doped scintillating optical fibers, read out by remotely located arrays of photo diodes. Test experiments with proton and carbon ion beams at the Heidelberg Ion Therapy center HIT have proven the new detector's potential to replace the costly multiwire proportional chambers widely used today in synchrotron based hadron therapy facilities. This work was supported by the Danish National Advanced Technology Foundation. A patent is pending.

Diamonds for Beam Instrumentation

Erich Griesmayer

CIVIDEC Instrumentation, Schottengasse 3A/1/41, Vienna 1010, Austria

Diamond is perhaps the most versatile, efficient and radiation tolerant material available for use in beam detectors with a correspondingly wide range of applications in beam instrumentation. Numerous practical applications have demonstrated and exploited the sensitivity of diamond to charged particles, photons and neutrons. A general description of diamond detectors is given together with several application examples.

IBA beam diagnostics: present and new developments

Vincent Eric Nuttens

Beam Production System, IBA s.a., Chemin du cyclotron 3, Louvain-La-Neuve B1348, Belgium

IBA is developing accelerators for a wide range of applications. Depending on the accelerator, the beam properties (particle type, energy, current, time structure) will be different, requiring specific diagnostics tools.

Medical accelerators are divided into two kinds of applications. The first one is dedicated to the production of radionuclides for nuclear imaging. Low energy (3-70MeV) cyclotrons are generally used with the highest beam currents possible (40-2000 μ A). The second one is dedicated to protontherapy. It deals with high energy cyclotrons or synchrocyclotrons (~250MeV) but provides low beam current (several nA). However, for quality assurance purposes, the beam properties must be well-known in order to ensure the quality of the patient treatment. It relies therefore on highly reliable beam diagnostic tools.

Industrial applications such as cable crosslinking and sterilization use Dynamitrons or Rhodotrons which produce several MeV electrons with currents up to 100mA.

IBA R&D teams have developed several tools to measure beam size, position and intensity at various positions in accelerators and beamlines. New developments are also in progress for online (i.e. during accelerator operation) and offline (i.e. during accelerator commissioning) beam diagnostic tools. A review of all the present and new developments is proposed.

Diagnostics for the optimization of an 11 keV inverse Compton scattering X-ray source

Anne-Sophie Chauchat¹, Jean-Pierre Brasile¹, Vincent Le Flanchec², Jean-Paul Nègre², Alain Binet²,
Jean-Michel Ortega³

⁽¹⁾THALES Communications & Security, 160 bd de Valmy, Colombes 92704, France

⁽²⁾CEA DAM DIF, Bruyères-Le-Châtel, Arpajon 91290, France

⁽³⁾LCP/CLIO, Université Paris-Sud, Bâtiment 201, Orsay 91405, France

In a scope of a collaboration between Thales Communications & Security and CEA DAM DIF, 11 keV X-rays were produced by inverse Compton scattering on the ELSA facility. In this type of experiment, X-rays observation lies in the use of accurate electron and laser beam interaction diagnostics and on fitted X-ray detectors. The low interaction probability, between <100 μ m width, 12 ps (rms) length electron and photon pulses, requires careful optimization of pulses spatial and temporal covering. Another issue was to observe 11 keV X-rays in the ambient radioactive noise of the linear accelerator. For that, we use a very sensitive detection scheme based on radio luminescent screens.

An innovative beam monitoring system for the research beam line of the new Bern PET cyclotron

Saverio Braccini

Albert Einstein Center for Fundamental Physics, Laboratory for High Energy Physics (LHEP), University of Bern, Sidlerstrasse 5, Bern CH-3012, Switzerland

The new cyclotron laboratory for radioisotope production and multi-disciplinary research in Bern (Switzerland) is based on a commercial IBA 18 MeV proton cyclotron, equipped with a specifically conceived 6 m long external beam line, ending in a separate bunker. It will provide beams for routine 18-F and other PET radioisotope production as well as for novel detector, radiation biophysics, radioprotection, radiochemistry and radiopharmacy developments. The accelerator is embedded into a complex building hosting two physics laboratories, four GMP radiochemistry and radiopharmacy laboratories, offices and two floors for patient treatment and clinical research activities. This project is the result of a successful collaboration among the University Hospital in Bern (Inselspital), the University of Bern and private investors, aiming at the constitution of a combined medical and research center able to provide the most cutting-edge technologies in medical imaging and cancer radiation therapy. For this purpose, the establishment of a proton therapy center on the campus of Inselspital is in the phase of advanced study. In this framework, an innovative beam monitor detector based on doped silica and optical fibres has been designed, constructed and tested. Scintillation light produced by Ce and Sb doped silica fibres moving across the beam is measured, giving information on beam position, shape and intensity. The doped fibres - constructed in collaboration with the Institute of Applied Physics (IAP) - are coupled to commercial optical fibres, allowing the read-out of the signal far away from the radiation source. This general-purpose device can be easily adapted for any accelerator used in medical applications and is suitable either for low currents used in hadrontherapy or for currents up to a few microAmpere for radioisotope production, as well as for both pulsed and continuous beams.

Development of long-lived thick carbon stripper foils for high energy heavy ion accelerators by a heavy ion beam sputtering method

Hideshi Muto¹, Yukimitsu Ohshiro², Katsunori Kawasaki³, Michihiro Oyaizu⁴, Toshiyuki Hattori⁵

⁽¹⁾*Center of General Education, Tokyo University of Science, Suwa, 5000-1 Toyohira, Chino Nagano 391-0292, Japan*

⁽²⁾*Center for Nuclear Study, University of Tokyo, 2-1 Hirosawa, Riken Campus, Wako Saitama 351-0198, Japan*

⁽³⁾*Van de Graaf Laboratory, Department of Physics, Tokyo Institute of Technology, 2-12-1 O-okayama, Meguro Tokyo 152-8551, Japan*

⁽⁴⁾*Institute of Particle and Nuclear Studies, High Energy Accelerator Research Organization (KEK), 1-1 Oho, Tsukuba Ibaraki 305-0801, Japan*

⁽⁵⁾*Heavy Ion Cancer Therapy Center, National Institute of Radiological Sciences, 4-9-1 Anagawa, Inage Chiba 263-855, Japan*

For over a decade, we have developed super long-lived carbon stripper foils of 1-50 $\mu\text{g}/\text{cm}^2$ thickness by the heavy ion beam sputtering method. Foils of this thickness are mainly used for heavy ion beams of 100 ~ 200 keV/u. Recently, high energy negative proton and heavy ion accelerators have started to use carbon stripper foils of over 100 $\mu\text{g}/\text{cm}^2$ in thickness. However, the heavy ion beam sputtering method was unsuccessful in production of foils thicker than 50 $\mu\text{g}/\text{cm}^2$ as resulted in the collapse of carbon particles from substrates during sputtering process. The reproduction probability was less than 25%. The samples of the carbon foil received had surface defects. However, the defects were eliminated by introduction of a substrate heater during sputtering process. In this manuscript we describe a highly reproducible method for thick carbon stripper foils by a heavy ion beam sputtering with krypton and xenon gases.

Detection of Special Nuclear Materials with the Associate Particle Technique

Cedric Carasco¹, Clément Deyglun¹, Bertrand Pérot¹, Stéphane Normand², Guillaume Sannicé², Karim Boudergui²,
Gwenolé Corre², Vladimir Kondrasovs², Philippe Pras³

⁽¹⁾CEA, DEN, Commissariat à l'Energie Atomique, Centre d'Etudes Nucléaires de Cadarache, Saint Paul Lez Durance 13108, France

⁽²⁾CEA, DRT, Commissariat à l'Energie Atomique, Centre d'Etudes Nucléaires de Saclay, Saclay 91400, France

⁽³⁾CEA, DAM, Commissariat à l'Energie Atomique, Centre d'Etudes Nucléaires de Bruyères le Châtel, Arpajon 91297, France

In the frame of the French trans-governmental R&D program against CBRN-E threats, CEA is studying the detection of Special Nuclear Materials (SNM) by neutron interrogation with fast neutrons produced by a sealed tube neutron generator. The deuterium-tritium fusion reaction produces an alpha particle and a 14 MeV neutron almost back to back. The principle of the Associated Particle Technique is to tag neutron emission, both in time and direction, with an alpha particle position-sensitive sensor embedded in the generator. After each fission induced by a tagged neutron in the SNM, several prompt neutron and gamma rays are detected in coincidence with the alpha particle in an array of plastic scintillators. To increase the selectivity between nuclear and benign materials, cross talk between adjacent plastic scintillators is filtered out. Indeed it produces false coincidences similar to fission events. We will present calculations performed with the MCNP-Polimi Monte Carlo code and with a post processing software developed with the ROOT package, showing the capability of the system to discriminate between SNM and benign materials such as iron and lead. The random noise due to accidental coincidences (not uncorrelated with the alpha particle) is taken into account in the calculation, as well as counting statistics to simulate realistic performances of the test bench under development by CEA laboratories.

IAEA Activities on Accelerator based Technologies and Applications

Françoise mulhauser, aliz simon, ralf kaiser, andrej zeman, danas ridikas
International Atomic Energy Agency, Vienna International Centre, Vienna A-1400, Austria

Accelerators can provide some of the best analytical techniques and applications in a diverse range of fields such as materials science, environmental science, cultural heritage and the biosciences. The effective utilization of accelerators is being promoted through participation in knowledge building activities, the development and application of innovative nuclear science, and the development of innovative nuclear energy systems. These areas offer a broad spectrum of activities for the development, and new applications of accelerators and accelerator based techniques.

This presentation will describe the latest developments as supported by the IAEA in the field of low-energy accelerators, especially the use for cultural heritage and material science, for medium energy accelerators and their use for the effective production of neutrons as well as material research. The main emphasis of the work of the IAEA is on training and education. In the field of education the IAEA is working together with the Abdus Salam International Center of Theoretical Physics (ICTP), Trieste, Italy. The new requirements on structural materials for fission and fusion request the use of accelerators and new modelling efforts. The IAEA has coordinated research projects on this topic, but would like to increase their efforts, on request by the Member States.

The IAEA has initiated several projects which outcomes are the strengthening of the nuclear technology contributions. Three main efforts should be highlighted: the training and qualification of a highly educated nuclear workforce using accelerators, the use of accelerators for materials research, and the development of innovative nuclear energy systems utilizing accelerators.

Strong-focusing 800 MeV cyclotron for high-current applications

Peter McIntyre¹, Saeed Assadi¹, Karie Badgley¹, Justin Comeaux¹, Joshua Kellams¹, Thomas Mann², Al McInturff¹,
Nathaniel Pogue¹, Akhdiyor Sattarov¹

⁽¹⁾Physics, Texas A&M University, College Station TX 77843, United States

⁽²⁾APS, Argonne National Lab, Argonne IL 60439, United States

A superconducting strong-focusing cyclotron (SFC) is being developed for high-current applications. It incorporates four innovations. Superconducting quarter-wave cavities are used to provide >20 MV/turn acceleration. The orbit separation is thereby opened so that bunch-bunch interactions between successive orbits are eliminated. Quadrupole focusing channels are incorporated within the sectors so that alternating-gradient strong-focusing transport is maintained throughout. Dipole windings on the inner and outer orbits provide enhanced control for injection and extraction of bunches. Finally each sector magnet is configured as a flux-coupled stack of independent apertures, so that any desired number of independent cyclotrons can be integrated within a common footprint.

Preliminary simulations indicate that each SFC should be capable of accelerating 10 mA CW to 800 MeV with very low loss and >50% energy efficiency. A primary motivation for SFC is as a proton driver for accelerator-driven subcritical fission in a molten salt core. The cores are fueled solely with the transuranics from spent nuclear fuel, and the beams from one SFC stack would destroy all of the transuranics and long-lived fission products that are produced by a GWe fission power reactor [1]. This capability offers the opportunity to close the nuclear fuel cycle and provide a path to green nuclear energy.

Neutronics and molten salt chemistry for accelerator-driven subcritical fission to close the nuclear fuel cycle

Akhdiyor Sattarov⁴, Elizabeth Sooby⁴, Michael Simpson³, Pavel Tsevkov², Marvin Adams², Supathorn Phongikaroon¹,
 Karie Badgley⁴, Peter McIntyre⁴, Prabhat Trepthy³, James Gerity⁴

⁽¹⁾Chemical Engineering, University of Idaho, Idaho Falls ID 83402, United States

⁽²⁾Nuclear Engineering, Texas A&M University, Spence St., College Station TX 77843, United States

⁽³⁾Idaho National Lab, P.O. Box 1625, Idaho Falls ID 83403, United States

⁽⁴⁾Physics, Texas A&M University, Spence St., College Station TX 77843, United States

The neutronics and core chemistry are presented for accelerator-driven subcritical fission in a molten salt core (ADSMS). The core is fueled solely with the transuranics and long-lived fission products from spent nuclear fuel. The neutronics and salt chemistry are optimized to destroy the transuranics by fission and the long-lived fission products by transmutation. The cores are driven by proton beams from a strong-focusing cyclotron stack, described in a separate paper. One such ADSMS system can destroy the transuranics and long-lived fission products and in the spent nuclear fuel produced by a GWe power reactor. It uniquely provides a method to close the nuclear fuel cycle for green nuclear energy.

Digital front-end electronics for a Tagged Neutron Inspection System

Davide Cester¹, Giancarlo Nebbia², Luca Stevanato¹, Giuseppe Viesti¹

⁽¹⁾*Dipartimento di Fisica ed Astronomia, Università di Padova, via Marzolo 8, Padova PD 35131, Italy*

⁽²⁾*Sezione di Padova, INFN, via Marzolo 8, Padova PD 35131, Italy*

In recent years a number of instruments based on the tagged neutron inspection technique have been developed i.e. the Euritrack portal [1] or the SMANDRA system [2]. For such systems it is mandatory to acquire the gamma ray spectra measured around the sample in coincidence with the associated alpha particle detected inside the neutron generator. The alpha-gamma time-of-flight is used to reconstruct the position of the inspected voxel. In the EURITRACK system a conventional VME was used, employing discriminators (CFTD), charge to digital converter (QDC) and time to digital converters (TDC) [3]. The development of fast digitizers offers the opportunity of deriving all information from the digitized signals, as done in the SMANDRA system.

We are presenting here a simple VME front-end electronics employing 3 FADC units (CAEN V1720 8 Channel 12bit 250 MS/s Digitizer) in which coincidence spectra are provided between two inputs in each card. This means that the system can host up to 21 independent detectors (7 per card) in coincidence with an alpha particle signal as trigger in each card. The coincident data are written in list mode and a specialized software checks the coincidence and builds the time-of-flight and energy spectra.

Different tests will be reported with detectors boosted up to the high count rates characteristic of this application.

[1] B. Perot et al., Nucl. Instr. Meth. B 261 (2007) 295.

[2] D. Cester et al., IEEE Proceedings of the 2011 2nd International Conference on Advancements in Nuclear Instrumentation, Measurement Methods and their Applications.

[3] M. Lunardon et al., Nucl. Instr. Meth. B 261 (2007) 391.

Measurements of Neutron Fluence from a Secondary Neutron Converter Irradiated with an 8 MeV Bremsstrahlung Pulsed Power Accelerator Beam

Lee J. Mitchell¹, Anthony L. Hutcheson¹, Bernard F. Philips¹, Eric A. Wulf¹, Chul S. Gwon¹, Jacob C. Zier²,

Joseph W. Schumer², Robert J. Commisso², Richard S. Woolf³, Frank C. Young⁵, Lori Jackson⁴, Stuart L. Jackson²

⁽¹⁾*Space Science Division - Radiation Detection Section, Naval Research Laboratory, 4555 Overlook Ave. S.W., Washington D.C. 20375, United States*

⁽²⁾*Plasma Physics Division, Naval Research Laboratory, 4555 Overlook Ave. S.W., Washington D.C. 20375, United States*

⁽³⁾*National Research Council, 500 Fifth St. N.W., Washington D.C. 20001, United States*

⁽⁴⁾*Praxis, Richmond Highway, Suite 700, Alexandria VA 22303, United States*

⁽⁵⁾*Consultant, L-3 Services, 3750 Centerview Dr., Chantilly VA 20151, United States*

The Mercury facility at the Naval Research Laboratory in Washington D.C., an 8 MV, 200 kA pulsed accelerator was used to produce ~50 ns intense bremsstrahlung pulses. A 10 cm thick by 33 cm diameter container of D₂O (heavy water) was placed in front of the beam and used as a neutron converter for the development of an intense pulsed mixed beam gamma and neutron source. Neutron fluence measurements were made by measuring the resulting neutron activation of 2.5 cm x 9.5 cm aluminum pucks placed near the D₂O converter with four 100% relative efficient high purity germanium detectors. The angular and linear response of the pulsed neutron burst in the presence of no target, a Pb surrogate, and depleted uranium was measured. The reactions of ²⁷Al(n,p)²⁷Mg with a threshold of approximately 1.1 MeV and the thermal neutron capture reaction of ²⁷Al(n,γ)²⁸Al were used to gauge the neutron fluence in two energy regimes. Monte Carlo simulations of the experimental setup were performed to determine the angular response of the neutron energy distribution in 2° bins. Simulations show a neutron energy spectrum with peak intensity near that of thermal neutrons. These spectra were then used to calculate a weighted cross section from the reactions. In the forward direction this was calculated to be 0.02 mb for the ²⁷Al(n,p)²⁷Mg reaction and 57 mb for the ²⁷Al(n,γ)²⁸Al. Accounting for germanium detector efficiency, absolute neutron fluences were determined from the weighted cross sections at the various puck positions. Based on the activation results, peak neutron fluences of 1.5x10¹¹ neutrons/sr were generated in the forward direction. Results show a steep decrease in fluence up to 100 cm from the source after which the fluence becomes fairly constant in intensity out to 200 cm. The angular dependence measured out to 60° was nearly uniform.

Neutronics of accelerator-driven subcritical fission for burning transuranics in used nuclear fuel

Akhdiyor I. Sattarov

Physics & Astronomy, Texas A&M University, College Station TX 77843, United States

A collaboration has been formed to develop accelerator-driven subcritical fission in a molten salt (ADSMS) core as a method to destroy the transuranics (TRU) contained in used nuclear fuel (UNF). The ADSMS core operates with criticality $k_{eff} = 0.96$; spallation of an 800 MeV proton beam to produce the balance of fast neutrons to sustain fission. The core neutronics is designed to achieve isoburning - all of the TRU isotopes are destroyed in the same proportion that they are produced in the thermal reactor of a PWR power station. The neutronics calculations, the fuel cycle over a century of operation, and the resulting 104 reduction in radiotoxicity of UNF will be presented.

TUE-ECR05-P1

#285 - Poster - Tuesday 5:30 PM - Rio Grande

Characterization of a Field Ionizing Charged Particle Source

Jordan W Watkins, Jose L Pacheco, Duncan L Weathers

Ion Beam Modification and Analysis Laboratory, University of North Texas, Department of Physics, 1155 Union Circle, #311427, Denton TX 76203, United States

High quality charged-particle beams obtained using a field-emission source can be used for plasma diagnostics or as ions sources for electrostatic accelerators. Also, in applications where differential pumping is not an option, the field-emission source can be employed because it is inherently ultra-high vacuum-compatible. A field-emission source capable of producing a bright, low-divergence electron beam has been designed and built. It is designed so that the spacing between the emitting tip and extraction electrode can be varied to maximize emission and optimize beam characteristics. The source design allows not only for electron emission, but with the introduction of a gas, could also produce ion emission. The design and initial characterization of the source performance are discussed, including optimal tip-electrode geometry, operating potentials, and conditioning procedures.

TUE-ECR05-P2

#299 - Poster - Tuesday 5:30 PM - Rio Grande

Effect of solenoid magnetic field on drifting laser plasma

Kazumasa Takahashi¹, Masahiro Okamura²

⁽¹⁾*Department of Energy Sciences, Tokyo Institute of Technology, 4259, Nagatsuta, Midori-ku, Yokohama 226-8502, Japan*

⁽²⁾*Collider-Accelerator Department, Brookhaven National Laboratory, 5th Ave. Bldg 930, Upton New York 11973, United States*

A laser ion source can provide various heavy ions using a simple apparatus. The ion beam extracted from a laser ablation plasma has high current and short pulse duration. The beam pulse length can be controlled by changing the plasma drift length between the surface of the target and the ion beam extraction point. However, the current decreases drastically due to three-dimensional expansion of plasma as the drift length becomes long. Longitudinal magnetic field during transportation of plasma can limit the expansion to transverse direction. Therefore, if the confinement technique with the magnetic field is applied to laser ion sources, increase of charge per pulse and extension of pulse length on keeping high current are expected.

To understand the fundamental effect of magnetic field on a drifting pulse plasma, we investigated behavior of ion beam currents extracted from a laser ablation plasma injected into magnetic field generated by a solenoid coil. Plasma was produced by Nd-YAG laser which has 850 mJ and 6ns pulse length. Ion beam currents were measured with a Faraday cup. We scanned the strength of magnetic field (~several hundreds gauss) and length of solenoid coil (50cm~3m) with various target material (Al, Cu, Ag, Au). In the conference, these effects on the beam current will be described.

Phase and Structured Stability in Ferritic Alloy 14YWT under High-dose Ion Irradiation

Yanwen Zhang¹, Zihua Zhu², Chad Parish¹, Philip D. Edmondson^{1,3}, Vaithiyalingam Shutthanandan², Michael Miller¹

⁽¹⁾Materials Science and Technology Division, Oak Ridge National Laboratory, Oak Ridge TN 37831-6136, United States

⁽²⁾Environmental Molecular Sciences Laboratory, Pacific Northwest National Laboratory, Richland WA 99352, United States

⁽³⁾Department of Materials, University of Oxford, Oxford OX1 3PH, United Kingdom

Increasing energy needs and the recent disaster at Fukushima nuclear power plants raises high demands for nuclear industry, structural materials in advanced nuclear reactor components and fuel cladding must demonstrate long-term stability and tolerance to high irradiation dose over extended lifetimes. Nanostructured Ferritic Alloys represents a new class of oxide dispersion strengthened steels. These mechanically alloyed steels containing a high density of dispersed nanoclusters have been considered as promising candidates for structural applications in future fission and fusion reactors. The highly desired strong resistance to radiation-induced property degradation is generally attributed to the presence of highly dispersed and stable oxide nanoparticles or solute nanoclusters.

Ion irradiation, due to much higher achievable dose rates than in nuclear reactors, can be used to simulate conventional collision-cascade damage to high doses across a wide range of temperatures over reasonable laboratory timescales and, therefore, provides an effective approach to evaluate the lifetime performance of materials in neutron irradiation environments. In this study, nanostructured ferritic alloy 14YWT samples were irradiated by 10 MeV Au/Pt to a penetration depth of $\sim 1.5 \mu\text{m}$ and doses up to $\sim 500 \text{ dpa}$ between -100 and 750°C . Heavy ions are used to maximize the deposited energy and minimize the ion content for a given displacement damage level. The irradiation-induced redistribution of Cr, W, C, N, O, Ti and Y and the response of the microstructure to high doses were characterized by complementary techniques of electron microscopy, atom probe tomography, and secondary ion mass spectrometry. Nanocluster stability in 14YWT under high-dose ion irradiation is evaluated. Significant change of Ti, Y and O are detected in the irradiated region that can be related to the predicted displacement and Au profiles. The radiation-induced modification needs to be taken into consideration for the structural stability evaluation of 14YWT in reactor environments.

Three-dimensional characterization of Au-implanted MBE grown CeO₂ thin films for plasmonic based chemical sensors

Arun Devaraj¹, Manjula I Nandasiri^{1,2}, N Joy³, T Varga¹, V Shutthanandan¹, W Jiang¹, P Nachimuthu¹,
S. V. N. T Kuchibhatla, M. A. Carpenter³, S Thevuthasan¹

⁽¹⁾Environmental Molecular Science Laboratory, Pacific Northwest National Laboratory, 902 Battelle Boulevard, Richland WA 99354, United States

⁽²⁾Physics Department, Western Michigan University, Kalamazoo MI 49008, United States

⁽³⁾College of Nanoscale Science and Engineering, University of Albany-SUNY, Rensselaer NY 12144, United States

Recently, Au doped cerium oxide (CeO₂) on Al₂O₃(0001) composite has been developed as a candidate gas sensor material for the detection of H₂, CO and NO₂ in harsh environments. The fabrication of the sensor material involved initial molecular beam epitaxial growth of CeO₂ thin films on Al₂O₃(0001) substrates followed by 2.0 MeV Au²⁺ ion irradiation in a tandem accelerator with high fluence of $1 \times 10^{17} \text{ ions/cm}^2$ at 600°C . Subsequent annealing at 600°C for 10 hours in air was performed to form well defined Au nanoclusters. As-grown, irradiated, and annealed CeO₂ thin films were characterized by Rutherford backscattering spectrometry (RBS), x-ray photoelectron spectroscopy (XPS), and x-ray diffraction (XRD). The final annealed sample after gas exposure experiments was also characterized by using cross sectional TEM and atom probe tomography (APT). Based on the XRD and RBS results, microstructure of the annealed Au-CeO₂ thin film before and after gas exposure experiments were shown to be identical. Focused Ion beam system was used for cross sectional TEM and APT sample preparation by lift-out process. Laser assisted APT is a recently developed 3D characterization capability with sub-nanometer spatial resolution and ppm level chemical sensitivity. Thus, unlike XPS or RBS which are characterization techniques with a large analytical spot size, suitable for obtaining average composition depth profiles, APT provides the compositional information of buried nanoscale volumes inside a matrix. Combining these multimodal characterization results, Au nanoparticles were shown to be structurally well defined and devoid of any impurities. Also the presence of an intermixed CeAlO₃ layer was noticed between the CeO₂ thin film and Al₂O₃ substrate. Application of such multimodal characterization capabilities not only help in providing a comprehensive understanding of the structure of complex technologically important material systems, but also help in subsequent process parameter optimization to achieve optimum end performance for targeted applications.

Electronic and Ionic Conductivity Study of a $\text{Sr}_{2-x}\text{VMoO}_{6-y}$ Solid Oxide Fuel Cell Anode ($x=0.0, 0.1, 0.2$)

Nicholas Brule Childs¹, Adam Weisenstein², Camas Key¹, Richard Smith¹, Stephen Sofie²

⁽¹⁾Physics, Montana State University, EPS Building Rm 264, Bozeman MT 59717-3840, United States

⁽²⁾Mechanical Engineering, Montana State University, EPS Building Rm 264, Bozeman MT 59717-3840, United States

The solid oxide fuel cell (SOFC) has many key advantages that make it stand out in the field of fuel cells. SOFCs are suited for high efficiency power generation, fuel flexibility, high temperature electrolysis, closed loop regenerative systems (reversible power/electrolysis), oxygen generation, and carbon dioxide reduction. Most notably, SOFCs have extremely high reversible efficiencies, thus the same stack can be used effectively for both electrolysis and power mode operation. These capabilities make the SOFC highly versatile for: primary/secondary power systems, advanced life support, and in-situ resource utilization which may all be desired for a forthcoming Lunar return and Mars Exploration.

A promising anode material for a SOFCs is the double perovskite $\text{Sr}_{2-x}\text{VMoO}_{6-y}$ ($x=0.0-0.2$), due to its stability, electronic, and ionic conduction. Anodes of this material were prepared via a tape casting technique, calcined in air at 1000 oC for 6 hrs and finally sintered in a reducing environment at 1300 oC for 20 hrs. RBS and XRD were used to determine elemental composition and crystal structure respectively. Electronic and ionic conductivities of the anodes were measured as a function of temperature (25-800 oC) in a reducing atmosphere. In conjunction with the conductivity measurements, XPS was performed after annealing in a vacuum environment with a controlled pressure of 10⁻⁶ Torr H₂ to determine valence states of Sr, V and Mo. Measurements for this double perovskite material have shown excellent electronic and ionic conductivity. Electron occupation in V and Mo d-shells is thought to be the mechanism for the electronic conductivity changes, while development of oxygen vacancies in the reducing environment provide for improved ionic conductivity.

This research is funded by a Montana NASA EPSCoR grant NNX09AP73A.

RBS Investigation of Volatile Gases Produced in Solid Oxide Fuel Cell Systems

C. F. Key¹, J. Eziashi², N. Childs¹, R. J. Smith¹, P. Gannon², W. Priyantha¹, J. Regar¹, S. Sofie³, P. Gentile³

⁽¹⁾Physics, Montana State University-Bozeman, EPS Building, Bozeman MT 59717, United States

⁽²⁾Chemical Engineering, Montana State University-Bozeman, Cobleigh Hall, Bozeman MT 59717, United States

⁽³⁾Mechanical Engineering, Montana State University-Bozeman, Roberts Hall, Bozeman MT 59717, United States

Solid oxide fuel cell (SOFC) development depends greatly on the use of readily available, inexpensive materials throughout SOFC systems. Ferritic stainless steel interconnects have been considered along with aluminosilicate insulation and gas-feed tubes to meet this demand. At SOFC operating temperatures (650-1000°C) these materials exhibit degradation due to interactions with water vapor and oxygen. Gaseous Cr and Si species are produced as a result that have been shown to form insulating phases in electrochemically active sites, limiting cell lifetime and performance.

A novel transpiration experiment has been developed to quantify the amount of volatile Cr and Si gases generated by these systems in a high temperature SOFC gas environment. Chemical reactions are facilitated by flowing humidified air or forming gas (5% H₂, N₂ balance) through quartz or aluminosilicate tubes and over samples located at the central hot-zone of the tube furnace. Downstream from the samples vapors are condensed on the surface of silicon or glassy carbon wafers mounted on a water-cooled heat-sink. Rutherford backscattering spectrometry (RBS) using a 2MV Van de Graaff accelerator is performed to determine the areal density (atoms/cm²) of Cr or Si atoms collected on the wafer. This density can then be converted to the total amount of Cr or Si on the wafer by knowing the area of the collecting surface and assuming uniform coverage over that area. During the course of an experiment wafers can be easily removed and replaced with new wafers, allowing one to monitor how volatility rates change with time.

Work supported under DOE SECA Cooperative Agreement No. DE-FC26-05NT42613 and NASA EPSCoR NNX09AP73A.

Electronic stopping power for heavy ions in silicon dioxide

Ke Jin¹, Yanwen Zhang^{1,2}, William J Weber^{1,2}

⁽¹⁾Department of Materials Science & Engineering, University of Tennessee, Knoxville TN 37920, United States

⁽²⁾Materials Science & Technology Division, Oak Ridge National Laboratory, Oak Ridge TN 37831, United States

Silicon dioxide (SiO₂) is widely used in electronic, nuclear and space applications. Accurate information of electronic stopping power is crucial to not only precisely control the dopant concentration over well defined depth distribution but also provide predictive performance models for materials under harsh environment. However, measuring electronic stopping power for heavy ions in materials is a long standing challenge. In this work, electronic stopping powers for ³⁵Cl, ⁸⁰Br, ¹²⁷I, and ¹⁹⁷Au ions in SiO₂ are measured in continuous medium energy range from 3 to 18 MeV based on a single ion technique utilizing a high-resolution time-of-flight spectrometer and a silicon detector. It is indicated that the predictions from the Stopping and Range of Ions in Matter (SRIM) code which has been widely used for decades underestimate the electronic stopping powers for heavy ions with energies over 30keV/u. The electronic stopping power for Au ions in silicon carbide (SiC) is also studied, Rutherford backscattering spectrometry (RBS) and secondary ion mass spectrometry (SIMS) are applied to measure the depth profiles of implanted ions in 6H-SiC with energies from 700 keV to 15 MeV.

The measured projectile ion ranges exhibit large discrepancies with SRIM predictions but agree well with the predictions based on the combination of measured stopping powers at medium energies and reciprocity theory predicted electronic stopping powers at low energy range. These results indicate that improved models and predictions for the electronic stopping power are necessary for more reliable predictions on damage and ion profiles.

High Resolution Depth Profiling using a Combination of Atom Probe Tomography and High-resolution Rutherford Backscattering Spectrometry

V Shutthanandan¹, Fang Liu², Huang Li², C M Wang¹, D K Schreiber³, D E Perea¹, A Devaraj¹, SVNT Kuchibhatla⁴, R F Davis², L M Porter², S Thevuthasan¹

⁽¹⁾EMSL, PNNL, Box 999, MSIN K8-93, Richland WA 99352, United States

⁽²⁾Department of Materials Science and Engineering, Carnegie Mellon University, 5000 Forbes Ave., Pittsburgh PA 15213, United States

⁽³⁾PNNL, Box 999, Richland WA 99352, United States

⁽⁴⁾Battelle Science and Technology India, MH-411057, Pune, India

Despite the significant improvements in instrumentation in the recent past, characterizing interfaces with ultra-high resolutions still poses challenges to research community as a result of inherent shortcomings in various techniques. In this context, it is imperative to intelligently combine more than one analytical technique and as appropriate use new techniques with improved spatial and chemical resolutions (better chemical sensitivity and improved mass resolution) to achieve such a goal. EMSL at Pacific Northwest National Laboratory has been focusing on "integrating multiple techniques to understand the otherwise impossible complex material systems". Laser assisted Atom Probe Tomography (APT), a relatively new addition to the surface and interfacial analysis suite at EMSL, is capable of providing 3D-chemical images of various materials including multi-layer thin films with sub-nanometer spatial and a ppm level chemical resolution.

The convergence of information from various analytical techniques, while highlighting the unique features that 3D-chemical imaging with atom probe tomography can offer, to study nanoscale interfaces is the focus of this study. Multi-quantum well (MQW) structures consisting of GaN, InGaN multi-layers, are prepared using metal-organic chemical vapor deposition. The microstructural and compositional information of the MQW structures is quite essential to understand and improve the efficiency of green LEDs. High-resolution scanning transmission electron microscopy (HRSTEM), high-resolution Rutherford backscattering spectrometry (HRRBS) and APT have been used to analyze these MQW structures. Information such as layer thickness, elemental composition, diffusion of elements across interfaces and interfacial roughness/mixing have been studied in detail. The concentration profiles obtained from atom probe tomography will be compared with high-resolution Rutherford backscattering spectrometry data to confirm the nature of the interfaces. Layer thickness values obtained from APT are compared to those from HRSTEM and HRRBS data.

Energy loss of proton beams in biological materials

Rafael Garcia-Molina¹, Isabel Abril², Pablo de Vera², Ioanna Kyriakou³, Dimitris Emfietzoglou³
⁽¹⁾*Departamento de Física - Centro de Investigación en Óptica y Nanofísica, Universidad de Murcia, Murcia, Spain*
⁽²⁾*Departament de Física Aplicada, Universitat d'Alacant, Alacant, Spain*
⁽³⁾*Medical Physics Laboratory, University of Ioannina, Medical School, Ioannina, Greece*

We study the energy deposited by swift proton beams on materials of biological interest, such as liquid water, DNA and PMMA. An appropriate description of the target Energy Loss Function (ELF), which provides its electronic excitation spectrum, is obtained from experimental optical data properly extended to non vanishing momentum transfers. The main magnitudes characterizing the stopping of the projectile with the biological media are calculated analytically (in the dielectric formalism framework) and compared with available experimental data. The differences of the proton stopping in several biological targets are discussed.

The spatial distribution of the delivered energy by a proton beam is evaluated by the code SEICS (Simulation of Energetic Ions and Clusters through Solids), which combines molecular dynamics and Monte Carlo techniques and includes the main interaction phenomena between the projectile and the target constituents. The proton energy-distribution at several depths in these biological materials is also simulated as well as the evolution of the beam energy and its geometrical dispersion.

Bridging the Gap between the Quasi-Molecular-Orbital World and Perturbative Ion-Energy-loss Treatments

Gregor Schiwietz¹, Pedro Luis Grande²
⁽¹⁾*Institute G-I2, Helmholtz-Zentrum Berlin für Materialien und Energie GmbH, Hahn-Meitner-Platz 1, Berlin Berlin 14109, Germany*
⁽²⁾*Inst. de Física, Universidade Federal do Rio Grande do Sul, Caixa Postal 15051, Porto Alegre RS 91500-970, Brazil*

Investigations of the energy losses of charged particles interacting with gases and solids started about a century ago. A profound qualitative knowledge on inelastic processes of charged particles in matter has evolved since then [1]. Classical and quantum effects have been investigated for the adiabatic low-energy limit as well as in the asymptotic (perturbative) high-energy limit. Intermediate energies are most important for applications, however, but turn out to be most problematic from the theoretical point of view.

Here we will show, using the UCA (unitary convolution approximation) stopping-power model, that it is possible to predict energy losses to localized-electron systems for ions of some 10 keV/u up to relativistic speeds. Starting from quantum perturbation theory of excitation and ionization and including various correction terms as well as electron-capture processes, all important energy-loss mechanism are considered. Reasonable precision is reached even for specific details, such as non-equilibrium charge states, channeling or backscattering [2,3].

[1] P.L. Grande and G. Schiwietz; in "Advances in Quantum Chemistry", Vol. 45, pp.7-46 (book article ed. by J. Sabin, 2004, Elsevier Inc.)

[2] G. Schiwietz and P.L. Grande; Nucl. Instr. Meth. B273, 1-5 (2012)

[3] G. Schiwietz and P.L. Grande; Phys.Rev. A84, 052703 (2011)

Quantitative analysis of ultra thin layer growth by Low Energy Ion Scattering

Daniel Primetzhofer^{1,2}, Dominik Goebel¹, Wolfgang Roessler¹, Peter Bauer¹

⁽¹⁾*Institut fuer Experimentalphysik, Johannes Kepler University, Altenberger Strasse 69, Linz 4040, Austria*

⁽²⁾*Institutionen för Fysik och Astronomi, Uppsala Universitet, Box 516, Uppsala S-751 20, Sweden*

The potential of low energy ion scattering (LEIS) for quantitative analysis of nanometer layers is highlighted. With noble gas ions at energies of several keV the use of spectrometers leads to an information depth close to one monolayer [1]. To obtain subsurface information, scattered neutrals may be detected by TOF-LEIS. Since 1 - 2 keV H or He ions are slow, monolayer depth resolution can easily be reached. A further advantage of TOF-LEIS is that the spectrum can be recorded simultaneously in a broad range, with very low damage to the sample. To some extent, quantification is a challenge, since for this purpose electronic stopping has to be known, and the influence of multiple scattering must be taken into account properly. The former may be an excessive demand for available stopping power tabulations, since band structure effects may lead to pronounced deviations from velocity proportionality [2]. The latter is in principle possible since the scattering potential is known sufficiently well, but cannot be done analytically. Therefore, simulations must be performed which allow for multiple scattering and include realistic electronic stopping [3] to quantitatively model the nanometer film of interest on the basis of the information deduced from the measured TOF-LEIS spectrum.

We present some recent applications of TOF-LEIS in studies of the properties of nanometer films, like growth of Au on boron [4] and of Ag on PET. Additionally, results on nanometer layers of metals and oxides on various substrates are shown.

[1] HH. Brongersma et al., Surface Science Reports 62, 3, 63-109 (2007).

[2] J. E. Valdés et al., Phys. Rev. A49 (1994) 1083.

[3] J.P. Biersack et al., Nucl. Instr. & Meth. B61 (1991) 77.

[4] D. Primetzhofer, S. N. Markin, P. Zeppenfeld and P. Bauer, S. Prusa, M. Kolibal, and T. Sikola, Appl. Phys. Lett. 92 (2008) 011929.

A simple approach for simulating the 2D MEIS spectrum in crystalline materials

A. Hentz¹, D. P. Woodruff²

⁽¹⁾*Instituto de Física, Universidade Federal do Rio Grande do Sul, Av. Bento Gonçalves, 9500, Porto Alegre RS 91501-970, Brazil*

⁽²⁾*Physics Dept, University of Warwick, Gibbet Hill Road, Coventry CV4 7AL, United Kingdom*

We have recently shown [1] the effect of trajectory-dependent energy-loss in Medium Energy Ion Scattering (MEIS) experiments for the clean Cu(111) surface under shadowing/blocking conditions. Specifically, the results show the influence of "skimming" trajectories suffered by ions scattered from sub-surface layers and emerging close to a blocking dip after passing close to near-surface atoms. One key component of this previous result was the use of the impact-parameter dependent energy-loss distribution called *Coupled-Channel* calculations. However the Coupled-channel calculations are computationally very time-consuming and their use requires one to deal with large tables of data (energy-loss distributions as a function of ion and target atomic species, ion energy, and impact parameter). In the present work we have tackled this issue by using an analytical asymmetric distribution function, called EMG -Exponentially Modified Gaussian [2], to model the energy-loss distribution according to the results from *ab-initio* calculations as well as from experimental data [3,4]. This information is used in a modified version of the standard VEGAS program to predict the scattered ion energy spectrum, as a function of scattering angle for a specific incidence direction at a crystalline surface.

Here we present the results of a combined experimental and theoretical investigation that shows direct experimental evidence of the influence of trajectory-dependent inelastic energy-loss in the detected energy of ions back-scattered from the outermost few atomic layers of a single crystal. We demonstrate this effect can be correctly modeled computationally, by comparing the simulated spectra for analytical (EMG fitting) and calculated (Coupled-channel calculations) energy-loss distributions.

[1] A. Hentz, et al. Phys. Rev. Lett. 102 (2009) 096103.

[2] P.L. Grande, et al. Nucl. Instr. And Meth. B 256 (2007) pp 92-96.

[3] A. Hentz, et al. Phys. Rev. B 74 (2007) 125408.

[4] M. Hazama, et al. Phys. Rev. B 78 (2008) 193402.

The energy loss straggling of ions in matter

Claudia C Montanari, Jorge E Miraglia

Institute of Astronomy and Space Physics, Consejo Nacional de Investigaciones Científicas y Tecnológicas and University of Buenos Aires, IAFE, Buenos Aires 1428, Argentina

The energy loss straggling is an interesting parameter for the theoretical study. It represents a sensitive input for many calculations and computer simulations for material analysis of technological and biological interest (SIMNRA, SEICS) [1,2]. The straggling in the energy loss is statistical: when swift charged particles penetrate matter, they lose energy in a great number of collisional events, giving rise to the dispersion in the ion energy loss spectrum. However, experimental measurements include also roughness-inhomogeneity contribution [3-4], clear in some data [5]. Since 1980, measurements began to take this effect into account [6], both in the sample preparation and in the final values. There are a great number of recent measurements from different laboratories and techniques that show less spread and a tendency to a single band.

In this contribution we present theoretical results using a collective model, the SLPA [7], for different ions and targets, together with a comparison with the available data. A scaling of the square energy loss straggling normalized to Bohr high energy limit is proposed, which allows to represent the straggling data and theoretical curves for different ions (H to B) and targets (Cu to Bi), is almost a single curve, and introduces the possibility of a simple universal function for the energy loss straggling.

- [1] M Mayerl, Nucl. Instrum. Methods. Phys. Res. B **194**, 177 (2002)
- [2] R Garcia-Molina *et al*, Phys. Med. Biol **56**, 6475 (2011)
- [3] Y Kido, Phys. Rev. B **34**, 73 (1986)
- [4] J C Eckardt and G. H. Lantschner, Thin Solid Films **249**, 11 (1994)
- [5] Q Yang *et al*, Nucl. Instrum. Methods. Phys. Res. B **61**, 149 (1991)
- [6] F Besenbacher *et al*, Nucl. Instrum. Methods **168**, 1 (1980)
- [7] C C Montanari *et al*, Phys. Rev. A **75**, 022903 (2007); Phys. Rev. A **79**, 032903 (2009)

Barkas effect in stopping power and energy-loss straggling for dressed projectiles

Claudio Archubi¹, Isabel Abril², Rafael Garcia-Molina³, Néstor R. Arista⁴

⁽¹⁾*Departamento de Física, Universidad de Buenos Aires, Buenos Aires, Argentina*

⁽²⁾*Departament de Física Aplicada, Universitat d'Alacant, Alacant, Spain*

⁽³⁾*Departamento de Física - Centro de Investigación en Óptica y Nanofísica, Universidad de Murcia, Murcia, Spain*

⁽⁴⁾*Centro Atómico Bariloche and Instituto Balseiro, Comisión Nacional de Energía Atómica, San Carlos de Bariloche, Argentina*

The deviation in the stopping power from the quadratic dependence on projectile charge predicted by the Bethe theory [1], called Barkas effect, was first experimentally measured by Barkas and co-workers [2] as a difference in the penetration range for positive and negative pions in matter. During the last four decades an important collection of theoretical studies has been developed to explain the Barkas effect. However, all these analysis were made assuming bare projectiles. On the other hand, it is well known that the degree of ionization of a projectile depends on its velocity [3]. Therefore, the effect of the bound electrons in the energy loss of an ion must be considered at low and intermediate velocities.

In this work we evaluate the Barkas effect in the stopping power and the energy-loss straggling for dressed projectiles moving in a free electron gas. The projectile trajectories were calculated by a numerical simulation, where the potential is described by a sum of two Yukawa potentials related to the screening of the projectile by the electron gas and the binding electrons. Then, following the classical model of the transport cross section [4], we calculate the Barkas factor for H, He, Li and C projectiles in an Al target in a wide velocity range. Applying a scaling law analogous to that proposed by Lindhard [5] for bare projectiles, we conclude that the Barkas factor increases with the degree of ionization for low and intermediate velocities.

- [1] H. Bethe, Ann. Phys. 5 (1930) 325.
- [2] W.H. Barkas *et al*, Phys. Rev. 101 (1956) 778; Phys. Rev. Lett. 11 (1963) 26.
- [3] W. Brandt, M. Kitagawa, Phys. Rev. B 25 (1982) 5631.
- [4] N.R. Arista, P.L. Grande, A.F. Lifschitz, Phys. Rev. A 70 (2004) 042902.
- [5] J. Lindhard, Nucl. Instr. and Meth. 132 (1976) 1.

Energy distributions of proton beams interacting with multi-walled carbon nanotubes

Rafael Garcia-Molina¹, Jorge E. Valdés^{2,3}, Carlos Celedón², Rodrigo Segura^{2,5}, Cristian D. Denton³, Néstor R. Arista⁴,
Patricio Vargas², Isabel Abril³

⁽¹⁾*Departamento de Física - Centro de Investigación en Óptica y Nanofísica, Universidad de Murcia, Murcia, Spain*

⁽²⁾*Departamento de Física-Laboratorio de Colisiones Atómicas, Centro para el Desarrollo de la Nanociencia y la Nanotecnología, Centro de Nanociencia de Valparaíso, Universidad Técnica Federico Santa María, Valparaíso, Chile*

⁽³⁾*Departament de Física Aplicada, Universitat d'Alacant, Alacant, Spain*

⁽⁴⁾*División Colisiones Atómicas, Centro Atómico de Bariloche, San Carlos de Bariloche, Argentina*

⁽⁵⁾*Departamento de Química y Bioquímica, Universidad de Valparaíso, Valparaíso, Chile*

The irradiation with energetic proton beams impinging normal to the axis of a multi-walled carbon nanotube (MWCNT) is studied, both experimentally and by simulations. The proton energy distribution measurements were performed after the protons have passed through the nanotubes, for proton beam with incident energies less than 10 keV. Nanotubes samples were dispersed and supported on a holey amorphous carbon (a-C) coated TEM grid. The simulation followed the trajectories of each projectile by solving its classical equation of motion, where the electronic structure of the nanotube and the stopping force was obtained through ab-initio models and the local density approximation.

The experimental energy spectra in the forward direction show two well differentiated peaks, whose origin is elucidated by using the simulation of the proton trajectory through the nanotube. We conclude that only protons that travel in quasi-planar channeling between the outer walls of the MWCNT are detected, due to small angular deflections. The low-energy loss peak comes from MWCNTs lying on the holes of the a-C substrate, whereas the high energy-loss peak originates mainly in the MWCNTs supported on the a-C substrate.

Medium Energy Ion Scattering applied to investigate planar buried nanostructured systems

Dario Sanchez¹, Flavio Luce¹, Mauricio Sortica¹, Francio Rodrigues¹, Jerome Leveneur², John Kennedy²,
Pedro Luis Grande¹, Paulo Fichtner¹

⁽¹⁾*Institute of Physics, UFRGS, Av. Bento Gonçalves 9500, Porto Alegre Select State 90460-080, Brazil*

⁽²⁾*National Isotope Centre, GNS Science, 30 Gracefield Road, Lower Hutt Select State, New Zealand*

Medium energy ion scattering (MEIS) is an ion beam characterization technique capable to determine with subnanometric depth resolution elemental composition and concentration-depth profiles in thin films. Also, MEIS measurements were recently used as an additional tool for the characterization of shape, composition, size distribution and stoichiometry nanoparticle (NP) systems, and also for determination of depth distributions of different elements in a single nanoparticle. Through the use of a Monte Carlo simulation and fitting software that we have developed, the PowerMeis, that considers any geometry, size distribution, composition and density of the nanostructures and also the asymmetry of the energy loss-distribution, we have explored the MEIS potentiality to investigate 2-dimensional nanostructured systems buried into a solid matrix, which has attracted interest in connection e.g. with plasmonic and magnetic applications. For both, the NP system properties are strongly dependent on size, shape, areal number density and spatial order of the NP set. In this work we show the capability of the MEIS analysis combined with synchrotron techniques and Transmission Electron Microscopy (TEM) to investigate several systems, namely: (i) a condensed arrangement of Pb nanoparticles (NPs) located under a silica layer at SiO₂/Si interface, where through TEM and Grazing Incidence X-rays Small Angle Scattering (GISAXS) the size distribution, the geometrical shape parameters and degree of organization were very well characterized, and, taken into account these features in the MEIS analysis it was obtained in additional the non-nucleated Pb distribution in the SiO₂ matrix around the NPs; (ii) a planar set of Fe@Fe_x(SiO₂)_y core@shell NPs near the surface into the SiO₂, where the NPs geometrical features were characterized through TEM analysis, and the shell stoichiometry obtained combined the TEM results with the MEIS analysis.

Structural characterization of CdSeZnS quantum dots using Medium Energy Ion Scattering

Mauricio Sortica¹, Pedro Luis Grande¹, Claudio Radtke², Lais Almeida¹, Rafaela Debastiani¹, Johnny Ferraz Dias¹

⁽¹⁾*Institute of Physics, UFRGS, Av. Bento Gonçalves 9500, Porto Alegre RS 90460-080, Brazil*

⁽²⁾*Institute of Chemistry, UFRGS, Av. Bento Gonçalves 9500, Porto Alegre RS 90460-080, Brazil*

Compound quantum dots QDs are promising materials that can be used in many fields of the technological development, but the accurate knowledge of compositional depth profiling inside of them is still a technological challenge. Medium energy ion scattering (MEIS) is an ion beam analysis technique, capable of elemental depth profiling with subnanometric depth resolution. Recently, the MEIS technique was optimized for nanostructured materials analysis and became a promising tool for structural characterization inside of QDs. In this work, we use the MEIS technique to characterize a core-shell nanostructure of CdSe/ZnS QDs. The crystal size of 5.2 nm, determined by MEIS, is in good agreement with optical measurements and TEM images. The core-shell structure is resolved by the present configuration of MEIS in contrast to the present TEM measurements. The commercial CdSe/ZnS QDs has non-stoichiometric Cd and Se concentrations. The sample selected for this work have a Cd:Se ratio of 0.69:0.31. Our investigation shows that there is Cd present on the shell and the CdSe core tends to be a stoichiometric crystal. That indicates that, despite the unbalance of material, the CdSe crystal is preserved during the industrial process that allows the control of the QDs diameters. This study shows the power of the MEIS technique, that combined with other analytical techniques, is a powerful method to determine elemental distribution profiles, inside nanoparticles with diameter about 5 nanometers. This allows for studies of the formation and stability of the internal structure of the QDs when exposed to several kind of processes, like heating and ion irradiation.

Investigation of deuteron dynamic deposition and retention by in-situ NRA and ex-situ ERDA

Tieshan Wang¹, Jiangtao Zhao¹, Qiang Wang¹, Kaihong Fang¹, Mingcong Lan¹, Xinxin Xu¹, Taw Kuei Chan², Thomas Osipowicz², Jirohta Kasagi³

⁽¹⁾*School of Nuclear Science and Technology, Lanzhou University, Tianshuinan Road 222, Lanzhou Gansu 730000, China*

⁽²⁾*Center of Ion Beam Application, Department of Physics, National University of Singapore, Singapore, Singapore*

⁽³⁾*Research Center of Electron Photon Science, Tohoku University, Sendai 980-8578, Japan*

The study on micro-dynamic behavior of hydrogen isotopes in metals is always a challenge due to limitations inherent to available analytical techniques. In this work, the **in-situ** analysis with D(d,p)T reaction combined with **ex-situ** high resolution Elastic Recoiled Detection Analysis (ERDA) are used to study the deuterium (D) micro-dynamics of deposition and retention in metals. Tungsten (W), molybdenum (Mo), beryllium (Be) and other metal (purity >99.9%) samples are investigated. D-deposition and concentration are measured by deuteron implantation and simultaneous measurement of the D-D reaction in the energy region below 20keV. The proton (p) and triton (t) yields from D(d,p)T are used to monitor in real-time D-concentrations in targets. A dynamically saturated D-concentration is been reached in each metal after a certain implantation fluence, but the saturation concentrations and the related critical fluences are material dependent, due to differences of diffusion coefficients and solubilities in the metals. Such experiments are performed with D₃⁺ beams with different energies in the range of 10~20 keV in 1.0 keV/amu steps. The saturated D-concentrations show a slight energy dependence, which is caused by the changing D-depth profile at each deuteron energy. The ratio of proton yield to triton yield (p/t-ratio) is monitored in the experiments as well. By comparing the experimental p/t-ratio with theoretical calculations that include multiple-scattering of deuterons, an approximation to the dynamical D-depth-profile is obtained at each energy point. The influence of radiation damage to the saturation D-concentration and distribution is also studied. The saturation concentration drops significantly in all metals after a certain implantation dose, but this reduction is material and fluence dependent. In order to study the D-retention after the experiments, the D-depth profile at nano-scales has been measured by high resolution ERDA. Lastly, significant deuterium loss and an inhomogenous distribution are found in the samples after one year.

H Uptake in Zr-Based Reactor Fuel Claddings Studied With ERD

Barney L. Doyle, David Enos, Shreyas Rajesekhara, Blythe G. Clark

Radiation Solid Interactions Department, Sandia National Laboratories, MS1056, Albuquerque NM 87104, United States

Zirconium-based alloys are currently the most prevalent material used as the cladding for the containment of uranium oxide nuclear fuel pellets for domestic light water reactors. While in service, hydrogen generated at the metal-solution interface diffuses into the cladding, where it can precipitate in the form of a brittle hydride, and impact mechanical properties. The Zr cladding is bombarded with high energy neutrons which cause displacement damage within the metal. This damage potentially either impedes or accelerates the accumulation of H in the cladding. A study has been undertaken at Sandia to elucidate the kinetics with which H incursion occurs in pure Zr and three common Zr alloys: Zircaloy-2, Zircaloy-4 and Optimized ZIRLO™. In this study, the H was introduced by electrochemically charging. The H accumulation rate was studied for these materials vs. displacement damage using 25 MeV Au and 34 MeV Si implants, producing dpa's ranging from 0 to 25. 10 MeV He Elastic recoil detection (ERD) and 34 MeV Si ERD were used to measure H concentration profiles vs. electrochemical charging time. TEM evaluation of the near-surface region demonstrated that hydrogen is present as a nearly continuous layer of hydride which grows into the material. Preliminary results indicate that a diffusion controlled mechanism is responsible for the incursion of H and progression of the hydride layer into these materials. The effective H diffusion coefficients through the hydrides are greatest for Zircaloy-2, lower for Zircaloy-4, and lowest for the ZIRLO. The same experiments on displacement damaged samples suggest that this damage tends to reduce the diffusion coefficients at lower damage levels (.1-1 dpa), but has little effect at higher damage levels (25 dpa).

Sandia National Laboratories is a multi-program laboratory managed and operated by Sandia Corporation, a wholly owned subsidiary of Lockheed Martin Corporation, for the U.S. Department of Energy's National Nuclear Security Administration under contract DE-AC04-94AL85000.

Accurate Determination of the Quantity of Material in Thin Films by Ion Beam Analysis

Chris Jeaynes³, Nuno P Barradas¹, E Szilagyi², Julian L Colaux³, Roger P Webb³

⁽¹⁾*Instituto Superior Tecnico/ITN, Universidade Tecnica de Lisboa, Lisbon, Portugal*

⁽²⁾*Institute for Particle and Nuclear Physics, Wigner Research Centre for Physics, Budapest, Hungary*

⁽³⁾*Surrey Ion Beam Centre, University of Surrey, Guildford Surrey GU12 5LY, United Kingdom*

Ion beam analysis (IBA) is a cluster of techniques including Rutherford and non-Rutherford backscattering spectrometry, and particle-induced X-ray emission (PIXE). Recently, the ability to treat multiple IBA techniques (including PIXE) self-consistently has been demonstrated. The utility of IBA for accurately depth profiling thin films is critically reviewed. As an important example of IBA, three laboratories have independently measured a silicon sample implanted with a fluence of nominally 5.10^{15}As/cm^2 at an unprecedented absolute accuracy. Using 1.5 MeV $^4\text{He}^+$ Rutherford backscattering spectrometry (RBS), each lab has demonstrated a combined standard uncertainty around 1% (coverage factor $k=1$) traceable to an Sb-implanted certified reference material through the silicon electronic stopping power. The Uncertainty Budget shows that this accuracy is dominated by the knowledge of the electronic stopping, but that special care must also be taken to accurately determine the electronic gain of the detection system and other parameters. This RBS method is quite general and can be used routinely, to accurately validate ion implanter charge collection systems, to certify SIMS standards, and for other applications. The generality of application of such methods in IBA is emphasised: if RBS and PIXE data are analysed self-consistently then the resulting depth profile inherits the accuracy and depth resolution of RBS and the sensitivity and elemental discrimination of PIXE.

In this presentation we will include details of how to obtain an accurate determination of (i) the machine energy, (ii) the electronic gain, and (iii) the pulse height defect correction from close analysis of calibration data using the 3038 keV resonance in the $^{16}\text{O}(\alpha,\alpha)^{16}\text{O}$ scattering cross-section function, and how this is very convenient for the RBS analysis. We will also show the construction of the Uncertainty Budget.

Implantation and characterization of helium in nuclear materials at Jannus-Saclay (France)

Lucile BECK¹, Patrick TROCELLIER¹, Sandrine MIRO¹, Sylvain VAUBAILLON², Yves SERRUYS¹

⁽¹⁾DEN-DMN-SRMP-Laboratoire JANNUS, CEA, CEA Saclay, Gif sur Yvette 91191, France

⁽²⁾INSTN-Laboratoire JANNUS, CEA, CEA Saclay, Gif sur Yvette 91191, France

The Jannus facility was recently commissioned at CEA-Saclay (France). The main goal of this project is to investigate ion irradiation damage mechanisms, synergistic effects of multi-beam irradiation and ion beam modification of materials. For that purpose, three electrostatic accelerators have been coupled in order to perform single, dual and triple beam irradiations in a dedicated triple beam chamber [1]. In addition, the facility is equipped with two lines for ion beam analysis. The complementarity of these techniques provides a relevant tool for implantation and characterization of helium in nuclear materials.

The performance of structural materials in nuclear applications is strongly influenced by the presence of helium. Helium can be produced in these materials by neutron reactions for fission reactors or by direct injection into the near surface region of the first wall for fusion reactor. As a consequence, the study of helium interactions with these materials is an important issue for present and future energy production reactors.

One of the means to study helium migration in ceramics and metals is to implant $^3\text{He}^+$ or $^4\text{He}^+$ by using ion beams. After implantation and various temperature annealing, ^3He profiles can be measured by nuclear reaction analysis using the $^3\text{He}(d, p)^4\text{He}$ reaction [2,3] and ^4He profiles by heavy ion ERDA using 15 MeV ^{16}O as incident particle. All these steps can be now performed at the JANNUS platform. In this contribution, the facility will be described, and first results of helium behaviour studies in SiC and Fe matrices will be presented.

[1] Y. Serruys *et al.*, J. Nucl. Mater 386-388 (2009) 967 - 970.

[2] S. Miro *et al.*, J. Nucl. Mater 415 (2012) 5-12.

[3] H. Lefaix-Jeuland, accepted for DIMAT proceedings (Dijon, 3-8 juillet 2011)

Ion Microscopy of Hydrogen retention in heavy metals

Katrin Peeper¹, Marcus Moser¹, Patrick Reichart¹, Elena Markina², Matej Mayer², Zhijie Jiao³, Gary Was³,
Guenther Dollinger¹

⁽¹⁾Institute for Applied Physics and Metrology, Universitat der Bundeswehr, Munich, Germany

⁽²⁾EURATOM Association, Max-Planck-Institute for Plasma Physics, Garching, Germany

⁽³⁾Nuclear Engineering and Radiological Sciences, University of Michigan, Ann Arbor, United States

Degradation of wall materials used in fission and fusion reactors due to extreme conditions and radiation is investigated in order to develop improved materials. Hydrogen plays a key role in metal embrittlement and is trapped at various natural and ion induced defects.

We present detailed study of the hydrogen retention in heavy metals in 3 dimensions and its correlation with structural features e.g. grain boundaries and blisters performed by proton-proton-scattering at the proton microprobe SNAKE. For low Z sample material like diamond, sensitivity of 5×10^{13} at/cm² is possible, resolving hydrogen enhancement even on grain boundaries of diamond [1]. High Z material is much more complex to analyse due to strong background from accidental coincidences induced by nuclear reactions.

We show that we obtain a sensitivity better than $\sim 10^{15}$ at/cm² (~ 2 at-ppm) is possible even for steel or tungsten. At SNAKE with high proton energies up to 25 MeV we are able to analyse up to 50 μm thick tungsten targets. We utilised 22 MeV protons to study hydrogen distributions in 50 μm Stainless Steel and 25 μm Tungsten samples. We irradiate the samples under conditions, which mimic the conditions in future fusion and fission reactors, blisters and cracks are created in the near-surface layer due to hydrogen-induced stress in the material. With pp-scattering at SNAKE we are able to image the damaged area and quantify the retained hydrogen.

[1] P. Reichart, *et al.* Science 306 (2004) 1537

Elastic and Inelastic Neutron Scattering Cross Sections for Fission Reactor Applications

S. F. Hicks¹, L. J. Kersting¹, P. J. McDonough¹, C. J. Lueck¹, A. J. Sigillito¹, J. R. Vanhoy⁴, E. E. Peters³, B. C. Crider²,
A. Kumar², M. T. McEllistrem², A. Chakraborty², F. M. Prados-Estevz², S. W. Yates^{2,3}

⁽¹⁾*Department of Physics, University of Dallas, Irving TX 75062, United States*

⁽²⁾*Department of Physics and Astronomy, University of Kentucky, Lexington KY 40506, United States*

⁽³⁾*Department of Chemistry, University of Kentucky, Lexington KY 40506, United States*

⁽⁴⁾*Department of Physics, United States Naval Academy, Annapolis MD 21402, United States*

Nuclear data important for the design and development of the next generation of light-water reactors and future fast reactors include elastic and inelastic neutron scattering cross sections on important structural materials, such as Fe, and on coolant materials, such as Na. These reaction probabilities are needed since neutron reactions impact fuel performance during irradiations and the overall efficiency of reactors. While neutron scattering cross sections from these materials are available for certain incident neutron energies, the fast neutron region, particularly above 2 MeV, has large gaps for which no measurements exist, or the existing uncertainties are large. Measurements have been made at the University of Kentucky Accelerator Laboratory to measure neutron scattering cross sections on both ^{nat}Fe and ²³Na in the region where these gaps occur and to reduce the uncertainties on scattering from the ground state and first excited state of these nuclei. Results from measurements on ^{nat}Fe at incident neutron energies between 2 and 4 MeV will be presented and comparisons will be made to model calculations available from data evaluators.

Using implantation and ion beam analysis methods to develop quantitative figures of merit for interface radiation response

Michael J Demkowicz¹, Amit Misra²

⁽¹⁾*Department of Materials Science and Engineering, MIT, room 4-142, 77 Massachusetts Ave., Cambridge MA 02139, United States*

⁽²⁾*Center for Integrated Nanotechnologies, Los Alamos National Laboratory, Los Alamos NM 87545, United States*

Ion implantation and ion beam analysis techniques have been indispensable in building a better understanding of how grain boundaries and heterophase interfaces interact with radiation-induced vacancies and interstitials as well as with implanted gasses such as He. This talk will give examples of composite design for radiation resistance that was enabled by ion implantation and ion beam analysis techniques.

This material is based upon work supported by the Los Alamos LDRD program and the **Center for Materials at Irradiation and Mechanical Extremes**, an Energy Frontier Research Center funded by the U.S. Department of Energy, Office of Science, Office of Basic Energy Sciences under Award Number 2008LANL1026.

Radiation Tolerance Interfaces

V. Shutthanandan, C Svoboda, S Vardney, S Manandhar, A Devaraj, A F Cohen, T F Kaspar, C M Wang,
A G Joly, R J Kurtz

Pacific Northwest National Laboratory, 902 Battelle Blvd, Richland WA 99352, United States

A systematic study of a wide range of interface types is underway to determine how variation in interface properties such as misfit-dislocation density affect radiation induced defect absorption and recombination. Epitaxial thin films of metallic Cr, V and their alloys deposited on MgO(001) substrates were used as model systems. By controlling the composition of Cr-V alloys, the lattice mismatch with MgO can be adjusted so that the misfit dislocation density varies over a wide range. In this paper, we present our experimental results of application of heavy ion beam radiation to study the stability of a well ordered interface between a Cr-V alloy films and an oxide (MgO) substrate. Three 100 nm thick Cr-V alloy films with different compositions were epitaxially grown on an MgO substrate using the molecular beam epitaxy method. Ion radiation experiments have been performed on these films at 300 K using 1 MeV Au⁺ ions at normal incidence over fluences ranging from 0.3 to 300 dpa. The experimental conditions were selected in order to produce maximum damage levels near the interface. The accumulation of damage in both film (Cr and V) and substrate (Mg) as well as the depth profiles of implanted gold ions have been investigated using Rutherford backscattering spectrometry in channeling and random geometries with 2 MeV He⁺ ions. In general, the degree of disorder in the Cr-V/MgO interface slightly increases with increasing irradiation damage, but the degree of disorder was far below the random level expected. There is a clear correlation exists between the dislocation densities and the damage levels: the larger the misfit dislocation density, the lower the damage levels are. These results show that the Cr-V/MgO interface appears to withstand the high dose of gold radiations.

Structure and Properties of the Y₂O₃/Fe Interface from First Principles Calculations

Samrat Choudhury, Christopher R Stanek, Blas P Uberuaga

Material Science and Technology Division, Los Alamos National Laboratory, Material Science and Technology Division, MST-8, MS G755, Los Alamos NM 87545, United States

Nanostructured ferritic alloys (NFAs) are considered excellent candidate materials for structural applications in nuclear reactors as they exhibit exceptionally high creep strength due to the presence of highly stable nanometer sized Y-Ti-O oxide precipitates within the primarily iron matrix. NFAs have also shown particular promise for their high radiation tolerance and ability to manage very high level of helium generated by transmutation reactions. It is believed that most of the radiation tolerance and He management properties in NFAs occurs at the metal/oxide interface. Thus an insight about the atomic structure of the metal/oxide interface is critical in understanding the origin of the enhanced properties of this material and ultimately designing new radiation resistant alloys.

Y₂O₃ has also been shown to form nanoprecipitates in iron and is a simpler surrogate for the Y-Ti-O precipitates. In this work, we present the behavior of the interface between the iron matrix and Y₂O₃ using density functional theory. In particular, the atomic structure of the interface will be presented. It was observed that, depending on the external partial pressure of oxygen, a critical number of defects -- iron-vacancies and/or interstitial oxygens -- are essential in stabilizing the metal/oxide interface. Importantly, the accommodation of these defects is very sensitive to the atomic structure of the interface, being enhanced at misfit dislocations at the interface. We discuss the implications of He storage at the interface in presence of such interfacial defects. Finally, we show the role of alloying elements, orientation relationship and interface misfit dislocations on the atomic structure of the metal/oxide interface, and segregation energies of the alloying elements. The insight gained in this research provides the fundamental science-based understanding needed to develop new NFAs tailored to meet challenges in fission and fusion applications, including safer operation of the current fleet of light water reactors.

Radiation Response of Nanostructured Oxide Ceramics

Yanwen Zhang^{1,2}, Tamas Varga³, Philip Edmondson^{1,4}, Sandra Moll⁵, Vaithiyalingam Shutthanandan³, Arun Devaraj³, William J. Weber^{1,2}

⁽¹⁾*Oak Ridge National Laboratory, Oak Ridge Tennessee, United States*

⁽²⁾*University of Tennessee, Knoxville Tennessee, United States*

⁽³⁾*Pacific Northwest National Laboratory, Richland Washington, United States*

⁽⁴⁾*Department of Materials, University of Oxford, Oxford, United Kingdom*

⁽⁵⁾*CEA /DMN, Service de Recherche de Metallurgie Physique, 91191 Gif sur Yvette, France*

As the world increases its reliance on nuclear energy, there is an ever-increasing demand for radiation-tolerant materials that can withstand the extreme radiation environments in nuclear reactors, accelerator-based nuclear systems, and nuclear waste forms. Understanding radiation effects in nanomaterials is an urgent challenge, since it may hold the key to unlock the design of tailored materials for advanced nuclear energy systems. Cubic ceria (CeO₂) and zirconia (ZrO₂) are well known ionic conductors that are also isostructural with urania, plutonia, and thoria-based nuclear fuels. Understanding role of nanograined structures under ion beam modification has, therefore, significant implication in advanced nuclear energy systems.

Response of nanostructured CeO₂ and ZrO₂ to heavy ion bombardments has been investigated. Grain growth, oxygen stoichiometry and phase stability of nanostructurally-stabilized cubic ZrO₂ and CeO₂ are investigated under ion bombardment at 160, 300 and 400 K to doses up to 35 displacements per atom. The initial grains size of ~8 nm increases with irradiation dose to a saturation value that is temperature dependent. Slower grain growth is observed in ZrO₂ under irradiation at 400 K irradiations, as compared to 160 K irradiation, indicating that thermal grain growth is not activated and irradiation-induced grain growth is the dominating mechanism. Faster grain growth in CeO₂ is observed with increasing temperature, indicating thermally-enhanced dynamics. Significant loss of oxygen in nanocrystalline ZrO₂ suggests an increase of oxygen vacancies under ion irradiation and the oxygen deficiency may be essential in stabilizing the cubic phase to larger grain sizes. Three dimensional distribution of oxygen along grain boundaries and grain interiors in nanocrystalline ZrO₂ as a function of irradiation is evaluated using atom probe tomography. Although grain growth in CeO₂ is observed with increasing irradiation dose, no significant change of stoichiometry is observed, which may be due to stability of the +4 valence state.

In-situ Observation of Point Defect Cluster Formation in Irradiated Nanocrystalline Iron

Mitra L Taheri¹, Greg A Vetterick¹, Chris M Barr¹, Jon Kevin Baldwin², Khalid Hattar³, Marquis Kirk⁴, Pete Baldo⁴, Amit Misra²

⁽¹⁾*Materials Science and Engineering, Drexel University, 3141 Chestnut Street, Philadelphia PA 19104, United States*

⁽²⁾*Center for Integrated Nanotechnologies, Los Alamos National Laboratory, Los Alamos NM 87545, United States*

⁽³⁾*Ion Beam Laboratory, Sandia National Laboratories, Albuquerque NM 87185, United States*

⁽⁴⁾*IVEM-Tandem Facility, Argonne National Laboratory, Argonne IL 60439, United States*

Despite extensive study, a fundamental understanding of how point defects contribute to radiation hardening, swelling, and radiation induced segregation (RIS) in ferritic steels is still lacking. Among these materials are ferritic and ferritic/martensitic alloys such as HT-9 and ODS steel which are being developed for future fusion and advanced fission reactors. Understanding and predicting the behavior of the complex microstructure of these materials is essential to the safe operation of the reactor over its 30-80 year lifetime. Using ion beam irradiation, the effects of radiation damage incurred over the life of the reactor may be studied on laboratory time scales. An ion accelerator coupled with a transmission electron microscope permits the direct observation of dislocation loop formation under irradiation. In doing so, one may study the effect of high sink density on the annihilation of point defects on length scales beyond those observed in molecular dynamics simulations.

This work presents the use of **in-situ** irradiation of nanocrystalline iron as an analogue for high sink density ferritic reactor steels in order to understand the contribution of the high grain boundary sink density found in these alloys to the behavior of the material under irradiation. The microstructure of nanocrystalline iron deposited by physical vapor deposition is a dense network of grain boundary sinks in an otherwise clean microstructure, allowing a systematic study of the aggregation of point defect clusters as a function of grain size. Free-standing nanocrystalline Fe films have been irradiated to approximately 5dpa at 300°C using 1MeV Kr^{2+} ions at Argonne. Dislocation loops in nanocrystalline iron displayed strong size dependence with grain size, and mechanisms responsible for such behavior have been observed.

Sandia National Laboratories is a multi-program laboratory managed and operated by Sandia Corporation, a wholly owned subsidiary of Lockheed Martin Corporation, for the U.S. Department of Energy's National Nuclear Security Administration under contract DE-AC04-94AL85000.

TUE-IBM05-6

#376 - Contributed Talk - Tuesday 8:30 AM - Pecos II

Effect of interface spacing on radiation damage tolerance of metallic nanolaminates

Rama Sesha R Vemuri, Arun Devaraj, Tamas Varga, Shutthanandan Vaithialingam, Chongmin Wang,
Thevuthasan Suntarampillai, Charles H Henager

Enviromental molecular sciences laboratory, pacific northwest national laboratory, Box 999 3335 Q ave MSIN K8-93, richland wa 99354, United States

Recent discovery and research indicate that materials can be designed to have higher radiation damage tolerance by building nanoscale -multilayered structures with an optimized interface spacing to increase point defect recombination relative to a non-layered structure and that can self-heal. In this study, we investigate whether scaling down the interface spacing to nano dimensions has effect on radiation damage mitigation in miscible metallic and metal nitride-metal multilayer systems. Ti/Al and TiN/Al multilayers (total stack thickness ~ 400nm) with varying interface spacing were fabricated by using DC magnetron sputtering with optimized growth parameters to achieve high quality films. These films were irradiated using 1MeV Au ions and 30KeV He ions at fluencies of $1E15$, $1E16$ and $1E17$ ions/cm² to emulate the radiation damage with heavy and light ions. The interface and crystal lattice damage, amorphization, and defect density were studied as a function of layer spacing and type of ion by using rutherford backscattering spectrometry, transmission electron microscopy and atom probe tomography.

TUE-IBM05-P1

#328 - Poster - Tuesday 5:30 PM - Rio Grande

Influence of native silicon oxide on formation of surface structures on single-crystalline silicon under the irradiation by high power ion beam nanosecond duration

Vladimir S. Kovivchak, Tatjana V. Panova, Oleg V. Krivozubov, Nadim A. Davletkildeev, Egor V. Knjazev
Physics Department, Omsk State University, Pr. Mira 55a, Omsk, Russia

The surface damage of silicon caused by the high power ion beam (HPIB) irradiation was investigated. It was established that the irradiation by a single HPIB pulse with a current density exceeding 20 A/cm^2 (at which no intense melting on the surface layer takes place) leads to the formation of surface structures with various shapes, from involved curves to stars with wedge like "rays" outgoing from a common center. The observed complicated surface structures were interpreted as a frozen state of the convective flow caused by the development of instability in melted silicon with native oxide thin film. The surface damage of silicon caused by HPIB exhibits a more complicated character and differs significantly from a laser pulse induced damage. This difference is related primarily to the volume character of energy deposition in a near surface layer and the implantation of impurities during ion irradiation. This investigation showed evidence that a native oxide layer plays a determining role in the formation of surface structures on single crystalline silicon under the action of a HPIB nanosecond duration.

Features of surface morphology of polycrystalline bismuth irradiated by high power ion beam

Vladimir S. Kovivchak, Tatjana V. Panova, Kirill A. Mikhailov
Physics Department, Omsk State University, Pr. Mira 55a, Omsk 644077, Russia

Specific features of surface relief formation on a polycrystalline bismuth target under the action of a high power ion (proton-carbon) beam (HPIB) of nanosecond duration have been studied. Local melt extrusion from subsurface layers and its crystallization on the surface is observed, which is explained by a significant (3.35%) thermal expansion of bismuth during the transition from liquid to solid state. The presence of extruded and solidified material on the surface of a bismuth target exposed to HPIB pulses indicates that crystallization of the ion beam melted layer begins simultaneously at both the melt-solid and vacuum-melt interfaces. As is known, the process of crystallization requires removal of a latent heat from the interfacial region. The heat of crystallization liberated at the moving boundary between liquid and solid phases is removed by heat exchange with the substrate. The heat of crystallization liberated in the surface layer can also be removed by thermal radiation, but this contribution in the case under consideration is insignificant because of a relatively low temperature of the heated surface layer. It is probable that a significant short term over cooling of the melted surface layer can also take place immediately after termination of the irradiation pulse because of the intensive vaporization of bismuth, which has a high vapor pressure even at relatively low temperatures (~ 10 Pa at 575°C). However, this assumption requires additional verification.

The Northern Illinois and Loma Linda University Proton CT Project

George Coutrakon¹, Victor Rykalin¹, Reinhard Schulte², Vladimir Bashkirov², Ford Hurley², Vishnu Zutshi¹,
 Nicholas Karonis¹, Hartmut Sadrozinski³

⁽¹⁾*Physics, Northern Illinois University, LaTourette Hall 202, DeKalb IL 60115, United States*

⁽²⁾*Radiation Medicine, Loma Linda University Medical Center, 11234 Anderson St., Loma Linda CA 92354, United States*

⁽³⁾*Santa Cruz Institute of Particle Physics, University of California at Santa Cruz, 505 High St., Santa Cruz CA 95064, United States*

Since 2009, Northern Illinois University has collaborated with Loma Linda University Medical Center and UC Santa Cruz to build the first large area (9 x 18 cm) proton CT scanner. In 2011, the first 3D images of a 14 cm spherical phantom were reconstructed using this first generation scanner. The scanner was constructed with 4 planes of X-Y silicon strip detectors and a segmented CsI calorimeter operating at a maximum particle data rate of 20 KHz. In this paper, we present details of the scanner hardware, calibration procedures, and method of image reconstruction. Work is currently in progress to build a 2nd generation scanner which will be capable of imaging an entire adult head in less than 10 minutes with up to 1 billion proton events. Highlights of this design and recent progress will be also presented.

A Double Photomultiplier Compton Camera and its Readout System for Mice Imaging

Cristiano Lino Fontana^{1,5}, Kostiantyn Atroshchenko^{1,6}, Giuseppe Baldazzi^{2,7}, Michele Bello⁶, Nikolay Uzunov^{3,6}, Giovanni Di Domenico^{4,8}

⁽¹⁾Physics Department "Galileo Galilei", University of Padua, Via Marzolo 8, Padova 35131, Italy

⁽²⁾Physics Department, University of Bologna, Viale Bertini Pichat 6/2, Bologna 40127, Italy

⁽³⁾Department of Natural Sciences, Shumen University, 115 Universitetska str., Shumen 9712, Bulgaria

⁽⁴⁾Physics Department, University of Ferrara, Via Saragat 1, Ferrara 44122, Italy

⁽⁵⁾INFN Padova, Via Marzolo 8, Padova 35131, Italy

⁽⁶⁾INFN Legnaro, Viale dell'Università 2, Legnaro PD 35020, Italy

⁽⁷⁾INFN Bologna, Viale Bertini Pichat 6/2, Bologna 40127, Italy

⁽⁸⁾INFN Ferrara, Via Saragat 1, Ferrara 44122, Italy

We have designed a Compton Camera (CC) to image the bio-distribution of gamma-emitting radiopharmaceuticals in mice. A CC employs the "electronic collimation", i.e. a technique that traces the gamma-rays instead of selecting them with physical lead or tungsten collimators. To perform such a task, a CC measures the parameters of the Compton interaction that occurs in the device itself. At least two detectors are required: one (tracker), where the primary gamma undergoes a Compton interaction and a second one (calorimeter), in which the scattered gamma is completely absorbed. Eventually the polar angle and hence a "cone" of possible incident directions are obtained (event with "incomplete geometry").

Different solutions for the two detectors are proposed in the literature: our design foresees two similar Position Sensitive Photomultipliers (PMT, Hamamatsu H8500). Each PMT has 64 output channels that are reduced to 4 using a charge multiplexed readout system, i.e. a Series Charge Multiplexing net of resistors. Triggering of the system is provided by the coincidence of fast signals extracted at the last dynode of the PMTs. Assets are the low cost and the simplicity of design and operation, having just one type of device; among drawbacks there is a lower resolution with respect to more sophisticated trackers and full 64 channels Readout.

This paper does compare our design of our two-hama CC to others solutions and shows how the spatial and energy accuracy is suitable for the inspection of radioactivity in mice.

Calibration and Operational Data for a Compact Photodiode Detector Useful for Monitoring the Location of Moving Sources of Positron Emitting Radioisotopes

Maryn Grace Marsland¹, Morgan Patrick Dehnel¹, Stefan Johansson², Joseph Theroux¹, Tue Christensen¹, Thomas Maxwell Stewart¹, Craig Hollinger¹, Olof Solin², Johan Rajander²

⁽¹⁾D-Pace, Inc., PO Box 201, Nelson BC V1L5P9, Canada

⁽²⁾Turku PET Centre, Abo Akademi University, Porthansgatan 3, Turku FI-20500, Finland

D-Pace has developed a compact cost-effective gamma detector system based on technology licensed from TRIUMF [1]. These photodiode detectors are convenient for detecting the presence of positron emitting radioisotopes, particularly for the case of transport of radioisotopes from a PET cyclotron to hotlab, or from one location to another in an automated radiochemistry processing unit. This paper describes recent calibration experiments undertaken at the Turku PET Centre for stationary and moving sources of F18 and C11 in standard set-ups. The practical diagnostic utility of using several of these devices to track the transport of radioisotopes from the cyclotron to hotlab is illustrated. For example, such a detector system provides: a semi-quantitative indication of total activity, speed of transport, location of any activity lost enroute and effectiveness of follow-up system flushes, a means of identifying bolus break-up, feedback useful for deciding when to change out tubing.

[1] S.K. Zeisler et al, A Photodiode Radiation Detector for PET Chemistry Modules, *Appl. Radiat. Isot.*, Vol. 45, No. 3, pp. 377-378, 1994.

In-Situ PET Scanning for Depth-Dose Verification

Richard Levy

Advanced Beam Cancer Treatment Foundation, PO Box 2356 (887 Wildrose Circle), Lake Arrowhead CA 92352, United States

Depth-dose distribution within patients can be calculated with fairly good reliability for protons, by correlating tissue stopping-power algorithms with measured electron-density data obtained from treatment-planning CT scans. However, similar range calculations for heavier ions in heterogeneous tissue may be more problematic, especially with ongoing treatment-related density changes in both normal and target tissues. As effective treatment with heavier ions may require very heterogeneous physical dose distributions to deliver uniform bio-equivalent doses calculated from voxel-based RBE modeling, greater certainty of the depth-dose distribution is of crucial importance. Here, PET imaging with the patient in treatment position can be used to verify range accuracy and/or to adjust beam energy more precisely. A variety of positron-emitting isotopes of carbon and/or oxygen are produced by the interaction of the heavier ions with the patient tissues, or these isotopes can be produced by transiently interposing a beryllium filter in the beam path. Imaging these short-half-life species in situ as an immediate precursor to treatment can serve as a very valuable method for range verification and/or beam-energy adjustment.

Current Status of Beam Scanning and Dealing with Organ Motion

Richard Levy

Advanced Beam Cancer Treatment Foundation, PO Box 2356 (887 Wildrose Circle), Lake Arrowhead CA 92352, United States

Beam scanning utilizes two unique properties of heavy charged particles: (1) they can be laterally deflected precisely by magnets linked to modulating power supplies; and (2) their range can be modified precisely by adjusting their kinetic energy. This technique has proved especially useful in aiming at irregularly shaped target volumes in close proximity to critical normal tissues, while concurrently producing sharper lateral dose fall-off and minimizing secondary neutron production. Scanning strategies employed have included step-and-shoot spot scanning (wherein the ion beam is turned off transiently as it is moved between adjacent voxels), and digitized Raster scanning (wherein the beam is deflected continuously between adjacent voxels). As the lateral penumbra of the beam decreases with increasing mass of the particle, it is of crucial importance to integrate the specific lateral dose penumbra in the treatment-planning algorithm. Even slight movement of physiologically mobile targets (e.g., liver, lung) can introduce potential hot or cold spots at positions of transient spatial overlap or offset of adjacent voxels. Potential solutions include beam-gating in sync with respiratory phase, multi-painting the fields, and active online tracking of the position of the target volume.

The ERHA (Enhanced Radiotherapy with HAdrons) project beam delivery system

Annarita Lacalamita¹, Vincenzo Dimiccoli², Vincenzo Variale³, Antonio Cosimo Rainò¹

⁽¹⁾Departement of Physics Bari University, Bari University, Via Amendola 173, Bari 70126, Italy

⁽²⁾Itel Telecomunicazioni, Itel Telecomunicazioni, Via Labriola 39, Ruvo di Puglia 70037, Italy

⁽³⁾INFN, Ba-INFN, Via Amendola 173, Bari 70126, Italy

A new proton therapy beam delivery system has been studied in a new project called ERHA. It is characterized by an active scanning system which irradiates target with a pencil beam. The challenge of this project is the linear accelerator and the Robotized Patient Positioning System instead of the traditional gantry. The transport guide, the scanning system and the moving target are described.

Two Dimensional Beam Monitor System

Augustine Ei-fong Chen⁵, Siou-yin Cai⁵, Pei-rong Tsai⁵, Ya-wen Tsai⁵, Ping-kun Teng⁴, Ming-lee Chu⁴,
Fu-xiong Chang⁴, Chung-hsiang Wang⁶, Chi-wen Hsieh³, Ting-shien Duh¹, Jeng-hung Lee¹, Tsi-chian Chao²,
Shu-jhen Dai², Chung-chi Lee², Chuang-jong Tung², Chih-hsun Lin⁴

⁽¹⁾*Institute of Nuclear Energy Research, Lung-tan, Taiwan*

⁽²⁾*Medical Imaging and Radiological Sciences department, Chang Gung University, Lin-ko Tao-Yuan, Taiwan*

⁽³⁾*Electrical Engineering department, National Chiayi University, Chia-yi, Taiwan*

⁽⁴⁾*Institute of Physics, Academia Sinica, Taipei, Taiwan*

⁽⁵⁾*Physics Department, National Central University, Jong-li, Taiwan*

⁽⁶⁾*Optical Engineering Department, National United University, Miao-li, Taiwan*

A simple two dimensional beam monitor system has been constructed based on ionization chamber technology. PCB with segmented strips or pads serves as measurements in space. Designs of related electronics are based commercial available products. Chambers with different strip widths are tested with proton and electron beams. Their performances are as expected. In practice, broad field method used in proton therapy usually implies low current density which means small signals to our system. High gain or current integrator electronics are preferred. The other Pencil Beam Scan method means high current density and fast scan, such that less gain and DAQ rate greater than 20,000 Hz electronics is necessary. System with pad has been tested with Co-60 source as dose calibration. Our system is still under developing to meet needs from proton therapy.

Evaluation of Image Reconstruction Methods for Compton SPECT Camera in Incomplete Geometry

Cristiano Lino Fontana^{1,4}, Giuseppe Baldazzi^{2,3}, Michele Bello⁷, Dante Bollini³, Giovanni Di Domenico^{6,8},
Giuliano Moschini^{1,4,7}, Nikolay Uzunov^{7,9}, Gianluigi Zampa⁵, Nicola Zampa⁵, Paolo Rossi^{1,4}

⁽¹⁾*Physics Department "Galileo Galilei", University of Padua, Via Marzolo 8, Padova 35131, Italy*

⁽²⁾*Physics Department, University of Bologna, Viale Berti Pichat 6/2, Bologna 40126, Italy*

⁽³⁾*INFN Bologna, Viale Berti Pichat 6/2, Bologna 40127, Italy*

⁽⁴⁾*INFN Padova, Via Marzolo 8, Padova 35131, Italy*

⁽⁵⁾*INFN Trieste, Via Valerio, 2, Trieste 34127, Italy*

⁽⁶⁾*INFN Ferrara, Via Saragat 1, Ferrara 44122, Italy*

⁽⁷⁾*INFN Legnaro, Viale dell'Università 2, Legnaro PD 35020, Italy*

⁽⁸⁾*Physics Department, University of Ferrara, Via Saragat 1, Ferrara 44122, Italy*

⁽⁹⁾*Department of Natural Sciences, Shumen University, 115 Universitetska str., Shumen 9712, Bulgaria*

A "Compton Camera" is an X-ray detector that can trace the photon trajectory by measuring the parameters of the Compton interaction occurring inside the device. This technique is known as "electronic collimation," since a real collimator is not needed. The Compton Camera consists of two position-sensitive X-ray detectors. In the first detector (tracker) the photon undergoes a Compton interaction, whose position and deposited energy are measured. In the second detector (calorimeter) the scattered photon is completely absorbed and again position and energy are measured. Having these measurements, with no information about the recoiled electron in the tracker, only the scattering polar angle can be deduced. Hence only a cone of possible incoming trajectories can be defined. A camera that performs such trajectory reconstructions without the measurement of the electron velocity is assumed to work in the so-called "incomplete geometry."

In the Laboratory for Radiopharmaceuticals and Molecular Imaging (LRMI) we have designed a Compton camera to perform SPECT (Single Photon Emission Computed Tomography) on small animals, treated with radio-pharmaceuticals. The camera dimensions, the object dimensions, as well as the object-to-camera distances are of a comparable size, which is quite different from the large distance pathways in the case of image reconstructions with Compton cameras, used for astronomy applications.

We have developed an algorithm that performs a reconstruction of the spatial bio-distribution of the radiopharmaceuticals by employing the Compton Camera information about the incoming "cones" (in incomplete geometry). The reconstruction can be performed selecting one of the tomographic methods: Filtered Back-Projection (FBP) and Penalized-Likelihood Reconstruction (PLR). A GEANT4 simulation of the apparatus to test the different methods and the feasibility of our approach has been developed. A comparison between the reconstruction algorithm exploiting FBP and PLR has been conducted.

TUE-MA05-P4

#402 - Poster - Tuesday 5:30 PM - Rio Grande

Feasibility Tests of a Dual Modality System for Imaging Using Gamma Rays and NIR Light

Nikolay Uzunov^{1,3}, Kostiantyn Atroshchenko^{3,5}, Yanka Baneva⁴, Michele Bello³, Matteo De Rosa⁵,
Cristiano Lino Fontana^{2,5}, Giuliano Moschini^{3,5}, Paolo Rossi^{2,5}

⁽¹⁾*Department of Natural Sciences, Shumen University, 115 Universitetska str., Shumen 9712, Bulgaria*

⁽²⁾*INFN Padova, Via Marzolo 8, Padova 35131, Italy*

⁽³⁾*INFN Legnaro, Viale dell'Università 2, Legnaro PD 35020, Italy*

⁽⁴⁾*Department of Physics and Biophysics, Medical University, Varna, Bulgaria*

⁽⁵⁾*Physics Department "Galileo Galilei", University of Padua, Via Marzolo 8, Padova 35131, Italy*

A dual system for small-animal imaging, compounded by a high-spatial resolution gamma-camera and a scanner for Near-Infra-Red(NIR) light is under development. The gamma-camera is assembled from a position-sensitive photomultiplier and segmented Yttrium-Aluminum-Perovskite(YAP) scintillation-crystal with a parallel-hole collimator. This system performs gamma-ray images as well as camera-to-object distance measurements using the so-called tilted-collimator(TC) technique. The imaging-system for NIR light can perform object scanning in the interval of 900nm-1700nm. It is based on InGaAs array-sensor Hamamatsu G9203-256D and is designed for near-object scanning. A first mode of scanning is performed in transmitted linearly-polarized NIR-light, traversed through the scanned object. Five fixed-wavelengths Light-Emitting-Diodes of NIR-light are used. The scanning process is realized by a consecutive repositioning of the NIRsensor. In a second scanning mode the fluorescence emission of nanoparticles, such as single-walled carbon nanotubes(SWCNTs) administrated in the imaged object, is excited using different laser-wavelengths: 705nm,785nm,808nm and 830nm.

Assessments on sensitivity, energy and spatial resolution of the gamma-camera have been conducted. The spatial resolution at different camera-to-object distances, have been studied using specially-designed phantoms: a parallel capillary-system filled with a solution of Tc-99m and volumetric phantoms containing Tc-99m-filled cavities with different shapes and dimensions. The NIR-scanner spatial resolution has been determined along two perpendicular directions using USAF1951 resolution-standard, placed at different distances from the sensor. Experiments on the sensitivity to the concentration of optical-active agents at different wavelengths have been conducted. The results indicated that both NIR scanning-system and the gamma-camera possess good imaging-parameters and can be applied for multimodality studies.

TUE-MA06-1

#489 - Invited Talk - Tuesday 1:00 PM - Pecos I

Proton Therapy for Pediatric Cancer: Current status and ongoing issues

Anita Mahajan

Radiation Oncology, MD Anderson Cancer Center, 1515 Holcombe Blvd. Unit 097, Houston TX 77030, United States

Proton radiotherapy (PRT) is a powerful tool in the management of cancer in children. Because of the physical characteristics of the proton beam interactions, typically there is a lower dose delivered to the uninvolved normal organs that are close to the target area. The potential benefit of a lower integral dose to the body of the patient may lead to a reduction in both acute and late toxicities.

The delivery of radiotherapy to children can be challenging for many reasons: 1) young children are unable to cooperate for the radiotherapy delivery; 2) immobilization devices may not fit the smaller size of the child; 3) most pediatric cancers require multidisciplinary care requiring clear communication with other care providers; 4) the spectrum of pediatric cancer diagnosis is quite different than the typical adult cancers; 5) children are more sensitive to radiotherapy and long term follow up is required to monitor and address late effects if they occur.

The issues listed above need to be recognized for any radiotherapy delivery, but some are of additional importance for proton therapy. The neutron scatter that occurs in the room and in the patient may have more impact in a child. Inadequate immobilization will lead to more dose disturbance and uncertainties for PRT than XRT. Uncertainty margins that are required to account for appropriate PRT planning can be large relative to the size of a small child. These issues must be recognized when developing a program for pediatric PRT. They should be acknowledged when creating a treatment plan to have a realistic approach that can have the optimal outcome.

There is growing evidence that PRT yields equivalent results to XRT with regards to tumor control. Ongoing efforts are required to monitor these patients to confirm the reduction of late effects.

TUE-MA06-2

#479 - Contributed Talk - Tuesday 1:00 PM - Pecos I

Summary of Ongoing Clinical Protocols for Proton and Heavier-Ion Therapy

Richard Levy

Advanced Beam Cancer Treatment Foundation, PO Box 2356 (887 Wildrose Circle), Lake Arrowhead CA 92352, United States

Since 1954 when the very first patient was treated at LBNL with heavy-charged particles, some 84,000 patients in total have now been treated with protons, and another 13,000 patients have been treated with carbon and other heavier ions. During the first several decades of this endeavor, particle therapy was accessible only at a small number of programs. More recently, however, this therapy has become available at a rapidly increasing number of facilities worldwide. This expansion of the discipline has led to the development of many more clinical trials, designed to optimize particle-beam therapy and to compare the results achieved with those resulting from other treatment methods.

Presently, more than 50 clinical protocols worldwide are actively involved in the effort to improve our understanding of these clinical guidelines. The purpose of this presentation is to offer a broad overview of these protocols, highlighting the specific disease categories that are now being studied using proton and/or heavier-ion therapy, and how the parameters of dose-escalation, beam conformity, and RBE modeling are being evaluated for various disease sites and stages.

TUE-MA07-1

#86 - Invited Talk - Tuesday 3:30 PM - Pecos I

Current Status and Future Prospects for Carbon Ion Therapy at NIRS

tadashi kamada

Research Center for Charged Particle Therapy, National Institute of Radiological Sciences, 4-9-1 anagawa, inage-ward, Chiba 2638555, Japan

Carbon ion radiotherapy (CIRT) is a unique radiotherapy, which possesses well localized, and superior depth dose distribution in addition to less repairable radiobiological effects. The use of CIRT for various diseases has been explored as clinical trials at the Heavy Ion Medical Accelerator in Chiba (HIMAC), Japan. Since 1994, when the first clinical study of cancer therapy with carbon ion beams was started, about 50 clinical studies have been completed safely and effectively. These studies revealed that intractable cancers such as inoperable bone and soft tissue sarcomas can be cured and so can be cancers in the head and neck, lung, liver, pancreas, prostate, and postoperative pelvic recurrence of rectal cancer in a safe manner in a shorter overall treatment time. The number of patients receiving CIRT has reached 6,500 and the therapy was approved as a highly advanced medical technology in 2003. Based on these experiences, we embarked on the research and development of a new generation beam delivery facilities such as a 3D-scanning method with a pencil beam and a compact rotating gantry. A clinical research using the pencil beam scanning was in operation since May 2011.

Particle Therapy at the Heidelberg Ion Therapy Center: Clinical Concepts, Research Approaches and Networking within a European Framework

Stephanie E. Combs, Jürgen Debus

Department of Radiation Oncology, Heidelberg University Hospital, Im Neuenheimer Feld 400, Heidelberg 69120, Germany

Particle therapy as an innovative and relatively new technique is of increasing interest in radiation oncology. Compared to standard radiation therapy (RT) with photons, the main advantages lie in the distinct physical characteristics of particles enabling a more precise dose delivery to the target. Heavier ions, such as carbon ions, additionally offer distinct biological characteristics leading to an increase in relative biological effectiveness (RBE). For several further indications, clinical results of particle therapy have been shown to be beneficial. For others, clinical trials are required to define the role of particle therapy in their treatment.

While proton therapy is more widespread, especially in the United States, carbon ion radiotherapy was only available in Japan and Germany. Beginning in 1997, treatment was performed at the Gesellschaft für Schwerionenforschung (GSI) in Darmstadt, and since November 2009, treatment is available at the Heidelberg Ion-Beam Therapy Center (HIT). Other European Centers will take up clinical operation. Recently, the CNAO in Pavia, Italy, started patient treatment.

Since several European particle therapy initiatives are underway, and since clinical data, still remains scarce, the logical consequence is to combine all efforts in the field of particle therapy and to generate a common platform for all patients treated with particle beams. Therefore, within the transnational access (TNA) pillar of the ULICE project (Union of Light Ions Centers in Europe) funded by the European Commission, the generation of a common database has been a main focus. Additionally, training opportunities are available in a parallel Marie-Curie-Project - PARTNER, also funded by the European Union. Beamtime is available for experimental work within these frameworks.

A HIT, currently 12 clinical trials are recruiting patients for several indications (see: www.ClinicalTrials.gov), and prospective evaluation of clinical and pre-clinical data is underway.

Particle radiotherapy for patient with hepatocellular carcinoma

Masao Murakami¹, Kazuki Terashima², Yusuke Demizu², Naoki Hashimoto², Dongcun Jin², Masayuki Araya², Masayuki Mima², Osamu Fujii², Yasue Niwa², Nobukazu Fuwa²

⁽¹⁾Radiation Oncology, Dokkyo Medical University, 880 Kitakobayashi, Mibu-machi, Shimotsuga-gun Tochigi 321-0293, Japan

⁽²⁾Radiology, Hyogo Ion Beam Medical Center, 1-2-1, Kouto, Shingu-cho, Tatsuno Hyogo 679-5165, Japan

The HIBMC is the world's first institution capable of applying both proton (PRT) and carbon ion radiotherapy (CiRT). More than 4,600 patients have been treated since its opening in 2001, and about 800 patients with hepatocellular carcinoma (HCC) have been treated. Recently, we published 3 papers dealing with the treatment results of HCC. In the first paper of **Cancer117:4890-904,2011**, 343 consecutive patients, including 242 who received PRT and 101 who received CiRT, were treated on 8 protocols of PRT (52.8-84.0 GyE / 4-38 fr) and on 4 protocols of CiRT (52.8-76.0 GyE / 4-20 fr). The 5-year local control (LC) and overall survival (OS) rates for all patients were 90.8% and 38.2%, respectively. Regarding PRT and CiRT, the 5-year LC / OS rates were 90.2% / 38% and 93% / 36.3%, respectively with no significant difference between the 2 therapies. No patients died of treatment-related toxicities. In the second paper of **Br J Surg 98: 558-564, 2011**, we confirmed that 5-year LC / OS rates were 92.3 % / 50.9% in 150 patients with a single HCC smaller than 5 cm in diameter. In the third paper **in submitting**, we compared the results of particle radiotherapy in 140 patients with HCC as a first-line treatment with the other treatments of surgical resection and radiofrequency ablation (RFA). We confirmed that OS rates of 71.6% at 4 years for <3 cm tumors were comparable to those of RFA and 66.7% at 5 years for operable stage was superior to, and more 46.7% at 5 years for inoperable stage was comparable to those of surgical resection. We concluded that particle radiotherapies may represent innovative alternatives to conventional local therapies for HCC regardless of sorts of ions. We are now going on a prospective randomized clinical trial for HCC between PRT and CiRT.

Acute Toxicity of Carbon-ion Radiotherapy for Localized Prostate Cancer at the Gunma University Heavy-ion Medical Center

Yoshiyuki Suzuki¹, Hiroyuki Katoh¹, Hitoshi Ishikawa¹, Takuya Kaminuma¹, Tomoaki Tamaki¹, Katsuyuki Shirai¹, Hiroshi Matsui¹, Tatsuya Ohno¹, Kazuto Ito², Kazuhiro Suzuki², Takashi Nakano¹

⁽¹⁾*Gunma University Heavy-ion Medical Center, Gunma University, 3-39-22, Showa-machi,, Maebashi 3718511, Japan*

⁽²⁾*Department of Urology, Gunma University Graduate School of Medicine, 3-39-22, Showa-machi,, Maebashi 3718511, Japan*

<Objection> Carbon-ion radiotherapy (C-ion RT) has been started at the Gunma University Heavy-ion Medical Center in March 2010. This time, we evaluated the acute toxicity of C-ion RT for localized prostate cancer.

<Materials and Methods> Seventy-six patients with T1-4N0M0 prostate cancer were treated with C-ion RT between March 2010 and January 2011. The prescribed dose of C-ion RT was 57.6 GyE in 16 fractions over 4 weeks. Seven patients (9%) received C-ion RT alone, and the other 69 patients (91%) received a combination therapy of C-ion RT and androgen deprivation therapy. Common Terminology Criteria for Adverse Events v4.0 were used for evaluating acute toxicities (the worst degree of toxicity experienced within 90 days after the initiation of therapy was computed for each patient.) All 76 patients completed the treatment as planned and the follow-up of 90 days.

<Results> Neither grade 3 nor severer acute toxicity at the genito-urinary system and the rectum was observed. Three patients (3.9%) presented with grade 2 acute toxicity at the genito-urinary system and the other patients presented grade 0-1 acute toxicity at the genito-urinary system and/or rectum. Any other acute toxicity was not seen in all patients.

<Conclusion> With regard to acute toxicity, 57.6 GyE in 16 fractions over 4 weeks of C-ion RT for localized prostate cancer is well tolerated. Further follow-up is ongoing to evaluate the late toxicity and the efficacy of C-ion RT.

Construction of SAGA HIMAT for Carbon Ion Cancer Therapy

Sho Kudo, Yoshiyuki Shioyama, Masahiro Endo, Mitsutaka Kanazawa, Hirohiko Tsujii, Tadahide Totoki
Ion Beam Therapy Center, SAGA HIMAT Foundation, 1-802-3 Hondori-machi, Tosu Saga 841-0033, Japan

The SAGA HIMAT (Saga Heavy Ion Medical Accelerator in Tosu) is now under construction in Tosu, Saga Prefecture, Japan and will become the fourth carbon ion cancer therapy center in Japan. The facility locates at the cross-point of railroads and high ways.

The project has been based upon a collaborative effort among the Saga prefectural government, regional industries and universities in Kyushu District. The project started in 2008, and the completion of construction will be in October 2012. Then, after several months of beam tests and measurement of dose distribution it will open sometime in the spring of 2013. At present, the ion beam therapy is not covered by the medical insurance system in Japan, and its cost should be paid by the patients. However, many companies sell medical insurance products to cover it.

The facility has no beds and all the patients will be treated as out-patients. There are three treatment rooms, where the first one is equipped with horizontal and 45° oblique beam lines, the second has horizontal and vertical beam lines, and the third is for future preparation of scanning beam delivery. The maximum beam energy is 400 MeV/u and maximum beam intensity is 1.3×10^9 pps. We are planning to treat about 200 patients in the first year then to increase the number up to >800 per year in the near future.

We will collaborate with the three preceding carbon ion beam institutes in Japan, including National Institute of Radiological Sciences to obtain the technical assistance and training of the personnel. We also collaborate with the universities and medical centers in Kyushu area to get the patients referral.

A Prefectural Plan to Install "i-ROCK" (Ion-Beam Radiation Oncology Center in Kanagawa) at Kanagawa Cancer Center

Tetsuo Nonaka¹, Yuko Nakayama¹, Nobutaka Mizoguchi¹, Miho Shiomi¹, Shinichi Minohara², Yohsuke Kusano², Makoto Akaike³, Osamu Kobayashi³

⁽¹⁾*Radiation Oncology, Kanagawa Cancer Center, 1-1-2 Nakao, Asahi-ku, Yokohama, Japan*

⁽²⁾*Radiotherapy Quality Assurance, Kanagawa Cancer Center, 1-1-2 Nakao, Asahi-ku, Yokohama, Japan*

⁽³⁾*Kanagawa Cancer Center, 1-1-2 Nakao, Asahi-ku, Yokohama, Japan*

Kanagawa Cancer Center (KCC) is preparing to install a heavy charged particle (carbon ion) radiotherapy system and start its operation as the fifth heavy ion radiotherapy facility in Japan. The project of installation Ion-beam Radiation Oncology Center in Kanagawa, "i-ROCK", started in 2004 at KCC, and the basic frame work and design of i-ROCK were completed in 2010. The final detail designs of the facility and building are now carrying out. The location of this center benefits from an excellent and efficient public transportation network covering the entire area of Kanagawa Prefecture and extending into Tokyo Metropolitan District. The KCC stands at an ideal location for receiving outpatients from local, regional, and even distant areas. One of the major missions of the forthcoming radiotherapy facility is to provide the latest medical treatment in an outpatient setting. This facility will be managed and operated in close cooperation and coordination with other department in the KCC, with the help of its cancer specialist surgeons, who will design high-level medical treatment for various types of cancer. The combination of i-ROCK and the high-precision radiation therapy units of the KCC will provide the full range of radiation oncology center services, from which appropriate treatment strategies will be selected for each patient. Moreover, a spot scanning irradiation method will be included in the treatment options from the start of the facility operation in addition to conventional irradiation techniques (the wobblers method). The combination allows a wider selection of irradiation methods depending on patient conditions. The state-of-the-art facility, i-ROCK, will start its operation in the winter of 2015.

Treaty Verification Opportunities in a Post-Cold-War Environment

Robert Runkle

Radiation Detection and Nuclear Sciences, Pacific Northwest National Laboratory, 902 Battelle Blvd., Richland WA 99336, US

With the reduction of nuclear weapons stockpiles in the United States and Russia alongside the growing breadth of civilian nuclear power, there exists an increasing need for technology that can confidently verify existing and emerging nuclear security treaties. The new Strategic Arms Reduction Treaty (START) entered into force on 5 February 2011, and it mandates significant reductions in strategic deployed nuclear weapons. The treaty also requires negotiation of a future treaty that will further reduce stockpiles. As the number of warheads falls, the required confidence of verification measures increases, thus increasing the need for higher performance technology. This reality creates an opportunity for non-destructive evaluation methods specifically in the realm of dismantlement verification. Similar opportunities exist under the auspices of the Treaty on the Nonproliferation of Nuclear Weapons where significant improvements are possible in safeguarding growing stocks of plutonium-possessing spent nuclear fuel. On the horizon is the Fissile Material Cutoff Treaty that will drive even greater technology requirements for confirming the absence of undeclared production of nuclear materials. This presentation will discuss these treaties and present potential opportunities for active interrogation technology as part of a verification regime.

Analysis Techniques for Intense Pulsed Active Detection

Joseph W Schumer¹, John P Apruzese², Robert J Commisso¹, Stuart L Jackson¹, David Mosher², Stephen B Swanekamp¹,
Bruce V Weber¹, Jacob C Zier¹

⁽¹⁾*Pulsed Power Physics Branch, Plasma Physics Division (Code 6770), Naval Research Laboratory, 4555 Overlook Avenue SW,
Washington DC 20375, United States*

⁽²⁾*Independent contractor for NRL, L-3 Services, Inc., 3750 Centerview Drive, Chantilly VA 20151, United States*

Intense pulsed active detection (IPAD)^a uses a high power (~TW) pulsed accelerator to produce a short (<100 ns) pulse of fission-inducing radiation, temporarily elevating the emissions from fissile materials and improving the signal-to-natural-background ratio by reducing counting times. Analysis techniques relying upon sequential probability ratio test (SPRT)^b provide a more sensitive means of extracting and differentiating these fission signatures from both passive and active backgrounds. In this presentation, the SPRT is compared to the minimum detectable activity (MDA^b) technique for laboratory-based IPAD experiments utilizing pulsed bremsstrahlung and neutron irradiation sources. Because both induced fission and active background scale linearly with the number of source particles (i.e. photons or neutrons) but scale non-linearly with source particle type, source-particle energy spectrum, and detector recovery following an irradiation, a quantitative analysis technique is required to compare sources and improve the confidence in the measurement. SPRT is known to be superior in flexibility and sensitivity to the "Currie Equation"^b. Examples of the utility of SPRT analysis will be shown, applied to laboratory-based IPAD experiments with intense pulsed bremsstrahlung and/or neutron sources.

^aS.B. Swanekamp, J.P. Apruzese, R.J. Commisso, **et al.**, IEEE Trans. Nucl. Sci. **58**, 2047 (2011).

^bA. Wald, The Annals of Math. Stat. **16** (2), June 1945, pp. 117-186; L. A. Currie, Anal. Chem. **40** (3), March 1968, pp. 586 - 593.

*Work supported by ONR and DTRA.

Active-induced Time Correlation Signatures for the Characterization of Shielded HEU using D-T Neutron Generators

Seth McConchie, Brandon Grogan, Jason Crye, John Mihalcz, Jeffrey Johnson
Oak Ridge National Laboratory, 1 Bethel Valley Rd, Oak Ridge TN 37831, United States

Unlike plutonium, the detection and characterization of uranium has long been considered a difficult technical challenge for the general nonproliferation problem, especially when uranium is in a shielded configuration. Plutonium emits orders of magnitude more signature radiation than uranium due to the shorter half-lives of ²³⁹Pu and ²⁴⁰Pu, and commonly used shielding like polyethylene can provide other signatures to indicate the presence of plutonium. Using time correlated neutrons and gammas as the observable for detecting fissioning material, an alternative approach for HEU detection is to actively induce fissions at rates much higher than its spontaneous fission rate. Measurement methodologies like differential die-away analysis, active multiplicity counting, and delayed neutron and gamma-ray counting can then be applied. A variety of radiation sources have been the subject of research, such as ²⁵²Cf sources, AmLi and AmBe sources, pulsed or continuous D-D and D-T neutron generators, and pulsed bremsstrahlung electron linacs. All of these sources have different strengths and weaknesses depending upon aspects of the measurement scenario like shielding. In support of a continuing effort to understand the capabilities of D-T neutron generators for HEU detection, measurements were performed with 18 kg of 93.15 wt% HEU metal in the Nuclear Detection Sensor Test Center (NDSTC) at the Y-12 National Security Complex. Various types of shielding were used, including up to tens of centimeters of polyethylene. For each shielding configuration, a pulsed neutron generator and an associated particle imaging (API) neutron generator were used with arrays of plastic scintillators and arrays of moderated ³He proportional tubes to measure the time correlation signatures. The results of these measurements are presented.

Assessment of Delayed Gamma-Ray Technique for Special Nuclear Materials Assay

Vladimir Mozin¹, Alan W. Hunt², Edward Reedy², Bernhard Ludewigt³

⁽¹⁾*Lawrence Livermore National Laboratory, 7000 East Ave., L-211, Livermore CA 94550, United States*

⁽²⁾*Idaho Accelerator Center, Idaho State University, 1500 Alvin Ricken Drive, Pocatello ID 83209, United States*

⁽³⁾*Lawrence Berkeley National Laboratory, 1 Cyclotron Rd., Berkeley CA 94720, United States*

High-energy, beta-delayed gamma-ray spectroscopy is investigated with a focus on developing non-destructive assay instrumentation for inventory quantification of special nuclear materials. Results obtained up to date indicate that individual isotope-specific signatures contained in the delayed gamma-ray spectra can potentially be used to quantify the total fissile content and individual weight fractions of fissile and fertile nuclides present in multi-component samples. The assay precision that is adequate for the inventory analysis can be obtained using a neutron generator of sufficient strength and currently available detection technology.

Effects of the assay system parameters on the delayed gamma-ray response are analyzed. Experimental measurements from fissionable material samples activation and high-fidelity modeling results are investigated to evaluate the importance of the interrogation time pattern. Relative merits of the more practical "single-pass" assay mode that is focused on the long-lived responses are compared with the "pulsed" mode that captures the more isotope-specific, short-lived signatures. Active neutron source and spectrometry setup requirements are established for a set of assay scenarios, corresponding response analysis and instrument calibration approaches are outlined.

Fission Detection and Competing Interferences at High Bremsstrahlung Endpoint Energies

E. S. Cardenas¹, M. T. Kinlaw³, E. T. E. Reedy¹, H. A. Seipel¹, B. W. Blackburn⁴, A. W. Hunt^{1,2}

⁽¹⁾*Department of Physics, Idaho State University, Campus Box 8106, Pocatello ID 83209-8288, United States*

⁽²⁾*Idaho Accelerator Center, Idaho State University, 1500 Alvin Ricken Drive, Pocatello ID 83201, United States*

⁽³⁾*Idaho National Laboratory, 2525 Fremont Avenue, Idaho Falls ID 83415, United States*

⁽⁴⁾*Raytheon Company, 870 Winter Street, Waltham MA 02451, United States*

In a bremsstrahlung based active interrogation technique, both β^- delayed neutrons and γ -rays have yielded reliable signatures of fissionable materials. These signatures rely on the detection of neutrons and high-energy γ -rays emitted tens to hundreds of milliseconds after the probing bremsstrahlung pulse resulting in relatively short detection timescales. At bremsstrahlung energies up to ~20 MeV, the fission signatures are unique and reliable, however, at higher bremsstrahlung energies a multitude of photonuclear reaction channels in non-fissionable materials open up resulting in reaction products whose emissions interfere with the β^- delayed neutron and γ -ray fission signatures. In the experiments discussed in this presentation, signature interferences at bremsstrahlung energies from 19 to 45 MeV were investigated from a variety of non-fissionable isotopes including but not limited to ^{18}O , Ca, ^9Be , NaCl and LiF. While most of the non-fissionable isotopes studied produced interferences at the highest bremsstrahlung energies, reaction products from ^{18}O and ^{19}F both strongly interfered with both the delayed neutron and γ -ray fission signatures. For ^{18}O , neutrons were emitted on long timescales from ^{17}N produced by the well-known $^{18}\text{O}(\gamma, p)^{17}\text{N}$ reaction and high-energy γ -rays were emitted from ^{16}N produced by $^{18}\text{O}(\gamma, np)^{16}\text{N}$ reactions. In ^{19}F , these same reaction products are produced in $^{19}\text{F}(\gamma, 2p)^{17}\text{N}$ and $^{19}\text{F}(\gamma, n+2p)^{16}\text{N}$ reaction. Mitigation of these interferences as well as others to the fission signatures is discussed.

A Design Study for the Analysis of ^{90}Sr and $^{135,137}\text{Cs}$ by ISA-AMS

Jean-Francois Alary¹, Lisa M Cousins², John Eliades³, Changtong Hao¹, Gholamreza Javahery², William E Kieser⁴,
Albert E Litherland³, Xiao-Lei Zhao⁴

⁽¹⁾Isobarex Corp., 32 Nixon Road Unit #1, Bolton Ontario L7E 1W2, Canada

⁽²⁾IONICS Mass Spectrometry Group, 32 Nixon Road Unit #1, Bolton Ontario L7E 1W2, Canada

⁽³⁾Department of Physics, University of Toronto, 60 St. George St., Toronto Ontario M5S 1A7, Canada

⁽⁴⁾Department of Physics, University of Ottawa, 150 Louis Pasteur, Ottawa Ontario K1N 6N5, Canada

Extending the range of Accelerator Mass Spectrometry (AMS) to the fission products ^{90}Sr and $^{135,137}\text{Cs}$ would offer numerous advantages for non-proliferation surveillance activities. A new method for suppressing the interfering isobars ^{90}Zr and $^{135,137}\text{Ba}$ using low kinetic energy (<20 eV) gas-phase reactions in an AMS injection line may help achieving this goal in a cost effective way [1]. The reactions occur in a radiofrequency quadrupole (RFQ) cell filled with a thin gas, the Isobar Separator for Anions (ISA). Combined with fluoride-matrix assisted ionization, this method considerably improves the analytical capabilities of AMS for ^{90}Sr and should enable the direct analysis of $^{135,137}\text{Cs}$ at sub-parts per trillion. The ISA alone provides interference suppression factors of 4×10^{-6} for $\text{ZrF}_3^+/\text{SrF}_3^+$ and 2×10^{-5} for $\text{BaF}_2^+/\text{CsF}_2^+$. The general performance improvement provided by the ISA, however, critically depends on the capacity of this device to transmit the wanted anions at a high stable efficiency. Based on recent SIMION-8.1 studies and on results of a parallel study on the attenuation of other anions, we have developed a pre-commercial design for the ISA. In this design, RFQ rods and split-flow turbo molecular pumps are configured to achieve full control of reaction time, energy and fragmentation pathways (chemical and kinetic reactions), and to optimize beam transmission through the cell. The mechanical layout will be presented in 3D models using SolidWorks; SIMION-8.1 simulations using a hard-sphere collision model were used to illustrate the gas-anion dynamics in the gas cell and in the deceleration and acceleration stages. Results of confirmatory tests obtained on an improved version of the experimental ISA setup at the IsoTrace laboratory (operated by the University of Ottawa) will also be reported.

[1] J. Eliades, X-L Zhao, A. E. Litherland and W. E. Kieser, Nucl. Instr. Meth. B (2011),
doi:10.1016/j.nimb.2011.11.030

The ReA electron-beam ion trap charge breeder for reacceleration of rare isotopes

Alain Lapierre, Stefan Schwarz, Kritsada Kittimanapun, Walter Wittmer, Daniela Leitner, Georg Bollen,
for the ReA team

NSCL, Michigan State University, 640 South Shaw Lane, East Lansing Michigan 48824, United States

ReA is a post-accelerator at the National Superconducting Cyclotron Laboratory at Michigan State University intended to reaccelerate rare isotopes to energies of ~0.3-6 MeV/u (light ions) following production by fast-projectile fragmentation and thermalization in a gas cell. Rare-isotope beams at such energies are particularly in demand for the study of capture reactions in nuclear astrophysics. ReA is being commissioned and consists of four main components: an electron-beam ion trap (EBIT), an achromatic charge-over-mass separator, a radio-frequency quadrupole (RFQ) pre-accelerator, and a superconducting radio-frequency linear accelerator (SRF-LINAC).

The EBIT employs electron-impact ionization with a quasi-monoenergetic electron beam to charge breed ions. It is designed to efficiently capture a rare-isotope singly charged ion beam injected at low energy and produce a narrow charge-state distribution of trapped highly charged ions. Such ions are subsequently extracted and a given charge state is selected according to its mass-to-charge ratio for reacceleration through the RFQ and SFR-LINAC. The use of charge-bred highly charged ions to reach high beam energies is a key aspect that makes ReA a compact and cost-efficient post-accelerator.

The EBIT is equipped with an electron-gun designed to generate an electron beam current of a few amperes. It is characterized by a unique dual magnet configuration to provide both the high electron-beam current density necessary for fast charge breeding of short-lived isotopes as well as high acceptance for injected beams. This talk will present an overview and the status of the ReA EBIT, which is presently in the commissioning phase. It has extracted for reacceleration tests charge-bred highly charged Ne^{8+} ion beams of stable isotopes produced from injected gas and more recently K^{16+} ion beams by injecting stable K^+ ions from an external ion source.

Development of Ion Beams for Space Effects Testing Using an ECR Ion Source

Janilee Benitez, Adrian Hodgkinson, Mike Johnson, Tim Loew, Claude Lyneis, Larry Phair

Nuclear Science Division, Lawrence Berkeley National Lab, One Cyclotron Road MS88R0192, Berkeley CA 94720, United States

At LBNL's 88-Inch Cyclotron and Berkeley Accelerator Space Effects (BASE) Facility, a range of ion beams at energies from 1 to 55 MeV/nucleon are used for radiation space effects testing. By bombarding a component with ion beams the space environment can be simulated and single event effects (SEEs) determined. The performance of electronic components used in space flight and high altitude aircraft can then be evaluated. The 88-Inch Cyclotron is coupled to the three electron cyclotron resonance ion sources (ECR, AECR-U, VENUS). These ion sources provide a variety of ion species, ranging from protons to heavy ions such as bismuth, for these tests. In particular the ion sources have been developed to provide "cocktails", a mixture of ions of similar mass-to-charge ratio, which can be simultaneously injected into the cyclotron, but selectively extracted from it. The ions differ in both their linear energy transfer (LET) deposited to the part and in their penetration depth into the tested part. The current heavy ion cocktails available are the 4.5, 10, 16, and 30 MeV per nucleon.

To provide the optimum range of LET a variety of ion beams and charge states is required. In order to produce a broad range of heavy ion cocktails, several methods to inject various metals and gases simultaneously have been developed, including sputter probes and ovens. Cocktail beams, first developed in 1985 in Berkeley, continue to evolve along with the capabilities of the accelerator system. The newest ECR source at Berkeley, VENUS, is capable of producing high charge state heavy ions, delivering heavier ions with increased range and LET. The most recent example is the acceleration of Bi^{56+} to 9.5 MeV per nucleon. This paper will discuss the progress and gains still underway with the ECR ion sources and how they support radiation space effects testing.

Production of Rare Isotope Beams at the Texas A&M University Cyclotron Institute

Gabriel Tabacaru¹, Donald P May¹, Juha Arje², Greg Chubarian¹, Henry Clark¹, George Kim¹, Robert E Tribble¹

⁽¹⁾*Cyclotron Institute, Texas A&M University, University Dr., MS 3366, College Station TX 77843, United States*

⁽²⁾*Accelerator Laboratory, University of Jyväskylä, Jyväskylä, Finland*

The Cyclotron Institute at Texas A&M is currently configuring a scheme for the production of radioactive-ion beams that incorporates a light-ion guide (LIG) and a heavy-ion guide coupled (HIG) with an ECRIS constructed for charge-boosting (CB-ECRIS). This scheme is part of an upgrade to the facility and is intended to produce radioactive beams suitable for injection into the K500 superconducting cyclotron. The current status of the project and details on the ion sources used in the project is presented.

High-Flux Neutron Source Based on Liquid-Lithium Target

Shlomi Halfon^{1,2}, Gitai Fienberg^{1,2}, Michael Paul², Alex Arenshtam¹, Dan Berkovits¹, Daniel Kijel¹, Ami Nagler¹,
Ilan Eliyahu¹, Ido Silverman¹

⁽¹⁾*Soreq Nuclear Research Center, Road 4111, Yavne 81800, Israel*

⁽²⁾*Racah Institute of Physics, Hebrew University, Jerusalem 91904, Israel*

A prototype of a compact Liquid Lithium Target (LiLiT), which will be able to constitute an accelerator-based intense neutron source was built. The neutron source is intended to be used for nuclear astro-physical research, boron neutron capture therapy (BNCT) in hospitals and material studies for fusion reactors. The LiLiT setup is presently being commissioned at Soreq Nuclear research Center (SNRC). The lithium target will produce neutrons through the ${}^7\text{Li}(\text{p},\text{n}){}^4\text{He}$ reaction and it will overcome the major problem of removing the thermal power generated by a high-intensity proton beam (1.91-2.5 MeV, >3 mA), necessary for sufficient therapeutic neutron flux.

The liquid-lithium loop of LiLiT is designed to generate a stable lithium jet at high velocity on a concave supporting wall with free surface for the incident proton beam (up to 10 kW). The liquid-lithium flow at a temperature of ~200°C is driven by an electromagnetic (EM) induction pump. The lithium flow is collected into a containment tank where a heat exchanger dissipates the beam power. Radiological risks due to the ^7Be produced in the reaction will be handled though cold trap and appropriate shielding.

In off-line tests, liquid lithium was flown through the loop and generated a stable jet at velocity higher than 5 m/s on the concave supporting wall. The target is now under extensive test program using a high-power 20-kW electron-gun. By now, up to 2 kW electron beam was applied on the lithium flow at velocity of 3 m/s without any instabilities of excessive evaporation. High-intensity proton beam irradiation (1.91- 2.5 MeV, 2-4 mA) will take place at SARAF (Soreq Applied Research Accelerator Facility) superconducting linear accelerator currently in construction at SNRC.

TUE-NP03-5

#188 - Contributed Talk - Tuesday 8:30 AM - Triniity Central

DIANA - A Deep Underground Accelerator for Nuclear Astrophysics Experiments

Alberto Lemut¹, Daniela Leitner³, Manoel Couder², Uwe Greife⁴, Adrian Hodgkinson¹, Joseph Saba¹, Paul Vetter, William Waldron¹, Daniel Winklehner³, Michael Wiescher², Matthaeus Leitner³

⁽¹⁾*Lawrence Berkeley National Laboratory, Berkeley CA 94720, United States*

⁽²⁾*University of Notre Dame, South Bend IN 46556, United States*

⁽³⁾*Michigan State University, East Lansing MI 48824, United States*

⁽⁴⁾*Colorado School of Mines, Golden CO 80401, United States*

A novel nuclear astrophysics facility is being designed in a collaboration of Lawrence Berkeley National Laboratory, the University of Notre Dame, Michigan State University, Western Michigan University, Colorado School of Mines, and the University of North Carolina. The goal is to develop a next generation deep underground facility to measure cross-sections of thermo nuclear reactions in the sun and pre-supernova stars. However, because of the low stellar temperatures associated with these environments and the high Coulomb barrier, the reaction cross-sections are extremely low. The experimental difficulties in determining these low energy cross-sections are caused by the vanishing small signal rates in comparison to the large background rates associated with cosmic ray-induced reactions.

One way to address this background issue is by going underground. This presentation describes the design of the proposed deep underground facility DIANA (Dakota Ion Accelerator for Nuclear Astrophysics). The facility is designed to be built and operated about one km underground in an existing or new laboratory. The basic concept of DIANA consists of two coupled electrostatic accelerators: a low energy (50 kV - 400 kV), high intensity accelerator and a flexible high energy (300 kV - 3 MV) accelerator, target stations, and detector systems. The focus of this presentation will lie on the design of the lower energy machine of the two proposed accelerators. Several technical challenges needed to be overcome in order to create, accelerate, and transport the desired beams in sufficient intensities (e.g. space-charge of beams with currents of up to 100 mA). The design with ion source, high voltage platform with variable width acceleration gap, and solenoid focusing scheme will be presented and simulations of the beam transport will be shown.

TUE-NP03-6

#193 - Contributed Talk - Tuesday 8:30 AM - Triniity Central

Historical and Climatological Research in the Himalaya Region by ^{14}C AMS Dating of Wooden Drill Cores from Historic Buildings

Wolfgang Kretschmer¹, Achim Bräuning², Andreas Scharf¹, Frederique Daragon²

⁽¹⁾*Physics, University of Erlangen, Erwin-Rommel-Str. 1, Erlangen 91058, Germany*

⁽²⁾*Geography, University of Erlangen, Kochstr. 4, Erlangen 91054, Germany*

In recent years, the Geographical Institute of the University Erlangen could sample numerous wooden drill cores from historic buildings in four regions of High Asia and could evaluate them dendrochronologically. Part of the drill cores were collected from monasteries and temples in the Dolpo region of western Nepal, a barely studied region in the Inner Himalaya and situated in the rain shadow of the main Himalayan crest line. Another major part came from temples in Central Tibet. In many cases tree-ring dating of these drill cores was not possible, indicating that the sample woods exhibit a higher age than the present range of the existing tree-ring chronologies which only reach back to the 11th century. So these samples can be used to extend the tree-ring chronologies of this region, which could help to detect suggested monsoon variations during the Middle Ages.

The historic tower buildings of Tibet and Sichuan are a special cultural heritage which has been rarely studied up to now. The knowledge of their exact age could help to better understand the cultural and historical context of their development and their function, and could support the effort to declare them a UNESCO World Heritage site. The Erlangen AMS laboratory has performed ^{14}C - datings via accelerator mass spectrometry on 200 samples of 74 of these drill cores. Using wiggle-matching these drill cores could be dated with enhanced precision, and in many cases important information about the time of construction of these important historic buildings could be obtained for the first time.

TUE-NP03-P1

#340 - Poster - Tuesday 5:30 PM - Rio Grande

Quasi-Monoenergetic Protons Accelerated from a Thin Multi-Ion Foil by Laser Radiation Pressure

Tung-Chang Liu, Jao-Jang Su, Xi Shao, Chuan-Sheng Liu

East-West Space Science Center, University of Maryland, College Park, University of Maryland, College Park MD 20742, United States

Radiation pressure acceleration is considered as an efficient way to produce quasi-monoenergetic ions, where an ultra-thin foil is accelerated by high intensity circular polarized laser. However, along with the rapid acceleration is the fast growing rate of the instabilities. A crucial factor limiting this acceleration scheme is the Rayleigh-Taylor instability, which results in the exponential growth of the perturbation of the foil density during the acceleration and hence the induced transparency of the foil and the broadening of the particle energy spectrum. We study the radiation pressure acceleration of a multi-ion thin foil made of a mixture of carbon and hydrogen and investigate the possibility of using abundant electrons supplied from carbon to delay the foil from becoming transparent, enhance the acceleration of protons from the carbon ion layer fallen behind and therefore improve the energy of quasi-monoenergetic proton beam. Particle-in-cell simulations have been used to find energy dependencies of quasi-monoenergetic protons on concentration of carbon and hydrogen in the foil and optimal conditions for obtaining higher proton energies. Our simulation shows that a quasi-monoenergetic proton beam of 60 MeV and 100 MeV can be produced by circular polarized laser of normalized amplitude a_0 being 5 and 10, respectively, corresponding to laser power of less than 300 TW.

TUE-NP04-1

#303 - Invited Talk - Tuesday 3:30 PM - Trinity Central

Facility upgrades and research developments at the Brookhaven Linac Isotope Producer (BLIP)

Leonard F Mausner

Collider Accelerator Department, Brookhaven National Laboratory, Building 801, Upton NY 11973, United States

Now over 40 years old the Brookhaven Linac Isotope Producer continues to operate effectively due to many enhancements, big and small. For example, the Linac can now incrementally vary beam energy pulse to pulse. It provides protons to BLIP at energies of 66, 92, 117, 139, 160, 181, or 200 MeV while simultaneously delivering low intensity polarized protons at 200 MeV for nuclear physics experiments in the Relativistic Heavy Ion Collider (RHIC). Recent modifications to the low energy beam transport line upstream of the Linac have improved beam transmission and led to an increase in integrated intensity up to a maximum 120 μA (42mA pulse, 430 μs , at 6.67Hz repetition rate). The increased average and instantaneous beam current as well as a sharply peaked Gaussian shaped beam intensity profile have caused target reliability and lifetime issues. Therefore we plan to implement a beam raster system in BLIP with a rapid ($\sim 3\text{kHz}$) scan frequency. This will require better beam diagnostics in the BLIP beam line, including a laser profile monitor and a plunging multiwire device, and require rapid cycling magnets and power supplies to continuously move the beam spot. The isotopes Sr-82, Ge-68, Zn-65, Rb-83 and Be-7 are now routinely produced and distributed. Radioisotopes under development include Cu-67, and Y-86. These require the use of an expensive enriched stable isotope target material that must be recovered, purified and recycled into new targets. After first use the material will be radioactive. Similarly we plan to make Ac-225 with a Th-232 target. Therefore a capsule design that could be sealed remotely in a hot cell rather than simply fabricated and welded in a machine shop was developed.

Cyclotron Production of Radioisotopes at Washington University

Suzanne Lapi, Tom Voller, Evelyn Madrid, Deborah Sultan, Paul Eisenbeis
Radiology, Washington University, 510 S. Kingshighway Blvd, St. Louis MO 63110, United States

The common isotopes used for positron emission tomography (PET), ^{18}F , ^{11}C , ^{15}O and ^{13}N , have relatively short half-lives (less than 2 hours) which only allow for imaging of biological processes that occur on a rapid timescale. For imaging of the biodistribution of larger molecules such as antibodies or nanoparticles which have a long blood circulation time (hours-days) PET isotopes with longer half-lives must be produced. Our group has focused on the production of positron emitters ^{64}Cu , ^{86}Y , ^{76}Br and ^{89}Zr and the distribution of these isotopes to other research centers. This involves the irradiation of appropriate solid target materials on our 15 MeV proton cyclotron, purification of the isotopes from the target and often recycling of the isotopically enriched target material. We have developed semi-automated systems for those isotopes which we routinely produce in large quantities to minimize dose to personnel. We currently supply ^{64}Cu to 15-20 research facilities per week and support 3 clinical trials with agents involving this isotope. An overview of the current status and future plans for the isotope production program at Washington University will be presented.

Accelerator Based Isotope Production and R&D at LANL

Kevin D John, Eva R Birnbaum, Beau D Ballard, Jonathan W Engle, Michael E Fassbender, F Meiring Nortier,
 Wayne A Taylor
Los Alamos National Laboratory, PO Box 1663, Los Alamos NM 87544, United States

The Los Alamos National Laboratory (LANL) has an almost four decade long history of producing radioisotopes for applications in medicine, industry and science. Starting in 1974, a wide variety of isotopes were made available through production via spallation, using the 800 MeV proton beam of the Los Alamos Meson Physics Facility (LAMPF), now called the Los Alamos Neutron Science Center (LANSCE). This capability was decommissioned in the late nineties but shortly afterwards replaced with the commissioning of a new state-of-the-art 100 MeV facility in 2005, which provided new impetus to the advancement of the program's international leading role.

In the past half decade, the program has developed a world-leading production capability for $^{82}\text{Sr}/^{82\text{m}}\text{Rb}$ and $^{68}\text{Ge}/^{68}\text{Ga}$ Positron Emission Tomography (PET) radionuclide generators. Strontium-82/ $^{82\text{m}}\text{Rb}$ is utilized for cardiac imaging mainly in North America, while $^{68}\text{Ge}/^{68}\text{Ga}$ serves as calibration source for PET instruments worldwide, and LANL's supply record for these isotopes is unmatched in terms of quality and reliability. In 2008 the DOE Office of Science, Office of Nuclear Physics took ownership of the LANL isotope program and began to assert the need to expand the program's R&D component. This move has catalyzed research efforts in highly specialized technical areas such as high current targetry, nuclear data measurements, complex radiochemical separations, and novel applications of the program's portfolio of unique radioisotope products. A few examples of isotopes currently under investigation at Los Alamos include ^{225}Ac , ^{186}Re and $^{72,74}\text{As}$ for medical imaging and therapy. A variety of other isotopes are presently being considered to support our focus on therapeutic applications and in support of our core nuclear physics mission. This talk provides an overview of the present status of LANL's production capabilities, current isotope portfolio and emerging R&D efforts.

Production of Th-229 with low energy protons

Cara U Jost¹, Rose A Boll², Stephanie H Bruffey², Justin R Griswold², Saed Mirzadeh², Daniel W Stracener³,
Cecil L Williams⁴

⁽¹⁾*Department of Physics and Astronomy, University of Tennessee, Knoxville TN 37996, United States*

⁽²⁾*Fuel Cycle & Isotopes Division, Oak Ridge National Laboratory, Oak Ridge TN 37831, United States*

⁽³⁾*Department of Physics, Oak Ridge National Laboratory, Oak Ridge TN 37831, United States*

⁽⁴⁾*Oak Ridge Associated Universities, Oak Ridge TN 37831, United States*

The α -emitters Ac-225 and Bi-213 are of great interest for α -radioimmunotherapy where radioisotopes attached to cancer-seeking antibodies can be used to efficiently treat various types of cancers. Both radioisotopes are daughters of the long-lived Th-229 ($t_{1/2} = 7880\text{y}$). This isotope can be obtained either from the decay of stockpiles of U-233, a currently inaccessible resource, or from irradiation of Ra-226 targets in a high flux nuclear reactor.

Alternatively, Th-229 can be produced by proton irradiation of Th-232 and Th-230, either directly via (p,pxn) reactions, through a (p,xn) reaction producing Pa-229, which decays to Th-229 with a half-life of 1.5 days, or through the (p, α) reaction on Th-232 to Ac-229, which decays to Th-229 with a half-life of one hour. The excitation functions for the relevant nuclear reactions are mostly unknown. To obtain these excitation functions, stacks of Th-232 foils and Th-230 electrodeposited on Al foils were irradiated at the On-Line Test Facility at the Holifield Radioactive Ion Beam Facility at ORNL. The maximum proton current on target was 50 nA, with a maximum beam energy of 40 MeV. The yield of reaction products was determined by gamma-ray spectroscopy, in some cases after chemical separation.

Benchmark tests of well-measured cross-sections for isotopes produced via proton induced reactions on Cu and Ni foils, show very good agreement with literature results. The experiments with thorium targets were focused on the production of Pa-229 and its daughter Ac-225 from both Th-232 and Th-230 targets. Differential cross-sections for the production of Pa-229 and other Pa isotopes have been obtained and will be presented.

BEST Medical Radioisotope Production Cyclotrons

Vasile Sabaiduc, Bruce Milton, Richard Johnson, Krishnan Suthanthiran
Best Cyclotron Systems Inc., #7-8765 Ash Street, Vancouver British Columbia V6P 6T3, Canada

Best Cyclotron Systems Inc (BCSI) is currently developing 14MeV, 25MeV, 35MeV and 70MeV cyclotrons for radioisotope production and research applications as well as the entire spectrum of targets and nuclear synthesis modules for the production of the PET, SPECT and radiation therapy isotopes. The company is a subsidiary of Best Medical International renowned in the field of medical instrumentation and radiation therapy. All cyclotrons have external negative hydrogen ion sources, four radial sectors with two dees in opposite valleys, cryogenic vacuum system and simultaneous beam extraction on opposite lines. The beam intensity ranges between 400 μA to 1000 μA depending on the cyclotron energy and application. The BEST14p is designed for fixed 14MeV extraction with a combined beam current of 400 μA . The main application is for the production of PET isotopes and $^{99\text{m}}\text{Tc}$ production. All higher energy cyclotrons, BEST25p, BEST35p and BEST70p are designed for variable energy extraction with a combined beam current in excess of 1000 μA . While BEST25p and BEST35p cyclotrons extend the capability to producing more medical radioisotopes for diagnostics and therapy the BEST70p reaches radioisotope production for heavy radionuclides most notable the production of ^{82}Sr , the parent for ^{82}Rb generators. The BEST70p cyclotron may also be used as injector to a post-accelerator or for the production of the radioactive beams. Beam lines are optional on the 14MeV and 25MeV cyclotron and standard supply for the 35MeV and 70MeV cyclotrons (custom designed beam lines).

Multi-Ion Beam Lithography of Graphene on SiC by Low-Temperature Annealing

Bill R. Appleton^{1,2}, Sefaattin Tongay^{2,3}, Maxime Lemaitre¹, Arthur F. Hebard³, Brent Gila^{1,4}, Joel Fridmann⁵, Achim Nadzeyka⁶, Fan Ren⁷, Xiaotie Wang⁷, Dinesh K. Venkatachalam⁸, Robert G. Elliman⁸, Joseph Klingfus⁵

⁽¹⁾*Department of Material Science and Engineering, University of Florida, Gainesville FL, United States*

⁽²⁾*Nanoscience Institute for Medical and Engineering Technologies, University of Florida, Gainesville FL, United States*

⁽³⁾*Department of Physics, University of Florida, Gainesville FL, United States*

⁽⁴⁾*Nanoscale Research Facility, University of Florida, Gainesville FL, United States*

⁽⁵⁾*Raith USA, Ronkonkoma NY, United States*

⁽⁶⁾*Raith GmbH, Dortmund, Germany*

⁽⁷⁾*Department of Chemical Engineering, University of Florida, Gainesville FL, United States*

⁽⁸⁾*Department of Electronic Materials Engineering, Australian National University, Canberra, Australia*

Promising techniques for growing graphene on SiC single crystals for electronic device fabrication include heating in UHV above the graphitization temperature (T_G)¹; or processing them in vacuum using pulsed excimer laser².

Here we report an approach that combines ion implantation, thermal or pulsed laser annealing (PLA), and multi-ion beam lithography (MIBL) to both pattern and synthesize graphene nanostructures on SiC single crystals at low temperatures. This approach utilizes a MIBL system developed at the University of Florida in collaboration with Raith for implantation/nanofabrication, in combination with thermal annealing in vacuum or PLA with a 25 ns pulsed ArF laser in air. To investigate the mechanisms and the effects of the implanted species, ion damage, and annealing, samples were also subjected to broad-area ion-implantations using facilities at the Australian National University.

We show that implantation of Si, Ge, Au, or Cu followed by thermal annealing in vacuum below the T_G of SiC can selectively grow graphene only where the ions are implanted, and that graphene nanoribbons a few nanometers to microns wide can be formed using MIBL. Additionally, we will show that graphene can be formed on implanted and/or unimplanted SiC by ArF PLA in air, at fluences from 0.4-1.2 J/cm². AES, SEM, X-sectional TEM, micro-Raman analyses and heat flow simulations are presented to verify graphene growth and explain the effects and mechanisms involved.

We also report recent findings on graphitization of SiC using patterned Ga implantation, in which the implanted regions exhibit reduced T_G .

1. Conrad, P. N. First, and W. A. de Heer, J. Phys. Chem. 108, 19912 (2004).

2. Sangwon Lee, Michael F. Toney, Wonhee Ko, Jason C. Randel, Hee Joon Jung, Ko Munakata, Jesse Lu, Theodore H. Geballe, Malcolm R. Beasley, Robert Sinclair, Hari C. Manoharan, and Alberto Salleo; ACS Nano Vol.4, No. 12, 7524-7530 (2010).

Towards a regular array of single swift heavy ion impact sites

Sjoerd Roorda

physique, Université de Montréal, 2900 Boulevard Edouard Montpetit, Montréal Québec H3C 3J7, Canada

What happens during the passage of a swift ion through a solid is of interest to both technology (e.g., nanopores, radium exposure dosimetry) and science (e.g. does the track melt or not). A difficulty in studying ion tracks is that they are highly localized in both time and space, so that one can only study "post-mortem" effects. In this work, we have attempted to limit the effect of the random spatial distribution of ion tracks. Self-organized anodic porous alumina masks were made and positioned in front of oxide and a-Si samples. The sample+mask sandwich was aligned with the ion beam and exposed to low fluences of ions, chosen so as to optimize the probability of only one ion passing through a single pore. Atomic force microscopy of the irradiated sample shows that the lateral distribution of the single ion impact sites is nearly equidistant with a most probable distance between first neighbouring impact sites corresponding to the inter-pore distance in the mask. The signal from grazing incidence small angle x-ray scattering is greatly enhanced and exhibits a feature corresponding to the average distance between single impact sites.

Microscale fabrication and functionalization of single-crystal diamond with focused MeV ion beams

Paolo Olivero^{1,2,3,4}

⁽¹⁾*Physics Department, University of Torino, via P. Giuria 1, Torino 10125, Italy*

⁽²⁾*"Nanostructured Interfaces and Surfaces" Centre of Excellence, University of Torino, Torino 10125, Italy*

⁽³⁾*Sezione di Torino, INFN, Torino 10125, Italy*

⁽⁴⁾*Sezione di Torino, Consorzio Nazionale Interuniversitario per le Scienze Fisiche della Materia, Torino 10125, Italy*

Diamond exhibits a set of outstanding physical properties: high mechanical and radiation hardness, chemical inertness, spectrally wide transparency, high carrier mobility, high dielectric strength, bio-compatibility. These features make diamond appealing for many applications, ranging from micro-optical devices to particle detectors, and from micro-fluidics to nano-electromechanical systems and photonic devices. Remarkably, the same properties also pose a major challenge in the fabrication of this material. MeV and keV ions represent a powerful tool for fabrication and functionalization of diamond, particularly if it is considered that the structural modification of the diamond crystal offers access to alternative allotropic forms of carbon (diamond, amorphous carbon, graphite) with significantly different physical properties. This results in the possibility of tailoring the electrical, optical and structural properties of this material. Such structural modification process can be carried with high spatial resolution in both lateral and depth dimensions, thanks to the availability of focused ion beams and to the peculiar damage density profile of highly energetic ions in matter, respectively.

In the present contribution, an overview will be given on our activity in the development of deep ion beam lithography in diamond carried at the University of Torino in collaboration with several partner institutions:

- fabrication of three-dimensional conductive structures in the bulk material by means of variable-thickness masks for applications in bio-sensing and radiation detection;
- fabrication of waveguiding structures by means of a controlled modification of the material's refractive index;
- fabrication of microfluidic channels with the selective removal of sacrificial graphitic layers;
- production of optically active luminescent centers by direct ion implantation.

NanoScale Performance Enhancement for Ion Beam Lithography, using Guided Self-Assembly

John Baglin

IBM Almaden Research Center, 650 Harry Road, San Jose CA 95120, United States

Despite the narrow width of an ion track in a typical polymer resist layer, it has proved to be problematic to develop techniques for ion based lithography whose performance could satisfy the requirements of the ITRS Roadmap for commercial fabrication with spatial fidelity that is acceptable beyond the CMOS 22 nm node. For future device patterning, for example, the Roadmap requires not only lateral resolution of a few nanometers or less, but also line edge roughness (LER) below 2 nm, and stable critical dimensions. For practical adoption of ion beam lithography, exposure of a resist layer must not cause distortion of adjacent features due to proximity effects in the resist. And patterning must not create thermal or radiation damage to device layers beneath the resist. And processing throughput for an entire wafer must retain or exceed the speed currently offered by standard UV or e-beam processing of traditional photoresists. The LER and resolution criteria would apparently demand very high local doses of focused ions for edge regions, in order to avoid pattern defects due to stochastic shot noise - a process inconsistent with commercial manufacturing criteria.

In this presentation, we explore possible solutions to these problems, based on the concept of applying sparse ion exposure in order to seed directed self assembly of critical pattern features having clean geometrical definition. We also discuss the potential applicability of such approaches for fabrication of integrated 3-D device structures.

Surface nanopattern formation by ion-beam sputtering: recent developments

Rodolfo Cuerno

Departamento de Matemáticas, Universidad Carlos III de Madrid, Avenida de la Universidad 30, Leganés Madrid 28911, Spain

Ion beam sputtering of monoelemental targets that become amorphous under low to medium energy irradiation has attracted much interest as a technique to produce high quality surface nanopatterns. However, although reports on modifications of surface topography thus achieved date back to the 1960s, a physical picture that allows us to understand and eventually control this route to nanostructuring is being elucidated only in the recent few years [1]. To date, many questions still remain to be answered. Among other, they include the physical nature of the microscopic processes that control the evolution of the surface morphology over macroscopic times, the correct space-time description of the complex surface topographies that ensue, and the capability of the technique to produce textures than differ from the usual spontaneous arrays of nanometric sized features, like ripples and dots, and that may have a similar interest for electronic, magnetic, or optical applications. In this talk we will present recent experimental and theoretical results that tackle some of these issues.

[1] For a recent overview, see e.g. R. Cuerno, M. Castro, J. Munoz-Garcia, R. Gago, and L. Vazquez, Nucl. Instr. Meth. Phys. Res. B 269, 894 (2011).

Self-Assembled Nanoscale Patterns Produced by Ion Bombardment of Binary Compounds

R. Mark Bradley¹, Patrick D. Shipman², Francis C. Motta²

⁽¹⁾*Department of Physics, Colorado State University, Fort Collins Colorado 80523, United States*

⁽²⁾*Department of Mathematics, Colorado State University, Fort Collins Colorado 80523, United States*

We review our recent work which demonstrates that a surface layer of altered composition can have a crucial effect on pattern formation induced by ion bombardment of a solid surface. First, we discuss a theory that explains the genesis of the strikingly regular hexagonal arrays of nanodots that can form when the binary material GaSb is bombarded at normal incidence. In our theory, the coupling between a surface layer of altered stoichiometry and the topography of the surface is the key to the observed pattern formation. For a certain range of the parameters, we find that nanodot arrays with strong short range hexagonal order emerge spontaneously. Our theory also predicts that remarkably defect-free ripples can be produced by oblique-incidence bombardment of a binary material if the ion species, energy and angle of incidence are appropriately chosen. This high degree of order cannot be achieved by bombarding an elemental material.

A related theory yields insight into pattern formation induced by deposition of impurities during ion bombardment of an elemental material. We show that if the impurities are deposited obliquely during normal- or near-normal-incidence ion bombardment, a novel instability can yield surface ripples. This instability can set in even if the curvature dependence of the sputter yields is negligible and the two atomic species are completely miscible.

Is sputter erosion relevant for ion induced self-organized surface patterns?

Hans Hofsäss, Kun Zhang, Omar Bobes, André Pape

Faculty of Physics, 2nd Institute of Physics, University Göttingen, Friedrich-Hund-Platz 1, Göttingen 37077, Germany

Ion induced self-organized surface patterns have attracted much attention in the last years. Several experimental studies have demonstrated that co-deposited atoms during ion beam erosion of a substrate have a tremendous impact on the pattern formation. Furthermore, the dominant role of curvature dependent sputter erosion was put into question and other processes like collision cascade prompt mass redistribution (the Carter-Vishnyakov effect), crater formation etc. were proposed as decisive mechanisms leading to topographical surface instabilities and self-organized nano pattern formation. Novel theoretical approaches and computer simulation studies were introduced to take into account co-deposited surfactant atoms in the pattern formation process.

In this contribution we discuss pattern formation under the presence of co-deposited atoms as well as systematic studies on pattern formation on pure substrates. Ion beam surface pattern formation in the presence of co-deposited metal impurities is investigated for Si and amorphous carbon (a-C) substrates and for keV Xe ions incident at normal and near normal direction. Ion induced phase separation and metal silicide formation are seen as the relevant processes leading to dot and ripple patterns. Pattern formation on pure Si, a-C and Pt substrates is investigated for grazing incidence (45° to 85°) Xe and Ne ion irradiation with energies varied between 100 eV and 10 keV. Our results indicate that both sputter erosion and mass transport are relevant for pattern formation. The contribution of each mechanism can be evaluated from the ion incidence angle marking the transition between perpendicular and longitudinal ripple orientation.

Creating sharp features by colliding shocks on uniformly ion-bombarded surfaces

Miranda Holmes-Cerfon, Michael J Aziz, Michael P Brenner

School of Engineering and Applied Science, Harvard University, 29 Oxford Street, Cambridge MA 02138, United States

We investigate the nonlinear dynamics of surface evolution under ion bombardment, with the goal of finding a dynamical way to create sharp, small-scale structures. We show, through theory, numerical simulations, and experiment, that if a surface is patterned initially to have finite slopes on the macroscale, then it evolves under uniform bombardment to a pattern made of identical knife-edge-like ridges, with scales much smaller than those in the initial condition or achievable through linear instabilities. The ridges are predicted by the governing macroscopic equations in which they arise as a special kind of traveling wave solution with a very large basin of attraction. We derive asymptotically a one-dimensional equation for the nonlinear evolution of level sets of surface slope, and show how this can be used to predict the final location of the ridges. Our hope is that one can eventually invert this equation to answer the inverse problem: can we find an easily-achievable initial patterning of the surface, so that it evolves under uniform irradiation to a target small-scale pattern?

Self-Organized Nanoscale Pattern Formation Using Ion Beams

Michael J. Aziz

School of Engineering and Applied Sciences, Harvard University, 29 Oxford Street, Cambridge MA 02138, United States

Focused and unfocused ion beam irradiation of a solid changes the surface morphology by sputter erosion, ballistic mass redistribution, and material relaxation processes. Their interplay can result in self-organized nanoscale corrugation, dot, or hole patterns with periodicities down to 7 nm; self-sharpening high-sloped shock fronts that propagate instead of dissipating and evolve to the same slope from a range of initial slopes; and controlled closure of nanopores with applications to single biomolecule detection. Current understanding of these phenomena will be reviewed from an experimental and a theoretical perspective. The prospects for using guided self-organization for large-area patterning of functional nanostructures will be discussed.

Recent Analytical Progress on Low-Energy Ion Irradiation

Scott A Norris

Mathematics, Southern Methodist University, 208 Clements Hall, Dallas TX 75275-0156, United States

Despite more than 40 years of research since the first observation of patterns on ion-irradiated surfaces, a predictive model explaining these patterns has remained elusive -- models based directly on physical principles have struggled to agree with experiment, while more phenomenological models with good agreement have remain ungrounded in physics. In particular, since the observation of highly-ordered hexagonal nanodots on various materials irradiated in the 1 keV range, a primary problem has been to identify a mechanism for the **finite-wavelength bifurcation** typically associated with such patterns in other branches of science

In this talk we present recent advances in the understanding of amorphous solids irradiated at low ion energies. Two primary physical mechanisms once proposed to cause dot structures are discussed. On the timescale of individual ion impacts ($\sim 10^{-12}$ sec), target atoms involved in the collision cascade but not sputtered away from the surface undergo **mass redistribution**, often forming small craters with rims. Understanding the long-time effect of these craters requires careful multi-scale analysis to connect with the much longer timescale in which patterns emerge. Additionally, on the timescale of tens of seconds, stress is generated in the solid, the relaxation of which is investigated using a viscoelastic continuum model.

Together, these studies have greatly improved our understanding of the pure amorphous system, such that quantitative comparisons with experiment are now possible. Interestingly, neither effect produces the finite-wavelength bifurcation required for ordered dot formation, which was originally accepted as a deficiency in the theory. However, more recently, it has been discovered that all experiments observing dot structures on pure materials ultimately suffered from contamination, and such structures are now widely believed to occur only in systems with two different target atoms, in which concentration effects come into play. Hence, for pure systems, theory and experiment are finally beginning to converge.

Nanoscale topography formation on Ge surfaces bombarded by low-energy Kr^+ ions

Joy C. Perkinson, Charbel S. Madi, Michael J. Aziz

School of Engineering and Applied Sciences, Harvard University, 29 Oxford Street, Cambridge MA 02138, United States

Ion irradiation of surfaces has been shown to create ripples, dots, holes, and ultrasmoothering on a variety of materials. Features as small as 7 nm have been observed, leading to interest in ion irradiation as a technique for large-scale production of devices with sub-lithographic features. It is thus of interest to develop a working model to predict and understand the behavior of surfaces under ion bombardment. The nanoscale pattern formation of Ge surfaces uniformly irradiated by Kr^+ ions was studied in a low-contamination environment at ion energies of 250 and 500 eV and at angles of 0° through 85° . We present a phase diagram of domains of pattern formation occurring as these two control parameters are varied. Flat surfaces are stable from normal incidence up to an incidence angle of $\theta=55^\circ$ from normal. At higher angles, the surface is linearly unstable to the formation of parallel-mode ripples, in which the wave vector is parallel to the projection of the ion beam on the surface. For $\theta>75^\circ$ we observe perpendicular-mode ripples, in which the wave vector is perpendicular to the ion beam. This behavior is qualitatively similar to those of Madi et al. for Ar^+ -irradiated Si but is inconsistent with those of Ziberi et al. for Kr^+ -irradiated Ge. The existence of a window of stability is qualitatively inconsistent with the erosion-based theory of Bradley and Harper and qualitatively consistent with the theory of ion impact-induced mass redistribution as well as crater function theory. The critical transition angle between stable and rippled surfaces occurs $10\text{--}15^\circ$ above the value predicted by the simple Carter-Vishnyakov model of mass redistribution. Implications for theory will be discussed.

Real-Time X-ray Investigations of Semiconductor Surface Stability and Instability during Ion Bombardment

Karl F. Ludwig, Jr.¹, Eitan Anzenberg¹, Joy Perkinson², Charbel S. Madi², Michael J. Aziz²

⁽¹⁾*Physics, Boston University, 590 Commonwealth Ave., Boston MA 02215, United States*

⁽²⁾*School of Engineering and Applied Sciences, Harvard University, Cambridge MA 02138, United States*

Grazing-incidence small-angle x-ray scattering can quantitatively examine evolving surface morphology on lateral length scales of 1-100 nm during a wide range of surface processes. Using a facility developed at the National Synchrotron Light Source (Brookhaven National Laboratory), we have carefully examined the initial stages of self-organized nanostructure formation or ultra-smoothing during 1 keV Ar^+/Si and Kr^+/Ge bombardment at room temperature. Our measurements determine the linear theory amplification factor $\mathbf{R}(\mathbf{q})$ as a function of surface modulation wavenumber \mathbf{q} and ion incidence angle. The amplification factor reflects the surface stability/instability during ion bombardment: if $\mathbf{R}(\mathbf{q})$ is negative, the surface is stable to small perturbations, if it is positive, the surface is unstable to the growth of perturbations. For Ar^+/Si , the amplification factor behavior is consistent with lateral mass redistribution both driving surface smoothing at low bombardment angles, and driving the surface instability at bombardment angles above a critical angle of 45° [1,2]. The general surface behavior for Kr^+/Ge is qualitatively similar to that for Ar^+/Si , but the critical angle of transition between stability and instability increases to approximately 62° [3].

This is difficult to quantitatively explain within the simplest theory of lateral mass redistribution. A more sophisticated crater function approach combining redistributive and erosive effects can exhibit more complex phase behavior [4], but our experimental results also provide critical tests of its accuracy independent of the exact shape of the assumed crater function response of the surface to an ion impact.

[1] C. Madi et al., **Phys. Rev. Lett.** **106**, 066101 (2011).

[2] E. Anzenberg et al., **Phys. Rev. B** **84**, 214108 (2011).

[3] E. Anzenberg, et al., in preparation.

[4] S.A. Norris et al., **Nature Comm.** **2**, 276 (2011).

The BU and Harvard components of this research were supported by NSF DMR-1006538 and DE-FG02-06ER46335 respectively.

Self-assembled nano-patterns by off-normal gas cluster ion beam bombardment

Buddhi Tilakaratne, Dharshana Wijesundera, Xuemei Wang, Wei-Kan Chu

Department of Physics and Texas Center for Superconductivity, University of Houston, 3201 Cullen Blvd, Ste 202 Houston Science Center, Houston TX 77204, United States

Surface nano-pattern formation has generated promising applications in semiconductor, medical related industries. We use 3000 Ar atoms per cluster ion beam to irradiate surfaces at an off-normal angle to generate self-assembled nano-patterns on surfaces of Au, Ag, polystyrene polymer thin films and bulk materials (e.g. Si, SiO₂). When a cluster ion collide off-normal to the surface target atoms gain forward momentum and nano patterns start to develop on the surface and highest surface instability depends on the cluster ion incident angle, energy and the target material. During irradiation process surface atoms undergo three sputtering processes: (i) target atoms having similar or higher energies as of atoms of the cluster would gain the necessary work potential to dissipate into the vacuum, (ii) atoms having lesser amount of energy would redeposit on the surface, which are known as hopping atoms, and (iii) atoms with a fraction of energy diffuse close to the surface in the direction of cluster ion incident direction. In this presentation we will discuss experimental results of surface evolution during the cluster ion beam off-normal irradiation and compare results with a theoretical model.

Use of ion irradiation to study void swelling of ferritic and ferritic-martensitic steels at damage levels of 50 to 600 dpa at 400-580°C

Frank A. Garner¹, V. N. Voevodin², V. V. Bryk², V. V. Melnichenko², O. V. Borodin², P. Hosemann³, L. Hsiung⁴

⁽¹⁾*Radiation Effects Consulting, 2003 Howell Avenue, Richland WA 99354, United States*

⁽²⁾*Kharkov Institute of Physics and Technology, Kharkov 61072, Ukraine*

⁽³⁾*University of California, Berkeley, Berkeley CA 94720, United States*

⁽⁴⁾*Lawrence Livermore National Laboratory, Livermore CA 94551, United States*

Void swelling is often the life-limiting concern for austenitic steels in fission, fusion and spallation environments. Therefore research is directed toward ferritic and ferritic-martensitic steels known to swell less during irradiation. Oxide-dispersion-strengthened (ODS) variants are also under development, with the expectation that they will exhibit higher strength at elevated temperatures, with a reduction in swelling due to oxide-metal interfaces acting as sinks for radiation-generated point defects, helium and hydrogen. Due to the limited data from reactors, current activities focus on HT9 in the USA (≤ 208 dpa in FFTF) and EP-450 in Russia (≤ 160 dpa in BOR-60). Both are 12Cr alloys with HT9 in fully tempered condition (decomposed martensite grains with small fractions of delta ferrite and carbides) and EP-450 tempered to produce a 1:1 duplex grain structure of ferrite and decomposed martensite. There is additional interest in MA957, an ODS alloy (≤ 110 dpa in FFTF) and an ODS variant of EP-450, both ferritic only.

To explore the swelling of these alloys at doses >100 dpa and beyond, ion bombardment at 1×10^{-2} dpa/sec were conducted using 1.8 MeV chromium ions at 400-550°C, extracting microscopy data at 150 nm below the surface, far from the influence of the injected chromium, which not only suppresses swelling by its physical presence as an injected interstitial but by its chemical accumulation, reaching 20% additional Cr when 500 dpa is reached in the examined area. In non-ODS alloys swelling exhibits a bilinear behavior where the transient regime varies from 150-400 dpa depending on grain structure, followed by a steady-state swelling regime of $\sim 0.2\%$ per dpa, one-fifth the rate of austenitic alloys. Ferrite grains enter the steady-state regime sooner (~ 150 dpa) than decomposed martensite grains, which resist to 300-400 dpa. Swelling of ODS alloys is strongly variable, dependent on local dispersoid level.

Microstructural Evolution of Nanocrystalline Nickel Thin Films due to High-Energy, Heavy-Ion Irradiation

Khalid Hattar, Shreyas Rajasekhara, Paulo J Ferreira

Radiation Solid Interactions, Sandia National Laboratories, PO Box 5800, Albuquerque New Mexico 87185, United States

Nanocrystalline metals have been extensively investigated over the last several decades and are reported to have some promising and unexpected thermal and mechanical properties. Recently, it has been speculated that the wealth and type of grain boundaries and interface structures in nanostructured metals provides an appreciable density of rapid diffusion pathways. The increase in diffusion pathways has been theorized to result in decreased accumulation of radiation defects and subsequently radiation tolerant structures.

This presentation will highlight results from an initial investigation into the structural stability under extreme radiation environments of a well-studied nanocrystalline nickel thin film. The film produced by pulsed laser deposition is comprised of a nearly monodispersed nanocrystalline structure whose thermal and mechanical properties have been extensively characterized. These free-standing thin films, of nominal 90 nm thickness, were irradiated with 35 MeV Ni⁶⁺ ions at doses ranging from nominally 1 dpa to 10 dpa using a 6 MV Tandem accelerator. In addition to the expected point defect substructure grain growth was seen in samples with at least two dpa of radiation damage. Samples subjected to greater than 10 dpa damage with 35 MeV Ni⁶⁺ ions exhibited a large percentage of metastable hcp Ni phase identified by precession electron microscopy. The radiation stability of these nanocrystalline films in light of the thermal and mechanical stability and insight gained into potential radiation tolerant materials will be discussed.

This research was funded by the U.S. Department of Energy, Office of Science, Office of Basic Energy Sciences, Division of Materials Sciences and Engineering. Sandia National Laboratories is a multi-program laboratory managed and operated by Sandia Corporation, a wholly owned subsidiary of Lockheed Martin Corporation, for the U.S. Department of Energy's National Nuclear Security Administration under contract DE-AC04-94AL85000.

Ion-irradiation induced damage in FeCr alloys characterized by nanoindentation

Cornelia Heintze¹, Frank Bergner¹, Mercedes Hernández-Mayoral²

⁽¹⁾*Institute of Ion Beam Physics and Materials Research, Helmholtz-Zentrum Dresden-Rossendorf, Bautzner Landstrasse 400, Dresden 01328, Germany*

⁽²⁾*Technology Department, CIEMAT, Avenida de la Complutense 40, Madrid 28040, Spain*

Self-ion irradiation in combination with nanoindentation offers the possibility to characterize irradiation damage in a broad range of irradiation temperature and fluence. Nanoindentation results are reported for binary FeCr alloys of commercial purity with nominal chromium contents of 2.5, 9 and 12 at%. The irradiation conditions considered include irradiations at room temperature, 300°C and 500°C. Special features of this work are roughly rectangular damage profiles produced by multi-step irradiations with different ion energies and exploitation of the load dependence of hardness for indentation loads in the range of 2 to 500 mN. The effects of Cr content, fluence and irradiation temperature are discussed. Irradiation-induced changes of the microstructure were characterized by means of transmission electron microscopy (TEM). Hardening features and their contribution to the observed irradiation-induced hardness changes will be discussed in the framework of a tentative two-feature hardening model. Small-angle neutron scattering (SANS) data reported for neutron-irradiated conditions of the same alloys will be taken into account.

Accelerator-Driven Subcritical Fission in a Molten Salt Core: Closing the Nuclear Fuel Cycle for Green Nuclear Energy

Akhdiyov Sattarov², Saeed Assadi², Karie Badgley², Justin Comeaux², Joshua Kellams², Thomas Mann⁴, Al McInturff², Peter McIntyre², Nathaniel Pogue², Elizabeth Sooby², Michael Simpson⁵, Prabhat Trepahy⁵, Supathorn Phongikaroon¹, Pavel Tsvetkov³, Marvin Adams³

⁽¹⁾Chemical Engineering, University of Idaho, Idaho Falls ID 83402, United States

⁽²⁾Physics, Texas A&M University, Spence St., College Station TX 77843, United States

⁽³⁾Nuclear Engineering, Texas A&M University, Spence St., College Station TX 77843, United States

⁽⁴⁾APS, Argonne National Lab, Argonne IL 60439, United States

⁽⁵⁾Idaho National Lab, Idaho Falls ID 83403, United States

A technology for accelerator-driven subcritical fission in a molten salt core (ADSMS) is being developed as a basis for the destruction of all transuranics and long-lived fission products in spent nuclear fuel. The molten salt fuel is a eutectic mixture of NaCl and the chlorides of the transuranics and fission products. The core is driven by proton beams from a strong-focusing cyclotron stack, described in a separate paper. This approach uniquely provides an intrinsically safe means to drive a core fueled only with transuranics, thereby eliminating competing breeding terms.

The ADSMS technology uniquely provides a means to destroy all transuranics and long-lived fission products in spent nuclear fuel and recover the 95% uranium still in it so that it can be re-used, thereby closing the nuclear fuel cycle for the first time.

Simultaneous irradiation and corrosion of HT-9 F/M steel in lead-bismuth coolant - The ICE-II Experiment

Staffan Qvist¹, Peter Hosemann¹, Yongqiang Wang², Joseph Tesmer², Magdalena Caro², Mark Bourke²

⁽¹⁾Department of Nuclear Engineering, University of California, 2430 Dwight Way, Berkeley CA 94704, United States

⁽²⁾Materials Science and Technology Division, Los Alamos National Laboratory, P.O. Box 1663, Los Alamos NM 87545, United States

Lead-bismuth eutectic (LBE) has been selected as candidate coolant for fast reactor concepts, accelerator driven systems (ADS), spallation targets and hybrid systems. As a fast reactor coolant, LBE offers significant advantages over available alternatives. It does not have any violent chemical reaction with air, water or steam, and has a very high boiling point (1670 deg. C) and excellent natural circulation cooling capability. However, corrosion, liquid metal embrittlement and liquid metal enhanced creep challenge the lifetime of steel structural components in contact with LBE.

In this work, we describe the irradiation/corrosion experiment ICE-II, performed at Ion Beam Materials Laboratory in Los Alamos within the Los Alamos National Laboratory -University of California Berkeley (LANL-UCB) collaboration. The purpose of this work is to study synergistic effects of irradiation on steel corrosion, and investigate if and how a steady state concentration of defects continuously created by displacement cascades affects surface chemistry such as oxidation or dissolution. In the ICE-II experimental setup, a 3 MV Pelletron tandem accelerator is used to irradiate a steel surface with an energetic proton beam. During the irradiation, the surface is kept in contact with high-temperature LBE.

ICE-II constitutes a natural continuation of ICE-I experiment, where HT-9 ferritic martensitic steel was exposed to proton irradiation in the presence of LBE at high temperature. ICE-II improved capabilities include monitoring oxygen content in LBE and the ability to reach higher temperatures and dose values. ICE-II demonstrated long-term routine irradiations using the operating experimental set-up are possible allowing for systematic studies of combined effects (chemistry, dose, and temperature).

Dual-Beam Irradiation of HT-9 Ferritic Stainless Steel: Preliminary Results

Marilyn E. Hawley¹, Ming Tang¹, Joseph R. Tesmer¹, Feng Ren², Yongqiang Wang¹

⁽¹⁾Materials Science and Technology Division, Los Alamos National Laboratory, Los Alamos NM 87545, United States

⁽²⁾Department of Physics, Wuhan University, Wuhan, Hubei Province 87545, China

A fundamental issue in nuclear energy, fission, fusion, and fusion-fission hybrids, is the changes in material properties as a consequence of time, temperature, and neutron fluence. Candidate materials for nuclear energy applications are usually tested in nuclear reactors to understand and model the changes that arise from a combination of atomic displacements, helium and hydrogen production, and nuclear transmutations, however, such an approach takes much too long for many high neutron fluence scenarios expected in reactors of the next generation. Alternatively, irradiation with ions can be utilized to initiate the processes of radiation damage similar to that expected in the next generation nuclear energy systems, but at much higher rates (a factor of $\sim 10^3$ or higher) than available neutron sources. Ion-beam irradiation brings several advantages to the problem of understanding radiation damage in materials, including performing critical scientific studies on reasonable time scales. Furthermore, ion irradiated samples have much lower residual activation, allowing post irradiation examination to be performed much more quickly. HT-9 is of considerable interest for elevated-temperature in-core applications (cladding, wrappers, and ducts) for fast reactors, and as structural materials for fusion reactors because of its excellent thermal properties and irradiation resistance (low swelling) relative to austenitic stainless steels. Los Alamos has recently implemented a dual radiation capability in the Ion Beam Materials Laboratory with sample heating capability making it possible to study the synergistic effects resulting from irradiation using a dual beam of two different ions and at elevated temperatures relevant to reactor conditions. We will present preliminary results from dual beam irradiation experiments on HT-9 at >200 dpa, and temperatures between 450°C and 480°C using 150 keV He^+ ions and 2 MeV Cr^{2+} ions.

Comparative study of intrinsic and helium defects production due to collision cascades in bcc iron and tungsten

Chunping Xu^{1,3}, Xiang-Yang Liu¹, Fei Gao², Yongqiang Wang¹

⁽¹⁾Materials Science and Technology Division, Los Alamos National Laboratory, Los Alamos NM 87545, United States

⁽²⁾Pacific Northwest National Laboratory, Richland WA 99352, United States

⁽³⁾School of Nuclear Science and Technology, Lanzhou University, Lanzhou Gansu 730000, China

We used molecular dynamics (MD) method to simulate displacement cascades in bcc iron (Fe) and tungsten (W) containing different concentrations of substitutional helium (He) atoms. The MD program used in this work is the LAMMPS code. Primary knock-on atom (PKA) energies, are from 1 to 10 keV, with varying He concentrations. The influences of He atoms and PKA energy on defect production are investigated. The interstitial clusters, vacancy clusters, and the He-vacancy clusters produced directly within displacement cascades, as well as the nucleation mechanisms of these clusters are studied.

The Use of Accelerated Radiation Testing for Avionics

Heather Marie Quinn

ISR3, MSD440, LANL, Los Alamos NM 87545, United States

High-altitude airplanes experience the highest neutron flux in the terrestrial environment. Furthermore, as the terrestrial neutron flux also changes with latitude, longitude and altitude, most airplanes experience a widely varying radiation environment. This radiation environment is known to cause single-event effects in analog and digital components. In particular, single-event upsets can cause bitflips in memory components, single-event transients in gates, single-event latchup in components, or single-event gate rupture in power MOSFETs. While most of these single-event effects are not permanently destructive, many of them can cause data reliability or availability issues. For unmanned aerial vehicles, which often include science and/or military payloads, radiation effects in the analog and digital components can make fault-tolerant processing difficult.

Testing components for single-event effects in a neutron accelerator, such as Los Alamos National Laboratory's (LANL) Los Alamos Neutron Science Center (LANSCE), can provide aircraft designers valuable information about how well the components will work in deployed radiation environment. This type of testing can allow designers to determine if component selection needs to be modified or mitigation of radiation-induced errors will be necessary to meet their mission goals. In this talk, we will explore how accelerated radiation testing can be useful at reducing risk and increasing availability and reliability of the deployed mission.

Atmospheric Radiation Effects on Avionics Systems

Laura Dominik^{1,2}

⁽¹⁾*Honeywell, 8840 Evergreen Blvd, Minneapolis MN 55433, United States*

⁽²⁾*Aerospace Vehicle Systems Institute (AVSI), 102 Graphic Services Bldg., College Station TX 77843-3126, United States*

Natural atmospheric radiation effects have been recognized in recent years as key safety and reliability concerns for avionics systems. Atmospheric radiation causes Single Event Effects (SEE) in electronics. The resulting single event effects can cause various failure conditions, including hazardous misleading information and system failures in avionics equipment. As technology trends continue to achieve higher densities and lower voltages, semiconductor devices are becoming more susceptible to atmospheric radiation effects. Government and customer specifications increasingly require assessments of the single event effects probability in electronics from atmospheric neutrons.

To ensure a system meets all its safety and reliability requirements, SEE induced upsets and potential system failures need to be considered. Testing is needed when it has been determined that a part is both critical to system performance and susceptible to radiation, no test data is available, and initial conservative estimates do not meet system safety/reliability requirements. Testing of ICs and systems for use in radiation environments requires the utilization of highly advanced laboratory facilities that can run evaluations on microcircuits for the effects of radiation.

Radiation-Induced Effects in High Performance Computing Platforms

Sarah Michalak

Statistical Sciences Group, Los Alamos National Laboratory, PO Box 1663, MS F600, Los Alamos NM 87544, United States

High performance computing (HPC) platforms may include thousands of nodes, ten of thousands of processors, and hundreds of terabytes of memory. These systems are frequently used to perform large-scale scientific calculations, which can require thousands of processors and take weeks to months to complete. Radiation-induced errors can affect both application runtimes and the accuracy of scientific results. Radiation-induced failures, e.g. those detected by a parity check, can cause a node involved a calculation to crash. In this case, the entire calculation may need to be restarted from a previously-saved state, increasing the time until the calculation is completed. Radiation-induced errors may also occur in regions without error protection, e.g. parity checks or error-correcting codes. In this case, they may result in silent data corruption (SDC), which occurs when incorrect results are delivered without any accompanying error or warning message. Because HPC platforms contain many replicates of different devices, e.g. microprocessors or DRAM, they are more susceptible to radiation-induced effects than smaller systems.

This talk focuses on studies of neutron-induced effects on HPC hardware that were undertaken at the Los Alamos Neutron Science Center (LANSCE) Irradiation of Chips and Electronics (ICE) House facility at Los Alamos National Laboratory. In one case, the results of neutron-beam testing are consistent with the rate of parity errors observed in the field that are presumed to be neutron-induced. A second study permits estimation of rates of neutron-induced crashes and SDCs and considers whether different applications and different replicates of the hardware under test have differing susceptibilities to neutron-induced errors.

Are mono-atomic amorphous semiconductors inhomogeneous on the nanoscale?

Sjoerd Roorda

physique, Université de Montréal, 2900 Boulevard Edouard Montpetit, Montréal Québec H3C 3J7, Canada

Amorphous silicon and germanium are widely considered to be a near perfect realization of a continuous random network. However, a recent publication claims otherwise [1] and presents reverse Monte Carlo models of amorphous silicon that, so it is claimed, fit diffraction data as well as 4-particle correlations deduced from fluctuation electron microscopy. These models consist of nanoscale crystalline matter ("paracrystallites") embedded in a disordered (but non-CRN) matrix and thus imply that a-Si and a-Ge are inhomogeneous on the nm scale. I will show recent, very high resolution, x-ray diffraction data on a-Ge [2] and re-analyze older diffraction data on a-Si and demonstrate that the models presented in [1] do **not** fit the diffraction data. I will also discuss the intermediate and long-range ordering observed upon thermal annealing.

[1] M. M. J. Treacy and K. B. Borisenko, Science 335, 950 (2012).

[2] S. Roorda et al, Phys. Rev. Lett., in press.

Combined theoretical-experimental studies of defect-interface interactions in oxidesBlas Pedro Uberuaga*Materials Science and Technology Division, Los Alamos National Laboratory, MS G755, Los Alamos NM 87545, United States*

It is well established that interfaces and grain boundaries can act as efficient sinks for radiation-induced defects. However, many details of how interfaces interact with defects and how this interaction depends on the structure of the interface are still uncertain. Here, we examine two types of coherent interfaces in oxides -- thin film hetero-bilayers and non-stoichiometric planar defects -- to determine how radiation-induced defects interact with such interfaces and modify the radiation tolerance of the material. In particular, we focus on the interface between thin film oxides and the SrTiO₃ substrate on which they are grown as well as non-stoichiometric SrTiO₃ in which the non-stoichiometry is accommodated by extra planes of SrO, forming a type of multilayer structure. Even though these interfaces are nearly fully coherent, with no special atomic structure that leads to thermodynamic trap states at the interface, the interface nevertheless greatly influences how the materials respond to the produced defects, at least in a transient regime where only some of the kinetic processes are active. Both enhancement and degradation of radiation tolerance is observed, depending on which region of the material is examined. We complement irradiation experiments with atomistic calculations and kinetic Monte Carlo simulations to gain insight into the origins of the behavior, identifying differences in the bulk behavior of defects on each side of the interface as the important determiners. In particular, differences in chemical potential and bulk migration of defects in each phase are hypothesized to be the controlling factors for this behavior.

Irradiation induced effects in nano- and microcrystalline ZrO₂ ceramicsAdam Georg Balogh*Institute of Materials Science, Technische Universität Darmstadt, Petersenstr. 23, Darmstadt Hessen 64287, Germany*

Defect formation and stability have been studied systematically on nano- and microcrystalline ceramic (ZrO₂) samples. Experiments focusing on defect formation in nano and coarse grained ZrO₂ showed agglomeration of defect clusters (vacancies or interstitials) triggered by heavy ion irradiation. The density of the clusters clearly depends on temperature and grain size. A dependence on the ion dose was also observed. Near grain boundary areas free of defects were observed. From the evaluation of the defect free regions different diffusion mechanisms could be determined. Electron irradiation experiments were also performed to investigate a different process of defect cluster formation. In this case, defect clusters could not be formed immediately by the irradiation, but only after short-range diffusion. This is a consequence of the lower deposition rates of the atoms during electron irradiation.

Additionally, systematic experiments have been performed to investigate the phase stability of the tetragonal phase of nanocrystalline ZrO₂ samples after the unexpected phase transition from monoclinic ZrO₂ to tetragonal ZrO₂ under heavy ion irradiation. A dependence of the relative volume of the tetragonal phase on the ion dose was observed. In order to investigate the thermal stability of the tetragonal phase, heat treatments of similar samples have been performed up to 1300°C. For samples that had been irradiated with high doses (1•10¹⁶ ions/cm² and higher) the tetragonal phase was stable up to 900°C which is in good agreement with the sintering temperature. At higher temperatures a residual content of the tetragonal phase of less than 5% was observed. Significant grain growth could not be observed after the irradiation procedure.

Radiation effects in nanocrystalline intermetallics

Askar R. Kilmametov^{1,3}, Adam G. Balogh², Mohammad Ghafari^{1,2}, Ruslan Z. Valiev³, Horst Hahn^{1,2}

⁽¹⁾*Institute of Nanotechnology, Karlsruhe Institute of Technology (KIT), Hermann-von-Helmholtz-Platz 1, Eggenstein-Leopoldshafen 76344, Germany*

⁽²⁾*Institute for Materials Science, Technical University of Darmstadt, Petersen str. 23, Darmstadt 64287, Germany*

⁽³⁾*Institute of Physics of Advanced Materials, Ufa State Aviation Technical University, K. Marx Str. 12, Ufa 450000, Germany*

Nanocrystalline metals and alloys are attractive for advanced structural use under irradiation due to the expectation of their increased irradiation tolerance. The annihilation of point defects produced by high energy irradiation depends critically on the concentration of internal sinks. It is expected that nanocrystalline metals exhibit enhanced irradiation resistance due to the large volume fraction of internal defects, such as grain boundaries, phase boundaries, triple junctions and dislocation walls. Bulk ordered nanocrystalline TiNi and FeAl alloys with various grain sizes were processed using severe plastic deformation, namely high pressure torsion technique. Fully-dense nanocrystalline and coarse-grained counterparts which possess a long-range chemical ordering studied by X-ray diffraction and Mössbauer spectroscopy methods to examine irradiation effects on the stability or degradation of crystal superlattice. Comparative analysis of long-range disordering and amorphisation kinetics revealed essentially enhanced irradiation resistance of nanocrystalline intermetallic alloys demonstrating their potential under irradiation conditions. It was shown that at the equal damage dose nanocrystalline samples are able to retain a long-range ordering while the coarse-grained counterparts were substantially disordered or amorphised. The present experimental studies verify that fully-dense ordered intermetallic alloys are promising candidate materials for radiation environments.

Ion irradiation-induced multishell nanoparticles

Feng Ren, Changzhong Jiang

Physics, Wuhan University, Luojiashan, Wuchang, Wuhan Hubei 430072, China

Ion irradiation technology is a powerful method to fabricate and tailor nanomaterials. In this talk, we present the fabrication of multishell nanoparticles (NPs) by ion irradiation. Ag NPs embedded in silica were irradiated by N⁺, Si⁺, Ar⁺, Cu⁺ at 300 keV, by Cu⁺ ions at varying energies from 110 to 500 keV, or by Cu⁺ ions at 400 keV to fluences varying from 1x10¹⁶ to 1x10¹⁷ ions/cm². The size of the irradiation-induced nanocavities increases with increasing ion mass and energy, and also depends on the nuclear and electronic energy losses of irradiation ions. The composition of the multishell NPs are characterized by TEM technologies (HRTEM, HAADF, STEM-EDS, STEM-EELS). A model is set up to reproduce the process of the ion-nanoparticle interaction and the formation of these multishell NPs. The behavior of the multishell NPs under high temperature heating are observed by in-situ TEM.

Optimal Conditions for High Current Proton Irradiations at the University of Wisconsin's Ion Beam Laboratory

C. J. Wetteland¹, O. Albakri², K. G. Field¹, K. Sridharan², T. R. Allen²

⁽¹⁾*Materials Science, University of Wisconsin Madison, 1509 University Avenue, Madison WI 53706-1595, United States*

⁽²⁾*Engineering Physics, University of Wisconsin Madison, 1500 Engineering Drive, Madison WI 53706-1646, United States*

The National Electrostatics Corporation's (NEC) Toroidal Volume Ion Source (TORVIS) source is known for exceptionally high proton currents with minimal service downtime as compared to traditional sputter sources. 150 μA of proton beam current are readily achievable within 10 minutes of source startup. For over-scanned target areas of approximately 2 cm^2 , it has been possible to achieve 70 μA of proton current on the target stage. Using beam currents of this magnitude may have many undesirable effects, especially for insulators. This may include high temperature gradients at the surface, sputtering, surface discharge, cracking or even disintegration of the sample. A series of experiments were conducted to examine the role of sample charging in amorphous and single crystal SiO_2 under high proton fluxes. Results show the optimal proton irradiation conditions and target mounting strategies needed to minimize unwanted damage.

Destructive Malfunctions in Silicon Carbide Metal-Oxide-Semiconductor Devices Induced by Ion Beams

Takeshi Ohshima¹, Manato Deki^{1,2}, Takahiro Makino¹, Naoya Iwamoto¹, Shinobu Onoda¹, Kazutoshi Kojima³, Takuro Tomita², Shigeki Matsuo², Shuichi Hashimoto², Toshio Hirao¹

⁽¹⁾*Japan Atomic Energy Agency, Watanuki, Takasaki Gunma 370-1292, Japan*

⁽²⁾*The University of Tokushima, Tokushima Tokushima 770-8506, Japan*

⁽³⁾*National Institute of Advanced Industrial Science and Technology, Tsukuba Ibaraki 305-8568, Japan*

Metal-Oxide-Semiconductor (MOS) capacitors were fabricated on n-type 4H-SiC epitaxial layers, and the leakage current through the gate oxide during heavy ion irradiation was investigated in order to evaluate dielectric breakdown induced by heavy ions (Single Event Gate Rupture: SEGR). The samples used in this study were 4H-SiC MOS capacitors fabricated on n-type epitaxial layers grown on Si-face n-type 4H-SiC substrates. The gate oxide at thickness ranges between 60 and 80 nm was formed using pyrogenic oxidation ($\text{H}_2 : \text{O}_2 = 1:1$) at 1100 C for 60 min. Circular electrodes with 180 μm diameter were formed using Al evaporation and a lift-off technique. The leakage current observed through the gate oxide was monitored during 18 MeV oxygen (O) or nickel (Ni) ions. As a result, although no significant difference in the value of the electric field at the dielectric breakdown (around 8.2 MV/cm) was observed between non-irradiated and 18MeV-O irradiated samples, the value decreased to be 7.3 MV/cm in the case of 18 MeV-Ni ion incidence. The Linier Energy Transfer (LET) for 18 MeV-O is 7 MeVcm²/mg, and this value is smaller than that for 18MeV-Ni (24 MeVcm²/mg). Also, 18 MeV-Ni ions deposit energy in narrower regions than 18 MeV-O ions. Thus, it can be concluded that the high density of charge induced by 18 MeV-Ni ions triggers SEGR in SiC MOS capacitors.

Structure and magnetic properties of irradiated Fe/Fe oxide core-shell nanoclusters

John S. McCloy¹, Weilin Jiang¹, Jennifer Sundararajan², You Qiang², Edward Burks³, Kai Liu³

⁽¹⁾*Pacific Northwest National Laboratory, Richland WA 99352, United States*

⁽²⁾*University of Idaho, Moscow ID 83844, United States*

⁽³⁾*University of California, Davis CA 95616, United States*

A cluster deposition method was used to produce a film of loosely aggregated particles of Fe-Fe₃O₄ core-shell nanoclusters with an 8 nm iron core size and 2 nm oxide shell thickness. The film of particles on a silicon substrate was irradiated by 10¹⁶ cm⁻² Si²⁺ ions at room temperature, and computer simulations (SRIM, Stopping and Range of Ions in Matter) show that the implanted Si species penetrate through the entire film and into the substrate. The ion irradiation creates a structural change in the film with corresponding chemical and magnetic changes. X-ray diffraction shows that the core size and chemistry stay the same but the shell becomes FeO that grows to a thickness of 17 nm. Helium ion microscopy shows that the previously separate particles have densified into a nearly continuous film. Major loop magnetic hysteresis measurements show a decrease in saturation magnetization that we attribute to the presence of the antiferromagnetic (AFM) FeO shell. First order reversal curve measurements on the irradiated film performed with a vibrating sample magnetometer show that the AFM shell prevents the particles from interacting magnetically, leading to low coercivity from the iron core and little bias field from the core interactions. These results, and others presented previously on different chemistries (Fe₃O₄ or FeO+Fe₃N nanoclusters), show that the ion irradiated behavior of nanocluster films such as these depend strongly on the initial nanostructure and chemistry.

Study of the monoclinic-tetragonal phase transition of zirconia by 1.5 MeV proton bombardment

S.C. Yang¹, Y.H. Shen¹, R.T. Huang¹, Y.C. Yu²

⁽¹⁾*Institute of Materials Engineering, National Taiwan Ocean University, Keelung 20224, Taiwan*

⁽²⁾*Institute of Physics, Academia Sinica, Taipei 11529, Taiwan*

Zirconium alloys generally are used as cladding elements in nuclear plants because of the low absorption cross-section of zirconium. This oxide layer drastically modified the mechanical and thermal behavior of cladding elements could diminishes the lifetime of the nuclear core, and the behavior of zirconia under irradiation also has been attracted great attention. The implantation parameters (energy, ion dose, substrate temperature, and ex-situ annealed temperature) play a vital role in the resultant phase transition of zirconia. In this study, zirconia of monoclinic (m) phase was first prepared by commercial purchase and the internal oxidation of Ag-AgZr₂ alloys, respectively, to study the phase transition of zirconia under irradiation with free surface and nano-confinement situations. Here, the particles size or grains size of pure monoclinic zirconia are ranging from 20 to 60 nm. 1.5 MeV protons were following implanted into the two kinds of specimens, i.e., pure monoclinic zirconia free particles and internal oxides, with fluences from 1×10¹⁴ to 1×10¹⁶ ions/cm² by using a NEC 3 MV tandem accelerator. The effect of implanted doses, were studied and characterized by using transmission electron microscopy (TEM) and x-ray diffractometer (XRD). Accordingly, tetragonal (t) zirconia characteristic peak appeared with the proton doses above 1×10¹⁵ ions/cm² for the free particles of zirconia, while tetragonal zirconia characteristic peak all appeared at the proton doses range from 1×10¹⁴ to 1×10¹⁶ ions/cm². Apparently, the m to t phase transition for zirconia free particle can be accomplished with the above threshold of requiring dose (1×10¹⁵ ions/cm²), while the internally oxidized zirconia could show the m to t phase transition at lower proton dose (1×10¹⁴ ions/cm²) due to nanoconfinement effect. The further results and study on the m to t phase transition to the two kinds of zirconia will be presented.

National and International Standards for the Imaging Performance of Gamma-ray or X-ray Cargo and Vehicle Inspection Systems

Paul M Bergstrom

Physical Measurement Laboratory, National Institute of Standards and Technology, 100 Bureau Dr, Gaithersburg MD 20899, United States

While cargo and vehicles have been subjected to non-intrusive inspection (NII) by x-rays or gamma-rays for some time, there have been no standards providing test methods to measure image quality indicators (IQIs) until recently. The first such standard IEEE/ANSI N42.46, published in 2008, specifies test objects and provides test methods for simple penetration, contrast sensitivity, spatial resolution and wire resolution for transmission systems and similar objects for back-scatter systems. The more recently published standard IEC 62523 provides for different objects and test methods for these IQIs and also provides a test for materials discrimination. The work presented here discusses the similarities and differences between these standards, results obtained for IQIs using the test objects and methods and attempts to harmonize the standards. In addition, current efforts to modify the IEEE/ANSI standard will be discussed.

Z-SPEC: Bremsstrahlung Transmission Spectroscopy for Z-Determination

Tsahi Gozani, Craig Brown, Mashal Elsalim, Willem G.J. Langeveld, Michael J. King, Joseph Bendahan
Rapiscan Laboratories, Rapiscan Systems Inc., 520 Almanor, Sunnyvale CA 94085, United States

The most common method of luggage or cargo inspection is X ray radiography. The basic information it provides is a two-dimensional projection image of the areal density of the material traversed by the beam of x-rays. The human screener (aided by computer image enhancements) then tries to identify anomalous shapes that could be an object of interest, such as drugs, explosives, nuclear material or some other specific items. Radiographic images, however, do not provide material composition, which is needed to detect most potential threats.

Over the years, attempts were made, with differing degrees of success, to extract material information from the x-rays. For cargo inspection, the most common method is dual-energy imaging (e.g. 6 and 9 MeV). In recent years, significant progress was achieved in automatic detection of high-Z elements (typically $Z > 70$) employing algorithmic image analysis, high-energy backscattered x-ray-generated electron bremsstrahlung and transmitted x-ray statistical ("noise") analysis ("Z-SCAN").

Transmission x-ray spectroscopy, called "Z-SPEC", was studied extensively over the last few years. It extracts in the fullest possible way the Z information contained in x-rays transmitted through a cargo. The basic physics is quite straightforward. The transmitted x-ray bremsstrahlung spectrum is being shaped by the three key photon-atom interaction processes: the photoelectric effect, Compton scattering and pair production, each with very different Z dependence. Thus, measuring the actual transmitted energy spectra provides information on the areal density of the various substances traversed by the x-ray beam. These spectra can be unfolded to yield the Z distribution of the inspected cargo. The principles and measurement results demonstrating the capabilities and range of applicability of the method, employing existing and future detectors, will be shown.

Methods for Evaluating the Active Neutron Interrogation Detection Limits of Shielded Highly Enriched Uranium

Scott J. Thompson, Edward H. Seabury, David L. Chichester
Idaho National Laboratory, 2525 Fremont Avenue, Idaho Falls ID 83415, United States

An extensive modeling campaign was recently performed to study the utility of active neutron interrogation of heavily shielded highly enriched uranium (HEU). This study spanned a wide parameter space that included HEU mass, shielding materials and thicknesses, incident particle energy, source duty cycle and operating frequency, measurement duration, and environmental background detection rates. Scenario performance comparisons of several detection signatures were performed in this effort, bringing about the development of a set of automated tools and algorithms that utilize standard statistical methods to evaluate detection outcome likelihoods. These tools allow for the behavior of false-detection rates, both false-positive and missed detection outcomes, to be monitored not only as a function of measurement time, but with respect to one another as well. A summary of these automated tools and the statistical methods behind them is provided.

Neutron detection in a high gamma ray background with liquid scintillators

Luca Stevanato¹, Davide Cester¹, Giancarlo Nebbia², Giuseppe Viesti¹
⁽¹⁾*Dipartimento di Fisica e Astronomia Galileo Galilei, Università degli studi di Padova, Via Marzolo 8, Padova 35131, Italy*
⁽²⁾*Sezione di Padova, INFN, Via Marzolo 8, Padova 35131, Italy*

One of the current problems in Homeland Security applications is the quest for neutron detectors that would represent a suitable alternative to the standard ^3He proportional counters[1]. The requested characteristics of neutron detectors include the capability of maintaining a good selection of neutron signals when operated in a very high gamma ray field (corresponding to 100 $\mu\text{Sv/h}$). This particular performance is demanded in order to avoid the possibility of masking Special Nuclear Material with commercial gamma emitters. This requirement has been normally translated into "gamma ray insensitivity" of the neutron detectors, using simple devices with high sensitivity to neutrons and low efficiency for gamma rays. As a consequence, organic liquid scintillators have not been considered for such applications not only for the chemical hazard (toxicity and flammability) but also for their intrinsically good gamma ray efficiency. Nowadays with the development of new materials intrinsically more secure in the field of liquid scintillators, it is interesting to reconsider the possibility offered by these detectors. On the other hand, a recent work has shown how difficult it would be detecting neutrons in very high gamma ray field by using standard analogic front-end electronics[2]. We have explored the capability of liquid scintillators (2"x2" cells of EJ301 and EJ309) of detecting neutrons in a very high gamma ray background by using digitizers with a hybrid Pulse Shape Discrimination technique. A CAEN-V1720 (250MS/s Digitizer) has been used to perform digital pulse processing by FPGA. By filtering the FPGA data with a fast off-line algorithm, a weak ^{252}Cf source has been detected in a high ^{137}Cs gamma ray background corresponding to 300 $\mu\text{Sv/h}$ with probability of detection in compliance with IEC requirements for hand held instruments.

[1] R.T. Kouzes et al., NIMA 623 (2010) 1035-1045

[2] L. Swiderski et al., NIMA 652 (2011) 330-333

A Whole-System Approach towards X-Ray Spectroscopy in Cargo Inspection Systems

Willem G J Langeveld, Tsahi Gozani, Peter Ryge, Shrabani Sinha, Tim Shaw, Dan Strellis
Rapiscan Laboratories, Inc., 520 Almanor Ave, Sunnyvale CA 94085, United States

The bremsstrahlung x-ray spectrum used in high-energy, high-intensity x-ray cargo inspection systems (CIS) is attenuated and modified by the materials in the cargo in a Z-dependent way. Therefore, spectroscopy of the detected x rays yields information about the Z of the x-rayed cargo material. It has previously been shown that such Z-Spectroscopy (Z-SPEC) is possible under certain circumstances. A statistical approach, Z-SCAN (Z-determination by Statistical Count-rate ANalysis), has also been shown to be effective, and it can be used either by itself or in conjunction with Z-SPEC when the x-ray count rate is too high for individual x-ray spectroscopy. Both techniques require fast x-ray detectors and fast digitization electronics. It is desirable (and possible) to combine all techniques, including x-ray imaging of the cargo, in a single detector array, to reduce cost, weight, and overall complexity.

In this presentation, we take a whole-system approach to x-ray spectroscopy in x-ray cargo inspection systems, and show how the various parts interact with one another. Faster detectors and read-out electronics are beneficial for both techniques. A higher duty-factor x-ray source allows lower instantaneous count rates at the same overall x-ray intensity, improving the range of applicability of Z-SPEC in particular. Using an intensity-modulated advanced x-ray source (IMAXS) allows reducing the x-ray count for cargoes with higher transmission, and a stacked-detector approach may help material discrimination for the lowest attenuations. Image processing and segmentation allow derivation of results for entire objects, and subtraction of backgrounds.

We discuss R&D performed under a number of different programs, showing progress made in each of the interacting subsystems. We discuss results of studies into faster scintillation detectors, suitable photo-detectors, read-out and digitization electronics, high-duty-factor x-ray sources, image processing techniques, and how these elements work together to enable spectroscopic techniques. In sum, we present an integrated picture of CIS optimization for x-ray spectroscopy.

Large Area Liquid Argon Detectors for Interrogation Systems

Charles K Gary¹, Steve Kane¹, Craig Brown², John Kwong², Tsahi Gozani², Michael King², Daniel McKinsey³,
 James Nikkel³, Greg Smith¹, Murray Firestone¹

⁽¹⁾*2003 East Bayshore Rd, Redwood City CA 94303, United States*

⁽²⁾*Rapiscan Systems, 520 Amanor Avenue, Sunnyvale CA 94085, United States*

⁽³⁾*Department of Physics, Yale University, P.O. Box 208120, New Haven CT 06520, United States*

Measurements of time resolution, energy resolution and detection efficiency for gamma rays are presented for two prototype liquid argon (LAr) detectors that were fabricated and tested. Originally developed to provide massive, sensitive detectors for dark matter experiments, liquid noble gas detectors are ideally suited for large interrogation systems. Liquid argon (LAr) is potentially the lowest cost technology for large area detectors, and its fast response, good energy resolution and excellent neutron/gamma discrimination make it an ideal technology for portal interrogation systems, including those to detect special nuclear materials (SNM). Of all noble gas-based scintillators, liquid xenon (LXe) detectors have the fastest response time with a scintillation light decay of 20 ns. However, a xenon-doped liquid argon detector (LAr(Xe)) can achieve similar timing by introducing a small concentration (~0.2%) of xenon into the argon. This shortens the normal decay time of 1500 ns for LAr to close to 100 ns. The small necessary amount of Xe allows a scintillator with the speed and light yield of LXe, but with the cost of LAr. In addition, LAr detectors can provide energy resolution approaching that of NaI and can have excellent gamma ray detection efficiencies due to the large detection volumes that can be achieved.

Design Considerations for a Liquid Krypton Detector of Gammas below 12 MeV

Michael Hosack, David Koltick

Department of Physics, Purdue University, 525 Northwestern Avenue, West Lafayette IN 47907-2036, United States

Liquid krypton has been used widely for electromagnetic calorimeters for charged particles and gamma rays above 100 MeV. Despite the significant price advantage of krypton over xenon, little work has been done with liquid krypton detectors for energies in the range 200 keV to 12 MeV, important for neutron elemental analysis applications. We present the estimated energy resolution and rate capabilities of a LKr gamma ray detector including the effects of beta decays arising from Kr-85, scintillation light acceptance and decay time on signal analysis. These difficulties can be overcome with careful optimization of the detector dimensions, doping the Kr with Xe to improve its timing characteristics, and fast trigger electronics to eliminate dead-time from beta decays. While the presence of Kr-85 does not allow charge collection over the full volume, the effect of charge sampling over a limited volume to improve energy resolution and rates are presented.

Signal simulations are presented to show the expected impact of beta decays on gamma energy resolution and photo-peak efficiency and also allow the investigation of simple pile-up rejection strategies to be implemented with an FPGA. We provide a systems-level overview of electronics that could be used for such measurements. Initial measurements of the activity of our krypton supply are also presented.

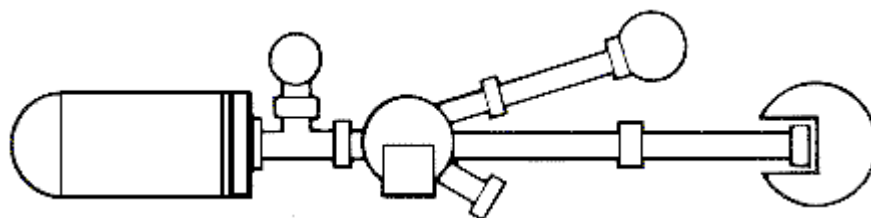
Effect of Hydrogen Contents of Bulk Samples on High Energy Gamma Ray Response of a $\text{LaCl}_3\text{:Ce}$ Detector

Akhtar A. Naqvi¹, Faris A. Al-Matouq¹, Fatah Z. Khiari¹, A. A. Issab²

⁽¹⁾*Physics, King Fahd University of Petroleum and Minerals, Dhahran, Dhahran Eastern Province 31261, Saudi Arabia*

⁽²⁾*Chemistry, King Fahd University of Petroleum and Minerals, Dhahran, Dhahran Eastern Province 31261, Saudi Arabia*

The response of a cylindrical 3 inches x 3 inches (height x diameter) $\text{LaCl}_3\text{:Ce}$ detector was measured for high energy prompt gamma rays from hydrogen, carbon and oxygen in the bulk samples produced through inelastic scattering of 14 MeV neutrons from benzene, water, toluene, propanol, ethanol and methanol bulk samples. Strong interference has been observed between chlorine prompt gamma rays from the $\text{LaCl}_3\text{:Ce}$ detector material and oxygen prompt gamma ray from the samples for samples containing higher concentration of hydrogen. Despite of the chlorine and oxygen prompt gamma rays interference, the experimental yield of high energy prompt gamma ray of hydrogen, carbon and oxygen measured with the $\text{LaCl}_3\text{:Ce}$ detector based PGNA setup has an excellent agreement with the results of Monte Carlo calculations. The agreement indicates excellent performance of the $\text{LaCl}_3\text{:Ce}$ detector for detection of hydrogen, carbon and oxygen in bulk samples.



WEDNESDAY

Atomic data of tungsten for current and future uses in fusion and plasma science

Peter Beiersdorfer, Joel Clementson

Physics Division, Lawrence Livermore National Laboratory, 7000 East Ave, L-260, Livermore CA 94550, United States

Atomic physics has played a very important role throughout the history of experimental plasma physics. For example, accurate knowledge of atomic properties has been crucial for understanding the plasma energy balance and for diagnostic development. With the shift in magnetic fusion research toward the very high-temperature burning plasmas like those expected to be found in the ITER tokamak, the atomic physics of tungsten has become of high importance. Tungsten will be a constituent of ITER plasmas because of its use as a plasma-facing component able to withstand high heat loads and with a lower tritium retention than other possible materials. Already, ITER diagnostics are being developed based on using tungsten radiation. In particular, the ITER Core Imaging X-ray Spectrometer (CIXS), which is designed to measure the core ion temperature and bulk plasma motion, is being based on the x-ray emission of neonlike tungsten ions (W64+).

In addition, tungsten emission will be measured by extreme ultraviolet (EUV) and optical spectrometers to determine its concentration in the plasma and to assess power loss and the tungsten sputtering rate. Moreover, tungsten is used on present-day tokamaks in preparation for ITER. The Wolfram Project at Livermore produces data for tungsten in various spectral bands: L-shell x-ray emission for CIXS development, soft x-ray and EUV M-shell and N-shell tungsten emission for understanding the edge radiation from ITER plasmas, and O-shell EUV emission for developing spectral diagnostics of the ITER divertor. Here, we present some of the atomic data we have measured using spectrometers on various plasma devices.

Work was performed under the auspices of the DOE by LLNL under contract DE-AC52-07NA27344 as part of the IAEA Coordinated Research Project "Spectroscopic and Collisional Data for Tungsten from 1 eV to 20 keV".

Charge Exchange and Atom-Surface Collisions in Astrophysics

Ara Chutjian¹, John A. MacAskill¹, Stojan M. Madzunkov¹, Jurij Simcic¹, David R. Schultz²

⁽¹⁾*Atomic and Molecular Physics Group, Jet Propulsion Laboratory/Caltech, 4800 Oak Grove Drive, Pasadena CA 91109, United States*

⁽²⁾*Department of Physics, University of North Texas, Denton TX 76203, United States*

Molecular effects involving highly charged ions, atoms, and collisions with dust grains are present in, for example, the solar wind-comet interaction, the interplanetary region, circumstellar clouds, and the interstellar medium. The relevant astrophysical objects will be presented and recent results given for charge exchange, X-ray emission, and atom-surface collisions leading to formation of larger molecules. Observations using the Herschel Space Telescope have raised the question of why there is so much water in the Universe. Laboratory experiments for water formation on dust grains will be discussed.

Collisional-radiative modeling for neutral beams in fusion plasmas

Yuri Ralchenko¹, Olexander Marchuk², Wolfgang Biel², David R. Schultz³

⁽¹⁾*National Institute of Standards and Technology, 100 Bureau Dr, MS 8422, Gaithersburg MD 20899, United States*

⁽²⁾*Institute of Energy and Climate Research, Forschungszentrum Juelich, Juelich 52425, Germany*

⁽³⁾*University of North Texas, Denton TX 76203, United States*

Powerful beams of neutral particles are extensively used in fusion devices, such as tokamaks and stellarators, to heat and diagnose the magnetically confined plasmas. The radiative spectra due to interactions between the neutral beam and the plasma particles provide valuable information on plasma fields, temperatures and densities, and other important parameters. I will present the recently developed collisional-radiative (CR) models used for analysis of two of the widely used spectroscopic techniques. First, a fully time-dependent CR model for charge exchange recombination spectroscopy was used to study important physical processes resulting in emission between highly-excited states of H-like Ar. Then, a new CR model for m-resolved parabolic states of hydrogen which has been successfully applied to explain motional Stark effect (MSE) spectra from tokamak plasmas is presented.

A new method for calculation of collisional cross sections between parabolic states was developed and used to compute the required atomic data. It is shown that the sigma- and pi-component intensities under typical fusion conditions cannot be described by statistical (Boltzmann) distribution and therefore require a complete CR analysis. I will also discuss non-statistical behavior of parabolic state populations in a wide range of plasma parameters.

WED-AP06-3

#354 - Invited Talk - Wednesday 8:30 AM - Elm Fork

An accelerator-based in-situ surface diagnostic for plasma-wall interactions science on the Alcator C-Mod magnetic fusion tokamak

Zachary S Hartwig, Dennis G Whyte, Harold S Barnard, Brandon N Sorbom, Peter W Stahle

Plasma Science and Fusion Center, Massachusetts Institute of Technology, 77 Massachusetts Ave, Cambridge MA 02139, United States

Boundary science in magnetic fusion devices is severely hindered by a dearth of in-situ diagnosis of plasma facing component (PFC) surfaces. The ideal in-situ PFC diagnostic would perform surface composition measurements on a plasma shot-to-shot time scale with 1 μm depth and 1 cm spatial resolution over large PFC areas. To this end, the customary laboratory surface diagnostic - nuclear scattering of MeV ions - is being adapted to the Alcator C-Mod tokamak. A compact (~ 1 m), high-current ($\sim \text{mA}$) radio-frequency quadrupole accelerator will inject 0.9 MeV deuterons into the vacuum vessel. The deuterons are then steered to PFC surfaces with the tokamak's magnetic fields in between plasma shots, where the deuterons induce high-Q nuclear reactions with low-Z isotopes in the first 10 μm of PFC material. The induced gammas and neutrons are detected using custom-designed, compact scintillation detectors, with energy spectroscopy providing quantitative surface analyses. Techniques to measure the thickness of low-Z PFC film coatings as well as the quantity of retained hydrogenic plasma fuel are presented along with simulated measurements by ACRONYM, a comprehensive Geant4 synthetic diagnostic for in-situ ion beam analysis of PFCs. Provided that the diagnostic is installed on schedule in early summer of 2012, validation efforts and first physics results will also be discussed.

WED-AP06-4

#398 - Invited Talk - Wednesday 8:30 AM - Elm Fork

The application of atomic physics within fusion plasma impurity diagnostics

Stuart Loch¹, Connor Ballance¹, Mitch Pindzola¹, Don Griffin²
(¹)*Physics, Auburn University, 206 Allison Lab, Auburn AL 36849, United States*
(²)*Physics, Rollins College, Winter Park FL 32789, United States*

A brief overview is presented of the electron-impact processes commonly used in fusion plasma diagnostics. Applications for use in impurity influx and impurity transport are given, along with examples of recent atomic data that have been generated. With the focus of ITER on the transport and emission properties of tungsten, generating atomic data for complex species has received a lot of interest. Perturbative approaches do not work well for near neutral systems, so calculating non-perturbative collision data for near neutral complex species presents a particular challenge. Recent results on Mo^+ are given as an illustration of how the diagnostics applications can guide the theoretical calculations for such systems.

Electrostatic Storage Ring With Focusing Provided by the Space Charge of an Electron Plasma

Jose L. Pacheco, Carlos A. Ordonez, Duncan L. Weathers

Department of Physics, University of North Texas, 1155 Union Circle #311427, Denton Texas 76203-5017, United States

Electrostatic storage rings are used for a variety of atomic physics studies. An advantage of electrostatic storage rings is that heavy ions can be confined. Described here is the concept of an electrostatic storage ring that employs the space charge of an electron plasma for focusing confined ions. An additional advantage of the present concept is that slow ions, as well as stationary ion plasma, can be confined. The concept employs an artificially structured boundary which is defined as a boundary that produces a spatially periodic static electromagnetic field, where the spatial period and range of the field are much smaller than the dimensions of a plasma or charged-particle beam that is confined by that field. An artificially structured boundary is used to confine a non-neutral electron plasma along the storage ring. The electron plasma is effectively unmagnetized, except near an outer boundary where the confining electromagnetic field resides. The electron plasma produces a radially inward electric field, which focuses the ion beam. Self-consistently computed radial beam profiles are reported. Results of preliminary experimentation are also reported.

$2p_{3/2}^{-1}3x^{-1}3x^{-1}3d^{-1}$ Coster Kroing transitions and Shake off process of La_1 X-Ray Satellites spectra in 3d, 4d and 5d transition elements.

Surendra Poonia

Division of Natural Resources and Environment, Central Arid Zone Research Institute, Jodhpur - 342003, Rajasthan, India, Central Arid Zone Research Institute, Jodhpur - 342003, Rajasthan, India, Dr. Surendra Poonia, S/O Dr. Fateh Singh Poonia, 10-C, Mahaveer Colony, Ratanada, Jodhpur - 342001, Rajasthan, Jodhpur Rajasthan 342001, India

The X-ray satellite spectra arising due to $2p_{3/2}^{-1}3x^{-1}3x^{-1}3d^{-1}$ ($x = s, p, d$) transition array, in elements with $Z = 40$ to 92, have been calculated. The energies of various transitions of the array have been determined by using available HFS data on $1s^{-1}2p^{-1}3x^{-1}$ and $2p_{3/2}^{-1}3x^{-1}3x^{-1}$ Auger transition energies and their relative intensities have been estimated by considering cross - sections of singly ionized $2x^{-1}$ ($x = s, p$) states and then of subsequent CK and shake off processes. The calculated spectra have been compared with the measured satellite energies in La_1 spectra. Their intense peaks have been identified as the observed satellite lines. It has been established that six satellites observed in the La region of the X-ray spectra of various elements and named $a_3, a_4, a_5, a', a^{ix}$ and a^x in order of increasing energy are mainly emitted by $2p_{3/2}^{-1}3d^{-1}3d^{-2}$ transitions. On the basis of agreement between computed spectra and measured satellites, It is observed that the satellite a_3 in $_{40}Zr$ to $_{48}Cd$ and a' in $_{74}W$ to $_{92}U$ is emitted by the superposition of the most intense transition $^3F_4-^3F_4$, contributing in order of decreasing intensity. It has been well established that the transition $^1F_3-^1G_4$ is the main source of the emission of the satellite a_4 in the spectra of elements with $Z = 40-48$. The same transition $^1F_3-^1G_4$ and other two transitions namely $^1P_1-^1D_2$ and $^1F_3-^1D_2$ have been proved to be the main origin of the satellite, a^{ix} , reported in the range $Z = 74-92$. Further, the line a_5 in the spectra of elements with $Z = 40 - 48$ has been assigned to mainly the $^3D_3-^3F_4, ^3D_2-^3F_3, ^1P_1-^1D_2$ and $^1F_3-^1D_2$ transitions. Finally, the satellite a^x , reported in the spectra of elements with $Z = 74-92$, has been associated with the transition $^3D_3-^3F_4$.

Accelerator-Based Fusion with a Low Temperature Target

Ryan E. Phillips, Carlos A. Ordonez

Department of Physics, University of North Texas, 1155 Union Circle #311427, Denton Texas 76203-5017, United States

Neutron generators are in use in a number of scientific and commercial endeavors. They function by triggering fusion reactions between accelerated ions (usually deuterons) and a stationary cold target (usually containing tritium). This setup has the potential to generate energy. It has been shown that if the energy transfer between injected ions and target electrons is sufficiently small, net energy gain can be achieved. Three possible avenues are: (a) a hot target with high electron temperature, (b) a cold non-neutral target with an electron deficiency, or (c) a cold target with a high Fermi energy. A study of the third possibility is reported in light of recent research that points to a new phase of hydrogen, which is hypothesized to be related to metallic hydrogen. As such, the target is considered to be composed of nuclei and delocalized electrons. The electrons are treated as conduction electrons, with the average minimum excitation energy being approximately equal to 40% of the Fermi energy. The Fermi energy is directly related to the electron density. Preliminary results indicate that if the claimed electron densities in the new phase of hydrogen were achieved in a target, the energy transfer to electrons would be small enough to allow net energy gain.

Classical Trajectory Monte Carlo Code for Simulating Ion Beam Focusing or Defocusing With Magnetic Elements Modeled as Current Loops or Current Lines

Ryan A. Lane, Carlos A. Ordonez

Department of Physics, University of North Texas, 1155 Union Circle #311427, Denton Texas 76203-5017, United States

A computational tool is described that can be used for designing magnetic focusing or defocusing systems. A fully three-dimensional classical trajectory Monte Carlo simulation has been developed. Ion trajectories are simulated in the presence of magnetic elements that can be modeled as any combination of current loops and current lines. Each current loop or line may be located anywhere in the system and oriented along any of the three coordinate axes. The configuration need not be axisymmetric. The solutions are obtained using normalized parameters, which can be used for easily scaling the results. Examples are provided of the utility of the code.

Formation of Magneto-Bound States of Positronium and Protonium

Jose R. Correa, Carlos A. Ordonez

Department of Physics, University of North Texas, 1155 Union Circle #311427, Denton Texas 76203-5017, United States

A magneto-bound state is defined as a matter-antimatter two-particle quasi-bound system that has positive total energy, where the energy of the system is defined to be zero when the two particles are at rest with infinite separation. A magneto-bound state is a state in which the two particles have equal mass and opposite charge, and the two particles are temporarily bound due to the presence of an external magnetic field. The formation and dissociation of magneto-bound positronium and protonium is investigated via three-dimensional classical trajectory simulations. The investigation yields information on the formation cross-section, the lifetime (before dissociation occurs), and the drift velocity of magneto-bound states of positronium and protonium. Various timescales are compared, including the magneto-bound formation timescale, the lifetime, and a loss timescale (due to drifting to a wall). These timescales are also compared to the timescale for annihilation to occur for unmagnetized positronium and protonium.

Simulation of an Antihydrogen Gravity Experiment Utilizing Multiple Apertures

Ryan M. Hedlof, Carlos A. Ordonez

Department of Physics, University of North Texas, 1155 Union Circle #311427, Denton Texas 76203-5017, United States

A classical trajectory Monte Carlo simulation of an antihydrogen gravity experiment that would employ multiple apertures is presented. Such an experiment may be possible at the CERN Antiproton Decelerator facility. The simulation was developed with the primary goal of reducing the experimental run time necessary to determine the direction of free fall acceleration for antimatter in the gravitational field of the earth. The experiment would confine a cryogenic antihydrogen plasma for producing antihydrogen (e.g., by three-body recombination). A cylindrical drift tube would have a horizontal axis of symmetry, with two series of coaxial apertures positioned on either side of the region for antihydrogen production. The experiment would employ a detector capable of distinguishing between cosmic rays and antihydrogen annihilations. The distribution of annihilations on the drift-tube would be azimuthally asymmetric for a short distance beyond each aperture depending on the direction of the gravitational acceleration of antimatter. The Monte Carlo simulation is used to determine the number of azimuthally asymmetric annihilations that could be expected for specified experimental parameters.

Dual Levitated Coils for Antihydrogen Production

Joshua D. Wofford, Carlos A. Ordonez

Department of Physics, University of North Texas, 1155 Union Circle #311427, Denton Texas 76203-5017, United States

Two coaxial superconducting magnetic coils that carry currents in the same direction and that are simultaneously levitated may serve for antihydrogen plasma confinement. The configuration may be suitable for use by a collaboration at the CERN Antiproton Decelerator facility to test fundamental symmetries between the properties of hydrogen and antihydrogen. Nested Penning traps are currently used to confine recombining antihydrogen plasma. Symmetry studies require the production of sufficiently cold antihydrogen. However, plasma drifts within nested Penning traps can increase the kinetic energy of antiprotons that form antihydrogen atoms. Dual levitated coils may serve to confine relatively large, cold, dense non-drifting recombining antihydrogen plasmas. A minimum-B magnetic field that is produced by the coils could provide for atom trapping. The possibility of using the configuration for other applications, such as for confining fusion plasmas, is discussed. A toroidal plasma is confined between the coils. High density plasmas may be possible, by allowing plasma pressure to balance mechanical pressure to keep the coils apart. Progress is reported on theoretical and experimental efforts. The theoretical effort includes the development of a classical trajectory Monte Carlo simulation of confinement. The experimental effort includes levitation of a NdFeB permanent ring magnet, which produces a magnetic field that is qualitatively similar to the field that would be produced by the two coaxial superconducting magnetic coils. Liquid-nitrogen-cooled Bi-2223 high-temperature-superconducting components, with a critical temperature of 108 K, were used to levitate the ring magnet. The experimental results indicate that, to avoid tilts, the two coaxial superconducting magnetic coils must be surrounded with a superconducting cavity.

Simulations of Charged Particles Trapped by a Cylindrically-Symmetric Artificially Structured Boundary

Allen S. Kiester, Jose L. Pacheco, Carlos A. Ordonez, Duncan L. Weathers

Department of Physics, University of North Texas, 1155 Union Circle #311427, Denton Texas 76203-5017, United States

The ALPHA Collaboration's trapping of antihydrogen has brought antimatter research to the forefront of scientific interest [Andresen et al., Nature Physics DOI:10.1038/NPHYS2025]. Antihydrogen is currently produced by the three-body recombination of positron and antiproton plasmas that interact in a Penning-Malmberg trap at cryogenic temperatures. The antiproton plasma contained in a Penning-Malmberg trap is subject to ExB drifts. Because the produced antihydrogen has a similar kinetic energy distribution to the antiproton plasma, an ExB drift can increase the average kinetic energy of the antihydrogen and make it less likely to be confined with the minimum-B configuration used in the Penning-Malmberg trap. A simulation of an alternative trapping configuration that could reduce plasma kinetic energy is presented. A three-dimensional cylindrically-symmetric artificially structured boundary-i.e., a boundary that produces periodic short-range static fields to reflect charged particles-is studied by computational simulations that calculate single particle trajectories for particles of different mass and charge. The results show that both positively and negatively charged particles can be contained simultaneously.

Simulations of Charged Particle Reflection by an Artificially Structured Boundary

Aimee L. E. Ayton, Jose L. Pacheco, Carlos A. Ordonez, Duncan L. Weathers

Department of Physics, University of North Texas, 1155 Union Circle #311427, Denton Texas 76203-5017, United States

In an effort to identify an alternative to existing two-species charged particle traps, such as the Penning-Malmberg trap used by the ALPHA Collaboration to study antihydrogen, an artificially structured boundary that could serve as a trap wall is investigated. The artificially structured boundary consists of a spatially periodic sequence of magnetic cusps, with nested electrostatic barriers in each cusp. The intent is to simultaneously reflect, and hence confine within the volume bounded by the surface, charged particles of either sign of charge that have completely random incident trajectories. Trajectories in the vicinity of the boundary have been simulated and analyzed to identify the conditions where particles begin to escape confinement. Three parameters are varied, relative to the energy of the incident particles: the voltages on the positive and negative electrodes producing the electrostatic barriers, and the current generating the magnetic fields. The goal is to identify a region within this three-dimensional parameter space for which particles of both signs of charge are simultaneously confined, and use this information to optimize the trap design. Preliminary results suggest that particles of equal mass but opposite sign of charge cannot be simultaneously confined by a short, symmetric electrode configuration. However, there is an overlap in the regions of confinement in the parameter space for particles of opposite sign of charge with different masses. For example, it is possible to confine both protons and electrons.

Lgamma₁ X-Ray satellites spectra of elements ₄₁Nb to ₅₁Sb

Surendra Poonia

Division of Natural Resources and Environment, Central Arid Zone Research Institute, Jodhpur - 342003, Rajasthan, India, Central Arid Zone Research Institute, Jodhpur - 342003, Rajasthan, India, Dr. Surendra Poonia, S/O Dr. Fateh Singh Poonia, 10-C, Mahaveer Colony, Ratanada, Jodhpur - 342001, Rajasthan, Jodhpur Rajasthan 342001, India

The X-ray satellite spectra arising due to $2p_{1/2}^{-1}3x^{-1}3x^{-1}4d_{3/2,5/2}^{-1}$ ($x = s, p, d$), i.e. $L_2M_x-M_xN_{4,5}$ transition array, in elements with $Z = 41$ to 51 , have been calculated, using available Hartree-Fock-Slater (HFS) data on $K-L_2M_x$ and $L-M_xN_{4,5}$ Auger transition energies. The relative intensities of all the possible transitions have been estimated by considering cross-sections for the Auger transitions simultaneous to a hole creation and then distributing statistically the total cross sections for initial two hole states L_2M_x amongst various allowed transitions from these initial states to $M_xN_{4,5}$ final states by Coster-Kronig (CK) and shake off processes.

In both these processes initial single hole creation is the prime phenomenon and electron bombardment has been the primary source of energy. Each transition has been assumed to give rise to a Gaussian line and the overall spectrum has been computed as the sum of these Gaussian curves. The computed satellite spectra have been compared with the experimentally reported measured $L\gamma_{\text{sat}}$ satellite energies. On the basis of agreement between computed spectra and measured satellites, It is observed that the satellite $L\gamma_{\text{sat}}$ in $_{41}\text{Nb}$ to $_{51}\text{Sb}$ is emitted by the superposition of the most intense transitions namely A ($L_2M_1^1P_1-M_1N_4^1D_2$), D ($L_2M_1^3P_0-M_1N_4^3D_1$), F ($L_2M_3^3D_1-M_3N_5^3D_1$) and H ($L_2M_3^3D_1-M_3N_4^3P_0$) contributing in order of decreasing intensity.

WED-AP07-1

#174 - Invited Talk - Wednesday 1:00 PM - Elm Fork

New directions in electrostatic ion beam traps

Oded Heber

Department of Particle Physics and Astrophysics, Weizmann Institute of Science, Rehovot 76100, Israel

Electrostatic Ion Beam Trap (EIBT) devices have been used extensively in many laboratories around the world for the last 15 years. The uniqueness of such traps is the usage of only electrostatic fields to store ions with no mass limit and no mass dependent tuning. EIBT devices have been used in many scientific applications in atomic and molecular physics such as lifetime measurement of metastable ions, ion collision with electrons and gas targets, molecular ionization fragmentation and radiative decay. Applications in mass spectrometry and isotope separation also exist.

In this presentation some new applications will be revealed. The first one will be a new use for large biological molecules where the trapping time is correlated to the molecular structure. The second example will be the usage of the EIBT as a trap for radioactive beams enabling to detect decays like beta decay with fully kinematic data of the recoil ion and the emitted electron. Therefore the correlation with the neutrino is obtained for checking the standard model or physics beyond the standard model. Other new applications will be briefly discussed as well.

WED-AP07-2

#456 - Invited Talk - Wednesday 1:00 PM - Elm Fork

Electron-Ion Recombination Measurements by TOF from an EBIT

S. Mahmood, I. Orban, E. Lindroth, S. Ali, S. Tashenov, R. Schuch

Department of Physics, Stockholm University, S-106 91, Stockholm, Sweden

Dielectronic and radiative recombination (DR) and (RR) are important electron ion recombination processes in high temperature plasmas, where they strongly affect the charge/energy balance and emit photons for diagnostics. These processes were studied by a new method with highly charged Si and S ions at the Stockholm Electron Beam Ion Trap (S-EBIT). After breeding the ions in the trap by electron bombardment at around 10 keV to the desired charge state distribution, the electron beam energy was scanned from 1.4 keV to 3.0 keV. The X rays emitted from RR and DR processes were observed during the scan by a Si(Li) detector placed at 90° to the electron beam direction. For every step of the scan, the charge state distribution was monitored by fast ion extraction from the trap and TOF detection $\sim 3\text{m}$ from the trap. Thus, a combination of X-ray and TOF technique allowed for charge state resolved X-ray measurement at an EBIT[1]. Additionally, the electron-impact excitation rates could be determined[1]. The temperature dependent recombination rate coefficients will be presented as well.

[1] I Orban et al., to be publ., S. Mahmood et al., to be publ. in The Astrophysical Journal

3D imaging of molecular-ion dissociation induced by slow atom impact: alignment and orientation dependence in soft and hard collisions

Itzik Ben-Itzhak

J.R. Macdonald Laboratory, Department of Physics, Kansas State University, Manhattan Kansas 66506, United States

Hard collisions between few keV molecular ions and atoms can lead to vibrational excitation and subsequent dissociation as well as target ionization. Previous experimental efforts were unable to resolve the vibrational process from the competing electronic excitation complicating comparison with theory [1]. Moreover, target ionization has been largely ignored. Employing 3D coincidence imaging of the ion-beam fragments and recoil ions, we study collision induced dissociation (CID), where vibrational (vCID) and electronic (eCID) processes are experimentally separated, giving new insight into the vibrational mechanism. In particular, vCID occurs predominantly for molecular ions aligned perpendicular to their velocity and when the momentum transfer is along the molecular axis. Similarities and differences between CID and other processes occurring in collisions between slow atoms and HeH^+ and H_2^+ (and their isotopologues) will be discussed.

Other contributors to this work with J.R. Macdonald Laboratory affiliation: Nora G. Johnson, Ben Berry, A. Max Saylor, Dag Hathiramani, Jack W. Maseberg, Sam Fahrenholtz, and Kevin D. Carnes. In collaboration with Wania Wolff, Instituto de Fisica, Universidade Federal do Rio de Janeiro, Rio de Janeiro, 21945-970, RJ, Brazil

This work was supported by the Chemical Sciences, Geosciences, and Biosciences Division, Office of Basic Energy Sciences, Office of Science, U.S. Department of Energy.

1. J. Los and T. R. Govers, *Collision-Induced Dissociation of Diatomic Ions*, Collision Spectroscopy (Plenum Press, New York and London, 1978), pp. 289-343

Intense decelerated ion beams for the study of low-energy charge transfer

Vola M Andrianarijaona¹, Jonathan G King¹, Merl F Martin¹, Xavier Urbain²

⁽¹⁾*Department of Physics, Pacific Union College, Angwin CA 94508, United States*

⁽²⁾*Institute of Condensed Matter and Nanosciences, Université Catholique de Louvain, Chemin du Cyclotron 2, Louvain-la-Neuve B-1348, Belgium*

Using a 3-D imaging technique, the vibrational distributions of slow H_2^+ and D_2^+ produced by charge transfer (CT) between an H_2 or D_2 target and various fast atomic and molecular ions were measured from 10 eV to few keV energies in the laboratory frame. The atomic or molecular ions are extracted from a standard duoplasmatron ion source, accelerated and decelerated to enter the collision cell hosting neutral molecules from an effusive jet. The CT daughter molecular ions are extracted sideways and accelerated to 2 keV before crossing an effusive potassium jet to undergo resonant dissociative charge exchange. The positions and flight time difference of the two resulting particles give access to the vibrational distribution of the CT products. At 50 eV and above, our results on the (H_2, H^+) system benchmark state-to-state calculations [1]. At lower energies, the deviations from theory are not understood yet but may suggest that rovibrational modes start to play an important role in the CT dynamics. CT measurements have also been performed with H_2^+ , D_2^+ , He^+ , and H_3^+ on H_2 and on D_2 from 10 eV to few keV.

[1] L. F. Errea, L. Fernandez, L. Mendez, B. Pons, I. Rabadan, and A. Riera, *Phys. Rev. A* **75** 032703 (2007).

Research supported by the Fund for Scientific Research FNRS through IISN Grant No. 4.4504.10, and the National Science Foundation through Grant No. PHY-106887.

Peripheral collisions of fast electrons with highly charged ions

J. H. Macek¹, S. J. Ward²

⁽¹⁾*Physics and Astronomy, University of Tennessee, 401 Nielsen Physics Building, Knoxville TN 37996-1200, United States*

⁽²⁾*Physics and Astronomy, University of North Texas, Denton TX 76203-1427, United States*

Vortices are a novel feature of time-dependent atomic wave functions. A general discussion of vortices is given which relates them to nodes in the real and imaginary parts of complex functions, the isolated zeros in such functions, the probability current \mathbf{j} , the velocity field \mathbf{v} , the integral of the current around isolated zeros, the density of atomic wave functions in the neighborhood of isolated zeros and the mean angular momentum averaged over the same regions. The imaging theorem shows that vortices may appear as observable structures in the momentum distributions of electrons ejected from atoms by photons or by electron or positive ion impact. It is also shown that angular momentum transfer is needed in order for complex functions to exhibit isolated zeros. This unexpected connection between purely analytic properties, namely zeros, and the transfer of a physical quantity, namely angular momentum, is examined for electron impact on C^{5+} . This connection is studied for the special case of peripheral collisions where the dipole force between incident and ejected electrons dominates [1].

1. S.J.W. acknowledges NSF support under grant no 0968638.
2. J.H.M. acknowledges DOE support under grant no. FG02 02ER15283.
3. J. Botero and J. H. Macek, Phys. Rev. A **45**, 54 (1992).

Angular distribution of bremsstrahlung produced by 50-keV electrons incident on a thick Au target

Daniel Gonzales, Scott Williams

Department of Physics, Angelo State University, ASU Station #10904, San Angelo Texas 76909, United States

We compare of the relative intensities of thick-target bremsstrahlung produced by 50-keV electrons incident on Au at forward angles ranging from 0 to 55 degrees. Following corrections of the data for photon absorption within the target, an anisotropical distribution of the detected radiation appears to occur only for photon energies, k , that are approximately equal to the initial energy of the incident electrons, E_0 . As the ratio k/E_0 approaches 0, the results indicate that the detected radiation essentially takes on an isotropic distribution. This is primarily attributed to electron-scattering within the target. The results are compared to the theoretical shape functions of Kissel *et al.* [At. Data Nucl. Data Tables **28**, 381 (1983)]. Comparisons suggests that when k/E_0 is approximately equal to 1, the angular distribution of bremsstrahlung emitted by electrons incident on thick targets is in agreement with the theoretical angular distribution of bremsstrahlung emitted by electrons incident on free-atom targets.

The Stockholm Electron Beam Ion Trap for Highly Charged Ions

Yao Ke¹, M. Hobein¹, S. Tashenov¹, A. Safdar¹, T. Mohamed¹, I. Orban¹, S. Trotsenko², R. Schuch¹

⁽¹⁾*Physics Department, Stockholm University, Stockholm, Sweden*

⁽²⁾*GSI Helmholtzzentrum, Darmstadt, Germany*

Recent years have witnessed remarkable accomplishments in developing advanced accelerator- and laser facilities along with significant progress in experimental instrumentation. It should now-a-days be possible to provide ions of all elements up to uranium at rest, with all electrons stripped off, even in a table top machine such as an EBIT¹. These allow investigations of electrons in extremely strong electromagnetic fields, testing QED at its limits. Precision mass measurements in a Penning trap that use the benefit of a single, but cold highly-charged ion. The higher the charge, the higher is the mass accuracy that is achieved. Examples for the transport of highly-charged ions through nano-capillaries for new focusing devices will be given; and, of spectroscopy of electron-ion processes through photon and ion detection from the EBIT for fusion and astro-physical plasma.

¹¹ S. Böhm *et al.*, J. of Phys. **58**, 303 (2007) and R. Schuch *et al.*, J. of Instr. **5**, C12018 (2010)

Few Body Quantum Dynamics of high-Z Ions studied at the Future Relativistic HESR Storage Ring and the ESR/Cryring

Siegbert Hagmann^{1,2}, Thomas Stoeckler^{2,3,4}, Yuri Litvinov², Christophor Kozhuharov², Pierre-Michel Hillenbrand², Dieter Schneider⁶, Vladimir Shabaev⁵, Michael Lestinsky²

⁽¹⁾*Inst. f. Kernphysik, Univ Frankfurt, Frankfurt, Germany*

⁽²⁾*GSI, Gesellschaft für Schwerionenforschung, Darmstadt, Germany*

⁽³⁾*Helmholtz Institut, Helmholtz Institut, Jena, Germany*

⁽⁴⁾*Physikalisches Institut, Universität Jena, Jena, Germany*

⁽⁵⁾*Dept. of Physics, St Petersburg State University, St Petersburg, Russia*

⁽⁶⁾*LLNL, Lawrence Livermore National Laboratory, Livermore, United States*

At the FAIR facility for antiprotons and ion research the high energy storage ring HESR, originally conceived for experiments using antiprotons, will be configured to also provide highly-charged heavy ions up to beam energies corresponding to $\gamma=5$. This opens a wealth of opportunities for in-ring atomic physics experiments on few-body quantum dynamics ranging from e.g. dynamics of various e^+e^- pair creation processes to quasi-photoionisation of inner shells of the highest-Z ions. Additionally to the HESR the low energy storage ring Cryring ($B\rho=1.44\text{Tm}$) will be installed at the ESR storage ring. This will considerably extend the range of available collision energies down to 0.1 AMeV for heavy ions up to bare U^{92+} . This opens up new windows for adiabatic collisions and high resolution spectroscopy. We will discuss various in-ring spectrometers permitting characterization of the pertaining fundamental processes in a kinematically complete fashion for HESR and new adiabatic experiments on superheavy quasimolecules now possible at the Cryring.

Electron impact phenomena for the process of projectile excitation in ion-atom collisions

Alexandre Gumberidze^{1,2}, Daniel Bristol Thorn, Andrey Surzhykov^{3,4}, Stephan Fritzsche^{2,3,5}, Christopher J. Fontes⁶, Hong Lin Zhang⁶, Alexander Voitkiv⁷, Bennaceur Najjari⁷, Dariusz Banas⁸, Heinrich Beyer^{3,9}, Weidong Chen³, Robert D. DuBois^{1,10}, Sabrina Geyer^{3,11}, Robert Grisenti^{3,11}, Siegbert Hagmann^{3,11}, Myke Hegewald^{3,11}, Sebastian Hess^{3,11}, Paul Indelicato¹², Christophor Kozhuharov³, Renate Martin^{3,9}, Istvan Orban¹³, Nikos Petridis^{3,11}, Regina Reuschl^{1,2,14}, Anna Simon¹⁵, Uwe Spillmann³, Martino Trassinelli¹⁴, Sergiy Trotsenko^{3,9}, Günter Weber^{3,9}, Danyal F. A. Winters^{3,4}, Natalya Winters^{3,4}, Deyang Yu^{3,16}, Thomas Stöhlker^{3,4,9}

⁽¹⁾*ExtreMe Matter Institute EMMI, GSI Helmholtzzentrum für Schwerionenforschung, Planckstrasse 1, Darmstadt 64291, Germany*

⁽²⁾*FIAS Frankfurt Institute for Advanced Studies, Frankfurt am Main 60438, Germany*

⁽³⁾*GSI Helmholtzzentrum für Schwerionenforschung, Darmstadt 64291, Germany*

⁽⁴⁾*Physikalisches Institut, Ruprecht-Karls-Universität, Heidelberg 69120, Germany*

⁽⁵⁾*Department of Physics, University of Oulu, Oulu Fin-90014, Finland*

⁽⁶⁾*Los Alamos National Laboratory, Los Alamos NM 87545, United States*

⁽⁷⁾*Max-Planck-Institut für Kernphysik, Saupfercheckweg 1, Heidelberg 69117, United States*

⁽⁸⁾*Institute of Physics, Jan Kochanowski University, Kielce PL-25-406, Poland*

⁽⁹⁾*Helmholtz-Institut Jena, Jena 07743, Germany*

⁽¹⁰⁾*Department of Physics, Missouri University of Science and Technology, Rolla Missouri 65409, United States*

⁽¹¹⁾*Institut für Kernphysik, University of Frankfurt, Frankfurt am Main 60486, Germany*

⁽¹²⁾*Laboratoire Kastler Brossel, Ecole Normale Supérieure, CNRS, Université Pierre et Marie Curie-Paris 6, Paris F-75252, France*

⁽¹³⁾*Department of Physics, University of Stockholm, Stockholm S-106 91, Sweden*

⁽¹⁴⁾*Inst. des NanoSciences de Paris, CNRS UMR7588 and UMPC-Paris 6, Paris F-75015, France*

⁽¹⁵⁾*Michigan State University, East Lansing Michigan 48824, United States*

⁽¹⁶⁾*Institute of Modern Physics, Lanzhou 730000, China*

In this contribution, we present a study of the K-shell excitation in hydrogen-like uranium in relativistic collisions with different gaseous targets. The experiment was conducted at the ESR storage ring of the GSI accelerator facility in Darmstadt, Germany. By performing measurements with different targets as well as with different collision energies, we were able to gain access to both; proton (nucleus) impact excitation (PIE) and electron impact excitation (EIE) processes in the relativistic collisions. The large fine-structure splitting in H-like uranium allowed us to unambiguously resolve excitation to different L-shell levels. Moreover, information about the population of different magnetic sublevels has been obtained via an angular differential study of the decay photons associated with the subsequent de-excitation process. A comparison with recent relativistic calculations which include excitation mechanisms due to both; the protons (nucleus) and the electrons will be presented.

Polarimetry of electron beams by means of bremsstrahlung

Stanislav Tashenov¹, Torbjörn Bäck², Roman Barday³, Bo Cederwall², Joachim Enders³, Anton Khaplanov², Yulia Poltoratska³, Kai-Uwe Schüssler², Andrey Surzhykov^{1,4}

⁽¹⁾Physikalisches Institut Universität Heidelberg, Im Neuenheimer Feld 226, Heidelberg 69120, Germany

⁽²⁾Nuclear Physics, Royal Institute of Technology, Stockholm SE-10691, Sweden

⁽³⁾Institut für Kernphysik, Technische Universität Darmstadt, Schlossgartenstraße 2, Darmstadt 64289, Germany

⁽⁴⁾GSI Helmholtzzentrum für Schwerionenforschung GmbH, Planckstr 1, Darmstadt 64291, Germany

Linear polarization of hard x-rays emitted in the process of the atomic field electron bremsstrahlung has been measured with a polarized electron beam. The correlation between the initial orientation of the electron spin and the angle of photon polarization has been systematically studied by means of Compton and Rayleigh polarimetry techniques applied to a segmented germanium detector. The results are in a good agreement with the fully-relativistic calculations. They are also explained classically and in a unique way manifest that due to the spin-orbital interaction the electron scattering trajectory is not confined to a single scattering plane. The developed photon polarimetry technique with a passive scatterer is very efficient and accurate and thus allows for novel applications. Bremsstrahlung polarization correlations lead to a new method of polarimetry of electron beams. Such a method is sensitive to all three components of the electron spin. It can be applied in a broad range of the electron beam energies from 100 keV up to a few 10 MeV. The results of the test measurement at 100 keV will be shown. The optimum scheme for electron polarimetry will be analyzed and the relevant theoretical predictions will be presented.

Nuclear Excitation by Electron Capture (NEEC) Experiments at GSI, LBNL, and Omega

Andrea L. Kritcher¹, Lee Bernstein¹, Darren Bleuel¹, Jack Caggiano¹, Wolfgang Stoeffl¹, Dan Sayre¹, Robert Hatarik¹, Dieter Schneider¹, Carsten Brandau^{2,4}, Christopher Kozhuharov², Thomas Stoeckler^{2,3}, Alex Mueller², Alex Gumberidze^{2,4}, Michael Heil², Haik Simon², Yu Litvinov^{2,5}, V. Bagnoud², Thomas Kuehl², Adriana Palffy⁵, Christoph Keitel⁵, Vincent Meot¹⁰, Gilbert Gosselin¹⁰, Eric Bauge¹⁰, Rene Reifarh⁶, Rod Clark⁷, Phil Walker⁸, Mathis Wiedeking⁹, Pascal Morel¹⁰

⁽¹⁾Lawrence Livermore National Laboratory, Livermore CA, United States

⁽²⁾GSI-Helmholtzzentrum, Darmstadt, Germany

⁽³⁾Helmholtzzentrum Jena, GSI-Helmholtzzentrum, Jena, Germany

⁽⁴⁾EMMI/FIAS (extreme Matter Institute/Frankfurt Institute for Advanced Science), GSI-Helmholtzzentrum, Darmstadt, Germany

⁽⁵⁾Max Planck Institute of Nuclear Physics, Heidelberg, Germany

⁽⁶⁾University of Frankfurt, Frankfurt, Germany

⁽⁷⁾Lawrence Berkeley National Laboratory, Berkeley CA, United States

⁽⁸⁾University of Surrey, Guildford CA, United Kingdom

⁽⁹⁾iThemba LABS, Somerset West, South Africa

⁽¹⁰⁾CEA/DAM, Bruyères-le-Châtel, France

The effect of high energy density plasma (HEDP) environments on capture cross-sections in high-energy-density laboratory astrophysics experiments is expected to play an important role. With the recent commissioning of the National Ignition Facility (NIF) at LLNL, there has been a renewed interest in the study of these HEDP environments on nuclear plasma interactions. For example, the excitation of low lying nuclear states ($E_x \sim k_B T$) such as Nuclear Excitation by Electron Capture (NEEC) can effect neutron capture probabilities by modifying the spin and parity of the target nucleus, changing the density of states available to the decaying compound nucleus. Although there have been extensive theoretical studies on this subject, previous attempts to measure NEEC have been unsuccessful. This experiments discussed in this presentation are part of a multi-year scientific collaboration to demonstrate NEEC on an array of science facilities, including Lawrence Berkeley National Laboratory (LBNL), Gesellschaft für Schwerionenforschung (GSI), the Facility for Anti-proton and Ion Research (FAIR), and the Omega laser facility. The study of this mechanism will provide information on models used to predict excitation rates in high energy density plasmas.

Current status of the 1s-Lamb Shift Experiments at High-Z

Regina Reuschl^{1,2}, Heinrich F. Beyer², Alexandre Gumberidze^{1,2}, Siegbert Hagmann^{2,3}, Paul Indelicato⁴, Dieter Liesen², Renate Maertin^{2,5}, Uwe Spillmann², Martino Trassinelli⁶, Sergiy Trotsenko^{2,5}, Guenter Weber^{2,5}, Danyal Winters², Thomas Stoeckler^{2,5}

⁽¹⁾*ExtreMe Matter Institute EMMI, Planckstrasse 1, Darmstadt Hessen 64291, Germany*

⁽²⁾*Atomic Physics, GSI Helmholtzzentrum fuer Schwerionenforschung, Planckstrasse 1, Darmstadt Hessen 64291, Germany*

⁽³⁾*IKF, Johann Wolfgang Goethe University, Max-von-Laue-Str.1, Frankfurt Hessen 60438, Germany*

⁽⁴⁾*LKB, ENS, CNRS UMR 8552, Universite Pierre et Marie Curie Paris 6, Paris 75005, France*

⁽⁵⁾*Helmholtz-Institut Jena, Froebelstieg 3, Jena 07743, Germany*

⁽⁶⁾*INSP, CNRS UMR 7588, Universite Pierre et Marie Curie Paris 6, Paris 75005, France*

Atomic electrons bound to a very heavy nucleus experience extremely strong electromagnetic fields of up to 10^{16} V/cm. Hence, electrons under such extreme conditions are subject to pronounced relativistic and quantum-electrodynamics (QED) effects. As one of the best and most successful fundamental theories in contemporary physics, quantum electrodynamics has been the subject of many rigorous tests.

One of the most important experiments is the measurement of the 1s Lamb Shift in the most highly charged, one-electron ion available in the laboratory, uranium (U^{91+}). In H-like uranium the electric field strength begins to approach the critical value for the spontaneous emission of electron-positron pairs which makes it ideal for testing the limits of our understanding of bound state QED. In recent years, tremendous progress has been achieved in the theoretical treatment and evaluation of higher order QED corrections, which requires refined experimental methods to cope with the precision reached in the theoretical calculations.

At the Experimental Storage Ring (ESR) a series of experiments has been performed on the topic of the 1s-Lamb Shift during the last decade. By exploiting the luminosity of the stored and cooled ion-beams, the experimental accuracy could be improved considerably over the years. Nowadays, the study of the 1s-Lamb Shift in high-Z ions can be regarded as the most accurate test of strong field QED for simple one-electron systems. In these experiments different approaches have been applied and thus provide profound knowledge for anticipated future scenarios. Only recently, a high-precision x-ray crystal spectrometer has been setup at the internal gas-jet target of the ESR. With this installation we envisage an experimental accuracy of better than 1 eV.

An overview on the current status of experimental results and the progress in technical developments for future installations will be given.

Electron Beams, Wood and Bio-Fuels and Chemicals

Mark S Driscoll³, Mellony S Manning¹, Arthur J Stipanovic¹, Vincent Barber², John P Hassett¹, Craig Kenny¹

⁽¹⁾*Chemistry, State University of New York College of Environmental Science and Forestry, One Forestry Drive, Syracuse NY 13210, United States*

⁽²⁾*Paper and Bioprocess Engineering, State University of New York College of Environmental Science and Forestry, One Forestry Drive, Syracuse NY 13210, United States*

⁽³⁾*UV/EB Technology Center, State University of New York College of Environmental Science and Forestry, One Forestry Drive, Syracuse NY 13210, United States*

Cellulose is the major structural component of wood and plant fibers and is the most abundant polymer synthesized by nature. Despite this great abundance, cellulosic biomass has seen limited application outside of the paper industry. Its use as a feedstock for fuels and chemicals has been limited because of its highly crystalline structure, inaccessible morphology and limited solubility (recalcitrance). Any economic use of lignocellulosic resources for the production of fuels or chemicals will require a "pretreatment" technology to enhance the accessibility of the biomass to enzymes and/or chemical reagents. Electron beams (EB), X-rays or gamma rays produce ions in a material which can then initiate chemical reactions and cleavage of chemical bonds. Such ionizing radiation predominantly scissions and degrades or depolymerizes cellulose. This study looked at how electron beam irradiation of wood, wood pulp and microcrystalline cellulose changed the recalcitrance and how that change affects the economics of lignocellulosic fuel and chemical production.

Dimensional Stability of Natural Fibers

Mark S Driscoll¹, Jennifer L Smith², Sean Sean Woods², Kenneth J Tiss², L. Scott Larsen³

⁽¹⁾*UV/EB Technology Center, State University of New York College of Environmental Science and Forestry, One Forestry Drive, Syracuse NY 13210, United States*

⁽²⁾*Sustainable Construction Management and Engineering, State University of New York College of Environmental Science and Forestry, One Forestry Drive, Syracuse NY 13210, United States*

⁽³⁾*NYSERDA, 17 Columbia Circle, Albany NY 12203, United States*

One of the main problems associated with the use of natural fibers as reinforcing agents in composites is their uptake of moisture. Many natural fibers are lignocellulosic, which causes the fibers to swell and shrink as the amount of available moisture changes. Swelling and shrinking can cause composites to prematurely fail. This paper will present results of a research study that focuses on the use of low molecular weight monomers polymerized by electron beam ionizing radiation to dimensionally stabilize cellulose-based material. Tests will be conducted to evaluate the shrinking and swelling of fibers prior to their use in a composite. Results will be presented for different natural fibers.

Advancements in Facilities for Irradiated Materials and Ion Beam Analysis at the University of Wisconsin Ion Beam Laboratory

Kevin G Field¹, Chris J Wetteland¹, Guoping Cao¹, Chris R Field², Kim Kriewaldt¹, Kumar Sridharan¹, Todd R Allen¹

⁽¹⁾*University of Wisconsin - Madison, 1500 Engineering Drive, Madison WI 53706, United States*

⁽²⁾*Naval Research Laboratory, 4555 Overlook Avenue, Washington DC 20375, United States*

The University of Wisconsin Ion Beam Laboratory (UW-IBL) has recently undergone significant infrastructure upgrades to facilitate graduate level research in irradiated materials phenomena and ion beam analysis. A high current, National Electrostatics Corp. (NEC) Torodial Volume Ion Source (TORVIS) capable of emittance of hydrogen ions up to - 200 μ A and helium ion emittance of -5 μ A production is the keystone upgrade for the facility. Recent upgrades also include RBS analysis packages, end station developments for irradiation of relevant material systems, and the development of an in-house touch screen based graphical user interface for ion beam monitoring. Key research facilitated by these upgrades include irradiation of nuclear fuels, studies of interfacial phenomena under irradiation, and clustering dynamics of irradiated oxide dispersion strengthened steels. The UW-IBL has also partnered with the Advanced Test Reactor National Scientific User Facility (ATR-NSUF) to provide access to the irradiation facilities housed at the UW-IBL as well as access to post irradiation facilities housed at the UW Characterization Laboratory for Irradiated Materials (CLIM) facility and other ATR-NSUF partner facilities. Partnering allows for rapid turnaround from proposed research to finalized results through the ATR-NSUF rapid turnaround proposal system. An overview of the UW-IBL including CLIM and relevant research is summarized.

Three dimensional finite element methods: their role in the design of DC accelerators systems

Nicolae C. Podaru, A. Gottdang, D.J.W. Mous

High Voltage Engineering B.V., P.O. Box 99, Amersfoort 3800AB, Netherlands

Over the last years, High Voltage Engineering (HVE) has expanded its know-how and software tools for the detailed design of DC linear particle accelerators. Three dimensional (3D) finite element methods (FEM) are applied in the design stage to optimize complex electrostatic, magnetostatic (or combinations of these two) field distributions. The ray-tracing capabilities of the 3D FEM design tool is used to understand the origin of aberrations in ion optical components like analyzing magnets, electrostatic lenses and accelerator tubes and to minimize these aberrations. In addition, 3D FEM is used for Singletron™/Tandetrion™ power supply design which provides a precise prediction of their essential characteristics like required RF input power, electrical losses and accelerator voltage holding capability. The 3D design tools have been applied in the design of a dual-beam irradiation facility. Two Singletron™ accelerators with a rated terminal voltage of 2 MV, one for electrons (e^-) and one for protons (H^+), share a common end chamber to simultaneously irradiate samples of up to $300 \times 300 \text{ mm}^2$.

This work describes both the 3D FEM design and operational performance of the system, with emphasis on accelerator performance and charged-particle beam optics. A detailed overview of the accelerator system is also given. The terminal voltage ripple measured on both Singletron™ accelerators is below 27 V (RMS) at a terminal voltage of 1.5 MV. Particle transmission above 90% was measured over the entire beam energy range of 100 keV up to 2 MeV. Electron beam transmission is supported down to 100 keV, and below, which is achieved by shielding the 5 m long beamline by mu-metal to reduce the DC magnetic field to 1-10 mG.

WED-AT05-P1

#165 - Poster - Wednesday 5:30 PM - Rio Grande

Accelerator Driven Photon Sources for Material Irradiation Studies

Carol Haertling¹, Joseph Tesmer¹, Yongqiang Wang¹, Chelsea D'Angelo^{1,2}

⁽¹⁾*Material Science & Technology, Los Alamos National Laboratory, M/S G770, Los Alamos NM 87545, United States*

⁽²⁾*Advanced Engineering Analysis, Los Alamos National Laboratory, M/S T080, Los Alamos NM 87545, United States*

We have used a particle accelerator in our Ion Beam Materials Laboratory to produce characteristic photons at desired energies for use in material irradiation studies. The photons are desired to mimic radioactive sources. Metal targets were irradiated with a proton beam, in one case producing characteristic x-rays (PIXE), and in another case producing gammas by nuclear reaction (PIGE). Both techniques result in reasonably monoenergetic photon sources. This presentation discusses the development and characteristics of these photon sources as well as how they are used in experiments.

WED-ECR04-1

#418 - Contributed Talk - Wednesday 8:30 AM - Post Oak

Defect mitigation by ion induced amorphousization and solid-phase epitaxy

L. C. Phinney, K. Hossain, R. J. Cottier, O. W. Holland, T. Golding

Amethyst Research Inc., 123 Case Circle, Ardmore OK 73401, United States

Ion implantation is a common technique in the semiconductor industry used to modify the electrical properties of materials, usually silicon. Some dopant ions are sufficiently light, such as boron, that they do not create a continuous amorphous layer in silicon over the range of the ions. In the presence of such a layer, most of the ion-induced damage can be removed by solid-phase epitaxy growth (SPEG), which results in recrystallization of the amorphous damage. However, end-of-range defects at the amorphous-crystal interface give rise to threading dislocations during SPEG that degrade the quality of the recrystallized Si. We have studied the end of range defects in silicon with two different implantations. The first was with 80 keV ³⁰Si with a dose of 3×10^{15} Si/cm², and the second was a double implant of 100 keV ⁷²Ge at a dose of 1×10^{15} Ge/cm² followed by 340 keV ²⁸Si at a dose of 3×10^{14} Si/cm². Annealing at 600° C was done to recrystallize the implanted samples, and the end of range defects were studied using channeled Rutherford Backscattering Spectrometry (RBS). The effects of photon-assisted hydrogenation on amorphization and recrystallization were also studied.

WED-ECR04-2

#411 - Contributed Talk - Wednesday 8:30 AM - Post Oak

Nano-engineered GeSi-on insulator for Heteroepitaxy

Khalid Hossain¹, Orin W Holland¹, Mukul C Debnath², T D Mishima², M B Santos²

⁽¹⁾*Amethyst Research Inc, 123 Case Circle, Ardmore OK 73401, United States*

⁽²⁾*Homer L. Dodge Department of Physics and Astronomy, University of Oklahoma, 440 West Brooks Street, Norman OK 73019 United States*

A compliant substrates has been prepared to grow metamorphic semiconductor films on a Si-based platform. It involves the synthesis of a patterned off-axis Ge-on-insulator (GeOI) heterostructure to achieve the "holy grail" of optoelectronics. A dilute GeSi layer is initially formed by implanting Ge⁺ into a silicon-on-insulator (SOI) substrate. Thermal oxidation segregates the Ge at the growing oxide interface to form a distinct Ge_xSi_{1-x} thin-film with a composition that can be tailored by controlling the oxidation parameters. In addition, the film thickness can be controlled by the implantation fluence, which is important since the film forms pseudomorphically below 2×10^{16} Ge/cm². Continued oxidation consumes the underlying Si leaving the nearly pure Ge film encapsulated by the two oxide layers, i.e. the top thermal oxide and the buried oxide. Removal of the thermal oxide by a dilute HF etch completes the process.

This technique combines the demonstrated compliancy of a thin ($< 3\text{nm}$) Ge nano-film (on insulator) with that of patterning to yield an obedient substrate with unsurpassed ability to accommodate lattice mismatch strain during thin-film growth with reduced dislocation that can thread through.

The technical challenges in fabricating device-quality epitaxial layers of II-V or III-V semiconductors on Si also include the reduction of anti-phase domains (APDs) due to growth of polar semiconductor on non-polar substrate besides the 14-20% lattice mismatch between the materials. The APDs have been handled with the use of off-axis substrate, and the utilization of sub-monolayer arsenic as wetting layer, which has been incorporated by co-implanting As^+ with Ge^+ on SOI. The GeOI thin film has been characterized with Raman spectroscopy, Rutherford backscattering spectroscopy, SEM and x-TEM. The patterning of GeOI is done with e-beam lithography. This work is supported by Oklahoma Center for Advancement in Science and Technology contract # ONAP-09-008.

WED-ECR04-3

#360 - Contributed Talk - Wednesday 8:30 AM - Post Oak

Investigation of diffusion of low energy Silver ions implanted in Silicon

Mangal S Dhoubhadel, Venkata C Kummari, Bibhudutta Rout, Gary A Glass, Jerome L Duggan, Floyd D McDaniel
Ion Beam Modification And Analysis Laboratory, Department of Physics, University of North Texas, 1155 Union Circle, #311427, Denton Texas 76203, United States

Transitional metal (e.g. Au, Ag) nanoparticles have recently found attractive applications in a variety of fields involving plasmonic effects in optics, photo-voltaics, and tracing the delivery of drugs in nano-medicine. In all these study, the size, shape and location of the metallic nano-particles play a key role in the application. Low energy silver ions were implanted at shallow depths at various fluences in the crystalline silicon substrates. The samples were annealed at temperatures below the eutectic point to prevent the formation of silicide. These samples were characterized to study the diffusion behavior of silver ions in the amorphous/polycrystalline silicon medium. The silver ions were implanted in silicon with energies of 35 keV, 55 keV, and 78 keV in the fluences of 5×10^{14} , 2×10^{15} , 4×10^{15} , 6×10^{15} , 1×10^{16} atom/cm² respectively. The samples were annealed at 500 °C for periods of 30, 60 and 90 minutes in vacuum and in Forming gas (96% argon 4% hydrogen). The diffusion behavior of the silver ions in silicon was characterized by using RBS, RBS-Channeling, RAMAN, XRD and TEM measurements. The results show that the diffusion of silver was asymmetric and showed strong preferential direction. The study shows that initially (30 minutes annealing) silver ions diffuse at a higher rate at 500 °C. The length of annealing time also influences in the formation of different sizes of silver nanoparticles.

WED-ECR04-4

#373 - Contributed Talk - Wednesday 8:30 AM - Post Oak

Improvements of the research infrastructure at the tandem laboratory at IFIN-HH

Dan Gabriel Ghita, Marius Dogaru, Marius Marin Gugiu, Ion V. Popescu, Catalin Ionut Calinescu, Gheorghe Catalin Danil, Mihaela Enachescu, Anisoara Pantelica, Dan Pantelica, Alexandru Petre, Tiberiu Bogdan Sava, Corina Anca Simion, Catalin Stan-Sion, Mihai Stasescu, Paul Ionescu, Nicolae Victor Zamfir
Nuclear Physics Department, Horia Hulubei National Institute for R&D in Physics and Nuclear Engineering, 30 Reactorului street, Magurele Ilfov 077125, Romania

An extensive process of modernizing the particle accelerators infrastructure started 5 years ago at the tandem laboratory in IFIN-HH. Major improvements of the 9 MV FN tandem accelerator installed in IFIN-HH in '73 were done in the late years, making it a very reliable machine, suited for basic and applied research experiments. Many developments opened the way for new experiments made for the first time in our laboratory. Some of the main research directions and original results will be presented.

Two new Cockcroft-Walton tandem accelerators were also installed this year. The 1 MV HVE Tandetron accelerator is dedicated for AMS measurements, especially for ^{14}C dating, and the 3 MV HVE Tandetron accelerator has the reaction chambers and detection system prepared for Ion Beam Analysis measurements, microprobe experiments and ion implantation.

Investigation of beam transmission in a 9SDH-2 3.0 MV NEC Pelletron® tandem accelerator

Naresh T. Deoli, Jose L. Pacheco, Venkata C. Kummari, Tilo Reinert, Bibhudutta Rout, Duncan L. Weathers,
Jerome L. Duggan, Gary A. Glass, Floyd D. McDaniel

Ion Beam Modification and Analysis Laboratory, Department of Physics, University of North Texas, Denton TX 76203, United States

Electrostatic tandem accelerators are widely used to accelerate ions for experiments in materials science such as high energy ion implantation, materials modification and micro-analyses. Many applications require high beam current as well as high beam brightness at the target; thus, maximizing the beam transmission through such electrostatic accelerators becomes important. The Ion Beam Modification and Analysis Laboratory (IBMAL) at University of North Texas is equipped with four accelerators, one of which is a 9SDH-2 3.0 MV National Electrostatic Corporation (NEC) Pelletron® tandem accelerator. The tandem accelerator is equipped with two Cs-sputter type (Source of Negative Ions using Cesium Sputter (SNICS) and Trace-Element AMS) ion sources and a radio frequency-He (Alphatross) ion source.

This work presents a detailed study of the beam transmission through this accelerator using the SNICS ion source for injection energy ranging from 20 to 60 keV for ions of different masses. The beam transmission is quantified for three different terminal voltages: 1, 1.5 and 2.0 MV. For a given terminal voltage, it has been found that beam transmission is strongly dependent on the ion source injector voltage. Details of experiments and data analysis are presented.

Heavy-ion energy resolution measurement of the F series ORTEC SSB detector

Zdravko Siketic, Iva Bogdanovic Radovic, Milko Jaksic

Division of Experimental Physics, Ruder Boskovic Institute, Bijenicka c. 54, Zagreb 10000, Croatia

In the Elastic Recoil Detection Analysis (ERDA) and Heavy Ion Rutherford Backscattering Spectrometry (HIRBS), silicon surface barrier detectors (SSBD) are commonly used for the energy detection. The energy resolution of the SSBD detectors for ions heavier than Li is usually significantly worse than for H and He, which limits both the mass and depth resolution of the experiment. There are three main contributions to the intrinsic energy resolution (pulse height defect) of the SSBD detector: a) entrance window effect (energy loss and straggling through the entrance window), b) nuclear collision effect (non-ionizing energy loss) and c) plasma effect which contributes the most (dense cloud of produced electron-hole pairs creates a zero initial electric field region and consequently recombination of the charge carriers can occur).

One of the solutions for this problem is to use a gas ionization chamber for energy detection instead of SSBD (in gas ionization chamber plasma effect is reduced). If gas ionization detector is not available, other possibility is to increase the value of the internal electric field in the SSBD. Effects coming from the formation of plasma are decreasing with increasing of the electric field (delay time and plasma time decrease). This should improve overall intrinsic energy resolution of the SSBD.

In this work we will study commercially available F series ORTEC SSBD detector designed especially for heavy ion spectroscopy, which is characterized with a high electric field under the entrance window (>15 kV/cm). Detector energy resolution for a wide range of ion mass and energy (Li, O, Si, Cl, Br and I ions with energy range 1-25 MeV) will be measured and compared with the existing experimental results for the gas ionization chambers. Performance of the detector concerning radiation hardness will be also studied.

Effect of c irradiation on the resistivity of Ru oxide thin films

C. Duk Lim¹, V. Ukirde¹, B. P. Sharma¹, L. Mitchell², F. D. McDaniel², M. El Bouanani^{1,3}

⁽¹⁾*Materials Science and Engineering, University of North Texas, 3940 North Elm Street-suite E-132, Denton TX 76207, United States*

⁽²⁾*Department of Physics, University of North Texas, 1115 Union Circle # 311427, Denton TX 76203, United States*

⁽³⁾*Center for Advanced Research and Technology, University of North Texas, 3940 North Elm street-suite E-132, Denton TX 76207, United States*

Conducting Ruthenium dioxide thin films are potential candidates for a number of advanced applications for next generation Si devices. Potential applications of thin films ruthenium oxides are: (a) metal-based gate electrodes that to maintain scaling and performance of future high-k based CMOS devices, and (b) diffusion barriers for copper interconnect. Good thermal stability, low resistivity, suitable work function and diffusion barrier properties are some of the required properties for future CMOS applications. Carbon irradiation and modification is used to explore the possibility of fine-tuning the resistivity of ruthenium dioxide thin films. RBS, XPS and four probe measurements are used to correlate resistivity, composition and carbon irradiation dose.

RBS and XPS studies of CH₄ plasma irradiated TaN for Cu Diffusion Barriers

V. Ukirde¹, B. P. Sharma¹, M. El Bouanani^{1,2}

⁽¹⁾*Materials Science and Engineering, University of North Texas, 3940 North ELM street-Suite E-132, Denton TX 76207, United States*

⁽²⁾*Center for Advance Research and Technology, University of North Texas, 3940 North ELM street-Suite E-132, Denton TX 76207, United States*

One of the crucial issues for the use of Copper in metallization applications in the semiconductor industry is its detrimental fast diffusion into Silicon. Therefore a suitable diffusion barrier is necessary between Cu metallization and Si and SiO₂. Tantalum nitride (TaN) is an established material for diffusion barriers against copper diffusion. However, Cu suffers from poor adhesion to TaN and many ongoing research activities are focused on using wet chemistry to alter the surface chemistry of the ultra-thin TaN diffusion barrier layer to overcome adhesion issue during Cu electroplating. The aim of this study is to modify the TaN surface via plasma processing in methane and incorporate different levels of carbon. Significant modification of surface chemistry of TaN was demonstrated by X-ray Photoelectron Spectroscopy, especially the Ta-C and C-C bonding configurations. Rutherford backscattering Spectrometry was used to evaluate the thermal stability of Cu/TaN/C/Si structure. Correlation between CH₄ plasma processing conditions of TaN and its effects on diffusion barrier properties for Cu will be presented.

Efficiency Calibration of a HPGe X-ray Detector for Quantitative PIXE Analysis

Stephen J Mulware, Wickramaarachchige Lakshantha, Bibhudutta Rout, Tilo Reinert

Ion Beam Modification And Analysis Laboratory, Department of Physics, University of North Texas, 1155 Union Circle #311427, Denton Texas 76203, United States

Particle Induced X-ray Emission (PIXE) is an analytical technique, which provides reliably and accurately quantitative results without the need of standards when the efficiency of the X-ray detection system is calibrated. The ion beam microprobe of the Ion Beam Modification and Analysis Laboratory at the University of North Texas has recently purchased a 100 mm² high purity germanium X-ray detector (Canberra GUL0110 Ultra-LEGe). In order to calibrate the efficiency of the detector for standardless PIXE analysis we have measured the X-ray yield of a set of commercially available X-ray fluorescence standards. The set contained elements from low atomic number $Z=11$ (sodium) to higher atomic numbers to cover the X-ray energy region from 1 keV to about 20 keV where the detector is most efficient. The charge measurement was done by collected charge integration as well as from the proton backscattering yield of a calibrated particle detector. The calibration is tested on reference samples.

PIXE simulation: models, methods and technologies

Matej Batic^{1,2}, Maria Grazia Pia¹, Paolo Saracco¹, Georg Weidenspointner³

⁽¹⁾*INFN Sezione di Genova, Istituto Nazionale di Fisica Nucleare, Via Dodecaneso 33, Genova 16146, Italy*

⁽²⁾*Experimental Particle Physics Department, Jožef Stefan Institute, Jamova cesta 39, Ljubljana 1000, Slovenia*

⁽³⁾*Max-Planck-Institut für extraterrestrische Physik, Institute Max-Planck, Giessenbachstraße, Garching 85748, Germany*

The simulation of PIXE (Particle Induced X-ray Emission) is discussed in the context of general-purpose Monte Carlo systems for particle transport.

Dedicated PIXE codes are mainly concerned with the application of the technique to elemental analysis, but they lack the capability of dealing with complex experimental configurations. General-purpose Monte Carlo codes provide powerful tools to model the experimental environment in great detail, but so far they have provided limited functionality for PIXE simulation. Despite the simplicity of its nature as a physical effect, PIXE represents a conceptual challenge for general-purpose Monte Carlo codes for particle transport, since it involves an intrinsically discrete effect (the atomic relaxation) intertwined with a process (ionization) affected by infrared divergence.

This presentation will provide an overview of the Geant4 simulation toolkit, and of recent developments that have endowed it with advanced capabilities for PIXE simulation. It will also report results of an extensive effort for quantitative validation of cross sections and other physical parameters relevant to PIXE simulation. Open issues in PIXE modeling will be discussed.

New Results about Stopping Power for positive Ions

Helmut Paul

Atomic and Surface Science, University of Linz, Altenbergerstrasse 69, Linz A 4040, Austria

The following points will be discussed:

- New stopping results for water
- New experimental and theoretical stopping results by Argentine-Brasil group
- New theoretical results using program CasP
- A comparison of new experimental data obtained by different methods
- The importance of the nuclear stopping contribution
- The solid-gas difference in stopping powers

High Resolution K X-ray PIXE spectra of 3d transition metals and their compounds

Stjepko Fazinic¹, Luka Mandic², Matjaz Kavcic³, Iva Bozicevic¹

⁽¹⁾*Rudjer Boskovic Institute, Bijenicka c. 54, Zagreb 10000, Croatia*

⁽²⁾*Physics Department, University of Rijeka, Omladinska 14, Rijeka 51000, Croatia*

⁽³⁾*Josef Stefan Institute, Jamova 39, Ljubljana SI-1000, Slovenia*

PIXE is usually performed with detectors not capable to resolve fine structure of **K** x-ray lines. When measured with wavelength dispersive x-ray spectrometers, this fine structure of **K α** and **K β** x-ray lines is observed. Many studies were performed to observe variations of relative intensities and/or positions of individual **K** x-ray components as a function of chemical effects. Attempts were made to use observed variations in **K** X-ray intensity ratios and relative positions for applications, including chemical speciation. **K α** spectra of **3d** transition elements are not so sensitive to chemical effects since they are emitted through transitions between inner shells. **K β** band components are related to valence electron transitions, influencing higher sensitivity to chemical effects. This is because the outermost **3d** level in **3d** transition metals becomes a broad band forming in chemical compounds the valence shells. However, the yield of **K β** x-rays is much lower compared to **K α** components. In order to study chemical effects on **K α** and **K β** spectra of **3d** transition elements and their compounds, a database of **K α** and **K β** spectra of selected **3d** metals and their compounds was collected.

The **K β** spectra were used to perform simple parameterization of crossover and valence band **K β** x-rays' relative positions and intensities over the range of **3d** metal compounds. Here a discussion will be presented about high resolution **K α** and **K β** x-ray spectra of **3d** transition elements and their compounds measured by wavelength dispersive spectrometers and obtained by MeV proton excitation. Chemical effects on **K α** and **K β** spectra will be discussed. Possibilities for using the spectra for chemical speciation will be discussed, as well as for improved interpretation of **K** x-ray spectra of **3d** transition metal compounds measured by solid state detectors, which could be important for PIXE in some special cases where samples contain high quantities of **3d** metals.

WED-IBA07-4

#104 - Contributed Talk - Wednesday 1:00 PM - Brazos I

A capillary microbeam for STIM and PIXE

M. J. Simon, M. Doebeli, M. Schulte-Borchers, A. M. Müller
Ion Beam Physics, ETH Zurich, HPK H32 Schafmattstrasse 20, Zurich 8093, Switzerland

Technical details and performance of an MeV ion microprobe based on glass micro-capillaries are presented. The ion beam is collimated by custom produced glass capillaries with outlet diameters in the range of 0.7 to 10 microns. Transmission properties for proton and helium ions have been measured and compared to Monte Carlo simulations. Due to the small gas leakage through the capillary opening, the beam can be taken into air without membrane. The setup procedure of the capillary micro beam is extremely fast and simple and virtually independent of particle type and energy. In-air STIM and PIXE raster imaging is performed by means of a piezo-driven XY stage. For STIM, the energy of the transmitted particles is measured by a miniaturized and radiation hard high resolution gas ionisation detector.

WED-IBA07-5

#108 - Contributed Talk - Wednesday 1:00 PM - Brazos I

PIXE analysis of aerosol samples at GIC4117 tandem accelerator laboratory of Beijing Normal University

Guangfu Wang^{1,2}, Lingda Yu¹, Junhan Chu¹, Xufang Li¹, Renjian Zhang³, BingBing Wu¹
⁽¹⁾*Key Laboratory of Beam Technology and Materials Modification of Ministry of Education, College of Nuclear Science and Technology, Beijing Normal University, Beijing 100875, China*
⁽²⁾*Beijing Radiation Center, Beijing 100875, China*
⁽³⁾*Key Laboratory of Regional Climate-Environment Research for Temperate East Asia(RCE-TEA), Institute of Atmospheric Physics, Chinese Academy of Sciences, Beijing 100029, China*

PIXE Analysis of concentrations of elements with Z>11 in aerosol samples is one of major applications of GIC4117 tandem accelerator in Beijing Normal University, and an external-beam facility for PIXE/PIGE analysis has been installed. PIXE analysis results and source apportionment of PM2.5 aerosol fractions collected on Teflon filters on daily basis over 2010 at one site in north city of Beijing will be shown. This is the first annual daily PM2.5 PIXE results of Beijing. Positive matrix factorization techniques identified that the major sources contributions to the PM2.5 are automobiles and transport (44.4%), windblown soil (8.9%), smoke from biomass burning (13.7%), road dust resuspended by the mobile transportation (11.1%), industrial emission (8.7%) and coal combustion (13.2%) during the 2010. Influences of some special events, such as set off firecrackers during Spring Festival, sand storm in spring and straw burning were also discussed.

Combinatory laser-catapult microdissection (LCM), high-sensitivity native protein Western blotting, and microPIXE spectrometry for selenoprotein characterization in pure nerve cell populations

Karen P. Briski¹, Baher A. Ibrahim¹, Jack E. Manuel², Venkata C. Kummari², Gary A. Glass²

⁽¹⁾*Basic Pharmaceutical Sciences, The University of Louisiana at Monroe College of Pharmacy, 1800 Bienville Drive, Monroe LA 71201, United States*

⁽²⁾*Ion Beam Modification and Analysis Laboratory, Physics Department, University of North Texas, Denton TX 76203, United States*

The essential trace element, selenium (Se), exerts critical biological effects via incorporation into the selenoproteome in the form of the amino acid, selenocysteine. Selenoproteins reduce cellular oxidative stress, regulate redox-sensitive gene transcription, and control thyroid hormone metabolism. Oxidative stress is implicated in bioenergetic and neurodegenerative damage to the brain. Development of strategies for manipulation of these distinct proteins for therapeutic benefit is hampered by a lack of fundamental knowledge of regional and cellular patterns of selenoprotein expression across regions and cell types within the brain. In this work laser-catapult microdissection (LCM), high-sensitivity native protein Western blotting, and microPIXE spectrometry are combined to characterize selenoprotein expression in separate cell populations in brain regions typified by vulnerability versus resistance to oxidative stress.

Trace Element Analysis of Mineral Water Samples through XRF, ICP-MS and PIXE

Akshar Dash^{1,3}, Casey Thurber², Venkata C Kummari¹, Wickramaarachchige Lakshantha¹, Guido F. Verbeck², Jerome L. Duggan¹, Bibhudutta Rout¹, Gary A. Glass¹, Floyd Del McDaniel¹

⁽¹⁾*Ion Beam Modification and Analysis Laboratory, Department of Physics, University of North Texas, 1155 Union Circle, Denton TX 76203, United States*

⁽²⁾*Department of Chemistry, University of North Texas, 1155 Union Circle # 305070, Denton TX 76203, United States*

⁽³⁾*Texas Academy of Mathematics and Science, University of North Texas, 1155 Union Circle #305309, Denton TX 76203, United States*

This study aims to determine the trace elemental composition of natural mineral water samples using three widely-used concentration analysis techniques: X-Ray Fluorescence (XRF), Inductively Coupled Plasma-Mass Spectrometry (ICP-MS) and Particle Induced X-ray Emission (PIXE). The XRF and PIXE analyses are non-destructive techniques, while the ICP-MS is a destructive technique but highly sensitive to the concentration levels of different elements and compounds. About 200 ml samples of natural hot spring water from Hot Springs, Arkansas, were collected during the winter season in 2011. A part of the water samples were prepared through dilution for ICP-MS analysis and through filtration for XRF analysis. Elemental concentration analyses of the hot spring water samples were compared to that of tap water samples prepared through the same dilution and filtration methods. We speculate that the mineral water sample will contain a smaller concentration (in parts per million levels) of trace elements like Co, Mg, and Pb than tap water, since the mineral water is in an environmentally natural state. The ICP-MS and XRF results showed the presence of the elements Co, As, Se, Kr, Mo, Cd, Sn, and W in the hot spring water samples. The respective concentrations of these trace elements were significantly lower in the natural mineral water samples than in the tap water samples. We plan to investigate the presence and concentrations of trace elements using also the quantitative analysis technique PIXE. PIXE provides accurate analyses and can be used to analyze liquid and solid samples alike; therefore, we want to compare the analytical results with the two other techniques.

Nanoscale manipulation of the properties of solids at high pressures and irradiated by relativistic heavy ions

Maik Lang

Earth and Environmental Sciences, University of Michigan, 1100 N University Av, Ann Arbor Michigan 48109, United States

During the past few years, research on materials at extreme conditions has become a vibrant field worldwide in many universities and research institutions. Relativistic heavy ions provide a unique opportunity to access a physical regime quite apart from thermodynamic equilibrium conditions [1]. These projectiles exhibit exceptional properties because they deposit their kinetic energy (GeV), within an exceedingly short interaction time (sub fs) into nanometer-sized sample volumes, resulting in extremely high energy densities (up to tens of eV/atom). Here, we describe a new strategy of combining such ion beams with high-pressure techniques by injecting relativistic ions from one of the world's largest accelerator facilities (GSI - Helmholtz Center for Heavy Ion Research - Darmstadt, Germany) through a mm-thick diamond anvil of a high-pressure cell into a pressurized target [2]. This experimental approach allows for the investigation of the behavior of materials at extreme conditions and opens up unprecedented possibilities for the synthesis of new materials.

Ion-beam exposure of different ceramic oxides revealed that radiation-induced energy deposition into highly compressed materials (several tens of GPa) are able to modify dramatically phase-transformation pathways. For example, the combined use of advanced **in situ** (synchrotron X-ray diffraction and Raman spectroscopy) and **ex situ** (transmission electron microscopy) characterization techniques evidenced after irradiation under a pressure up to 65 GPa: (i) the stabilization of a new metastable high-pressure phase of gadolinium-zirconate pyrochlore ($\text{Gd}_2\text{Zr}_2\text{O}_7$) [2] and (ii) the transformation into high-pressure and high-temperature phases of ceria (CeO_2) and zirconia (ZrO_2) at unexpected low pressures and/or radiation fluences.

[1] J.M. Zhang, M. Lang, M. Toulemonde, R. Devanathan, R.C. Ewing, W.J. Weber, **J. Mater. Res.** **25** (2010) 1344.

[2] M. Lang, F.X. Zhang, J.M. Zhang, J.W. Wang, B. Schuster, C. Trautmann, R. Neumann, U. Becker, R.C. Ewing, **Nature Materials** **8** (2009) 793.

Study of the radiation effects in borosilicate glasses

Tieshan Wang, Kunjie Yang, Haibo Peng, Limin Zhang, Genfa Zhang, Liang Chen

School of Nuclear Science and Technology, Lanzhou University, Tianshuinan Road 222, Lanzhou Gansu 730000, China

In order to study the radiation effects of borosilicated glasses in high level radioactive field, various ions and electron beams were used to simulate the radiation irradiation, and nano-indentation test, micro-Raman spectroscopy, electron paramagnetic resonance and transmission microscopy etc methods, were employed to study the micro-structure evaluation versus irradiation. Different kinds of borosilicate glasses are studied in this work. Proton and He^+ , Kr^{q+} and Xe^{q+} etc. ion beams were used for simulating alpha particle, recoiled nuclei and also fission fragments, and 1.2MeV electron beam was used for simulating the beta-decay irradiation in the experiments. The irradiation dose is in the range of 10^6Gy - 10^{10}Gy . The average hardness of borosilicate glasses decreases significantly versus the ion irradiation dose and reaches to a saturation about -14% above a critical dose of $3 \times 10^7\text{Gy}$. But there is almost no change up to a dose of $2 \times 10^8\text{Gy}$ by electron irradiation, and only 4% decrease is found after $1 \times 10^9\text{Gy}$ electron irradiation. A decrease of the average Si-O-Si angle and an increase in number of three-membered SiO_4 ring are observed. The polymerization of the silicate network increases with the electronic energy deposition according to the Raman spectra. These have been correlated to the densification process of glass. The minor effects of ion irradiation on structure modifications mainly attribute to the recovery caused by thermal quenching during ion irradiation as a consequence of local heat associated with thermal spike effect. The radiation effects are also observed by EPR. It is evidently dose-dependent. The results indicate that the nuclear energy deposition is the major factor of the evolution in the plastic response of the borosilicate glass, while the electronic energy deposition affects to the silicate network and migration of the alkaline results in changes of mechanical properties.

Application of pyroelectric crystal to metal ion beam

Susumu Imashuku, Akira Imanishi, Jun Kawai

Materials Science and Engineering, Kyoto University, Sakyo, Kyoto 606-8501, Japan

When a temperature change under a vacuum condition is applied to a pyroelectric crystal, an electric field around 50 kV is produced due to uncompensated charges on the surface of the pyroelectric crystal. In the present study, applying the produced electric field, we tried to field-emit metal ions by dropping ionic liquid containing metal ion on the pyroelectric crystal. In the experiments, ionic liquid (EMI-Tf₂N, EMI = 1-Ethyl-3-methylimidazolium (C₆H₁₁N₂) Tf = CF₃SO₂) containing zinc ions was dropped on the pyroelectric crystal of LiTaO₃ and electric field was applied between the ionic liquid and silicon or silver substrate. By XPS measurement, it was confirmed that Zn(Tf₂N)₂, EMI-Tf₂N, and ZnF₂ were deposited on silicon substrate. In contrast, Zn(Tf₂N)₂, EMI-Tf₂N, and ZnS were deposited on silver substrate. The results that deposited compounds were different from substrates is considered to be related to affinities of fluorine and sulfur to silicon and silver. We can say that silicon has a high affinity for fluorine and that silver has a high affinity for sulfur. From these results, it is considered that various kinds of ions such as Zn²⁺, EMI⁺, ZnF⁺, Zn₂S²⁺, Tf₂N⁻ were emitted by applying an electric field with 50 kV between EMI-Tf₂N containing zinc ions and substrates.

Microstructures of barium titanate irradiated with 1.5 GeV ²³⁸U ions

Weilin Jiang¹, Ram Devanathan¹, Kazuhisa Sato², Manabu Ishimaru³, Tamas Varga¹, Abdenacer Benyagoub⁴

⁽¹⁾*Pacific Northwest National Laboratory, Richland WA 99352, United States*

⁽²⁾*Tohoku University, Sendai Miyagi 980-8577, Japan*

⁽³⁾*Osaka University, Ibaraki Osaka 567-0047, Japan*

⁽⁴⁾*Grand Accélérateur National d'Ions Lourds, Laboratoire CIMAP, 14070 Caen cedex 5, France*

Barium titanate (BaTiO₃) has been extensively studied for a wide range of potential applications in ferroelectric, dielectric, semiconducting, and optical devices. Although a few irradiation studies of the material with MeV ions have been reported in the literature, those using swift heavy ions (SHI) are still absent to date. Such studies are needed to understand the physical processes associated with the ion track formation and heat transport. Single-crystal BaTiO₃ exhibits different crystalline phases in different temperature ranges and is an excellent model material for study of microstructures due to phase transformation induced by thermal spikes in the transient process.

Irradiation of tetragonally structured BaTiO₃ was performed at the GANIL facility using 1.5 GeV ²³⁸U ions to ion fluences of 1.0x10⁷, 5.0x10¹⁰ and 1.4x10¹² ions/cm² at nominal room temperature. Subsequent sample characterizations have been carried out using various methods, including helium ion microscopy (HIM), x-ray diffraction (XRD), and transmission electron microscopy (TEM). From TEM, we observed an amorphous core at the ion-entry spot with a diameter of ~10 nm. The spot is surrounded by a strained lattice structure. Cross-sectional TEM examinations exhibit a similar feature. We also observed satellite-like defects around the ion track. HIM study shows that the highest-fluence sample was broken into pieces at the surface, probably due to phase-transformation induced local stress. In-situ XRD data suggest that phase transformation in a perfect BaTiO₃ crystal from tetragonal structure at room temperature to cubic structure at 403 K is reversible. In addition, we have also developed interatomic potentials for this system and have performed molecular dynamics (MD) simulations of thermal spikes for various electronic stopping power values. The simulations show similar damage structures and reveal the stages in microstructural evolution under SHI irradiation. The experimental and computational results, along with data analysis and discussion, will be presented.

Charge changing cross-section of 300 A MeV Fe²⁶⁺ ion beam in Al target

Renu Gupta, Ashavani Kumar

Department of Physics, National Institute of Technology, Kurukshetra, India

A stack was composed of CR39 and Makrofol foils of size $11.5 \times 11.5 \text{ cm}^2$ and aluminum as target for the beam exposure. The stack was then exposed to Fe²⁶⁺ ion beam with energy 300 A MeV at Brookhaven National Laboratory (BNL) NSRL, USA in 2005 at normal incidence with total ion density of $\sim 2000/\text{cm}^2$. Partial charge changing cross-section of 300 A MeV Fe²⁶⁺ ion beam was calculated in aluminum target for $\Delta Z = -1, -2, \dots, -23$ by using track etch technique. Etched cone tracks due to ion beam and their fragments were analysed by using automated optical microscope under the magnification 20X with Leica QWin Plus software after etching the detectors in 6N NaOH solution at $(70 \pm 0.1)^\circ\text{C}$. Very new technique of single side etching was used in the present work to prevent the development of the tracks from the other side surfaces of the detectors. For calculating charge changing cross-section, the diameter distributions of tracks due to beam and fragments for the detectors before and after the target were obtained and fitted by multiple Gaussians. From Gaussian fittings, the number of fragments before and after the target was calculated within 95.5% confidence levels and number of incident projectile ions and survived projectile ions were calculated within 99.7% confidence levels. Total charge changing cross-section was calculated and compared with the experimental results of others and was also fitted by Bradt-Peters theoretical geometrical cross-section. Charge of the fragments was detected with better charge resolution. To show the consistency in measurements, the response of two detectors was given by a relation between etch-rate ratio p and restricted energy loss (REL) and was found within the limits of experimental error. The response of the detectors was fitted by a first degree polynomial.

Optimizing the Composition Measurement of Ultra-Thin Metal Oxide Films Through the Combination of Recoil and Forward Scattering

Gregory J Stein, Barney L Doyle

Radiation Solid Interactions, Sandia National Labs, 1515 Eubank SE, Albuquerque NM 87185-1056, United States

Ion Beam Analysis (IBA) has routinely been used to characterize this composition of thin films because of its broad elemental sensitivity and its quantitative approach. Sandia has recently developed a new IBA technique especially well suited for the composition measurement of metal-oxide memristive materials, particularly Ta₂O_{5-x} that combines simultaneous Rutherford Forward Scattering (RFS) and Elastic Recoil Detection (ERD), called RFSEERD. This new technique utilizes high energy heavy ions from tandem-style accelerators, and a standard ERD geometry where both the heavy ions that are scattered by the sample atoms, and the atoms recoiled by the Si beam are energy analyzed using a single surface barrier detector mounted in the forward direction. Before detection, all of the scattered heavy ions and target recoils pass through a Mylar range foil.

This talk will describe a theoretical treatment of the RFSEERD ion-atom collision physics that has led to the optimal selection, for a 6MV tandem accelerator, of the incident beam ion (Si or Cl), its energy ($\sim 46 \text{ MeV}$), range foil thickness ($\sim 13 \text{ microns}$) and scatter/recoil angle (30 degrees). This treatment has also indicated that the reproducibility of the scattering angle dominates the propagation of error in the measurement of stoichiometry, and suggests the need for control of this angle to ~ 0.1 degree or standards when the RFSEERD technique is used. We will also use this ion-atom collision theory to suggest optimum beam and detector geometries for a wide range of other particle accelerators typically used in IBA labs.

* Sandia National Laboratories is a multi-program laboratory managed and operated by Sandia Corporation, a wholly owned subsidiary of Lockheed Martin Corporation, for the U.S. Department of Energy's National Nuclear Security Administration under contract DE-AC04-94AL85000.

BINP projects for cancer therapy and other medical applications

Eugene Levichev

Accelerator, Budker Institute of Nuclear Physics, Lavrentiev 11, Novosibirsk 630090, Russia

Budker Institute of Nuclear Physics (BINP) is a well-known scientific center located in Novosibirsk city, Russia. The BINP fields of research include high energy physics, accelerator science and technology, synchrotron radiation generation and utilization, plasma and thermonuclear studies. Besides fundamental science activity, BINP is developing equipment for application in different areas of medicine, industry, material science, etc. In this talk I discuss BINP projects and achievements for medical applications including carbon ion synchrotron with electron cooling, X-ray scanners with extremely low radiation dose, small electron accelerators for sterilization, BNCT electrostatic tandem accelerator, etc.

Development of the new IBA S2C2

Patrick Verbruggen¹, Michel Abs¹, Sebastien Henrotin¹, Yves Jongen¹, Wiel Kleeven¹, Sebastien Quets¹, Matthieu Conjat², Jerome Mandrillon², Pierre Mandrillon²

⁽¹⁾*Ion Beam Applications s.a., Chemin du Cyclotron, 3, Louvain-la-Neuve 1348, Belgium*

⁽²⁾*AIMA Developpement, Nice 06200, France*

In 2009, IBA took the decision to start the development of a compact superconducting synchrocyclotron as an alternative, compact source of protons for protontherapy. This new accelerator will be integrated to future small footprint proton therapy centers called Proteus One ®. This ambitious project, driven by a small dedicated team and run on a tight schedule and budget, is challenging in numerous aspects. For instance, several Beam Physics codes needed to be developed or modified to handle the variable frequency during acceleration. In addition, due to the compactness of the machine, even the slightest modification on one of its subsystem may have an impact on others. Besides that, the S2C2 is a unique opportunity to start from a blank page, bring new technologies into the company, create new partnerships and incorporate novel ideas in the system architecture. This communication covers the evolution of the project from initial requirements and sketches to the latest pictures of assembly and testing in our factory, describing all major sub-systems.

Application of Novel Acceleration Concepts for Medical Applications

Chandrashekhar Joshi

Electrical Engineering, UCLA, 405 Hilgard Ave, Los Angeles CA 90095, United States

New concepts for particle acceleration have made a great strides in recent years. One can now envision extremely compact few hundred MeV electron and ion accelerators that are powered by laser pulses in the near future. Consequently researchers are beginning to develop new concepts for very high energy electron therapy and hadron therapy using laser-driven accelerators. I will discuss the principles behind these new acceleration schemes, show the state of the art results on electron and ion acceleration and present some ideas on how these ideas might be applied in the medical field.

New techniques and technology for cancer treatment with a proton beam

Vladimir Balakin

ZAO "PROTOM", Akademicheskoy proezd 2, 110, Protvino 142280, Russia

It is known for several decades that the use of proton beams has significant advantages over gamma-radiation from electron accelerators. However, currently there are a few thousand electron accelerators in use, and only two or three tens of proton accelerators. The aim of our many-years-long work is an attempt to correct this inconsistency - to develop and promote the proton beams as the main tool instead of electron beams. To make this happen, the cost of the techniques and technology of radiation therapy with a proton beam has to be reduced many of times. New technology of treatment: fast immobilisation system, multi-field irradiation and optimised IMPT allow with one treatment room to have higher efficiency and productivity than any existing proton facility. Maximal energy of proton beam 330 MeV gives the possibility to have proton tomography in the future. We hope that in not so far future most of the treatment will be on the proton facilities instead of electron accelerators.

Compact Superconducting Cyclotrons for Medical Applications

Timothy A. Antaya

Ionetix Corporation, Hampton NH 03842, United States

Proton Beam Radiotherapy (PBRT) is now beginning to make transition from large regional facilities to more affordable and more widely distributed local one room and two room facilities. This is both in the US and Europe and is driven by patients and medical groups. Superconducting synchrocyclotrons, owing to their ability to operate at high magnetic fields and the resulting exceptional compactness are the accelerator of choice for these next generation facilities. In addition, PBRT treatment gantries need to be more compact and more open, and here again superconducting gantries with high momentum acceptance appear favorable for scanned beams and are now under development for operation by 2014. The recent supply instability in SPEC isotopes for cardiac imaging, and the need for advanced imaging agents for Alzheimer's disease diagnosis, is driving imaging to short lived PET isotopes, and a recently commissioning high field cyclotron appears ready to make possible point of use on demand availability of C11, N13 and O15 tracers. A survey of recent advances in superconducting technology in these areas will be made in this talk, with emphasis on present status, current limitations and future prospects.

Startup of the Kling Center for Proton Therapy

Charles Bloch, Patrick Hill, Kuan Ling Chen, Akito Saito, Eric E Klein

Radiation Oncology, Washington University School of Medicine, 4921 Parkview Place, Campus Box 8224, Saint Louis MO 63110, United States

In November of 2011 Mevion (formerly Still River Systems) delivered the S250 Proton Therapy system accelerator to the Kling Center for Proton Therapy at the Siteman Cancer Center in Saint Louis. The Mevion system is unique, with an in-room gantry-mounted superconducting synchro-cyclotron. This is the first true single-room proton therapy system and has greatly reduced size as well as cost. A month after its arrival, the installation was complete and the superconducting magnet was ramped up to full current (~2000 amperes). In March of 2012, full energy beam was extracted and radiation surveys were performed to verify the shielding. Once that was shown to be sufficient, Mevion began fine-tuning the system to provide a highly isocentric beam from the 50 ton system. In June the field-shaping system (energy degraders, contoured scatterers and range modulators) will be installed and clinical beam measurements will commence. Monte Carlo simulations (MCNPX) have been performed for the system and validated with beam measurements done at the factory. Those simulations have been used for a preliminary commissioning of our treatment planning system. Additionally predictions of the neutron background have been made and validated with factory measurements. Final commissioning of the treatment planning system and verification of the neutron background will be accomplished with measurements made later in 2012. Based on current progress, patient treatments are scheduled to begin later this year. Beam and radiation background data will be presented.

Associated Particle Neutron Imaging for Elemental Analysis in Medical Diagnostics

Haoyu Wang¹, David Koltick¹, Huiling Nie²

⁽¹⁾*Physics Department, Purdue University, 525 Northwestern Avenue, West Lafayette Indiana 47907, United States*

⁽²⁾*School of Health Sciences, Purdue University, 550 Stadium Mall Drive, West Lafayette Indiana 47907, United States*

Associated particle neutron elemental imaging (API) for in vivo and invitro diagnostic analysis is a candidate to measure elemental disease signatures. Results are presented of phantoms that suggest API can produce elemental images with spatial features as small as a few millimeters even when limiting patient radiation exposure to 5-rem and with elemental sensitivity relevant to medical diagnostics. While the human body is composed of complex mechanical, chemical and organizational interactions involving molecules with up to 100s of billions of atoms, it is surprising localized elemental content presents diagnostic information on disease presence. Anomalous elemental concentrations have been observed to depend on cancer location for breast, liver, colon, kidney, lung and prostate. In vivo observation of these elemental anomalies would provide a diagnostic tool for disease presence. In vitro observation may provide rapid margin analysis during surgery to reduce the need for surgical reintervention. Investigation into the pathways underlying these anomalous elemental concentrations may provide new and possible novel therapeutic targets. Measured elemental disease signatures range from 1-ppm to over 1000-ppm.

WED-MA04-1

#139 - Invited Talk - Wednesday 1:00 PM - Pecos I

The iRCMS rapid cycling synchrotron

Joseph Lidestri³, Dejan Trbojevic², Derek Lowenstein², Richard Johnson³, Stephen Peggs¹

⁽¹⁾*Superconducting Magnet Division, Brookhaven National Laboratory, Building 902, Upton NY 11973, United States*

⁽²⁾*Collider-Accelerator Department, Brookhaven National Laboratory, Building 902, Upton NY 11973, United States*

⁽³⁾*Best Medical International, 7643 Fullerton Road, Springfield VA 22153, United States*

I will describe the status and plans for the iRCMS -- the ion Rapid Cycling Medical Synchrotron - being designed and developed under a Cooperative Research and Development Agreement (CRADA) between Best Medical International, and Brookhaven National Accelerator.

WED-MA04-2

#157 - Invited Talk - Wednesday 1:00 PM - Pecos I

Dielectric Wall Accelerator for Proton Therapy

Yu-Jiuan Chen

Lawrence Livermore National Laboratory, 7000 East Ave., L-410, Livermore CA 94550, United States

We are developing a compact dielectric wall accelerator (DWA) for the intensity modulated proton therapy with a goal of fitting the DWA in a single room. We have developed a transport scheme to transport the proton bunch in the DWA and to focus the charge bunch on the patient without using any external focusing lenses. The transport scheme allows us change the proton beam spot size on the patient easily and rapidly. Slanting the conductors of high-gradient insulator stack with an angle provides a dipole field and an acceleration field. We are using this fact to develop an intra-DWA beam scanning method. These beam transport developments will be presented.

The Compact Particle Accelerator Corporation has developed an architecture to produce pulsed proton bunches suitable for cancer treatment. Subsystems include a RFQ injection system with a pulsed kicker to select the desired proton bunch and a linear DWA with stacked Blumleins to produce the required voltage. The Blumleins are switched with solid state laser driven optical switches, which are an integral part of the Blumlein assemblies. A master timing system to synchronize the RFQ with the DWA has been successfully developed. Other subsystems include a laser, a fiber optic distribution system, an electrical charging system and beam diagnostics. An engineering prototype has been constructed and it has been fully characterized. Results obtained from the engineering prototype support the development of an extremely compact 150 MeV system capable of modulating energy, beam current and spot size on a shot to shot basis within the next two years. The engineering prototype and experimental results will be presented.

*This work performed under the auspices of the U. S. Department of Energy by Lawrence Livermore National Laboratory under Contract DE-AC52-07NA2A27344.

Cyclotron-Based Neutron Source for Boron Neutron Capture Therapy

Toshinori Mitsumoto¹, Hiroshi Tsutsui¹, Satoru Yajima¹, Hiroki Tanaka², Yoshinori Sakurai², Akira Maruhashi²

⁽¹⁾*Quantum Equipment Division, Sumitomo Heavy Industries, Ltd., 2-1-1 Yato-Cho, NishiTokyo Tokyo 188-8585, Japan*

⁽²⁾*Research Reactor Institute, Kyoto University, 2, Asashiro-Nishi, Kumatori-cho, Sennan-gun Osaka 590-0494, Japan*

Kyoto University Research Reactor Institute (KURRI) and Sumitomo Heavy Industries, Ltd. have developed a cyclotron-based neutron source for Boron Neutron Capture Therapy (BNCT). It was installed at KURRI campus in Osaka prefecture. The neutron source consists of a proton cyclotron named HM-30, a beam transport system and an irradiation & treatment system. In the cyclotron, H⁺ ions are accelerated and extracted as 30 MeV proton beam of 1 mA. The proton beam is transported to the neutron production target made by beryllium plate. Emitted neutrons are moderated by lead, iron, aluminum and calcium fluoride. Aperture diameter of neutron collimator is in the range from 100 mm to 250 mm. The peak neutron flux in the water phantom is 1.8×10^9 neutrons/cm²/sec at 20mm from the surface at 1 mA proton beam. The neutron source has been stably operated for 3 years with 30 kW proton beam. Various pre-clinical tests including animal tests have been done by using the cyclotron-based neutron source with ¹⁰B-p-Boronophenylalanine. Clinical trials of malignant brain tumors will be started in this year.

A new type of accelerator for charged particle cancer therapy

Thomas Robert Edgecock

ASTeC, STFC Rutherford Appleton Laboratory, Chilton, Didcot Oxon OX11 0QX, United Kingdom

So-called non-scaling Fixed Field Alternating Gradient accelerators (ns-FFAGs) show great potential for the acceleration of protons and light ions for the treatment of certain cancers. They have unique features as they combine techniques from the existing types of accelerators, cyclotrons and synchrotrons, and hence look to have advantages over both for this application. However, these unique features meant that it was necessary to build one of these accelerators to show that it works and to undertake a detailed conceptual design of a medical machine. Both of these have now been done. This presentation will describe the concepts of this type of accelerator, show results from the proof-of-principle machine (EMMA) and describe the medical machine (PAMELA).

Compact CW FFAGs for combined Proton and Carbon Therapy and Proton Computed Tomography

Carol Joanne Johnstone¹, Hywel Owen², George Coutrakon³

⁽¹⁾*Particle Accelerator Corporation, 809 Pottawatomie Trail, Batavia IL 60510, United States*

⁽²⁾*University of Manchester, Manchester, United Kingdom*

⁽³⁾*Northern Illinois University, 1120 East Diehl Rd, Naperville IL 60563, United States*

The advantage of the cyclotron in proton therapy is its continuous (CW) beam output which reduces complexity and response time in the dosimetry requirements and beam controls along with a clear advantage in pencil beam scanning. Present compact isochronous cyclotrons for proton therapy reach only 250 MeV as required for patient treatment, but this energy is low for full proton Computed Tomography (pCT) capability. PCT specifications require 300-330 MeV in order for protons to transit the human body. Recent innovations in non-scaling FFAG design have achieved isochronous (CW) performance in compact machine designs at these higher energies. Further, lower energy beams can be efficiently extracted for proton therapy thus avoiding the beam loss associated with degrading the higher energy 330-MeV beam down to treatment energies. These advances in CW accelerator technology have been extended successfully to include carbon therapy machine designs and a combined proton/carbon system has also been successfully integrated. These new advances in CW accelerators for proton and carbon therapy are presented here.

Improvement of Extraction Efficiency from a Compact Synchrotron for Proton Beam Therapy by Applying Particle Tracking Analysis

Futaro Ebina, Masumi Umezawa, Kazuo Hiramoto

Hitachi Research Laboratory, Hitachi, Ltd, 2-1, Omika-cho 7-chome, Hitachi-shi Ibaraki-ken 319-1221, Japan

Various types of synchrotrons are used for particle beam therapy. In particle beam therapy, especially in proton beam therapy, downsizing of the accelerator system is major concern. A compact synchrotron dedicated for proton beam therapy is presented. The synchrotron is horizontally weak focusing and consists of 4 H-type zero-gradient dipole magnets and 4 quadrupole magnets. The circumference of the ring is a little shorter than 18 m, and the energies are up to 230MeV.

Beam extraction from the synchrotron is performed by RF-driven slow extraction technology. Two sextupole magnets set in adjacent straight sections form a horizontal separatrix which is fixed during the beam extraction. Horizontal RF voltage excites betatron oscillation of the circulating beam, and protons exceeding the separatrix are extracted by an electrostatic deflector and a horizontal septum dipole magnet. To achieve adequately high extraction efficiency, the relationship between the extraction efficiency and the horizontal chromaticity of the ring was analyzed by particle tracking simulation. The horizontal chromaticity with maximum extraction efficiency is half of the theoretical value because of the distortion of the horizontal separatrix for the extraction. With this chromaticity, the spiral-step of the extracted particle is independent of the momentum deviation of the particle, and the separatrix across the electrostatic septum electrodes is superpositioned.

Automated Beam Tuning Function to Correct Beam Axis Shift with High Accuracy in Proton Beam Therapy System

Masumi Umezawa¹, Satoshi Totake², Koji Matsuda², Chihiro Nakashima², Kiminori Iga², Kazuo Hiramoto¹, Kazumichi Suzuki³, Michael T Gillin³

⁽¹⁾*Hitachi Research Laboratory, Hitachi, Ltd., 7-2-1 Omika-cho, Hitachi Ibaraki 319-1221, Japan*

⁽²⁾*Hitachi Works, Hitachi, Ltd., 3-1-1 Saiwai-cho, Hitachi Ibaraki 317-8511, Japan*

⁽³⁾*Department of Radiation Physics, The University of Texas, MD Anderson Cancer Center, 1840 Old Spanish Trail, Houston Texas 77054-2002, United States*

Purpose: In order to maintain the desired dose distribution in clinical irradiation field of proton beam therapy system, automated beam tuning(ABT) function, which enables to maintain the high accuracies of beam position and gradient at the irradiation nozzle, had been developed and applied to the passive scattering nozzles employed in Proton Therapy Center Houston(PTC-H).

Method: The passive irradiation nozzles employed in PTC-H utilizes dual-ring double scattering method to expand the irradiation fields laterally. In this expansion method, the required beam axis accuracy is quite high. On the other hand, in hospital-based proton center such as PTC-H, there may be no time to tune all of the beam parameters during treatment. Therefore, ABT function had been developed and applied to correct the beam axis shift at the irradiation nozzle and the entrance of the rotating gantry. Beam axis correction algorithm, which had been developed originally by Hitachi, calculates the exciting current of two sets of steering magnets installed in beam line based on the measurement results of two beam position sensitive monitors.

Results: Before applying this ABT function to daily treatment session, we had conducted verification test. The results showed the beam axis shift can be corrected as expected. In daily clinical sessions, beam checking procedure is performed prior each patient treatment field. In the procedure, small portion of the beam is irradiated to the beam monitors and checked its properties while beam block in the nozzle stop the entire proton beam. In the case that the beam axis is outside of tolerance, ABT function runs automatically and corrects the beam shift. From the trend of recorded values of steering magnet, it was clear that the beam properties from synchrotron have been stable and reproducible.

Conclusion: The ABT function had been developed and successfully applied to daily treatment in PTC-H.

Production of High Specific Activity ^{186}Re for Cancer Therapy Using a WO_3 Target in a Proton Beam

Michael E Fassbender¹, Beau D Ballard¹, Jonathan W Engle¹, F Meiring Nortier¹, Kevin D John¹, Eva R Birnbaum¹,
Cathy S Cutler², Silvia S Jurisson², Alan R Ketring², D Scott Wilbur³

⁽¹⁾Chemistry Division, Los Alamos National Laboratory, PO Box 1663, Los Alamos NM 87544, United States

⁽²⁾University of Missouri-Columbia, Columbia MO 65211, United States

⁽³⁾University of Washington, Seattle WA 98105, United States

Rhenium-186 is a β^- emitter with a half-life of 90.64 h and a β^- end-point energy of 1.07 MeV. The isotope is suitable to treat cancers with small dimensions (mm range). Moreover, its γ -emission at 137.15 keV is in the energy range suitable for both γ -camera and SPET imaging. Current production methods rely on the neutron capture induced reaction $^{185}\text{Re}(n,\gamma)$ in a reactor and are associated with low specific activities ($0.6 \text{ kCi}\cdot\text{mmol}^{-1}$), thereby limiting the application of the isotope to palliative treatments. Production via charged particle irradiation of enriched ^{186}W results in a ^{186}Re product with a much higher specific activity; allowing its use in therapeutic nuclear medicine. A test target of pressed, sintered $^{\text{nat}}\text{WO}_3$ (25.2 g; 2.54 mm thick) was proton irradiated at the Los Alamos Isotope Production Facility (LANL-IPF) to evaluate radionuclide product yields, impurities, irradiation parameters and wet chemical Re recovery for a bulk production. We demonstrated that ^{186}Re can be isolated in 97% yield from irradiated $^{\text{nat}}\text{WO}_3$ targets within 12 h of end of bombardment (EOB) via an alkaline dissolution followed by anion exchange. Tungsten (VI) oxide can be easily recycled for recurrent irradiations. A ^{186}Re batch yield of $42.7 \pm 2.2 \text{ mCi}/\text{mAh}$ ($439 \pm 23 \text{ MBq}/\text{C}$) (with respect to ^{186}W content) was obtained after 24 h in an 18.5 mA proton beam. The target entrance energy was determined to be 15.6 MeV. The specific activity of ^{186}Re at EOB was measured to be 1.9 kCi (70.3 TBq) $\times\text{mmol}^{-1}$. Based upon our studies of $^{\text{nat}}\text{WO}_3$, we anticipate the utilization of enriched $^{186}\text{WO}_3$; and a proton beam of 250 mA for 24h will provide batch volumes of 256 mCi (9.5 GBq) of ^{186}Re at EOB with a specific activity approaching the theoretical value of $35 \text{ kCi}\times\text{mmol}^{-1}$ ($1295 \text{ TBq}\times\text{mmol}^{-1}$).

Development of the Mini-SHINE/MIPS experiment at the Low Energy Accelerator Facility, Argonne National Laboratory

Sergey Chemerisov, Charles Jonah, Amanda Youker, Andrew Hebden, Nicholas Smith, Peter Tkac, James Bailey, Vakhtang Makarashvili, Bradley Micklich, Elizabeth Krahn, John Krebs, Delbert Bowers, Allen Bakel, George Vandegrift

Chemical Science and Engineering, Argonne National Laboratory, 9700 S Cass Ave, Lemont IL 60439, United States

Argonne National Laboratory (ANL) is conducting experiments to support Babcock and Wilcox Technical Services Group (B&W) and Morgridge Institute for Research (MIR) as part of the National Nuclear Security Administration (NNSA) Global Threat Reduction Initiative's (GTRI) program to accelerate the establishment of a reliable domestic supply of Mo-99 produced without the use of high enriched uranium (HEU).

B&W is developing the Medical Isotope Production System (MIPS); in this system, Mo-99 is produced in an LEU-fueled aqueous homogenous reactor (AHR) by the fission of U-235. MIR is currently developing the Subcritical Hybrid Intense Neutron Emitter (SHINE), which creates Mo-99 by neutron-induced fission of LEU in an aqueous solution contained in a sub-critical accelerator driven reaction vessel. Both uranyl nitrate and sulfate solutions are being considered for use in these systems.

The mini-SHINE/MIPS experiments planned at Argonne's Low Energy Accelerator Facility (LEAF) will provide important design data for both systems. We will measure the production rate and composition of radiolytic gases generated during operation of the system under varying conditions of power density, solution temperature, and start-up conditions; monitor changes of solution composition (peroxide concentration, iodine, and nitrogen speciation, pH, conductivity, solids formation), vs. time, temperature, and fission power; and demonstrate Mo-recovery from the irradiated solution at the end of irradiation.

This presentation will review the design of the main components of the mini-SHINE/MIPS setup, results of the Monte Carlo computer simulations, and the current status of these activities.

Work supported by the U.S. Department of Energy, National Nuclear Security Administration's (NNSA's) Office of Defense Nuclear Nonproliferation, under Contract DE-AC02-06CH11357.

Design and Experimental Activities Supporting Commercial U.S. Electron Accelerator Production of Mo-99

Gregory E. Dale¹, Segey D. Chemerisov², George F. Vandegrift², Keith A. Woloshun¹, Charles T. Kelsey IV¹, Peter Tkac², Charles D. Jonah², Eric R. Olivas¹, Ken P. Hurtle¹, Frank P. Romero¹, Dale A. Dalmás¹, James T. Harvey, Vakhtang Makarashvili

⁽¹⁾Los Alamos National Laboratory, PO Box 1663, Mail Stop H851, Los Alamos NM 87544, United States

⁽²⁾Argonne National Laboratory, 9700 S. Cass Avenue, Argonne IL 60439, United States

Los Alamos National Laboratory (LANL) and Argonne National Laboratory (ANL) are working together with NorthStar Medical Technologies, LLC as part of the National Nuclear Security Administration (NNSA) Global Threat Reduction Initiative's (GTRI) program to accelerate the establishment of a reliable domestic supply of Mo-99 for nuclear medicine, produced without the use of highly enriched uranium (HEU). The metastable daughter product of Mo-99, Tc-99m, is the most commonly used radioisotope in nuclear medicine. This radioisotope is used in approximately two-thirds of all nuclear medicine imaging procedures, amounting to approximately 50,000 diagnostic nuclear medicine procedures performed every day in the United States (US). Until recently, the entire US supply of Mo-99 for nuclear medicine has been produced in aging foreign reactors using HEU targets. Recent maintenance and repair shutdowns of these reactors have significantly disrupted the supply of Mo-99 in the US and much of the rest of the world.

Experiments are being performed by LANL and ANL to demonstrate and validate the technology for producing Mo-99 using high-power electron accelerators utilizing the Mo-100(γ,n)Mo-99 reaction in an enriched Mo-100 target. The photons for this reaction are generated by bremsstrahlung as the electron beam from the accelerator collides with the target. Subjects currently under investigation include target cooling, maximizing the production rate, quantification of side-reaction products, and processing targets after irradiation. To date, five scaled target irradiations have been performed using the electron accelerator facility at ANL. Following an upgrade of the accelerator, a scaled production run is scheduled over the summer to produce greater than 30 Ci of Mo-99 in a 24-hour irradiation using an enriched Mo-100 target. This presentation will review the current status of these activities.

Development of the Compact Proton Beam Therapy System dedicated to Spot Scanning with Real Time Tumor Tracking Technology

Masumi Umezawa¹, Rintaro Fujimoto¹, Tooru Umekawa¹, Yuusuke Fujii¹, Taisuke Takayanagi¹, Futaro Ebina¹, Takamichi Aoki¹, Yoshihiko Nagamine², Koji Matsuda², Kazuo Hiramoto¹, Taeko Matsuura³, Naoki Miyamoto³, Hideaki Nihongi³, Kikuo Umegaki⁴, Hiroki Shirato⁴

⁽¹⁾Hitachi Research Laboratory, Hitachi, Ltd., 7-2-1 Omika-cho, Hitachi Ibaraki 319-1221, Japan

⁽²⁾Hitachi Work, Hitachi, Ltd., 3-1-1 Saiwai-cho, Hitachi Ibaraki 317-8511, Japan

⁽³⁾Department of Medical Physics, Hokkaido University Graduate School of Medicine, Kita 15 Nishi 7, Sapporo Hokkaido 060-0815, Japan

⁽⁴⁾Department of Radiation Medicine, Hokkaido University Graduate School of Medicine, Kita 15 Nishi 7, Sapporo Hokkaido 060-0815, Japan

Purpose: The spot scanning technique in proton therapy has advantage such as superior controllability for the irradiation dose distribution. In order to maximize its advantages, Hokkaido University and Hitachi Ltd. has started the joint development of the Real-time Tumor-tracking Proton Therapy (RTPT) system by integrating real-time tumor-tracking technology and proton therapy system dedicated to discrete spot scanning techniques.

Method: In order to realize compact and cost-reduced proton therapy system, Hitachi has concentrated to develop the synchrotron-based accelerator system by taking advantages of spot scanning technique, for example, the quantity of proton beam and maximum energy can be reduced less than that for the passive scattering technique. In order to control the dose distribution irradiated to the moving tumors with spot scanning, RTPT system have the ability to gate the proton beams from the synchrotron only when the actual positions of fiducial markers are within the planned position. In this gated irradiation, we have focused on the issues to maximize irradiation efficiency and minimize motion dose errors.

Results: This integrated system consists of the newly-designed synchrotron accelerator, beam transport system, the one compact rotating gantry treatment room with robotic couch, and one experimental room for the future research. The maximum range of 30g/cm² and irradiation field size of 30×40cm. The synchrotron has its circumference of 18m, which is 20% less than that of the Hitachi's conventional synchrotron design. From the viewpoint to improve irradiation efficiency, the new control function which enables multiple gated irradiations per synchrotron operation cycle has been applied and confirmed its efficacy by the irradiation time estimation.

Conclusion: The RTPT system has been designed under the collaborative study of Hokkaido University and Hitachi, Ltd. This newly-designed system will be able to maximize the advantages of spot scanning technique from the view of both clinical and economical point.

WED-NBAE06-1

#246 - Invited Talk - Wednesday 1:00 PM - Brazos II

Review of FELs and Synchrotrons as Accelerator Applications in Industry and Research

William A. Barletta

Dept of Physics & US Particle Accelerator School, Massachusetts Institute of Technology, 77 Massachusetts Avenue, Cambridge MA 02139, United States

Synchrotron radiation sources have had a profound effect on both science and technology from their beginnings decades ago as parasitic operations on accelerators for high energy physics. Now the general area of photon science has opened up new experimental techniques which have become the mainstay tools of materials science, surface, protein crystallography, and nanotechnology. With the promise of ultra-bright beams from the latest generation of storage rings and free electron lasers with full coherence, the tools of photon science promise to open a new area of mesoscale science and technology as well as prove to be a disruptive wildcard in the search for sustainable energy technologies. This review will survey a range of applications and explore in greater depth the potential applications to EUV lithography and to technologies for solar energy.

WED-NBAE06-2

#243 - Invited Talk - Wednesday 1:00 PM - Brazos II

Time-Resolved X-Ray Photoelectron Spectroscopy Techniques for Real-Time Studies Of Intramolecular And Interfacial Charge Transfer Dynamics

Oliver Gessner¹, Andrey Shavorskiy¹⁰, Amy Cordones⁴, Josh Vura-Weis⁴, Katrin Siefertmann¹, Daniel Slaughter¹, Felix Sturm¹, Fabian Weise¹, Matthew Strader¹, Hana Cho¹, Ming-Fu Lin^{1,4}, Camila Bacellar^{1,4}, Champak Khurmi¹, Marcus P. Hertlein¹⁰, Travis Wright¹, Jinghua Guo¹⁰, Hendrik Bluhm², Tolek Tylliszczak¹⁰, Giacomo Coslovich³, Joseph Robinson^{3,6}, Robert Kaindl³, Robert W. Schoenlein¹, Ali Belkacem¹, Daniel M. Neumark^{1,4}, Stephen R. Leone^{1,4,5}, Dennis Nordlund⁶, Hirohito Ogasawara⁶, Anders Nilsson⁶, Oleg Krupin⁶, William F. Schlotter⁶, Joshua J. Turner⁶, Philip A. Heimann⁶, Marc Messerschmidt⁶, Michael P. Minitti⁶, Martin Beye⁷, Sheraz Gul⁸, Jin Zhang⁸, Nils Huse⁹

⁽¹⁾*Ultrafast X-ray Science Laboratory, Chemical Sciences Division, Lawrence Berkeley National Laboratory, 1 Cyclotron Road, Berkeley CA 94720, United States*

⁽²⁾*Chemical Sciences Division, Lawrence Berkeley National Laboratory, 1 Cyclotron Road, Berkeley CA 94720, United States*

⁽³⁾*Materials Sciences Division, Lawrence Berkeley National Laboratory, 1 Cyclotron Road, Berkeley CA 94720, United States*

⁽⁴⁾*Department of Chemistry, University of California Berkeley, Berkeley CA 94720, United States*

⁽⁵⁾*Department of Physics, University of California Berkeley, Berkeley CA 94720, United States*

⁽⁶⁾*SLAC National Accelerator Laboratory, 2575 Sand Hill Road, Menlo Park CA 94025, United States*

⁽⁷⁾*Helmholtz-Zentrum Berlin fuer Materialien und Energie GmbH, Berlin 12489, Germany*

⁽⁸⁾*Department of Chemistry, University of California Santa Cruz, 1156 High Street, Santa Cruz CA 95064, United States*

⁽⁹⁾*Max Planck Research Department for Structural Dynamics at the University of Hamburg, Center for Free Electron Laser Science (CFEL), Notkestrasse 85, Hamburg 22607, Germany*

⁽¹⁰⁾*Advanced Light Source, Lawrence Berkeley National Laboratory, 1 Cyclotron Road, Berkeley CA 94720, United States*

X-ray based spectroscopy techniques are particularly well suited to gain access to local oxidation states and electronic dynamics in complex systems with atomic pinpoint accuracy. Traditionally, these techniques are applied in a quasi-static fashion that usually highlights the steady-state properties of a system rather than the often fast dynamics that define the system function on a molecular level. Novel x-ray spectroscopy techniques enabled by free electron lasers (FELs) and synchrotron based pump-probe schemes provide the opportunity to monitor intramolecular and interfacial charge transfer processes in real-time and with element and chemical specificity. Two complementary time-domain x-ray photoelectron spectroscopy techniques are presented that have been applied at the Advanced Light Source (ALS) and the Linac Coherent Light Source (LCLS) to study charge transfer processes in dye-sensitized nanostructured semiconductor films, which are at the heart of emerging light-harvesting technologies.

Materials Processing R&D with a Free Electron Laser

Michael J. Kelley¹, Richard F. Haglund, Jr.²

⁽¹⁾*Free Electron Laser Division, Thomas Jefferson National Accelerator Facility, 12000 Jefferson Avenue, Newport News VA 23606, United States*

⁽²⁾*Dept. of Physics and Astronomy, Vanderbilt University, 6301 Stevenson Center Lane, Nashville TN 37235-1807, United States*

A unique light source to explore and develop laser-based processes may be based on a free electron laser driven by an energy-recovering linac. It can address much of the vast "white space" between the output wavelengths of conventional fixed-frequency lasers. The greatest success of conventional lasers is in delivering great energy intensity for ever-shorter pulse duration with increasing average power. They serve as sources of spatio-temporally dense electronic excitation, which can be converted to heat, especially in metals. In contrast, the inherent tunability of the FEL provides opportunity for channeling energy into specific vibrational pathways in a material to achieve desired effects. Organic materials offer a significant example, attracting as they do growing attention for next-generation photonics and electronics, with some applications already commercialized. Present fabrication techniques based on solvents or evaporation set limits on materials selection. Tuning the FEL to an IR absorption band, on the other hand, offers a path to molecule-selective energy deposition, enabling pulsed laser deposition, processing, and analysis of otherwise intractable materials. The UV FEL now coming into operation at JLab will offer further opportunities, as it will be able to drive electronic transition directly as well as the vibrational transitions accessible with the IR FEL.

Authored by Jefferson Science Associates LLC under U.S.DOE Contract No. DE-AC05-06OR23177

X-PEEM reveals novel biomineral properties at the nano-scale

Rebecca Ann Metzler

Physics and Astronomy, Colgate University, 13 Oak Dr., Hamilton New York 13346, United States

The ability to collect both spectroscopic and micrographic data simultaneously through the use of the synchrotron based techniques x-ray absorption near-edge structure (XANES) spectroscopy and x-ray photoemission electron microscopy (X-PEEM) enables an unprecedented view of biomaterials in general and biominerals in particular. Biominerals are complex composite materials consisting of both mineral and organic components that are arranged in unique and extraordinary structures. Here we demonstrate the capabilities of X-PEEM and XANES by examining two different biomineral systems, sea urchin spicules and red abalone nacre, and revealing that XANES spectroscopy at the calcium L-edge is sensitive to calcium carbonate polymorph and at the carbon K-edge is able to detect orientation of individual calcium carbonate crystals. Through the use of X-PEEM and XANES spectroscopy we are able to obtain great insight into the systems being studied.

The Francium Facility at TRIUMF

S. Aubin¹, J. A. Behr², R. A. Collister³, E. Gomez⁹, G. Gwinner³, V. V. Flambaum⁴, D. G. Melconian⁸, L. A. Orozco⁷,
M. R. Pearson², G. D. Sprouse⁵, M. Tandecki^{2,3}, J. Zhang⁷, Y. Zhao⁶

⁽¹⁾Dept. Physics, College of William and Mary, Williamsburg VA 23185, United States

⁽²⁾TRIUMF, 4004 Wesbrook Mall, Vancouver BC V6T 2A3, Canada

⁽³⁾Dept. of Physics and Astronomy, University of Manitoba, Winnipeg MB R3T 2N2, Canada

⁽⁴⁾School of Physics, University of New South Wales, Sydney 2052, Australia

⁽⁵⁾Department of Physics and Astronomy, Stony Brook University, Stony Brook NY 11794, United States

⁽⁶⁾Laser Spectroscopy Laboratory, Shanxi University, Taijuan Shanxi, China

⁽⁷⁾Joint Quantum Institute, Dept. of Physics and NIST, University of Maryland, College Park MD 20742, United States

⁽⁸⁾Physics Department, Texas A&M University, College Station TX 77843, United States

⁽⁹⁾Instituto de Fisica, Universidad Autonoma de San Luis Potosi, San Luis Potosi SLP 78290, Mexico

The Francium Facility at TRIUMF is a dedicated instrument for trapping Fr atoms on-line in the ISAC hall. TRIUMF produces Fr by bombarding targets of uranium carbide with protons. Yields of hundreds of millions per second of the longer-lived isotopes (20 minutes) enter the facility, which includes a Faraday cage to isolate from RF and microwave interferences. It is currently under construction but we expect commissioning in the late summer of 2012. The facility should prepare samples of neutral Fr for atomic spectroscopy studies of the weak nuclear interaction. The approximately 15 KeV Fr ions will land on an Yt foil for neutralization and then proceed to be captured in a magneto optical trap where their temperature should be a few tens of microkelvins. These cold atoms will be moved into a science chamber where the environment should facilitate precision measurements of the anapole moment of a series of Fr isotopes. The results should provide information about the neutral weak currents inside the nucleus at very low energies. Work supported by NSERC and NRC from Canada, NSF and DOE from the USA.

Nuclear Structure Studies with Radioactive Ion Beams in the Mass A = 80 Region

E. Padilla-Rodal¹, R. F. Garcia-Ruiz¹, A. Galindo-Uribarri², J. M. Allmond³, J. C. Batchelder⁴, J. R. Beene², C. Bingham⁵,
K. B. Lagergren³, P. E. Mueller², D. C. Radford², D. W. Stracener², R. L. Varner², C. -H. Yu²

⁽¹⁾Instituto de Ciencias Nucleares, UNAM, Circuito Exterior de C.U., S/N, Mexico City Mexico City 04510, Mexico

⁽²⁾Physics Division, Oak Ridge National Laboratory, 1 Bethel Valley Road, Oak Ridge TN 37831, United States

⁽³⁾Joint Institute for Heavy Ion Research, Oak Ridge National Laboratory, 1 Bethel Valley Road, Oak Ridge TN 37831, United States

⁽⁴⁾Oak Ridge Associated Universities, Oak Ridge National Laboratory, 1 Bethel Valley Road, Oak Ridge TN 37831, United States

⁽⁵⁾Department of Physics and Astronomy, University of Tennessee, 401 Nielsen Physics Building, Knoxville TN 37996, United States

To get a comprehensive picture on how the shell structure evolves when we move towards neutron-rich nuclei in the $A = 80$ region, we have measured a series of spectroscopic properties: $E(2^+)$, $B(E2)$, Q and g -factors at the Holifield Radioactive Ion Beam Facility (HRIBF). The beams, instrumentation and techniques developed at HRIBF specifically for this purpose have allowed us to systematically study the behavior of these observables along isotopic and isotonic chains using both stable and radioactive nuclei under almost identical experimental conditions. Recent results on Coulomb Excitation of n -rich nuclei along the $N = 50$ shell closure and the static quadrupole moment of the first 2^+ in ^{78}Ge will be presented.

Development of the SuperORRUBA detector array and the measurement of single particle states in ^{81}Ge

S. AHN^{1,2}, A. S. ADEKOLA³, D. W. BARDAYAN², J. C. BLACKMON⁶, K. Y. CHAE², K. A. CHIPPS⁵, J. A. CIZEWSKI³, J. ELSON⁸, S. HARDY³, M. E. HOWARD³, K. L. JONES¹, R. L. KOZUB⁷, B. MANNING³, M. MATOS⁶, C. D. NESARAJA², P. D. O'MALLEY³, S. D. PAIN², W. A. PETERS⁴, S. T. PITTMAN¹, B. C. RASCO⁶, M. S. SMITH², L. SOBOTKA⁸, I. SPASSOVA⁴

⁽¹⁾University of Tennessee at Knoxville, Knoxville Tennessee 37996, United States

⁽²⁾Oak Ridge National Laboratory, Oak Ridge Tennessee 37831, United States

⁽³⁾Rutgers University, New Brunswick New Jersey 08903, United States

⁽⁴⁾Oak Ridge Associated Universities, Oak Ridge Tennessee 37830, United States

⁽⁵⁾Colorado School of Mines, Golden Colorado 80401, United States

⁽⁶⁾Louisiana State University, Baton Rouge Louisiana 70803, United States

⁽⁷⁾Tennessee Technological University, Cookeville Tennessee 38505, United States

⁽⁸⁾Washington University in St. Louis, St. Louis Missouri 63130, United States

The study of nuclei far from stability elucidates the evolution of nuclear shell structure, and also affects estimates of heavy element nucleosynthesis in supernova explosions. Studying transfer reactions in inverse kinematics with radioactive ion beams is a powerful technique for these types of studies. Rare isotope beams often have relatively low beam intensities, and this places difficult requirements on detection systems for reaction products. The detectors must provide large solid angle coverage in the laboratory along with good position and energy resolution. The SuperORRUBA (Oak Ridge Rutgers University Barrel Array) detector array has been developed for such measurements and is comprised of 24 double-sided non-resistive silicon strip detectors. This configuration features low thresholds and improved resolution over detectors employing charge division. As a first implementation of this system, the $^2\text{H}(^{80}\text{Ge}, \text{p})^{81}\text{Ge}$ neutron transfer reaction was measured at the Holifield Radioactive Ion Beam Facility (HRIBF) at Oak Ridge National Laboratory (ORNL). The construction, commissioning, and performance of the array will be presented, as well as the status of the analysis of the ^{81}Ge data.

*This work was supported in part by the U.S. Department of Energy Office of Nuclear Physics, Stewardship Science Academic Alliance of the National Nuclear Security Administration and the National Science Foundation.

Single-neutron levels near the N=82 shell gap

B. Manning¹, J. A. Cizewski¹, R. L. Kozub², S. H. Ahn³, J. M. Allmond⁴, D. W. Bardayan⁵, J. R. Beene, K. Y. Chae⁵, K. A. Chipps⁶, A. Galindo-Uribarri^{3,5}, M. E. Howard¹, K. L. Jones³, J. F. Liang⁵, M. Matos⁷, C. D. Nesaraja⁵, P. D. O'Malley¹, S. D. Pain⁵, E. Padilla-Rodal⁸, W. A. Peters⁹, S. T. Pittman⁵, D. C. Radford⁵, A. Ratkiewicz¹, K. T. Schmitt⁵, D. Shapira⁵, M. S. Smith⁵

⁽¹⁾Department of Physics and Astronomy, Rutgers University, Piscataway NJ 08854, United States

⁽²⁾Department of Physics, Tennessee Technological University, Cookeville TN 38505, United States

⁽³⁾Physics Division, University of Tennessee, Knoxville TN 37996, United States

⁽⁴⁾JHIR, Oak Ridge National Laboratory, Oak Ridge TN 37831, United States

⁽⁵⁾Physics Division, Oak Ridge National Laboratory, Oak Ridge TN 37831, United States

⁽⁶⁾Physics Department, Colorado School of Mines, Golden CO 80401, United States

⁽⁷⁾Department of Physics and Astronomy, Louisiana State University, Baton Rouge LA 70803, United States

⁽⁸⁾Instituto de Ciencias Nucleares, UNAM, AP 70-543, 04510 México D.F., Mexico

⁽⁹⁾Oak Ridge Associated Universities, Oak Ridge TN 37830, United States

Nuclei with a few nucleons beyond shell closures are important in understanding the evolution of single-particle structure, which is critical to the benchmarking of nuclear models. With radioactive ion beams, studies near the double shell closure ^{132}Sn have been made possible. While the single-neutron states in ^{133}Sn with N=83 have recently been verified to be highly pure [1], it is important to study further from the N=82 closed shell. The (d,p) reaction was measured with the radioactive ion beams of ^{126}Sn and ^{128}Sn in inverse kinematics at the Holifield Radioactive Ion Beam Facility (HRIBF) at Oak Ridge National Laboratory, utilizing the SuperORRUBA silicon detector array. Angular distributions of reaction protons were measured for several states in ^{127}Sn and ^{129}Sn in order to determine angular momentum transfers and deduce spectroscopic factors. Such information is critical for calculating direct (n, γ) cross sections for the r-process and for constraining shell model parameters in the A=130 region.

Additional work was conducted to measure the ($^9\text{Be}, ^8\text{Be} \gamma$) reaction at HRIBF using a HPGe and CsI array (CLARION+HyBall) to obtain more precise energy levels. Combined with previous experiments on ^{130}Sn and ^{132}Sn , these results provide a complete set of (d,p) reaction data on even tin isotopes between stable ^{124}Sn and doubly magic ^{132}Sn . This work is supported in part by the U.S. Department of Energy and National Science Foundation.

[1] K.L. Jones, et al., Nature 465, 454 (2010) and Phys. Rev. C 84, 034601 (2011).

WED-NP05-5

#359 - Invited Talk - Wednesday 8:30 AM - Trinity Central

New high detection efficiency discovery tools for decay studies

Robert Grzywacz

Physics and Astronomy, University of Tennessee, 1408 Circle Dr, Knoxville TN 37996, United States

One of the several challenges of experimental studies of exotic nuclei, the low production rates requires the use of high detection efficiency detectors. Three such detectors have been developed recently with the main focus on ultra-efficient beta decay studies with a particular focus on studies of very neutron rich isotopes. Modular Total Absorption Spectrometer (MTAS) is a very large gamma-ray spectrometer, Versatile Array of Neutron Detectors at Low Energy (VANDLE) is a high-efficiency device for energy-resolved neutron spectroscopy and 3Hen is a high-efficiency neutron counter. Each of the three detectors was used in experiments with ^{238}U fission products at the Holifield Radioactive Ion Beam Facility (HRIBF) at Oak Ridge National Laboratory. Overview of the essential properties of these devices and examples of the most interesting discoveries will be presented.

This talk is given on behalf of MTAS, VANDLE and 3Hen collaborations. This work was supported by the U.S. Department of Energy Office of Nuclear Physics and National Nuclear Security Agency

WED-NP06-1

#465 - Invited Talk - Wednesday 1:00 PM - Trinity Central

On the production of exotic nuclei for nuclear physics and accelerator mass spectrometry

Meghan S. Janzen^{1,2,3}, Alfredo Galindo-Uribarri^{1,2,3}, Yuan Liu¹, Elizabeth Padilla-Rodal⁴

⁽¹⁾*Physics Division, Oak Ridge National Laboratory, Bethel Valley Rd, Oak Ridge TN 37831, United States*

⁽²⁾*Department of Physics and Astronomy, University of Tennessee, 401 Nielsen Physics Building, Knoxville TN 37996, United States*

⁽³⁾*Department of Earth and Planetary Sciences, University of Tennessee, 1412 Circle Dr, Knoxville TN 37996, United States*

⁽⁴⁾*Instituto de Ciencias Nucleares, Universidad Nacional Autonoma de Mexico, A.P. 70-543, Mexico D.F. 04510, Mexico*

The fields of AMS and RIB science share some common challenges and complement each other in techniques. I will give a brief description of some of the experimental tools and specialized techniques developed at the Holifield Radioactive Ion Beam Facility (HRIBF) which can broaden the range of radionuclides that can be detected at ultra-low levels. I will describe the on-going research activities aimed at the studies of environmental radioactivity (oceanography, rock erosion, climatic events and fuel cycles). I will report on the performance of aluminum nitride AlN as a source material compared with aluminum oxide (Al₂O₃) studied at the off-line ion source test facility and the 25MV-Tandem high-voltage platform at HRIBF and its impact in the production of ^{26}Al for radioactive ion beam science and AMS studies of geological samples.

Research sponsored by the Office of Nuclear Physics, U.S. Department of Energy and by PAPIIT grant IN-121209

Investigation of the Origin of Environmental Compounds from Indoor Air Samples via Accelerator Mass Spectrometry

Wolfgang Kretschmer, Matthias Schindler, Andreas Scharf, Alexander Stuhl
Physics, University of Erlangen, Erwin-Rommel-Str. 1, Erlangen 91058, Germany

Many organic environmental compounds are potentially dangerous due to their allergic or carcinogen impact on humans. For an effective program to reduce their concentration in houses, their sources have to be detected. Our investigation is focussed on aldehyde compounds since their indoor concentration is relatively high and since they originate from biogenic or anthropogenic sources. Both types of sources can be distinguished by their different ^{14}C content which can be measured via accelerator mass spectrometry (AMS).

For the collection and separation of these gaseous substances they have to be converted into liquid or solid phase by derivatization. This leads to the incorporation of up to six additional carbon atoms into the derivatized sample and hence to a reduced ^{14}C content and to an increased uncertainty for the deduced ^{14}C concentration. To reduce the number of additional carbon atoms, different derivatization compounds and methods have been tested with acet- and formaldehyde of known ^{14}C content.

The Erlangen AMS facility, based on an EN tandem accelerator and a hybrid sputter ion source for solid and gaseous samples, is well suited for the measurement of isotope ratios $^{14}\text{C}/^{12}\text{C} = 10^{-12} - 10^{-15}$. The ^{14}C concentration of the calibration samples and from various indoor air samples have been determined by AMS, the corresponding results are discussed with regard to potential sources of aldehydes.

Resonant scattering experiments with radioactive nuclear beams - Recent results and future plans

Takashi Teranishi
Department of Physics, Kyushu University, 6-10-1 Hakozaki, Higashi-ku, Fukuoka-shi, Fukuoka 812-8581, Japan

Measurement of proton resonances in unstable nuclei is useful for studying exotic nuclear structure and astrophysical nuclear reactions. We have performed proton resonant scattering experiments with radioactive beams at CNS, University of Tokyo and at RIKEN. In this presentation, our recent results of $^{14}\text{O}+p$ and $^{17}\text{Ne}+p$ will be reported together with some earlier results. Next, we will discuss future plans of resonant scattering experiments with polarized proton targets. We will also briefly introduce a project of a small-scale radioactive beam facility using a tandem accelerator at Kyushu University.

Nuclear fragmentation measurements for hadrontherapy and space radiation protection

Marzio De Napoli, C. Agodi, A. Blancato, G.A.P. Cirrone, G. Cuttone, F. Giacoppo, D. Nicolosi, L. Pandola, G. Raciti, E. Rapisarda, F. Romano, D. Sardina, C. Sfienti, S. Tropea
Sezione di Catania e Laboratori Nazionali del Sud, Istituto Nazionale di Fisica Nucleare (INFN), Via S. Sofia 64, Catania 95125, Italy

Nuclear fragmentation measurements are extremely important for hadrontherapy and space radiation protection. An effective shielding of space vehicles and an evaluation of the radiological risks for the astronauts require a correct prediction of the galactic cosmic rays fragmentation inside the space vehicles and the human body. In hadrontherapy the fragmentation of Carbon ions within the patient body produces lighter nuclei, resulting in the irradiation of healthy tissues, an attenuation of the primary beam, and the creation of a mixed radiation field in the tumor region. These effects have to be correctly evaluated by using Monte Carlo codes that, however, are presently affected by large uncertainties in the description of ion's nuclear interactions. Experimental cross section measurements are therefore mandatory to tune and validate Monte Carlo simulations.

In order to fill the gap of data in the intermediate energy region, we have measured the double-differential cross-sections of different isotopes produced in the fragmentation of a 12C beam at 62 AMeV on a thin Carbon target at the INFN - LNS in Catania. The measured cross sections have been used to test the GEANT4 hadronic models. This comparison is the only one performed so far with a 12C beam impinging on a thin Carbon target at intermediate energies. In this contribution the results on the measured fragmentation cross-sections and the comparison with GEANT4 predictions will be presented.

WED-NP06-5

#379 - Contributed Talk - Wednesday 1:00 PM - Trinity Central

Neutron-Induced Fission Cross Section Measurements for Uranium Isotopes and Other Actinides at LANSCE

F. Tovesson¹, A. B. Laptev¹, T. S. Hill²

⁽¹⁾LANSCE-NS, Los Alamos National Laboratory, P.O. Box 1663, MS H855, Los Alamos NM 87545, United States

⁽²⁾Idaho National Laboratory, P.O. Box 1625, Idaho Falls ID 83415, United States

A well established program of neutron-induced fission cross section measurement at Los Alamos Neutron Science Center (LANSCE) is supporting the Fuel Cycle Research program (FC R&D). The incident neutron energy range spans from sub-thermal up to 200 MeV by combining two LANSCE facilities, the Lujan Center and the Weapons Neutron Research center (WNR). The time-of-flight method is implemented to measure the incident neutron energy. A parallel-plate fission ionization chamber was used as a fission fragment detector. The event rate ratio between the investigated foil and a standard ²³⁵U foil is translated into a fission cross section ratio. Thin actinide targets with deposits of <200 µg/cm² on stainless steel backing were loaded into a fission chamber. In addition to previously measured data for ²³⁷Np, ²³⁹⁻²⁴²Pu, ²⁴³Am, new measurements include the recently completed ^{233,238}U isotopes, ²³⁶U data which is being analyzed, and ²³⁴U data acquired in the 2011-2012 LANSCE run cycle. The new data complete the full suite of Uranium isotopes which were investigated with this experimental approach. When analysis of the new measured data is completed, data will be delivered to evaluators. Having data for multiple Uranium isotopes will support theoretical modeling capabilities and strengthens nuclear data evaluation.

This work has benefited from the use of the Los Alamos Neutron Science Center at the Los Alamos National Laboratory. This facility is funded by the US Department of Energy and operated by Los Alamos National Security, LLC under contract DE-AC52-06NA25396.

WED-NP06-6

#434 - Invited Talk - Wednesday 1:00 PM - Trinity Central

Neutron-induced reactions relevant for Inertial-Confinement Fusion Experiments

M S Boswell², Anna Hayes¹, Gerry Hale¹, Jerry Jungman¹, Gary Grim², Andi Klein², Carl Wilde², Mac Fowler³, Bob Rundberg³, Jerry Wilhelemy³, Anton Tonchev⁴, Werner Tornow⁵, Frank Merrill²

⁽¹⁾Theory Division, Los Alamos National Laboratory, P.O. Box 1663, MS-H803, Los Alamos New Mexico 97544, United States

⁽²⁾Physics Division, Los Alamos National Laboratory, P.O. Box 1663, MS-H803, Los Alamos New Mexico 97544, United States

⁽³⁾Chemistry Division, Los Alamos National Laboratory, P.O. Box 1663, MS-H803, Los Alamos New Mexico 97544, United States

⁽⁴⁾Physics Division, Livermore National Laboratory, 7000 East Avenue, , Livermore CA 94550, United States

⁽⁵⁾Triangle Universities Nuclear Laboratory, Duke University, Durham NC 27708-0308, United States

The typical NIF DT implosion shot generates a high flux of 14-MeV neutrons from the d(t,n)α reaction. There is some spread in the energy of these primary neutrons, which is mainly attributable to the temperature of the DT burn. Neutrons created during this reaction have a 10% chance of scattering before escaping the capsule. Neutrons emerging from the capsule with energy less than 14-MeV represent neutrons that have scattered once, and hence give a direct measure of the areal density of the capsule. Neutrons emerging with an energy greater than the reaction energy are generated by neutrons transferring momentum to a deuteron or tritium ion, these enhanced energy ions then react in flight to produce higher energy neutrons; some of these neutrons have energies in excess of 30 MeV. Measuring the fluencies of both the low- & high-energy neutrons is a powerful mechanism for studying the implosion process, and the various parameters that drive inertial confinement fusion. We have developed a number of tools to measure the spectral characteristics of the NIF neutron spectrum. Most of these methods rely on exploiting the energy dependence of (n,γ), (n,2n), (n,3n) and (n,p) reactions on a variety of materials either implicitly present in the NIF implosion or through doping the target capsule or holraum.

I will be discussing both prompt activation measurements, and debris activation measurements of these materials currently under development at LANL. Focusing specifically on the development of an in-situ detector to measure short-lived activation products, as well as a low-background counting facility we are developing at the Waste Isolation Pilot Plant (WIPP) to study longer-lived activation products. Furthermore, I will also be discussing several cross section measurements that are important for the interpretation of the data collected from these activation products.

WED-NP07-1

#11 - Invited Talk - Wednesday 3:30 PM - Trinity Central

Neutron research at the n_TOF facility (CERN): results and perspectives

Nicola Colonna, for the n_TOF Collaboration

Istituto Nazionale Fisica Nucleare - Sez. di Bari, V. Orabona 4, Bari 70125, Italy

Neutrons studies are of great importance for various fields of basic and applied Nuclear Physics. In Nuclear Astrophysics, new measurements are needed to refine the modeling of stellar nucleosynthesis of heavy elements, while in nuclear technology neutron cross section data are requested to improve safety and efficiency of current reactors, as well as to develop advanced systems for energy production and waste transmutation, such as Gen IV reactors, Accelerator Driven Systems and reactors based on innovative fuel cycles.

The need of new cross section data has recently triggered a renewed world-wide effort in neutron research. An important contribution is being provided since 2001 by the CERN neutron time-of-flight facility n_TOF. The wide energy range, high instantaneous flux and excellent energy resolution are the main features of the facility. In the first ten years of operation, a variety of results have been obtained on capture cross sections relevant to Nuclear Astrophysics, as well as on capture and fission reactions of interest for advanced nuclear energy systems. Following a recent upgrade of the target/moderation system and experimental area, a new program started in 2009. In the first part of this talk, a review of the most important results obtained so far at n_TOF will be presented.

To further expand the range of measurements, a second experimental area at the shorter flight path of 20 m is now being proposed. The increased flux and shorter time-of-flight would result in a much higher signal to radioactive background ratio, thus allowing to measure radioactive isotopes with half-lives as short as a few years, samples of very small mass, down to μg , and (n,charged particle) reactions on very thin samples.

The design and main features of the second experimental area will be shown in the second part of the talk, and the foreseen experimental program discussed.

WED-NP07-2

#18 - Invited Talk - Wednesday 3:30 PM - Trinity Central

Some Results of (n, γ) Experiments on Tin Isotopes

Bayarbadrakh Baramsai¹, G. E. Mitchell¹, C. L. Walker¹, T. A. Bredeweg², A. Couture², R. C. Haight², M. Jandel², J. M. O'Donnell², R. S. Rundberg², J. L. Ullmann², D. J. Vieira², F. Becvar³, M. Krlicka³, U. Agvaanluvsan⁴, D. Dashdorj⁴, E. Batchuluun⁴, T. Tseren⁴

⁽¹⁾North Carolina State University, Raleigh NC 27695, United States

⁽²⁾Los Alamos National Laboratory, P. O. Box 1663, Los Alamos NM 87545, United States

⁽³⁾Faculty of Mathematics and Physics, Charles University in Prague, Prague, Czech Republic

⁽⁴⁾MonAme Scientific Research Center, Ulaanbaatar, Mongolia, United States

Neutron capture experiments on highly enriched ^{117, 119}Sn isotopes were performed with the DANCE detector array located at the Los Alamos Neutron Science Center. The DANCE detector provides detailed information about the multi-step γ -ray cascade following neutron capture.

The major goals of this experiment are: to improve understanding of the neutron capture reaction including a test of the statistical model in medium mass nuclei, to assign spins and parities of the neutron resonances, and to study the Photon Strength Function (PSF) and Level Density (LD) below the neutron separation energy. Preliminary results for the (n, γ) reaction on ^{117, 119}Sn will be presented. Neutron resonance spins of the odd-A tin isotopes are almost completely unknown. Resonance spins and parities have assigned via analysis of the multi-step γ -ray spectra and the application of our pattern recognition method. Discrepancies between nuclear data libraries such as ENDF, JEFF and JENDL are addressed based on the relative cross section and on analysis with the R-matrix code SAMMY.

This work was supported in part by the U. S. Department of Energy Grants No. DE-FG52-09NA29460 and No. DE-FG02-97-ER41042 and performed under the auspices of the U.S. DOE under contracts No. DE-AC52-06NA25396.

Precision lifetime measurements of exotic nuclei based on Doppler-shift techniques

Hironori Iwasaki

National Superconducting Cyclotron Laboratory, Michigan State University, Cyclotron, 640 S. Shaw Lane, East Lansing Michigan 48824-1321, United States

The study of the internal structure of atomic nuclei with extreme proton-to-neutron ratios represents one of major frontiers of fundamental research in nuclear science. The increasing availability of rare isotope (RI) beams as well as the development of large segmented gamma-ray detector arrays has opened a new opportunity to study deformation or collectivity of exotic nuclei. Recently, drastic changes of nuclear shell structure and possible emergence of neutron decoupling phenomena in nuclear deformation have extensively been studied both experimentally and theoretically, calling for an alternative verification by experiments with new sensitive techniques.

In this talk, the recent progress in precision lifetime measurements at the National Superconducting Cyclotron Laboratory (NSCL), Michigan State University will be presented. The lifetimes of excited nuclear levels in the range from about 1ps to 1000ps are measured with the Recoil Distance Doppler-shift technique, which is applied to nuclear reactions involving intermediate-energy RI beams. As such example, recent lifetime measurements of the 2^+ states in neutron-rich $^{62,64,66}\text{Fe}$ isotopes at and around $N=40$ (W.Rother, A.Dewald, H.Iwasaki, et al., Phys. Rev. Lett. 106 (2011) 022502) will be introduced. As a direct measure of quadrupole collectivity, we deduced the reduced E2 transition probabilities $B(E2)$ from the measured lifetime. The experiment was performed at the Coupled Cyclotron Facility at NSCL using a combination of several experimental instruments; the Segmented Germanium Array (SeGA), the plunger device, and the S800 spectrograph. The observed trend of $B(E2)$ clearly demonstrates that an enhanced collectivity persists in ^{66}Fe despite the semi-magic number $N=40$. The present results will also be discussed in comparison with the large-scale shell model calculations as well as the empirical scheme of the valence proton symmetry among the $N=40$ isotones.

Physics with Cold and Ultracold Neutrons

Pieter Mumm

Physical Measurements Laboratory, National Institute of Standards and Technology, 100 Bureau Dr., Gaithersburg MD 20899, United States

The National Institute of Standards and Technology (NIST) operates a national user facility for neutron based research, the NIST Center for Neutron Research (NCNR). Neutrons can be used to address a very broad range of topics including condensed matter physics, materials science, nuclear chemistry, biological and fundamental particle physics. The Neutron Physics Group group at NIST operates two high-intensity polychromatic beams, a number of monochromatic beams, and a neutron interferometer and optics facility. I will present an overview of these capabilities and then focus on some of the fundamental physics aspects of our work. Particularly interesting are precision measurements of neutron decay parameters which, for example, play an important role in our understanding of the early universe. The neutron lifetime dominates the uncertainty in theoretical predictions of the primordial abundance of He-4 in Big Bang Nucleosynthesis, while detailed studies of decay correlations may shed light on the matter-antimatter asymmetry of the universe by providing precise tests of time-reversal invariance. Neutron decay correlations, on the other hand, provide consistency checks of the Standard Model. I will discuss illustrative examples of these measurements.

NUCLEAR STRUCTURE AND DEPLETION OF NUCLEAR ISOMERS USING ELECTRON LINACS

J. J. Carroll¹, M. S. Litz¹, K. Netherton^{1,2}, S. Henriquez¹, N. Pereira³, D. Burns¹, S. A. Karamian⁴

⁽¹⁾US Army Research Laboratory, 2800 Powder Mill Road, Adelphi MD 20783, United States

⁽²⁾Drexel University, 3141 Chestnut Street, Philadelphia PA 19104, United States

⁽³⁾Ecopulse, Inc., P. O. Box 528, Springfield VA 22150, United States

⁽⁴⁾Flerov Laboratory of Nuclear Reactions, JINR, Dubna 19180, Russia

Nuclear isomers are long-lived excited states of atomic nuclei, with lifetimes ranging from several nanoseconds to millennia, and energies from a few eV to MeV. Their existence relies on decays that are hindered by specific features of nuclear structure, e. g. the angular momenta and symmetries of nuclear states. As such, they have provided important clues and touchstones in the development of shell and collective models. In the case of truly metastable isomers, like $^{180\text{m}}\text{Ta}$ ($T_{1/2} > 10^{15}$ years) and $^{108\text{m}}\text{Ag}$ ($T_{1/2} = 438$ years), the intrinsic energy storage of these states has been suggested for possible applications. The feasibility of applications based on isomers will depend sensitively on the ability to induce a depletion of metastable populations upon demand, due to the interaction of external agents. So far, induced depletion has been demonstrated experimentally for $^{180\text{m}}\text{Ta}$ (with real photons and Coulomb excitation), $^{68\text{m}}\text{Cu}$ (Coulomb excitation), and $^{177\text{m}}\text{Lu}$ and $^{178\text{m2}}\text{Hf}$ (by superelastic scattering of thermal neutrons). This presentation will discuss new experiments using bremsstrahlung produced by electron linacs to investigate the induced depletion of $^{108\text{m}}\text{Ag}$ and $^{166\text{m}}\text{Ho}$ ($T_{1/2} = 1200$ y). For the silver isomer, a transient excess in sample activity was detected after irradiation by 6 MeV bremsstrahlung, and was consistent with the 2.37 min half-life of $^{108\text{g}}\text{Ag}$. This demonstrated the depletion of some isomeric population to the ground state by the decay of intermediate states, following their excitation from the isomer. An experiment to study depletion of the holmium isomer is in development, and will utilize the natural pulse characteristics of a 2 MeV electron linac. The status of this experiment will also be discussed.

Relativistic masses of secondary neutrons in fission and fragments in fusion

ajay sharma

Physics, Fundamental Physics Society, Shimla, POST BOX 107 GPO SHIMLA 171001 INDIA, SHIMLA Not Applicable 171001, India

The fission is initiated by thermal neutron (0.025eV or 2,185m/s). In the fission reactions neutrons produced are known as fast (secondary) or relativistic neutrons having energy 2MeV (1.954×10^7 m/s or $\sim 7\%$ speed of light). With help of moderator the velocity is reduced to thermal neutrons or in classical limits. The relativistic variation of mass of fast neutron has to be taken in account. The masses of thermal and fast neutrons are 1.0086649156u and 1.01080879u respectively from relativistic variation of mass. But in calculations of Q-value (energy of reactants - energy of products) the masses of fast (secondary) and slow neutrons are taken as same i.e. 1.0086649156u. Nonetheless, it is not justified to take the relativistic velocity (1.954×10^7 m/s) or relativistic mass is taken same as classical velocity (2,185m/s) or classical mass. Thus in the existing literature, then Q value is calculated as 166.728MeV, the masses of products in this case is 235.8736037u. If masses of fast neutrons are considered, then mass of the products must be 235.880035u. The mass of the reactants in both the cases in the i.e. 236.05255948u. The masses of fission fragments Ba^{144} and Kr^{89} are taken as classical masses due to non-availability of exact velocities. If the relativistic masses of secondary neutrons are taken in account correctly, then Q value of the reaction is 160.7373MeV. Thus the accepted Q-value is 5.99MeV (or 0.00643u), which is comparable with energy of gamma ray emitted in fission. There may be numerous such reactions involving fission and fusion. If velocity is found in relativistic region, then relativistic mass has to be taken in account in energy considerations. In fusion the energy is emitted is very high and hence velocity of products is comparable to c. So the conclusions must be drawn with all fission and fusion events

Exploring optoelectronic applications of graphene nanohybrids

Jianwei Liu¹, Guowei Xu¹, Rongtao Lu¹, Qian Wang², Ron Hui², Judy Wu¹

⁽¹⁾*Physics and Astronomy, University of Kansas, 1251 Wescoe Hall Drive, Room 1082 Malott Hall, Lawrence Kansas 66045, United States*

⁽²⁾*Electrical Engineering and Computer Science, University of Kansas, 3026 Eaton Hall, Lawrence Kansas 66045, United States*

The zero bandgap of graphene presents a challenge in its application for optoelectronics. Graphene nanohybrids with nanostructured sensitizers of metals and semiconductors may provide a unique pathway to address this challenge. The unique merits of the graphene nanohybrid include the superior wavelength selectivity and charge mobility, both being critical to high-performance optoelectronic applications. In this work, we explore both metallic (e.g. Ag, Au) plasmonic nanoparticle (NP) sensitizers and semiconductor (such as ZnO) aligned nanowire (NW) array sensitizers for applications in photodetectors and advanced transparent conductors with light trapping mechanism. On the plasmonic metal NP/graphene nanohybrids, strong plasmonic resonance in visible range was confirmed in both Raman and optical spectroscopy characterization. Using a transparent front gate field-effect transistor scheme, high photoresponse in exceeding 20 mA/W has been obtained in visible spectrum. On the aligned ZnO NW/graphene nanohybrids, UV detectors were assembled using graphene as anode. High sensitivity of 1.62 A/W-volt and fast response time ~300 ms have been obtained. These results suggest sensitized graphene nanohybrids may provide a promising scheme for graphene based optoelectronic applications.

Tunable magnetoresistance behavior in suspended graphitic multilayers through ion implantation

Carlos Diaz-Pinto, Xuemei Wang, Sungbae Lee, Viktor G. Hadjiev, Debtanu De, Wei-Kan Chu, Haibing Peng

Department of Physics and the Texas Center for Superconductivity, University of Houston, 4800 Calhoun Rd, Houston TX 77204-5005, United States

We report a tunable magnetoresistance (MR) behavior in suspended graphitic multilayers through point defect engineering by ion implantation. We find that ion implantation drastically changes the MR behavior: the linear positive MR in pure graphitic multilayers transforms into a negative MR after introducing significant short-range disorders (implanted boron or carbon atoms), consistent with recent non-Markovian transport theory. Our experiments suggest the important role of the non-Markovian process in the intriguing MR behavior for graphitic systems, and open a new window for understanding transport phenomena beyond the Drude-Boltzmann approach and tailoring the electronic properties of graphitic layers.

Surface Plasmon Resonances of Large-area Nanostructured Metallic Films Created by Gas Cluster Ion Beams

Jiming Bao¹, Buddhi Tilakaratne^{2,3}, Dharshana Wijesundera^{2,3}, Yang Li¹, Indrajith Rajapaksa⁴, Donna Stokes², Xuemei Wang^{2,3}, Wei-Kan Chu^{2,3}

⁽¹⁾*Electrical and Computer Engineering, University of Houston, N 308 Engineering Building 1, Houston Texas 77204-4005, United States*

⁽²⁾*Department of Physics, University of Houston, Houston Texas 77204, United States*

⁽³⁾*Texas Center for Superconductivity, University of Houston, Houston Texas 77204, United States*

⁽⁴⁾*Department of Electrical Engineering and Computer Science, University of California, Irvine CA 92697, United States*

We investigate surface plasmon resonances of self-assembled nano-ripples created on metallic films by gas cluster ion beam. In fabrication of nano ripples, we deposited Au and Ag metal films on silicon substrates and these films were irradiated with gas cluster ions consisting of 3000 Ar atoms per cluster with energy of 30keV per cluster at off-normal incidence up to a dose of 3×10^{16} clusters/cm². The forward momentum gained by surface atoms during irradiation results in self-assembly of the nano-ripples. By further adjusting the cluster ion dosage, beam angle of incidence as well as film material, we are able to tune the size and shape of nano-ripples, which exhibit tunable surface plasmon resonances with center wavelength ranging from 600 to 850 nm.

Multilayered nanoporous templates synthesized by nuclear track etching for nano-fabrication

Christopher Ortega¹, Shuangqi Song¹, Buddhi P Tilakaratne², Wei-Kan Chu², Li Sun^{1,2}

⁽¹⁾*Department of Mechanical Engineering, University of Houston, Houston TX 77204, United States*

⁽²⁾*Texas Center for Superconductivity (TcSUH), University of Houston, Houston TX 77204, United States*

Nanoporous templates play a significant role in traditional filtering and separation applications; it has been developed into a major synthesis method for the templating growth of various free-standing nanostructures with controllable diameter, aspect ratio and sometimes composition along the length direction. However, current available porous templates most contain pores with a uniform cylindrical shape throughout the length.

To take advantage of the nanomaterials dimension, shape and composition dictated physiochemical properties, we are developing multilayered nanoporous templates with adjustable pore diameter in individual layers using nuclear track etching technique. Utilizing the different ionization and chemical etching characteristics of insulating materials after high energy ion irradiation, membranes of different layers with controllable etching pore diameters have been fabricated. These membranes can then be used as templates for the electrochemical growth of multi-diameter and multi component nanostructures. Nanowires with controlled length and diameter as small as 15nm have been demonstrated. These nanomaterials can be extracted from the polymer template to become free-standing structures. Since these nanomaterials can have shape and morphology that cannot be obtained by other synthesizing methods, we are expecting them to have unique physicochemical properties to deliver novel application. We are currently developing an magnetic resonance imaging (MRI) contrast agent using these nanomaterials for signal enhancement.

Large Area Mapping of Graphene Grain Structure and Orientation

Herman Carlo Floresca, Ning Lu, Jinguo Wang, Moon J Kim

Materials Science and Engineering, The University of Texas at Dallas, 800 W. Campbell Road, RL10, Richardson Tx 75080, United States

Chemical vapor deposited (CVD) graphene grows as a polycrystalline sheet with grains that are oriented in many directions. There is a push to increase the size of these grains until a large single-crystal graphene sheet can be achieved. This can only be accomplished with a thorough understanding of the graphene growth process and its resulting grain and grain boundary structure. In our study, we demonstrate a simple method in conjunction with customized software for identifying and analyzing the orientations of graphene lattices within a sheet of CVD graphene. This process is scalable and able to grow with the increasing sizes of grown graphene grains. Selected area diffraction (SAD) patterns in the transmission electron microscope (TEM) were taken throughout the graphene sample and measured for the diffraction spot rotations which indicate the rotation of the selected graphene area. The information gathered from that was then plotted for a visual representation of the graphene's lattice structure. This process was supported by customized programs which decreased the time needed for the acquisition, measurement and plotting of the information. The resulting map revealed and identified two grain boundary types: grown grain boundaries and island grain boundaries. When applied to a growth series of graphene samples, the lattice orientations of islands were determined along with any misoriented lattices within. Statistics pulled from the software also provided quantitative data about orientation preferences that may be present due to the orientation of the copper substrate the graphene was grown on. These insights into the structure of graphene can lead to an understanding of the graphene growth mechanism, helping researchers reach the goal of large single crystal graphene sheets.

Acknowledgments: This work was supported by SWAN (GRC-NRI), AOARD-AFOSR (FA2385-10-1-4066) and the State of Texas ETF Fusion.

From Basic to application of Ion beam production of Pseudo-crystals¹

Daryush ILA

Department of Chemistry and Physics, Fayetteville State University, 1200 Murchison Rd., Fayetteville NC 28301-4297, United States

For the past eighteen years, we have studied and improved methodology for formation of nanostructure by the MeV ion beam in order to fabricate pseudo-crystals consisting of nanostructures. The focus of this talk will be on the change in the optical and thermoelectric properties of interacting nano-materials and their applications for capturing heat loss and energy efficiency. The success of this work is based on the formation of Pseudo-crystals of Nano-materials due to energy deposited by ionization in order to produce quantum dots or nano-structures with applications in optical devices as well as with applications in highly efficient thermoelectric Materials. The interacting nanocrystals enhance the electrical conductivity, reduce thermal conductivity and increase the Seebeck coefficient, in order to produce highly efficient thermoelectric materials. Theoretically, the regimented quantum dot superlattice/ pseudo-crystals consisting of nanostructures of any materials produces new physical properties such as new electrical band structure, phonon mini-bands, as well as improved mechanical properties. A proper choice of nanocrystals and host results in production of highly efficient thermoelectric generator (TEG) with efficiencies as high as 30% which correspond to figure of merit above 4.0.

In addition to above such systems are in a unique position to be used both as electrical generation from heat and/or other forms of radiation as well as cooling the structures, thus enhance the applicability of hybrid systems. The interaction of nanostructures results in phonon mini-bands formation reducing the thermal conductivity, while increasing the electrical conductivity resulted in synthesis of TEG with much higher efficiency than reported to this date. We will review a series of materials selected for investigation some operating at temperatures around 300K and some at about 1000K.

1- Patents Awarded

Next Generation MeV Proton Beam Focusing; what is required for sub 10 nm 3D lithography?

Jeroen Anton van Kan

Physics, CIBA, 2 Science Dr 3, Singapore 117542, Singapore

To overcome the diffraction constraints of traditional optical lithography, the next generation lithographies (NGLs) will utilize any one or more of EUV (extreme ultraviolet), X-ray, electron or ion beam technologies for producing deep sub-100nm features. Electron beam lithography (EBL), a candidate for direct-write technology at nanodimensions has extensively been investigated for the last four decades. However, proximity effects from high energetic secondary electrons initiating from adjacent and nearby features gives rise to structure broadening. Perhaps the most under-developed and under-rated is the utilisation of ions for lithographic purposes. Ion beam techniques like PBW, Focused Ion Beam (FIB) and Ion Projection Lithography (IPL) have the flexibility and potential to become leading contenders as next generation lithographies. Recently PBW has been incorporated in the Japanese governments road map for the nanotechnology business creation initiative which was updated in 2010.

A second generation proton beam writing line has been installed at the Centre for Ion Beam Applications at the National University of Singapore. Here we introduce this new system for proton beam writing (PBW), this system is able to focus MeV proton beams down to $13 \times 29 \text{ nm}^2$. PBW is a promising technique for proximity free structuring of high aspect ratio, high density 3D nano structures. The latest achievements in PBW of high aspect ratio metallic nanowires as well as the first lithographic results with the 2nd generation proton beam writing line will be presented. PBW and Ni electroplating will be introduced as a platform technique for the fabrication of 3D Nano Imprint Lithography (NIL) molds. Finally an outlook will be given how to achieve sub 10 nm focusing for fast 3D nano lithography using MeV light ion beams.

The authors acknowledge the support from A-Star (R-144-000-261-305), MOE Singapore (R-144-000-265-112) and the US Air Force.

Focused Ion Beam Mediated Assembly of Hierarchically Scaled Semiconductor Nanostructures for Potential Nanoelectronic Device Applications

Robert Hull

Materials Science and Engineering, Rensselaer Polytechnic Institute, 110 8th Street, Troy NY 12180, United States

We have combined the short range processes of strain-induced self assembly with longer range lithographic forcing functions to create semiconductor nanostructures arrays that can be controlled over many orders of magnitude of length scales. This work uses the input of positional maps from controlled arrays of focused ion beam pulses to locally modify Si substrate surfaces. This "template" then controls the subsequent assembly of (Si)Ge nanostructure arrays through epitaxial growth. We examine how information is transferred from the original template maps into the observed distributions of nanostructures that result, and show that it is possible to accurately template nanostructure arrays over length scales ranging from nanometers to macroscopic dimensions. We also discuss novel focused ion beam methods to deliver pulses of electronic or magnetic doping species with doses as small as a few ions per pulse and positional accuracy of order ten nm. With such methods we hope to functionalize ordered nanostructure arrays to develop prototype nanoelectronic devices based on motion of just a few units of electronic charge or spin.

Work in collaboration with J. Floro (UVA), J. Gray (U. Pittsburgh), Frances Ross (IBM), M. Gherasimova (S. Connecticut State), A. Portavoce (CNRS), J. Graham (FEI,) P. Balasubramanian, S. W. Chee and J. Murphy (RPI).

Construction of compact focused gaseous ion beam system to form 300 keV proton nanobeam

Takeru Ohkubo¹, Yasuyuki Ishii¹, Yoshinobu Miyake², Tomihiro Kamiya¹

⁽¹⁾*Department of Advanced Radiation Technology, Takasaki Advanced Radiation Research Institute, Japan Atomic Energy Agency, 1233 Watanuki-machi, Takasaki Gunma 370-1292, Japan*

⁽²⁾*Beam Seiko Instruments Inc., 2-10-1 Kamata, Ohta-ku Tokyo 144-0052, Japan*

Several hundreds of keV proton nanobeam have micrometer scale range and become great tools for high aspect ratio structure in proton lithography. Those beams are, however, generated from large accelerators with long beam transport chambers and, therefore, a compact system like FIB with higher energy is necessary for industrial applications. The focused gaseous ion beam (gas-FIB) system composed of a series of electrostatic lenses, called "acceleration lens system", has been developed to form nanobeams using gaseous ions generated from a plasma ion source. Ion beams are accelerated and focused simultaneously by a pair of electrodes. A beam diameter of 160 nm has been so far obtained with 46 keV proton beam focused by the compact acceleration lens system of 300 mm length. A new compact acceleration lens system including an acceleration tube was constructed to form 300 keV ion nanobeam. Since chromatic and spherical aberrations are hindrance to form nanobeams with their smaller sizes in diameter, a pair of electrodes working as a deceleration lens was introduced to downstream of the second stage acceleration part in the new acceleration lens system. A deceleration lens, which performs like a defocusing lens, is effective to reduce the aberrations, as we have already shown optical simulation results in CAARI 2010. Total acceleration length became 650 mm which was short enough to make the high energy gas-FIB compact. The experiments of micro- and nano-beam generations were carried out and the results will be discussed at the presentation.

PMMA as a potential dosimetry material for ion beam cancer therapy studies on a nanoscale

Harry J. Whitlow^{1,2,3}, Rattanaporn Norarat², Mari Napari², Nitipon Puttaraksa², Timo Sajavaara², Mikko Laitinen², Ananda A.R. Sagari², Mika Pettersson⁴, Orapin Chienthavorn³, Peerapong Yotprayoonsak⁵

⁽¹⁾*Institut des Microtechnologies Appliquées Arc, Haute Ecole Arc Ingénierie, Eplatures-Grise 17, la Chaux-de-Fonds CH-2300, Switzerland*

⁽²⁾*Department of Physics, University of Jyväskylä, PO Box 35 (YFL), Jyväskylä FI-40014, Finland*

⁽³⁾*Department of Chemistry, Kasetsart University, Bangkok, Thailand*

⁽⁴⁾*Nanoscience Center, Department of Chemistry, University of Jyväskylä, Jyväskylä FIN-40014, Finland*

⁽⁵⁾*Nanoscience Center, Department of Physics, University of Jyväskylä, Jyväskylä FIN-40014, Finland*

A commonly used phantom material in cancer therapy studies and resist material for lithography is PMMA (poly(methyl methacrylate)). It may be used as both a positive and negative resist depending on the ion fluence used. To investigate its lithographic properties for studying the dose distribution for single ion impacts on a scale of nanometers, which may provide important information for ion beam cancer therapy, we have investigated the lithographic process using Atomic Force Microscopy (AFM), μ -Raman Spectroscopy and Scanning Electron Microscopy (SEM). 2 MeV $^1\text{H}^+$, 3 MeV $^4\text{He}^{2+}$ and 6 MeV $^{12}\text{C}^{3+}$ ions from the Pelletron Accelerator in the Accelerator Laboratory of the University of Jyväskylä were used to irradiate PMMA samples which were then developed in 7:3 (vol.) solution of propan-2-ol in water. The results showed a monotonic increase in the C=C bonds with ion irradiation while the fluences for both chain scission and development are consistent with an overlapped ion track model. Void formation and topographical changes were markedly enhanced for ^{12}C ion impingement.

Microlithography in silicon with MeV ion irradiation

Jack E Manuel, Gary A Glass, Mangal Dhoubadel, Venkata Kummari

Physics Department, University of North Texas, 1155 Union Circle, Denton TX 76203, United States

Crystalline silicon displays a high degree of anisotropy when etched in strong alkaline solutions while amorphous silicon is relatively inert to the chemical etch process. By creating surface patterns of amorphous silicon on crystalline silicon substrates these amorphized areas can then serve as masks for wet-etching by anisotropic etchants. In this work, three dimensional microstructures have been created by chemical wet etching following patterned amorphization of silicon substrates with 3 MeV silicon ions. The addition of isopropyl alcohol alters the degree of anisotropy associated with the etching process. Results are presented for several substrates, including Si(100), Si (110) and Si(111).

The effect of grain boundary character on sink efficiency under irradiation

Michael J Demkowicz¹, Weizhong Han², Amit Misra²

⁽¹⁾*Department of Materials Science and Engineering, MIT, Cambridge MA 02139, United States*

⁽²⁾*Center for Integrated Nanotechnologies, Los Alamos National Laboratory, Los Alamos NM 87545, United States*

A reaction-diffusion model is used to demonstrate the effect of grain boundary (GB) sink efficiency on steady-state defect concentrations under irradiation. Next, transmission electron microscopy (TEM) is used to show that GB sink efficiency in polycrystalline Cu irradiated with He at high temperature depends on both GB misorientation and interface plane orientation. The consequences of these findings for design of radiation resistant materials is discussed.

This material is based upon work supported as part of the Center for Materials at Irradiation and Mechanical Extremes, an Energy Frontier Research Center funded by the U.S. Department of Energy, Office of Science, Office of Basic Energy Sciences under Award Number 2008LANL1026.

Computer Simulation of Microstructure Evolution in Irradiated Materials

Shenyang Hu

Pacific Northwest National Laboratory, P.O. Box 999, MSIN J4-55, Richland WA 99352, United States

Rich microstructure evolution, such as defect accumulation, the formation and growth of precipitates and voids, and solute segregation, takes place in fuels and structural components in nuclear reactors. In this work, we present a generic phase-field model to study the microstructure evolution kinetics. The model takes into account multiple material processes including the generation, diffusion and reaction of defects; nucleation of second phases, one dimensional motion of interstitials, volume change, and long-range elastic interaction. Volumetric swelling, which is one of important phenomena observed in irradiated materials, will be used to demonstrate the capability of the model. The effect of defect mobility, defect recombination rates, and sink strengths on void nucleation and growth kinetics is simulated. Results show that volumetric swelling has a quasi-bell shape distribution with temperature which is in agreement with experiments.

Microstructure Evolution of Heterogeneous Interfaces under Vacancy Supersaturation

Enrique Martinez, Alfredo Caro

MST-8, LANL, P.O.Box 1663, Los Alamos NM 87545, United States

A new hybrid Molecular Dynamics-kinetic Monte Carlo (MD-KMC) algorithm has been developed in order to study the microstructure evolution of heterogeneous systems in vacancy-supersaturated environments. The algorithm takes into account both chemical and stress fields. Migration barriers are calculated using either a linear approximation in which final and initial energies are obtained from MD or the nudged-elastic band method where the microstructure requires more accurate saddle point calculations. The approximation makes the algorithm fast enough to be able to handle hundreds of vacancies. Therefore, we are able to observe vacancy agglomeration at twist boundaries in Fe and Cu, characterized by different sets of screw dislocations. The mechanical properties of the sample with excess vacancies have been studied through shearing experiments. We observe an increase in the yield point due to vacancy preventing dislocation movement. The error is estimated comparing the final microstructure properties as given by the KMC algorithm with the same samples after MD annealing for 1 ns.

This material is based upon work supported as part of the Center for Materials at Irradiation and Mechanical Extremes, an Energy Frontier Research Center funded by the U.S. Department of Energy, Office of Science, Office of Basic Energy Sciences, and by the LANL LDRD Office.

Helium Trapping Behavior of Nanoprecipitate Interfaces

Niraj Gupta¹, Enrique Martinez², Srinivasan Srivilliputhur¹, Alfredo Caro²

⁽¹⁾*Materials Science and Engineering, University of North Texas, 1155 Union Circle #305310, Denton TX 76203-5017, United States*

⁽²⁾*MST-8, Los Alamos National Lab, Los Alamos NM 87545, United States*

Irradiation damage and helium generation pose a major challenge to the development of advanced materials for proposed fusion reactor designs. Recent experimental efforts have shown that nanostructured ferritic alloys exhibit exceptional helium tolerance due to defect recombination and helium trapping in small gas bubbles due to an ultrahigh density of oxide "nanofeatures." The trapping mechanism is believed to be geometric in nature, and is modeled in our work using a prototype Cu-Nb system. Helium addition to FCC Cu precipitates in a BCC Nb matrix and vice versa were simulated using MD and Monte Carlo simulations. Both these simulations yield preferential interfacial helium trapping, illustrating that this behavior is general to any stable high-interface density material systems irrespective of chemistry. The role of coherency of the interface is also explored by contrasting with helium behavior in the Fe-Cr system wherein both Fe and Cr have body-centered-cubic structure and similar lattice constants.

Micro-Raman analysis of the spatial distribution of radiation damage in He⁺-irradiated lithium niobate

Hsu-Cheng Huang¹, Ophir Gaathon¹, Richard M Osgood Jr.¹, Sasha Bakhru², Hassaram Bakhru²

⁽¹⁾Center for Integrated Science & Engineering, Columbia University, New York New York 10027, United States

⁽²⁾College of Nanoscale Science and Engineering, State University of New York at Albany, Albany New York 12222, United States

Radiation damage in insulating, complex oxides is important for a variety of technological applications and as well as for understanding the response of materials to extreme environments. The spatial distribution and crystallinity of He⁺-radiation-damage of implanted congruent lithium niobate (LiNbO₃) has been investigated by means of optical microscopy (OM), scanning electron microscopy (SEM) and confocal micro-Raman spectroscopy. The use of the tight optical excitation beam in this Raman tool allows mapping of the Raman spectra both laterally and normal to the irradiation axis with submicrometer spatial resolution. Point defects were observed after irradiation and surface deformation including blistering and microstress were observed in the stopping range. Careful polishing of a crystal facet enabled additional probing of the irradiation region. Micro-Raman analyses clearly show the very localized dislocation and compositional change. The effects of different He⁺ doses and energies, together with post-implantation treatments such as annealing and etching are also discussed.

Formation of optical waveguides using swift heavy ion irradiation

Jose Olivares^{1,2}, Miguel Luis Crespillo^{1,2}, Javier Manzano-Santamaria^{2,3}, Mariano Jubera⁵, Ovidio Peña-Rodriguez⁴, Mercedes Carrascosa⁵, Angel Garcia-Cabañes⁵, Fernando Agullo-Lopez²

⁽¹⁾Instituto de Optica, Consejo Superior de Investigaciones Cientificas, C/Serrano 121, Madrid 28006, Spain

⁽²⁾Centro de Microanálisis de Materiales (CMAM), Universidad Autónoma de Madrid, Campus Cantoblanco, Madrid 28049, Spain

⁽³⁾Euratom/CIEMAT Fusion Association, CIEMAT, Avda. de la Complutense, Madrid 28040, Spain

⁽⁴⁾Instituto de Fusión Nuclear, Universidad Politécnica de Madrid, Madrid 28006, Spain

⁽⁵⁾Departamento de Física de Materiales, Universidad Autónoma de Madrid, Campus Cantoblanco, Madrid 28049, Spain

A new route has been developed based on the use of high energy ions and their electronic excitation, suitable for the fabrication of micro and nano-structures. The method presents clear advantages compared with more classical ones like ion implantation. The aim is to process optical materials in order to fabricate novel optical waveguides. More precisely, we investigate the fabrication of thick (several microns) amorphous layers that allows to fabricate nonlinear optical waveguides showing large refractive index jump and step-like index profile. This is achieved in the so called regime of overlapping damage tracks. The fluences needed are of the order of 1e14 at/cm², two order of magnitude lower than those required by light ion implantation [1]. On the other hand, we research in the regime of isolated track impact generating nanostructured that allow also to produce light guiding. In this way optical waveguides are obtained with ultralow fluences of 1e11 at/cm² [2,3]. A current third topic of research is the fabrication of nanopores by means of selective chemical etching of the amorphous nanotracks produced in each high energy ion impact. The main optical materials being studied are LiNbO₃, KGW, TiO₂, BaMgF₄ and BGO. The research in the electronic damage is also being carried out on optical materials that are of interest for the fusion energy field, like amorphous and crystalline SiO₂ [4,5].

From the fundamental point of view, the group at CMAM-UAM has continued and extended its research activity in the area of modeling and simulation of the interaction of swift heavy ions with dielectric materials on the following topics:

- Non-radiative exciton model for point-defect generation,
- Ionoluminescence,
- Modeling Stress-strain halo around amorphous tracks in LiNbO₃,
- Kinetics of amorphization: MonteCarlo and analytical models.

Simulating ion tracks and controlled nanoparticle deformation using swift heavy ions

Olli H. Pakarinen¹, Aleksi A. Leino¹, Patrick Kluth², Mark C. Ridgway², Flyura Djurabekova¹, Kai Nordlund¹

⁽¹⁾*Department of Physics and Helsinki Institute of Physics, University of Helsinki, P.O. Box 43, University of Helsinki FI-00014, Finland*

⁽²⁾*Research School of Physics and Engineering, The Australian National University, Canberra ACT, Australia*

Swift heavy ion (SHI) irradiation leads to narrow trails of damage known as ion tracks in many materials, and can be used in modifying nanomaterials, for example in shape transformation of nanoparticles into well-controlled, non-equilibrium shapes. In a-Ge local melting around the ion path leads to void formation, due to volume contraction associated with the molten phase. MD simulations reproduce the void formation, but not the non-spherical shape seen in experiments. The analyses comparing different potentials show that the outcome depends sensitively on the relative volume changes during the phase transitions.

In a recent comparison of SAXS experiments and molecular dynamics (MD) simulations, a previously unresolved fine structure with a low-density core and a high-density shell in ion tracks in amorphous silica was found [1]. The origin of the fine structure is a picosecond time scale pressure wave out of the track center that freezes in, creating a permanent low-density region around the ion path.

Elongation of metal nanoclusters inside an insulating substrate has recently been demonstrated on several nanocluster materials under SHI irradiation, and shown to be related to SHI track formation properties of the substrate [2]. We present large-scale MD simulations of SHI irradiation into Au nanoclusters embedded in several insulator substrates and at interfaces between different materials, compared to experiments, showing the picosecond time scale dynamics of track formation and nanoparticle shape transformation. Both MD simulations and experiments at interfaces show that the cluster shape transformation is dependent on the low-density track formation in the substrates. Finally, we present novel simulation results on recurrent irradiation of particles at a varying angle, which forces metal nanoparticles into well-defined non-equilibrium shapes, promising for plasmonics applications.

[1] P. Kluth et al., Phys. Rev. Lett. 101 (2008) 175503

[2] M.C. Ridgway et al., Phys. Rev. Lett. 106 (2011) 095505

Observing the thermal annealing of unetched fission fragment tracks along the entire ion trajectories

Weixing Li¹, Maik Lang¹, Andrew J. W. Gleadow², Maxim V. Zdorovets³, Rodney C. Ewing^{1,4,5}

⁽¹⁾*Department of Earth & Environmental Sciences, University of Michigan, Ann Arbor MI 48109, United States*

⁽²⁾*School of Earth Sciences, The University of Melbourne, Melbourne Vic 3010, Australia*

⁽³⁾*Institute of Nuclear Physics, National Nuclear Centre, Astana 010008, Kazakhstan*

⁽⁴⁾*Department of Materials Science and Engineering, University of Michigan, Ann Arbor MI 48109, United States*

⁽⁵⁾*Department of Nuclear Engineering and Radiological Sciences, University of Michigan, Ann Arbor MI 48109, United States*

Tracks created by fission events in ceramics are randomly-oriented, linear radiation-damage regions about 10 to 25 μm in length but only several nm in diameter. In the absence of a method to observe the entire length of a latent, unetched fission track, the details of the structure and the process of the thermal-annealing of tracks have remained elusive, despite their importance to fission track thermochronology and radiation damage studies in nuclear materials. Here, we have used a novel microtome sample preparation technique, together with advanced transmission electron microscopy (TEM), to successfully image the entire length and in situ thermal annealing of latent tracks created by 80 MeV Xe ions (a typical fission fragment) implanted in apatite. By using the microtome method, we have avoided the possibility of modifying track morphology due to heating or further ion damage, as is highly possible for other common TEM preparation techniques, such as ion milling and focused ion beam cutting. Track annealing significantly increases as the track diameter decreases along the ion trajectory from an initial diameter of 8.9 nm to ~ 1.5 nm at the end of the track (total track length $\sim 8.1 \mu\text{m}$). For the first time, the initial, rapid reduction in etched length during isothermal annealing can be essentially explained by the rapid annealing of the sections of the track with smaller diameters, as observed directly by TEM.

Swift Heavy Ion Irradiation of Amorphous Metals

Matias Daniel Rodriguez¹, Christina Trautmann², Zohair S. Houssain³, Boshra Afra¹, Thomas Bierschenk¹, Nigel Kirby⁴, Patrick Kluth¹

⁽¹⁾Department of Electronic Materials Engineering, The Australian National University, The Australian National University, Canberra Australian Capital Territory ACT 0200, Australia

⁽²⁾Helmholtz Centre for Heavy Ion Research, GSI, Planckstraße 1, Darmstadt 64291, Germany

⁽³⁾Process Science and Engineering (CPSE), CSIRO, Clayton South MDC, Clayton Victoria ViC 3169, Australia

⁽⁴⁾Australian Synchrotron, 800 Blackburn Road, Clayton Victoria ViC 3168, Australia

Amorphous metals, also called metallic glasses, are metallic alloys with a disordered non-crystalline atomic structure. The amorphous structure is quenched from the liquid state by rapid cooling with rates of $\sim 10^6$ K/s. There is a high level of interest in metallic glasses due to their interesting physical properties such as high mechanical strength, great wear and corrosion resistance, and high elasticity. High electronic excitations generated by swift heavy ion irradiation (SHII) of a solid can lead to the formation of long columnar defects along the ion trajectories, termed "ion tracks". Ion tracks in amorphous materials are often characterized only by subtle differences in structure and density between track and matrix material. This lack of contrast leaves the complex structure of ion tracks inaccessible with most experimental techniques. At present, there is little information about the effect of ion tracks in metallic glasses while still in the amorphous phase.

For this study, ion tracks were generated in Fe-B and Ti-Zr based alloys using various heavy ion beams with energies ranging from 100 MeV to 2.2 GeV. Fluences ranged between 1×10^{10} and 3×10^{11} ions/cm² to form individual ion tracks with negligible overlap. The ion track morphology was studied using synchrotron based small angle x-ray scattering (SAXS). The tracks are well described by cylindrical objects with a density difference between the track and matrix material of approximately 0.1 %. By applying an inelastic thermal spike model we determined the track formation threshold for the selected alloys. The track annealing kinetics has been studied using SAXS combined with **ex situ** isochronal and **in situ** isothermal annealing experiments. The annealing of the samples leads to a change in the track radii due to the relaxation of the ion track boundaries. Such track recovery occurs while the material still is amorphous and gradually becoming brittle.

Ion Tracks produced by sub MeV C₆₀ ions in Amorphous Si₃N₄

Yosuke Morita¹, Kaoru Nakajima¹, Motofumi Suzuki¹, Kazumasa Narumi⁴, Yuichi Saitoh⁴, Norito Ishikawa³, Kiichi Hojou³, Masahiro Tsujimoto², Syoichi Isoda², Kenji Kimura¹

⁽¹⁾Department of Micro Engineering, Kyoto University, Yoshida-honmachi, Kyoto 6068501, Japan

⁽²⁾Institute for Integrated Cell-Material Sciences, Kyoto University, Yoshida-honmachi, Kyoto 6068501, Japan

⁽³⁾Japan Atomic Energy Agency, Tokai, Japan

⁽⁴⁾Takasaki Advanced Radiation Research Institute, Japan Atomic Energy Agency, Takasaki 3701292, Japan

The discovery of ion tracks dates back to 1959 when the tracks produced by single fission fragments from ²³⁵U in mica were observed by transmission electron microscopy (TEM). Since then, ion tracks have been observed in various materials irradiated with swift heavy ions, including insulators, semiconductors and metals. In case of crystalline materials, the structure of the ion track can be easily observed by TEM. The track interior is amorphized or comprised of defect clusters depending on the material. In case of amorphous materials, however, there has been no direct TEM observation of ion tracks. It is believed that direct TEM observation of ion tracks is difficult due to a lack of sufficient contrast. Only indirect methods, such as Fourier transform infrared spectroscopy and etching, have been used to study the ion tracks in amorphous materials. In this presentation, we will report on the first TEM observation of ion tracks produced in an amorphous material. Thin films of amorphous Si₃N₄ were irradiated with 120 - 720 keV C₆₀ ions and observed using TEM. The observed TEM images show circular structures and the number of the circular structures coincides with the number of the incident ions, indicating that the observed structures are ion tracks. For quantitative analysis, the ion tracks were also observed using high-angle annular dark field scanning transmission electron microscopy (HAADF-STEM). The observed ion track consists of a low density core (radius 2.5 nm) which is surrounded by a high density shell (width 2.5 nm). The role of the nuclear stopping power on the track formation will be also discussed.

In-situ resistivity monitoring of defects during swift heavy ion-irradiation of graphite

Sandrina Da Visitacao Fernandes¹, Mikhail Avilov¹, Markus Bender², Marine Boulesteix¹, Markus Krause², Wolfgang Mittig^{1,3}, Frederique Pellemoine¹, Mike Schein¹, Daniel Severin², Marilena Tomut^{2,4}, Christina Trautmann^{2,5}

⁽¹⁾Facility for Rare Isotope Beams, Michigan State University, 1 Cyclotron Lab, East Lansing MI 48824-1321, United States

⁽²⁾GSI Helmholtzzentrum für Schwerionenforschung, Planckstr. 1, Darmstadt 64291, Germany

⁽³⁾National Superconducting Cyclotron Lab NSCL, Michigan State University, 1 Cyclotron Lab, East Lansing MI 48824-1321, United States

⁽⁴⁾National Institute for Materials Physics NIMP, Bucharest, Romania

⁽⁵⁾Technische Universität Darmstadt, Darmstadt, Germany

For studying the feasibility of using graphite as a high-power target material for secondary nuclear beam production for the Facility for Rare Isotope Beams FRIB (USA) and the Facility for Antiproton and Ion Research FAIR (Germany) polycrystalline graphite thin foils were irradiated at GSI with a 8.6 MeV/u ¹⁹⁷Au beam with external electric ohmic heating up to 1600°C. The graphite radiation damage was monitored by in-situ electrical resistance measurements during and after irradiation until its stabilization and cooling to room temperature. The change of electrical resistance provided an assessment of electrical resistivity change and of the accumulation and recovery of irradiation-produced defects in graphite as a function of ion fluence and irradiation temperature. The results show that the saturation of defects occurs faster at low irradiation temperatures due to a less efficient recombination of the irradiation produced defects. The visual inspection of the irradiated graphite foils showed that the higher the irradiation temperature is, the less the observed swelling and dimensional change in the irradiated region. At irradiation temperatures higher than 1200°C no visible foil deformation was observed after irradiation. The annealing of radiation damage at high irradiation temperatures was also confirmed by measuring the thermal diffusivity and Young's modulus at room temperature. All these measurements showed a nearly complete recovering of the pristine graphite properties at high irradiation temperatures.

Highlights of TEM with in situ Ion Irradiation in 4D at the Argonne IVEM-Tandem Facility

Marquis Albert Kirk

Materials Science Division, Argonne National Laboratory, 9700 S. Cass Ave., Argonne Illinois 60439, United States

With results from our unique IVEM-Tandem Facility we will highlight recent research which features dynamic formation of defect structures in materials under **in situ** ion irradiation in real time at controlled temperature and applied stress, and in three spatial dimensions. Future directions and instrumentation for this research, with emphasis on materials for nuclear energy, will be discussed.

Recent Results from the Microscope and Ion Accelerator for Materials Investigations (MIAMI) Facility

Jonathan A Hinks¹, Graeme Greaves¹, Cheng-Ta Pan², Sarah Haigh², Stephen E Donnelly¹

⁽¹⁾Computing and Engineering, University of Huddersfield, Queensgate, Huddersfield HD4 5AD, United Kingdom

⁽²⁾Materials Science Centre, School of Materials, University of Manchester, Manchester M13 9PL, United Kingdom

The Microscope and Ion Accelerator for Materials Investigations (MIAMI) facility is located at the University of Huddersfield, United Kingdom. It features a 1-100 kV ion accelerator coupled to 200 kV JEOL JEM-2000FX transmission electron microscope (TEM). Ion beams of most ionic species can be generated across the available energy range allowing a variety of irradiation conditions from low-energy light ions such as He to high-energy heavier self-ions. Whilst observing **in situ** within the TEM, the temperature can be controlled from -173 to 1000°C allowing a wide range of radiation-induced nanoscale phenomena to be studied.

Recent experimental work using the MIAMI facility will be presented including: observation of the creation of bubbles and their self-ordering into superlattices in Cu under He irradiation giving insight into the underlying atomic mechanisms; and dimensional change in graphene under displacing irradiation which is of importance for understanding the radiation hardness of this material but also of relevance to similar effects observed in nuclear graphite.

In-situ Observation of Radiation Damage in Iron base alloys by means of HVEM-ion accelerator Facility

Somei Ohnuki¹, H Kinoshita², N Hashimoto¹, N Yamaguchi¹, T Shibayama¹, S Watanabe¹

⁽¹⁾*Graduate School of Engineering, Hokkaido University, Sapporo, Japan*

⁽²⁾*Fukushima Technological College, Iwaki, Japan*

Hokkaido University has installed multi-beam irradiation facility combining with an atomic resolution high voltage electron microscope and ion-accelerators. By using the facility several groups have used for in-situ observation of damage structure in fusion and fission reactor materials and synthesis of non-stoichiometric phases. An example of in-situ observation for radiation-damage in fusion and fission reactor materials will be introduced during an electron-helium ion irradiation.

Ferritic steels are candidate materials for fusion reactors, however, there are main materials issues such as irradiation embrittlement and elevation in ductile-brittle transition temperature. Migration energy of point defects influence evolution of irradiation-induced dislocation loops, and hydrogen and/or helium created by nuclear transmutation reaction are important terms in "Multi-scale modeling" for solving such macroscopic materials behavior.

In order to investigate the effect of helium on migration energy of vacancies or interstitials in Fe-Cr model alloys, two types of irradiations, electron single irradiation and electron-helium dual irradiation and their in situ observations were performed at 300 - 500 C. The acceleration voltage of electron in a HVEM was 1250 kV, and He ion was 100 kV. The damage rate was 10×10^{-4} dpa/s, and the injection rate was 10 He appm / dpa.

At the beginning of the electron-irradiation interstitial-type dislocation loops were nucleated and then grew on $\langle 001 \rangle$ and $\langle 111 \rangle$. In the case of dual-beam irradiation, the loops were nucleated with much higher number density, and the grown with continuing irradiation. By using simple method based on Kiritani and Yoshida [3], the migration energy of interstitials was evaluated as 0.2 eV in both types of irradiations, and that of vacancies was evaluated as 0.95 eV in electron-irradiation and 1.5 eV in dual beam irradiation, where the difference of two energies, 0.5 eV, could be assumed to be net binding energy of vacancy and helium atom.

In-Situ Ion Irradiation and Tomography of Gold Nanoparticles

Sarah M Hoppe, Khalid Hattar

Sandia National Laboratories, P.O. Box 5800, Albuquerque NM 87185, United States

Nanomaterials have become of interest in a variety of applications from radiotherapy to satellite components due to their unique physical and chemical properties in comparison to bulk materials. Gold nanoparticles (Au NP), in particular, have been used as a model system because of their monodispersity, well-understood properties, and ease of synthesis. However, little is known about how nanoparticles are affected by extreme radiation environments.

In this work, commercially available 10 nm citrate coated Au NP were deposited on holey carbon lace Transmission Electron Microscopy (TEM) grids. These grids were placed in an in-situ ion irradiation TEM that is connected to a 6 MV Tandem Accelerator and irradiated with 3 MeV Cu^+ ions to gain a fundamental understanding of radiation effects on nanostructured materials. Initial studies tracked various regions of Au NP over time to image the structural changes caused by ion irradiation. The studies show the particles coalesce into larger clusters and smaller particles sputter off the larger masses. Later studies followed a single region of Au NP during irradiation, and collected tomography tilt series to create 3D reconstructions of the particles to better view the damage caused through the whole material. These Au NP irradiation studies aid in understanding the structural stability of the nanoparticles and their radiation hardness. The results of the irradiation and tomography studies on Au NP, as well as the details of the unique in-situ ion irradiation TEM capabilities will be discussed.

This research was funded by the U.S. Department of Energy, Office of Science, Office of Basic Energy Sciences, Division of Materials Sciences and Engineering. Sandia National Laboratories is a multi-program laboratory managed and operated by Sandia Corporation, a wholly owned subsidiary of Lockheed Martin Corporation, for the U.S. Department of Energy's National Nuclear Security Administration under contract DE-AC04-94AL85000.

Ion Irradiation-induced Amorphization in RE Silicate with Apatite Structure

Jiaming Zhang, Fuxiang Zhang, Weixing Li, Maik Lang, Rodney C Ewing
Earth and Environmental Sciences, University of Michigan, 2534 CC Little Bld, Ann Arbor MI 48108, United States

The apatite-type structure, $A^I_4A^{II}_6(BO_4)_6(OH, O, F, Cl)_2$ ($A^I, A^{II} = Ca$, rare earths, fission products and/or actinides; $B = Si$ and/or P), offers unique structural advantages as an advanced waste form for complex waste streams because of its structural and chemical flexibility. Radiation effects in apatite compounds, specifically for natural minerals and fluorapatite, have been extensively studied for different types of irradiation sources to understand the process of irradiation damage and recovery in the structure. In this study, we performed ion beam irradiation using 1 MeV Kr^{2+} on the series of rare-earth silicates, $RE_{9.33}(SiO_4)_6O_2$, with the goal in understanding the effects of chemical composition on the damage production and defect annealing processes. The ion irradiations were conducted using IVEM-Tandem facilities at Argonne National Laboratory between room temperature and 1000 K, combined with in-situ TEM observations. The results show that the structures are susceptible to amorphization upon ion irradiation and T_c , the critical temperature for amorphization, varies with the composition. The variation of T_c dependent on the composition are related to the ratio of electronic to nuclear stopping power (ENSP) based on SRIM calculations, in which the ionization process resulting from electronic energy loss may lead to enhanced annealing of defects upon radiation damage. In addition, the results are compared to the previous studies on the synthetic britholites.

In-situ Heavy Ion Irradiation of Inconel X-750 with Pre-implanted Helium

Zhongwen Yao¹, Ken he Zhang¹, Mark Kirk²
⁽¹⁾*Mechanical and Materials Engineering, Queen's University, Union St 60, Kingston ON K7L 3N6, Canada*
⁽²⁾*Materials Science Division, Argonne National Lab, 9700 S. Cass Avenue, Argonne IL 60439, United States*

Inconel X-750 is a γ' $Ni_3[Al, Ti]$ precipitation strengthened Ni based superalloy used for commercial nuclear reactors as one of structure materials. In order to mimic neutron irradiation, in which atomic displacement damages and helium impurities from (n, α) transmutation reaction were generated, in-situ heavy ion (Kr^{2+}) irradiation with pre-implanted helium were performed under observation of an intermediate voltage electron microscope (IVEM). By comparing to our previous studies using Kr^{2+} irradiation without He, the pre-implanted helium was found to be essential in the development of irradiation induced cavities. Large amounts of voids were found in Kr^{2+} irradiated sample containing 200 appm helium irradiated to 10 dpa (displacements per atom) at 300 °C. Helium interstitials were found to stabilize the γ' precipitates, preventing disordering at temperatures <400°C. The dose level at which the γ' precipitates became disordered increase from 0.06 dpa to about 2 dpa due to the presence of pre-injected helium. The sizes and densities of irradiation induced stacking fault tetrahedras (SFTs) and loops were characterized by using weak beam dark field method in TEM.

Sources, Active Inspection Systems and Neutron Kinetics

Tsahi Gozani, Micheal J. King
Rapiscan Laboratories, Rapiscansystems, Inc., 520 Almanor Avenue, Sunnyvale CA 94085, United States

The efficient use of neutron sources and their moderators in active interrogation systems requires a good understanding of the neutron interactions in energy and time domains. The selection of source related parameters, such as the energy (e.g. (d,T), (d,D), (p,Li) or (γ,n)), source shielding and spectrum tailoring usually pertains to maximizing the signal i.e. detectable fission signatures. The neutron kinetics or time behavior is considered mostly in the context of obtaining temporal separation between the numerous source neutrons and the much weaker fission signatures, allowing the measurement of the latter with minimal interference from the former. An outstanding example for this is the Differential Die Away Analysis (DDAA) technique. The DDAA and other techniques based on pulsed neutron sources implicitly assume that the neutron population reaches asymptotic behavior and then extract the threat signature from the interaction of this population with the threat and its surrounding media.

Working in the asymptotic time domain, where there is a convenient separation between time and energy (or velocity) variables, makes the results much easier to interpret and validate. However, by ignoring the more difficult non-asymptotic domains one may be losing useful information which, when extracted, can enhance the overall system sensitivity. The very basics of non-asymptotic neutron kinetics, its relevance to the detection of nuclear materials and other threats and its potential to increase signal and to improve signal to background ratios in neutron based interrogation systems will be discussed and some actual examples will be shown.

^{*}) This work has been partially supported by the US Department of Homeland Security, Domestic Nuclear Detection Office, under competitively awarded contract HSHQDC-10-C-00122 and HSHQDC-10-C-00048. This support does not constitute an expressed or implied endorsement on the part of the Government.

WED-SSCD03-2

#227 - Invited Talk - Wednesday 8:30 AM - Pecos II

Characterization of an Intense Pulsed Photoneutron Source for Active Detection

Jacob C Zier¹, Raymond J Allen¹, John P Apruzese³, Robert J Commisso¹, David D Hinshelwood¹, Anthony L Hutcheson², Stuart L Jackson¹, Lee J Mitchell², David Mosher³, Donald P Murphy¹, David G Phipps¹, Bernard F Phlips², Joseph W Schumer¹, Stephen B Swaneekamp¹, Richard S Woolf⁴, Eric A Wulf², Frank C Young³

⁽¹⁾Plasma Physics Division, Naval Research Laboratory, 4555 Overlook Ave, SW, Washington DC 20375, United States

⁽²⁾Space Science Division, Naval Research Laboratory, 4555 Overlook Ave, SW, Washington DC 20375, United States

⁽³⁾Independent contractor for NRL through L-3 Services, Inc., Chantilly VA 20151, United States

⁽⁴⁾Research Associate, National Research Council, 500 Fifth St, NW, Washington DC 20001, United States

Detection of smuggled fissile materials can help prevent nuclear proliferation and limits the threat posed by nuclear terrorism. Active detection methods elevate natural signatures from these materials using fission-inducing radiation, making them easier to detect than using passive methods alone. Intense pulsed active detection (IPAD)* uses a high power (~TW) pulsed driver to produce a short (~50 ns) irradiation. This improves the signal-to-natural-background ratio by reducing counting times. One option for IPAD is a mixed bremsstrahlung and neutron source. Photoneutrons are generated by placing a D₂O "secondary converter" in front of the bremsstrahlung converter outside the accelerator, allowing simple coupling to the existing bremsstrahlung source. This source was fielded on NRL's Mercury generator (8 MV, 200 kA, 50 ns) to produce ~10¹² neutrons/pulse with energies up to 3 MeV. The < 50 ns bremsstrahlung pulse gives a neutron production rate > 10²⁰ neutrons/s per pulse. The source was optimized using MCNPX to predict neutron yields and energy spectra. The source was experimentally diagnosed using rhodium, aluminum, MnCu, and depleted uranium activation detectors. These measurements were compared to the same bremsstrahlung source with an H₂O secondary converter.

*S.B. Swaneekamp, J.P. Apruzese, R.J. Commisso, **et al.**, IEEE Trans. Nucl. Sci. **58**, 2047 (2011).

Work supported by the UK Atomic Weapons Establishment through DTRA. Distribution A: Approved for public release; distribution is unlimited.

WED-SSCD03-3

#43 - Invited Talk - Wednesday 8:30 AM - Pecos II

Negative Ion Associated Particle Imaging Neutron Generator

A. J. Antolak¹, D. H. Morse¹, K.-N. Leung¹, P. A. Hausladen²

⁽¹⁾Sandia National Laboratories, Livermore CA 94550, United States

⁽²⁾Oak Ridge National Laboratory, Oak Ridge TN 37831, United States

A neutron generator for associated particle imaging is being developed that has high neutron output, long lifetime, high spatial resolution, and wide field-of-view. These improvements are realized through use of a novel D⁻/T⁻ negative ion source that simultaneously loads and causes T(D, n)⁴He reactions to occur on the target surface, while enabling the generator to operate at low pressure and with high efficiency. The generator utilizes an RF inductively-coupled plasma source to create negative ions, a magnetic filter diode to remove electrons from the extracted ion beam, a specially designed titanium target that minimizes scattering of the exiting neutrons, and a position sensitive alpha-particle detector. Monatomic negative ion beams bombarding the positively biased target cause little or no sparking in the generator and reduce sputtering of the target surface to maintain small beam spot size and long lifetime. The neutron generator is designed to produce >10⁸ n/s from a 1 mm diameter beam spot for high resolution imaging.

*K.-N. Leung is also affiliated with the Nuclear Engineering Department, University of California, Berkeley CA 94720, United States.

This work was supported by the DOE/NA-22 Office of Nonproliferation Research and Development. Sandia National Laboratories is a multi-program laboratory managed and operated by Sandia Corporation, a wholly owned subsidiary of Lockheed Martin Corporation, for the U.S. Department of Energy's National Nuclear Security Administration under contract DE-AC04-94AL85000. Oak Ridge National Laboratory is managed for the U.S. Department of Energy by UT-Batelle, LLC under Contract No. DE-AC05-00OR22725.

WED-SSCD03-4

#248 - Invited Talk - Wednesday 8:30 AM - Pecos II

Adapting New Ion Source Technologies for use in Neutron Generators

Qing Ji¹, Arun Persaud¹, Amy Sy¹, Bernhard Ludewigt¹, Thomas Schenkel¹, Hannes Vainionpaa², Charles K Gary²,
Melvin A. Piestrup²

⁽¹⁾Lawrence Berkeley National Laboratory, 1 Cyclotron Road, MS 5R0121, Berkeley CA 94720, United States

⁽²⁾Adelphi Technology, Inc., 2003 East Bayshore Road, Redwood City CA 94603, United States

Research and development of adapting new ion source technologies in neutron generators with increased capabilities for homeland security applications is being conducted at the Lawrence Berkeley National Laboratory (LBNL). Penning ion sources have long been used because of their ease of operation, low power consumption and compactness. Recent work at LBNL indicates that the source performance, i.e., extracted beam current density and atomic ion fraction, can be improved for increased neutron yields by better magnetic confinement, optimization of electrode geometry, and choice of wall materials. To achieve ultra-compactness, a low-power field emission ionization source using nanotechnology is under development that does not consume RF or DC discharge power. They are easily portable and can serve as replacement for radiological sources. In pursuit of high yield of neutrons, permanent-magnet, microwave-driven ion sources have been developed to produce high extracted beam currents with high atomic fractions for high-output neutron generators. These sources are more power efficient than RF-driven ones while providing similar mono-atomic fractions and beam current densities. They operate also at lower gas pressure, which makes them more suitable for sealed tubes DT operation. Lately, permanent-magnet, microwave-driven ion source technology has also been adopted in the development of an API system with enhance spatial resolution and increase neutron yield for proliferation detection and nuclear safeguards applications.

*This work was performed under the auspices of the U.S. Department of Energy, NNSA Office of Nonproliferation and Verification Research & Development by Lawrence Berkeley National Laboratory under Contract No. DE-AC02-05CH11231.

WED-SSCD03-5

#417 - Contributed Talk - Wednesday 8:30 AM - Pecos II

Linear Accelerator X-Ray Sources with High Duty Cycle

Cathie Condrion¹, Craig Brown¹, Willem G.J. Langeveld¹, Tsahi Gozani¹, Mike Hernandez²

⁽¹⁾Labs, Rapiscan Systems, 520 Almanor Ave, Sunnyvale CA 84085, United States

⁽²⁾XScell Corp., 2134 Old Middlefield Way, Mountain View CA 94043, United States

Traditional x-ray cargo inspection systems use pulsed linear-accelerator based x-ray sources, which emit a bremsstrahlung spectrum of x-rays. These x-rays traverse the cargo and are detected by a detector array. During typical pulse durations of a few microseconds, an excessive amount of x-rays arrive at each detector, unless they are heavily absorbed/scattered by the cargo. Spectroscopy of the detected x-rays is allows one to determine the Z of the material the x-ray traversed. Unfortunately, spectroscopy is impractical in conventional cargo inspection systems for several technological reasons that will be discussed in the presentation. If one could develop an accelerator that eliminates these technological hurdles, Active Interrogation methods would be greatly improved.

We set a goal of designing an accelerator using Conventional Off the Shelf components capable of duty cycles greater than one percent. A matrix of available linac components that include all RF source options as well as a price comparison to a component level, where possible, was constructed. From the parameter/cost matrix a linac Figure Of Merit was defined as an aid in choosing the most appropriate linac for improving AI capabilities.

Another goal was to develop an accelerator capable of nano-pulsing, micro-pulsing, and macro-pulsing. The micro and macro-pulsing mode of this design will enhance spectroscopic applications by spreading out the bremsstrahlung x-rays over a longer beam burst thus reducing pileup and dead time in the detectors. The nano-pulsing mode will enable, via Time of Flight technique, new AI modalities such as photoneutron resonance spectroscopy, which is applicable to explosives, contraband, and SNM detection. The findings of this program will be presented and discussed.

Comparing Modern Measurements of the $^{11}\text{B}(\text{d}, \text{n}\gamma_{15.1})^{12}\text{C}$ Excitation Function with Previous Values

Kevin Wayson Cooper, Thomas N Massey, David C Ingram

Physics and Astronomy, Ohio University, Clipping Labs 251B, Athens Ohio 45701, United States

A possible means of active interrogation of special nuclear materials is detection of signature emissions following induced photofission. This method requires a probe gamma-ray beam to induce the photofission. The $^{11}\text{B}(\text{d}, \text{n}\gamma_{15.1})^{12}\text{C}$ reaction is a candidate for the source of this probe beam. The reaction is prolific and the produced 15.1 MeV gamma-ray is close to a photofission cross-section peak for $^{235,238}\text{U}$ and $^{238,239}\text{Pu}$. In order to model an active interrogation system using the $^{11}\text{B}(\text{d}, \text{n}\gamma_{15.1})^{12}\text{C}$ reaction as a source probe an accurate value for its differential cross-section must be included in data libraries. Measurements of the differential cross-section for the $^{11}\text{B}(\text{d}, \text{n}\gamma_{15.1})^{12}\text{C}$ reaction have been carried out with a BGO detector and found to differ from previous measurements reported by Kavanagh (1958) and Kuan (1964). The discrepancy in the measurements may be explained by examining the detector response function used by Kavanagh and presumably Kuan to that modeled with MCNP5. A comparison of the MCNP5 and Kavanagh detector response functions normalized to the 15.1 MeV gamma-ray peak pulse height shows a factor of approximately 1.7 difference in integrated counts. Applying this correction to the differential cross-section previously reported by Kuan brings the values into agreement, within uncertainties, to the more recent measurements. The evaluation of the detector response function for the 15.1 MeV gamma ray in the NaI detector reported by Kavanagh to that modeled by MCNP5 is shown. This result is applied to the comparison of recent measurements on the $^{11}\text{B}(\text{d}, \text{n}\gamma_{15.1})^{12}\text{C}$ reaction differential cross-section to those previously reported.

WED-SSCD04-1

#270 - Invited Talk - Wednesday 1:00 PM - Pecos II

Fusion driven gamma and fast neutron radiography test-bed at LLNL

Vincent Tang, Brian Rusnak, Steven Falabella, James McCarrick, Han Wang, Jennifer Ellsworth, James Hall, Phil Kerr

Lawrence Livermore National Laboratory, 7000 Eas Ave, Livermore CA 94588, United States

Fusion driven gammas and fast neutrons could provide unique radiography capabilities due to their ability to produce both high and low energy mono-energetic gammas and neutrons in contrast to broadband bremsstrahlung based x-ray sources. The possibility of simultaneously obtaining both gamma and neutron radiographs using one source could allow complex objects composed of a large range of low to high Z materials to be imaged. In this work we review a 4 MV RFQ accelerator driven radiography test-bed at LLNL designed to study the physics involved in applying these dual fusion driven reactions for radiography applications. First experimental neutron images along with simulated neutron and gamma radiographs will be presented.

This work was performed under the auspices of the U.S. Department of Energy by Lawrence Livermore National Laboratory under Contract DE-AC52-07NA27344 and partly supported by the U.S. Department of Energy NA-22 Office of Nonproliferation Research and Development under the Radiological Source Replacement Program

WED-SSCD04-2

#279 - Invited Talk - Wednesday 1:00 PM - Pecos II

Compact, Inexpensive X-Band Linacs as Radioactive Isotope Source Replacements

Salime Boucher, Ronald Agustsson, Luigi Faillace, Pedro Frigola, Alex Murokh, Marcos Ruelas, Scott Storms, Xiaodong Ding

RadiaBeam Technologies, LLC, 1717 Stewart Street, Santa Monica CA 90404, United States

Radioisotope sources are commonly used in a variety of industrial and medical applications. The US National Research Council has identified as a priority the replacement of high-activity sources with alternative technologies, due to the risk of accidents and diversion by terrorists for use in Radiological Dispersal Devices ("dirty bombs"). RadiaBeam Technologies is developing novel, compact, inexpensive linear accelerators for use in a variety of such applications as cost-effective replacements. The technology is based on the MicroLinac (originally developed at SLAC), an X-band linear accelerator powered by an inexpensive and commonly available magnetron. Prototypes are currently under construction. This paper will describe the design, engineering, fabrication and future testing of these linacs at RadiaBeam. Future development plans will also be discussed.

Radiobiological Studies Using Gamma and X Rays

Charles Potter¹, Bobby Scott², Katherine Gott², Yong Lin², Mabel Padilla², Julie Wilder²

⁽¹⁾*National Security Studies, Sandia National Laboratories, PO Box 5800, MS0425, Albuquerque NM 87123, United States*

⁽²⁾*Lovelace Respiratory Research Institute, 2425 Ridgecrest Dr. SE, Albuquerque NM 87108, United States*

In 2008, the National Academy of Science's Committee on Radiation Source Use and Replacement (National Research Council) published **Radiation Source Use and Replacement**. This report was driven by terrorism concerns following the Sept. 11, 2001 attacks on the United States and publicized the unique risks of the continued use radiation sources made of ¹³⁷CsCl. Irradiators in hospitals, universities, and research institutions frequently make use of ¹³⁷CsCl due to its long half-life and the relatively high energy and monoenergetic gamma emissions.

The National Nuclear Security Agency's Office of Proliferation Detection (NA-221) within the Office of Nonproliferation Research and Development has funded a study out of the Radiological Source Replacement Program to explore the possibility of replacing ¹³⁷CsCl irradiators with X-ray irradiators for biological applications. Sandia National Laboratories is teaming with the Lovelace Respiratory Research Institute to compare the effects on biological systems exposed to 662 keV ¹³⁷CsCl gamma rays and X rays produced in a 320 kV irradiator. It is hoped that the results of this research will show (1) the viability of using X-ray irradiators as alternatives to ¹³⁷CsCl irradiators and reduce the use of ¹³⁷CsCl nationwide, ideally making ¹³⁷CsCl less available for detrimental uses, and (2) identify how gamma and x-rays effect some biological tissues differently.

Sandia National Laboratories is a multi-program laboratory managed and operated by Sandia Corporation, a wholly owned subsidiary of Lockheed Martin Corporation, for the U.S. Department of Energy's National Nuclear Security Administration under contract DE-AC04-94AL85000.

Pulsed Pyroelectric Crystal-Powered Gamma Source

Allan Xi Chen, Arlyn J. Antolak, Ka-Ngo Leung, Thomas N. Raber, Dan H. Morse

Sandia National Laboratories, 7011 East Ave., Livermore CA 94550, United States

A compact pulsed gamma generator is being developed at Sandia National Laboratories to replace existing radiological sources. Mono-energetic gammas are produced in the 0.4 - 1.0 MeV energy range using either D-⁹Be or D-⁶Li nuclear reactions. The gamma generator employs a RF-driven inductively coupled plasma ion source to produce deuterium current densities up to 2 mA/mm² and ampere-level current pulses are attained by utilizing an array extraction grid. The extracted deuterium ions are accelerated to approximately 300 keV via a compact stacked pyroelectric crystal system which subsequently bombards the production target to generate gammas. The resulting microsecond pulse of gammas is equivalent to a radiological source with Curie-level activity.

^aA.X. Chen is also affiliated with Department of Mechanical Engineering, University of California, Berkeley, CA 94720

^bK.-N. Leung is also affiliated with Department of Nuclear Engineering, University of California, Berkeley, CA 94720

This work was supported by the DOE/NA-22 Office of Nonproliferation Research and Development. Sandia National Laboratories is a multi-program laboratory managed and operated by Sandia Corporation, a wholly owned subsidiary of Lockheed Martin Corporation, for the U.S. Department of Energy's National Nuclear Security Administration under contract DE-AC04-94AL85000.

Alternative Neutron Sources for Well Logging

Gregory E Dale¹, James T Rutledge¹, Christen M Frankle¹, Michele E DeCroix¹, Scott D Kovaleski², Peter Norgard², James A VanGordon², Emily A Baxter², Brady B Gall², Baek Huyn Kim², Jae Wan Kwon², Avneet Sood

⁽¹⁾*High Power Electrodynamics, Accelerator Operations and Technology, Los Alamos National Laboratory, PO Box 1663, Mail Stop H851, Los Alamos NM 87544, United States*

⁽²⁾*Electrical Engineering, University of Missouri, Columbia Mo 65211, United States*

The 2008 National Academies report on radiation source use and replacement found that Am-241, Cs-137, Co-60, and Ir-192 account for greater than 90% of the sealed sources that pose the highest security risks in the United States. In the case of Am-241, the highest activity sealed sources are found in AmBe neutron sources used in the petroleum industry for characterizing oil wells, known as well logging. The National Academies report also encouraged the government to facilitate the replacement of high-risk radiation sources and improve radiation source safety and security. Therefore, Los Alamos National Laboratory and the University of Missouri (MU) are working with NNSA to develop and explore alternative neutron sources for use in the well-logging industry. To be considered a viable alternative by industry, the neutron source must have similar response characteristics to the sources presently in use, must be compact to fit in the small well bore, and be extremely rugged to survive extremes of pressure, temperature, and vibration. The utilization of compact accelerator sources generating neutrons through hydrogen fusion reactions, such as D-T, D-D, and T-T, is one approach. In most instances, however, the energy spectra of the neutrons emitted in these reactions are substantially different than the energy spectra of neutrons emitted from an AmBe source, leading to different response characteristics. To make this comparison, we have been modeling the neutron output spectra from these reactions and comparing them to radioisotope neutron sources in the measurement of formation porosity and carbon to oxygen ratio. We are also investigating the ion emitter and the power supply of these accelerators to reduce the size and increase the neutron yield. As part of this project we are investigating a novel high-voltage piezoelectric transformer neutron generator (PTNG) under development at MU as a compact alternative neutron source for well-logging applications.

Progress in Field Ionization Sources for Compact Neutron Generators

Arun Persaud¹, Rehan Kapadia², Kuniharu Takei², Ali Javey², Thomas Schenkel¹

⁽¹⁾*Accelerator and Fusion Research Division, Lawrence Berkeley National Laboratory, 1 Cyclotron Rd, Berkeley CA 94720, United States*

⁽²⁾*Department of Electrical Engineering and Computer Sciences, University of California, Berkeley CA 94720, United States*

The replacement of radiological sources, such as AmBe, in oil-well logging applications requires small, compact and energy efficient neutron generators. In this talk, we report on our progress to utilize field ionization in a diode-like structure to generate deuterium/tritium ions. Neutrons are then generated in a fusion reaction (D/D, D/T or T/T reaction). To achieve field ionization, local electrical fields of the order of 20 V/nm [1] are necessary. These are achieved by applying a strong external electric field, which at the same time supplies the acceleration voltage, and using field enhancement effects created by microscopic tips, such as carbon nano-fibers (CNF). The challenge in this approach is to achieve high uniformity across a large array of field-emitter, so that many tips contribute to the ion current, and to achieve long life time of the tip structures in a harsh hydrogen environment. We will show results from different sample geometries: forest samples, patterned arrays of small islands of CNF and arrays of single tips. We will also talk about coating of these structure to prevent etching effect in a hydrogen environment. The approach can lead to a plasma free neutron generator with very compact dimensions and low energy consumption.

Work performed under the auspices of the US Department of Energy, NNSA Office of Nonproliferation Research and Engineering (NA-22) by Lawrence Berkeley National Laboratory under Contract DE-AC02-05CH11231.

[1] R. Gomer, "Field Emission and Field Ionization", AIP, 1993

Coaxial Electron Cyclotron Resonance Neutron Source

William Johnson, Arlyn Antolak, Ka-Ngo Leung, Tom Raber

Rad/Nuc Detection Materials & Analysis, Sandia National Laboratories, 7011 East Avenue, Livermore California 94550, United States

A compact D-D neutron generator is being developed at Sandia National Laboratories to replace radiological neutron sources used in research, industry and national security applications. The neutron generator utilizes a novel coaxial permanent dipole magnet electron cyclotron resonance (ECR) plasma ion source that can operate at low pressure, produce a high fraction of atomic species, and is scalable to high current densities using multiple ion beamlets. Unlike conventional microwave-driven ion sources in which plasma is obtained by applying the microwave electric field with a linear applicator, the present system consists of a permanent-magnet that is azimuthally symmetric around its magnetization axis and a microwave applicator in the form of a coaxial line. This approach avoids the propagation of microwaves within the plasma (which leads to non-uniform plasma) and, in addition, provides a large ion beam extraction area (leading to high neutron yield). Multiple D^+ ion beamlets are extracted from the ion source, accelerated and subsequently bombard a titanium target at high voltage to cause D-D fusion reactions at the beam-loaded target surface. Hydrogen plasma has been successfully ignited at a microwave power of 25 W and 0.375 mTorr gas pressure. The neutron generator is designed to produce $>10^7$ n/s when operating at an average power of 100 W.

Sandia National Laboratories is a multi-program laboratory managed and operated by Sandia Corporation, a wholly owned subsidiary of Lockheed Martin Corporation, for the U.S. Department of Energy's National Nuclear Security Administration under contract DE-AC04-94AL85000.

High Voltage Pyroelectric-Driven Acceleration System

Allan Xi Chen, Arlyn J. Antolak, Ka-Ngo Leung, Thomas N. Raber, Dan H. Morse

Sandia National Laboratories, 7011 East Ave., Livermore CA 94550, United States

A novel method of powering a high voltage pulsed gamma generator in atmospheric pressure using lithium tantalate ($LiTaO_3$) pyroelectric crystals is being developed. A stack of twenty $LiTaO_3$ crystals (50 mm diameter x 1 mm thick) are used as temperature-induced self-charging capacitors by maximizing their capacitive energy storage potential. The crystals were immersed in a small bath of dielectric fluid and utilized Peltier thermoelectric modules to provide rapid heating/cooling. A maximum voltage of 22 kV was observed for a single 1 mm thick crystal using a surface DC voltmeter during the heating phase from 25°C to 70°C before breakdown occurred in the dielectric fluid. This is the experimental maximum coercive field that can be generated by a $LiTaO_3$ crystal without inducing polar domain reversal. The harvested electrical energy was approximately 0.18 J which is equivalent to an energy density of ~ 95 kJ/m³ per crystal. Several crystals are configured in a stack arrangement to take advantage of the Marx bank principle, resulting in a final pulsed voltage output of ~ 300 kV and joule-level energy per pulse. The pyroelectric crystal powering system is well suited to pulsed accelerator applications requiring high peak voltage.

^aA.X. Chen is also affiliated with Department of Mechanical Engineering, University of California, Berkeley, CA 94720

^bK.-N. Leung is also affiliated with Department of Nuclear Engineering, University of California, Berkeley, CA 94720

This work was supported by the DOE/NA-22 Office of Nonproliferation Research and Development. Sandia National Laboratories is a multi-program laboratory managed and operated by Sandia Corporation, a wholly owned subsidiary of Lockheed Martin Corporation, for the U.S. Department of Energy's National Nuclear Security Administration under contract DE-AC04-94AL85000.

A COMPACT ION SOURCE AND ACCELERATOR BASED ON A PIEZOELECTRIC DRIVER

Peter Norgard¹, Scott D. Kovaleski¹, James A VanGordon¹, Emily A Baxter¹, Brady B Gall¹, Jae Won Kwan¹,
Baek Hyun Kim¹, Gregory E Dale²

⁽¹⁾*Department of Electrical and Computer Engineering, University of Missouri, 349 Engineering Bldg. West, Columbia MO 65211, United States*

⁽²⁾*High Power Electrodynamics Group, Los Alamos National Laboratory, PO Box 1663, Los Alamos NM 87545, United States*

Compact ion sources and accelerators using piezoelectric devices for the production of energetic ion beams are being evaluated. A coupled source-accelerator is being tested as a neutron source to be incorporated into oil-well logging diagnostics. Two different ion sources are being investigated, including a piezoelectric transformer-based plasma source and a silicon-based field ion source. The piezoelectric transformer plasma ion source uses a cylindrical, resonantly driven piezoelectric crystal to produce high voltage inside a confined volume filled with low pressure deuterium gas. The plasma generated in the confined chamber is ejected through a small aperture into an evacuated drift region. The silicon field ion source uses localized electric field enhancement produced by an array of sharp emitters etched into a silicon blank to produce ions through field desorption ionization. A second piezoelectric device of a different design is used to generate an accelerating potential on the order of 130 kV; this potential is applied to a deuterated target plate positioned perpendicular to the ion stream produced by either plasma source. This paper shall discuss the results obtained from the integrated neutron source.

Work supported by Qynergy and Los Alamos National Laboratory

WED-TA01-1

#421 - Invited Talk - Wednesday 1:00 PM - Bur Oak

Undergraduate Experiment on the Kinematics of Elastic and Inelastic Scattering for 1.5 MeV Protons on Thin LiF Targets

Randolph S. Peterson¹, Prashanta Kharel^{1,3}, Derrith A. Roberson^{1,4}, Jerome L. Duggan²

⁽¹⁾*Department of Physics, The University of the South, 735 University Avenue, Sewanee TN 37383, United States*

⁽²⁾*Department of Physics, University of North Texas, 1155 Union Circle, Denton TX 76203, United States*

⁽³⁾*Department of Physics, Columbia University, 538 West 120th Street, New York NY 10026, United States*

⁽⁴⁾*Woodside Priory School, 302 Portola Road, Portola Valley CA 94028, United States*

Rutherford Scattering of protons and alpha particles from thin films is an exciting experiment for undergraduate physics students. The theoretical models for binary collisions and Rutherford scattering are taught in introductory and intermediate physics courses. An interesting variation in these experiments is the mixture of elastic scattering with inelastic (p,α) interactions for 1.5 MeV protons on thin film targets of ⁷Li¹⁹F. The challenges with the kinematic measurements involving exceeding the detector's calibration range and struggling with the statistics of the small number of events will be discussed.

WED-TA01-2

#176 - Invited Talk - Wednesday 1:00 PM - Bur Oak

Student research with 400keV beams: ¹³N radioisotope production target development

Andrew D. Roberts

Department of Physics and Astronomy, Minnesota State University-Mankato, Trafton Science Center N141, Mankato MN 56001, United States

The AN400 Van de Graaff accelerator at the Minnesota State University, Mankato, Applied Nuclear Science Lab has demonstrated utility as an accessible and versatile platform for student research. Despite the limits of low energy, the research team successfully developed projects with applications to the wider radioisotope production community. A target system has been developed for producing and extracting ¹³N by the ¹²C(d,n)¹³N reaction below 400keV. The system is both reusable and robust, with future applications to higher energy machines producing this important radioisotope for physiological imaging studies with Positron Emission Tomography.

Undergraduate research involving accelerator and radiation physics at Angelo State University

Scott Williams

Department of Physics, Angelo State University, ASU Station #10904, San Angelo Texas 76909, United States

Undergraduate research is an important component of our students' education at Angelo State University. A long-term project involving the construction of a relatively low energy (~25 keV) electron accelerator will be discussed, along with several short-term projects involving various radiative processes (bremsstrahlung, characteristic X-rays, gamma rays, etc.). Desired learning outcomes associated with the construction of the accelerator and the short-term projects will be described, with emphasis on ensuring that students are introduced to both the practical, hands-on aspects of research (working with amplifiers, detectors, vacuum systems, etc.), as well as the theoretical/computational aspects (data processing, Monte Carlo simulations, etc.).

Conceptual Demonstration of Hypervelocity Dust Particle Detection

Nicholas Childs¹, Anthony Shu², Andrew Collette², Keith Drake², Mihaly Horanyi^{2,3}

⁽¹⁾*Physics, Montana State University, Bozeman MT 59715, United States*

⁽²⁾*Colorado Center for Lunar Dust and Atmospheric Studies, University of Colorado at Boulder, Boulder CO 80309, United States*

⁽³⁾*Laboratory for Atmospheric and Space Physics, University of Colorado at Boulder, Boulder CO 80309, United States*

We describe the principles of charged dust grain detection in the laboratory, and their connections to the physics classroom. Electrostatic dust accelerator systems, capable of launching charged dust grains at hypervelocities (1-100 km/sec), are a critical tool for space exploration. Dust grains in space typically have large speeds relative to the probes or satellites which encounter them. Development and testing of instruments which look for dust in space therefore depends critically on the availability of fast, well-characterized dust grains in the laboratory. One challenge for the experimentalist is how to measure the speed and mass of laboratory dust particles without disturbing them. Detection systems currently in use exploit the well known effect of image charge to register the passage of dust grains without changing their speed or mass. We describe the principles of image charge detection and provide a simple classroom demonstration of the technique using soup cans and pith balls.

Simulation of ion beam transport through the 400-keV ion implanter at MIBL

Fabian U Naab, Ovidiu F Toader, Gary S Was

Nuclear Engineering and Radiological Sciences, University of Michigan, 2600 Draper Road, Ann Arbor Mi 48109, United States

The Michigan Ion Beam Laboratory houses a 400-kV ion implanter. An application that simulates the ion beam trajectories through the implanter from the ion source to the target was developed using the SIMION[®] code. The goals were to have a tool to develop intuitive understanding of abstract physics phenomena and diagnose ion trajectories. Using this application, new implanter users of different fields in science quickly understand how the machine works and quickly learn to operate it. In this article we describe the implanter application and compare the parameters of the implanter components obtained from the simulations with the measured ones. The overall agreement between the measured and simulated values of the magnetic fields and electric potentials for the implanter components is ~10%.

Analysis of Russian kopecks (1877-1933) using X-ray fluorescenceBrandon Cavness, Scott Williams*Department of Physics, Angelo State University, ASU Station #10904, San Angelo, Texas 76909, United States*

We have analyzed several Russian kopecks minted between the years of 1877 and 1933 (spanning eras associated with Alexander II, Alexander III, Nicholas II, Lenin, and Stalin) using X-ray fluorescence (XRF) as part of an undergraduate research project. The intensities of the Cu K-shell X-rays were studied in order to compare the relative purities of the Cu used to mint the kopecks. The economic conditions under which each of the kopecks were minted is discussed as well as impurities discovered during XRF analysis (notably, Hg). In addition to XRF analysis, kopecks produced just before (1915) and after (1924) the October Revolution of 1917 were weighed and measured in order to determine whether or not the Decree of February 22, 1924 was carried out. The legislation (enacted by the Central Executive Committee and the Council of the People's Commissaries) decreed that the proportions of pure Ag and Cu used in the minting of new coins should be the identical to those produced before the revolution and that the diameters and weights of the kopecks should also remain the same.

Construction of a Scattering Chamber for Ion-Beam Analysis of Environmental Materials in Undergraduate Physics ResearchScott LaBrake, Michael Vineyard, Colin Turley, Christopher Johnson, Robert Moore*Physics & Astronomy, Union College, 807 Union Street, Schenectady New York 12308, United States*

We have developed a new scattering chamber for ion-beam analysis of environmental materials with the 1.1-MV Pelletron accelerator at the Union College Ion-Beam Analysis Laboratory. The chamber was constructed from a ten-inch, Conflat, multi-way cross and includes a three-axis target manipulator and target ladder assembly, an eight-inch turbo pump, an Amptek X-ray detector, and multiple charged particle detectors. Recent projects performed by our undergraduate research team include proton induced X-ray emission (PIXE) and Rutherford backscattering (RBS) analyses of atmospheric aerosols collected with a nine-stage cascade impactor in Upstate New York. We will describe the construction of the chamber and discuss the results of some commissioning experiments.

Undergraduate Research and Teaching Using a Nuclear Physics LaboratoryDaniel Keith Marble*Engineering and Physics, Tarleton State University, Box T-390, Stephenville Texas 76402, United States*

In response to declining budgets for higher education, several states including Texas have recently began closing smaller undergraduate programs like physics that produce few graduates annually. This graduation threshold (presently 5 to 8 per year depending on the state and expected to rise) puts a large number of undergraduate physics programs potentially at risk. In order to remain viable in this environment, undergraduate physics programs especially at smaller public institutions are adjusting curriculum in order to prepare students for immediate employment in non-traditional physics areas in addition to pursuing graduate study in physics. Since nuclear physics techniques are used in a wide-range of fields, undergraduate nuclear physics laboratory experiments are an excellent mechanism for helping a small program achieve its goals. A discussion of the nuclear physics laboratory at Tarleton State University and its use in undergraduate research and teaching to support the physics program with its medical physics and nuclear engineering concentrations will be provided.

Undergraduate Research at the State University of New York College of Environmental Science and Forestry

Mark S Driscoll¹, Craig Kenny², Tyler C Kight², L. Scott Larsen³

⁽¹⁾*UV/EB Technology Center, State University of New York College of Environmental Science and Forestry, One Forestry Drive, Syracuse NY 13210, United States*

⁽²⁾*Chemistry, State University of New York College of Environmental Science and Forestry, One Forestry Drive, Syracuse NY 13210, United States*

⁽³⁾*NYSERDA, 17 Columbia Circle, Albany NY 12203, United States*

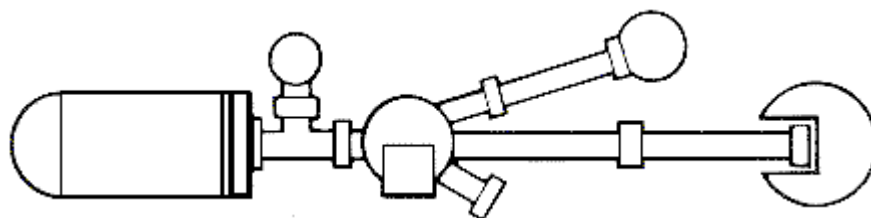
The State University of New York College of Environmental Science and Forestry is a small specialized, Ph.D. granting institution. The College encourages undergraduate students to conduct research and many departments require students to conduct a research project to meet graduation requirements. This presentation will present an overview of undergraduate research conducted utilizing both low and high energy electron beams.

Accelerator Base Nuclear and Materials Sciences Education and Training at the Fayetteville State University

Robert Lee Zimmerman, Daryush ILA

Department of Chemistry and Physics, Fayetteville State University, 1200 Murchison Rd, Fayetteville NC 28301-4297, United States

The materials science education and summer training using a particle accelerator was originally established by the authors in early 1990 at the Center for Irradiation of Materials (<http://cim.aamu.edu>) which was founded by D. ILA in order to enhance the education and research capabilities at AAMU and provide services needed by the Aero Space and Defense community and Industry at Huntsville, Alabama. As the result of establishment of the Center for Irradiation the annual grants at AAMU was increased to additional \$7M per year and annual contract because of the CIM was increased by nearly \$5M per year. The total number of summer students trained at this facility was between 10 to 20 students each summer and nearly two dozen graduate students per year used this facility regularly. The major focus of the accelerator based research is ion beam modification materials to change chemical, physical and mechanical properties. The optical, electrical, thermal and mechanical properties of materials are measured before and after ion beam induced change and the change in the chemical structure and stoichiometry is measured to understand the effect of ion beam on selected materials and for production of materials with new properties and for prototype devices. This team is now establishing a similar capability at the Fayetteville State University, a constituent of University of North Carolina, using a 9SDH-2 Pelletron Accelerator at the Research and Development Center of Excellence (RDCE) of FSU. In this talk we will present the historical perspective of this joint effort and plans for similar capability at the FSU.



THURSDAY

THU-AT06-1

#450 - Invited Talk - Thursday 8:30 AM - Bur Oak

Emerging High Power RF Accelerator Technologies

Chris Adolphsen

SLAC National Accelerator Laboratory, 2575 Sand Hill Rd., Menlo Park CA 94025, United States

This will be a survey talk detailing emerging technologies for RF accelerators. Focus will be on near-term (1-5 years) developments.

THU-AT06-2

#350 - Invited Talk - Thursday 8:30 AM - Bur Oak

RF Sources for Industrial and Research Accelerators

Peter E. Kolda, Stephan J. Lenci

Communications & Power Industries LLC, 607 Hansen Way, Palo Alto CA 94304, United States

CPI is a leader in the design and manufacture of high power RF sources including klystrons, Inductive Output Tubes (IOT), magnetrons, gyrotrons, power grid tubes, and coupled cavity traveling wave tubes (TWT). CPI has recently delivered high power klystrons and IOTs to TRIUMF, CERN, ESS Bilbao, Los Alamos National Laboratory, to name a few. CPI is also working on the next generation of high power high efficiency devices with the plan to provide them for ADS, CLIC, CSNS, ESS Lund and other accelerators requiring operation from 200 MHz to 12 GHz. CPI has a long history of providing devices for medical and research accelerator applications. CPI products fill the majority of the sockets at the Spallation Neutron Source at ORNL and LANSCE at LANL. Our multi-MW S-band klystrons are used in industrial and medical accelerators around the world. Recent developments include multi-MW, long-pulsed klystrons at 325, 352, and 500 MHz; a 10 MW peak, 1.3 GHz multiple beam klystron; an 80 kW CW IOT at 1.3 GHz, and a 5 MW peak, short-pulse klystron at 9.3 GHz. Presently in development are a 300 kW CW klystron at 1.3 GHz and a 50 MW peak klystron at 12 GHz.

THU-AT06-3

#233 - Invited Talk - Thursday 8:30 AM - Bur Oak

Pulsed Power Modulators for Modern Accelerator Facilities

David E Anderson

Spallation Neutron Source, Research Accelerator Division, Oak Ridge National Laboratory, 1 Bethel Valley Rd., MS6485, Oak Ridge TN 37831, United States

New and recent accelerator projects are establishing requirements for modulators driving high power RF sources that are increasingly challenging. Additionally, costs associated with developing and procuring these systems are significant. Fortunately, the development of solid-state switching and other enabling technologies has evolved to the point where incorporating semiconductors into modulator designs is achievable. This fact, combined with innovative system architectures stemming from power electronics and other disciplines, makes these goals achievable at reasonable cost. This talk will briefly discuss the evolution of pulsed power technology, drawing from a wide variety of applications, over the last half-century. Following that, it will review the major modulator technologies in use today and planned for the next decade at accelerators world-wide, including some of the challenges faced by modulator engineers at these facilities. Finally, the talk will review some of the concepts and enabling technologies under development which promise better modulator performance, efficiency and reliability.

SOLID STATE DIRECT DRIVE™ RF TECHNOLOGY - THE ROUTE TO 1W PER EURO CENTOliver Heid*Siemens AG, Erlangen, Germany*

In most particle accelerators RF power is a decisive design constraint due to high costs and relative inflexibility of current electron beam based RF sources, i.e. Klystrons, Magnetrons, Tetrodes etc. At VHF/UHF frequencies the transition to solid state devices promises to fundamentally change the situation. Recent progress brings 1 Watt per Euro cent installed cost within reach. We present a Silicon Carbide semiconductor solution utilising the Solid State Direct Drive™ technology at unprecedented efficiency, power levels and power densities. The proposed solution allows retrofitting of existing RF accelerators and opens the route to novel particle accelerator concepts.

Resonant Coupling Applied to Superconducting Accelerator StructuresJames M. Potter¹, Frank L Krawczyk²⁽¹⁾*JP Accelerator Works, Inc., 2245 47th Street, Los Alamos NM 87544, United States*⁽²⁾*Los Alamos National Laboratory, PO Box 1663, Los Alamos NM 87545, United States*

The concept of resonant coupling and the benefits that accrue from its application is well known in the world of room temperature coupled cavity linacs. Design studies show that it can be applied successfully between sections of conventional elliptical superconducting coupled cavity accelerator structures and internally to structures with spoked cavity resonators. The coupling mechanisms can be designed without creating problems with high field regions or multipactoring. The application of resonant coupling to superconducting accelerators eliminates the need for complex cryogenic mechanical tuners and reduces the time needed to bring a superconducting accelerator into operation.

This work was done by JP Accelerator Works, Inc. and Los Alamos National Laboratory under contract N00014-10-M-0328 with the Office of Naval Research.

The Klynac: An Integrated Klystron and Linear AcceleratorJames M. Potter¹, David Schwellenbach², Alfred Meidinger²⁽¹⁾*JP Accelerator Works, Inc., 2245 47th Street, Los Alamos NM 87544, United States*⁽²⁾*National Security Technologies, LLC, Los Alamos Operations, P.O. Box 809, Los Alamos NM 87544, United States*

The Klynac concept integrates an electron gun, a radio frequency (RF) power source, and a coupled-cavity linear accelerator into a single resonant system. The Klynac uses a unique cavity structure to resonantly couple the klystron output cavity to the accelerator cavities, locking the two in amplitude and phase, thereby eliminating the normal transmission line between klystron and accelerator. The system can be further simplified by using feedback to make a self-oscillating structure with a reduced gain klystron section. A single cathode is the electron source for both the klystron and the accelerator. Because the klystron output cavity is an integral part of the accelerator, the choice of frequency does not depend on the availability of commercial RF sources. The beam energy and current can be varied for a wide range of applications.

This work was done by National Security Technologies, LLC, under Contract No. DE-AC52-06NA25946 with the U.S. Department of Energy and supported by the Site-Directed Research and Development Program.

Picosecond Narrow Bandwidth X-ray Pulses from a Laser-Thomson-Backscattering

Sergiy Trotsenko^{1,2}, Arie Irman³, Axel Jochmann³, Thomas Cowan³, Michael Kuntzsch³, Ulf Lehnert³, Roland Sauerbrey³, Andreas Wagner³, Jurjen Pieter Couperus³, Alexander Debus³, Hans-Peter Schlenvoigt³, Ulrich Schramm³, Kenneth Ledingham⁴, Daniel Thorn⁵, Thomas Stöhlker^{1,2}

⁽¹⁾Atomic Physics, GSI Helmholtzzentrum für Schwerionenforschung, Planckstr. 1, Darmstadt 64291, Germany

⁽²⁾Helmholtz Institute Jena, Froebelstieg 3, Jena 07743, Germany

⁽³⁾Helmholtz Zentrum Dresden-Rossendorf, Bautzner Landstraße 128, Dresden 01328, Germany

⁽⁴⁾Department of Physics, University of Strathclyde, Glasgow G4 0NG, United Kingdom

⁽⁵⁾ExtreMe Matter Institute EMMI/GSI, Planckstr. 1, Darmstadt 64291, Germany

Intense, ultimately coherent, ultra-short hard X-ray pulses can serve as a novel tool for structural analysis of complex systems with unprecedented temporal and spatial resolution. With the simultaneous availability of a high power short-pulse laser system it provides unique opportunities for a number of subsequent research steps at the forefront of relativistic light-matter interactions. At HZDR we demonstrated the generation of such a light source by colliding picosecond electron bunches from the ELBE linear accelerator with counter-propagating femtosecond laser pulses from the 150 TW Draco Ti:Sapphire laser system. The generated narrowband X-rays are highly collimated and can be reliably adjusted from 5.5 to 23.5 keV by tuning the electron energy (24 MeV to 30 MeV) and the laser intensity. Ensuring the spatio-temporal overlap and suppressing the bremsstrahlung background we used an X-ray camera (resolution of 250 eV(FWHM)) to record the spectrum, we were able to resolve the angular-energy correlation and to study the influence of the beam emittance on the observed bandwidth.

Ion beam analysis of photon-assisted surface passivation of semiconductors

Eric Smith^{1,2}, Floyd McDaniel¹, Khalid Hossain², Wayne Holland², Terry Golding²

⁽¹⁾Ion Beam Modification and Analysis Laboratory, University of North Texas, Denton TX 76203, United States

⁽²⁾Amethyst Research, Inc., 123 Case Circle, Ardmore OK 73401, United States

Hydrogen passivation of semiconductor materials strongly affects their electronic properties and surface chemistry for material growth. More stable passivation can be achieved by the use of deuterium instead of hydrogen. A low temperature, photon-assisted deuterium passivation, which is inherently cleaner than traditionally used chemical or plasma-assisted techniques, is under investigation. Among other surface sensitive techniques, elastic recoil detection analysis (ERDA) and nuclear reaction analysis (NRA) will be used to study the surface passivation and contamination.

A 1.5 MeV $^4\text{He}^+$ beam incident on a deuterium passivated surface yields an ERDA spectrum with hydrogen (H) and deuterium (D) concentration profiles separated in recoil energy. This allows differentiating the D passivation from H, giving better understanding of the photon-assisted passivation process. The effect of varying passivation parameters on the isotopic exchange of hydrogen to deuterium will be presented. This work is supported by Oklahoma Center for Advancement in Science and Technology contract # OARS-7959.

PIXE as a complementary technique to RBS in thin film characterization

Johan Meersschaet¹, Marko Kayhko¹, Haraprasanna Lenka^{1,2}, Qiang Zhao², André Vantomme², Wilfried Vandervorst^{1,2}

⁽¹⁾Materials and Components Analysis, imec, Kapeldreef 75, Leuven BE-3001, Belgium

⁽²⁾Instituut voor Kern- en Stralingsfysica, K.U.Leuven, Celestijnenlaan 200 D, Leuven BE-3001, Belgium

To support further technological advancements, a continuous improvement of measurement and characterization techniques is essential. In certain cases, the thickness information obtained via Rutherford backscattering spectrometry (RBS) is limited, either due to a limited sensitivity (light elements), or due to signal interference from elements with a small mass difference. The potential contribution of particle induced X-ray emission (PIXE) in complement to RBS in characterizing thin films has been demonstrated before. We have explored the potential capabilities of PIXE on samples that are of importance in the microelectronics industry. For the PIXE measurements, we used 2.5 MeV He⁺ or 2.3 H⁺ beams, and a 30 mm² HPGe detector located at 45 degrees with the incoming beam. The PIXE results will be compared to Rutherford backscattering measurements obtained using (primarily) 1.5 MeV He and a standard PIPS detector at a scattering angle of 170 degrees.

Using a set of selected examples, we will illustrate the capability of PIXE in resolving and quantifying various elements in the sample, in situations where RBS has insufficient resolution or sensitivity. More particularly, the high sensitivity of PIXE will be illustrated in the case of samples containing trace amounts of S, Cl, Ar or As. The potential of PIXE to resolve the constituents with comparable elementary mass is illustrated on samples containing Co, Ni, and Cu. We will give an overview of the potential and the limitations of the PIXE technique, and of its complementarity to RBS and ERD. The use of PIXE to reduce the solution space of the RBS analyses will be illustrated.

Depth profiling of nitrogen within ¹⁵N-incorporated ultrananocrystalline diamond thin film

Elias Garratt¹, Salem AlFaify¹, David Cassidy¹, Amila Dissanayake¹, Derrick Mancini², Zihua Zhu³,
Manjula Nandasiri^{1,3}, Suntharampillai Thevuthasan³, Asghar Kayani¹

⁽¹⁾Physics, Western Michigan University, Kalamazoo MI 49008, United States

⁽²⁾Center of Nanoscale Materials, Argonne National Lab, Argonne IL 60439, United States

⁽³⁾EMSL, Pacific Northwest National Lab, Richland WA 99354, United States

In order to obtain a lucid picture of nitrogen distribution within nitrogen doped ultrananocrystalline diamond (UNCD) a direct measurement of nitrogen content and depth profiling was performed on a UNCD film deposited on a silicon substrate. This sample was prepared within a microwave plasma chemical vapor deposition (MPCVD) system with isotopic nitrogen, ¹⁵N, diluted within a highly ionized argon-methane growth atmosphere. To assess the elemental concentrations of the film ion beam analysis techniques were employed. The ion beam analysis determined the concentration of carbon to be 94.2 at% and hydrogen concentration to be 5.7 at%. To obtain a depth profile of ¹⁵N within the material proton induced gamma-ray emission, an ion beam analysis technique, and secondary ion mass spectrometry were performed. Additionally, proton induced gamma-ray emission, likely the first analysis of this kind used within this context, determined ¹⁵N concentration within the film to be on average 0.20 at%.

Detection and Profiling of carbon via the $^{13}\text{C}(\text{p},\text{g})^{14}\text{N}$ resonant reaction

Hassaram Bakhru^{1,2}, Arthur W Haberl¹, Wayne G Skala¹

⁽¹⁾*Ion Beam laboratory, University at Albany, 1400 Washington Avenue, Albany NY 12222, United States*

⁽²⁾*College of Nanoscale Science and Engineering, University at Albany, 1400 Washington Avenue, Albany NY 12222, United States*

We have tested and standardized the profiling of ^{13}C in various substrates, including silicon, by use of the $^{13}\text{C}(\text{p},\text{g})^{14}\text{N}$ resonance at 1.748 MeV. Depth resolution and interference factors will be shown. The large background due to silicon is not a significant difficulty for atomic concentrations of ^{13}C greater than 1%. Background from elements heavier than Si are present but not significant. We show the mechanical details and results of the analysis program ALLPROF which also develops depth profiles for the light elements H, Li, ^{11}B , ^{13}C , ^{14}N , ^{15}N , F, Na, Al and P. By extension, the program and our system can profile natural B, C and N via the assumed natural ratio of isotopes.

Preliminary experiments of hydrogen profiling on Carbon nanowalls using Resonant Nuclear Reaction Analysis

Ion Burducea^{1,2}, Liviu Stefan Craciun^{1,2}, Cristina Ionescu^{1,2}, Mihai Straticiu^{1,2}, Silviu Daniel Stoica^{2,3}, Alexandru Jipa², Petru Mihai Racolta¹

⁽¹⁾*Applied Nuclear Physics Department, Horia Hulubei National Institute of Physics and Nuclear Engineering IFIN-HH, 30 Reactorului St, Magurele Ilfov 077125, Romania*

⁽²⁾*Faculty of Physics, University of Bucharest, 405 Atomistilor St, Magurele Ilfov 077125, Romania*

⁽³⁾*National Institute for Laser, Plasma and Radiation Physics Bucharest, 409 Atomistilor St, Magurele Ilfov 077125, Romania*

The presence of hydrogen can have dramatic effects on the electrical, mechanical and chemical properties of many materials. Thus more precise knowledge of its presence in samples to be analyzed has a great importance. Carbon nanowalls (CNWs) are considered to be one of the most promising material for a wide range of applications including gas sensors, hydrogen storage devices and field emission displays. Among many possible techniques for hydrogen analysis, ion beam techniques have become popular and satisfy most analysis needs. However, the Resonant Nuclear Reaction Analysis (RNRA) technique is particularly attractive and powerful because of its inherent capability of providing an accurate and simple analysis of the hydrogen content in a sample. CNWs were obtained using an expanding argon radiofrequency discharge and injected with a small amount of acetylene in the presence of hydrogen as active gas. RNRA was applied on CNWs for hydrogen depth profiling.

[1] S. Vizireanu, L. Nistor, M. Haupt, V. Katzenmaier, C. Oehr, G. Dinescu, Carbon Nanowalls Growth by Radiofrequency Plasma-Beam-Enhanced Chemical Vapor Deposition, **Plasma Process. Polym.** 2008, 5, 263-268

[2] F. Xiong, F. Rauch, C. Shi, Z. Zhou, R. P. Livi and T. A. Tombrello, Hydrogen depth profiling in solids: A comparison of several resonant nuclear reaction techniques, **Nuclear Instruments and Methods in Physics Research B**, 27, 1987, pp. 432-441

[3] C. A. Barnes, J. C. Overley, Z. E. Switkowski and T. A. Tombrello, Measurement of hydrogen depth distribution by resonant nuclear reactions, **Applied Physics Letters**, Vol. 31, No. 3, 1977, pp. 239-241.

A full range detector for the HIRRBS high resolution RBS magnetic spectrometer

Wayne G Skala¹, Arthur W Haberl¹, Hassaram Bakhru^{1,2}, William Lanford^{1,3}

⁽¹⁾*Ion Beam Laboratory, University at Albany, 1400 Washington Avenue, Albany NY 12222, United States*

⁽²⁾*College of Nanoscale Science and Engineering, University at Albany, 1400 Washington Avenue, Albany NY 12222, United States*

⁽³⁾*Physics Department, University at Albany, 1400 Washington Avenue, Albany NY 12222, United States*

The UALBANY HIRRBS (High Resolution RBS) system has been updated for better use in rapid analysis. The focal plane detector now covers the full range from U down to O using a linear stepper motor to translate the 1-cm detector across the 30-cm range. Input is implemented with zero-back-angle operation in all cases. The chamber has been modified to allow for quick swapping of sample holders, including a channeling goniometer. A fixed standard surface-barrier detector allows for normal RBS simultaneously with use of the magnetic spectrometer. The user can select a region on the standard spectrum or can select an element edge or an energy point for collection of the expanded spectrum portion. The best resolution currently obtained is about 2-to-3 keV, probably representing the energy width of the incoming beam. Calibration is maintained automatically for any spectrum portion and any beam energy from 1.0 to 3.5 MeV. Element resolving power, sensitivity and depth resolution are shown using several examples. Examples also show the value of simultaneous conventional RBS.

Depth profiling of nitrogen within ¹⁵N-incorporated UNCD thin film deposited in Cr coated Silicon substrate

Salem AlFaify¹, Elias Garratt¹, Amila Dissanayake¹, David Cassidy¹, Derrick Mancini², Asghar Kayani¹

⁽¹⁾*Physics, Western Michigan University, Kalamazoo MI 49008, United States*

⁽²⁾*Center of Nanoscale Materials, Argonne National Lab, Argonne IL 60439, United States*

In order to obtain a picture of nitrogen distribution within N-doped ultrananocrystalline diamond (UNCD) film a content analysis and depth profiling of nitrogen was performed on UNCD sample. This sample was prepared with a microwave-plasma chemical-vapor deposition (MPCVD) system with isotopic nitrogen, ¹⁵N₂, diluted into a highly ionized argon-methane growth atmosphere. The sample was grown on Cr coated Si substrate. To investigate the micro and bonding structure of the sample, Raman spectroscopy and ion beam analysis techniques were employed. Analysis of the spectra confirmed the presence of crystalline carbon structures within the film. The ion beam analysis determined that the concentrations of nitrogen, carbon, and hydrogen were, for the UNCD film deposited on Si with Cr interlayer less than 1, greater than 75, and greater than 20 atomic percent respectively. Additionally, for the sample grown on a Cr interlayer, IBA techniques, specifically proton-induced gamma-ray emission, revealed there had been diffusion of chromium into the bulk of the material; which lead to a greater nitrogen incorporation; which was found to vary as a function of depth.

RBS diffusion-like elemental profiles and the degradation of thermally processed Ru and RuO₂/HfO₂/Si structures

V. Ukirde¹, C. Duk Lim¹, B. P. Sharma¹, M. El Bouanani^{1,2}

⁽¹⁾Material Science and Engineering, University of North Texas, 3940 North ELM street -Suite E-132, Denton TX 76207, United States

⁽²⁾Center for Advanced Research and Technology, University of North Texas, 3940 North ELM street -Suite E-132, Denton TX 76207, United States

Rutherford Backscattering Spectrometry (RBS) is a versatile and powerful tool used successfully for the characterization of thin films in the semiconductor industry. RBS depth profiling capabilities are routinely used for interfacial reaction and diffusion studies of multi-layered structures. It's often assumed that the elemental depth profiles extracted using RBS are from homogeneous structures and sometime may take into account roughness. A case study of pinhole formation following high temperature anneals of Ru/HfO₂/Si and RuO₂/HfO₂/Si and artifacts in RBS depth profiles will be presented. Special emphasis on pinhole formation-diffusion like profiles will be highlighted. Use of complementary characterization methods such as SEM and AFM are critical in elucidating interfacial reactions and diffusion phenomena in multi-layered nano-structures.

Development of MeV-SIMS imaging system with Electrostatic Quadrupole Lens

Toshio Seki^{1,4}, Sho Shitamoto¹, Shunichiro Nakagawa¹, Takaaki Aoki^{3,4}, Jiro Matsuo^{2,4}

⁽¹⁾Department of Nuclear Engineering, Kyoto University, Sakyo, Kyoto Kyoto 606-8501, Japan

⁽²⁾Quantum Science and Engineering Center, Kyoto University, Gokasyo, Uji Kyoto 611-0011, Japan

⁽³⁾Department of Electronic Science and Engineering, Kyoto University, Nishikyo, Kyoto Kyoto 615-8510, Japan

⁽⁴⁾CREST, Japan Science and Technology Agency (JST), Chiyoda, Tokyo 102-0075, Japan

The importance of imaging mass spectrometry (MS) for visualizing the spatial distribution of molecular species in biological tissues and cells is growing. SIMS imaging has been used to visualize elemental distribution at the cellular level because of its low molecular ion yield. In conventional SIMS with keV-energy ion beams, elastic collisions occur between projectiles and atoms in constituent molecules. The collisions break the molecules and produce fragments, which makes acquisition of molecular information difficult. In contrast, MeV-energy ion beams excite electrons and enhance the ionization of high-mass molecules, and a SIMS spectrum of ionized molecules can be obtained. In a previous study, we have developed a new system for imaging mass spectrometry using MeV-energy heavy ion beams, termed MeV-secondary ion mass spectrometry (MeV-SIMS), and demonstrated more than 1000-fold increase in molecular ion yield from a peptide sample (1154 Da), compared to keV ion irradiation. In addition, we successfully obtained mass spectrometric imaging of the deprotonated peptides (m/z 1153) without any matrix enhancement [1]. However, obtaining molecular imaging data at present, takes a long time, because the current density of the primary beam is not high enough. We have developed an electrostatic quadrupole lens to focus the swift heavy ion beam and reduce measurement time. Using this quadrupole lens, the current density increased by a factor of ~60 and we obtained an MeV-SIMS image of 100 x 100 pixels of protonated distearoyl phosphatidylcholine (DSPC) (m/z = 790.6) over a 4 mm x 4 mm field of view with a pixel size of 40 nm within 5 min, showing that the Q lens reduces measurement time of current imaging by a factor of ~30.

[1] Y. Nakata, et al. J. Mass Spectrom. (2009) 44, 128-136

Ambient Pressure Molecular Concentration Mapping Using Simultaneous MeV-SIMS and PIXE

Brian N Jones, Vladimir Palitsin, Geoff W Grime, Luke D Antwis, Roger P Webb
Surrey Ion Beam Centre, University of Surrey, Guildford Surrey GU12 5LY, United Kingdom

There has been a resurgence of interest in Plasm Desorption Mass Spectrometry¹ (PDMS -renamed MeV-SIMS) when it was shown that it can be used with a focussed beam² to produce images with a much higher spatial resolution than is currently possible with laser techniques such as MALDI (Matrix Assisted Laser Desorption Ionisation). It has also been demonstrated that the technique can be performed simultaneously with Heavy Ion PIXE measurements³. One of the limitations of SIMS techniques (including MALDI) is the effects of the matrix on the secondary ion yield which can make even relative measurements difficult and isotopic isomers which can even make trace elemental identification difficult, the combination with the PIXE elemental signals removes some of the ambiguity in these measurements.

A further recent development has been the demonstration that the Mass Spectrometry can be performed at pressures above the vapour pressure of water enabling SIMS to be performed on wet samples⁴.

We describe the new equipment being commissioned, which will allow simultaneous MeV-SIMS and PIXE to be collected in full ambient pressures with a micron beam resolution. We show examples of the work performed so far in vacuum as well as the preliminary results from the new instrument performed at atmospheric pressure.

1. J.Bergquist, P.Hakansson, B.Sunqvist, R.Zubarev, **Int J. Mass Spec.** **268**, 73-82, (2007)
2. Y.Wakamatsu, H.Yamada, S.Ninomiya, B.N.Jones, T.Seki, T.Aoki, R.P.Webb, J.Matsuo, **NIMB**, **269**, 2251-2253, (2011)
3. B.N.Jones, V.Palitsin, R.P.Webb, **NIMB**, **268**, 1714-1717, (2010)
4. J. Matsuo, S. Ninomiya, H. Yamada, K. Ichiki, Y. Wakamatsu, M. Hada, T. Seki, & T. Aoki, *Surf. & Interface Anal.*, **42**, 2010, 1612-1615

2D and 3D Quantitative Element Mapping using a Nuclear Microprobe

Tilo Reinert

Ion Beam Modification and Analysis Laboratory, Physics Department, University of North Texas, 1155 Union Circle #311427, Denton TX 76203, United States

There are not many analytical techniques that have the capability of quantitatively mapping elemental distributions with high sensitivity and lateral resolutions of about one micrometer or even below. Particle Induced X-ray Emission (PIXE) is often the method of choice when quantitative element mapping or microanalyses of trace elements are required. Therefore, PIXE studies are a major part of research projects on nuclear microprobes with increasing numbers of collaborations especially in the field of biomedical research. Consequently, the growing beam time requests increased the need for high throughput 2D element mapping capabilities. Today, state of the art nuclear microprobe systems provide the technology of mapping elemental distributions within a few minutes at high resolution. This advancement enabled the development of 3D quantitative analysis techniques like PIXE tomography, confocal PIXE, and PIXE stacking, or even high definition element mapping.

This contribution presents the current developments in the field of 2D and 3D quantitative element mapping with related applications.

MicroPIXE mapping of the metal content of microbial communities

Paolo Rossi^{1,2}, Bryan Carson¹, Barney L. Doyle¹, Cristiano Lino Fontana², Conrad D. James¹, Elebeoba May¹, Amy J. Powell¹, Eric Ackerman¹

⁽¹⁾Sandia National Laboratories, PO Box 5800, Albuquerque NM 87185, United States

⁽²⁾Department of Physics, University of Padua and INFN, Padova 35131, Italy

We have employed an ion microbeam to map the metal content in infectious disease applications (macrophage response to *Francisella tularensis* LVS infection) and samples from distinct microhabitats of the Sevilleta Long Term Ecological Research site in central NM. The dynamics and properties of both systems are traced through the measurement of variations in the metal concentration and location during various states of the system. The microbeam, part of the new Sandia Ion Beam Laboratory (IBL), is based on an Oxford focusing triplet of magnetic quadrupoles and delivers a 3 MeV proton beam. The line is served by a high intensity Pelletron that allows a current of 1 nA on sample. Analysis is performed by a very large solid angle PIXE Silicon Drift Detector, consisting of a circular crown of 12 separate low noise detectors placed upstream at 6 mm from the sample. The SDD, unique for its high sensitivity, has been jointly designed by the German Roentec company and the Sandia Department 1111 (Radiation-Solid Interactions). A measurement of scattered protons establishes the matrix composition and thickness, and allows the correction for the self-absorption of X-rays in the sample. Multi-elemental analysis allows accurate ratios among metals as required by this biological program, which are impossible to obtain with alternate methods. The proton irradiation has taken place in vacuum inside a scattering chamber, where both aqueous and dried samples (cells) are analyzed within a suitable holder. Aqueous samples are sandwiched between a 1 micrometer thick silicon-nitride membrane and a Kapton film. Charge gathered on the insulating sample during irradiation is neutralized by a thermo-ionic emission filament in order to lower the bremsstrahlung background. The paper describes the new IBL microPIXE system, its performance, including sensitivity and spatial resolution, and features that allow measurements of diverse biological samples. Early results are presented.

Sandia National Laboratories is a multi-program laboratory managed and operated by Sandia Corporation, a wholly owned subsidiary of Lockheed Martin Corporation, for the U.S. Department of Energy's National Nuclear Security Administration under contract DE-AC04-94AL85000.

Analysis of Roman glass from Illyricum

Ziga Smit^{1,2}, Deyan Lesigysarski³, Tina Milavec⁴, Milica Maric Stojanovic⁵, Fatos Tartari⁶

⁽¹⁾Faculty of mathematics and physics, University of Ljubljana, Jadranska 19, Ljubljana SI-1001, Slovenia

⁽²⁾Jozef Stefan institute, Jamova 39, Ljubljana SI-1001, Slovenia

⁽³⁾Faculty of chemistry, University of Sofia, James Bouchier 1, Sofia 1164, Bulgaria

⁽⁴⁾Department of archaeology, Faculty of arts, University of Ljubljana, Askerceva 2, Ljubljana SI-1001, Slovenia

⁽⁵⁾National museum Belgrade, Trg republike 1a, Belgrade, Yugoslavia

⁽⁶⁾Archaeological Institute, Tirana, Albania

The combined PIXE-PIGE analysis provides an efficient method for investigation of ancient glass - it is nondestructive and covers a wide range of elements from sodium to uranium, which represent major and trace constituents of glass in the form of oxides. Investigation of Roman glass should mainly answer the question of production centers. At least in Late Antiquity, the production of raw glass was concentrated in the region of Palestine and Egypt, while in the imperial age, glass could have also been produced in central Italy, south France, Spain and England. It is therefore interesting to inspect the Roman glass finds eastward of the Italian peninsula, in the region that was commonly known as Illyricum. During recent years, our analysis involves glasses from Albania, Bulgaria, Serbia and Slovenia. The analytical results match with the established groups of Roman glass, but also show smaller specific groups with different siliceous sand contribution, which may indicate small scale local production of raw glass.

Shear Modulus SEM Analysis of Leg Bones Exposed to Simulated Microgravity by Hind Limb Suspension (HLS)

Niravkumar D. Patel¹, Rahul Mehta¹, Nawab Ali², Michael Soulsby³, Parimal Chowdhury³

⁽¹⁾*Department of Physics and Astronomy, University of Central Arkansas, 201 Donaghey Avenue, Lewis Science Center 171, Conway AR 72035, United States*

⁽²⁾*Graduate Institute of Technology, University of Arkansas at Little Rock, 2801 S. University Avenue, Little Rock AR 72204, United States*

⁽³⁾*Department of Physiology and Biophysics, University of Arkansas for Medical Sciences, 4301 W. Markham St., Little Rock AR 72205, United States*

The aim of this study was to determine composition of the leg bone tissue of rats that were exposed to simulated microgravity by Hind-Limb Suspension (HLS) by tail for one week. The leg bones were cross sectioned, cleaned of soft tissues, dried and sputter coated, and then placed horizontally on the stage of a Scanning Electron Microscope (SEM) for analysis. Interaction of a 17.5 keV electron beam, incident from the vertical direction on the sample, generated images using two detectors. X-rays emitted from the sample during electron bombardment were measured with an Energy Dispersive Spectroscopy (EDS) feature of SEM using a liquid-nitrogen cooled Si(Li) detector with a resolution of 144 eV at 5.9 keV ($^{25}\text{Mn K}_\alpha$ x-ray). K_α - x-rays from carbon, oxygen, phosphorus and calcium formed the major peaks in the spectrum. Relative percentages of these elements were determined using a software that could also correct for ZAF factors namely Z(atomic number), A(X-ray absorption) and F(characteristic fluorescence). The x-rays from the control groups and from the experimental (HLS) groups were analyzed on well-defined parts (femur, tibia and knee) of the leg bone. The SEM analysis shows that there are definite changes in the hydroxyl or phosphate group of the main component of the bone structure, hydroxyapatite $[\text{Ca}_{10}(\text{PO}_4)_6(\text{OH})_2]$, due to hind limb suspension.

In a separate experiment, entire leg bones (both from HLS and control rats) were subjected to mechanical shear stress by mean of a variable force. The stress vs. strain graph was fitted with linear and polynomial function, and the parameters reflecting the mechanical strength of the bone, under increasing shear stress, were calculated. From the slope of the linear part of the graph the shear modulus for HLS bones were calculated and found to be 2.3 times smaller than those for control bones.

Ionic Liquid Matrix-Enhanced Secondary Ion Mass Spectrometry

Jennifer J Dertinger, Paul Kunnath, Amy V Walker

Materials Science and Engineering, University of Texas at Dallas, 800 W. Campbell Drive, RL 10, Richardson TX 75080, United States

Imaging mass spectrometry (MS) has the unique ability to acquire the spatial distribution of a wide range of atoms and molecules including polymers, pharmaceuticals, lipids, proteins, and semiconductors without the use of labels such as fluorescent tags. In recent years, the performance of SIMS for molecular analysis has greatly improved, but their application in imaging MS remains limited by the small number of analyte-specific ions that are obtained per sub-micron pixel. Here we describe our current work in using room temperature ionic liquids (ILs) as matrices for the enhancement of SIMS signals. ILs have many uses including in microextraction, and as solvents, lubricants and as matrices in matrix assisted laser desorption/ionization mass spectrometry (MALDI MS). Initial studies focused on the use of two different ionic liquids (ILs), derived from the MALDI matrix α -cyano-4-hydroxycinnamic acid (CHCA). The data clearly showed that ILs are extremely effective matrices in SIMS. Increases in molecular ion intensities of more than 2 orders of magnitude have been observed, as well as ~3 orders magnitude improvements in detection limits. Since the IL remains a liquid in vacuum, no "hot spots" are observed and so can be easily employed in imaging MS experiments. We shall also discuss our progress in understanding the mechanism of the molecular ion intensity enhancement, which involves proton transfer between the analyte and the ionic liquid.

Studying Liquid Interface In Situ by ToF-SIMS

Xiao-Ying Yu¹, Li Yang², Zihua Zhu³, Theva Thevuthasanand³, James Cowin²

⁽¹⁾*Atmospheric Sciences and Global Climate Change, Pacific Northwest National Laboratory, 760 6th St., Richland WA 99354, United States*

⁽²⁾*Chemical and Materials Sciences Division, Pacific Northwest National Laboratory, 760 6th St., Richland WA 99354, United States*

⁽³⁾*W. R. Wiley Environmental Molecular Science Laboratory, Pacific Northwest National Laboratory, 760 6th St., Richland WA 99354, United States*

A self-contained microfluidic-based device was designed and fabricated for **in situ** imaging of aqueous surfaces using vacuum techniques. The device is a hybrid between a microfluidic PDMS block and external accessories, all portable on a small platform (10 cm×8 cm). The key feature is that a small aperture with a diameter of 2-3 micrometers is opened to the vacuum, which serves as a detection window for **in situ** imaging of aqueous surfaces. Vacuum compatibility and temperature drop due to water vaporization are the two most important challenges in this invention. Theoretical calculations and fabrication strategies are presented from multiple design aspects. Results from the scanning electron microscope and time-of-flight secondary ion mass spectrometry (ToF-SIMS) of aqueous surfaces are presented. Newer devices are being developed to enable direct probing the electrode-electrolyte interface and the biofilm in its native liquid environment. Preliminary results will be presented to illustrate the potential of this new technique.

Molecular Imaging with Focused Cluster Ion Beams

Jiro Matsuo^{1,4}, Shinichiro Nakagawa¹, Matthieu Py^{1,4}, Takaaki Aoki^{3,4}, Toshio Seki^{2,4}

⁽¹⁾*Quantum Science and Engineering Center, Kyoto University, Gokasho, Uji 611-0011, Japan*

⁽²⁾*Department of Nuclear Engineering, Kyoto University, Sakyo, Kyoto 606-8501, Japan*

⁽³⁾*Department of Electronic Science and Engineering, Kyoto University, Nishikyo, Kyoto 615-8510, Japan*

⁽⁴⁾*CREST, Japan Science and Technology Agency (JST), Chiyoda, Tokyo 102-0075, Japan*

Molecular depth profiling and molecular imaging with Ar cluster beam is one of the most promising applications for SIMS, because the cluster ion beams have a high secondary ion yield and induce less damage on surfaces than other techniques [1]. A new SIMS imaging system with focused Ar cluster ion beam has been developed [2]. An orthogonal acceleration time-of-flight (oa-TOF) mass spectrometer, which allows the use of a continuous beam, was employed in a new bio-imaging system. Because there is no need to use the ion-bunching technique in this system, it is possible to eliminate tradeoff between beam diameter and mass resolution, which is inevitable in mass-imaging with conventional ToF-SIMS system. SIMS spectra of biological samples obtained with Ar cluster ions are quite different from those obtained with Bi₃ ions. Lipid molecular ions found in the mass range over 600 Da, are clearly observed with Ar cluster ions. Furthermore, the background level of the spectra obtained with Ar cluster ions is much lower than with Bi₃ ions, and this is attributed to the lower velocity of the primary ions.

The latest results obtained with this system and its performance in molecular imaging of cells and tissues will be presented and discussed in comparison of .

This work is supported by the Core Research of Evolutional Science and Technology (CREST) of Japan Science and Technology Agency (JST).

[1] J. Matsuo, S. Ninomiya, H. Yamada, K. Ichiki, Y. Wakamatsu, M. Hada, T. Seki and T. Aoki, *Surf. Interface Anal.*, 42, (2011), 1612

[2] K. Ichiki, J. Tamura, T. Seki, T. Aoki and J. Matsuo, *Surf. Interface Anal.* (accepted)

Ag Diffusion in Single Crystal Silicon Carbide

Haizhou Xue¹, Yanwen Zhang^{1,2}, Zihua Zhu³, Shuttha Shutthanandan³, Lance L Snead², William J Weber^{1,2}

⁽¹⁾Department of Materials Science and Engineering, University of Tennessee, Knoxville Tennessee 37996, United States

⁽²⁾Materials Science & Technology Division, Oak Ridge National Laboratory, Oak Ridge Tennessee 37831, United States

⁽³⁾Pacific Northwest National Laboratory, P.O. Box 999, Richland Washington 99352, United States

For the application of the tristructural isotropic (TRISO) fuel particles in high-temperature gas cooled nuclear reactors (HTGRs), it is a key issue to understand the release mechanism of radioactive ^{110m}Ag through the SiC coating. In this work, Ag ion implantation in 4H single crystal SiC implantation was carried out to produce Ag profiles at different depths from the sample surface. High temperature annealing was performed on the as-irradiated samples to study the possible out-surface diffusion of Ag. Before and after annealing, Rutherford backscattering spectrometry (RBS) and secondary ion mass spectrometer (SIMS) measurements were employed to obtain the elemental profiles of the irradiated samples. An out-surface diffusion is observed that suggests Ag prefers moving to the surface rather than diffusing into the SiC bulk. During annealing, SiO₂ layers are formed on top of the SiC surfaces, and no Ag concentration is found in the SiO₂ layers. The results indicate that SiO₂ may serve as an effective barrier to keep ^{110m}Ag from release from the TRISO coated particles.

Development of Advanced SIMS Single Stage Accelerator Mass Spectrometer Instrument at the Naval Research Laboratory

K. Fazel, K. Grabowski, D. Knies, G. Hubler

Naval Research Laboratory, Bldg. 74, Rm. 110 4555 Overlook Ave. S.W., Washington DC 20375, United States

The Naval Research Laboratory (NRL) will be constructing a SIMS Single Stage Accelerator Mass Spectrometer (SSAMS) instrument starting at the end of 2013 for use with nuclear forensics, cosmology, and other applications. The instrument will enable analysis of both positive and negative ions, and will have a molecular destruction capability. These features will address our goal to improve sensitivity and precision of select species, broaden the range of elements and isotopes to measure, and ease sample chemical pre-processing requirements.

To provide these features, the front portion of a Cameca IMS 6f will be combined with an NEC SSAMS system. The NEC SSAMS system will include a bipolar 300-kV air insulated single stage accelerator, custom multi-port 90° high mass resolution injection magnet ($ME/Z^2 = 2.6 \text{ amu-MeV}$), 90° double focusing analysis magnet ($ME/Z^2 = 75 \text{ amu-MeV}$), electrostatic spherical analyzer, and a molecular ion dissociator. High-speed electrostatic switching is also included in both magnets to allow high efficiency and precision of measurements of small sample particles. The multi-port injector magnet enables nearly continuous matrix normalization over a large mass range without having to change the magnetic field of the injector. The bipolar power supply for the accelerator allows measurement of both electropositive and electronegative elements, while the molecule destruction feature minimizes molecular interferences. Access to electropositive elements should provide improved sensitivity for rare earth elements, Uranium, and Plutonium. Before NRL can apply the instrument, the fundamentals of the instrument must be established.

The fundamentals include establishing molecular destruction cross sections of anticipated molecular ions, charge state distributions, overall transmission, and molecule fragment patterns. Upon establishing the performance characteristics of the instrument, the NRL SIMS-SSAMS will be unique tool able to better understand the constituents of an unknown material in nuclear forensics, cosmology, and other applications.

ToF-SIMS and NanoSIMS Imaging of Uranium Distributions in the Sediment of Hanford Site

Zihua Zhu, Zheming Wang

Environmental Molecular Sciences Laboratory, Pacific Northwest National Laboratory, 902 Battelle Boulevard, P.O. Box 999, MSIN K8-93, Richland WA 99352, United States

Nuclear materials processing over the past seventy years has left approximately 55 million gallons of nuclear wastes stored in underground tanks at Hanford site. Some of these wastes are leaking into the ground and the DOE has been working on developing remediation technologies. As a part of these activities, sediment samples have been extensively studied to understand chemical speciation and aqueous mineral chemistry. Although concentrations and distributions of radioactive elements, such as uranium (U), plutonium (Pu), and technetium (Tc) are of great interest, U is the most important one because its concentration in the wastes is significantly higher compared to other radioactive elements. Previous studies show that the sediment samples contain low concentration of U (<10 ppm). However, non-uniform distribution of U is found, and the U appears to be mainly in micron- or sub-micron-size particles. Although an understanding of the chemistry and speciation of these particles is important, it is extremely difficult to obtain the composition of these particles using conventional analytical capabilities such as AES, XPS, and SEM/EDX because of the low concentration of U in the samples. Secondary ion mass spectrometry (SIMS) can be effectively used to discover the chemical components of these U-containing particles with excellent sensitivity and decent spatial resolution. We used ToF-SIMS and Nano-SIMS to image some of these U-containing particles in the sediment samples. Preliminary results indicated that U was present across the sample at lower concentrations, while spots of sub-micron particles with much higher U concentrations were irregularly distributed. The major elements in these "hot" spots appeared to be uranium, sodium, phosphorus, and oxygen.

Nuclear stopping power and its impact on ion beam modification

Helmut Paul

Atomic and Surface Science, University of Linz, Altenbergerstrasse 69, Linz A 4040, Austria

As already noted by Behar et al. in the nineties, the penetration depth of heavy ions into light targets is often much larger than predicted by Ziegler's SRIM program. Evidently, SRIM stopping power must be too high at low energy in these cases. This leads to the question: are there any stopping power measurements that show this directly? There are a few, indeed. We first discuss the description of nuclear stopping in SRIM, and then discuss these examples. Naturally, the contribution of nuclear stopping is large in these cases. Assuming that SRIM nuclear stopping is correct, we find that indeed, SRIM electronic stopping is much too high at low energy.

Controlling the structure and size of nanoparticles by ion modification

Weixing Li¹, Yanbin Chen², Jiaming Zhang³, Lumin Wang⁴, Rodney C. Ewing⁵

⁽¹⁾*Departments of Earth & Environmental Sciences, Materials Science & Engineering, and Nuclear Engineering & Radiological Sciences, University of Michigan, Ann Arbor Michigan 48109, United States*

⁽²⁾*Department of Nuclear Engineering and Radiological Sciences, University of Michigan, Ann Arbor Michigan 48109, United States*

⁽³⁾*Departments of Earth & Environmental Sciences, University of Michigan, Ann Arbor Michigan 48109, United States*

⁽⁴⁾*Departments of Materials Science & Engineering, and Nuclear Engineering & Radiological Sciences, University of Michigan, Ann Arbor Michigan 48109, United States*

⁽⁵⁾*Departments of Earth & Environmental Sciences, Materials Science & Engineering, and Nuclear Engineering & Radiological Sciences, University of Michigan, Ann Arbor Michigan 48109, United States*

The performance of nanoparticles in the near-surface regions of a matrix depends strongly on two factors: the size of the nanoparticles, and the contact structure of the nanoparticles with the matrix. By combining *in situ* thermal annealing with transmission electron microscopy, we have directly observe that Au nanoparticles, which were originally fully embedded in the near-surface region of Au ion-implanted TiO₂, can be tailored into hemispheres exposed at the surface that are favorable for catalytic applications. Precise control of the size of the Au hemispheres can be achieved by subsequent low-energy ion sputtering. Control over the microstructure and size of nanocrystals by thermal processing and ion sputtering provides a new method by which the catalytic properties of these nanocomposites can be improved. The same technique can be used to create novel devices that have similar spatial and size requirements at the nanoscale.

Ion Irradiation effects on Mn-doped ZnO films

N. Matsunami¹, S. Okayasu², M. Sataka², H. Kakiuchida³

⁽¹⁾*EcoTopia Science Institute, Nagoya University, Furo-cho, Chikus-ku, Nagoya 464-8603, Japan*

⁽²⁾*Japan Atomic Energy Agency, Naka-gun, Shirakata, Tokai 319-1195, Japan*

⁽³⁾*National Institute of Advanced Industrial Science and Technology, Shidami, Nagoya 463-8560, Japan*

Mn(5%)-doped ZnO films, which were grown on SiO₂ and Al₂O₃ substrates by means of sputter deposition method are irradiated with 100 MeV Xe ions at room temperature. We have measured X-ray diffraction (XRD), optical absorption and magnetic property as the function of the ion fluence. We find the reduction of the XRD intensity to 1/5 of the unirradiated intensity at the ion fluence of $2 \times 10^{15} \text{ cm}^{-2}$, the lattice compaction of 0.6 % at $2 \times 10^{15} \text{ cm}^{-2}$, little bandgap shift ($< 0.02 \text{ eV}$ at $2 \times 10^{14} \text{ cm}^{-2}$). We also find that temperature (T) dependence of the magnetic susceptibility (χ) follows the Curie law: $\chi = \chi_0 + C/T$ and the Curie constant C increases to $8 \times 10^{-3} \text{ emu cm}^{-3} \text{ K}^{-1}$ at 10^{15} cm^{-2} . Measurements of electrical properties are under way.

Three-dimensional characterization of Heavy ion irradiation effects using Atom Probe Tomography

Arun Devaraj, Robert Colby, Shutthanandan Vaithiyalingam, Suntharampillai Thevuthasan
Environmental Molecular science Laboratory, Pacific Northwest National Laboratory, 902 Battelle Boulevard, Richland WA 99354, United States

The development of three-dimensional, high spatial and mass resolution characterization techniques is important for several materials in energy and environmental applications. The recently developed laser assisted atom probe tomography (APT) technique offers the opportunity to perform analysis of materials including metals, semiconductors and dielectrics, with sub-nanometer spatial resolution and ppm-level mass resolution. Heavy ion irradiation of thin films and bulk oxides, using Au or Ag ions, is expected to generate radiation induced intermixing, point defects and incorporation of metallic ions into the host lattice. Short duration, high temperature annealing of such irradiated structures leads to the formation of embedded metallic nanoparticles and nanoscale defect clusters. With about 0.2 nm spatial resolution in three dimensions and ppm-level mass sensitivity, APT is uniquely suited to characterize such heavy ion irradiation effects in a variety of materials. Samples for APT are prepared by a focused ion beam lift-out procedure, facilitating analysis of an entire ion implantation profile using a single sample. To demonstrate the application of APT, case studies from heavy ion irradiations in thin films and bulk oxides will be presented. APT studies on Au irradiated, MBE grown single crystal Cr thin films on MgO substrates will be utilized to highlight the benefits of APT in terms of spatial resolution and composition sensitivity over Rutherford backscattering. Additionally, the unique benefit of APT in distinguishing the chemical intermixing and topography at rough interfaces will be presented. Another case study presented will be high resolution characterization of metal nanoparticles and vacancy clusters embedded in bulk oxides generated by Au ion implantation and subsequent annealing, using a combination of aberration-corrected STEM and APT. With these case studies an overview of the procedure, advantages and challenges towards characterizing heavy ion irradiation effects using APT will be provided.

New Cluster Ion Beams or Traditional Monatomic Ion Beam -Primary Ion Beam Choices in ToF-SIMS Analysis

Zihua Zhu, Vaithiyalingam Shutthanandan, Ponnusamy Nachimuthu, Mark Engelhard
Environmental Molecular Sciences Laboratory, Pacific Northwest National Laboratory, 902 Battelle Boulevard, P.O. Box 999, MSIN K8-93, Richland WA 99352, United States

Time-of-flight secondary ion mass spectrometry (ToF-SIMS) is a powerful surface analysis tool. It has been used in scientific research and semiconductor industry for more than 30 years. Traditionally, liquid metal ion sources (Ga^+ , In^+) are used as analysis ion sources, and O_2^+ / Cs^+ sources are used as sputtering ion sources if depth profiling analysis is performed. During the last 10 years, cluster ion sources, such as metal cluster ions (Au_n^+ , Bi_n^+), SF_5^+ , C_{60}^+ , C_nH_m^+ and Ar cluster ions (Ar_n^+ , $n>500$), have been developed. They can provide 10-1000 times enhancement for organic molecule ion signals if used as analysis beams. More important, molecular depth profiling is possible if SF_5^+ , C_{60}^+ , C_nH_m^+ and Ar_n^+ are used as sputtering ions. Almost all new ToF-SIMS instruments on current market are equipped with one or more these cluster ion sources. However, the cluster ion source option may lead to some new questions: Are cluster ion analysis beams are better choices than traditional monatomic ion beams for all ToF-SIMS analysis? If not, are there any basic rules to select primary ion beam? In this presentation, I will use my personal experience to describe how to choose primary ion beams in ToF-SIMS analysis. Three representative scenarios will be discussed: (1) Surface spectra and imaging, (2) Traditional elemental depth profiling, and (3) Molecular depth profiling.

Electrical activation and electron spin resonance measurements of implanted bismuth in silicon-28

Thomas Schenkel¹, Christoph D. Weis¹, Cheuk Chi Lo², Jeffrey Bokor², Steven A. Lyon⁴, Alexei M. Tyryshkin⁴,
John J. L. Morton³, Volker Lang³, Richard E. George³, Kin M. Yu¹

⁽¹⁾*Lawrence Berkeley National Laboratory, 1 Cyclotron Road, 5-121, Berkeley CA 94720, United States*

⁽²⁾*Department of Electrical Engineering and Computer Sciences, University of California, Berkeley, Berkeley CA 94720, United States*

⁽³⁾*University of Oxford, Oxford OX1 3PH, United Kingdom*

⁽⁴⁾*Department of Electrical Engineering, Princeton University, Princeton NJ 08544, United States*

Spins of donor electrons and nuclei in silicon exhibit long coherence times and their potential integration with nanoscale spin readout devices and control electrodes make them attractive quantum bit candidates. Most studies on donor spins in silicon have been performed with phosphorus. Bismuth, the heaviest donor in silicon, has potential advantages due to its high mass (which reduces straggling during ion implantation) and larger nuclear spin and hyperfine coupling (enabling complex nuclear spin memory schemes and rapid nuclear spin initialization). But much less is known about the electrical activation and damage repair of bismuth following ion implantation into silicon, compared to more common donors. We have performed continuous wave and pulsed electron spin resonance measurements of implanted bismuth donors in isotopically enriched silicon-28. Donors are electrically activated via thermal annealing with minimal diffusion. Damage from bismuth ion implantation is repaired during thermal annealing as evidenced by narrow spin resonance line widths (~12 micro Tesla) and long spin coherence times ($T_2=0.7$ ms, at a temperature $T=8$ K). The results qualify ion implanted bismuth as a promising candidate for spin qubit integration in silicon [1, 2].

This work was supported by the U.S. National Security Agency under 100000080295 and by DOE under Contract No. DE-AC02-05CH11231.

[1] C. D. Weis, et al., Appl. Phys. Lett. 100, 172104 (2012)

[2] T. Schenkel, et al., arXiv: 1110.2228v1

Power Coupling Effect on Microwave Plasma Ion source Utilizing Double-port Rectangular Cavity Resonator

Yuna Lee, Yeong-shin Park, Jeong-jeung Dang, Kyoung-Jae Chung, Y. S. Hwang

*Energy System Engineering, Seoul National University, 30-117, Dept. of Nuclear Engineering, Seoul National University,
599 Gwanak-Ro, Gwanak-Gu, Seoul 151-744, Korea*

Microwave plasma ion source with a rectangular cavity resonator utilizing double-port wave launchers have been examined to enhance ion beam current by varying cavity length. The rectangular cavity resonator is designed to make TE-103 mode, maximizing the resonance electric field for generating plasma efficiently, and control the cavity length by installing movable doors. Plasma densities are measured by Langmuir probe, and the ratio of the forward power to magnetron power (power coupling efficiency) is measured by directional coupler installed between resonator and magnetron, as varying the cavity length at fixed magnetron power. It is found that optimal cavity length for maximum power coupling efficiency is shorter than that for plasma generation. Plasma density is also found to be proportional to the power coupling efficiency. As changing the cavity length, the ion beam currents are obtained by Faraday cup, at different magnetron power and gas pressure. Regardless of the operating power and pressure, the higher current ion beams are extracted at optimal cavity length. In this study, the length-tunable cavity resonator is shown to enhance the ion beam current with increasing the power coupling efficiency.

C irradiation of Ru ultra-thin films for enhanced Cu diffusion barrier

B. P. Sharma¹, V. C. kummari², P. R. Paudel¹, B. Rout², F. D. McDaniel², M. El Bouanani^{1,3}

⁽¹⁾Material Science and Engineering, University of North Texas, 3940 N. Elm Street-suite E-132, Denton TX 76207, United States

⁽²⁾Department of Physics, University of North Texas, 1115 Union Circle # 311427, Denton TX 76203, United States

⁽³⁾Center for Advanced Research and Technology, University of North Texas, 3940 N. Elm Street- suite E-132, Denton TX 76207, United States

Thin film stacked layers of Ta/TaN are well established diffusion barrier material for copper interconnects applications in semiconductor industries. However, aggressive demand for downscaling integrated circuit technology to giga-scale feature sizes requires ultrathin diffusion barrier of thickness below 5 nm. This presents many challenges for the current Ta/TaN stack and a concerted effort has been going on in many laboratories to ideally develop a single effective diffusion barrier layer without the need for a currently used seed layer for copper electro fill. One attractive solution is to use less than 5 nm Ru thin films that are demonstrated to be good for copper plating but not effective as a diffusion barrier beyond 300C anneals. The failure of these ultra thin Ru diffusion barriers was speculated to be due to Ru silicide formation.

The aim of the present investigation is to show that the crystalline structure of the Ru thin films is a critical parameter. The most desirable diffusion barriers are expected to be stable amorphous materials that are free from grain boundaries. The amorphization of 5 nm Ru on SiO₂/Si samples was carried out using a 60 keV carbon irradiation at a fluence of 1×10^{17} atoms/cm². A 20 nm Cu layer was thermally evaporated on the Ru/SiO₂/Si samples and subsequently annealed in nitrogen at temperatures up to 400 °C. X-ray diffraction (XRD) was used to determine the Ru crystalline structure and Rutherford backscattering spectroscopy (RBS) to evaluate the effectiveness of the carbon amorphized Ru diffusion barrier. The performance and enhancement of amorphized Ru diffusion barrier for copper interconnect will be presented.

Session Overview: The Future of Particle Therapy in Medicine; The Next Likely Steps

Richard P Levy

Advanced Beam Cancer Treatment Foundation, PO Box 2356 (887 Wildrose Circle), Lake Arrowhead CA 92352-2356, United States

As conformal irradiation has become more widely accepted, treatment with protons and heavier charged particles has gained widespread use. All charged particles have intrinsic 3-D dose distribution properties, tightly conforming to targets with rapid dose fall-off in surrounding tissues. After almost four decades and more than 75,000 patients, protons and helium nuclei, with relatively low linear-energy-transfer (LET) properties similar to X-rays, have demonstrated good results for many tumor types. However, up to 20% of tumors have proven resistant to low-LET irradiation. For these tumors, high-LET treatment with heavier-ions (e.g., carbon) offers great potential benefit. High-LET particles have increased relative biological effectiveness (RBE), reaching maximum effect within the Bragg peak at the target volume. Irradiation with heavier ions offers the unique combination of excellent 3D-dose distribution and increased RBE at the target. Dose-fractionation studies have demonstrated that high-LET radiation can treat some tumors with fewer fractional doses than is safe with lower-LET particles.

More cost-efficient and compact design of proton systems will make treatment available to more patients. In parallel, heavier ion therapy provides further tools for treatment of radioresistant tumors, as well as for treatment with fewer fractions for many tumor types. Some cancers may be better treated with a combination of lower-LET particles for the clinical target volume, and high-LET particles to treat the gross tumor. The future of heavy charged particle therapy will be best realized by clinical trials with ready access to top-quality delivery of both protons and heavier ions, and which will permit randomized-trial comparison of various ions for different diseases. Optimal results will require: (1) sophisticated target delineation that integrates CT, MRI and PET imaging; (2) reliable RBE modeling algorithms; (3) efficient beam-scanning technology that compensates for organ movements; (4) online beam control proximal to and within the patient; and (5) better understanding of dose-fractionation parameters.

Positron differential studies: comparison to photoionizationANTONIO C F SANTOS¹, ROBERT DEAN BUBOIS²⁽¹⁾*Departamento de Física Nuclear, Universidade Federal do Rio de Janeiro, Caixa Postal 68528, Rio de Janeiro, RJ, Rio de Janeiro RJ 21941-972, Brazil*⁽²⁾*Department of Physics, Missouri University of Science and Technology, 102 Physics Bldg, 1315 N Pine St., Rola Mo 65409, United States*

Differential studies of double ionization of atomic and molecular systems by positron and electron impact and their comparison to photoionization data provides a peculiar mode to examine the effects of electron-electron interaction. One approach is based on separating the physical mechanisms which provides peculiar signatures in the associated cross sections. In the TS-1 mechanism also termed adiabatic double ionization, it is assumed that the first electron absorbs the energy lost by the projectile and afterwards collides with the second electron. The TS-1 mechanism is dominant at lower energy excess above the double ionization threshold. Another mechanism, the shake-off (SO) or sudden ionization. It explains the finite constant value that the double-to-single ionization cross sections ratio approaches asymptotically. In this work, we attempt to clarify the roles of SO and TS-1 mechanisms by studying the differential double ionization cross sections by 500 eV positron impact on argon and comparing it to photoionization data.

Recent progress in understanding resonant annihilation of positrons on moleculesAdric C. L. Jones, James R. Danielson, Mike R. Natisin, Cliff M. Surko*Physics Department, University of California, San Diego, 9500 Gilman Drive, La Jolla, San Diego CA 92093-0319, United States*

At energies below the positronium formation threshold, the annihilation of positrons on most molecules is dominated by a resonant attachment process. This process is facilitated by the excitation of a vibration and the existence of a positron bound state, and it enhances annihilation rates by orders of magnitude. Major features of this process are well predicted by a vibrational Feshbach resonance model (VFR) [1] that predicts resonant annihilation at energies corresponding to those of the fundamental vibrational modes, downshifted by the binding energy. This process involves a positron with energy ε , incident on a molecule with a bound state of energy ε_b , exciting a vibrational mode of energy ε_v . This reaction is resonant when the incident energy of the positron is equal to that of the vibration, minus the binding energy, **i.e.**, when $\varepsilon = \varepsilon_v - \varepsilon_b$.

For small molecules the model generally predicts most of the observed spectral weight [2], while enhancements are seen in larger molecules, presumably due to intramolecular vibrational redistribution (IVR) [2]. Recently, a new, and seemingly ubiquitous, broad spectral component has been observed, apparently due to VFRs involving multimode vibrations. A model incorporating these modes, statistical multimode resonant annihilation (SMRA) [3], predicts such a spectrum. This feature is seen, at some level, in the spectra of all molecules with bound states studied to date. The broader implications of these resonant annihilation phenomena, and particularly the SMRA, will be discussed.

This work is supported by NSF grant no. PHY 1068023.

[1] G. F. Gribakin & C. M. R. Lee, (2006) **Phys. Rev. Lett.** **97**, 193201.

[2] G. F. Gribakin, J. A. Young & C. M. Surko, (2010) **Rev. Mod. Phys.** **82**, 2557.

[3] A. C. L. Jones, **et al.** (2012) **Phys. Rev. Lett.** **108**, 093201.

Measurement of the spectra of low energy electrons resulting from Auger transitions induced by the annihilation of low energy positrons implanted at the Ag(100) surface

Karthik Shastry, Prasad Joglekar, A. H. Weiss, N. G. Fazleev

Physics, The University of Texas at Arlington, Box 19059, Arlington TX 76019-0059, United States

A few percent of positrons bound to a solid surface annihilate with core electrons resulting in highly excited atoms containing core holes. These core holes may be filled in an auto-ionizing process in which a less tightly bound electron drops into the hole and the energy difference transferred to an outgoing "Auger electron." Because the core holes are created by annihilation and not impact it is possible to use very low energy positron beams to obtain annihilation induced Auger signals that have little or none of the large impact induced secondary electron background that interferes with measurements of the low energy Auger spectra obtained using the much higher incident energies necessary when using electron or photon beams. In this talk we present the results of measurements of the energy spectrum of low energy electrons emitted as a result of Positron Annihilation Induce Auger Electron Emission [1] from a clean Ag (100) surface. The measurements were performed using the University of Texas Arlington Time of Flight Positron Annihilation induced Auger Electron Spectrometer (T-O-F-PAES) System [2]. A strong double peak was observed at ~35eV corresponding to the N2VV and N3VV Auger transitions in agreement with previous PAES studies [3]. The T-O-F system allowed us to observe for the first time, much less intense, PAES peaks, at ~260eV, and 350eV, which we attribute to the M4,5N1V, and M4,5VV Auger transitions, respectively. Measurements of the intensities of the peaks were used to estimate of the annihilation probabilities of positrons trapped in an image potential state at the Ag(100) surface with the 3d and 4p core levels of Ag.

[1] A. Weiss, R. Mayer, M. Jibaly, C. Lei, D. Mehl, and K.G. Lynn, **Phys. Rev. Lett.** **61**, 2245 (1988).

[2] S. Xie, Ph.D. thesis, University of Texas at Arlington, (2002).

Materials Characterization of Free Volume and Void Properties by Two-Dimensional Positron Annihilation Spectroscopy

Hongmin Chen¹, J. David Van Horn¹, Y.C. Jean¹, Wei-Song Hung^{2,3}, Kuier-Rarn Lee^{2,3}

⁽¹⁾*Department of Chemistry, University of Missouri - Kansas City, 5009 Rockhill Road, Kansas City MO 64110, United States*

⁽²⁾*Department of Chemical Engineering, Chung Yuan Christian University, Chung Li, Taiwan*

⁽³⁾*R&D Center for Membrane Technology, Chung Yuan Christian University, Chung Li, Taiwan*

Positron annihilation spectroscopy (PAS) has been widely used to determine the free volume and void properties in polymeric materials. Recently, a two dimensional positron annihilation spectroscopy (2D-PAS) system has been developed for membrane applications. The system measures the coincident signals between the lifetime and the energy which could separate the 2γ and 3γ annihilations and improve the accuracy in the determination of the free volume and void properties. When 2D-PAS is used in coupling with a variable mono-energy slow positron beam, it could be applied to a variety of material characterization. An example of multi-layer polymer membrane characterization using 2D-PAS will be presented.

INTERACTION OF LIGHT PARTICLES WITH CAPILLARIES

K. Tokesi¹, R. D. DuBois²

⁽¹⁾*Institute of Nuclear Research of the Hungarian Academy of Sciences (ATOMKI), Debrecen H-4001, Hungary*

⁽²⁾*Department of Physics, Missouri University of Science and Technology, Rolla MO, United States*

Since the discovery of the new phenomenon, namely "guiding" of charged particles through insulating capillaries, the research activities in the field of charged particle physics have turned to the investigation of charged particles interactions with inner surfaces based on various insulating capillaries from nano- to micrometer size. Work in this field is strongly motivated because the new knowledge holds the possibility of many technical applications for surface diagnostics and spectroscopy in understanding material damage and surface modification. It can also be useful in medical research like in cancer therapy using focused charged particle beam and last but not least in producing antimatter.

Ion guiding through the capillary ensues as soon as a dynamical equilibrium of self-organized charge-up by the ion beam, charge relaxation and reflection is established. We believe that our knowledge of guiding by highly charged ions (HCI) is adequate. At the same time, however, although during the past few years many research groups joined to this field of research many details of light particle guiding are still unknown.

In this work we focus on the transmission of light particles, like positrons and electrons, through a single cylindrical and tapered glass capillary with large aspect ratio. A unique feature of our investigations is the use of the combination of light projectiles with single capillaries. We try to get the answer whether the guiding-effect is still observable for low intensity positron beams. In other words, can the required electric field inside a macroscopic capillary be generated in order for guiding to occur? If the guiding field can form, what are the maximum capillary tilt angles for the transmission of positrons? Our results for positron guiding will be compared with the corresponding electron and HCI data.

This work supported by the Hungarian Scientific Research Fund OTKA No. NN 103279.

The Intense Slow Positron Beam Facility at the PULSTAR Reactor and Applications in Nano-Materials Study

Ming Liu¹, Jeremy Moxom¹, Ayman I. Hawari¹, David W. Gidley²

⁽¹⁾*Nuclear Reactor Program, Department of Nuclear Engineering, North Carolina State University, P.O. Box 7909, Raleigh NC 27695, United States*

⁽²⁾*Department of Physics, The University of Michigan, 450 Church Street, Ann Arbor MI 48109, United States*

An intense slow positron beam has been established at the PULSTAR nuclear research reactor of North Carolina State University. The slow positrons are generated by pair production in a tungsten moderator from gamma-rays produced in the reactor core and by neutron capture reactions in cadmium. The moderated positrons are electrostatically extracted and magnetically guided out of the region near the core. Subsequently, the positrons are used in two spectrometers that are capable of performing positron annihilation lifetime spectroscopy (PALS) and positron Doppler broadening spectroscopy (DBS) to probe the defect and free volume properties of materials. One of the spectrometers (e+PALS) utilizes an rf buncher to produce a pulsed beam and has a timing resolution of 277ps. The second spectrometer (PsPALS) uses a secondary electron timing technique and is dedicated to positronium lifetime measurements with a ~0.5ns timing resolution. PALS measurements have been conducted in the e+PALS spectrometer on a series of nano-materials including organic photovoltaic thin films, membranes for filtration, and polymeric fibers. The results have illustrated the utility of positrons in understanding some critical issues related to the development of the examined nano-materials.

Positron production using a 1.7 MV Pelletron Accelerator

KATIANNE F ALCANTARA, PAOLO CRIVELLI, ANTONIO C F SANTOS

Departamento de Física Nuclear, Universidade Federal do Rio de Janeiro, Caixa Postal 68528, Rio de Janeiro, RJ, Rio de Janeiro RJ 21941-972, Brazil

We report the foremost phase of a fourth generation positron source, being constructed at Universidade Federal do Rio de Janeiro. Positron yields are reported by making use of the $^{19}\text{F}(p,a)^{16}\text{O}$ reaction, where the fluorine target is in the form of a CaF_2 target. Although the idea of obtaining this source of positrons was proposed in 2001 [1], it had not been tested so far. Positron production has been observed by detecting 511 keV annihilation gamma rays emerging from the irradiated CaF_2 target. The source is based on the reaction $^{19}\text{F}(p,a)$, which has resonances around 2.0 MeV [2]. Positrons and electrons pairs are produced via the nuclear decay of a state of short-lived (70 ps) of a core. The fluorine target in the form of CaF_2 . In the internal nuclear conversion, the decay energy is shared equally between the electron and positron due to their equivalent masses. The most probable energy of the positron is 2.5 MeV, with a broad distribution due to the conservation of energy and momentum. The advantages of this source is the absence of intense background radiation due to bremsstrahlung as observed in high energy electrons induced sources. It also mimics long life sources like ^{22}Na if one continues the proton bombardment. Another advantage of this source is the fact that it can be turned off in the sense that after the proton beam is turned off, the source activity drops significantly. In this paper, we report positron yields as a function of the incident proton energy for the reaction $^{19}\text{F}(p,a)^{16}\text{O}$ using a 1.7 MV Pelletron accelerator.

[1] N. A. Guardala, J. P. Farrell, V. Dudnikov, AIP Conference Proceedings, **576**, 741 (2001).

[2] W. A. Ranken, T. W. Bonner, J. H. McCrary, Phys. Rev. **109**, 1646 (1958).

Status of the Linac based positron source at Saclay

Jean-Michel G Rey, Gilles Coulloux, Pascal Debu, Philippe Hardy, Laszlo Liskay, Paul Lotrus, Patrice Pérez, Jean-Yves Roussé, Nicolas Ruiz, Yves Sacquin, Gilles Dispau
IRFU, CEA, CE - Saclay, Gif sur Yvette 91191, France

Low energy positron beams are of major interest for fundamental science and materials research. IRFU has developed and build a slow positron source based on a small, low energy (4.3 MeV) electron linac. The system includes a magnetic system to separate MeV positrons from electrons, which allows the development of a solid neon moderator. We successfully tested both the fast positron production rate and the electron-positron separator by an array of Faraday cup detectors in the high noise environment of the linac target zone. In the present version of the positron source a positron moderator, made of a stack of thin tungsten meshes and placed directly behind the electron target, was used to produce slow positrons that are subsequently extracted from the concrete shielding. The slow positron intensity was measured at the beam exit point, outside of the biological shield. The detected intensity is comparable to that of the current sodium-22 based slow positron sources which uses solid neon moderator. The linac-based source will provide positrons for a magnetic storage trap and represents the first step of the Gbar experiment (Gravitational Behaviour of Antimatter in Rest) recently recommended by the CERN-SPSC committee for an installation in the Antiproton Decelerator hall at CERN (CERN-SPSC-P-342, September 2011). The installation built in Saclay will be described with its main characteristics. The ultimate target of the Gbar experiment will be briefly presented as well as the foreseen development of an industrial positron source dedicated for material science laboratories.

LIGHT-INDUCED METASTABLE DEFECTS IN Cu_2O STUDIED BY POSITRON ANNIHILATION LIFETIME AND DOPPLER BROADENING SPECTROSCOPY

Fnu Aameena, Carroll Quarles², Michael Jin³

⁽¹⁾Physics, University of Texas at Arlington, Texas 76019, USA, Arlington TX 76019, United States

⁽²⁾Physics and Astronomy, Texas Christian University, Fort Worth, Texas 76129, USA, Fort Worth, Texas 76129, USA, Fort worth TX 76129, United States

⁽³⁾Department of Materials Science and Engineering, University of Texas, Arlington, Texas 76019, USA, Arlington, Texas 76019, USA, Arlington TX 76019, United States

Persistent photo conductivity (PPC) in Cu_2O describes the increase in its electrical conductivity upon light illumination and the extremely slow decay of the conductivity under dark at room temperature. The PPC effect is also important to Cu_2O -based solar cells as it influences their junction characteristics including open circuit voltage, short circuit current, and series resistance [1, 2]. Although a few theoretical models [3-5] have been proposed to explain the PPC effect based on the dissociation of defect complexes under light and their thermally activated association under dark, none of them have been verified by the experimental observation of the change in defect population. By using positron annihilation lifetime spectroscopy (PALS) together with Doppler broadening spectroscopy (DBS) this study has experimentally shown the change in the characteristic positron lifetimes associated with open defects in Cu_2O , which supports the conclusion that the light dissociates copper vacancy complexes into smaller size meta-stable copper vacancies and the meta-stable vacancies recover back to bigger size under dark. The DBS results showed no change in the chemical environment around the defects where the annihilation of the positrons occurred and it further supported the conclusion by excluding the major presence of copper vacancy-oxygen vacancy complexes. A part of this study also includes a systematic analysis of positron annihilation in Cu, Cu_2O , and CuO, which has revealed the common presence of copper vacancies in all three materials, and is consistent with the low formation energy of the copper vacancy particularly in copper oxides. Besides, the DBS data showed that the density of low- and high-momentum electrons respectively increases and decreases as the degree of covalency in the material increases.

Theoretical studies of positron states and annihilation characteristics at the oxidized Cu(100) surface

N. G. Fazleev^{1,2}, A. H. Weiss¹

⁽¹⁾Physics, University of Texas at Arlington, Department of Physics, Box 19059, UT Arlington, Arlington Texas 76019-0059, United States

⁽²⁾Physics, Kazan Federal University, Kremlevskaya 18, Kazan 420008, Russia

In this work we present the results of theoretical studies of positron surface and bulk states and annihilation probabilities of surface-trapped positrons with relevant core electrons at the oxidized Cu(100) surface under conditions of high oxygen coverage. **An ab-initio** study of the stability and electronic properties of the Cu(100) missing row reconstructed surface at various on surface and sub-surface oxygen coverages ranging from 0.5 to 2 monolayers has been performed using the density functional theory (DFT). The observed decrease in the positron work function and increase in the surface dipole moment when oxygen atoms occupy subsurface sites have been attributed to significant charge redistribution within the first two layers, buckling effects within each layer and interlayer expansion. Calculations of positron surface and bulk states and positron annihilation characteristics have been also performed for the on-surface adsorption of oxygen on the Cu(100) surface for oxygen coverages up to one monolayer to use for comparison. The computed positron binding energy, positron surface state wave function, and annihilation probabilities of surface trapped positrons with relevant core electrons demonstrate their sensitivity to oxygen coverage, elemental content, atomic structure of the topmost layers of surfaces, and charge transfer effects. Theoretical results are compared with experimental data obtained from studies of oxidation of the Cu(100) surface using positron annihilation induced Auger electron spectroscopy (PAES) [1]. Possible explanation is proposed for the observed behavior of the intensity of the Cu $M_{2,3}VV$ and O KLL Auger peaks and probabilities of annihilation of surface trapped positrons with Cu **3p** and O **1s** core electrons with changes of the annealing temperature [1,2].

This work was supported in part by the National Science Foundation Grant DMR-0907679.

[1] N.G. Fazleev et al., Surface Science **604**, 32 (2010).

[2] N.G. Fazleev, W.B. Maddox, A.H. Weiss, J. Phys.: Conf. Ser. **262**, 012019 (2011).

Characterization of defects in ZnO thin films by Positron Annihilation Spectroscopy

Mihai Straticiuc^{1,2}, Tudor Bogdan Coman³, Ion Burducea^{1,2}, Petru Mihai Racolta¹, Alexandru Jipa², Florin Ovidiu Caltun³

⁽¹⁾*Applied Nuclear Physics, Horia Hulubei National Institute of Physics and Nuclear Engineering - IFIN HH, 30 Reactorului St., Magurele Ilfov 077125, Romania*

⁽²⁾*Faculty of Physics, University of Bucharest, 405 Atomistilor St., Magurele Ilfov 077125, Romania*

⁽³⁾*Faculty of Physics, "Al.I.Cuza" University, Carol I Blvd, No.11, Iasi 700506, Romania*

The study of intrinsic defects in zinc oxide (ZnO) has become a particularly interesting subject following reports of ferromagnetism (FM) in undoped zinc oxide, an otherwise non-FM semiconductor. Theoretical computations as well as experimental data seem to support the idea that vacancies and interstitials can indeed possess magnetic moments and be at the origin of long-range magnetic ordering in this material. We applied the positron annihilation spectroscopy for a better understanding of point defects present in ZnO. Using lifetime and coincidence Doppler broadening techniques in zinc oxide thin layers (up to 250 nm thickness) synthesized by pulsed laser deposition followed by annealing in the temperature range of 400⁰ C to 800⁰ C we observed a migration of the vacancy clusters for the samples exposed to higher temperature. Coincidence Doppler spectra indicate the presence of Zn or Zn-O vacancies. For temperatures higher than 600⁰ C the shape parameter (S parameter) and the lifetime (τ_2) increase with temperature. The effect of the annealing on the concentration of observed defects is discussed. Positron annihilation spectroscopy is an effective tool for analyzing defects in ZnO thin films.

THU-NP08-1

#483 - Invited Talk - Thursday 8:30 AM - Trinity Central

Upgrade of CEBAF from 6 GeV to 12 GeV: Status*

Leigh Harwood

Jefferson Laboratory, 12000 Jefferson Ave, Newport News VA 23692, United States

The CEBAF accelerator is being upgraded from 6 GeV to 12 GeV by the US Department of Energy. The accelerator upgrade is being done within the existing tunnel footprint. The accelerator upgrade includes: 10 new srf-based high-performance cryomodules plus RF systems, doubling the 2K helium plant's capability, upgrading the existing beamlines to operate at nearly double the original performance envelop, and adding a beamline to a new experimental area. Construction is over 75% complete with final completion projected for late FY13. Details of the upgrade and status of the work will be presented.

* Notice: Authored by Jefferson Science Associates, LLC under U.S. DOE Contract Nos. DE-AC05-84ER40150 and DE-AC05-06OR23177. The U.S. Government retains a non-exclusive, paid-up, irrevocable, world-wide license to publish or reproduce this manuscript for U.S. Government purposes.

THU-NP08-2

#485 - Invited Talk - Thursday 8:30 AM - Trinity Central

Performance in the RHIC II Era

Vahid Ranjbar

Collider Accelerator, Brookhaven National Labs, Upton NY 11973, United States

RHIC is a high-luminosity heavy ion collider, and the only collider of spin-polarized beams. We are coming to the end of a series of significant upgrades to the RHIC accelerator complex which have already yielded an order of magnitude increase in luminosity performance for both heavy ions and polarized protons as well as significant increases to polarization. Operation is possible over a wide range of species and collision energies. The most notable advancements in accelerator technology include the first ever application of bunched stochastic cooling, the operational use beam-based feedback control for orbits, tunes and chromaticities.

Gamma-ray induced reactions pertinent for neutrino physicsMelissa Boswell¹, Hiro Ejiri³, Albert Young²⁽¹⁾*Physics Division, Los Alamos National Laboratory, P.O. Box 1663, MS-H803, Los Alamos New Mexico 97544, United States*⁽²⁾*Physics Department, North Carolina State University, Box 8202, Raleigh North Carolina 27695, United States*⁽³⁾*Physics Department, Osaka University, 1-1 Machikaneyama, Toyonaka Osaka 560-0043, Japan*

I will be presenting several measurements that are pertinent to neutrino physics. These measurements will primarily focus on the unique features of the Duke High Intensity Gamma-Ray Source. The tight collimation and limited angular momentum range of this nuclear probe makes it an ideal tool for studying the low-angular momentum states that are typically excited by neutral current interactions from supernovae neutrinos. Furthermore, I will discuss a potential measurement of beta decay matrix elements by studying photo-nuclear excitation of isobaric analog states (IAS) in ⁷⁶As in ⁷⁶Se. Such measurements are important to constrain and possibly help normalize calculations of double beta-decay matrix element calculations.

12 GeV Era Detector Technology at Jefferson LabJohn Leckey*Jefferson Lab, Indiana University, 908 Tabb Lakes Dr, Yorktown VA 23693, United States*

The Thomas Jefferson National Accelerator Facility (Jlab) is presently in the middle of an upgrade to increase the energy of its CW electron beam from 6 GeV to 12 GeV along with the addition of a fourth experimental hall. Driven both by necessity and availability, novel detectors and electronics modules have been used in the upgrade. One such sensor is the Silicon Photomultiplier (SiPM), specifically a Multi-Pixel Photon Counter (MPPC), that is an array of avalanche photodiode pixels operating in Geiger mode that are used to sense photons. The SiPMs replace conventional photomultiplier tubes and have several distinct advantages including the safe operation in a magnetic field and the lack of need for high voltage. Another key to 12 GeV success is advanced fast electronics.

Jlab will use custom 250 MHz and 125 MHz 12-bit analog to digital converters (ADC) and time to digital converters (TDC) that all take advantage of VME Switched Serial (VXS) bus with its GB/s high bandwidth readout capability. These new technologies will be used to readout drift chambers, calorimeters, spectrometers and other particle detectors at Jlab once the 12 GeV upgrade is complete. The largest experiment at Jlab utilizing these components is ~SGlueX~T - an experiment in the newly constructed ~SHall D~T that will study the photoproduction of light mesons in the search for hybrid mesons. The performance of these components and their respective detectors will be presented.

Plans for Proof-of-principle Experiment for Coherent Electron Cooling

I. Pinayev, S. A. Belomestnykh, I. Ben-Zvi, J. Bengtsson, A. Elizarov, A. V. Fedotov, Y. Hao, D. Kayran, V. Litvinenko, G. J. Mahler, W. Meng, T. Roser, B. Sheehy, R. Than, J. E. Tuozzolo, G. Wang, S. D. Webb, V. Yakimenko, G. I. Bell, D. L. Bruhwiler, V. H. Ranjbar, B. T. Schwartz, A. Hutton, G. A. Krafft, M. Poelker, R. A. Rimmer, M. A. Kholopov, P. Vobly

Collider-Accelerator Department, Brookhaven National Lab, Mail Stop 911, Upton NY 11792, United States

Coherent electron cooling (CEC) has a potential to significantly boost luminosity of high-energy, high-intensity hadron colliders. To verify the concept we conduct proof-of-the-principle experiment at RHIC. In this paper, we present the current experimental setup to be installed in the RHIC. We describe current design, status of equipment acquisition, estimates for the expected beam parameters and planned experiments.

Direct Reaction Studies by Particle-Gamma Coincidence Spectroscopy Using HPGe-CsI and HPGe-Si Arrays

James Mitchell Allmond

Joint Institute for Heavy Ion Research, Oak Ridge National Laboratory, Oak Ridge TN 37831, United States

Particle-gamma coincidence spectroscopy has several advantages in the study of direct reactions (particularly in inverse kinematics) since it can allow determination of: decay paths by particle-gamma-gamma; high-precision level energies; multipolarities of transitions by particle-gamma angular correlations; and cross sections through gamma-ray intensity balances. Techniques for studying direct reactions by particle-gamma coincidence spectroscopy are presented for two cases: (1) heavy-ion reactions with HPGe-CsI [1], and (2) light-ion reactions with HPGe-Si [2]. For the heavy-ion reaction, a radioactive-ion-beam (RIB) of ^{134}Te ($N=82$) at 565 MeV is used to study single-particle neutron states in the $N=83$ nucleus ^{135}Te by ($^{13}\text{C}, ^{12}\text{C}$ -gamma) and ($^9\text{Be}, ^8\text{Be}$ -gamma) direct reactions in inverse kinematics. In particular, the heavy-ion reaction is used here to gain selectivity to the high-spin single-particle neutron state $i13/2$ above the $N=82$ shell closure. For the light-ion reaction, a proton beam at 25 MeV is used to study low-spin neutron single-quasiparticle states in the $N=91$ nucleus ^{155}Gd by the (p, d -gamma) reaction. The use of Si detectors with light ions provides the ability to measure the entrance channel in normal or inverse kinematics. Because of the limited resolution, direct-reaction studies with Si are often limited to near-spherical nuclei with low level densities. This hurdle can be overcome by coupling Si-HPGe, which simultaneously measures entrance-channel energies and high-precision gamma-ray energies. The deformed nucleus ^{155}Gd with a relatively large level-density provides an excellent demonstration in how particle-gamma spectroscopy can be used to effectively study direct reactions. Future direct-reaction studies with RIBs will mostly involve inverse kinematics, which eliminates the traditional use of magnetic spectrometers. Particle-gamma spectroscopy provides the most viable method to study direct reactions with RIBs of any level density.

[1] J.M. Allmond et al., to be published; D.C. Radford et al., *Eur. Phys. J. A* 15, 171 (2002).

[2] J.M. Allmond et al., *Phys. Rev. C* 81, 064316 (2010).

Distance calculation methods used in linearization for particle identification in multi-detector arrays

Larry W May^{1,2}, Zachary Kohley², Sara Wuenschel², Kris Hagel², Sherry J Yennello^{1,2}

⁽¹⁾*Chemistry Department, Texas A&M University, College Station Tx 77843, United States*

⁽²⁾*Cyclotron Institute, Texas A&M University, College Station Tx 77843, United States*

Interest in the influence of the neutron-to-proton (N/Z) degree of freedom on multifragmentation has demanded an improvement in the capabilities of multidetector arrays as well as the particle identification methods. Excellent isotopic identification of particles through a linearization analysis is achieved with various algorithms for calculating the distance between a point and a polynomial function. A new Point-to-Curve method of distance determination is introduced. Descriptions of various methods as well as their performance is presented.

ANASEN: a new Array for Nuclear Astrophysics Studies with Exotic Nuclei

E. Koshchiy¹, G. V. Rogachev¹, I. Wiedenhöver¹, E. Johnson¹, L. Baby¹, J. Belarge¹, A. Kuchera¹, D. Santiago-Gonzalez¹, J. C. Blackmon², M. Matoš², L. E. Linhard², L. L. Mondello², D. Bardayan³

⁽¹⁾*Department of Physics, Florida State University, Tallahassee FL 32306, United States*

⁽²⁾*Department of Physics and Astronomy, Louisiana State University, Baton Rouge LA 70803, United States*

⁽³⁾*Physics Division, Oak Ridge National Laboratory, Oak Ridge TN 37831, United States*

The Array for Nuclear Astrophysics Studies with Exotic Nuclei (ANASEN) is a new active target detector designed for direct and indirect measurements of the key astrophysical nuclear reaction rates and to study structure of exotic nuclei using rare isotope beams. ANASEN has cylindrically symmetric geometry and consists of 48 detector telescopes and gas proportional counter. 19-anodes position-sensitive proportional counter surrounds the beam axis and enables an active-target mode by using the target gas (helium, hydrogen, deuterium, etc.) as an active detector volume.

The solid state telescopes are constructed from the 1-mm thick position sensitive silicon detectors and the 20-mm-thick CsI(Tl) crystals. The 36 rectangular Micron Semiconductor Super-X3 design position sensitive detectors form 3 rings of 12 detectors. These are backed by 20-mm-thick trapezoid-shaped CsI(Tl) scintillator crystals in a barrel configuration. Annular quadrants of DSSD detectors QQQ3 type (still under development) backed by 16 CsI(Tl)-scintillators cover the forward scattering angles. ANASEN covers almost 3π steradian solid angle providing high efficiency for experiments with low intense radioactive beams. The high-density ASICs (Application-Specific Integrated Circuits) electronics [1] is used for silicon array readout (total of 480 channels). Conventional electronics is used for proportional counter and CsI scintillators.

ANASEN is designed by Florida State University and Louisiana State University and it aims at direct measurement of the astrophysically important reaction cross-sections (such as (α, p) reactions), proton and alpha elastic and inelastic scattering and (d, p) reactions with exotic nuclei in inverse kinematics. ANASEN is currently used at the RESOLUT radioactive beam facility at the John D. Fox Superconducting Linear Accelerator Laboratory at FSU. The first commissioning experiments with ^{17}F , ^{19}O and ^6He beams have been performed. It is planned to move ANASEN to the new ReA3 accelerator facility at the National Superconducting Cyclotron Laboratory at Michigan State University in late 2012.

I.G.Engel et al. NIM A573(2007)418

The PARIS calorimeter

David Jenkins¹, Adam Maj², Iolanda Matea³, Olivier Dorvaux⁴

⁽¹⁾*Department of Physics, University of York, York, United Kingdom*

⁽²⁾*IFJ PAN, Krakow, Poland*

⁽³⁾*IPNO Orsay, Orsay, France*

⁽⁴⁾*IPHC, Strasbourg, France*

Gamma-ray detection is a very important tool in experimental nuclear physics. In general, the two approaches to this technique are to use scintillator detectors with high efficiency but low intrinsic resolution or high-purity germanium detectors with excellent resolution but low efficiency and high relative cost. Recent developments in scintillator technology have provided materials which bridge the gap between these two regimes, for example, scintillators such as lanthanum bromide which have very high energy resolution ($\sim 3\%$ at 667 keV). The PARIS calorimeter is intended to be an instrument for use at the next-generation ISOL facility, SPIRAL2, under construction in France. PARIS will be an array comprising around 200 detector elements and will profit from the heavy employment of novel scintillators such as lanthanum bromide. The Physics case for PARIS ranges from studies of giant resonances to exotic nuclei and nuclear astrophysics.

The intention is for PARIS to cover the gamma ray energy range from 1 to 50 MeV but high resolution is needed only for the lower part of this range. Given the high cost of the material, this has led to the concept of PARIS comprised of two shells - an inner shell of lanthanum bromide and an outer shell of standard material such as sodium iodide. The evolution of this concept has led to the development of phoswich detectors where these two crystal materials are directly coupled and the scintillation light collected with a single photomultiplier tube. Initial tests have validated this approach. To achieve the best resolution, digital algorithms will need to be developed. The status and perspectives for the PARIS project will be presented.

This work is presented on behalf of the PARIS collaboration comprising around 100 scientists from a wide range of institutions in France, Poland, India, the UK and elsewhere.

A Gas Jet Target for Radioactive Ion Beam Experiments

K. A. Chipps¹, D. W. Bardayan², J. C. Blackmon³, M. Couder⁴, L. Erikson⁵, U. Greife¹, U. Hager¹, A. Lemut⁶, L. Linhardt³, Z. Meisel⁷, F. Montes⁷, S. D. Pain², D. Robertson⁴, F. Sarazin¹, H. Schatz⁷, K. T. Schmitt², M. S. Smith², P. Vetter⁶, M. Wiescher⁴

⁽¹⁾Colorado School of Mines, Golden Colorado 80401, United States

⁽²⁾Oak Ridge National Laboratory, Oak Ridge Tennessee 37831, United States

⁽³⁾Louisiana State University, Baton Rouge Louisiana 70803, United States

⁽⁴⁾University of Notre Dame, Notre Dame Indiana 46556, United States

⁽⁵⁾Pacific Northwest National Laboratory, Richland Washington 99352, United States

⁽⁶⁾Lawrence Berkeley National Laboratory, Berkeley California 94720, United States

⁽⁷⁾National Superconducting Cyclotron Laboratory, Michigan State University, East Lansing Michigan 48824, United States

New radioactive ion beam (RIB) facilities, like FRIB in the US or FAIR in Europe, will push further away from stability and enable the next generation of nuclear physics experiments. Thus, the need for improved RIB targets is more crucial than ever: developments in exotic beams should coincide with developments in targets for use with those beams, in order for nuclear physics to remain on the cutting edge.

Of great importance to the future of RIB physics are scattering, transfer and capture reaction measurements of rare, exotic, and unstable nuclei on light targets such as hydrogen and helium. These measurements require targets that are dense, highly localized, and pure, and conventional targets often suffer too many drawbacks to allow for such experimental designs. Targets must also accommodate the use of large area, highly-segmented silicon detector arrays, high-efficiency gamma arrays and novel heavy ion detectors to efficiently measure the reaction products.

To address this issue, the Jet Experiments in Nuclear Structure and Astrophysics (JENSA) Collaboration led by the Colorado School of Mines (CSM) is in the process of designing, building and testing a supersonic gas jet target for use at existing and future RIB facilities. The gas jet target provides a high density and high purity of target nuclei within a tightly confined region, without the use of windows or backing materials. The design also enables the use of multiple state-of-the-art detection systems. A discussion of the motivation, specifications and status of the JENSA gas jet target system will be discussed.

Polymer Composites for Radiation Scintillation

Qi Chen, Qibing Pei

Department of Materials Science and Engineering, University of California, Los Angeles, 420 Westwood Plaza, Los Angeles CA 90095, United States

I will present the synthesis of conjugated polymer composites for radiation scintillation. The composites exploit the high optical density and photoluminescent efficiency of conjugated polymers in solid-state bulk. High-Z organometallic compounds and nanoparticles are dissolved in the luminescent polymer matrix to enhance the deposition of gamma ray energy. Bulk polymerization is employed to obtain transparent composite at high loading contents. Bulk composites have been synthesized exhibiting high photoluminescence efficiency. The photophysics and performance of the composites for efficient beta and gamma scintillation will be described.

Using Nanoparticles to Enable Radiotherapy and Photodynamic Therapy For Deep Cancer Treatment

Wei Chen

*Department of Physics, The University of Texas at Arlington, 108 Science Hall, 502 Yates Street, Arlington Texas 7601900059
United States*

Photodynamic therapy (PDT) is a promising recipe for cancer treatment. However, the difficulty of light penetration into deep tissue has hitherto prevented the application of photodynamic therapy for deep cancer treatment. PDT efficiency is largely determined by the yield of singlet oxygen, which is a product of photosensitizer structure, light absorption characteristics (intensity and wavelength), and oxygen concentration. Light must be delivered to the photosensitizers to activate them. Light in the near infrared range of 700-900 nm, provides best tissue penetration. All current porphyrin-derived PDT compounds, such as Photofrin, have a strong absorption band near 400 nm called the Soret band. The Soret band absorption is more than 10 times stronger in intensity than the absorption at 630 nm. Unfortunately, attempting to activate porphyrins through absorption at the Soret band is not practical because blue light has minimal penetration into tissue; thus, direct photodynamic therapy is not efficient for deep cancer treatment.

To solve the problem of light penetration and to enhance the PDT treatment for deep cancers, I have proposed a new PDT system in which the light is provided by afterglow nanoparticles with attached photosensitizers. When the nanoparticle-photosensitizer conjugates are targeted to tumor and stimulated by X-ray during radiotherapy, the particles will generate light to activate the photosensitizers for photodynamic therapy. Therefore, the radiation and photodynamic therapies are combined and occur simultaneously, and the tumor destruction will be more efficient. More importantly, it can be used for deep tumor treatment as X-ray can penetrate deep into the tissue such as Breast and prostate cancers. This novel modality is called nanoparticle self-lighting photodynamic therapy (NSLPDT). In this presentation, I will report the progress of the research in my group on the design, synthesis and evaluation of nanoparticle conjugates for photodynamic therapy.

The Tri-modal Imager: Imaging and Source Identification at Standoff Distances

S. Tornga¹, M. Galassi¹, A. Hoover¹, M. Mocko¹, D. Palmer¹, L. Schultz¹, M. Wallace¹, B. Harris², M. Hynes², M. Toolin², D. Wakeford³, B. Horn⁴, R. Lanza⁴, D. Wehe⁵, M. Squillante⁶, J. Christian⁶

⁽¹⁾*Los Alamos National Laboratory, Los Alamos NM, United States*

⁽²⁾*Raytheon Integrated Defense Systems, Tewksbury MA, United States*

⁽³⁾*Bubble Technology Industries, Chalk River Ontario, Canada*

⁽⁴⁾*Massachusetts Institute of Technology, Cambridge MA, United States*

⁽⁵⁾*University of Michigan, Ann Arbor MI, United States*

⁽⁶⁾*Radiation Monitoring Devices Inc, Watertown MA, United States*

The Standoff Radiation Detection System (SORDS) Tri-modal Imager (TMI) is a mobile truck-based, hybrid gamma-ray imaging system able to quickly detect and identify, in position and energy, illicit radiation sources at standoff distances while minimizing the false alarm rate. The TMI consists of 35 NaI crystals each 5" x 5" x 2" arranged in a random mask array, followed by an array of 30 NaI position sensitive bars each 24" x 2.5" x 3". Reconstruction of gamma-ray sources is performed using a combination of two imaging modalities: coded aperture and Compton imaging. A third modality is offered by a shadow algorithm that provides directional information about sources that are not in the field of view of the imager. The active random array acts as both a coded aperture mask and scattering detector for Compton events. Coded aperture and Compton algorithms will be described as well as fusion of the two modalities, and image and energy refinement techniques. Both maximum likelihood and back-projection algorithms have been evaluated and will be compared. Extensive simulations using GEANT4 have been performed and validated against measured data and demonstrate the usefulness of such simulations. Results of image reconstruction algorithms at various speeds and distances will be presented. Utilizing imaging information will also show signal-to-noise gains on energy spectra. The TMI was developed for the SORDS program conducted by the Department of Homeland Security's (DHS) Domestic Nuclear Detection Office (DNDO).

Enhanced Luminescent Properties of Plastic Scintillators by Incorporation of CeF₃ Nanoparticles

Wei Chen, Ke Jiang

Physics, University of Texas at Arlington, 502 Yates Street, Arlington TX 76019, United States

The development of competent scintillating materials for radiation detection is essential for public health and security. The drawbacks of conventional inorganic and organic scintillators necessitate a new generation of scintillators with good energy resolution, high production rate, low cost, and capability to work at room temperature. One practical approach is to make composite materials which consist of high-performance scintillating nanoparticles embedded in a transparent polymer matrix. Ideally, the high-Z nanoparticles could not only improve the stopping power of the polymer scintillator, but also enhance the light yield of the polymer matrix based on the fluorescent resonance energy transfer (FRET).

Cerium fluoride (CeF₃) is an appealing scintillating material due to its high γ -ray sensitivity and short decay time. In this work, CeF₃ nanoparticles were synthesized by a straightforward wet chemistry route. A capping agent was utilized to confine growth of CeF₃ crystals so that small particle sizes were achieved for minimizing light scattering. Polyvinyl toluene (PVT) was chosen as the polymer matrix because of its superior light transmission properties. CeF₃ nanoparticles were incorporated into PVT matrix which was doped with 2,5-diphenyloxazol (PPO) as an energy acceptor. Due to the small size of CeF₃ nanoparticles (<20 nm), the PVT/PPO/CeF₃ nanocomposites are transparent at high loading levels (~30wt%). The subsequent photoluminescence and X-ray luminescence characterizations show that the emission intensity of PVT/PPO scintillators is significantly enhanced after incorporation of CeF₃ nanoparticles. It was then proposed that such a strategy could be applied to prepare composite scintillators with tunable emission wavelengths by rational design of appropriate combinations of energy donors and acceptors. In summary, incorporation of scintillating nanomaterials into transparent polymer matrix represents a promising route to construct novel scintillators for high-energy radiation detection.

Tomographic study of ion tracks by ion loss energy spectroscopy

Jiri Vacik, Vladimir Havranek, Vladimir Hnatowicz, Dietmar Fink

Nuclear Physics Institute, Academy of Sciences of the Czech Republic, Husinec - Rez, Rez 250 68, Czech Republic

Structural changes of ion-irradiated thin film polymers are visualized after etching treatment. Several tomographic studies of ion track structure (radial density distributions) by ion energy loss spectroscopy have been performed using divergent monoenergetic (or quasimonoenergetic) ion beams. The method of ion energy loss spectroscopy is based on the analysis of residual energy of ions transmitted through the ion track density inhomogeneities. To evaluate the polymer density alterations a set of Monte Carlo simulation codes of ion transmission through the modified samples was developed. To obtain more reliable results of a sufficiently good accuracy, low ion fluences and smallest possible angular beam is required. This can be fulfilled using microprobe systems. Here, an application of ion microbeam in tomographic examination of ion tracks is presented and discussed.

The relevance of particle flux monitors in accelerator-based activation analysis

Chr. Segebade, M. Maimaitimin, Sun Zaijing

Idaho Accelerator Centre, Idaho State University, Pocatello ID 83201, United States

One of the most critical parameters in activation analysis is the flux density of the activating particles, its spatial distribution in particular. The validity of the basic equation for calculating the activity induced to the exposed item depends upon the fulfilment of several conditions, the most relevant of them being equal doses of incident activating radiation received by the unknown sample, the calibration material and the reference material, respectively. This fact is most problematic if accelerator-produced radiation is used for activation. Whilst nuclear research reactors usually are equipped with exposure positions that provide fairly homogenous activation fields for thermal neutron activation analysis accelerator-generated particle beams (neutrons, photons, charged particles) exhibit sharp axial and, in particular, radial flux gradients. Different experimental procedures have been developed to fulfil the condition mentioned above.

In this paper, three variants of the application of flux monitors in photon activation analysis is discussed (external monitor, inherent and additive internal monitor). Experiments have indicated that the latter technique yields highest quality of the analytical results.

 σ^* -Mediated Photoprotection of Ammonia and Heteroaromatics Studied by Time-resolved Photoelectron and Photofragmentation Spectroscopy

Susanne Ullrich, Nicholas L Evans, Hui Yu

Department of Physics and Astronomy, University of Georgia, Athens GA 30602, United States

The UV photostability of molecules is determined by excited state electronic relaxation mechanisms that must operate on ultrafast time scales in order to dominate over competing photochemical processes that potentially lead to destruction of the molecule. Electronic excited states with notable σ^* character, centered at X - H (where X = O or N) bonds, may play a particular important role in efficient photoprotection of many molecules.

We have investigated the photochemistry of UV excited ammonia and imidazole using three complementary femtosecond (fs) pump-probe techniques: time-resolved photoelectron (TRPES), ion-yield (TRIY) and photofragment translational spectroscopy (TRPTS).

Ammonia, a prototypical amine group which appears in a number of organic molecules, is resonantly excited to specific vibrational levels of its first electronic excited state of $n\sigma^*$ character. Three deactivation paths are available along the N-H stretching coordinate: Non-adiabatic crossing through a conical intersection leads to either repopulation of the NH_3 ground state or dissociation into ground state NH_2 and H photoproducts whereas adiabatic avoidance correlates with excited state NH_2 and ground state H. TRPES spectra give direct spectroscopic evidence of σ^* mediated relaxation in form of combination bands of the umbrella mode and symmetric stretch. TRPTS measurements of H-atom appearance times provide time constants of < 75 fs to 350 fs for the relaxation, which increase with the amount of internal energy partitioned into the NH_2 co-fragment.

Imidazole, a common chromophore in biomolecules, is shown to undergo similarly efficient $\pi\sigma^*$ mediated relaxation in competition with ring puckering and ring opening pathways following 200nm excitation to its lowest electronically excited $^1\pi\pi^*$ state. Appearance times of the photoproducts from the NH-stretching and ring deformation pathways can roughly be placed at 82 fs and 107-162 fs, respectively. Similar deactivation pathways are active in related heteroaromatic molecules such as pyrazole and adenine.

Multiscale approach to the physics of radiation damage with ions

Eugene Surdutovich¹, Andrey V. Solov'yov²

⁽¹⁾*Physics Department, Oakland University, 2200 N. Squirrel Rd., Rochester MI 48309, United States*

⁽²⁾*Frankfurt Institute for Advanced Studies, Goethe University, Ruth-Moufang-Str. 1, Frankfurt am Main D60438, Germany*

The scientific interest in obtaining a deeper understanding of radiation damage is motivated by the development of ion-beam cancer therapy and other applications of ions interacting with biological targets. This field has attracted much attention from the scientific community, atomic and molecular physics in particular. Among these studies is the multiscale approach to the assessment of radiation damage induced by irradiation with ions. This method combines many spatial, temporal, and energy scales. The multiscale approach raised questions about the nature of the effects that take place and lead to survival curves and the calculation of RBE and other macroscopic quantities. The main issues addressed by the multiscale approach are ion stopping in the medium, the production and transport of secondary electrons produced as a result of ionization and excitation of the medium, the interaction of secondary particles with biological molecules, the most important being DNA, the analysis of induced damage, and the evaluation of the probabilities of subsequent cell survival or death. The milestones in the development of the multiscale approach were the calculations of the Bragg peak, the estimation of DSB yield by secondary electrons, and assessment of the complex DNA damage. A special investigation was devoted to DNA damage as a result of thermomechanical effects caused by ions. These effects can be described as a dynamical change in temperature and pressure in the medium, due to ions passage, causing forces that may rupture bonds in DNA molecules. The understanding of such a possibility evolved from the estimates of the temperature increase in the medium as a result of ion propagation to the analysis of thermal and pressure spikes in liquid water and further to the analysis of the shockwave in the medium and its effect on biomolecules.

Ionization by Dressed Ions: Projectile and Target Scaling

Robert D DuBois

Department of Physics, Missouri University of Science and Technology, 1315 N Pine, Rolla MO 65409, United States

According to the Born approximation, target ionization for bare ion-atom collisions scales as $(Z/v)^2$, where Z and v are the projectile charge and velocity. For collisions involving dressed projectiles where both the target and the projectile can be ionized, Bates and Griffing¹ showed that for ionization of the target/projectile, the bound projectile/target electrons act passively to partially screen the projectile/target nuclear charge and actively where they directly interact with target/projectile electrons. These are often referred to as the screening and antiscreening contributions. The respective target/projectile cross sections now scale as $(Z_{\text{eff}}^2 + N_{\text{eff}})/v^2$, where for ionization of one of the collision partners Z_{eff} and N_{eff} are the screened nuclear charge and the number of active electrons of the other partner. The difficulty in applying this scaling is in determining Z_{eff} and N_{eff} , as they depend on the collision velocity plus, for target ionization, on the projectile charge state. The other difficulty is that these scalings are based on perturbative models and break down when Z/v becomes large. Recently, in a collaboration between the Missouri University of Science and Technology and the Federal and Catholic Universities in Rio de Janeiro, we modeled projectile ionization in fast, heavy ion collisions with atoms². We have now turned our attention to target ionization. Here the emphasis is on dressed ion impact on atomic and molecular targets and on a model that is applicable from approximately 10 keV/u to several MeV/u. This talk will give an overview of our results.

Acknowledgements: this work supported by the National Science Foundation.

1. D.R. Bates and G. Griffing, Proc. Phys. Soc. London, Sect. A 66, 961 (1953); 67, 663 (1954); 68, 90 (1955).

2. R.D. DuBois, A.C.F. Santos, G.M. Sigaud and E.C. Montenegro, Phys. Rev. A 84, 022702 (2011).

ANGULAR INTEGRATED ELECTRON SPECTRA IN COLLISION BETWEEN CARBON IONS AND NEON ATOMS

K. Tokesi¹, P. Sigmund², A. Schinner³, L. H. Toburen⁴, J. L. Shinpaugh⁴

⁽¹⁾*Institute of Nuclear Research of the Hungarian Academy of Sciences, Debrecen 4001, Hungary*

⁽²⁾*Dept. of Physics, Chemistry and Pharmacy Univ. Southern Denmark, Odense M DK-5230, Denmark*

⁽³⁾*Dept. of Exp. Physics and Surface Physics, Johannes-Kepler-University, Linz A-4040, Austria*

⁽⁴⁾*Department of Physics, East Carolina University, Greenville NC 27858, United States*

In this work we present angular-integrated electron-emission spectra from 0.8 - 2.4 MeV C⁺ and C²⁺ ions interacting with neon. We used the classical trajectory Monte Carlo (CTMC) method and binary theory. Both theories deliver separate spectra for electrons emitted from the target and the projectile. By summing these two components in the rest frame of the target we may make a comparison with available experimental data. Generally we find good agreement with both calculations. Minor differences between the theoretical results are found, which only partly may be computational. Although tabulated shell binding energies enter both codes, binary theory also contains shell-wise I-values. A more interesting source of differences is Fermi-shuttle ionization, since multiple interactions are not taken into account in binary theory. For the collision system in question, a significant contribution from Fermi-shuttle ionization has to be expected in the spectra at energies higher than $E=0.5 m_e (nV)^2$, where m_e is the mass of the electron, V the projectile velocity and n an integer greater than 1. We found enhanced electron yields compared to binary theory in this region of measured and CTMC spectra, which can be directly attributed to the contribution of Fermi-shuttle type multiple scattering.

This work was supported in part by the Hungarian Scientific Research Fund OTKA No. NN 103279 and by the Danish Natural Science Research Council (FNU).

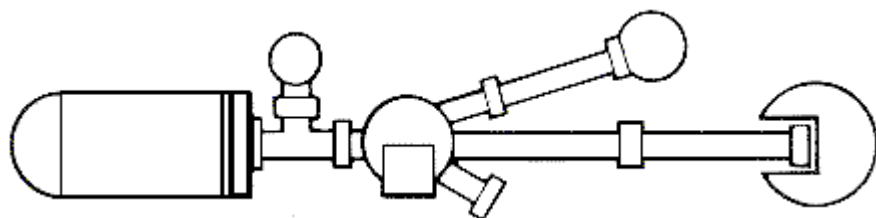
Outgassing Studies of Irradiated Lithium Hydride

Carol Haertling¹, Joseph Tesmer¹, Yongiang Wang¹, Chelsea D'Angelo¹, T. William McAlexander²

⁽¹⁾*Material Science & Technology, Los Alamos National Laboratory, M/S G770, Los Alamos NM 87545, United States*

⁽²⁾*University of Tennessee, Material Science & Engineering, 434 Dougherty Hall, Knoxville TN 37996, United States*

Lithium hydride (LiH) is a highly reactive solid that is used in nuclear applications, where radiation environments are present that can disrupt the structure of a material. This disruption creates defects and can produce gases, most obviously H₂ gas. We have performed experiments to determine the effects of long-term irradiation on LiH, using both alpha particle radiation and photon radiation. Alpha radiation at a specific energy was produced directly from an accelerator. Photon radiation was produced by accelerator-driven proton bombardment of metal targets, which then emit photons at desired energies. Outgassing from the LiH was measured during irradiation and quantified.



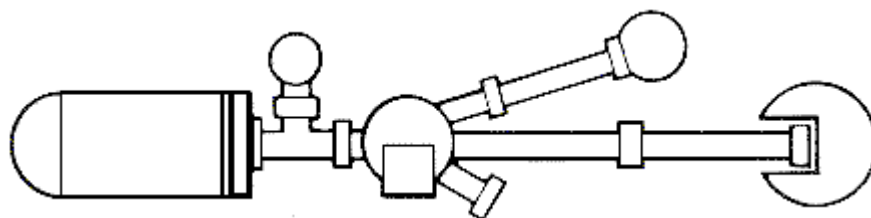
FRIDAY

The Evolving Role of HEP Stewardship for Accelerator R&D - Overview and Highlights of the HEP Task Force Report

Stephen Gourlay

AFRD, Lawrence Berkeley National Laboratory, 1 Cyclotron Road, MS: 50-4049, Berkeley CA 94720, United States

Accelerator science and technology have a significant impact on many fields in our society. Initially developed as tools for discovery science by the Department of Energy Office of Science and the National Science Foundation, the use of accelerators extends to many other applications, with potential for continued innovation that can help drive US economic competitiveness. A number of applications were clearly identified in the 2009 workshop on Accelerators for America's Future organized by the DOE Office of High Energy Physics (HEP), the acknowledged steward of long-term accelerator R&D. A number of accelerator R&D areas that would help the US to maintain its competitive edge were singled out to help develop a coherent program. In September 2011, in recognition of these opportunities, the Senate Appropriations Committee requested that the DOE develop a 10-year strategic plan for accelerator technology research and development to advance accelerator applications in energy and the environment, medicine, industry, national security, and discovery science for accelerator stewardship by June 2012. The DOE Office of High Energy Physics then established the current task force, made up of representatives from the national laboratories, universities and industry, to provide input for that plan. This talk will give an overview of the Task Force report and cover some of the key highlights.



AUTHOR INDEX

(Alphabetical by Author Last Name)

Abril, Isabel	TUE-IBA04-1
Abril, Isabel	TUE-IBA04-P1
Abril, Isabel	TUE-IBA04-P2
Abs, Michel.....	WED-MA03-2
Ackerman, Eric	THU-IBA06-4
Adams, Marvin	TUE-ECR05-4
Adams, Marvin	TUE-REP02-4
ADEKOLA, A. S.	WED-NP05-3
Adolphsen, Chris	THU-AT06-1
Adoui, Lamri.....	MON-AP01-2
Aflakian, Nafiseh.....	MON-AT02-4
Afra, Boshra.....	MON-IBM02-4
Afra, Boshra.....	WED-REP06-4
Agodi, C.....	WED-NP06-4
Agullo-Lopez, Fernando.....	WED-REP06-1
Agustsson, Ronald	WED-SSCD04-2
Agvaanluvsan, U.....	WED-NP07-2
AHN, S.	WED-NP05-3
Ahn, S. H.	MON-NP02-1
Ahn, S. H.	WED-NP05-4
Akaike, Makoto	TUE-MA07-6
Akinlua, Akinsehinwa	MON-IBA01-P9
Al-Amoudi, Omar O. S.....	MON-NBAE02-5
Al-Matouq, Faris A.....	MON-NBAE02-5
Al-Matouq, Faris A.....	MON-NBAE02-P1
Al-Matouq, Faris A.....	TUE-SSCD02-P1
Alarcon, FB.....	MON-AP01-P1
Alary, Jean-Francois	TUE-NBAE03-6
Albakri, O.	TUE-REP04-5
ALCANTARA, KATIANNE F.....	THU-NBAE04-P1
AlFaify, Salem.....	THU-ECR03-3
AlFaify, Salem.....	THU-ECR03-P1
Ali, Nawab	THU-IBA06-P1
Ali, S.	WED-AP07-2
Alkemade, Paul F.A.....	MON-NST07-2
Allen, Raymond J	WED-SSCD03-2
Allen, T. R.	TUE-REP04-5
Allen, Todd R	WED-AT05-3
Allmond, J. M.	WED-NP05-2
Allmond, J. M.	WED-NP05-4
Allmond, James Mitchell.....	THU-NP09-1
Almaraz-Calderon, Sergio	MON-NP02-4
Almeida, Lais.....	TUE-IBA04-P4
Aloni, Shaul	MON-IBM01-3
Alonso, Jose R	MON-NP01-2
AlShammari, Suliman M.	TUE-AP05-P2
Amaral, L.	MON-AT02-2
Amaro, Pedro	TUE-AP05-3
Ameena, Fnu.....	THU-NBAE05-1

Anderson, David E.....	THU-AT06-3
Andreiou, C.....	TUE-AP05-2
Andrianarijaona, V M.....	TUE-AP04-P1
Andrianarijaona, Vola M.....	WED-AP07-4
Antaya, Timothy A.	WED-MA03-5
Antolak, A. J.	WED-SSCD03-3
Antolak, Arlyn	WED-SSCD04-7
Antolak, Arlyn J.....	TUE-AT03-P1
Antolak, Arlyn J.....	WED-SSCD04-4
Antolak, Arlyn J.....	WED-SSCD04-P1
Antonenko, A. H.....	MON-IBM01-6
Antwis, Luke D.....	THU-IBA06-2
Anzenberg, Eitan	TUE-NST09-4
Aoki, Takaaki	THU-IBA06-1
Aoki, Takaaki	THU-IBM03-3
Aoki, Takamichi	WED-MA09-P1
Apodaca, Mac D	TUE-AT03-4
Appleton, Bill R.....	TUE-NST05-1
Aprahamian, Ani.....	MON-NP02-4
Apruzese, John P	TUE-NBAE03-2
Apruzese, John P	WED-SSCD03-2
Araujo, Leandro	MON-IBM02-4
Araya, Masayuki.....	TUE-MA07-3
Archubi, Claudio.....	TUE-IBA04-P1
Arenshtam, Alex	TUE-NP03-4
Arista, Néstor R.	TUE-IBA04-P1
Arista, Néstor R.	TUE-IBA04-P2
Arje, Juha.....	TUE-NP03-3
Asaithamby, Aroumougame	MON-MA01-2
Assadi, Saeed	TUE-ECR05-3
Assadi, Saeed	TUE-REP02-4
Atroshchenko, Kostiantyn	TUE-MA05-2
Atroshchenko, Kostiantyn	TUE-MA05-P4
Attili, Andrea	MON-MA02-3
Aubin, S.	WED-NP05-1
Avasthi, Devesh Kumar	MON-IBM02-2
Avilov, Mikhail.....	MON-NP01-P2
Avilov, Mikhail.....	WED-REP06-6
Ayton, Aimee L. E.....	WED-AP06-P7
Ayyad, A.....	TUE-AP03-5
Aziz, Michael J	TUE-NST06-4
Aziz, Michael J.	TUE-NST09-1
Aziz, Michael J.	TUE-NST09-3
Aziz, Michael J.	TUE-NST09-4
B, Sundaravel.....	MON-IBM02-5
Babu, N Manikantha.....	MON-IBM02-P2
Baby, L.	THU-NP09-3
Bacellar, Camila	WED-NBAE06-2
Badgley, Karie	TUE-ECR05-3

Badgley, Karie	TUE-ECR05-4
Badgley, Karie	TUE-REP02-4
Baglin, John	TUE-NST05-4
Bagnoud, V.	WED-AP08-5
Bailey, James	WED-MA09-4
Bailey, M. J.	MON-AT02-1
Bajpai, Parmendra Kumar	MON-IBM02-3
Bakel, Allen	WED-MA09-4
Bakhru, Hassaram	WED-REP05-5
Bakhru, Hassaram	THU-ECR03-4
Bakhru, Hassaram	THU-ECR03-6
Bakhru, Sasha	WED-REP05-5
Balakin, Vladimir	WED-MA03-4
Baldazzi, Giuseppe	TUE-MA05-2
Baldazzi, Giuseppe	TUE-MA05-P3
Baldo, Pete	TUE-IBM05-5
Baldwin, Jon Kevin	TUE-IBM05-5
Baldwin, Matthew	MON-REP01-4
Ballance, Connor	WED-AP06-4
Ballard, Beau D	TUE-NP04-3
Ballard, Beau D	WED-MA09-3
Balogh, Adam G.	TUE-REP04-3
Balogh, Adam Georg	TUE-REP04-2
Banas, D.	TUE-AP05-5
Banas, Dariusz	WED-AP08-3
Baneva, Yanka	TUE-MA05-P4
Bao, Jiming	WED-NST03-3
Baramsai, Bayarbadrakh	WED-NP07-2
Barber, Powell	MON-IBA02-4
Barber, Vincent	WED-AT05-1
Barday, Roman	WED-AP08-4
Bardayan, D.	THU-NP09-3
Bardayan, D. W.	MON-NP02-1
Bardayan, D. W.	MON-NP02-3
BARDAYAN, D. W.	WED-NP05-3
Bardayan, D. W.	WED-NP05-4
Bardayan, D. W.	THU-NP09-5
Barletta, William A.	WED-NBAE06-1
Barnard, Harold S	WED-AP06-3
Barr, Chris M	TUE-IBM05-5
Barradas, Nuno P	TUE-IBA05-3
Barton, Joseph	MON-REP01-4
Bashkirov, Vladimir	TUE-MA05-1
Batchelder, J. C.	WED-NP05-2
Batchuluun, E.	WED-NP07-2
Batic, Matej	WED-IBA07-1
Bauer, Peter	TUE-IBA04-3
Bauge, Eric	WED-AP08-5
Baurichter, Arnd	TUE-AT04-1

Bax, Daniel V	MON-NST01-2
Baxley, Jacob D	MON-MA01-P1
Baxter, Emily A	WED-SSCD04-5
Baxter, Emily A	WED-SSCD04-P2
Bazin, D.	MON-NP02-1
Bech, J.	MON-AP01-4
BECK, Lucile	TUE-IBA05-4
Becvar, F.	WED-NP07-2
Beene, J. R.	WED-NP05-2
Beene, J. R.	WED-NP05-4
Behr, J. A.	WED-NP05-1
Beiersdorfer, Peter	TUE-AP04-4
Beiersdorfer, Peter	WED-AP06-1
Belarge, J.	THU-NP09-3
Belkacem, Ali	WED-NBAE06-2
Bell, G. I.	THU-NP08-5
Bello, Michele.....	TUE-MA05-2
Bello, Michele.....	TUE-MA05-P3
Bello, Michele.....	TUE-MA05-P4
Belomestnykh, S. A.	THU-NP08-5
Ben-Itzhak, Itzik	WED-AP07-3
Ben-Zvi, I.	THU-NP08-5
Bendahan, Joseph	TUE-SSCD01-2
Bender, Markus.....	WED-REP06-6
Bengtsson, J.	THU-NP08-5
Benitez, Janilee	TUE-NP03-2
BENYAGOUB, Abdenacer	TUE-AP03-3
Benyagoub, Abdenacer.....	WED-IBM04-4
Bereczky, R. J.	TUE-AP03-6
Bergner, Frank	TUE-REP02-3
Bergstrom, Paul M.....	TUE-SSCD01-1
Berkovits, Dan	TUE-NP03-4
Bernstein, Lee	WED-AP08-5
Bertrand, Damien.....	MON-MA02-3
Beye, Martin	WED-NBAE06-2
Beyer, H. F.....	TUE-AP05-5
Beyer, Heinrich.....	TUE-AP05-4
Beyer, Heinrich.....	WED-AP08-3
Beyer, Heinrich F.....	WED-AP08-6
Bharuth-Ram, Krish.....	MON-IBM01-4
Biel, Wolfgang.....	WED-AP06-2
Bierschenk, Thomas	MON-IBM02-4
Bierschenk, Thomas	WED-REP06-4
Bilek, Marcela MM	MON-NST01-2
Binet, Alain.....	TUE-AT04-4
Bingham, C.	WED-NP05-2
Birnbaum, Eva R	TUE-NP04-3
Birnbaum, Eva R	WED-MA09-3
Blackburn, B. W.	TUE-NBAE03-5

Blackmon, J. C.....	MON-NP02-3
BLACKMON, J. C.	WED-NP05-3
Blackmon, J. C.....	THU-NP09-3
Blackmon, J. C.....	THU-NP09-5
Blackston, Matthew	MON-NBAE02-3
Blancato, A.	WED-NP06-4
Blank, Ina.....	MON-AP01-P4
Bleuel, Darren.....	WED-AP08-5
Bloch, Charles.....	WED-MA03-6
Bluhm, Hendrik	WED-NBAE06-2
Bobes, Omar	TUE-NST06-3
Bogdanovic Radovic, Iva.....	WED-ECR04-6
Bokor, Jeffrey	THU-IBM06-6
Boll, Rose A.....	TUE-NP04-4
Bollen, Georg.....	TUE-NP03-1
Bollini, Dante.....	TUE-MA05-P3
Bonnerup, Chris A.....	MON-AT02-3
Borodin, O. V.	TUE-REP02-1
Boswell, M S	WED-NP06-6
Boswell, Melissa.....	THU-NP08-3
Bouanani, M. El.....	WED-ECR04-P1
Bouanani, M. El.....	WED-ECR04-P2
Bouanani, M. El.....	THU-ECR03-P2
Bouanani, M. El.....	THU-IBM06-P2
Boucher, Salime.....	WED-SSCD04-2
Boudergui, Karim	TUE-ECR05-1
Boulesteix, Marine.....	WED-REP06-6
Bourke, Mark.....	TUE-REP02-5
Bowers, Delbert	WED-MA09-4
Bozicevic, Iva	WED-IBA07-3
Braccini, Saverio.....	TUE-AT04-5
Bradley, R. Mark	TUE-NST06-2
Brandau, Carsten.....	TUE-AP05-4
Brandau, Carsten.....	WED-AP08-5
Brasile, Jean-Pierre	TUE-AT04-4
Bredeweg, T. A.....	WED-NP07-2
Brenner, Michael P	TUE-NST06-4
Briski, Karen P.....	WED-IBA07-P1
Brown, Craig.....	TUE-SSCD01-2
Brown, Craig.....	TUE-SSCD02-3
Brown, Craig.....	WED-SSCD03-5
Brown, Gregory V.	TUE-AP04-4
Bruffey, Stephanie H	TUE-NP04-4
Bruhwieler, D. L.....	THU-NP08-5
Brunner, T.....	TUE-AP05-2
Bryk, V. V.....	TUE-REP02-1
Bräuning, Achim.....	TUE-NP03-6
Bräuning-Demian, Angela	TUE-AP05-4
BUBOIS, ROBERT DEAN.....	THU-NBAE04-1

Burducea, Ion.....	THU-ECR03-5
Burducea, Ion.....	THU-NBAE05-3
Burks, Edward	TUE-REP04-P1
Burns, D.....	WED-NP07-5
Bylinski, Yuri	MON-NP01-4
Byrne, Aidan.....	MON-IBM02-4
Bäck, Torbjörn.....	WED-AP08-4
Caffrey, Augustine J	MON-NBAE02-P3
Caggiano, Jack.....	WED-AP08-5
Cai, Siou-yin	TUE-MA05-P2
Calinescu, Catalin Ionut.....	WED-ECR04-4
Caltun, Florin Ovidiu.....	THU-NBAE05-3
Campbell, John L.....	MON-PS02-1
Cao, Guoping	MON-REP01-2
Cao, Guoping	WED-AT05-3
Capece, Angela	MON-IBA02-2
Capron, Michael	MON-AP01-2
Carabe, Alejandro	MON-MA02-4
Carasco, Cedric.....	MON-NBAE02-P2
Carasco, Cedric.....	TUE-ECR05-1
Cardenas, E. S.....	TUE-NBAE03-5
Caro, Alfredo	MON-REP01-3
Caro, Alfredo	WED-REP05-3
Caro, Alfredo	WED-REP05-4
Caro, Magdalena.....	MON-REP01-3
Caro, Magdalena.....	TUE-REP02-5
Carpenter, M. A.	TUE-IBA03-2
Carrascosa, Mercedes	WED-REP06-1
Carroll, J. J.....	WED-NP07-5
Carson, Bryan	THU-IBA06-4
Cassidy, David.....	THU-ECR03-3
Cassidy, David.....	THU-ECR03-P1
Cassimi, A.....	MON-AP01-4
CASSIMI, Amine	TUE-AP03-3
Cata-Danil, Gheorghe	WED-ECR04-4
Caussyn, Dave D	MON-IBA02-4
Cavness, Brandon	WED-TA01-P1
Cederquist, Henrik.....	MON-AP01-2
Cederwall, Bo	WED-AP08-4
Celedón, Carlos.....	TUE-IBA04-P2
Cester, D.	MON-NBAE02-2
Cester, Davide.....	TUE-ECR05-5
Cester, Davide.....	TUE-SSCD02-1
Chae, K. Y.	MON-NP02-1
CHAE, K. Y.....	WED-NP05-3
Chae, K. Y.	WED-NP05-4
Chajecki, Z.....	MON-NP02-1
Chakraborty, A.	TUE-IBA05-6
Chan, Taw Kuei	TUE-IBA05-1

Chang, Fu-xiong	TUE-MA05-P2
Chang, Long	MON-NST07-3
Chao, Tsi-chian.....	TUE-MA05-P2
Charnvanichborikarn, S.	MON-IBA02-1
Chartkunchand, K.	MON-IBA01-P1
Chauchat, Anne-Sophie	TUE-AT04-4
Chaudhuri, A.....	TUE-AP05-2
Chemerisov, Segey D.	WED-MA09-5
Chemerisov, Sergey	WED-MA09-4
Chen, Allan Xi	TUE-AT03-P1
Chen, Allan Xi	WED-SSCD04-4
Chen, Allan Xi	WED-SSCD04-P1
Chen, Augustine Ei-fong	TUE-MA05-P2
Chen, Benjamin	MON-MA01-4
Chen, David J.....	MON-MA01-2
Chen, Fengfeng.....	MON-IBA01-6
Chen, Hongmin.....	THU-NBAE04-4
Chen, Kuan Ling.....	WED-MA03-6
Chen, Liang.....	WED-IBM04-2
Chen, Qi	THU-REP08-1
Chen, Wei	THU-REP08-2
Chen, Wei	THU-REP08-4
Chen, Weidong	WED-AP08-3
Chen, Yanbin	THU-IBM06-2
Chen, Yu-Jiuan	WED-MA04-2
Cherkov, A. G.....	MON-IBM01-6
Cherkova, S. G.....	MON-IBM01-6
Chesnel, Jean-Yves.....	MON-AP01-2
Chichester, David L.	TUE-AT03-1
Chichester, David L.	TUE-SSCD01-P1
Chienthavorn, Orapin	WED-NST04-5
Childs, N.	TUE-IBA03-4
Childs, Nicholas.....	WED-TA01-4
Childs, Nicholas Brule.....	TUE-IBA03-3
Chin, Yu-Chung.....	MON-IBA01-6
Chipps, K. A.	MON-NP02-3
CHIPPS, K. A.	WED-NP05-3
Chipps, K. A.	WED-NP05-4
Chipps, K. A.	THU-NP09-5
Cho, Hana	WED-NBAE06-2
Choi, Bill.....	MON-REP01-5
Choudhury, Samrat	TUE-IBM05-3
Chowdhury, Parimal	THU-IBA06-P1
Chowdhury, U.....	TUE-AP05-2
Christensen, Tue	TUE-MA05-3
Christian, J.	THU-REP08-3
Chu, Junhan	WED-IBA07-5
Chu, Ming-lee	TUE-MA05-P2
Chu, Wei-Kan	MON-IBA01-5

Chu, Wei-Kan	TUE-NST09-5
Chu, Wei-Kan	WED-NST03-2
Chu, Wei-Kan	WED-NST03-3
Chu, Wei-Kan	WED-NST03-4
Chubarian, Greg	TUE-NP03-3
Chung, Kyoung-Jae	THU-IBM06-P1
Chutjian, Ara.....	WED-AP06-1
Ciapetti, Gabriela	MON-NST01-1
Cirrone, G.A.P.	WED-NP06-4
Cizewski, J.....	MON-NP02-1
Cizewski, J. A.	MON-NP02-3
CIZEWSKI, J. A.	WED-NP05-3
Cizewski, J. A.	WED-NP05-4
Clark, Blythe G.	TUE-IBA05-2
Clark, Henry	TUE-NP03-3
Clark, Rod.....	WED-AP08-5
Clement, R. R.C.....	MON-NP02-1
Clementson, Joel.....	TUE-AP04-4
Clementson, Joel.....	WED-AP06-1
Cohen, A F.....	TUE-IBM05-2
Colaax, J. L.....	MON-AT02-1
Colaax, Julian L.....	TUE-IBA05-3
Colby, Robert.....	MON-IBM01-2
Colby, Robert.....	THU-IBM06-4
Cole, Philip	MON-NBAE01-2
Cole, Philip Lawrence	MON-NBAE01-1
Colgan, J	MON-AP02-3
Collaboration, for the n_TOF	WED-NP07-1
Collette, Andrew	WED-TA01-4
Collister, R. A.	WED-NP05-1
Colonna, Nicola	WED-NP07-1
Coman, Tudor Bogdan.....	THU-NBAE05-3
Combs, Stephanie E.....	TUE-MA07-2
Comeaux, Justin.....	TUE-ECR05-3
Comeaux, Justin.....	TUE-REP02-4
Commisso, Robert J.....	TUE-NBAE03-2
Commisso, Robert J.....	WED-SSCD03-2
Commisso, Robert J.....	TUE-ECR05-6
Condron, Cathie	WED-SSCD03-5
Conjat, Matthieu	WED-MA03-2
Cooper, Kevin Wayson.....	WED-SSCD03-P1
Cordones, Amy	WED-NBAE06-2
Corre, Gwenolé.....	TUE-ECR05-1
Correa, Jose R.	WED-AP06-P3
Coslovich, Giacomo	WED-NBAE06-2
Costa-Fraga, R.	MON-AP01-4
Costes, Ph.D., Sylvain	MON-MA01-3
Cottier, R. J.....	WED-ECR04-1
Couder, M.	THU-NP09-5

Couder, Manoel	MON-NP01-3
Couder, Manoel	TUE-NP03-5
Coulloux, Gilles	THU-NBAE04-P2
Couperus, Jurjen Pieter	THU-AT06-P1
Coupland, D.	MON-NP02-1
Cousins, Lisa M	TUE-NBAE03-6
Coutrakon, George	TUE-MA05-1
Coutrakon, George	WED-MA04-5
Couture, A.	WED-NP07-2
Couture, Aaron	MON-NP02-2
Coventry, Matthew D.	TUE-AT03-3
Covington, A. C.	MON-IBA01-P1
Cowan, Thomas	THU-AT06-P1
Cowin, James	THU-IBM03-2
Craciun, Liviu Stefan	THU-ECR03-5
Cremer, Jay T	TUE-AT03-4
Crespillo, Miguel Luis	WED-REP06-1
Crider, B. C.	TUE-IBA05-6
CRIVELLI, PAOLO	THU-NBAE04-P1
Crye, Jason	TUE-NBAE03-3
Cuerno, Rodolfo	TUE-NST06-1
Cutler, Cathy S	WED-MA09-3
Cuttone, G.	WED-NP06-4
Czasch, A.	MON-AP01-4
D'Angelo, Chelsea	WED-AT05-P1
D'Angelo, Chelsea	THU-REP09-5
DAEdALUS Collaboration, for the	MON-NP01-2
Dagci, Taner	MON-NST01-P2
Dagci, Taner	MON-NST01-P3
Dai, Shu-jhen	TUE-MA05-P2
Dale, Gregory E	WED-SSCD04-P2
Dale, Gregory E	WED-MA09-5
Dale, Greogry E	WED-SSCD04-5
Dalmas, Dale A.	WED-MA09-5
Dang, Jeong-jeung	THU-IBM06-P1
Danielson, James R.	THU-NBAE04-2
Daragon, Frederique	TUE-NP03-6
Dash, Akshar	WED-IBA07-P2
Dashdorj, D.	WED-NP07-2
Dassanayake, B S	TUE-AP03-5
Dassanayake, Buddhika Senarath	TUE-AP03-4
Davis, D. D.	MON-IBA01-P1
Davis, R F	TUE-IBA03-P1
Davis, V. T.	MON-IBA01-P1
Davletkildeev, Nadim A.	TUE-IBM05-P1
de Azevedo, G. M.	MON-AT02-2
De Napoli, Marzio	WED-NP06-4
De Rosa, Matteo	TUE-MA05-P4
de Vera, Pablo	TUE-IBA04-1

De, Debtanu	WED-NST03-2
Debastiani, Rafaela	TUE-IBA04-P4
Debnath, Mukul C	WED-ECR04-2
Debu, Pascal	THU-NBAE04-P2
Debus, Alexander	THU-AT06-P1
Debus, Jürgen	TUE-MA07-2
DeCroix, Michele E	WED-SSCD04-5
Defay, X	TUE-AP04-P1
Dehnel, Morgan Patrick	TUE-MA05-3
Deki, Manato	TUE-REP04-6
Delheij, P.	TUE-AP05-2
Demirci, Utkan	MON-NST01-3
Demizu, Yusuke	TUE-MA07-3
Demkowicz, Michael J	TUE-IBM05-1
Demkowicz, Michael J	WED-REP05-1
Denton, Cristian D.	TUE-IBA04-P2
Deoli, Naresh T.	MON-AT02-4
Deoli, Naresh T.	WED-ECR04-5
Dertinger, Jennifer J	THU-IBM03-1
Devanathan, Ram	WED-IBM04-4
Devaraj, A	TUE-IBA03-P1
Devaraj, A	TUE-IBM05-2
Devaraj, Arun	MON-IBM01-2
Devaraj, Arun	TUE-IBA03-2
Devaraj, Arun	TUE-IBM05-4
Devaraj, Arun	TUE-IBM05-6
Devaraj, Arun	THU-IBM06-4
Devlin, Matthew	MON-NP02-2
Deyglun, Clément	TUE-ECR05-1
Dhoubadel, Mangal	WED-NST04-P2
Dhoubhadel, Mangal	MON-AT02-4
Dhoubhadel, Mangal S	WED-ECR04-3
Dhoubhadel, Mangal S	MON-IBM01-5
Di Domenico, Giovanni	TUE-MA05-2
Di Domenico, Giovanni	TUE-MA05-P3
Di, Zengfeng	MON-IBA01-3
Dias, J. F.	MON-AT02-2
Dias, Johnny Ferraz	TUE-IBA04-P4
Diaz-Pinto, Carlos	WED-NST03-2
Dilling, J.	TUE-AP05-2
Dimiccoli, Vincenzo	TUE-MA05-P1
Ding, Xiaodong	WED-SSCD04-2
Dispau, Gilles	THU-NBAE04-P2
Dissanayake, Amila	THU-ECR03-3
Dissanayake, Amila	THU-ECR03-P1
Ditrói, Ferenc	MON-NBAE01-4
Djurabekova, Flyura	WED-REP06-2
Doebeli, M.	WED-IBA07-4
DOEBELI, Max	TUE-AP03-3

Doerner, R.....	MON-AP01-4
Doerner, Russell	MON-REP01-4
Dogaru, Marius	WED-ECR04-4
Dollinger, Guenther	TUE-IBA05-5
Dollinger, Günther	MON-MA02-2
Domaracka, Alicja	MON-AP01-2
Dominik, Laura.....	TUE-REP03-2
Donnelly, Stephen E	WED-REP07-2
Dorvaux, Olivier	THU-NP09-4
dos Remedios, Christobal G	MON-NST01-2
Doyle, Barney L.....	WED-IBM04-6
Doyle, Barney L.....	TUE-IBA05-2
Doyle, Barney L.....	THU-IBA06-4
Draganic, I N	TUE-AP04-P1
Draganic, Ilija	TUE-AP04-3
Drake, Keith.....	WED-TA01-4
Driscoll, Mark S.....	WED-AT05-1
Driscoll, Mark S.....	WED-AT05-2
Driscoll, Mark S.....	WED-TA02-2
DuBois, R. D.....	THU-NBAE04-5
DuBois, Robert D	THU-REP09-3
DuBois, Robert D.	WED-AP08-3
Duggan, Jerome L.....	WED-ECR04-3
Duggan, Jerome L.....	MON-AT02-4
Duggan, Jerome L.....	WED-ECR04-5
Duggan, Jerome L.....	WED-IBA07-P2
Duggan, Jerome L.....	WED-TA01-1
Duh, Ting-shien	TUE-MA05-P2
Dunne, Michael.....	MON-REP01-5
Durante, Marco	MON-MA02-1
Ebina, Futaro.....	WED-MA09-1
Ebina, Futaro.....	WED-MA09-P1
Edgecock, Thomas Robert.....	WED-MA04-4
Edmondson, Philip.....	TUE-IBM05-4
Edmondson, Philip D.....	TUE-IBA03-1
Eisenbeis, Paul	TUE-NP04-2
Ejiri, Hiro	THU-NP08-3
El Ghazaly, Mohamed O. A.	TUE-AP05-P2
Eliades, John	TUE-NBAE03-6
Eliyahu, Ilan.....	TUE-NP03-4
Elizarov, A.	THU-NP08-5
Elkafrawy, T.	TUE-AP04-5
Elliman, Robert G.....	TUE-NST05-1
Ellsworth, Jennifer	WED-SSCD04-1
Ellsworth, Jennifer L	TUE-AT03-7
Elsalim, Mashal	TUE-SSCD01-2
ELSON, J.	WED-NP05-3
Emfietzoglou, Dimitris	TUE-IBA04-1
Enachescu, Mihaela	WED-ECR04-4

Enders, Joachim	WED-AP08-4
Endo, Masahiro	TUE-MA07-5
Engelhard, Mark	THU-IBM06-5
Engle, Jonathan W	TUE-NP04-3
Engle, Jonathan W	WED-MA09-3
Enos, David	TUE-IBA05-2
Erikson, L.	THU-NP09-5
Errea, L. F.	MON-AP01-P3
Ettenauer, S.	TUE-AP05-2
Evans, Nicholas L	THU-REP09-1
Ewing, Rodney C	WED-REP07-5
Ewing, Rodney C	WED-REP06-3
Ewing, Rodney C	THU-IBM06-2
Eziashi, J	TUE-IBA03-4
Faillace, Luigi	WED-SSCD04-2
Falabella, Steven	TUE-AT03-7
Falabella, Steven	WED-SSCD04-1
Famiano, M. A.	MON-NP02-1
Fang, Kaihong	TUE-IBA05-1
Fassbender, Michael E	TUE-NP04-3
Fassbender, Michael E	WED-MA09-3
Fazel, K.	THU-IBM03-5
Fazinic, Stjepko	WED-IBA07-3
Fazleev, N. G.	THU-NBAE04-3
Fazleev, N. G.	THU-NBAE05-2
Fedotov, A. V.	THU-NP08-5
Fei, Zejie	TUE-AP05-P1
Fernandes, Sandrina	MON-NP01-P2
Fernandes, Sandrina Da Visitacao	WED-REP06-6
Ferreira, Paulo J	TUE-REP02-2
Fichtner, P. F.	MON-AT02-2
Fichtner, Paulo	TUE-IBA04-P3
Field, Chris R	WED-AT05-3
Field, K. G.	TUE-REP04-5
Field, Kevin G	WED-AT05-3
Fienberg, Gitai	TUE-NP03-4
Fink, Dietmar	THU-REP08-5
Firestone, Murray	TUE-SSCD02-3
Flambaum, V. V.	WED-NP05-1
Fletcher, Neil R	MON-IBA02-4
Floresca, Herman Carlo	WED-NST03-5
Fluss, Michael J.	MON-REP01-5
Fogle, M	TUE-AP04-P1
Fontana, Cristiano Lino	TUE-MA05-2
Fontana, Cristiano Lino	TUE-MA05-P3
Fontana, Cristiano Lino	TUE-MA05-P4
Fontana, Cristiano Lino	THU-IBA06-4
Fontes, Christopher J.	WED-AP08-3
Fowler, Mac	WED-NP06-6

Frankle, Christen M.....	WED-SSCD04-5
Fridmann, Joel	TUE-NST05-1
Friedrich, Thomas.....	MON-MA02-1
Frigola, Pedro	WED-SSCD04-2
Fritzsche, S.	TUE-AP05-5
Fritzsche, Stephan.....	WED-AP08-3
Fu, E.G.....	MON-IBA01-4
Fu, Engang.....	MON-REP01-3
Fuentes, BE.....	MON-AP01-P1
Fujii, Osamu	TUE-MA07-3
Fujii, Yuusuke.....	WED-MA09-P1
Fujimoto, Rintaro.....	WED-MA09-P1
Fuwa, Nobukazu	TUE-MA07-3
G, Devaraju.....	MON-IBM02-5
G, Devaraju.....	MON-IBM02-P1
G, Devaraju.....	MON-IBM02-P2
Gaathon, Ophir	WED-REP05-5
Galassi, M.	THU-REP08-3
Galindo-Uribarri, A.	WED-NP05-2
Galindo-Uribarri, A.	WED-NP05-4
Galindo-Uribarri, Alfredo.....	WED-NP06-1
Gall, Brady B	WED-SSCD04-5
Gall, Brady B	WED-SSCD04-P2
Gallant, A. T.	TUE-AP05-2
Gannon, P.	TUE-IBA03-4
Gao, Fei.....	TUE-REP02-P1
Garcia-Cabañes, Angel	WED-REP06-1
Garcia-Molina, Rafael	TUE-IBA04-1
Garcia-Molina, Rafael	TUE-IBA04-P1
Garcia-Molina, Rafael	TUE-IBA04-P2
Garcia-Ruiz, R. F.....	WED-NP05-2
Garner, Frank A.	TUE-REP02-1
Garratt, Elias	THU-ECR03-3
Garratt, Elias	THU-ECR03-P1
Garry, Charles K.....	TUE-AT03-4
Gary, Charles K	TUE-SSCD02-3
Gary, Charles K	WED-SSCD03-4
Gassert, H.	MON-AP01-4
Gentile, P.	TUE-IBA03-4
George, Richard E.	THU-IBM06-6
Gerity, James	TUE-ECR05-4
Gessner, Oliver	WED-NBAE06-2
Geyer, Sabrina	WED-AP08-3
Ghafari, Mohammad.....	TUE-REP04-3
Ghita, Dan Gabriel.....	WED-ECR04-4
Ghosh, T. K.....	MON-NP02-1
Giaccia, Amato J.....	MON-MA01-1
Giacoppo, F.....	WED-NP06-4
Gidley, David W.....	THU-NBAE04-6

Gila, Brent.....	TUE-NST05-1
Gillin, Michael T	WED-MA09-2
Girst, Stefanie	MON-MA02-2
Gislason, Haflidi	MON-IBM01-4
Giulian, Raquel	MON-IBM02-4
Glass, Gary A.....	WED-ECR04-3
Glass, Gary A.....	WED-NST04-P2
Glass, Gary A.....	MON-AT02-4
Glass, Gary A.....	WED-ECR04-5
Glass, Gary A.....	WED-IBA07-P1
Glass, Gary A.....	WED-IBA07-P2
Gleadow, Andrew J. W.....	WED-REP06-3
Goebl, Dominik	TUE-IBA04-3
Goerres, Joachim	MON-NP01-3
Golding, T.....	WED-ECR04-1
Golding, Terry	THU-ECR03-1
Goldman, Rachel S.	MON-IBA01-1
Gomez, E.	WED-NP05-1
Gondal, M. A.	MON-NBAE02-P1
Gonzales, Daniel.....	WED-AP07-P1
Gonzalez, Aleida C.....	MON-IBA02-4
Gosselin, Gilbert	WED-AP08-5
Gott, Katherine	WED-SSCD04-3
Gott dang, A.....	MON-IBA01-P4
Gott dang, A.....	WED-AT05-4
Gourlay, Stephen	FRI-PS04-1
Gozani, Tsahi	TUE-SSCD01-2
Gozani, Tsahi	TUE-SSCD02-2
Gozani, Tsahi	TUE-SSCD02-3
Gozani, Tsahi	WED-SSCD03-1
Gozani, Tsahi	WED-SSCD03-5
Grabowski, K.	THU-IBM03-5
Grande, P. L.....	MON-AT02-2
Grande, Pedro Luis	TUE-IBA04-2
Grande, Pedro Luis	TUE-IBA04-P3
Grande, Pedro Luis	TUE-IBA04-P4
Greaves, Graeme.....	WED-REP07-2
Greife, U.	THU-NP09-5
Greife, Uwe.....	TUE-NP03-5
Greubel, Christoph.....	MON-MA02-2
Griesmayer, Erich	TUE-AT04-2
Griffin, Don	WED-AP06-4
Grim, Gary	WED-NP06-6
Grime, G. W.	MON-AT02-1
Grime, Geoff W	THU-IBA06-2
Grisenti, R.....	MON-AP01-4
Grisenti, Robert.....	TUE-AP05-4
Grisenti, Robert.....	WED-AP08-3
Griswold, Justin R	TUE-NP04-4

Grogan, Brandon.....	TUE-NBAE03-3
Grossheim, A.	TUE-AP05-2
GRYGIEL, Clara	TUE-AP03-3
Grün, Rebecca.....	MON-MA02-1
Grzywacz, Robert	WED-NP05-5
Guerra, Mauro.....	TUE-AP05-3
Gugiu, Marius Marin	WED-ECR04-4
Guillen, C I	TUE-AP04-P1
GUILLOUS, Stéphane.....	TUE-AP03-3
Gul, Sheraz	WED-NBAE06-2
Gumberidze, A.....	TUE-AP05-5
Gumberidze, Alex.....	TUE-AP05-3
Gumberidze, Alex.....	WED-AP08-5
Gumberidze, Alexandre	TUE-AP05-4
Gumberidze, Alexandre	WED-AP08-3
Gumberidze, Alexandre	WED-AP08-6
Gunnlaugsson, Haraldur Palle	MON-IBM01-4
Guo, Jinghua.....	WED-NBAE06-2
Gupta, Niraj	WED-REP05-4
Gupta, Renu	WED-IBM04-5
Gurkan, Umut Atakan.....	MON-NST01-3
Gwilliam, R. M.	MON-AT02-1
Gwinner, G.	TUE-AP05-2
Gwinner, G.	WED-NP05-1
Gwon, Chul S.....	TUE-ECR05-6
Haberl, Arthur W	THU-ECR03-4
Haberl, Arthur W	THU-ECR03-6
Hable, Volker.....	MON-MA02-2
Hadjiev, Viktor G.	WED-NST03-2
Haertling, Carol	WED-AT05-P1
Haertling, Carol	THU-REP09-5
Hagel, Kris.....	THU-NP09-2
Hager, U.....	THU-NP09-5
Haglund, Jr., Richard F.....	WED-NBAE06-3
Hagmann, S.....	TUE-AP05-5
Hagmann, Siegbert	TUE-AP05-4
Hagmann, Siegbert	WED-AP08-2
Hagmann, Siegbert	WED-AP08-3
Hagmann, Siegbert	WED-AP08-6
Hahn, Horst.....	TUE-REP04-3
Haigh, Sarah	WED-REP07-2
Haight, R. C.	WED-NP07-2
Hale, Gerry	WED-NP06-6
Halfon, Shlomi.....	TUE-NP03-4
Hall, James.....	WED-SSCD04-1
Han, Weizhong	WED-REP05-1
Hao, Changtong	TUE-NBAE03-6
Hao, Y.....	THU-NP08-5
Hara, Masanori	MON-REP01-2

Hardy, Philippe	THU-NBAE04-P2
Hardy, S.	MON-NP02-3
HARDY, S.	WED-NP05-3
Harmon, Frank	MON-NBAE01-3
Harris, B.	THU-REP08-3
Harris, Jack L.	TUE-AT03-4
Hartwig, Zachary S.	WED-AP06-3
Harvey, James T.	WED-MA09-5
Harwood, Leigh	THU-NP08-1
Hashimot, N.	WED-REP07-3
Hashimoto, Naoki	TUE-MA07-3
Hashimoto, Shuichi.	TUE-REP04-6
Hassett, John P.	WED-AT05-1
Hatano, Yuji	MON-REP01-2
Hatarik, Robert	WED-AP08-5
Hattar, Khalid	TUE-IBM05-5
Hattar, Khalid	TUE-REP02-2
Hattar, Khalid	WED-REP07-4
Hattori, Toshiyuki	TUE-AT04-6
Hausladen, P. A.	WED-SSCD03-3
Hausladen, Paul	MON-NBAE02-3
Havener, C C	TUE-AP04-P1
Havener, Charles.	TUE-AP04-3
Havenith, Andreas	MON-NBAE02-P2
Havranek, Vladimir	THU-REP08-5
Hawari, Ayman I.	THU-NBAE04-6
Hawley, Marilyn E.	TUE-REP02-6
Hayes, Anna.	WED-NP06-6
Heasman, K. C.	MON-AT02-1
Hebard, Arthur F.	TUE-NST05-1
Hebden, Andrew	WED-MA09-4
Heber, Oded	WED-AP07-1
Hedlof, Ryan M.	WED-AP06-P4
Hegewald, Myke.	WED-AP08-3
Heid, Oliver	THU-AT06-4
Heil, Michael	WED-AP08-5
Heimann, Philip A.	WED-NBAE06-2
Heintze, Cornelia	TUE-REP02-3
Henager, Charles H.	TUE-IBM05-6
Henriquez, S.	WED-NP07-5
Henrotin, Sebastien	WED-MA03-2
Hentz, A.	TUE-IBA04-4
Herfurth, Frank	TUE-AP05-4
Hernandez, Mike.	WED-SSCD03-5
Hernández-Mayoral, Mercedes.	TUE-REP02-3
Hertlein, Marcus P.	WED-NBAE06-2
Hess, S.	TUE-AP05-5
Hess, Sebastian	WED-AP08-3
Hicks, S. F.	TUE-IBA05-6

Hill, Patrick.....	WED-MA03-6
Hill, T. S.	WED-NP06-5
Hillenbrand, Pierre-Michel	WED-AP08-2
Hinks, Jonathan A.....	WED-REP07-2
Hinshelwood, David D	WED-SSCD03-2
Hippler, Rainer	MON-IBA01-P2
Hiramoto, Kazuo.....	WED-MA09-1
Hiramoto, Kazuo.....	WED-MA09-2
Hiramoto, Kazuo.....	WED-MA09-P1
Hirao, Toshio	TUE-REP04-6
Hirsh, Stacey L.	MON-NST01-2
Hnatowicz, Vladimir.....	THU-REP08-5
Hobein, M.	WED-AP08-1
Hodges, R.	MON-NP02-1
Hodgkinson, Adrian.....	TUE-NP03-2
Hodgkinson, Adrian.....	TUE-NP03-5
Hoef, F.L. van de	MON-IBA01-P4
Hoekstra, Ronnie	MON-AP01-P4
Hofsäss, Hans	TUE-NST06-3
Hojou, Kiichi	WED-REP06-5
Hokin, Mitchell.....	TUE-AP04-3
Holland, O. W.....	WED-ECR04-1
Holland, Orin W	WED-ECR04-2
Holland, Wayne	THU-ECR03-1
Hollinger, Craig	TUE-MA05-3
Holm, Ann IS	MON-AP01-2
Holmes-Cerfon, Miranda.....	TUE-NST06-4
Hong Liao, Chijing	MON-IBA01-6
Hoover, A.	THU-REP08-3
Hoppe, Sarah M.....	WED-REP07-4
Horanyi, Mihaly.....	WED-TA01-4
Horbatsch, Marko	MON-AP01-5
Horbatsch, Marko	MON-AP01-P2
Horn, B.	THU-REP08-3
Hosack, Michael	TUE-SSCD02-4
Hosemann, P.	TUE-REP02-1
Hosemann, Peter	MON-REP01-5
Hosemann, Peter	TUE-REP02-5
Hossain, K.....	WED-ECR04-1
Hossain, Khalid.....	WED-ECR04-2
Hossain, Khalid.....	THU-ECR03-1
Houssain, Zohair S.....	WED-REP06-4
Howard, M. E.	MON-NP02-3
HOWARD, M. E.	WED-NP05-3
Howard, M. E.	WED-NP05-4
Howard, Meredith.....	MON-NP02-1
Hsieh, Chi-wen	TUE-MA05-P2
Hsiung, L.	TUE-REP02-1
Hsiung, Luke.....	MON-REP01-5

Hu, Shenyang.....	WED-REP05-2
Huang, Hsu-Cheng	WED-REP05-5
Huang, Mengbing	MON-IBA01-2
Huang, R.T.....	TUE-REP04-P2
Huber, Bernd A.....	MON-AP01-2
Hubler, G.	THU-IBM03-5
Hui, Ron.....	WED-NST03-1
Hull, Robert	WED-NST04-3
Hung, Wei-Song	THU-NBAE04-4
Hunt, A. W.....	TUE-NBAE03-5
Hunt, Alan W.....	TUE-NBAE03-4
Hurley, Ford.....	TUE-MA05-1
Hurtle, Ken P.	WED-MA09-5
Huse, Nils	WED-NBAE06-2
Hutcheson, Anthony L.....	WED-SSCD03-2
Hutcheson, Anthony L.....	TUE-ECR05-6
Hutton, A.	THU-NP08-5
Hutton, Roger	TUE-AP05-1
Hutton, Roger	TUE-AP05-P1
Hwang, Y. S.....	THU-IBM06-P1
Hynes, M.....	THU-REP08-3
Iannotti, Laura.....	MON-MA02-3
Ibrahim, Baher A.	WED-IBA07-P1
Iga, Kiminori.....	WED-MA09-2
Ikeda, Tokihiro	TUE-AP03-1
IKEDA, Tokihiro	TUE-AP03-3
Ikeda, Tokihiro	TUE-AP03-4
ILA, Daryush	MON-NP01-P1
ILA, Daryush	WED-NST04-1
ILA, Daryush	WED-TA02-3
Illescas, Clara.....	MON-AP01-3
Illescas, Clara.....	MON-AP01-P3
Imanishi, Akira	WED-IBM04-3
Imashuku, Susumu.....	WED-IBM04-3
Indelicato, Paul	TUE-AP05-3
Indelicato, Paul	WED-AP08-3
Indelicato, Paul	WED-AP08-6
Inertial Confinement Fusion Team, on behalf of The National.....	MON-PS01-1
Ingram, David C	WED-SSCD03-P1
Ionescu, Cristina	THU-ECR03-5
Ionescu, Paul.....	WED-ECR04-4
Irman, Arie.....	THU-AT06-P1
Ishii, Yasuyuki.....	WED-NST04-4
Ishikawa, Hitoshi	TUE-MA07-4
Ishikawa, Norito	WED-REP06-5
Ishimaru, Manabu	WED-IBM04-4
Isoda, Syoichi	WED-REP06-5
Issab, A. A.	MON-NBAE02-P1
Issab, A. A.	TUE-SSCD02-P1

Ito, Kazuto	TUE-MA07-4
Iwamoto, Naoya.....	TUE-REP04-6
Iwasaki, Hironori	WED-NP07-3
Jackson, Lori.....	TUE-ECR05-6
Jackson, Stuart L.....	TUE-NBAE03-2
Jackson, Stuart L.....	WED-SSCD03-2
Jackson, Stuart L.....	TUE-ECR05-6
Jagodzinski, P.	TUE-AP05-5
Jagutzki, O.	MON-AP01-4
Jahnke, T.....	MON-AP01-4
Jaksic, Milko.....	WED-ECR04-6
James, Conrad D.....	THU-IBA06-4
Jandel, M.....	WED-NP07-2
Janzen, Meghan S.	WED-NP06-1
Javahery, Gholamreza.....	TUE-NBAE03-6
Javey, Ali	WED-SSCD04-6
Jean, Y.C.....	THU-NBAE04-4
Jenkins, David.....	THU-NP09-4
Jeynes, C.	MON-AT02-1
Jeynes, Chris	TUE-IBA05-3
Jeynes, J. C.	MON-AT02-1
Ji, Qing.....	TUE-AT03-4
Ji, Qing.....	TUE-AT03-5
Ji, Qing.....	WED-SSCD03-4
Jiang, Changzhong.....	TUE-REP04-4
Jiang, Ke	THU-REP08-4
Jiang, W	TUE-IBA03-2
Jiang, Weilin.....	MON-IBM01-5
Jiang, Weilin	TUE-REP04-P1
Jiang, Weilin.....	WED-IBM04-4
Jiao, Zhijie	TUE-IBA05-5
Jin, Dongcun	TUE-MA07-3
Jin, Ke	TUE-IBA03-5
Jin, Michael.....	THU-NBAE05-1
Jin, Xuelong	TUE-AP05-P1
Jipa, Alexandru	THU-ECR03-5
Jipa, Alexandru	THU-NBAE05-3
Jochmann, Axel	THU-AT06-P1
Joglekar, Prasad	THU-NBAE04-3
Johansson, Henrik AB	MON-AP01-2
Johansson, Stefan.....	TUE-MA05-3
John, Angelin Ebanezar	MON-IBA01-P2
John, Kevin D	TUE-NP04-3
John, Kevin D	WED-MA09-3
Johnson, Christopher	WED-TA01-P2
Johnson, E.....	THU-NP09-3
Johnson, Jeffrey	TUE-NBAE03-3
Johnson, Mike.....	TUE-NP03-2
Johnson, Richard.....	TUE-NP04-5

Johnson, Richard.....	WED-MA04-1
Johnson, William	WED-SSCD04-7
Johnston, Karl	MON-IBM01-4
Johnstone, Carol Joanne	WED-MA04-5
Joly, A G	TUE-IBM05-2
Jonah, Charles.....	WED-MA09-4
Jonah, Charles D.....	WED-MA09-5
Jones, Adric C. L.	THU-NBAE04-2
Jones, B. N.....	MON-AT02-1
Jones, Brian N.....	THU-IBA06-2
Jones, Glenn.....	TUE-AT03-4
Jones, K. L.	MON-NP02-3
JONES, K. L.	WED-NP05-3
Jones, K. L.	WED-NP05-4
Jongen, Yves.....	MON-MA02-3
Jongen, Yves.....	WED-MA03-2
Joshi, Chandrashekhar	WED-MA03-3
Jost, Cara U.....	TUE-NP04-4
Joy, N	TUE-IBA03-2
Joyce, James M.....	MON-AT02-3
Jubera, Mariano	WED-REP06-1
Julin, Jaakko	MON-IBA01-7
Julin, Jaakko	MON-IBA01-P5
Julin, Jaakko	MON-IBA01-P6
Jung, A.....	MON-AP01-4
Jungman, Jerry	WED-NP06-6
Jurczyk, Brian E.....	TUE-AT03-3
Jurisson, Silvia S.....	WED-MA09-3
Kachurin, G. A.....	MON-IBM01-6
Kaindl, Robert.....	WED-NBAE06-2
kaiser, ralf	TUE-ECR05-2
Kakiuchida, H.	THU-IBM06-3
Kalakada, Zameer	MON-NBAE02-5
kamada, tadashi.....	TUE-MA07-1
Kamaev, G. N.	MON-IBM01-6
Kaminuma, Takuya.....	TUE-MA07-4
Kamiya, Tomihiro.....	WED-NST04-4
Kanazawa, Mitsutaka.....	TUE-MA07-5
Kane, Steve	TUE-SSCD02-3
Kapadia, Rehan.....	WED-SSCD04-6
Karamian, S. A.	WED-NP07-5
Karonis, Nicholas	TUE-MA05-1
Kasagi, Jirohta	TUE-IBA05-1
Kaspar, T F	TUE-IBM05-2
Kato, Hiroyuki	TUE-MA07-4
Kavcic, Matjaz	WED-IBA07-3
Kawai, Jun	WED-IBM04-3
Kawano, Toshihiko.....	MON-NP02-2
Kawasaki, Katsunori.....	TUE-AT04-6

Kayani, Asghar	MON-IBM01-2
Kayani, Asghar	THU-ECR03-3
Kayani, Asghar	THU-ECR03-P1
Kayhko, Marko	THU-ECR03-2
Kayran, D.....	THU-NP08-5
KC, Bindu	MON-NBAE01-3
Ke, Yao	WED-AP08-1
Keerthisinghe, D.....	TUE-AP03-5
Keerthisinghe, Darshika	TUE-AP03-4
Keitel, Christoph.....	WED-AP08-5
Kellams, Joshua	TUE-ECR05-3
Kellams, Joshua	TUE-REP02-4
Kelley, Michael J.....	WED-NBAE06-3
Kelsey IV, Charles T.	WED-MA09-5
Kemper, Kirby W	MON-IBA02-4
Kennedy, J	MON-IBM01-P1
Kennedy, John	TUE-IBA04-P3
Kennedy, John Vedomuthu.....	MON-IBM01-1
Kenny, Craig.....	WED-AT05-1
Kenny, Craig.....	WED-TA02-2
Kerr, Phil.....	WED-SSCD04-1
Kersting, L. J.....	TUE-IBA05-6
Kester, Oliver.....	TUE-AP05-4
Ketring, Alan R.....	WED-MA09-3
Kettler, John.....	MON-NBAE02-P2
Key, C. F.....	TUE-IBA03-4
Key, Camas.....	TUE-IBA03-3
Khan, Saif Ahmad	MON-IBM02-2
Khaplanov, Anton.....	WED-AP08-4
Kharel, Prashanta.....	WED-TA01-1
KHEMLICHE, Hussein	TUE-AP03-3
Khiari, Fatah Z.....	TUE-SSCD02-P1
Khizroev, Sakhrat	MON-NST07-3
Kholopov, M. A.	THU-NP08-5
Khurmi, Champak.....	WED-NBAE06-2
Kieser, William E	TUE-NBAE03-6
Kiester, Allen S.....	WED-AP06-P6
Kight, Tyler C.....	WED-TA02-2
Kijel, Daniel.....	TUE-NP03-4
Kilmametov, Askar R.	TUE-REP04-3
Kim, Baek Huyn	WED-SSCD04-5
Kim, Baek Hyun	WED-SSCD04-P2
Kim, George	TUE-NP03-3
Kim, H.K.	MON-AP01-4
Kim, Moon J.....	WED-NST03-5
Kimura, Kenji	WED-REP06-5
King, Jonathan G	WED-AP07-4
King, Michael	TUE-SSCD02-3
King, Michael J.....	TUE-SSCD01-2

King, Micheal J.....	WED-SSCD03-1
Kinlaw, M. T.....	TUE-NBAE03-5
Kinoshita, H.....	WED-REP07-3
Kirby, Nigel	WED-REP06-4
Kirchner, Tom.....	MON-AP01-P2
Kirk, Mark	WED-REP07-6
Kirk, Marquis.....	TUE-IBM05-5
Kirk, Marquis Albert	WED-REP07-1
Kirkby, K. J.....	MON-AT02-1
Kittimanapun, Kritsada.....	TUE-NP03-1
Kleeven, Wiel	WED-MA03-2
Klein, Andi	WED-NP06-6
Klein, Eric E	WED-MA03-6
Klingfus, Joseph	TUE-NST05-1
Kloepper, Kim L.....	TUE-AT03-3
Kluth, Patrick.....	MON-IBM02-4
Kluth, Patrick.....	WED-REP06-2
Kluth, Patrick.....	WED-REP06-4
Knies, D.	THU-IBM03-5
Knjazev, Egor V.	TUE-IBM05-P1
Kobayashi, Makoto.....	MON-REP01-2
Kobayashi, Osamu.....	TUE-MA07-6
Kohley, Zachary	THU-NP09-2
Kojima, Kazutoshi	TUE-REP04-6
Kolasinski, Robert D	MON-IBA02-3
Kolda, Peter E.....	THU-AT06-2
Koltick, David.....	MON-NBAE02-4
Koltick, David.....	TUE-SSCD02-4
Koltick, David.....	WED-MA03-P1
Kondrasovs, Vladimir.....	TUE-ECR05-1
Kondyurin, Alexey	MON-NST01-2
Koshchiy, E.....	THU-NP09-3
Kosobrodova, Elena.....	MON-NST01-2
Kovaleski, Scott D.....	WED-SSCD04-5
Kovaleski, Scott D.....	WED-SSCD04-P2
Kovivchak, Vladimir S.	TUE-IBM05-P1
Kovivchak, Vladimir S.	TUE-IBM05-P2
Kozhuharov, C.....	TUE-AP05-5
Kozhuharov, Christopher.....	WED-AP08-5
Kozhuharov, Christophor	WED-AP08-2
Kozhuharov, Christophor	WED-AP08-3
Kozub, R. L.....	MON-NP02-3
KOZUB, R. L.	WED-NP05-3
Kozub, R. L.....	WED-NP05-4
Krafft, G. A.....	THU-NP08-5
Krahn, Elizabeth	WED-MA09-4
Krause, Markus.....	WED-REP06-6
Krawczyk, Frank L	THU-AT06-6
Krebs, John	WED-MA09-4

Kretschmer, Wolfgang.....	TUE-NP03-6
Kretschmer, Wolfgang.....	WED-NP06-2
Kriewaldt, Kim	WED-AT05-3
Kring, Thomas	MON-NBAE02-P2
Kritcher, Andrea L.....	WED-AP08-5
Krivozubov, Oleg V.....	TUE-IBM05-P1
Krticka, M.....	WED-NP07-2
Krug, C.	MON-AT02-2
Krupin, Oleg	WED-NBAE06-2
Kuchera, A.....	THU-NP09-3
Kucheyev, S. O.....	MON-IBA02-1
Kuchibhatla, S. V. N. T	TUE-IBA03-2
Kuchibhatla, SVNT	TUE-IBA03-P1
Kudo, Sho	TUE-MA07-5
Kuehl, Thomas.....	WED-AP08-5
Kumar, A.	TUE-AP05-5
Kumar, A.	TUE-IBA05-6
Kumar, Ashavani	WED-IBM04-5
kummari, V. C.	THU-IBM06-P2
Kummari, Venkata.....	WED-NST04-P2
Kummari, Venkata C.....	WED-ECR04-3
Kummari, Venkata C.....	WED-IBA07-P2
Kummari, Venkata C.....	MON-AT02-4
Kummari, Venkata C.....	MON-IBM01-5
Kummari, Venkata C.....	WED-ECR04-5
Kummari, Venkata C.....	WED-IBA07-P1
Kunnath, Paul	THU-IBM03-1
Kuntzsch, Michael	THU-AT06-P1
Kurtalan, Secil	MON-NST01-P2
Kurtz, R J.....	TUE-IBM05-2
Kusano, Yohsuke.....	TUE-MA07-6
Kwan, Jae Won.....	WED-SSCD04-P2
Kwiatkowski, Anna A.	TUE-AP05-2
Kwon, Jae Wan.....	WED-SSCD04-5
Kwong, John.....	TUE-SSCD02-3
Kühl, Thomas	TUE-AP05-4
Kyriakou, Ioanna	TUE-IBA04-1
LaBrake, Scott	WED-TA01-P2
Lacalamita, Annarita.....	TUE-MA05-P1
Lagergen, K. B.....	WED-NP05-2
Laitinen, Mikko	MON-IBA01-7
Laitinen, Mikko	MON-IBA01-P5
Laitinen, Mikko	MON-IBA01-P6
Laitinen, Mikko	WED-NST04-5
Lakshantha, W. J.....	MON-AT02-4
Lakshantha, Wickramaarachchige	MON-IBA01-P7
Lakshantha, Wickramaarachchige	WED-ECR04-P3
Lakshantha, Wickramaarachchige	WED-IBA07-P2
Lan, Mingcong.....	TUE-IBA05-1

Lane, Ryan A.	WED-AP06-P2
Lanford, William	THU-ECR03-6
Lang, Maik.....	WED-IBM04-1
Lang, Maik.....	WED-REP06-3
Lang, Maik.....	WED-REP07-5
Lang, Volker	THU-IBM06-6
Langeveld, Willem G J	TUE-SSCD02-2
Langeveld, Willem G.J.	TUE-SSCD01-2
Langeveld, Willem G.J.	WED-SSCD03-5
Langouche, Guido.....	MON-IBM01-4
Lanza, R.	THU-REP08-3
Lapi, Suzanne	TUE-NP04-2
Lapierre, A.	TUE-AP05-2
Lapierre, Alain	TUE-NP03-1
Laptev, A. B.....	WED-NP06-5
Larsen, L. Scott.....	WED-AT05-2
Larsen, L. Scott.....	WED-TA02-2
Latkowski, Jeff	MON-REP01-5
Lattouf, Elie	MON-AP01-2
Le Flanchec, Vincent	TUE-AT04-4
Le Tourneur, Philippe.....	TUE-AT03-2
LEBIUS, Henning.....	TUE-AP03-3
Leckey, John	THU-NP08-4
Ledingham, Kenneth.....	THU-AT06-P1
Lee, Chung-chi	TUE-MA05-P2
Lee, Hye Young.....	MON-NP02-2
Lee, J.	MON-NP02-1
Lee, Jeng-hung.....	TUE-MA05-P2
Lee, Kuier-Rarn	THU-NBAE04-4
Lee, Sungbae.....	WED-NST03-2
Lee, Teck Ghee.....	MON-AP02-3
Lee, Yuna.....	THU-IBM06-P1
Lehnert, Ulf.....	THU-AT06-P1
Leino, Aleks A.....	WED-REP06-2
Leitner, Daniela	TUE-NP03-1
Leitner, Daniela	TUE-NP03-5
Leitner, Matthaeus	TUE-NP03-5
LELIEVRE, Daniel.....	TUE-AP03-3
Lemaitre, Maxime.....	TUE-NST05-1
Lemut, A.	THU-NP09-5
Lemut, Alberto.....	TUE-NP03-5
Lenci, Stephan J.....	THU-AT06-2
Lenka, Haraprasanna	THU-ECR03-2
Lennarz, A.	TUE-AP05-2
Lenz, U.	MON-AP01-4
Leone, Stephen R.....	WED-NBAE06-2
Lesigyerski, Deyan	THU-IBA06-5
Lestinsky, Michael.....	WED-AP08-2
Leung, K.- N.	WED-SSCD03-3

Leung, Ka-Ngo	TUE-AT03-P1
Leung, Ka-Ngo	WED-SSCD04-4
Leung, Ka-Ngo	WED-SSCD04-7
Leung, Ka-Ngo	WED-SSCD04-P1
Leveneur, Jerome	TUE-IBA04-P3
Levichev, Eugene	WED-MA03-1
Levy, Richard	TUE-MA05-4
Levy, Richard	TUE-MA05-5
Levy, Richard	TUE-MA06-2
Levy, Richard P	THU-MA08-1
Li, Huang	TUE-IBA03-P1
li, Lin	MON-IBA01-6
Li, Weixing	WED-REP06-3
Li, Weixing	WED-REP07-5
Li, Weixing	THU-IBM06-2
Li, Xufang	WED-IBA07-5
Li, Yang	WED-NST03-3
Liang, J. F.	WED-NP05-4
Lidestri, Joseph	WED-MA04-1
Liendo, Jacinto A	MON-IBA02-4
Liesen, Dieter	WED-AP08-6
Liljeby, Leif	TUE-AP05-P1
Lim, C. Duk	WED-ECR04-P1
Lim, C. Duk	THU-ECR03-P2
Lin, Chih-hsun	TUE-MA05-P2
Lin, Hao-Hsiung	MON-IBA01-6
Lin, Ming-Fu	WED-NBAE06-2
Lin, Yong	WED-SSCD04-3
Lindroth, E.	WED-AP07-2
Linhard, L. E.	THU-NP09-3
Linhardt, L.	THU-NP09-5
Lister, C. J.	MON-NP02-3
Liszkay, Laszlo	THU-NBAE04-P2
Litherland, Albert E	TUE-NBAE03-6
Litvinenko, V.	THU-NP08-5
Litvinov, Dmitri	MON-NST07-3
Litvinov, Yu	WED-AP08-5
Litvinov, Yuri	TUE-AP05-4
Litvinov, Yuri	WED-AP08-2
Litz, M. S.	WED-NP07-5
Liu, Chuan-Sheng	TUE-NP03-P1
Liu, Fang	TUE-IBA03-P1
Liu, Jianwei	WED-NST03-1
Liu, Kai	TUE-REP04-P1
Liu, Ming	THU-NBAE04-6
Liu, Tung-Chang	TUE-NP03-P1
Liu, Xiang-Yang	TUE-REP02-P1
Liu, Yuan	WED-NP06-1
Lo, Cheuk Chi	THU-IBM06-6

Loch, Stuart.....	WED-AP06-4
Loew, Tim.....	TUE-NP03-2
Lotrus, Paul.....	THU-NBAE04-P2
Lowenstein, Derek.....	WED-MA04-1
Lu, Di.....	TUE-AP05-P1
Lu, Ning.....	WED-NST03-5
Lu, Rongtao.....	WED-NST03-1
Luce, Flavio.....	TUE-IBA04-P3
Ludewigt, Bernhard.....	TUE-AT03-5
Ludewigt, Bernhard.....	TUE-NBAE03-4
Ludewigt, Bernhard.....	WED-SSCD03-4
Ludewigt, Bernhard A.....	TUE-AT03-4
Ludwig, Jr., Karl F.....	TUE-NST09-4
Lueck, C. J.....	TUE-IBA05-6
Luedde, Hans Juergen.....	MON-AP01-P2
Lynch, W.....	MON-NP02-1
Lyneis, Claude.....	TUE-NP03-2
Lyon, Steven A.....	THU-IBM06-6
Ma, Jean-Luc.....	MON-NBAE02-P2
Ma, Ki.....	MON-IBA01-5
MacAskill, John A.....	WED-AP06-1
Macdonald, T. D.....	TUE-AP05-2
Macek, J. H.....	WED-AP07-5
Maclot, Sylvain.....	MON-AP01-2
Madi, Charbel S.....	TUE-NST09-3
Madi, Charbel S.....	TUE-NST09-4
MADI, Toiammou.....	TUE-AP03-3
Madrid, Evelyn.....	TUE-NP04-2
Madsen, Morten Bo.....	MON-IBM01-4
Madzunkov, Stojan M.....	WED-AP06-1
Maertin, Renate.....	TUE-AP05-4
Maertin, Renate.....	WED-AP08-6
Mahajan, Anita.....	TUE-MA06-1
Mahler, G. J.....	THU-NP08-5
Mahmood, S.....	WED-AP07-2
Maimaitimin, M.....	THU-REP08-6
Maisonny, Rémi.....	MON-AP01-2
Maj, Adam.....	THU-NP09-4
Majima, Takuya.....	MON-IBA01-P3
Makarashvili, Vakhtang.....	WED-MA09-4
Makarashvili, Vakhtang.....	WED-MA09-5
Makino, Takahiro.....	TUE-REP04-6
Maloy, S.A.....	MON-REP01-5
Mamtimin, Mayir.....	MON-NBAE01-1
Mamtimin, Mayir.....	MON-NBAE01-2
Manandhar, S.....	TUE-IBM05-2
Manandhar, Sandeep.....	MON-IBM01-2
Mancini, Derrick.....	THU-ECR03-3
Mancini, Derrick.....	THU-ECR03-P1

Mandic, Luka.....	WED-IBA07-3
Mandrillon, Jerome.....	WED-MA03-2
Mandrillon, Pierre.....	WED-MA03-2
Mane, E.....	TUE-AP05-2
Mann, Thomas	TUE-ECR05-3
Mann, Thomas	TUE-REP02-4
Manning, B.	MON-NP02-1
Manning, B.	MON-NP02-3
MANNING, B.	WED-NP05-3
Manning, B.	WED-NP05-4
Manning, Mellony S	WED-AT05-1
Mantovan, Roberto	MON-IBM01-4
Manuel, Jack E.....	WED-NST04-P2
Manuel, Jack E.....	MON-AT02-4
Manuel, Jack E.....	WED-IBA07-P1
Manzano-Santamaria, Javier.....	WED-REP06-1
Marble, Daniel Keith	WED-TA02-1
Marchetto, Flavio.....	MON-MA02-3
Marchuk, Olexander	WED-AP06-2
Marian, Jaime	MON-REP01-5
Marin, D. V.....	MON-IBM01-6
Markina, Elena.....	TUE-IBA05-5
Markwitz, A.....	MON-IBM01-P1
Marletta, Giovanni	MON-NST01-1
Marletta, Giovanni	MON-NST07-4
Marsland, Maryn Grace	TUE-MA05-3
Marsman, Alain	MON-AP01-5
Martin, Merl F	WED-AP07-4
Martinez, Enrique	WED-REP05-3
Martinez, Enrique	WED-REP05-4
Martinez, H.....	MON-AP01-P1
Maruhashi, Akira	WED-MA04-3
Masenda, Hilary.....	MON-IBM01-4
Maslehuddin, M.....	MON-NBAE02-5
Massey, Thomas N	WED-SSCD03-P1
Matea, Iolanda	THU-NP09-4
Matos, M.....	MON-NP02-3
MATOS, M.....	WED-NP05-3
Matos, M.....	WED-NP05-4
Matoš, M.....	THU-NP09-3
Matsuda, Koji	WED-MA09-2
Matsuda, Koji	WED-MA09-P1
Matsui, Hiroshi	TUE-MA07-4
Matsunami, N.	THU-IBM06-3
Matsuo, Jiro	THU-IBA06-1
Matsuo, Jiro	THU-IBM03-3
Matsuo, Shigeki	TUE-REP04-6
Matsuura, Taeko	WED-MA09-P1
Mauerhofer, Eric.....	MON-NBAE02-P2

Mausner, Leonard	MON-NP01-P2
Mausner, Leonard F.....	TUE-NP04-1
May, Donald P	TUE-NP03-3
May, Elebeoba	THU-IBA06-4
May, Larry W	THU-NP09-2
Mayer, Matej.....	TUE-IBA05-5
McAlexander, T. William.....	THU-REP09-5
McCammon, D	TUE-AP04-P1
McCammon, Dan.....	TUE-AP04-3
McCarrick, James	WED-SSCD04-1
McCloy, John S.	TUE-REP04-P1
McConchie, Seth.....	MON-NBAE02-3
McConchie, Seth.....	TUE-NBAE03-3
McDaniel, F. D.	WED-ECR04-P1
McDaniel, F. D.	THU-IBM06-P2
McDaniel, Floyd	THU-ECR03-1
McDaniel, Floyd D	WED-ECR04-3
McDaniel, Floyd D.	MON-AT02-4
McDaniel, Floyd D.	MON-IBM01-5
McDaniel, Floyd D.	WED-ECR04-5
McDaniel, Floyd Del	WED-IBA07-P2
McDonough, P. J.	TUE-IBA05-6
McEllistrem, M. T.	TUE-IBA05-6
McInturff, Al.....	TUE-ECR05-3
McInturff, Al.....	TUE-REP02-4
McIntyre, Peter	TUE-ECR05-3
McIntyre, Peter	TUE-ECR05-4
McIntyre, Peter	TUE-REP02-4
McKenzie, David R	MON-NST01-2
McKinsey, Daniel	TUE-SSCD02-3
Meckel, M.....	MON-AP01-4
Meersschaut, Johan.....	THU-ECR03-2
Mehta, Rahul.....	THU-IBA06-P1
Meidinger, Alfred	THU-AT06-6
Meisel, Z.	THU-NP09-5
Melconian, D. G.	WED-NP05-1
Melnichenko, V. V.	TUE-REP02-1
Méndez, L.	MON-AP01-P3
Meng, W.	THU-NP08-5
Meot, Vincent	WED-AP08-5
Merabet, H.	MON-AP01-4
Merchant, M.	MON-AT02-1
Merino, E.	MON-NP02-1
Merrill, Frank.....	WED-NP06-6
Méry, Alain.....	MON-AP01-2
MERY, Alain	TUE-AP03-3
Messerschmidt, Marc.....	WED-NBAE06-2
Metz, D.	MON-AP01-4
Metzler, Rebecca Ann	WED-NBAE06-4

Michalak, Sarah	TUE-REP03-3
Michalski, Dörte	MON-MA02-2
Micklich, Bradley	WED-MA09-4
Mihalczo, John.....	MON-NBAE02-3
Mihalczo, John.....	TUE-NBAE03-3
Mikellides, Ioannis	MON-IBA02-2
Mikhailov, Kirill A.	TUE-IBM05-P2
Milavec, Tina	THU-IBA06-5
Miller, Michael	TUE-IBA03-1
Milton, Bruce	TUE-NP04-5
Mima, Masayuki	TUE-MA07-3
Minitti, Michael P.	WED-NBAE06-2
Minohara, Shinichi	TUE-MA07-6
Miraglia, Jorge E	MON-AP02-4
Miraglia, Jorge E	TUE-IBA04-5
MIRO, Sandrine.....	TUE-IBA05-4
Mirzadeh, Saed	TUE-NP04-4
Mishima, T D.....	WED-ECR04-2
Misra, Amit.....	TUE-IBM05-1
Misra, Amit.....	TUE-IBM05-5
Misra, Amit.....	WED-REP05-1
Mitchell, G. E.	WED-NP07-2
Mitchell, L.	WED-ECR04-P1
Mitchell, Lee J	WED-SSCD03-2
Mitchell, Lee J.	TUE-ECR05-6
Mitra, Sudeep.....	MON-NBAE02-1
Mitsumto, Toshinori	WED-MA04-3
Mittig, Wolfgang	MON-NP01-P2
Mittig, Wolfgang	WED-REP06-6
Miyake, Yoshinobu.....	WED-NST04-4
Miyamoto, Naoki.....	WED-MA09-P1
Mizoguchi, Nobutaka	TUE-MA07-6
Mocko, M.	THU-REP08-3
Mohamed, T.....	WED-AP08-1
Molholt, Torben Esman	MON-IBM01-4
Moll, Sandra	TUE-IBM05-4
Molls, Michael.....	MON-MA02-2
Momotyuk, O. A.....	MON-IBA02-4
Mondello, L. L.	THU-NP09-3
MONNET, Isabelle.....	TUE-AP03-3
Montanari, Claudia C.....	MON-AP02-4
Montanari, Claudia C.....	TUE-IBA04-5
Montes, F.	THU-NP09-5
Moore, Robert.....	WED-TA01-P2
Morel, Pascal	WED-AP08-5
Morgan, K.....	TUE-AP04-P1
Morgan, Kelsey.....	TUE-AP04-3
Morita, Yosuke	WED-REP06-5
Morse, D. H.	WED-SSCD03-3

Morse, Dan H.....	WED-SSCD04-4
Morse, Dan H.....	WED-SSCD04-P1
Morton, John J. L.....	THU-IBM06-6
Moschini, Giuliano	TUE-MA05-P3
Moschini, Giuliano	TUE-MA05-P4
Moser, Marcus	TUE-IBA05-5
Mosher, David	TUE-NBAE03-2
Mosher, David	WED-SSCD03-2
Motta, Francis C.	TUE-NST06-2
Mous, D.J.W.....	MON-IBA01-P4
Mous, D.J.W.....	WED-AT05-4
Moxom, Jeremy	THU-NBAE04-6
Mozin, Vladimir	TUE-NBAE03-4
Ms Milian, Felix	MON-MA02-3
Mueller, Alex	WED-AP08-5
Mueller, P. E.	WED-NP05-2
mulhauser, Françoise	TUE-ECR05-2
Mullens, James	MON-NBAE02-3
Multhoff, Gabriele	MON-MA02-2
Mulware, Stephen J	MON-IBA01-P7
Mulware, Stephen J	WED-ECR04-P3
Mulware, Stephen J.	MON-AT02-4
Mumm, Pieter	WED-NP07-4
Murakami, Masao	TUE-MA07-3
Murakami, Mitsuko	MON-AP01-P2
Murmu, P P.....	MON-IBM01-P1
Murokh, Alex.....	WED-SSCD04-2
Murphy, Donald P	WED-SSCD03-2
Muto, Hideshi	TUE-AT04-6
Myers, M. T.	MON-IBA02-1
Müller, A. M.	WED-IBA07-4
MÜLLER, Arnold Milenko	TUE-AP03-3
Märting, Renate	WED-AP08-3
N, Srinivasa Rao	MON-IBM02-5
N, Srinivasa Rao	MON-IBM02-P1
N, Srinivasa Rao	MON-IBM02-P2
Naab, Fabian U	WED-TA01-5
Nachimuthu, P	TUE-IBA03-2
Nachimuthu, Ponnusamy	THU-IBM06-5
Nadzeyka, Achim	TUE-NST05-1
Nagamine, Yoshihiko	WED-MA09-P1
Nagler, Ami	TUE-NP03-4
Nagy, G.U. L.	TUE-AP03-6
Naidoo, Deena	MON-IBM01-4
Nair, K G M.....	MON-IBM02-5
Najjari, Bennaceur	WED-AP08-3
Nakagawa, Shinichiro.....	THU-IBM03-3
Nakagawa, Shunichiro	THU-IBA06-1
Nakajima, Kaoru.....	WED-REP06-5

Nakano, Takashi	TUE-MA07-4
Nakashima, Chihiro	WED-MA09-2
Nakayama, Yuko	TUE-MA07-6
Nandasiri, Manjula	THU-ECR03-3
Nandasiri, Manjula I	TUE-IBA03-2
Napari, Mari	WED-NST04-5
Naqvi, Akhtar A	MON-NBAE02-5
Naqvi, Akhtar A	MON-NBAE02-P1
Naqvi, Akhtar A	TUE-SSCD02-P1
Naranjo, Brian	TUE-AT03-7
Narumi, Kazumasa	WED-REP06-5
Nastasi, M.	MON-IBA01-4
Nastasi, Michael	MON-IBA01-3
Nastasi, Mike	MON-REP01-3
Natisin, Mike R.	THU-NBAE04-2
Nebbia, G.	MON-NBAE02-2
Nebbia, Giancarlo	TUE-ECR05-5
Nebbia, Giancarlo	TUE-SSCD02-1
Nègre, Jean-Paul	TUE-AT04-4
Neri, F.	MON-NBAE02-2
NESARAJA, C. D.	WED-NP05-3
Nesaraja, C. D.	WED-NP05-4
Netherton, K.	WED-NP07-5
Neumann, N.	MON-AP01-4
Neumark, Daniel M.	WED-NBAE06-2
Ng, Martin KC	MON-NST01-2
Nicolosi, D.	WED-NP06-4
Nie, Huiling	MON-NBAE02-4
Nie, Huiling	WED-MA03-P1
Nihongi, Hideaki	WED-MA09-P1
Nikkel, James	TUE-SSCD02-3
Nilsson, Anders	WED-NBAE06-2
Niwa, Yasue	TUE-MA07-3
Nonaka, Tetsuo	TUE-MA07-6
Norarat, Rattanaorn	WED-NST04-5
Nordlund, Dennis	WED-NBAE06-2
Nordlund, Kai	WED-REP06-2
Norgard, Peter	WED-SSCD04-5
Norgard, Peter	WED-SSCD04-P2
Normand, Stéphane	TUE-ECR05-1
Norris, Scott A	TUE-NST09-2
Nortier, F Meiring	TUE-NP04-3
Nortier, F Meiring	WED-MA09-3
Nosworthy, Neil J	MON-NST01-2
Nuttens, Vincent Eric	TUE-AT04-3
Nörtershäuser, Wilfried	TUE-AP05-4
O'Connor, Joseph	MON-NP01-P2
O'Donnell, J. M.	WED-NP07-2
O'Donnell, John M.	MON-NP02-2

O'Malley, P. D.	MON-NP02-1
O'MALLEY, P. D.	WED-NP05-3
O'Malley, P. D.	WED-NP05-4
Odenweller, M.	MON-AP01-4
Ogasawara, Hirohito	WED-NBAE06-2
Ogletree, Frank	MON-IBM01-3
Ohkubo, Takeru	WED-NST04-4
Ohno, Tatsuya	TUE-MA07-4
Ohnuki, Somei	WED-REP07-3
Ohshima, Takeshi	TUE-REP04-6
Ohshiro, Yukimitsu	TUE-AT04-6
Okamura, Masahiro	TUE-ECR05-P2
Okayasu, S.	THU-IBM06-3
Olafsson, Svein	MON-IBM01-4
Olaniyi, Hezekiah B.	MON-IBA01-P9
Olise, Felix S.	MON-IBA01-P9
Olivares, Jose	WED-REP06-1
Olivas, Eric R.	WED-MA09-5
Olivero, Paolo	TUE-NST05-3
Olson, Ronald E.	MON-AP01-P4
Olson, Ronald E.	TUE-AP04-2
Ongel, Senem	MON-IBM01-P3
Onoda, Shinobu	TUE-REP04-6
Onumajor, Adaeze C.	MON-IBA01-P9
Orban, I.	WED-AP07-2
Orban, I.	WED-AP08-1
Orban, Istvan.	WED-AP08-3
Ordonez, Carlos A.	MON-AP02-1
Ordonez, Carlos A.	WED-AP06-5
Ordonez, Carlos A.	WED-AP06-P1
Ordonez, Carlos A.	WED-AP06-P2
Ordonez, Carlos A.	WED-AP06-P3
Ordonez, Carlos A.	WED-AP06-P4
Ordonez, Carlos A.	WED-AP06-P5
Ordonez, Carlos A.	WED-AP06-P6
Ordonez, Carlos A.	WED-AP06-P7
Orozco, L. A.	WED-NP05-1
Ortega, Christopher.	WED-NST03-4
Ortega, Jean-Michel	TUE-AT04-4
Osgood Jr., Richard M.	WED-REP05-5
Osipowicz, Thomas	TUE-IBA05-1
Otranto, Sebastian	MON-AP01-P4
Otranto, Sebastian	TUE-AP04-2
Owen, Hywel	WED-MA04-5
Owoade, Oyediran K.	MON-IBA01-P9
Oya, Yasuhisa	MON-REP01-2
Oyaizu, Michihiro.	TUE-AT04-6
Oztarhan, Ahmet.	MON-IBM01-P3
Oztarhan, Mustafa Ahmet.	MON-NST01-P2

Oztarhan, Mustafa Ahmet.....	MON-NST01-P3
Öztürk, Orhan	MON-NST01-P3
Pacheco, Jose L.....	TUE-ECR05-P1
Pacheco, Jose L.....	MON-AT02-4
Pacheco, Jose L.....	WED-AP06-5
Pacheco, Jose L.....	WED-AP06-P6
Pacheco, Jose L.....	WED-AP06-P7
Pacheco, Jose L.....	WED-ECR04-5
Padilla, Mabel	WED-SSCD04-3
Padilla-Rodal, E.....	WED-NP05-2
Padilla-Rodal, E.....	WED-NP05-4
Padilla-Rodal, Elizabeth	WED-NP06-1
Pain, S. D.	MON-NP02-3
PAIN, S. D.	WED-NP05-3
Pain, S. D.	WED-NP05-4
Pain, S. D.	THU-NP09-5
Pakarinen, Olli H.	WED-REP06-2
Palffy, Adriana.....	WED-AP08-5
Palitsin, V. V.....	MON-AT02-1
Palitsin, Vladimir.....	THU-IBA06-2
Palmer, D.	THU-REP08-3
Pan, Cheng-Ta	WED-REP07-2
Pan, Huiping	MON-IBA01-6
Pandey, Archana	MON-IBM01-2
Pandey, Bimal.....	MON-IBM01-P2
Pandola, L.	WED-NP06-4
Panova, Tatjana V.....	TUE-IBM05-P1
Panova, Tatjana V.....	TUE-IBM05-P2
Pantelica, Anisoara	WED-ECR04-4
Pantelica, Dan	WED-ECR04-4
Papaleo, R.	MON-AT02-2
Pape, André.....	TUE-NST06-3
Parish, Chad.....	TUE-IBA03-1
Park, Yeong-shin	THU-IBM06-P1
Patel, Niravkumar D.	THU-IBA06-P1
Pathak, Anand P.....	MON-IBM02-5
Pathak, Anand P.....	MON-IBM02-P1
Pathak, Anand P.....	MON-IBM02-P2
Paudel, P. R.....	THU-IBM06-P2
Paul, Helmut	WED-IBA07-2
Paul, Helmut	THU-IBM06-1
Paul, Michael	TUE-NP03-4
Pavuluri, Sudhherbabu.....	MON-IBM02-2
Payan, Emmanuel	MON-NBAE02-P2
Pearson, M. R.	TUE-AP05-2
Pearson, M. R.	WED-NP05-1
Peeper, Katrin	TUE-IBA05-5
Peggs, Stephen.....	WED-MA04-1
Pei, Qibing	THU-REP08-1

Pellemoine, Frederique	MON-NP01-P2
Pellemoine, Frederique	WED-REP06-6
Peña-Rodriguez, Ovidio	WED-REP06-1
Peng, Haibing	WED-NST03-2
Peng, Haibo.....	WED-IBM04-2
Peng, N.	MON-AT02-1
Perea, D E	TUE-IBA03-P1
Pereira, N.	WED-NP07-5
Pérez, Patrice	THU-NBAE04-P2
Perkinson, Joy.....	TUE-NST09-4
Perkinson, Joy C.	TUE-NST09-3
Perot, Bertrand.....	MON-NBAE02-P2
Pérot, Bertrand.....	TUE-ECR05-1
Persaud, Arun	TUE-AT03-5
Persaud, Arun	WED-SSCD03-4
Persaud, Arun	WED-SSCD04-6
Peters, E. E.....	TUE-IBA05-6
Peters, W. A.....	MON-NP02-3
PETERS, W. A.	WED-NP05-3
Peters, W. A.....	WED-NP05-4
Peterson, Randolph S.....	WED-TA01-1
Petre, Alexandru	WED-ECR04-4
Petridis, N.	MON-AP01-4
Petridis, Nikos.....	TUE-AP05-4
Petridis, Nikos.....	WED-AP08-3
Petrucci, S.	MON-NBAE02-2
Petterson, Mika	WED-NST04-5
Phair, Larry	TUE-NP03-2
Phillips, Ryan E.	WED-AP06-P1
Phinney, L. C.	WED-ECR04-1
Phipps, David G.....	WED-SSCD03-2
Phlips, Bernard F	WED-SSCD03-2
Phlips, Bernard F.	TUE-ECR05-6
Phongikaroon, Supathorn	TUE-ECR05-4
Phongikaroon, Supathorn	TUE-REP02-4
Pia, Maria Grazia	WED-IBA07-1
Piestrup, Melvin A.....	TUE-AT03-4
Piestrup, Melvin A.....	WED-SSCD03-4
Pinayev, I.	THU-NP08-5
Pindzola, M S.....	MON-AP02-3
Pindzola, Mitch.....	WED-AP06-4
PITTMAN, S. T.	WED-NP05-3
Pittman, S. T.	WED-NP05-4
Podaru, Nicolae C.....	MON-IBA01-P4
Podaru, Nicolae C.....	WED-AT05-4
Poelker, M.....	THU-NP08-5
Pogue, Nathaniel.....	TUE-ECR05-3
Pogue, Nathaniel.....	TUE-REP02-4
Polk, James	MON-IBA02-2

Poltoratska, Yulia	WED-AP08-4
Pons, B.	MON-AP01-P3
Poonia, Surendra.....	WED-AP06-6
Poonia, Surendra.....	WED-AP06-P8
Popescu, Ion V.....	WED-ECR04-4
Porter, L M.....	TUE-IBA03-P1
Portillo, Federico E.....	MON-IBA02-4
Potter, Charles.....	WED-SSCD04-3
Potter, James M.	THU-AT06-6
Potter, James M.	THU-AT06-6
Poudel, Prakash R.....	MON-IBM01-P2
Pouilly, Jean-Christophe	MON-AP01-2
Powell, Amy J.....	THU-IBA06-4
Prados-Estevz, F. M.....	TUE-IBA05-6
Pras, Philippe	TUE-ECR05-1
Primetzhofer, Daniel.....	TUE-IBA04-3
Priyantha, W.	TUE-IBA03-4
Puttaraksa, Nitipon	WED-NST04-5
Putterman, Seth.....	TUE-AT03-7
Py, Matthieu.....	THU-IBM03-3
Qiang, You.....	TUE-REP04-P1
Quarles, Carroll.....	THU-NBAE05-1
Quets, Sebastien.....	WED-MA03-2
Quinn, Heather Marie	TUE-REP03-1
Quint, Wolfgang	TUE-AP05-4
Quintenz, Jeffrey P	MON-PS01-1
Qvist, Staffan	TUE-REP02-5
Rabadán, I.	MON-AP01-P3
Raber, Thomas N.	WED-SSCD04-4
Raber, Thomas N.	WED-SSCD04-P1
Raber, Tom	WED-SSCD04-7
Raciti, G.....	WED-NP06-4
Racolta, Petru Mihai	THU-ECR03-5
Racolta, Petru Mihai	THU-NBAE05-3
Radford, D. C.....	WED-NP05-2
Radford, D. C.....	WED-NP05-4
Radkte, C.	MON-AT02-2
Radtke, Claudio	TUE-IBA04-P4
Rainò, Antonio Cosimo	TUE-MA05-P1
Rajander, Johan.....	TUE-MA05-3
Rajapaksa, Indrajith	WED-NST03-3
Rajasekhara, Shreyas	TUE-REP02-2
Rajesekhara, Shreyas	TUE-IBA05-2
Rajta, I.....	TUE-AP03-6
Ralchenko, Yuri	WED-AP06-2
RAMILLON, Jean-Marc	TUE-AP03-3
Rangama, J.....	MON-AP01-4
Rangama, Jimmy	MON-AP01-2
Ranjbar, V. H.....	THU-NP08-5

Ranjbar, Vahid	THU-NP08-2
Rao, S V S Nageswara	MON-IBM02-P2
Rapisarda, E.	WED-NP06-4
RASCO, B. C.	WED-NP05-3
Ratkiewicz, A.	MON-NP02-3
Ratkiewicz, A.	WED-NP05-4
ReA team, for the	TUE-NP03-1
Reedy, E. T. E.	TUE-NBAE03-5
Reedy, Edward	TUE-NBAE03-4
Regar, J.	TUE-IBA03-4
Reichart, Patrick	TUE-IBA05-5
Reifarh, Rene	WED-AP08-5
Reinert, Tilo	MON-AT02-4
Reinert, Tilo	MON-IBA01-P7
Reinert, Tilo	MON-IBM01-5
Reinert, Tilo	MON-MA01-P1
Reinert, Tilo	WED-ECR04-5
Reinert, Tilo	WED-ECR04-P3
Reinert, Tilo	THU-IBA06-3
Ren, Fan	TUE-NST05-1
Ren, Feng	TUE-REP02-6
Ren, Feng	TUE-REP04-4
Reuschl, R.	TUE-AP05-5
Reuschl, Regina	WED-AP08-3
Reuschl, Regina	WED-AP08-6
Rey, Jean-Michel G	THU-NBAE04-P2
Ridgway, Mark	MON-IBM02-4
Ridgway, Mark C.	WED-REP06-2
ridikas, danas	TUE-ECR05-2
Rimmer, R. A.	THU-NP08-5
Ringle, R.	TUE-AP05-2
Roberson, Derrith A.	WED-TA01-1
Roberts, Andrew D.	WED-TA01-2
Robertson, D.	THU-NP09-5
Robertson, Daniel	MON-NP01-3
Robinson, Joseph	WED-NBAE06-2
Rodrigues, Francio	TUE-IBA04-P3
Rodriguez, Matias	MON-IBM02-4
Rodriguez, Matias Daniel	WED-REP06-4
Roeder, Brian T	MON-IBA02-4
Roessler, Wolfgang	TUE-IBA04-3
Rogachev, G. V.	THU-NP09-3
Romano, F.	WED-NP06-4
Romano, S L	TUE-AP04-P1
Romero, Frank P.	WED-MA09-5
RONCIN, Philippe	TUE-AP03-3
Ronningen, Reg	MON-NP01-P2
Roorda, Sjoerd	TUE-NST05-2
Roorda, Sjoerd	TUE-REP03-4

ROPARS, Frédéric	TUE-AP03-3
Rosen, Stefan	MON-AP01-2
Roser, T.....	THU-NP08-5
Rossi, Paolo	TUE-MA05-P3
Rossi, Paolo	TUE-MA05-P4
Rossi, Paolo	THU-IBA06-4
Roussé, Jean-Yves	THU-NBAE04-P2
Rousseau, Patrick.....	MON-AP01-2
Rout, B.....	THU-IBM06-P2
Rout, Bibhudutta.....	MON-AT02-4
Rout, Bibhudutta.....	MON-IBA01-P7
Rout, Bibhudutta.....	MON-IBM01-5
Rout, Bibhudutta.....	WED-ECR04-3
Rout, Bibhudutta.....	WED-ECR04-5
Rout, Bibhudutta.....	WED-ECR04-P3
Rout, Bibhudutta.....	WED-IBA07-P2
Rubanov, S.....	MON-IBM01-P1
Ruchhoeft, Paul.....	MON-NST07-3
Ruck, B J.....	MON-IBM01-P1
Ruelas, Marcos	WED-SSCD04-2
Ruiz, Nicolas.....	THU-NBAE04-P2
Rundberg, Bob	WED-NP06-6
Rundberg, R. S.....	WED-NP07-2
Runkle, Robert.....	TUE-NBAE03-1
Rusnak, Brian	WED-SSCD04-1
Russo, Germano.....	MON-MA02-3
Rutledge, James T.....	WED-SSCD04-5
Ryge, Peter.....	TUE-SSCD02-2
Rykalin, Victor	TUE-MA05-1
Saba, Joseph.....	TUE-NP03-5
Sabaiduc, Vasile	TUE-NP04-5
Sacquin, Yves	THU-NBAE04-P2
Sadrozinski, Hartmut	TUE-MA05-1
Safdar, A.	WED-AP08-1
Sagari, Ananda A.R.	WED-NST04-5
Saito, Akito	WED-MA03-6
Saitoh, Yuichi	WED-REP06-5
Sajavaara, Timo	MON-IBA01-7
Sajavaara, Timo	MON-IBA01-P5
Sajavaara, Timo	MON-IBA01-P6
Sajavaara, Timo	WED-NST04-5
Sajo-Bohus, Laszlo	MON-IBA02-4
Sakai, Hideyuki.....	MON-NP01-1
Sakurai, Yoshinori	WED-MA04-3
Salem, S.	TUE-AP05-5
Sanchez, Dario	TUE-IBA04-P3
Sanetullaev, A.....	MON-NP02-1
Sann, H.	MON-AP01-4
Sannié, Guillaume.....	TUE-ECR05-1

Santiago-Gonzalez, D.	THU-NP09-3
SANTOS, ANTONIO C F.....	THU-NBAE04-1
SANTOS, ANTONIO C F.....	THU-NBAE04-P1
Santos, Jose Paulo.....	TUE-AP05-3
Santos, M B	WED-ECR04-2
Saracco, Paolo.....	WED-IBA07-1
Sarazin, F.	THU-NP09-5
Sardina, D.	WED-NP06-4
Sarrao, John L.....	MON-PS03-1
Sataka, M.	THU-IBM06-3
Sato, Kazuhisa	WED-IBM04-4
Sattarov, Akhdiyor.....	TUE-ECR05-3
Sattarov, Akhdiyor.....	TUE-ECR05-4
Sattarov, Akhdiyor.....	TUE-REP02-4
Sattarov, Akhdiyor I.	TUE-ECR05-7
Sauerbrey, Roland.....	THU-AT06-P1
Sauter, Patrick.....	TUE-AP04-3
Sava, Tiberiu Bogdan	WED-ECR04-4
Sayre, Dan.....	WED-AP08-5
Scharf, Andreas.....	TUE-NP03-6
Scharf, Andreas.....	WED-NP06-2
Schatz, H.	THU-NP09-5
Schein, Mike	MON-NP01-P2
Schein, Mike	WED-REP06-6
Schenkel, Thomas.....	MON-IBM01-3
Schenkel, Thomas.....	TUE-AT03-5
Schenkel, Thomas.....	WED-SSCD03-4
Schenkel, Thomas.....	WED-SSCD04-6
Schenkel, Thomas.....	THU-IBM06-6
Schindler, Matthias	WED-NP06-2
Schinner, A.	THU-REP09-4
Schiwietz, Gregor	TUE-IBA04-2
Schlenvoigt, Hans-Peter	THU-AT06-P1
Schlessner, Sophie	TUE-AP05-3
Schlotter, William F.....	WED-NBAE06-2
Schmid, Ernst.....	MON-MA02-2
Schmid, Thomas E.....	MON-MA02-2
Schmidt, Henning	MON-AP01-2
Schmidt, L.....	MON-AP01-4
Schmidt-Boecking, H.	MON-AP01-4
Schmitt, K.	MON-NP02-1
Schmitt, K. T.....	WED-NP05-4
Schmitt, K. T.....	THU-NP09-5
Schneider, Dieter	WED-AP08-2
Schneider, Dieter	WED-AP08-5
Schoeffler, Markus S.	MON-AP01-4
Schoenlein, Robert W.....	WED-NBAE06-2
Schoessler, S.	MON-AP01-4
Scholz, Michael	MON-MA02-1

Scholz, Uwe.....	MON-MA02-1
Schramm, Ulrich.....	TUE-AP05-4
Schramm, Ulrich.....	THU-AT06-P1
Schreiber, D K.....	TUE-IBA03-P1
Schuch, R.....	WED-AP07-2
Schuch, R.....	WED-AP08-1
Schuch, Reinhold.....	TUE-AP05-4
Schulte, Reinhard.....	TUE-MA05-1
Schulte-Borchers, M.....	WED-IBA07-4
Schultz, B. E.....	TUE-AP05-2
Schultz, David R.....	WED-AP06-1
Schultz, David R.....	WED-AP06-2
Schultz, L.....	THU-REP08-3
Schumer, Joseph W.....	TUE-NBAE03-2
Schumer, Joseph W.....	WED-SSCD03-2
Schumer, Joseph W.....	TUE-ECR05-6
Schwartz, B. T.....	THU-NP08-5
Schwartz, Julian.....	MON-IBM01-3
Schwarz, Stefan.....	TUE-NP03-1
Schwellenbach, David.....	THU-AT06-6
Schwoebel, Paul R.....	TUE-AT03-6
Schässburger, Kai-Uwe.....	WED-AP08-4
Scott, Bobby.....	WED-SSCD04-3
Seabury, Edward H.....	MON-NBAE02-P3
Seabury, Edward H.....	TUE-SSCD01-P1
Sean Woods, Sean.....	WED-AT05-2
Seel, Judith.....	MON-MA02-2
Segebade, C.....	MON-NBAE01-5
Segebade, Chr.....	THU-REP08-6
Segebade, Christian.....	MON-NBAE01-1
Segebade, Christian.....	MON-NBAE01-2
Segebade, Christian.....	MON-NBAE01-6
Segura, Rodrigo.....	TUE-IBA04-P2
Seipel, H. A.....	TUE-NBAE03-5
Seitz, Fabien.....	MON-AP01-2
Seki, Toshio.....	THU-IBA06-1
Seki, Toshio.....	THU-IBM03-3
Selmi, S.....	MON-NBAE02-2
SERRUYS, Yves.....	TUE-IBA05-4
Severin, Daniel.....	WED-REP06-6
Seweryniak, D.....	MON-NP02-3
Sfienti, C.....	WED-NP06-4
Shabaev, Vladimir.....	WED-AP08-2
Shand, C.....	MON-NP02-3
Shao, L.....	MON-IBA02-1
Shao, Lin.....	MON-IBA01-5
Shao, Xi.....	TUE-NP03-P1
Shapira, D.....	MON-NP02-1
Shapira, D.....	WED-NP05-4

sharma, ajay	WED-NP07-P1
Sharma, B. P.	WED-ECR04-P1
Sharma, B. P.	WED-ECR04-P2
Sharma, B. P.	THU-ECR03-P2
Sharma, B. P.	THU-IBM06-P2
Shastry, Karthik	THU-NBAE04-3
Shavorskiy, Andrey	WED-NBAE06-2
Shaw, Tim.....	TUE-SSCD02-2
Sheehy, B.	THU-NP08-5
Shen, Y.H.....	TUE-REP04-P2
Shen, Yang.....	TUE-AP05-P1
Shibayama, T	WED-REP07-3
Shimada, Masashi	MON-REP01-2
Shinpaugh, J. L.	THU-REP09-4
Shinpaugh, Jefferson L	MON-AT02-3
Shiomi, Miho	TUE-MA07-6
Shioyama, Yoshiyuki.....	TUE-MA07-5
Shipman, Patrick D.....	TUE-NST06-2
Shirai, Katsuyuki	TUE-MA07-4
Shirato, Hiroki	WED-MA09-P1
Shitamoto, Sho	THU-IBA06-1
Shu, Anthony	WED-TA01-4
Shutthanandan, Shuttha	THU-IBM03-4
Shutthanandan, V.....	TUE-IBA03-2
Shutthanandan, V.....	TUE-IBA03-P1
Shutthanandan, V.....	TUE-IBM05-2
Shutthanandan, Vaithiyalingam.....	TUE-IBA03-1
Shutthanandan, Vaithiyalingam.....	TUE-IBM05-4
Shutthanandan, Vaithiyalingam.....	THU-IBM06-5
Siebenwirth, Christian	MON-MA02-2
Siefermann, Katrin.....	WED-NBAE06-2
Sielemann, Rainer.....	MON-IBM01-4
Sigillito, A. J.	TUE-IBA05-6
Sigmund, P.....	THU-REP09-4
Siketic, Zdravko.....	WED-ECR04-6
Silverman, Ido.....	TUE-NP03-4
Simcic, Jurij	WED-AP06-1
Simion, Corina Anca	WED-ECR04-4
Simon, A.	TUE-AP04-5
Simon, A.	TUE-AP05-5
simon, aliz.....	TUE-ECR05-2
Simon, Anna	WED-AP08-3
Simon, Haik	WED-AP08-5
Simon, M. C.....	TUE-AP05-2
Simon, M. J.....	WED-IBA07-4
SIMON, Marius Johannes	TUE-AP03-3
Simon, V. V.	TUE-AP05-2
Simos, Nickolas	MON-NP01-P2
Simpson, Michael	TUE-ECR05-4

Simpson, Michael	TUE-REP02-4
Singh, Bipin	MON-NST07-1
Sinha, Shrabani	TUE-SSCD02-2
Skala, Wayne G	THU-ECR03-4
Skala, Wayne G	THU-ECR03-6
Skuratov, V. A.	MON-IBM01-6
Slaughter, Daniel	WED-NBAE06-2
Smit, Ziga	THU-IBA06-5
Smith, Eric	THU-ECR03-1
Smith, Greg.....	TUE-SSCD02-3
Smith, Jennifer L	WED-AT05-2
SMITH, M. S.	WED-NP05-3
Smith, M. S.	WED-NP05-4
Smith, M. S.	THU-NP09-5
Smith, Nicholas.....	WED-MA09-4
Smith, R. J.....	TUE-IBA03-4
Smith, Richard	TUE-IBA03-3
Snead, Lance L	THU-IBM03-4
Soares, G. V.	MON-AT02-2
SOBOTKA, L.	WED-NP05-3
Sofie, S.....	TUE-IBA03-4
Sofie, Stephen	TUE-IBA03-3
Sokolov, Mihail	MON-REP01-2
Sokullu Urkac, Emel.....	MON-NST01-P2
Solin, Olof.....	TUE-MA05-3
Solov'yov, Andrey V.	THU-REP09-2
Song, Shuangqi	WED-NST03-4
Sooby, Elizabeth	TUE-ECR05-4
Sooby, Elizabeth	TUE-REP02-4
Sood, Avneet.....	WED-SSCD04-5
Sorbom, Brandon N.....	WED-AP06-3
Sortica, Mauricio	TUE-IBA04-P3
Sortica, Mauricio	TUE-IBA04-P4
Soulsby, Michael	THU-IBA06-P1
SPASSOVA, I.....	WED-NP05-3
Spillmann, U.	TUE-AP05-5
Spillmann, Uwe	TUE-AP05-4
Spillmann, Uwe	WED-AP08-3
Spillmann, Uwe	WED-AP08-6
Sprouse, G. D.....	WED-NP05-1
Squillante, M.....	THU-REP08-3
Sridharan, K.	TUE-REP04-5
Sridharan, Kumar.....	WED-AT05-3
Srivastava, Sanjeev Kumar	MON-IBM02-2
Srivilliputhur, Srinivasan	WED-REP05-4
Stahle, Peter W	WED-AP06-3
Stan-Sion, Catalin	WED-ECR04-4
Stancil, Phillip C.....	MON-AP01-1
Stanek, Christopher R.....	TUE-IBM05-3

Starovoitova, V.	MON-NBAE01-5
Starovoitova, Valerii N.	MON-NBAE01-3
Statescu, Mihai	WED-ECR04-4
Stech, Edward	MON-NP01-3
Stedile, F. C.	MON-AT02-2
Stein, Gregory J	WED-IBM04-6
Steinräter, Olaf	MON-MA02-1
Stevanato, L.	MON-NBAE02-2
Stevanato, Luca.....	TUE-ECR05-5
Stevanato, Luca.....	TUE-SSCD02-1
Stewart, Thomas Maxwell	TUE-MA05-3
Stipanovic, Arthur J	WED-AT05-1
Stoeffl, Wolfgang	WED-AP08-5
Stoehlker, Thomas	TUE-AP05-4
Stoehlker, Thomas	WED-AP08-2
Stoehlker, Thomas	WED-AP08-5
Stoehlker, Thomas	WED-AP08-6
Stoica, Silviu Daniel	THU-ECR03-5
Stojanovic, Milica Maric	THU-IBA06-5
Stokes, Donna	WED-NST03-3
Stolterfoht, N	TUE-AP03-5
Stoner, Jon	MON-NBAE01-3
Storms, Scott.....	WED-SSCD04-2
Stracener, D. W.....	WED-NP05-2
Stracener, Daniel W	TUE-NP04-4
Strader, Matthew.....	WED-NBAE06-2
Straticiu, Mihai	THU-ECR03-5
Straticiu, Mihai	THU-NBAE05-3
Strellis, Dan	TUE-SSCD02-2
Stubbers, Robert A.....	TUE-AT03-3
Stuck, C.....	MON-AP01-4
Stuhl, Alexander	WED-NP06-2
Sturm, Felix	WED-NBAE06-2
Stöhlker, Th.	TUE-AP05-5
Stöhlker, Thomas	WED-AP08-3
Stöhlker, Thomas	THU-AT06-P1
Su, Jao-Jang	TUE-NP03-P1
Sullivan, James	MON-IBM02-4
Sultan, Deborah	TUE-NP04-2
Sun, Li.....	WED-NST03-4
Sun, Z. J.	MON-NBAE01-5
Sundararajan, Jennifer	TUE-REP04-P1
Suntarampillai, Thevuthasan	TUE-IBM05-6
Surdutovich, Eugene.....	THU-REP09-2
Surko, Cliff M.....	THU-NBAE04-2
Surzhykov, Andrey	WED-AP08-3
Surzhykov, Andrey	WED-AP08-4
Suthanthiran, Krishnan	TUE-NP04-5
Suvorova, A A	MON-IBM01-P1

Suzuki, Kazuhiro	TUE-MA07-4
Suzuki, Kazumichi.....	WED-MA09-2
Suzuki, Motofumi.....	WED-REP06-5
Suzuki, Yoshiyuki.....	TUE-MA07-4
Svoboda, C.....	TUE-IBM05-2
Swanekamp, Stephen B	TUE-NBAE03-2
Swanekamp, Stephen B	WED-SSCD03-2
Sy, Amy	TUE-AT03-5
Sy, Amy	WED-SSCD03-4
Szabo, Csilla I.....	TUE-AP05-3
Szilagyi, E.....	TUE-IBA05-3
Tabacaru, Gabriel	TUE-NP03-3
Taheri, Mitra L.....	TUE-IBM05-5
Takács, Sándor.....	MON-NBAE01-4
Takahashi, Kazumasa	TUE-ECR05-P2
Takayanagi, Taisuke	WED-MA09-P1
Takei, Kuniharu	WED-SSCD04-6
Talou, Patrick.....	MON-NP02-2
Tamaki, Tomoaki.....	TUE-MA07-4
Tan, Wanpeng.....	MON-NP02-4
Tanaka, Hiroki	WED-MA04-3
Tandecki, M.	WED-NP05-1
Tang, Ming	TUE-REP02-6
Tang, Vincent	TUE-AT03-7
Tang, Vincent	WED-SSCD04-1
Tanis, J A	TUE-AP03-5
Tanis, J. A.	TUE-AP04-5
Tanis, John.....	TUE-AP03-4
TANIS, John A	TUE-AP03-3
Tárkányi, Ferenc	MON-NBAE01-4
Tartari, Fatos.....	THU-IBA06-5
Tashenov, S.....	WED-AP07-2
Tashenov, S.....	WED-AP08-1
Tashenov, Stanislav	WED-AP08-4
Taylor, Wayne A	TUE-NP04-3
Teng, Ping-kun	TUE-MA05-P2
Teranishi, Takashi.....	WED-NP06-3
Terashima, Kazuki.....	TUE-MA07-3
Tesmer, Joseph	TUE-REP02-5
Tesmer, Joseph	WED-AT05-P1
Tesmer, Joseph	THU-REP09-5
Tesmer, Joseph R.....	TUE-REP02-6
Than, R.	THU-NP08-5
Theroux, Joseph.....	TUE-MA05-3
Thevuthasan, S.....	TUE-IBA03-2
Thevuthasan, S.....	TUE-IBA03-P1
Thevuthasan, Suntharampillai	MON-IBM01-2
Thevuthasan, Suntharampillai	THU-ECR03-3
Thevuthasan, Suntharampillai	THU-IBM06-4

Thevuthasanand, Theva	THU-IBM03-2
Thompson, J. S.	MON-IBA01-P1
Thompson, Scott J.	TUE-SSCD01-P1
Thorn, Daniel	THU-AT06-P1
Thorn, Daniel Bristol	WED-AP08-3
Thurber, Casey	WED-IBA07-P2
Tilakaratne, Buddhi	TUE-NST09-5
Tilakaratne, Buddhi	WED-NST03-3
Tilakaratne, Buddhi P	MON-IBA01-5
Tilakaratne, Buddhi P	WED-NST03-4
Tintori, C.....	MON-NBAE02-2
Tiss, Kenneth J.....	WED-AT05-2
Titze, J.....	MON-AP01-4
Tkac, Peter	WED-MA09-4
Tkac, Peter	WED-MA09-5
Toader, Ovidiu F.....	WED-TA01-5
Toburen, L. H.	THU-REP09-4
Toburen, Larry H.....	MON-AT02-3
Tokesi, K.....	TUE-AP03-6
Tokesi, K.....	THU-NBAE04-5
Tokesi, K.....	THU-REP09-4
Tomita, Takuro	TUE-REP04-6
Tomut, Marilena	WED-REP06-6
Tonchev, Anton	WED-NP06-6
Tongay, Sefaattin	TUE-NST05-1
Toolin, M.	THU-REP08-3
Tornga, S.....	THU-REP08-3
Tornow, Werner	WED-NP06-6
Totake, Satoshi	WED-MA09-2
Totoki, Tadahide.....	TUE-MA07-5
Tovesson, F.....	WED-NP06-5
Tran, Clara TH.....	MON-NST01-2
Trassinelli, M.	TUE-AP05-5
Trassinelli, Martino.....	WED-AP08-3
Trassinelli, Martino.....	WED-AP08-6
Trautmann, Christina	WED-REP06-4
Trautmann, Christina	WED-REP06-6
Trbojevic, Dejan	WED-MA04-1
Trepathy, Prabhat.....	TUE-ECR05-4
Trepathy, Prabhat.....	TUE-REP02-4
Tribble, Robert E	TUE-NP03-3
Tribedi, L. C.	TUE-AP05-5
Trinter, F.	MON-AP01-4
TROCELLIER, Patrick.....	TUE-IBA05-4
Tropea, S.....	WED-NP06-4
Trotsenko, S.....	TUE-AP05-5
Trotsenko, S.....	WED-AP08-1
Trotsenko, Serge	TUE-AP05-4
Trotsenko, Sergiy.....	WED-AP08-3

Trotsenko, Sergiy.....	WED-AP08-6
Trotsenko, Sergiy.....	THU-AT06-P1
Tsai, Pei-rong.....	TUE-MA05-P2
Tsai, Ya-wen.....	TUE-MA05-P2
Tsang, M. B.	MON-NP02-1
Tseren, T.	WED-NP07-2
Tsevkov, Pavel.....	TUE-ECR05-4
Tsoutas, Kostadinos	MON-NST01-2
Tsuchida, Hidetsugu	MON-IBA01-P3
Tsujii, Hirohiko.....	TUE-MA07-5
Tsujimoto, Masahiro.....	WED-REP06-5
Tsutsui, Hiroshi.....	WED-MA04-3
Tsvetkov, Pavel.....	TUE-REP02-4
Tumey, Scott.....	MON-REP01-5
Tung, Chuang-jong	TUE-MA05-P2
Tuozzolo, J. E.	THU-NP08-5
Turanli, Ali Erdem.....	MON-NST01-P3
Turley, Colin.....	WED-TA01-P2
Turner, Joshua J.	WED-NBAE06-2
Tyliszczak, Tolek.....	WED-NBAE06-2
Tynan, George	MON-REP01-4
Tyryshkin, Alexei M.....	THU-IBM06-6
Uberuaga, Blas P	TUE-IBM05-3
Uberuaga, Blas Pedro	TUE-REP04-1
Ukirde, V.	WED-ECR04-P1
Ukirde, V.	WED-ECR04-P2
Ukirde, V.	THU-ECR03-P2
Ullmann, J. L.	WED-NP07-2
Ullmann-Pfleger, K.....	MON-AP01-4
Ullrich, Susanne.....	THU-REP09-1
Ulrich, B.	MON-AP01-4
Umegaki, Kikuo.....	WED-MA09-P1
Umekawa, Tooru	WED-MA09-P1
Umezawa, Masumi	WED-MA09-1
Umezawa, Masumi	WED-MA09-2
Umezawa, Masumi	WED-MA09-P1
Urbain, Xavier	WED-AP07-4
Urkac, Emel Sokullu.....	MON-IBM01-P3
Urkac, Emel Sokullu.....	MON-NST01-3
Urkac, Emel Sokullu.....	MON-NST01-P3
Uzunov, Nikolay.....	TUE-MA05-2
Uzunov, Nikolay.....	TUE-MA05-P3
Uzunov, Nikolay.....	TUE-MA05-P4
V, Saikiran	MON-IBM02-5
V, Saikiran	MON-IBM02-P1
V, Saikiran	MON-IBM02-P2
Vacik, Jiri.....	THU-REP08-5
Vainionpaa, Hannes	WED-SSCD03-4
Vainionpaa, Jaakko H.....	TUE-AT03-4

Vaithialingam, Shutthanandan.....	TUE-IBM05-6
Vaithiyalingam, Shutthanandan.....	MON-IBM01-2
Vaithiyalingam, Shutthanandan.....	THU-IBM06-4
Valdés, Jorge E.	TUE-IBA04-P2
Valiev, Ruslan Z.	TUE-REP04-3
Van Horn, J. David	THU-NBAE04-4
van Kan, Jeroen Anton	MON-NST01-4
van Kan, Jeroen Anton	WED-NST04-2
Van Reeth, P.	MON-AP02-2
Vandegrift, George	WED-MA09-4
Vandegrift, George F.	WED-MA09-5
Vandervorst, Wilfried	THU-ECR03-2
VanGordon, James A.....	WED-SSCD04-5
VanGordon, James A.....	WED-SSCD04-P2
Vanhoy, J. R.	TUE-IBA05-6
Vantomme, André.....	THU-ECR03-2
Vardney, S	TUE-IBM05-2
Varga, T	TUE-IBA03-2
Varga, Tamas	TUE-IBM05-4
Varga, Tamas	TUE-IBM05-6
Varga, Tamas	WED-IBM04-4
Vargas, Patricio.....	TUE-IBA04-P2
Variale, Vincenzo	TUE-MA05-P1
Varner, R. L.	WED-NP05-2
Vasantachart, A K	TUE-AP04-P1
VAUBAILLON, Sylvain	TUE-IBA05-4
Vemuri, Rama Sessa R.....	TUE-IBM05-6
Vendamani, V S.....	MON-IBM02-P2
Venkatachalam, Dinesh K.	TUE-NST05-1
Verbeck, Guido F.....	WED-IBA07-P2
Verbruggen, Patrick.....	WED-MA03-2
Vetter, P.	THU-NP09-5
Vetter, Paul	TUE-NP03-5
Vetterick, Greg A.....	TUE-IBM05-5
Vieira, D. J.	WED-NP07-2
Viesti, G.....	MON-NBAE02-2
Viesti, Giuseppe.....	TUE-ECR05-5
Viesti, Giuseppe.....	TUE-SSCD02-1
Vilayurganapathy, Subramanian.....	MON-IBM01-2
Vineyard, Michael	WED-TA01-P2
Vobly, P.	THU-NP08-5
Voigtsberger, J.	MON-AP01-4
Voitkiv, Alexander	WED-AP08-3
Voller, Tom.....	TUE-NP04-2
Volodin, V. A.	MON-IBM01-6
Volotka, A.....	TUE-AP05-5
Voyevodin, V. N.....	TUE-REP02-1
Vura-Weis, Josh.....	WED-NBAE06-2
Wagner, Andreas	THU-AT06-P1

Waitz, M.	MON-AP01-4
Wakeford, D.	THU-REP08-3
Waldron, William	TUE-NP03-5
Walker, Amy V.....	THU-IBM03-1
Walker, C. L.	WED-NP07-2
Walker, Phil	WED-AP08-5
Wallace, M.....	THU-REP08-3
Wampler, William R.....	MON-REP01-1
Wang, C M.....	TUE-IBA03-P1
Wang, C M.....	TUE-IBM05-2
Wang, Chongmin.....	TUE-IBM05-6
Wang, Chung-hsiang	TUE-MA05-P2
Wang, G.....	THU-NP08-5
Wang, Guangfu.....	WED-IBA07-5
Wang, Han	WED-SSCD04-1
Wang, Haoyu	WED-MA03-P1
Wang, Jinguo	WED-NST03-5
Wang, Lumin	THU-IBM06-2
Wang, Qian	WED-NST03-1
Wang, Qiang	TUE-IBA05-1
Wang, Tieshan	TUE-IBA05-1
Wang, Tieshan	WED-IBM04-2
Wang, Xaiotie	TUE-NST05-1
Wang, Xi.....	MON-IBA01-3
Wang, Xuemei	MON-IBA01-5
Wang, Xuemei	TUE-NST09-5
Wang, Xuemei	WED-NST03-2
Wang, Xuemei	WED-NST03-3
Wang, Y.....	MON-REP01-5
Wang, Y.Q.....	MON-IBA01-4
Wang, Yongqiang	THU-REP09-5
Wang, Yongqiang	MON-IBA01-3
Wang, Yongqiang	MON-REP01-3
Wang, Yongqiang	MON-REP01-4
Wang, Yongqiang	TUE-REP02-5
Wang, Yongqiang	TUE-REP02-6
Wang, Yongqiang	TUE-REP02-P1
Wang, Yongqiang	WED-AT05-P1
Wang, Zheming	THU-IBM03-6
Warczak, A.	TUE-AP04-5
Ward, S. J.....	MON-AP02-2
Ward, S. J.....	WED-AP07-5
Was, Gary	TUE-IBA05-5
Was, Gary S	WED-TA01-5
Watanabe, S	WED-REP07-3
Waterhouse, Anna.....	MON-NST01-2
Watkins, Jordan W.....	TUE-ECR05-P1
Weathers, Duncan L	MON-IBM01-P2
Weathers, Duncan L	TUE-ECR05-P1

Weathers, Duncan L.	MON-AT02-4
Weathers, Duncan L.	WED-AP06-5
Weathers, Duncan L.	WED-AP06-P6
Weathers, Duncan L.	WED-AP06-P7
Weathers, Duncan L.	WED-ECR04-5
Webb, R. P.	MON-AT02-1
Webb, Roger P.	MON-IBM02-1
Webb, Roger P.	TUE-IBA05-3
Webb, Roger P.	THU-IBA06-2
Webb, S. D.	THU-NP08-5
Weber, Bruce V.	TUE-NBAE03-2
Weber, G.	TUE-AP05-5
Weber, Guenter.	WED-AP08-6
Weber, Günter.	TUE-AP05-4
Weber, Günter.	WED-AP08-3
Weber, William J.	TUE-IBA03-5
Weber, William J.	THU-IBM03-4
Weber, William J.	TUE-IBM05-4
Wehe, D.	THU-REP08-3
Weidenspointner, Georg.	WED-IBA07-1
Weis, Christoph D.	THU-IBM06-6
Weise, Fabian.	WED-NBAE06-2
Weisenstein, Adam.	TUE-IBA03-3
Weiss, A. H.	THU-NBAE04-3
Weiss, A. H.	THU-NBAE05-2
Weiss, Anthony S.	MON-NST01-2
Wells, D.	MON-NBAE01-5
Wells, Douglas P.	MON-NBAE01-3
Welsch, Carsten P.	TUE-AP05-P2
Wetteland, C. J.	TUE-REP04-5
Wetteland, Chris J.	WED-AT05-3
Weyer, Gerd.	MON-IBM01-4
Whaley, Josh A.	MON-IBA02-3
Wharton, C Jayson.	MON-NBAE02-P3
Whitlow, Harry J.	WED-NST04-5
Whyte, Dennis G.	WED-AP06-3
Wickramarachchi, S.	TUE-AP03-5
Wickramarachchi, Samanthi Jayamini.	TUE-AP03-4
Wiedeking, Mathis.	WED-AP08-5
Wiedenhoeffer, Ingo.	MON-IBA02-4
Wiedenhöffer, I.	THU-NP09-3
Wiescher, M.	THU-NP09-5
Wiescher, Michael.	MON-NP01-3
Wiescher, Michael.	MON-NP02-4
Wiescher, Michael.	TUE-NP03-5
Wijesundera, Dharshana.	TUE-NST09-5
Wijesundera, Dharshana.	WED-NST03-3
Wijesundera, Dharshana Nayanajith.	MON-IBA01-5
Wilbur, D Scott.	WED-MA09-3

Wilde, Carl.....	WED-NP06-6
Wilder, Julie.....	WED-SSCD04-3
Wilhelemy, Jerry.....	WED-NP06-6
Williams, Cecil L.....	TUE-NP04-4
Williams, David L	TUE-AT03-4
Williams, G.V.M	MON-IBM01-P1
Williams, Scott	WED-AP07-P1
Williams, Scott	WED-TA01-3
Williams, Scott	WED-TA01-P1
Wimmer, Kathrin.....	MON-NP02-5
Winkelbauer, J.	MON-NP02-1
Winklehner, Daniel.....	TUE-NP03-5
Winters, D.....	TUE-AP05-5
Winters, Danyal	WED-AP08-6
Winters, Danyal F. A.	WED-AP08-3
Winters, Natalya	WED-AP08-3
Wittmer, Walter	TUE-NP03-1
Wofford, Joshua D.....	WED-AP06-P5
Woloshun, Keith A.	WED-MA09-5
Woodruff, D. P.	TUE-IBA04-4
Woods, Denton	MON-AP02-2
Woolf, Richard S	WED-SSCD03-2
Woolf, Richard S.	TUE-ECR05-6
Wright, Travis.....	WED-NBAE06-2
Wu, BingBing.....	WED-IBA07-5
Wu, Judy	WED-NST03-1
Wuenschel, Sara	THU-NP09-2
Wulf, Eric A.....	WED-SSCD03-2
Wulf, Eric A.....	TUE-ECR05-6
Xiao, Jun	TUE-AP05-1
Xiao, Jun	TUE-AP05-P1
Xu, Chunping.....	TUE-REP02-P1
Xu, Guowei.....	WED-NST03-1
Xu, Xinxin	TUE-IBA05-1
Xue, Haizhou	THU-IBM03-4
Yajima, Satoru	WED-MA04-3
Yakimenko, V.....	THU-NP08-5
Yamaguchi, N.....	WED-REP07-3
YAMAZAKI, Yasunori	TUE-AP03-3
Yang, Kunjie.....	WED-IBM04-2
Yang, Li	THU-IBM03-2
Yang, S.C.....	TUE-REP04-P2
Yang, Yang	TUE-AP05-P1
Yao, Ke	TUE-AP05-1
Yao, Shude.....	MON-IBA01-6
Yao, Zhongwen.....	WED-REP07-6
Yaqoob, Faisal	MON-IBA01-2
Yasuda, Keisuke	MON-IBA01-P3
Yates, S. W.	TUE-IBA05-6

Yennello, Sherry J	THU-NP09-2
Yin, Youngbai.....	MON-NST01-2
Yotprayoonsak, Peerapong	WED-NST04-5
Youker, Amanda.....	WED-MA09-4
Young, Albert	THU-NP08-3
Young, Frank C	WED-SSCD03-2
Young, Frank C.	TUE-ECR05-6
Youngs, M.	MON-NP02-1
Yousif, FB.....	MON-AP01-P1
Yu, C. -H.....	WED-NP05-2
Yu, Deyang	WED-AP08-3
Yu, Hui	THU-REP09-1
Yu, Kin M.	THU-IBM06-6
Yu, Lingda	WED-IBA07-5
Yu, Xiao-Ying	THU-IBM03-2
Yu, Y.C.....	TUE-REP04-P2
Zaijing, Sun.....	THU-REP08-6
Zamfir, Nicolae Victor.....	WED-ECR04-4
Zampa, Gianluigi	TUE-MA05-P3
Zampa, Nicola.....	TUE-MA05-P3
Zdorovets, Maxim V.....	WED-REP06-3
zeman, andrej	TUE-ECR05-2
Zettergren, Henning.....	MON-AP01-2
Zhang, Fuxiang	WED-REP07-5
Zhang, Genfa	WED-IBM04-2
Zhang, Hong Lin.....	WED-AP08-3
Zhang, J.....	WED-NP05-1
Zhang, Jiaming	WED-REP07-5
Zhang, Jiaming	THU-IBM06-2
Zhang, Jin	WED-NBAE06-2
Zhang, Ken he.....	WED-REP07-6
Zhang, Kun	TUE-NST06-3
Zhang, Limin	WED-IBM04-2
Zhang, Miao.....	MON-IBA01-3
Zhang, Renjian.....	WED-IBA07-5
Zhang, Wei	TUE-AP05-1
Zhang, Yanwen.....	TUE-IBA03-1
Zhang, Yanwen.....	TUE-IBA03-5
Zhang, Yanwen.....	TUE-IBM05-4
Zhang, Yanwen.....	THU-IBM03-4
Zhao, Jiangtao.....	TUE-IBA05-1
Zhao, Qiang	THU-ECR03-2
Zhao, Xiao-Lei.....	TUE-NBAE03-6
Zhao, Y.	WED-NP05-1
Zhou, C. L.....	MON-AP01-4
ZHOU, ChunLin	TUE-AP03-3
Zhu, Zihua.....	TUE-IBA03-1
Zhu, Zihua.....	THU-ECR03-3
Zhu, Zihua.....	THU-IBM03-2

Zhu, Zihua.....	THU-IBM03-4
Zhu, Zihua.....	THU-IBM03-6
Zhu, Zihua.....	THU-IBM06-5
Zier, Jacob C.....	TUE-NBAE03-2
Zier, Jacob C.....	WED-SSCD03-2
Zier, Jacob C.....	TUE-ECR05-6
Zimmerman, Robert Lee.....	MON-NP01-P1
Zimmerman, Robert Lee.....	WED-TA02-3
Zlobinskaya, Olga.....	MON-MA02-2
Zou, Yaming.....	TUE-AP05-1
Zou, Yaming.....	TUE-AP05-P1
Zutshi, Vishnu.....	TUE-MA05-1